

UNIVERSITY OF BIRMINGHAM

EVALUATION OF THE IMMUNE PHENOTYPE OF WOMEN WITH RECURRENT PREGNANCY LOSS

by

DANAI BAGKOU DIMAKOU

A thesis submitted to the University of Birmingham for the degree of

DOCTOR OF PHILOSOPHY

Institute of Immunology and Immunotherapy

College of Medical and Dental Sciences

University of Birmingham

December 2021

UNIVERSITY OF
BIRMINGHAM

University of Birmingham Research Archive

e-theses repository

This unpublished thesis/dissertation is copyright of the author and/or third parties. The intellectual property rights of the author or third parties in respect of this work are as defined by The Copyright Designs and Patents Act 1988 or as modified by any successor legislation.

Any use made of information contained in this thesis/dissertation must be in accordance with that legislation and must be properly acknowledged. Further distribution or reproduction in any format is prohibited without the permission of the copyright holder.

Abstract

The current working hypothesis in recurrent pregnancy loss (RPL) suggests an immune dysregulation in women with this condition, with most studies highlighting an increase in natural killer (NK) cell numbers and cytotoxicity and a shift towards T helper (T_H) cell pro-inflammatory cytokine secretion, termed “Type-1/Type-2 hypothesis”. Experimental findings however remain contentious, hindering the introduction of immunological testing into clinical practice, despite the increasing pressure from clinicians and couples affected.

Through a nationwide survey, a strong variation in clinical practice was observed, with different definitions of RPL used and multiple tests employed for the identification of potential risk factors. Immunological testing was offered in 3 (9.38%) clinics included, while several therapies, including immunomodulatory agents, were utilised for the management of idiopathic RPL, underlining the need for further research into the role of the immune system in this condition.

Using peripheral blood samples from non-pregnant women with RPL and healthy controls, a broad immunophenotypic analysis was performed, confirming the NK cell increase and revealing a reduction in T cell prevalence in women with RPL. Further examination by mass cytometry displayed a decrease in regulatory-like T and B cell subsets and an increase in a plasma cell-like subpopulation, although validation of these findings utilising additional markers is required.

The elevated NK cell cytotoxicity, often referenced in RPL, was undetectable in the present study, although an increased degranulation capacity of these cells was seen. Cytolytic molecule release by peripheral blood mononuclear cells (PBMCs)

appeared reduced in women with RPL, possibly counterbalancing the enhanced degranulation. A unique mass cytometry panel was employed for the detailed investigation of activating and inhibitory receptor expression on NK cells. Increased prevalence of mature cytotoxic $CD57^+$ NK cells was detected in the RPL population, accompanied by an increase in subsets lacking the expression of multiple inhibitory receptors, indicating an enhanced responsiveness of the NK cell population to activating signalling.

Furthermore, elevated pro-/anti-inflammatory cytokine-producing T_H cell ratios were detected in women with RPL, accompanied however by decreased pro-/anti-inflammatory cytokine expression intensity on these cells. NK cell cytokine production appeared deficient in women with this condition. Interestingly, the shift towards pro-inflammatory molecules was evident when the levels of cytokine secretion by PBMCs were assessed, in agreement to the Type-1/Type-2 hypothesis. Pro- and anti-inflammatory cytokine secretion by PBMCs also appeared elevated in women with RPL and a following miscarriage, compared to those that were either in the 3rd trimester of their subsequent pregnancy or had a live birth, highlighting a potential prognostic capacity of these markers.

The findings of the present study highlight a dysregulation in peripheral immunity of women with RPL, which cannot however be appropriately described using a pro-/anti-inflammatory dichotomy. Although certain immune parameters, such as elevated NK cell levels, could provide potential diagnostic biomarkers, with plausible prognostic markers also proposed, further research on both peripheral and uterine samples is required to fully elucidate the role of the immune system in RPL, allowing the introduction of immunological testing into clinical practice.

Acknowledgements

First and foremost I would like to thank my supervisors Dr Jennifer Tamblyn, Prof David Lissauer, Prof Arri Coomarasamy, and Prof Alex Richter for their invaluable contribution to this project. Their experience and continued support was inspiring and encouraged me to remain enthusiastic throughout the project.

I would like to thank the members of the Clinical Immunology Service of the University of Birmingham, including Dr Siân Faustini, Dr Ilaria Chicca, Mr Tim Plant, and Ms Sarah Terjesen for their assistance. I also want to thank Mr Steven Dix, Ms Genevieve Panaro, Ms Kamila Silverio Fernadez for their support with the TBNK and flow cytometry assays. I am particularly grateful to Dr Naeem Khan, Dr Shahram Golbabapour, and Dr Akshay Patel for their support with the mass cytometry assay development, execution, and data analysis. I am also thankful to Dr Animesh Acharjee and Prof Georgios Gkoutos for their willingness to impart their knowledge on biomarker identification. Additionally, I would like to thank Dr Farhat Latif Khanim's for providing us with the K562 cells for the cytotoxicity assay and Dr Sayeed Haque for his input on the statistical analysis.

I extend my gratitude to the Tommy's research team in the Birmingham Women's Hospital, and in particular to Ms Oonagh Pickering and Ms Racheal Boothe, without whom recruitment for this project would not be feasible. I would like to thank the CHIPP research team, and in particular Ms Phern Adams, for their contribution towards control women recruitment. I would also like to thank the CERM research team in the University Hospital Coventry & Warwickshire, particularly Prof Siobhan Quenby, Ms Nicola Flint, and Ms Natalie Morris, for their contribution towards

recruitment, which was critical to the completion of the project during the COVID-19 pandemic. I am especially grateful to Prof Jan Brosens for his valuable input.

Last but not least, I would like to thank the Tommy's National Centre for Miscarriage Research for generously funding this project and of course all the participants that were willing to contribute to research.

Declaration of COVID-19 impact

The present project took place during the coronavirus (COVID-19) pandemic. Recruitment through Tommy's miscarriage clinic in Birmingham Women's Hospital was thus halted for three months. To improve recruitment rate upon re-opening of non-emergency clinics, additional recruitment through Tommy's clinic in the University Hospital Coventry & Warwickshire was initiated. Fortunately, with the support of the Tommy's teams in both Birmingham Women's Hospital and the University Hospital Coventry & Warwickshire, the recruitment goal was achieved in a timely manner.

During the first COVID-19 lockdown, when recruitment was halted, we designed and distributed an online survey to clinicians across the UK to assess current practice regarding idiopathic recurrent pregnancy loss diagnosis and management. A relevant chapter has been added to the present thesis.

1 CONTENTS

1 Contents 1

1.1 Figure and table summary 9

1.2 Abbreviations 66

2 Introduction 70

2.1 Definition, prevalence, and impact 71

2.2 Risk factors 72

2.3 The role of the immune system in RPL 76

2.4 NK cells in RPL 85

2.4.1 NK cell numbers 87

2.4.2 NK cell receptors 91

2.4.3 NK cell cytotoxicity 102

2.4.4 NK cell cytokine and angiogenic factor production 104

2.5 T cells in RPL 107

2.5.1 Cytotoxic T cells 109

2.5.2 T helper cell cytokine profiling 110

2.5.3 Regulatory T cells 116

2.6 B cells in RPL 117

2.6.1 Antibody production 119

2.6.2 Regulatory B cells 120

2.7 Other immune cells in RPL 121

2.7.1 Dendritic cells 121

2.7.2 Monocytes/Macrophages 123

2.8 Immunological testing in idiopathic RPL 126

3 Aims and Objectives 131

4 Materials and Methods 133

4.1 Ethics 134

4.2 Survey 134

4.2.1 Development and distribution 134

4.2.2 Data analysis 136

4.3 Participants 136

4.4 Reagents 138

4.5 Peripheral blood sample collection, storage, and peripheral blood mononuclear cell isolation 142

4.6 Peripheral blood mononuclear cell storage at -80ºC 143

4.7 Peripheral blood mononuclear cell stimulation 143

4.8 T, B, and NK cell assay 145

4.9 Flow cytometry 147

4.9.1 Panel design 147

4.9.2 NK cell panel staining 150

4.9.3 T cell panel staining 150

4.9.4 Cytokine panel staining 151

4.9.5 Dead cell staining 152

4.9.6 Data analysis 152

4.10 Mass cytometry 158

4.10.1 Panel design 158

4.10.2 Mass cytometry panel staining 160

4.10.3 Data analysis 165

4.11 Cytotoxicity assay 169

4.11.1 Data analysis 173

4.12 Enzyme-linked immunosorbent assay 175

4.12.1 Data analysis 178

4.13 Statistical analysis and data presentation 179

4.13.1 Survey 179

4.13.2 Participant demographics 180

4.13.3 TBNK, flow, cytotoxicity assay, and ELISA 180

4.13.4 Subpopulation analysis 181

4.13.5 Mass cytometry 182

4.14 Statistical analysis for biomarker identification 184

5 National Survey Exploring the Current Practice for the Diagnosis and Management of Idiopathic RPL 187

5.1 Results 188

5.1.1 Respondent/institution demographics 188

5.1.2 RPL diagnosis 191

5.1.3 Investigation of RPL risk factors 192

5.1.4 Immunological investigations for RPL 200

5.1.5 Idiopathic RPL management 202

5.2 Discussion 212

5.2.1 Limitations and future research 216

6 Participant Demographics 218

6.1 Demographic data 219

6.2 Discussion 226

6.2.1 Limitations and future research 228

7 Immunophenotyping 232

7.1 Results 233

7.1.1 TBNK assay 233

7.1.2 Flow cytometry assay – NK cells 235

7.1.3 Flow cytometry assay – T cells 237

7.1.4 Mass cytometry assay – T cells 240

7.1.5 Mass cytometry assay – B cells 246

7.1.6 Immune cell subsets in RPL and control subpopulations 251

7.1.7 Summary 264

7.2 Discussion 264

7.2.1 Limitations and future research 276

8 NK cell Activation and Cytotoxicity Evaluation 278

8.1 Results 279

8.1.1 Cytotoxicity assay 279

8.1.2 ELISA – Perforin and granzyme secretion 284

8.1.3 Flow cytometry assay – NK cell activation and cytokine receptor expression 287

8.1.4 Mass cytometry assay – NK cells 297

8.1.5 NK cell activity in RPL and control subpopulations 307

8.1.6 Summary 316

8.2 Discussion 317

8.2.1 Limitations and future research 335

9 Cytokine Analysis 338

9.1 Results 339

9.1.1 Flow cytometry assay – T_H cell cytokine production 339

9.1.2 Flow cytometry assay – NK cell cytokine production 349

9.1.3 ELISA – Cytokine, chemokine, and colony-stimulating factor secretion 363

9.1.4 Cytokine balance in RPL and control subpopulations 374

9.1.5 Summary 409

9.2 Discussion 412

9.2.1 Limitations and future research 422

10 Immune Biomarkers for the Identification of Women with RPL 425

10.1 Results 426

10.2 Discussion 431

10.2.1 Limitations and future research 432

11 Final Discussion 434

12 List of References 443

13 Appendices 480

13.1 Questionnaire designed and distributed to explore current practice for the diagnosis and management of idiopathic RPL 481

13.2 Flow and mass cytometry 489

13.3 Flow cytometer set-up and quality control 491

13.4 Peripheral blood mononuclear cell isolation time optimization 491

13.5 Peripheral blood mononuclear cell stimulation optimization 495

13.6 Flow cytometry assay optimization 500

13.7 Flow cytometry assay validation 505

13.8 Cell death evaluation following staining with the different flow cytometry panels 506

13.9 Compensation tube preparation for flow cytometry 506

13.10 Mass cytometry antibody conjugations 507

13.11 Mass cytometry antibody titrations 510

13.12 Mass cytometry assay validation 515

13.13 Mass cytometry data analysis pipeline 515

13.14 Cytotoxicity assay optimization and troubleshooting 518

13.15 Cytotoxicity assay validation 529

13.16 Effect of NK cell:K562 cell ratio on specific target cell death 531

13.17 Enzyme-linked immunosorbent assay optimization and validation 533

13.18 Data utilised for biomarker identification 535

13.19 Effectiveness of models built for the identification of women with RPL .. 537

14 Publications arising from the present thesis 539

1.1 Figure and table summary

Figure summary		page
Introduction		
Figure 1.	**Risk factors associated with recurrent pregnancy loss (RPL).** The prevalence of underlying conditions in women with RPL is displayed. In around half of the cases no risk factors can be identified and the condition is termed "idiopathic".[9, 18, 37, 48, 82, 83]	75
Figure 2.	**Overview of decidual immunity during healthy pregnancy, at the stage of fetal growth.** The contribution of decidual immune cell populations in the establishment and maintenance of pregnancy is displayed. Ang-1: angiopoietin 1, CD: cluster of differentiation, DC: dendritic cell, GM-CSF: granulocyte-macrophage colony-stimulating factor, IFN: interferon, IL: interleukin, Mφ: macrophage, NK cell: natural killer cell, T_C cell: cytotoxic T cell, T_H cell: T helper cell, TNF: tumor necrosis factor, Treg cell: regulatory T cell, VEGF: vascular endothelial growth factor	78
Figure 3.	**Overview of peripheral immunity during healthy early pregnancy.** The activity of peripheral immune cell populations during the initial pregnancy stages is illustrated. CD: cluster of differentiation, DC: dendritic cell, IFN: interferon, IL: interleukin, Mo: monocyte, NK cell: natural killer cell, T_C cell: cytotoxic T cell, T_H cell: T helper cell, TNF: tumor necrosis factor, Treg cell: regulatory T cell	80
Figure 4.	**Overview of decidual immunity in women with recurrent pregnancy loss.** The suggested pro-inflammatory shift in the decidual immune cell activity of women with recurrent pregnancy loss is depicted. Ang-1: angiopoietin 1, CD: cluster of differentiation, DC: dendritic cell, GM-CSF: granulocyte macrophage colony-stimulating factor, IFN: interferon, IL: interleukin, Mφ: macrophage, NK cell: natural killer cell, T_C cell: cytotoxic T cell, T_H cell: T helper cell, TNF: tumor necrosis factor, Treg cell: regulatory T cell, VEGF: vascular endothelial growth factor	82
Figure 5.	**Overview of peripheral immunity in women with recurrent pregnancy loss.** The suggested pro-inflammatory shift in the peripheral immune cell activity of women with recurrent pregnancy loss is shown. CD: cluster of differentiation, DC: dendritic cell, IFN: interferon, IL: interleukin, Mo: monocyte,	83

	NK cell: natural killer cell, T_C cell: cytotoxic T cell, T_H cell: T helper cell, TNF: tumor necrosis factor, Treg cell: regulatory T cell	
Figure 6.	**Natural Killer (NK) cell genetic, phenotypic, and functional changes in healthy pregnancy and recurrent pregnancy loss (RPL).** Alterations in receptor expression, killer-cell immunoglobulin-like receptor (KIR) gene frequencies, cytolytic molecule production, and cytokine secretion detected in the periphery (P) and uterus (U) of pregnant vs non-pregnant women and in RPL vs healthy pregnancy are displayed. CD: cluster of differentiation, IFN: interferon, IL: interleukin, IL-2R: IL-2 receptor, ILT: immunoglobulin-like transcript, NKG2: natural killer group 2, Tim-3: T cell immunoglobulin and mucin domain-containing protein-3, TGF: transforming growth factor, TNF: tumor necrosis factor	86
Figure 7.	**Natural Killer (NK) cell receptors and their cognate ligands on target cells.** Receptors transmitting activating (green) and inhibitory (red) signals on NK cells are displayed. Molecules whose interaction with the respective receptors is not fully established are shown in parentheses. CD: cluster of differentiation, HLA: human leukocyte antigen, IgG: immunoglobulin G, ILT: immunoglobulin-like transcript, KIR: killer-cell immunoglobulin-like receptor, MIC: MHC class I chain-related protein, NKG2: natural killer group 2, PD-1: programmed cell death protein 1, PD-L1: programmed death-ligand 1, TIGIT: T cell immunoreceptor with Ig and ITIM domains, Tim-3: T cell immunoglobulin and mucin domain-containing protein-3, ULBP: UL16-binding protein	92
Figure 8.	**T helper (T_H) cell subset prevalence and cytokine secretion in non-pregnant and pregnant women and women with recurrent pregnancy loss (RPL).** Alterations in pro-inflammatory T_H1 and T_H17 and anti-inflammatory T_H2 and regulatory T cell (Treg) subpopulation levels, as well as changes in pro-inflammatory tumor necrosis factor (TNF)-α, TNF-β, interferon (IFN)-γ, interleukin (IL)-1β, IL-2, IL-12, IL-17, IL-18, IL-21, IL-22, IL-23, and granulocyte-macrophage colony-stimulating factor (GM-CSF) and anti-inflammatory IL-4, IL-10, IL-13, and transforming growth factor (TGF)-β secretion in the periphery and uterus of pregnant vs non-pregnant women and in RPL vs healthy pregnancy are depicted.	111

Materials and Methods		
Figure 9.	**Summary of the experimental pipeline for cytokine assessment.** The major steps of the protocols followed for A) peripheral blood mononuclear cell (PBMC) stimulation, B) examination of cytokine production by flow cytometry, and C) cytokine, chemokine, and colony-stimulating factor secretion quantification by enzyme-linked immunosorbent assay (ELISA) are outlined. Wash steps are not included. Ab: antibody, Fc block: Fc receptor blocking solution, Fix/perm: fixation/permeabilization, NK cell: natural killer cell, RT: room temperature, T_H cell: T helper cell	144
Figure 10.	**T, B, and Natural Killer (NK) cell (TBNK) assay gating strategy.** Following bead exclusion the leukocyte population was gated on based on their CD45 (PerCP-Cy5.5) expression and side scatter (SSC) properties. The CD3 (FITC) expression of leukocytes was examined and the $CD3^-$ cells were assessed for their CD16/CD56 (PE) and CD19 (APC) expression to measure $CD16/CD56^+CD19^-$ NK and $CD16/CD56^-CD19^+$ B cell levels. The CD4 (PE-Cy7) and CD8 (APC-Cy7) expression of the $CD3^+$ T cell population was further investigated to determine the levels of the $CD8^-CD4^+$ helper and $CD8^+CD4^-$ cytotoxic subpopulations.	146
Figure 11.	**Flow cytometry assay Natural Killer (NK) cell panel gating strategy.** The singlet population was selected based on the forward scatter height (FSC-H) and forward scatter area (FSC-A). In that gate lymphocytes were selected according to their side (SSC-A) and forward scatter area (FSC-A). In the lymphocyte gate the $CD3^-$ population was gated on and in that gate $CD56^+$ NK cells were identified. In the NK cell population the $CD56^{dim}CD16^+$ and $CD56^{bright}CD16^-$ subsets were selected. CD69 expression on total $CD3^-CD56^+$, $CD3^-CD56^{dim}CD16^+$, and $CD3^-CD56^{bright}CD16^-$ NK cells was evaluated.	154
Figure 12.	**Flow cytometry assay T cell panel gating strategy.** The singlet population was selected based on the forward scatter height (FSC-H) and forward scatter area (FSC-A). In that gate lymphocytes were selected according to their side (SSC-A) and forward scatter area (FSC-A). In the lymphocyte gate the $CD3^+$ T cell population was gated on and in that gate the helper $CD4^+CD8^-$ (T_H) and cytotoxic $CD4^-CD8^+$ (T_C) subsets were identified. In both these subsets the expression of CD45RA was assessed. In the $CD4^+CD8^-$ gate the $FoxP3^+$ population was	155

	also selected. The $CD25^{+}CD127^{low/-}$ regulatory (Treg) subpopulation in the $FoxP3^{+}$ cell gate was examined.	
Figure 13.	**Flow cytometry assay T helper cell cytokine panel gating strategy.** The singlet population was selected based on the forward scatter height (FSC-H) and forward scatter area (FSC-A). In that gate lymphocytes were selected according to their side (SSC-A) and forward scatter area (FSC-A). In the lymphocyte gate the $CD3^{+}CD8^{-}$ T helper cell population was gated on and in that gate the expression of the IL-2, IFN-γ, TNF-α, IL-10, and IL-17A cytokines was assessed.	156
Figure 14.	**Flow cytometry assay Natural Killer (NK) cell cytokine panel gating strategy.** The singlet population was selected based on the forward scatter height (FSC-H) and forward scatter area (FSC-A). In that gate lymphocytes were selected according to their side (SSC-A) and forward scatter area (FSC-A). In the lymphocyte gate the $CD3^{-}$ cell population was gated on and in that gate the $CD16^{+}$ and/or $CD56^{+}$ population was selected. In that $CD16^{+}/CD56^{+}$ population, the $CD56^{+}$ NK cells and the $CD56^{dim}CD16^{+}$ NK cell subpopulation were gated on and in these gates the CD215, CD25, IFN-γ, IL-10, and TNF-α expression was examined.	157
Figure 15.	**Summary of the experimental pipeline for detailed lymphocyte phenotypic assessment.** The major steps of the protocol followed for the examination of natural killer (NK), T, and B cells by mass cytometry are displayed. Peripheral blood mononuclear cell (PBMC) thawing steps and wash steps are not included. Ab: antibody, CyTOF: cytometry by time-of-flight, Fc block: Fc receptor blocking solution, PFA: paraformaldehyde, RT: room temperature	163
Figure 16.	**Mass cytometry data clean-up and debarcoding.** Calibration beads were initially excluded and outliers were then removed according to the residual, offset, width, and center parameters. The singlet population was gated on according to DNA staining. In the singlet population the live cells were gated on. To debarcode data, in the live cell gate the population positive for the barcode of interest was selected, while populations positive for the other barcodes were excluded.	166
Figure 17.	**Mass cytometry assay lymphocyte gating strategy.** The gating strategies used for the identification of the A) Natural Killer, B) T, and C) B cell subpopulations in the cleaned-up and debarcoded mass cytometry data are illustrated. More specifically, NK cells were identified through gating on $CD3^{-}$	168

	$CD45^+$ cells, followed by gating on $CD14^-CD19^-$ cells, and $CD56^+$ cell identification. T cells were detected through $CD3^+CD45^+$ cell gating, followed by $CD14^-CD19^-$ cell identification, and gating on the $CD56^-$ cell population. The B cell population was identified through gating on $CD3^-CD45^+$ cells, followed by $CD14^-CD56^-$ cell gating, and selection of $CD19^+$ cells.	
Figure 18.	**Summary of the experimental pipeline for Natural Killer (NK) cell cytotoxicity assessment.** The major steps of the protocols followed for A) alive K562 isolation and staining, B) NK cell enrichment, and C) NK-K562 co-culture for the evaluation of NK cell degranulation, using CD107a as a degranulation marker, and the examination K562 cell death, using propidium iodide (PI), are illustrated. Wash steps are not included. Ab: antibody, CD: cluster of differentiation, complete RPMI: Roswell Park Memorial Institute 1640 medium containing 10% FBS and 1% penicillin/streptomycin, PBMCs: peripheral blood mononuclear cells, RT: room temperature	172
Figure 19.	**Natural Killer (NK) cell cytotoxicity assay gating strategy.** The NK and K562 populations are displayed according to their side (SSC-A) and forward scatter (FSC-A) area. In the "FlowAIGoodEvent" population the singlet population was gated on, according to the forward scatter height (FSC-H) and FSC-A. In that gate the alive and dead NK and K562 cell populations were detected, according to the PKH67 membrane dye staining of K562 cells and the propidium iodide (PI) staining of dead cells. In the alive and dead NK cell gates the expression of CD107a was examined.	174
Figure 20.	**Delta area plot generated following FlowSOM clustering and ConsensusClusterPlus metaclustering.** The delta score, represented by the relative change in the area under the CDF curve, indicates the relative amount of additional cluster stability obtained when clustering into k groups, compared to clustering into k-1 groups, in each of the A) Natural Killer, B) T, and C) B cell datasets.	183
National Survey Exploring the Current Practice for the Diagnosis and Management of Idiopathic RPL		
Figure 21.	**Respondent geographical location.** The number of responses collected from clinics in different regions of England and Scotland is illustrated, alongside the clinics' approximate geographical location (stars).	189

	(Response rate=78.38%) Picture adapted from Wikipedia (https://en.wikipedia.org/wiki/File:English_regions_2009.svg)	
Figure 22.	**Diagnostic criteria for women review in recurrent pregnancy loss clinics.** Clinical criteria in regards to A) number of losses, B) presence of consecutive losses, and C) biochemical losses are illustrated. Both the number of responses (*N*) and percentage (%) calculated based on total responses obtained for each question is depicted. (A - Response rate=83.78%, B - Response rate=100.00%, C - Response rate=97.30%)	192
Figure 23.	**Summary of diagnostic tests performed for the investigation of anatomical risk factors potentially associated with recurrent pregnancy loss.** Both routine and clinically indicated investigations are included, with both the number of responses (*N*) and the percentage (%), calculated according to the total number of responses for the respective question (*N*=32). (Response rate=86.49%)	194
Figure 24.	**Summary of diagnostic tests performed for the investigation of genetic/chromosomal risk factors potentially associated with recurrent pregnancy loss.** Both routine and clinically indicated investigations are included, with both the number of responses (*N*) and the percentage (%), calculated according to the total number of responses for the respective question (*N*=32). (Response rate=86.49%)	195
Figure 25.	**Summary of diagnostic tests performed for the investigation of haematological risk factors potentially associated with recurrent pregnancy loss.** Both routine and clinically indicated investigations are included, with both the number of responses (*N*) and the percentage (%), calculated according to the total number of responses for the respective question (*N*=32). (Response rate=86.49%)	196
Figure 26.	**Summary of diagnostic tests performed for the investigation of hypothalamic-pituitary-adrenal axis-associated risk factors potentially linked to recurrent pregnancy loss.** Both routine and clinically indicated investigations are included, with both the number of responses (*N*) and the percentage (%), calculated according to the total number of responses for the respective question (*N*=32). (Response rate=86.49%)	197
Figure 27.	**Summary of diagnostic tests performed for the investigation of thyroid-associated risk factors potentially linked to recurrent pregnancy loss.** Both routine and	198

	clinically indicated investigations are included, with both the number of responses (*N*) and the percentage (%), calculated according to the total number of responses for the respective question (*N*=32). (Response rate=86.49%)	
Figure 28.	**Summary of diagnostic tests performed for the investigation of diabetes-associated risk factors potentially linked to recurrent pregnancy loss.** Both routine and clinically indicated investigations are included, with both the number of responses (*N*) and the percentage (%), calculated according to the total number of responses for the respective question (*N*=32). (Response rate=86.49%)	198
Figure 29.	**Summary of diagnostic tests performed for the investigation of infection-associated risk factors potentially linked to recurrent pregnancy loss.** Both routine and clinically indicated investigations are included, with both the number of responses (*N*) and the percentage (%), calculated according to the total number of responses for the respective question (*N*=32). (Response rate=86.49%)	199
Figure 30.	**Summary of diagnostic tests performed for the investigation of additional risk factors potentially associated with recurrent pregnancy loss.** Both routine and clinically indicated investigations are included, with both the number of responses (*N*) and the percentage (%), calculated according to the total number of responses for the respective question (*N*=32). (Response rate=86.49%)	199
Figure 31.	**Median effectiveness/likelihood to suggest different treatments for the management of idiopathic recurrent pregnancy loss.** Medians were calculated based on responses obtained using a five-point Likert scale. Friedman test was used, accompanied by the Dunn's test for multiple comparisons, *: p≤0.05	211
	Participant Demographics	
Figure 32.	**Number of controls and women with recurrent pregnancy loss (RPL) in relation to their gravidity.** The number of control women and women with RPL, subcategorised according to their past pregnancies is depicted.	221
Figure 33.	**Number of controls and women with recurrent pregnancy loss (RPL) in relation to their parity.** The number of control women and women with RPL, subcategorised according to their past live births is depicted.	221
Figure 34.	**Number of women with recurrent pregnancy loss (RPL) in relation to the number of miscarriages in their reproductive**	222

	history. The number of women with RPL, subcategorised according to their past miscarriages is illustrated	
Figure 35.	**Underlying risk factors detected in women with recurrent pregnancy loss RPL.** The number of women in the RPL cohort (*N*=100) exhibiting each of the underlying conditions potentially associated with RPL is displayed. The number of women with idiopathic RPL, in whom no underlying condition could be detected is also shown.	222
Figure 36.	**Subsequent pregnancy outcome of women with recurrent pregnancy loss (RPL).** The number of women with RPL, sub-categorised according to the outcome of their following pregnancy is illustrated. Women in the RPL group who have not conceived since their recruitment or who could not be reached during follow-up are not included.	226
Immunophenotyping		
Figure 37.	**TBNK assay results regarding lymphocyte subpopulation prevalence.** The prevalence of A) $CD3^+$, B) $CD3^+CD4^+CD8^-$ helper, C) $CD3^+CD4^-CD8^+$ cytotoxic, and D) $CD3^+CD4^+CD8^+$ T cells in the $CD45^+$ leukocyte population, as well as E) $CD3^-CD19^-CD56/CD16^+$ Natural Killer cell and F) $CD3^-CD19^+CD56/CD16^-$ B cell prevalence in the $CD45^+$ leukocyte population of healthy controls (*N*=79) and women with recurrent pregnancy loss (RPL) (*N*=96) is illustrated. Normally distributed datasets (A, B): Unpaired t test performed, mean and standard deviation displayed. Non-normally distributed datasets (C-F): Mann-Whitney test used, median illustrated. ns: non-significant, *: p≤0.05	234
Figure 38.	**TBNK assay results regarding lymphocyte subpopulation absolute counts.** The absolute counts of A) $CD3^+$, B) $CD3^+CD4^+CD8^-$ helper, C) $CD3^+CD4^-CD8^+$ cytotoxic, and D) $CD3^+CD4^+CD8^+$ T cells, E) the ratio between $CD4^+$ and $CD8^+$ T leukocytes, as well as the absolute counts of F) $CD3^-CD19^-CD56/CD16^+$ Natural Killer cells and G) $CD3^-CD19^+CD56/CD16^-$ B cells in healthy controls (*N*=79) and women with recurrent pregnancy loss (RPL) (*N*=96) is shown. Mann-Whitney test utilised, median displayed. ns: non-significant, **: p≤0.01	235
Figure 39.	**Natural Killer (NK) cell and NK cell subset prevalence in women with recurrent pregnancy loss (RPL) and controls.** The prevalence of $CD3^-CD56^+$ NK cells in the A) peripheral blood mononuclear cell (PBMC) and B) lymphocyte population, and the percentage of	237

	C) $CD56^{dim}CD16^{+}$ and D) $CD56^{bright}CD16^{-}$ cells in the NK cell population of healthy controls (*N*=77) and women with RPL (*N*=90) is displayed. E) The $CD56^{bright}CD16^{-}$ to $CD56^{dim}CD16^{+}$ NK cell ratio is also shown. F) Example gating summarizing the strategy used to identify NK cell population and subpopulations is included. Mann-Whitney test used, median illustrated. ns: non-significant, **: p≤0.01, ****: p≤0.0001	
Figure 40.	**T cell and T cell subset prevalence in women with recurrent pregnancy loss (RPL) and controls.** The prevalence of $CD3^{+}$ T cells in the A) peripheral blood mononuclear cell (PBMC) and B) lymphocyte population, the percentage of C) $CD4^{+}CD8^{-}$ helper (T_H) and D) $CD4^{-}CD8^{+}$ cytotoxic (T_C) cells in the T cell population, the prevalence of $CD45RA^{+}$ cells in E) $CD4^{+}CD8^{-}$ and the F) $CD4^{-}CD8^{+}$ T cells, and G) the regulatory T cell (Treg) prevalence in the $CD4^{+}CD8^{-}$ T cell subpopulation of healthy controls (*N*=80) and women with RPL (*N*=89) is illustrated. H) Example gating summarizing the strategy used to identify T cell population and subpopulations is included. Normally distributed dataset without significantly different variances (D): Unpaired t test used, mean and standard deviation displayed. Normally distributed dataset with significantly different variances (E): Unpaired t test with Welch's correction utilised, mean and standard deviation shown. Non-normally distributed datasets (A-C, F, G): Mann-Whitney test performed, median illustrated. ns: non-significant, ****: p≤0.0001	239
Figure 41.	**Relative abundance of each sample in the mass cytometry datasets used to analyse T and B cell marker expression in control women and women with recurrent pregnancy loss (RPL).** The relative frequency of each sample, calculated according to cell counts, in the total A) T cell and B) B cell populations of the control (*N*=80) and RPL (*N*=100) cohorts is depicted. Individual samples are represented by different colours, with patient_id also displayed (RPL: 0268-0439 and 1349-1456, Control: 920-1000).	241
Figure 42.	**Multi-dimensional scaling (MDS) plot of the control and recurrent pregnancy loss (RPL) T cell samples, summarizing the level of similarity between cohorts.** The distances between samples approximate the difference in median expression of all markers examined, including CD4, CD8, CD25, CD127, CD226, T-cell immunoreceptor with Ig and ITIM domains/T cell immunoglobulin and mucin	242

	domain-containing protein 3 (TIGIT/Tim-3), and programmed cell death protein 1 (PD-1), translating multi-dimensional data into a two-dimensional scatter plot. Labels displaying the sample identity are included.	
Figure 43.	**Multi-dimensional scaling and phenotyping of 20 T cell clusters identified by mass cytometry.** A) Multi-dimensional scaling (MDS) plot of pseudobulks generated, with each point on the plot representing a cluster-sample instance, coloured according to the cluster, shaped based on the condition, and with a size proportional to the number of cells it represents. Distances between instances indicate relative phenotypic differences between clusters and samples, taking into consideration all markers assessed. The major phenotypic subgroups are demonstrated. B) Heatmap of median cluster of differentiation (CD)4, CD8, CD25, CD127, CD226, T-cell immunoreceptor with Ig and ITIM domains/T cell immunoglobulin and mucin domain-containing protein 3 (TIGIT/Tim-3), and programmed cell death protein 1 (PD-1) expression intensity across the different T cell clusters, ranging from high (red) to low (blue).	243
Figure 44.	**Visualization of T cell cluster prevalence in women with recurrent pregnancy loss (RPL) as detected by mass cytometry.** The 20 clusters of interest in women with RPL and controls are illustrated using a A) uniform manifold approximation and projection (UMAP) plot, with cells coloured according to the respective clusters, a B) relative abundance box plot, depicting cluster proportion in each sample of the control (orange) and RPL (blue) groups, and a C) differential analysis heatmap, displaying the normalised proportion of each cluster in each sample. The heatmap colour varies from purple, suggesting relative under-representation, to orange, suggesting relative over-representation. The green/grey bar indicates significantly (green) or non-significantly (grey) differentially abundant clusters, accompanied by the adjusted p values. A bar representing the log fold change (logFC), indicating over-representation in RPL (blue) or controls (orange) is also included. Cluster phenotypes according to the expression of the CD4, CD8, CD25, CD127, CD226, T-cell immunoreceptor with Ig and ITIM domains/T cell immunoglobulin and mucin domain-containing protein 3 (TIGIT/Tim-3), and programmed cell death protein 1 (PD-1) markers of interest are depicted.	245

Figure 45.	**Multi-dimensional scaling (MDS) plot of the control and recurrent pregnancy loss (RPL) B cell samples, summarizing the level of similarity between cohorts.** The distances between samples approximate the difference in median expression of all markers examined, including CD5, CD25, CD27, CD38, T-cell immunoreceptor with Ig and ITIM domains/T cell immunoglobulin and mucin domain-containing protein 3 (TIGIT/Tim-3), and programmed cell death protein 1 (PD-1), translating multi-dimensional data into a two-dimensional scatter plot. Labels displaying the sample identity are included.	247
Figure 46.	**Multi-dimensional scaling and phenotyping of 20 B cell clusters identified by mass cytometry.** A) Multi-dimensional scaling (MDS) plot of pseudobulks generated, with each point on the plot representing a cluster-sample instance, coloured according to the cluster, shaped based on the condition, and with a size proportional to the number of cells it represents. Distances between instances indicate relative phenotypic differences between clusters and samples, taking into consideration all markers assessed. The major phenotypic subgroups are demonstrated. B) Heatmap of median cluster of differentiation (CD)5, CD25, CD27, CD38, T-cell immunoreceptor with Ig and ITIM domains/T cell immunoglobulin and mucin domain-containing protein 3 (TIGIT/Tim-3), and programmed cell death protein 1 (PD-1) expression intensity across the different B cell clusters, ranging from high (red) to low (blue).	248
Figure 47.	**Visualization of B cell cluster prevalence in women with recurrent pregnancy loss (RPL) as detected by mass cytometry.** The 20 clusters of interest in women with RPL and controls are illustrated using a A) uniform manifold approximation and projection (UMAP) plot, with cells coloured according to the respective clusters, a B) relative abundance box plot, depicting cluster proportion in each sample of the control (orange) and RPL (blue) groups, and a C) differential analysis heatmap, displaying the normalised proportion of each cluster in each sample. The heatmap colour varies from purple, suggesting relative under-representation, to orange, suggesting relative over-representation. The green/grey bar indicates significantly (green) or non-significantly (grey) differentially abundant clusters, accompanied by the adjusted p values. A bar representing the log fold change (logFC),	250

	indicating over-representation in RPL (blue) or controls (orange) is also included. Cluster phenotypes according to the expression of the CD5, CD25, CD27, CD38, T-cell immunoreceptor with Ig and ITIM domains/T cell immunoglobulin and mucin domain-containing protein 3 (TIGIT/Tim-3), and programmed cell death protein 1 (PD-1) markers of interest are depicted.	
Figure 48.	**Natural Killer (NK) and T cell population and subpopulation prevalence in women with idiopathic recurrent pregnancy loss (RPL) and controls.** The prevalence of A) $CD3^{-}CD56^{+}$ NK cells in the lymphocyte population and B) $CD56^{dim}CD16^{+}$ and C) $CD56^{bright}CD16^{-}$ cells in the NK cell population of healthy controls (*N*=77) and women with idiopathic RPL (*N*=48) is illustrated. The percentage of D) $CD3^{+}$ T cells in the lymphocyte population, E) $CD4^{+}CD8^{-}$ and F) $CD4^{-}CD8^{+}$ cells in the T cell population, and G) regulatory T cells (Tregs) in the $CD4^{+}CD8^{-}$ T cell subpopulation of healthy controls (*N*=80) and women with idiopathic RPL (*N*=47) is also displayed. Normally distributed dataset without significantly different variances (F): Unpaired t test used, mean and standard deviation shown. Non-normally distributed datasets (A-E, G): Mann-Whitney test performed, median illustrated. ns: non-significant, ***: p≤0.001, ****: p≤0.0001	252
Figure 49.	**Natural Killer (NK) and T cell population and subpopulation prevalence in women with non-idiopathic recurrent pregnancy loss (RPL) and controls.** The prevalence of A) $CD3^{-}CD56^{+}$ NK cells in the lymphocyte population and B) $CD56^{dim}CD16^{+}$ and C) $CD56^{bright}CD16^{-}$ cells in the NK cell population of healthy controls (*N*=77) and women with non-idiopathic RPL (*N*=42) is shown. The percentage of D) $CD3^{+}$ T cells in the lymphocyte population, E) $CD4^{+}CD8^{-}$ and F) $CD4^{-}CD8^{+}$ cells in the T cell population, and G) regulatory T cells (Tregs) in the $CD4^{+}CD8^{-}$ T cell subpopulation of healthy controls (*N*=80) and women with non-idiopathic RPL (*N*=42) is also depicted. Normally distributed dataset without significantly different variances (F): Unpaired t test used, mean and standard deviation displayed. Non-normally distributed datasets (A-E, G): Mann-Whitney test performed, median illustrated. ns: non-significant, *: p≤0.05, ****: p≤0.0001	253
Figure 50.	**Natural Killer (NK) and T cell population and subpopulation prevalence in women with recurrent pregnancy loss (RPL) with at least 5 past losses and controls.** The	254

	prevalence of A) $CD3^{-}CD56^{+}$ NK cells in the lymphocyte population and B) $CD56^{dim}CD16^{+}$ and C) $CD56^{bright}CD16^{-}$ cells in the NK cell population of healthy controls (*N*=77) and women with RPL with a minimum of 5 losses (*N*=14) is depicted. The percentage of D) $CD3^{+}$ T cells in the lymphocyte population, E) $CD4^{+}CD8^{-}$ and F) $CD4^{-}CD8^{+}$ cells in the T cell population, and G) regulatory T cells (Tregs) in the $CD4^{+}CD8^{-}$ T cell subpopulation of healthy controls (*N*=80) and women with RPL with a minimum of 5 losses (*N*=13) is also displayed. Normally distributed dataset without significantly different variances (F): Unpaired t test used, mean and standard deviation illustrated. Non-normally distributed datasets (A-E, G): Mann-Whitney test performed, median shown. ns: non-significant, *: p≤0.05, ***: p≤0.001	
Figure 51.	**Natural Killer (NK) and T cell population and subpopulation prevalence in control women belonging to different age-associated subgroups.** The prevalence of A) $CD3^{-}CD56^{+}$ NK cells in the lymphocyte population and B) $CD56^{dim}CD16^{+}$ and C) $CD56^{bright}CD16^{-}$ cells in the NK cell population of healthy controls belonging to the ≤30 (*N*=39), 31-35 (*N*=15), 36-40 (*N*=7), and >40 (*N*=15) age groups is shown. The percentage of D) $CD3^{+}$ T cells in the lymphocyte population, E) $CD4^{+}CD8^{-}$ and F) $CD4^{-}CD8^{+}$ cells in the T cell population, and G) regulatory T cells (Tregs) in the $CD4^{+}CD8^{-}$ T cell subpopulation of healthy controls belonging to the ≤30 (*N*=41), 31-35 (*N*=15), 36-40 (*N*=8), and >40 (*N*=15) age groups is also depicted. Normally distributed dataset (F): One-way ANOVA test used, accompanied by the Dunn's test for multiple comparisons, mean and standard deviation illustrated. Non-normally distributed datasets (A-E, G): Kruskal-Wallis test performed, accompanied by the Dunn's test for multiple comparisons, median displayed. ns: non-significant	256
Figure 52.	**Natural Killer (NK) and T cell population and subpopulation prevalence in women with recurrent pregnancy loss (RPL) belonging to different age-associated subgroups.** The prevalence of A) $CD3^{-}CD56^{+}$ NK cells in the lymphocyte population and B) $CD56^{dim}CD16^{+}$ and C) $CD56^{bright}CD16^{-}$ cells in the NK cell population of women with RPL belonging to the ≤30 (*N*=30), 31-35 (*N*=31), 36-40 (*N*=25), and >40 (*N*=4) age groups is depicted. The percentage of D) $CD3^{+}$ T cells in the lymphocyte population, E) $CD4^{+}CD8^{-}$ and F) $CD4^{-}CD8^{+}$ cells in the T cell population, and G) regulatory T cells (Tregs) in the	257

	$CD4^+CD8^-$ T cell subpopulation of women with RPL belonging to the ≤30 (*N*=30), 31-35 (*N*=31), 36-40 (*N*=24), and >40 (*N*=4) age groups is also illustrated. Kruskal-Wallis test performed, accompanied by the Dunn's test for multiple comparisons, median displayed. ns: non-significant	
Figure 53.	**Natural Killer (NK) and T cell population and subpopulation prevalence in control women belonging to different ethnic subgroups.** The prevalence of A) $CD3^-CD56^+$ NK cells in the lymphocyte population and B) $CD56^{dim}CD16^+$ and C) $CD56^{bright}CD16^-$ cells in the NK cell population of healthy controls belonging to the Asian (*N*=5), Black (*N*=8), White (*N*=56), and Mixed (*N*=5) ethnic groups is illustrated. The percentage of D) $CD3^+$ T cells in the lymphocyte population, E) $CD4^+CD8^-$ and F) $CD4^-CD8^+$ cells in the T cell population, and G) regulatory T cells (Tregs) in the $CD4^+CD8^-$ T cell subpopulation of healthy controls belonging to the Asian (*N*=5), Black (*N*=8), White (*N*=58), and Mixed (*N*=6) ethnic groups is also depicted. Kruskal-Wallis test performed, accompanied by the Dunn's test for multiple comparisons, median displayed. ns: non-significant	258
Figure 54.	**Natural Killer (NK) and T cell population and subpopulation prevalence in women with recurrent pregnancy loss (RPL) belonging to different ethnic subgroups.** The prevalence of A) $CD3^-CD56^+$ NK cells in the lymphocyte population and B) $CD56^{dim}CD16^+$ and C) $CD56^{bright}CD16^-$ cells in the NK cell population of women with RPL belonging to the Asian (*N*=19), Black (*N*=2), and White (*N*=53) ethnic groups is shown. The percentage of D) $CD3^+$ T cells in the lymphocyte population, E) $CD4^+CD8^-$ and F) $CD4^-CD8^+$ cells in the T cell population, and G) regulatory T cells (Tregs) in the $CD4^+CD8^-$ T cell subpopulation of women with RPL belonging to the Asian (*N*=19), Black (*N*=2), and White (*N*=53) ethnic groups is also illustrated. Kruskal-Wallis test performed, accompanied by the Dunn's test for multiple comparisons, median displayed. ns: non-significant	259
Figure 55.	**Natural Killer (NK) cell population and subpopulation prevalence and T cell levels in White women with recurrent pregnancy loss (RPL) and White controls.** The prevalence of $CD3^-CD56^+$ NK cells in A) the peripheral blood mononuclear cell (PBMC) and B) the lymphocyte population, C) the percentage of $CD56^{bright}CD16^-$ cells in the NK cell population, and D) the ratio of $CD56^{bright}CD16^-$ to	261

	$CD56^{dim}CD16^{+}$ NK cell prevalence in healthy controls (*N*=57) and women with RPL (*N*=53) of White ethnic origin is displayed. The percentage of $CD3^{+}$ T cells in the E) leukocyte, F) PBMC, and G) lymphocyte population of healthy controls (*N*=59) and women with RPL (*N*=56) of White ethnic origin is also shown. Normally distributed dataset without significantly different variances (E): Unpaired t test used, mean and standard deviation illustrated. Non-normally distributed datasets (A-D, F, G): Mann Whitney test performed, median depicted. *: p≤0.05, **: p≤0.01, ****: p≤0.0001	
Figure 56.	**Natural Killer (NK) cell population and subpopulation prevalence and T cell levels in women with recurrent pregnancy loss (RPL), consuming low levels of alcohol, and controls with similar alcohol consumption habits.** The prevalence of $CD3^{-}CD56^{+}$ NK cells in A) the peripheral blood mononuclear cell (PBMC) and B) the lymphocyte population, C) the percentage of $CD56^{bright}CD16^{-}$ cells in the NK cell population, and D) the ratio of $CD56^{bright}CD16^{-}$ to $CD56^{dim}CD16^{+}$ NK cell prevalence in healthy controls (*N*=27) and women with RPL (*N*=24), consuming low levels of alcohol, is depicted. The percentage of $CD3^{+}$ T cells in the E) leukocyte, F) PBMC, and G) lymphocyte population of healthy controls (*N*=29) and women with RPL (*N*=25), consuming low levels of alcohol, is also illustrated. Normally distributed dataset without significantly different variances (F): Unpaired t test used, mean and standard deviation shown. Non-normally distributed datasets (A-E, G): Mann-Whitney test performed, median displayed. ns: non-significant, *: p≤0.05, **: p≤0.01, ***: p≤0.001, ****: p≤0.0001	262
Figure 57.	**Natural Killer (NK) and T cell population and subpopulation prevalence in women with recurrent pregnancy loss (RPL), who were either in the 3rd trimester of their subsequent pregnancy or had a live birth, and in those with a subsequent miscarriage.** The prevalence of A) $CD3^{-}CD56^{+}$ NK cells in the lymphocyte population and B) $CD56^{dim}CD16^{+}$ and C) $CD56^{bright}CD16^{-}$ cells in the NK cell population and D) the ratio of $CD56^{bright}CD16^{-}$ to $CD56^{dim}CD16^{+}$ NK cell prevalence in women with RPL belonging to the 3rd trimester/Live birth subgroup (*N*=13) and in those belonging to the miscarriage subgroup (*N*=22) is depicted. The percentage of E) $CD3^{+}$ T cells in the lymphocyte population, F) $CD4^{+}CD8^{-}$ and G) $CD4^{-}CD8^{+}$ cells in the T cell	263

	population, and H) regulatory T cells (Tregs) in the $CD4^+CD8^-$ T cell subpopulation of women with RPL belonging to the 3rd trimester/Live birth subgroup (*N*=13) and of those belonging to the miscarriage subgroup (*N*=21) is also shown. Normally distributed datasets without significantly different variances (A, G): Unpaired t test used, mean and standard deviation illustrated. Non-normally distributed datasets (B-F, H): Mann-Whitney test performed, median displayed. ns: non-significant	
NK cell Activation and Cytotoxicity Evaluation		
Figure 58.	**Specific target cell death in Natural Killer (NK) cell:K562 cell co-cultures, derived from women with recurrent pregnancy loss (RPL) and controls.** The specific K562 cell death detected in co-cultures including A) 0.5:1, B) 1:1, and C) 2:1 NK cell:K562 cell ratios is illustrated, alongside the D) average target cell death in 0.5:1, 1:1, and 2:1 cultures. NK cells isolated from healthy controls (0.5:1 cultures: *N*=71, 1:1 cultures: *N*=69, 2:1 cultures: *N*=72, Average of cultures: *N*=76) and women with RPL (0.5:1 cultures: *N*=71, 1:1 cultures: *N*=72, 2:1 cultures: *N*=72, Average of cultures: *N*=72) were used. E) Example gating used to identify dead and alive K652 and NK cell populations is displayed. Mann-Whitney test performed, median shown. ns: non-significant	281
Figure 59.	**CD107a-expressing Natural Killer (NK) cell prevalence in NK cell:K562 cell co-cultures, derived from women with recurrent pregnancy loss (RPL) and controls.** The prevalence of A-D) dead and E-H) alive NK cells expressing CD107a in co-cultures including A, E) 0.5:1, B, F) 1:1, and C, G) 2:1 NK cell:K562 cell ratios is depicted, alongside the D, H) average prevalence of these cells in 0.5:1, 1:1, and 2:1 cultures. NK cells isolated from healthy controls (0.5:1 cultures: *N*=71, 1:1 cultures: *N*=69, 2:1 cultures: *N*=72, Average of cultures: *N*=76) and women with RPL (0.5:1 cultures: *N*=52, 1:1 cultures: *N*=53, 2:1 cultures: *N*=53, Average of cultures: *N*=53) were used. I) Example gating used to identify the $CD107^+$ degranulating population is displayed, using a control (orange) and an RPL (blue) sample and a CD107a-negative control (red). Mann-Whitney test performed, median included. ns: non-significant, *: p≤0.05	282
Figure 60.	**CD107a expression intensity on Natural Killer (NK) cells in NK cell:K562 cell co-cultures, derived from women with recurrent pregnancy loss (RPL) and controls.** The intensity of CD107a expression, represented by the median	283

	fluorescence intensity (MFI), on A-D) dead and E-H) alive NK cells in co-cultures including A, E) 0.5:1, B, F) 1:1, and C, G) 2:1 NK cell:K562 cell ratios is displayed, alongside the D, H) average expression intensity on these cells in 0.5:1, 1:1, and 2:1 cultures. NK cells isolated from healthy controls (0.5:1 cultures: *N*=71, 1:1 cultures: *N*=69, 2:1 cultures: *N*=72, Average of cultures: *N*=76) and women with RPL (0.5:1 cultures: *N*=52, 1:1 cultures: *N*=53, 2:1 cultures: *N*=53, Average of cultures: *N*=53) were used. Mann-Whitney test performed, median illustrated. ns: non-significant	
Figure 61.	**Granzyme and perforin concentration (pg/mL) in unstimulated peripheral blood mononuclear cell (PBMC) cultures derived from women with recurrent pregnancy loss (RPL) and controls.** The levels of A) granzyme A, B) granzyme B, and C) perforin secretion by PBMCs isolated from healthy controls (*N*=72) and women with RPL (*N*=99) is depicted. Mann-Whitney test performed, median illustrated. ns: non-significant, **: p≤0.01	285
Figure 62.	**Granzyme and perforin concentration (pg/mL) in unstimulated and simulated peripheral blood mononuclear cell (PBMC) cultures derived from women with recurrent pregnancy loss (RPL), controls, and total participants.** The levels of A-C) granzyme A, D-F) granzyme B, and G-I) perforin secretion by PBMCs isolated from women with RPL (*N*=99) (A, D, G), healthy controls (*N*=72) (B, E, H), and total participants (*N*=171) (C, F, I) in the absence and following stimulation with phorbol 12-myristate 13-acetate and ionomycin, is shown. Wilcoxon matched-pairs signed rank test used, median included. ****: p≤0.0001	286
Figure 63.	**Granzyme and perforin concentration (pg/mL) in stimulated peripheral blood mononuclear cell (PBMC) cultures derived from women with recurrent pregnancy loss (RPL) and controls.** The levels of A) granzyme A, B) granzyme B, and C) perforin secretion by PBMCs isolated from healthy controls (*N*=72) and women with RPL (*N*=99) is illustrated. Mann-Whitney test used, median depicted. **: p≤0.01, ***: p≤0.001, ****: p≤0.0001	287
Figure 64.	**CD69 expression by Natural Killer (NK) cells in women with recurrent pregnancy loss (RPL) and controls.** The prevalence of A) total, B) $CD56^{dim}CD16^{+}$, and C) $CD56^{bright}CD16^{-}$ NK cells expressing CD69 and the expression intensity of this marker, represented by the median	288

	fluorescence intensity (MFI), on D) total, E) $CD56^{dim}CD16^{+}$, and F) $CD56^{bright}CD16^{-}$ NK cells of healthy controls (*N*=77) and women with RPL (*N*=90) is displayed. G) Example gating used to identify the $CD69^{+}$ activated population is depicted, using two samples (orange, blue) and a CD69-negative control (red). Mann-Whitney test used, median included. ns: non-significant, *: p≤0.05, ***: p≤0.001, ****: p≤0.0001	
Figure 65.	**CD25- and CD215-expressing cell prevalence in the unstimulated total and $CD56^{dim}CD16^{+}$ Natural Killer (NK) cell population of women with recurrent pregnancy loss (RPL) and controls.** The prevalence of A) $CD25^{+}$ and B) $CD215^{+}$ cells in the NK cell population, as well as the percentage of C) $CD25^{+}$ and D) $CD215^{+}$ cells in the $CD56^{dim}CD16^{+}$ NK cell subpopulation of healthy controls (total NK cells: *N*=71, $CD56^{dim}CD16^{+}$ NK cells: *N*=22) and women with RPL (total NK cells: *N*=84, $CD56^{dim}CD16^{+}$ NK cells: *N*=26) is depicted. Mann-Whitney test used, median included. ns: non-significant	290
Figure 66.	**CD25 and CD215 expression intensity on unstimulated total and $CD56^{dim}CD16^{+}$ Natural Killer (NK) cells of women with recurrent pregnancy loss (RPL) and controls.** The intensity of A) CD25 and B) CD215 expression on individual NK cells, represented by the median fluorescence intensity (MFI), as well as the intensity of C) CD25 and D) CD215 expression on the $CD56^{dim}CD16^{+}$ NK cell subpopulation of healthy controls (total NK cells: *N*=71, $CD56^{dim}CD16^{+}$ NK cells: *N*=22) and women with RPL (total NK cells: *N*=84, $CD56^{dim}CD16^{+}$ NK cells: *N*=26) is illustrated. Mann-Whitney test performed, median depicted. ns: non-significant	291
Figure 67.	**CD25- and CD215-expressing cell prevalence in the unstimulated and the stimulated total and $CD56^{dim}CD16^{+}$ Natural Killer (NK) cell population of women with recurrent pregnancy loss (RPL), controls, and total participants.** The prevalence of A-C) $CD25^{+}$ and G-I) $CD215^{+}$ cells in the NK cell population, as well as the percentage of D-F) $CD25^{+}$ and J-L) $CD215^{+}$ cells in the $CD56^{dim}CD16^{+}$ NK cell subpopulation of women with RPL (total NK cells: *N*=84, $CD56^{dim}CD16^{+}$ NK cells: *N*=26) (A, D, G, J), controls (total NK cells: *N*=71, $CD56^{dim}CD16^{+}$ NK cells: *N*=22) (B, E, H, K), and total participants (total NK cells: *N*=155, $CD56^{dim}CD16^{+}$ NK cells: *N*=48) (C, F, I, L) in the absence and following	293

	stimulation with phorbol 12-myristate 13-acetate and ionomycin is depicted. Wilcoxon matched-pairs signed rank test performed, median shown. ns: non-significant, *: p≤0.05, **: p≤0.01, ***: p≤0.001, ****: p≤0.0001	
Figure 68.	**CD25 and CD215 expression intensity on unstimulated and stimulated total and CD56^{dim}CD16^{+} Natural Killer (NK) cells of women with recurrent pregnancy loss (RPL), controls, and total participants.** The intensity of A-C) CD25 and G-I) CD215 expression, represented by the median fluorescence intensity (MFI), on individual NK cells, as well as the intensity of D-F) CD25 and J-L) CD215 expression on the CD56^{dim}CD16^{+} NK cell subpopulation of women with RPL (total NK cells: *N*=84, CD56^{dim}CD16^{+} NK cells: *N*=26) (A, D, G, J), controls (total NK cells: *N*=71, CD56^{dim}CD16^{+} NK cells: *N*=22) (B, E, H, K), and total participants (total NK cells: *N*=155, CD56^{dim}CD16^{+} NK cells: *N*=48) (C, F, I, L) in the absence and following stimulation with phorbol 12-myristate 13-acetate and ionomycin is displayed. Wilcoxon matched-pairs signed rank test used, median illustrated. ns: non-significant, *: p≤0.05, **: p≤0.01, ***: p≤0.001, ****: p≤0.0001	294
Figure 69.	**CD25- and CD215-expressing cell prevalence in the stimulated total and CD56^{dim}CD16^{+} Natural Killer (NK) cell population of women with recurrent pregnancy loss (RPL) and controls.** The prevalence of A) CD25^{+} and B) CD215^{+} cells in the NK cell population, as well as the percentage of C) CD25^{+} and D) CD215^{+} cells in the CD56^{dim}CD16^{+} NK cell subpopulation, following stimulation with phorbol 12-myristate 13-acetate and ionomycin, of healthy controls (total NK cells: *N*=71, CD56^{dim}CD16^{+} NK cells: *N*=22) and women with RPL (total NK cells: *N*=84, CD56^{dim}CD16^{+} NK cells: *N*=26) is illustrated. Example gating used to identify the E) CD25^{+} and F) CD215^{+} population is depicted, using two samples (orange, blue) and a control negative for the marker of interest (red). Mann-Whitney test performed, median depicted. ns: non-significant	296
Figure 70.	**CD25 and CD215 expression intensity on stimulated total and CD56^{dim}CD16^{+} Natural Killer (NK) cells of women with recurrent pregnancy loss (RPL) and controls.** The intensity of A) CD25 and B) CD215 expression on individual NK cells, represented by the median fluorescence intensity (MFI), as well as the intensity of C) CD25 and D) CD215 expression on the	297

	$CD56^{dim}CD16^{+}$ NK cell subpopulation, following stimulation with phorbol 12-myristate 13-acetate and ionomycin, of healthy controls (total NK cells: *N*=71, $CD56^{dim}CD16^{+}$ NK cells: *N*=22) and women with RPL (total NK cells: *N*=84, $CD56^{dim}CD16^{+}$ NK cells: *N*=26) is depicted. Mann-Whitney test used, median displayed. ns: non-significant, *: p≤0.05	
Figure 71.	**Relative abundance of each sample in the mass cytometry datasets used to analyse Natural Killer (NK) cell marker expression in control women and women with recurrent pregnancy loss (RPL).** The relative frequency of each sample, calculated according to cell counts, in the total NK cell population of the control (*N*=80) and RPL (*N*=100) cohorts is displayed. Individual samples are represented by different colours, with patient_id also depicted (RPL: 0268-0439 and 1349-1456, Control: 920-1000).	298
Figure 72.	**Multi-dimensional scaling (MDS) plot of the control and recurrent pregnancy loss (RPL) Natural Killer cell samples, summarizing the level of similarity between cohorts.** The distances between samples approximate the difference in median expression of all markers examined, including CD56, CD16, CD57, CD69, CD94, CD4, CD5, CD8α, CD25, CD27, CD38, CD122, CD127, CD161, CD226, killer-cell immunoglobulin-like receptor (KIR)2DL1/2DS1/2DS3/2DS5, KIR2DL1/2DS5, KIR2DL2/2DL3/2DS2/2DS4, KIR2DS4, KIR2DL2/2DL3/2DL5, KIR2DL4, KIR3DL1/3DL2, immunoglobulin-like transcript (ILT)1, ILT2, ILT2/LIR6, ILT3/ILT4/ILT5, NKp30/NKp80, NKp44/NKp46, natural killer group (NKG)2A, NKG2C/NKG2D, C-X-C motif chemokine receptors (CXCR)1/CXCR2, CXCR3/CXCR4, CXCR5, CXCR6, CX3CR1, T-cell immunoreceptor with Ig and ITIM domains/T cell immunoglobulin and mucin domain-containing protein 3 (TIGIT/Tim-3), and programmed cell death protein 1 (PD-1), translating multi-dimensional data into a two-dimensional scatter plot. Labels displaying the sample identity are included.	299
Figure 73.	**Multi-dimensional scaling and phenotyping of 20 Natural Killer cell clusters identified by mass cytometry.** A) Multi-dimensional scaling (MDS) plot of pseudobulks generated, with each point on the plot representing a cluster-sample instance, coloured according to the cluster, shaped based on the condition, and with a size proportional to the number of cells it represents. Distances between	303

	instances indicate relative phenotypic differences between clusters and samples, taking into consideration all markers assessed. The major phenotypic subgroups are demonstrated. B) Heatmap of median cluster of differentiation (CD)56, CD16, CD57, CD69, CD94, CD4, CD5, CD8α, CD25, CD27, CD38, CD122, CD127, CD161, CD226, killer-cell immunoglobulin-like receptor (KIR)2DL1/2DS1/2DS3/2DS5, KIR2DL1/2DS5, KIR2DL2/2DL3/2DS2/2DS4, KIR2DS4, KIR2DL2/2DL3/2DL5, KIR2DL4, KIR3DL1/3DL2, immunoglobulin-like transcript (ILT)1, ILT2, ILT2/LIR6, ILT3/ILT4/ILT5, NKp30/NKp80, NKp44/NKp46, natural killer group (NKG)2A, NKG2C/NKG2D, C-X-C motif chemokine receptors (CXCR)1/CXCR2, CXCR3/CXCR4, CXCR5, CXCR6, CX3CR1, T-cell immunoreceptor with Ig and ITIM domains/T cell immunoglobulin and mucin domain-containing protein 3 (TIGIT/Tim-3), and programmed cell death protein 1 (PD-1) expression intensity across the different Natural Killer cell clusters, ranging from high (red) to low (blue).	
Figure 74.	**Visualization of Natural Killer cell cluster prevalence in women with recurrent pregnancy loss (RPL) as detected by mass cytometry.** The 20 clusters of interest in women with RPL and controls are illustrated using a A) uniform manifold approximation and projection (UMAP) plot, in which cells are coloured according to the respective clusters, showing the relative cluster size, and distances representing the degree of phenotypic differences between clusters, a B) relative abundance box plot, depicting cluster proportion in each sample of the control (orange) and RPL (blue) groups, and a C) differential analysis heatmap, displaying the normalised proportion of each cluster in each sample [z score normalisation per cluster: z=(observation-mean observation)/standard deviation]. The heatmap colour varies from purple, suggesting relative under-representation, to orange, suggesting relative over-representation. The green/grey bar indicates significantly (green) or non-significantly (grey) differentially abundant clusters, accompanied by the adjusted p values. A bar representing the log fold change (logFC), indicating over representation in RPL (blue) or controls (orange) is also included. Cluster phenotypes according to the expression of the CD56, CD16, CD57, CD69, CD94, CD4, CD5, CD8α, CD25, CD27, CD38, CD122, CD127, CD161, CD226, killer-cell immunoglobulin-like receptor (KIR)2DL1/2DS1/2DS3/2DS5,	306

	KIR2DL1/2DS5, KIR2DL2/2DL3/2DS2/2DS4, KIR2DS4, KIR2DL2/2DL3/2DL5, KIR2DL4, KIR3DL1/3DL2, immunoglobulin-like transcript (ILT)1, ILT2, ILT2/LIR6, ILT3/ILT4/ILT5, NKp30/NKp80, NKp44/NKp46, natural killer group (NKG)2A, NKG2C/NKG2D, C-X-C motif chemokine receptors (CXCR)1/CXCR2, CXCR3/CXCR4, CXCR5, CXCR6, CX3CR1, T-cell immunoreceptor with Ig and ITIM domains/T cell immunoglobulin and mucin domain-containing protein 3 (TIGIT/Tim-3), and programmed cell death protein 1 (PD-1) markers of interest are depicted.	
Figure 75.	**Specific target cell death in Natural Killer (NK) cell:K562 cell co-cultures, derived from women with idiopathic and non-idiopathic recurrent pregnancy loss (RPL), women with RPL and at least 5 past losses, and controls.** The average specific K562 target cell death in co-cultures including 0.5:1, 1:1, and 2:1 NK cell:K562 cell ratios is depicted. NK cells isolated from healthy controls (*N*=76) and A) women with idiopathic RPL (*N*=40), B) women with non-idiopathic RPL (*N*=32), and C) women with RPL with a minimum of 5 losses (*N*=9) were used. Mann-Whitney test performed, median illustrated. ns: non-significant	308
Figure 76.	**Specific target cell death in Natural Killer (NK) cell:K562 cell co-cultures, derived from women with recurrent pregnancy loss (RPL) and controls belonging to different age-associated subgroups.** The average specific K562 target cell death in co-cultures including 0.5:1, 1:1, and 2:1 NK cell:K562 cell ratios is shown. NK cells isolated from A) healthy controls belonging to the ≤30 (*N*=39), 31-35 (*N*=14), 36-40 (*N*=7), and >40 (*N*=15) age groups and B) women with RPL belonging to the ≤30 (*N*=19), 31-35 (*N*=25), 36-40 (*N*=23), and >40 (*N*=5) age groups were used. Kruskal-Wallis test performed, accompanied by the Dunn's test for multiple comparisons, median displayed. ns: non-significant	308
Figure 77.	**Specific target cell death in Natural Killer (NK) cell:K562 cell co-cultures, derived from women with recurrent pregnancy loss (RPL) and controls belonging in different ethnic subgroups.** The average specific K562 target cell death in co-cultures including 0.5:1, 1:1, and 2:1 NK cell:K562 cell ratios is depicted. NK cells isolated from A) healthy controls belonging to the Asian (*N*=5), Black (*N*=7), White (*N*=57), and Mixed (*N*=6) ethnic groups and B) women with RPL belonging to the Asian (*N*=15) and White (*N*=48)	309

	ethnic groups were used. A) Kruskal-Wallis test performed, accompanied by the Dunn's test for multiple comparisons, median illustrated, B) Mann-Whitney test used, median shown. ns: non-significant	
Figure 78.	**Natural Killer (NK) cell degranulation capacity in NK cell:K562 cell co-cultures and granzyme and perforin concentration (pg/mL) in peripheral blood mononuclear cell (PBMC) cultures derived from White women with recurrent pregnancy loss (RPL) and White controls.** A) The average prevalence of alive NK cells expressing CD107a in co-cultures including 0.5:1, 1:1, and 2:1 NK cell:K562 cell ratios is illustrated. NK cells isolated from healthy controls (*N*=57) and women with RPL (*N*=32) of White ethnic origin were used. The levels of B) granzyme A in unstimulated PBMC cultures and C) granzyme A, D) granzyme B, and E) perforin in stimulated PBMC cultures are also shown. PBMCs isolated from healthy controls (*N*=52) and women with RPL (*N*=57) of White ethnic origin were utilised. Mann-Whitney test used, median depicted. ns: non-significant, *: p≤0.05, ***: p≤0.001, ****: p≤0.0001	310
Figure 79.	**Natural Killer (NK) cell degranulation capacity in NK cell:K562 cell co-cultures and granzyme and perforin concentration (pg/mL) in peripheral blood mononuclear cell (PBMC) cultures derived from women with recurrent pregnancy loss (RPL), consuming low levels of alcohol, and controls with similar alcohol consumption habits.** A) The average prevalence of alive NK cells expressing CD107a in co-cultures including 0.5:1, 1:1, and 2:1 NK cell:K562 cell ratios is shown. NK cells isolated from healthy controls (*N*=28) and women with RPL (*N*=12), consuming low levels of alcohol, were used. The levels of B) granzyme A in unstimulated PBMC cultures and C) granzyme A, D) granzyme B, and E) perforin in stimulated PBMC cultures are also illustrated. PBMCs isolated from healthy controls (*N*=26) and women with RPL (*N*=27), consuming low levels of alcohol, were utilised. Normally distributed dataset without significantly different variances (A): Unpaired t test used, mean and standard deviation shown. Non-normally distributed datasets (B-E): Mann-Whitney test performed, median displayed. ns: non-significant, *: p≤0.05, ***: p≤0.001	311
Figure 80.	**CD69 and CD215 expression by Natural Killer (NK) cells in White women with recurrent pregnancy loss (RPL) and White controls.** The expression intensity of CD69,	313

	represented by the median fluorescence intensity (MFI), on A) total and B) $CD56^{dim}CD16^{+}$ NK cells and C) the prevalence CD69-expressing $CD56^{bright}CD16^{-}$ NK cells of healthy controls (*N*=57) and women with RPL (*N*=53) of White ethnic origin is displayed. The expression intensity of CD215 on stimulated D) NK cells of healthy controls (*N*=52) and women with RPL (*N*=52) and E) $CD56^{dim}CD16^{+}$ NK cells of healthy controls (*N*=17) and women with RPL (*N*=16) of White ethnic origin is also shown. Mann-Whitney test used, median included. ns: non-significant, *: p≤0.05, **: p≤0.01, ****: p≤0.0001	
Figure 81.	**CD69 and CD215 expression by Natural Killer (NK) cells in women with recurrent pregnancy loss (RPL)**, **consuming low levels of alcohol, and controls with similar alcohol consumption habits.** The expression intensity of CD69, represented by the median fluorescence intensity (MFI), on A) total and B) $CD56^{dim}CD16^{+}$ NK cells and C) the prevalence CD69-expressing $CD56^{bright}CD16^{-}$ NK cells of healthy controls (*N*=27) and women with RPL (*N*=24), consuming low levels of alcohol, is shown. The expression intensity of CD215 on stimulated D) NK cells of healthy controls (*N*=25) and women with RPL (*N*=23) and E) $CD56^{dim}CD16^{+}$ NK cells of healthy controls (*N*=12) and women with RPL (*N*=8), consuming low levels of alcohol, is also illustrated. Mann-Whitney test used, median depicted. ns: non-significant, **: p≤0.01	314
Figure 82.	**Specific target cell death in Natural Killer (NK) cell:K562 cell co-cultures and granzyme and perforin concentration (pg/mL) in peripheral blood mononuclear cell (PBMC) cultures derived from women with recurrent pregnancy loss (RPL), who were either in the 3rd trimester of their subsequent pregnancy or had a live birth, and from those with a subsequent miscarriage.** A) The average specific K562 target cell death in co-cultures including 0.5:1, 1:1, and 2:1 NK cell:K562 cell ratios is depicted. NK cells isolated from women with RPL belonging to the 3rd trimester/Live birth subgroup (*N*=12) and from those belonging to the miscarriage subgroup (*N*=16) were used. The levels of B) granzyme A, C) granzyme B, and D) perforin in unstimulated PBMC cultures and the levels of E) granzyme A, F) granzyme B, and G) perforin in stimulated PBMC cultures are also illustrated. PBMCs isolated from women with RPL belonging to the 3rd trimester/Live birth subgroup (*N*=13) and from those belonging	315

	to the miscarriage subgroup (*N*=23) were utilised. Mann-Whitney test performed, median displayed. ns: non-significant	
Cytokine Analysis		
Figure 83.	**Cytokine-expressing cell prevalence in the unstimulated T helper (T_H) cell population of women with recurrent pregnancy loss (RPL) and controls.** The prevalence of A) interleukin (IL)-2^+, B) interferon (IFN)-γ^+, C) tumor necrosis factor (TNF)-α^+, D) IL-10^+, and E) IL-$17A^+$ cells in the $CD4^+$ T_H cell population of healthy controls (*N*=76) and women with RPL (*N*=82) is illustrated. Due to low T_H cell number (<10), *N*=2 RPL samples were excluded. Example gating used to identify F) IL-2^+, G) IFN-γ^+, H) TNF-α^+, I) IL-10^+, and J) IL-$17A^+$ T_H cells using two samples (orange, blue) and a control negative for the marker of interest (red) is included. Mann-Whitney test used, median illustrated. ns: non-significant, ****: p≤0.0001	341
Figure 84.	**Cytokine expression intensity on unstimulated T helper (T_H) cells of women with recurrent pregnancy loss (RPL) and controls.** The intensity of A) interleukin (IL)-2, B) interferon (IFN)-γ, C) tumor necrosis factor (TNF)-α, D) IL-10, and E) IL-17A expression on individual $CD4^+$ T_H cells, represented by the median fluorescence intensity (MFI), of healthy controls (*N*=76) and women with RPL (*N*=82) is depicted. Due to low T_H cell number (<10), *N*=2 RPL samples were excluded. Mann-Whitney test used, median illustrated. ns: non-significant, ****: p≤0.0001	342
Figure 85.	**Cytokine-expressing cell prevalence in the unstimulated and the stimulated T helper (T_H) cell population of women with recurrent pregnancy loss (RPL), controls, and total participants.** The prevalence of A-C) interleukin (IL)-2^+, D-F) interferon (IFN)-γ^+, G-I) tumor necrosis factor (TNF)-α^+, J-L) IL-10^+, and M-O) IL-$17A^+$ cells in the $CD4^+$ T_H cell population of women with RPL (*N*=82) (A, D, G, J, M), controls (*N*=76) (B, E, H, K, N), and total participants (*N*=158) (C, F, I, L, O) in the absence and following stimulation with phorbol 12-myristate 13-acetate and ionomycin is depicted. Due to low T_H cell number (<10), *N*=2 RPL samples were excluded. Wilcoxon matched-pairs signed rank test used, median illustrated. ****: p≤0.0001	344
Figure 86.	**Cytokine expression intensity on unstimulated and stimulated T helper (T_H) cells of women with recurrent pregnancy loss (RPL), controls, and total participants.** The intensity of A-C) interleukin (IL)-2, D-F) interferon (IFN)-γ,	345

	G-I) tumor necrosis factor (TNF)-α, J-L) IL-10, and M-O) IL-17A expression, represented by the median fluorescence intensity (MFI), on individual $CD4^+$ T_H cells of women with RPL (*N*=82) (A, D, G, J, M), controls (*N*=76) (B, E, H, K, N), and total participants (*N*=158) (C, F, I, L, O) in the absence and following stimulation with phorbol 12-myristate 13-acetate and ionomycin is shown. Due to low T_H cell number (<10), *N*=2 RPL samples were excluded. Wilcoxon matched-pairs signed rank test used, median included. ****: p≤0.0001	
Figure 87.	**Cytokine-expressing cell prevalence in the stimulated T helper (T_H) cell population of women with recurrent pregnancy loss (RPL) and controls.** The prevalence of A) interleukin (IL)-2^+, B) interferon (IFN)-γ^+, C) tumor necrosis factor (TNF)-α^+, D) IL-10^+, and E) IL-$17A^+$ cells in the $CD4^+$ T_H cell population, following stimulation with phorbol 12-myristate 13-acetate and ionomycin, of healthy controls (N=76) and women with RPL (N=84) is displayed. Example gating used to identify F) IL-2^+, G) IFN-γ^+, H) TNF-α^+, I) IL-10^+, and J) IL-$17A^+$ T_H cells using two samples (orange, blue) and a control negative for the marker of interest (red) is included. Normally distributed datasets (C): Unpaired t test performed, mean and standard deviation depicted. Non-normally distributed datasets (A, B, D, E): Mann-Whitney test used, median illustrated. ns: non-significant, *: p≤0.05, **: p≤0.01, ****: p≤0.0001	346
Figure 88.	**Cytokine expression intensity on stimulated T helper (T_H) cells of women with recurrent pregnancy loss (RPL) and controls.** The intensity of A) interleukin (IL)-2, B) interferon (IFN)-γ, C) tumor necrosis factor (TNF)-α, D) IL-10, and E) IL-17A expression on individual $CD4^+$ T_H cells, represented by the median fluorescence intensity (MFI), following stimulation with phorbol 12-myristate 13-acetate and ionomycin, of healthy controls (*N*=76) and women with RPL (*N*=84) is shown. Mann-Whitney test performed, median included. ns: non-significant, *: p≤0.05, **: p≤0.01, ****: p≤0.0001	347
Figure 89.	**Cytokine-expressing cell prevalence ratios in the stimulated T helper (T_H) cell population of women with recurrent pregnancy loss (RPL) and controls.** The prevalence ratios of A) interleukin (IL)-2^+/IL-10^+, B) interferon (IFN)-γ^+/IL-10^+, C) tumor necrosis factor (TNF)-α^+/IL-10^+, D) IL-$17A^+$/IL-10^+, E) IL-2^+/IL-$17A^+$, F) IFN-γ^+/IL-$17A^+$, and	348

	G) TNF-α$^+$/IL-17A$^+$ cells in the CD4$^+$ T_H cell population, following stimulation with phorbol 12-myristate 13-acetate and ionomycin, of healthy controls (*N*=76) and women with RPL (*N*=82) are illustrated. Mann-Whitney test performed, median depicted. ns: non-significant, *: p≤0.05, ****: p≤0.0001	
Figure 90.	**Cytokine expression intensity ratios on stimulated T helper (T_H) cells of women with recurrent pregnancy loss (RPL) and controls.** The intensity ratios of A) interleukin (IL)-2/IL-10, B) interferon (IFN)-γ/IL-10, C) tumor necrosis factor (TNF)-α/IL-10, D) IL-17A/IL-10, E) IL-2/IL-17A, F) IFN-γ/IL-17A, and G) TNF-α/IL-17A expression on individual CD4$^+$ T_H cells, represented by the median fluorescence intensity (MFI), following stimulation with phorbol 12-myristate 13-acetate and ionomycin, of healthy controls (*N*=76) and women with RPL (*N*=82) are displayed. Mann-Whitney test used, median included. ns: non-significant, *: p≤0.05, **: p≤0.01, ****: p≤0.0001	349
Figure 91.	**Cytokine-expressing cell prevalence in the unstimulated total and CD56^{dim}CD16$^+$ Natural Killer (NK) cell population of women with recurrent pregnancy loss (RPL) and controls.** The prevalence of A) interferon (IFN)-γ$^+$, B) tumor necrosis factor (TNF)-α$^+$, and C) interleukin (IL)-10$^+$ cells in the NK cell population, as well as the percentage of D) IFN-γ$^+$, E) TNF-α$^+$, and F) IL-10$^+$ cells in the CD56^{dim}CD16$^+$ NK cell subpopulation of healthy controls (total NK cells: *N*=71, CD56^{dim}CD16$^+$ NK cells: *N*=22) and women with RPL (total NK cells: *N*=84, CD56^{dim}CD16$^+$ NK cells: *N*=26) is shown. Example gating used to identify G) IFN-γ$^+$, H) TNF-α$^+$, and I) IL-10$^+$ NK cells using two samples (orange, blue) and a control negative for the marker of interest (red) is included. Mann-Whitney test used, median depicted. ns: non-significant, *: p≤0.05, **: p≤0.01, ****: p≤0.0001	351
Figure 92.	**Cytokine expression intensity on unstimulated total and CD56^{dim}CD16$^+$ Natural Killer (NK) cells of women with recurrent pregnancy loss (RPL) and controls.** The intensity of A) interferon (IFN)-γ, B) tumor necrosis factor (TNF)-α, and C) interleukin (IL)-10 expression on individual NK cells, represented by the median fluorescence intensity (MFI), as well as the intensity of A) IFN-γ, B) TNF-α, and C) IL-10 expression on the CD56^{dim}CD16$^+$ NK cell subpopulation of healthy controls (total NK cells: *N*=71, CD56^{dim}CD16$^+$ NK cells: *N*=22) and women with RPL (total NK cells: *N*=84, CD56^{dim}CD16$^+$ NK	352

	cells: *N*=26) is displayed. Mann-Whitney test used, median illustrated. ns: non-significant, **: p≤0.01	
Figure 93.	**Cytokine-expressing cell prevalence in the unstimulated and the stimulated Natural Killer (NK) cell population of women with recurrent pregnancy loss (RPL), controls, and total participants.** The prevalence of A-C) interferon (IFN)-γ^{+}, D-F) tumor necrosis factor (TNF)-α^{+}, and G-I) interleukin (IL)-10^{+} cells in the NK cell population of women with RPL (*N*=84) (A, D, G), controls (*N*=71) (B, E, H), and total participants (*N*=155) (C, F, I) in the absence and following stimulation with phorbol 12-myristate 13-acetate and ionomycin is illustrated. Wilcoxon matched-pairs signed rank test used, median included. ns: non-significant, *: p≤0.05, **: p≤0.01, ****: p≤0.0001	354
Figure 94.	**Cytokine expression intensity on unstimulated and stimulated Natural Killer (NK) cells of women with recurrent pregnancy loss (RPL), controls, and total participants.** The intensity of A-C) interferon (IFN)-γ, D-F) tumor necrosis factor (TNF)-α, and G-I) interleukin (IL)-10 expression, represented by the median fluorescence intensity (MFI), on individual NK cells of women with RPL (*N*=84) (A, D, G), controls (*N*=71) (B, E, H), and total participants (*N*=155) (C, F, I) in the absence and following stimulation with phorbol 12-myristate 13-acetate and ionomycin is shown. Wilcoxon matched-pairs signed rank test performed, median depicted. ns: non-significant, **: p≤0.01, ****: p≤0.0001	355
Figure 95.	**Cytokine-expressing cell prevalence in the unstimulated and the stimulated CD56^{dim}CD16^{+} Natural Killer (NK) cell population of women with recurrent pregnancy loss (RPL), controls, and total participants.** The prevalence of A-C) interferon (IFN)-γ^{+}, D-F) tumor necrosis factor (TNF)-α^{+}, and G-I) interleukin (IL)-10^{+} cells in the CD56^{dim}CD16^{+} NK cell population of women with RPL (*N*=26) (A, D, G), controls (*N*=22) (B, E, H), and total participants (*N*=48) (C, F, I) in the absence and following stimulation with phorbol 12-myristate 13-acetate and ionomycin is displayed. Wilcoxon matched-pairs signed rank test used, median shown. ns: non-significant, *: p≤0.05, **: p≤0.01, ****: p≤0.0001	356
Figure 96.	**Cytokine expression intensity on unstimulated and stimulated CD56^{dim}CD16^{+} Natural Killer (NK) cells of women with recurrent pregnancy loss (RPL), controls, and total participants.** The intensity of A-C) interferon (IFN)-γ,	357

	D-F) tumor necrosis factor (TNF)-α, and G-I) interleukin (IL)-10 expression, represented by the median fluorescence intensity (MFI), on individual $CD56^{dim}CD16^{+}$ NK cells of women with RPL (*N*=26) (A, D, G), controls (*N*=22) (B, E, H), and total participants (*N*=48) (C, F, I) in the absence and following stimulation with phorbol 12-myristate 13-acetate and ionomycin is depicted. Normally distributed datasets (A, D): Paired t test used, mean and standard deviation illustrated. Non-normally distributed datasets (B-D, F-I): Wilcoxon matched-pairs signed rank test performed, median shown. ns: non-significant, *: p≤0.05, **: p≤0.01, ***: p≤0.001	
Figure 97.	**Cytokine-expressing cell prevalence in the stimulated total and $CD56^{dim}CD16^{+}$ Natural Killer (NK) cell population of women with recurrent pregnancy loss (RPL) and controls.** The prevalence of A) interferon (IFN)-γ^{+}, B) tumor necrosis factor (TNF)-α^{+}, and C) interleukin (IL)-10^{+} cells in the NK cell population, as well as the percentage of D) IFN-γ^{+}, E) TNF-α^{+}, and F) IL-10^{+} cells in the $CD56^{dim}CD16^{+}$ NK cell subpopulation, following stimulation with phorbol 12-myristate 13-acetate and ionomycin, of healthy controls (total NK cells: *N*=71, $CD56^{dim}CD16^{+}$ NK cells: *N*=22) and women with RPL (total NK cells: *N*=84, $CD56^{dim}CD16^{+}$ NK cells: *N*=26) is illustrated. Example gating used to identify G) IFN-γ^{+}, H) TNF-α^{+}, and I) IL-10^{+} NK cells using two samples (orange, blue) and a control negative for the marker of interest (red) is included. Mann-Whitney test used, median included. ns: non-significant, ***: p≤0.001, ****: p≤0.0001	359
Figure 98.	**Cytokine expression intensity on stimulated total and $CD56^{dim}CD16^{+}$ Natural Killer (NK) cells of women with recurrent pregnancy loss (RPL) and controls.** The intensity of A) interferon (IFN)-γ, B) tumor necrosis factor (TNF)-α, and C) interleukin (IL)-10 expression on individual NK cells, represented by the median fluorescence intensity (MFI), as well as the intensity of A) IFN-γ, B) TNF-α, and C) IL-10 expression on the $CD56^{dim}CD16^{+}$ NK cell subpopulation, following stimulation with phorbol 12-myristate 13-acetate and ionomycin, of healthy controls (total NK cells: *N*=71, $CD56^{dim}CD16^{+}$ NK cells: *N*=22) and women with RPL (total NK cells: *N*=84, $CD56^{dim}CD16^{+}$ NK cells: *N*=26) is depicted. Normally distributed datasets (E): Unpaired t test performed, mean and standard deviation shown. Non-normally distributed	360

	datasets (A-D, F): Mann-Whitney test used, median illustrated. ns: non-significant, *: p≤0.05, ***: p≤0.001, ****: p≤0.0001	
Figure 99.	**Cytokine-expressing cell prevalence ratios in the stimulated total and CD56^{dim}CD16^{+} Natural Killer (NK) cell population of women with recurrent pregnancy loss (RPL) and controls.** The prevalence ratios of A) interferon (IFN)-γ^{+}/interleukin (IL)-10^{+} and B) tumor necrosis factor (TNF)-α^{+}/IL-10^{+} cells in the NK cell population, as well as the C) IFN-γ^{+}/IL-10^{+} and D) TNF-α^{+}/IL-10^{+} cell ratios in the CD56^{dim}CD16^{+} NK cell subpopulation, following stimulation with phorbol 12-myristate 13-acetate and ionomycin, in healthy controls (total NK cells: *N*=61, CD56^{dim}CD16^{+} NK cells: *N*=17) and women with RPL (total NK cells: *N*=50, CD56^{dim}CD16^{+} NK cells: *N*=16) is depicted. Mann-Whitney test performed, median shown. ns: non-significant	361
Figure 100.	**Cytokine expression intensity ratios on stimulated total and CD56^{dim}CD16^{+} Natural Killer (NK) cells of women with recurrent pregnancy loss (RPL) and controls.** The intensity ratios of A) interferon (IFN)-γ/interleukin (IL)-10 and B) tumor necrosis factor (TNF)-α/IL-10 expression on individual NK cells, represented by the median fluorescence intensity (MFI), as well as the intensity of C) IFN-γ/IL-10 and D) TNF-α/IL-10 expression on the CD56^{dim}CD16^{+} NK cell subpopulation, following stimulation with phorbol 12-myristate 13-acetate and ionomycin, in healthy controls (total NK cells: *N*=61, CD56^{dim}CD16^{+} NK cells: *N*=17) and women with RPL (total NK cells: *N*=50, CD56^{dim}CD16^{+} NK cells: *N*=16) is displayed. Mann-Whitney test used, median illustrated. ns: non-significant, **: p≤0.01	362
Figure 101.	**Protein concentration (pg/mL) in unstimulated peripheral blood mononuclear cell (PBMC) cultures derived from women with recurrent pregnancy loss (RPL) and controls.** The levels of A) interleukin (IL)-2, B) interferon (IFN)-γ, C) tumor necrosis factor (TNF)-α, D) IL-17A, E) IL-10, F) IL-4, G) IL-5, H) IL-13, I) IL-8, J) granulocyte colony-stimulating factor (G-CSF), and K) granulocyte-macrophage colony-stimulating factor (GM-CSF) secretion by PBMCs isolated from healthy controls (*N*=72) and women with RPL (*N*=99) is depicted. Mann-Whitney test performed, median illustrated. ns: non-significant, *: p≤0.05, **: p≤0.01, ***: p≤0.001, ****: p≤0.0001	365
Figure 102.	**Pro-inflammatory cytokine concentration (pg/mL) in unstimulated and stimulated peripheral blood**	367

	mononuclear cell (PBMC) cultures derived from women with recurrent pregnancy loss (RPL), controls, and total participants. The levels of A-C) interleukin (IL)-2, D-F) interferon (IFN)-γ, G-I) tumor necrosis factor (TNF)-α, and J-L) IL-17A secretion by PBMCs isolated from women with RPL (*N*=99) (A, D, G, J), healthy controls (*N*=72) (B, E, H, K), and total participants (*N*=171) (C, F, I, L) in the absence and following stimulation with phorbol 12-myristate 13-acetate and ionomycin, is displayed. Wilcoxon matched-pairs signed rank test performed, median shown. ns: non-significant, ***: p≤0.001, ****: p≤0.0001	
Figure 103.	**Anti-inflammatory cytokine concentration (pg/mL) in unstimulated and stimulated peripheral blood mononuclear cell (PBMC) cultures derived from women with recurrent pregnancy loss (RPL), controls, and total participants.** The levels of A-C) interleukin (IL)-10, D-F) IL-4, G-I) IL-5, and J-L) IL-13 secretion by PBMCs isolated from women with RPL (*N*=99) (A, D, G, J), healthy controls (*N*=72) (B, E, H, K), and total participants (*N*=171) (C, F, I, L) in the absence and following stimulation with phorbol 12-myristate 13-acetate and ionomycin, is illustrated. Wilcoxon matched-pairs signed rank test used, median depicted. ns: non-significant, **: p≤0.01, ****: p≤0.0001	368
Figure 104.	**Chemokine and colony-stimulating factor concentration (pg/mL) in unstimulated and stimulated peripheral blood mononuclear cell (PBMC) cultures derived from women with recurrent pregnancy loss (RPL), controls, and total participants.** The levels of A-C) interleukin (IL)-8, D-F) granulocyte colony-stimulating factor (G-CSF), and G-I) granulocyte-macrophage colony-stimulating factor (GM-CSF) secretion by PBMCs isolated from women with RPL (*N*=99) (A, D, G), healthy controls (*N*=72) (B, E, H), and total participants (*N*=171) (C, F, I) in the absence and following stimulation with phorbol 12-myristate 13-acetate and ionomycin, is shown. Wilcoxon matched-pairs signed rank test used, median included. ns: non-significant, *: p≤0.05, **: p≤0.01, ****: p≤0.0001	369
Figure 105.	**Protein concentration (pg/mL) in stimulated peripheral blood mononuclear cell (PBMC) cultures derived from women with recurrent pregnancy loss (RPL) and controls.** The levels of A) interleukin (IL)-2, B) interferon (IFN)-γ, C) tumor necrosis factor (TNF)-α, D) IL-17A, E) IL-10, F) IL-4, G) IL-5,	372

	H) IL-13, I) IL-8, J) granulocyte colony-stimulating factor (G-CSF), and K) granulocyte-macrophage colony-stimulating factor (GM-CSF) secretion by PBMCs isolated from healthy controls (*N*=72) and women with RPL (*N*=99), following stimulation with phorbol 12-myristate 13-acetate and ionomycin, is illustrated. Mann-Whitney test used, median displayed. ns: non-significant, *: p≤0.05, **: p≤0.01	
Figure 106.	**Protein concentration ratios in stimulated peripheral blood mononuclear cell (PBMC) cultures derived from women with recurrent pregnancy loss (RPL) and controls.** The ratios of A) interleukin (IL)-2/IL-10, B) interferon (IFN)-γ/IL-10, C) tumor necrosis factor (TNF)-α/IL-10, D) IL-17A/IL-10, E) IL-2/IL-4, F) IFN-γ/IL-4, G) TNF-α/IL-4, H) IL-17A/IL-4, I) IL-2/IL-5, J) IFN-γ/IL-5, K) TNF-α/IL-5, L) IL-17A/IL-5, M) IL-2/IL-13, N) IFN-γ/IL-13, O) TNF-α/IL-13, and P) IL-17A/IL-13 secretion levels by PBMCs isolated from healthy controls (*N*=72) and women with RPL (*N*=99) is displayed. Mann-Whitney test performed, median illustrated. ns: non-significant, *: p≤0.05, **: p≤0.01, ****: p≤0.0001	373
Figure 107.	**Ratios of cytokine production by stimulated T helper (T_H) cells of women with idiopathic recurrent pregnancy loss (RPL) and controls.** The prevalence ratios of A) interleukin (IL)-2^+/IL-10^+, C) interferon (IFN)-γ^+/IL-10^+, E) tumor necrosis factor (TNF)-α^+/IL-10^+, G) IL-$17A^+$/IL-10^+, I) IL-2^+/IL-$17A^+$, K) IFN-γ^+/IL-$17A^+$, and M) TNF-α^+/IL-$17A^+$ cells in the stimulated $CD4^+$ T_H cell population, as well as the intensity ratios of B) IL-2/IL-10, D) IFN-γ/IL-10, F) TNF-α/IL-10, H) IL-17A/IL-10, J) IL-2/IL-17A, L) IFN-γ/IL-17A, and N) TNF-α/IL-17A expression, represented by the median fluorescence intensity (MFI), on stimulated $CD4^+$ T_H cells of healthy controls (*N*=76) and women with idiopathic RPL (*N*=44) are displayed. Mann-Whitney test performed, median depicted. ns: non-significant, *: p≤0.05, ****: p≤0.0001	375
Figure 108.	**Cytokine production by stimulated Natural Killer (NK) cells of women with idiopathic recurrent pregnancy loss (RPL) and controls.** The prevalence of A) interferon (IFN)-γ^+, C) tumor necrosis factor (TNF)-α^+, and E) interleukin (IL)-10^+ cells in the stimulated NK cell population, as well as the intensity of B) IFN-γ, D) TNF-α, and F) IL-10 expression, represented by the median fluorescence intensity (MFI), on stimulated NK cells of healthy controls (*N*=71) and women with idiopathic	376

	RPL (*N*=46) are illustrated. Mann-Whitney test performed, median shown. ns: non-significant, ****: p≤0.0001	
Figure 109.	**Ratios of cytokine production by stimulated T helper (T_H) cells of women with non-idiopathic recurrent pregnancy loss (RPL) and controls.** The prevalence ratios of A) interleukin (IL)-2^+/IL-10^+, C) interferon (IFN)-γ^+/IL-10^+, E) tumor necrosis factor (TNF)-α^+/IL-10^+, G) IL-$17A^+$/IL-10^+, I) IL-2^+/IL-$17A^+$, K) IFN-γ^+/IL-$17A^+$, and M) TNF-α^+/IL-$17A^+$ cells in the stimulated $CD4^+$ T_H cell population, as well as the intensity ratios of B) IL-2/IL-10, D) IFN-γ/IL-10, F) TNF-α/IL-10, H) IL-17A/IL-10, J) IL-2/IL-17A, L) IFN-γ/IL-17A, and N) TNF-α/IL-17A expression, represented by the median fluorescence intensity (MFI), on stimulated $CD4^+$ T_H cells of healthy controls (*N*=76) and women with non-idiopathic RPL (*N*=38) are depicted. Mann-Whitney test performed, median shown. ns: non-significant, *: p≤0.05, ***: p≤0.001, ****: p≤0.0001	378
Figure 110.	**Cytokine production by stimulated Natural Killer (NK) cells of women with non-idiopathic recurrent pregnancy loss (RPL) and controls.** The prevalence of A) interferon (IFN)-γ^+, C) tumor necrosis factor (TNF)-α^+, and E) interleukin (IL)-10^+ cells in the stimulated NK cell population, as well as the intensity of B) IFN-γ, D) TNF-α, and F) IL-10 expression, represented by the median fluorescence intensity (MFI), on stimulated NK cells of healthy controls (*N*=71) and women with non-idiopathic RPL (*N*=38) are displayed. Mann-Whitney test performed, median illustrated. ns: non-significant, ****: p≤0.0001	379
Figure 111.	**Ratios of cytokine production by stimulated T helper (T_H) cells of women with recurrent pregnancy loss (RPL) with at least 5 past losses and controls.** The prevalence ratios of A) interleukin (IL)-2^+/IL-10^+, C) interferon (IFN)-γ^+/IL-10^+, E) tumor necrosis factor (TNF)-α^+/IL-10^+, G) IL-$17A^+$/IL-10^+, I) IL-2^+/IL-$17A^+$, K) IFN-γ^+/IL-$17A^+$, and M) TNF-α^+/IL-$17A^+$ cells in the stimulated $CD4^+$ T_H cell population, as well as the intensity ratios of B) IL-2/IL-10, D) IFN-γ/IL-10, F) TNF-α/IL-10, H) IL-17A/IL-10, J) IL-2/IL-17A, L) IFN-γ/IL-17A, and N) TNF-α/IL-17A expression, represented by the median fluorescence intensity (MFI), on stimulated $CD4^+$ T_H cells of healthy controls (*N*=76) and women with RPL with a minimum of 5 losses (*N*=12) are displayed. Mann-Whitney test performed, median depicted. ns: non-significant, *: p≤0.05, **: p≤0.01, ***: p≤0.001	381

Figure 112.	**Cytokine production by stimulated Natural Killer (NK) cells of women with recurrent pregnancy loss (RPL) with at least 5 past losses and controls.** The prevalence of A) interferon (IFN)-γ$^+$, C) tumor necrosis factor (TNF)-α$^+$, and E) interleukin (IL)-10$^+$ cells in the stimulated NK cell population, as well as the intensity of B) IFN-γ, D) TNF-α, and F) IL-10 expression, represented by the median fluorescence intensity (MFI), on stimulated NK cells of healthy controls (*N*=71) and women with RPL with a minimum of 5 losses (*N*=12) are illustrated. Mann-Whitney test performed, median shown. ns: non-significant, **: p≤0.01	382
Figure 113.	**Ratios of cytokine production by stimulated T helper (T_H) cells of control women belonging to different age-associated subgroups.** The prevalence ratios of A) interleukin (IL)-2$^+$/IL-10$^+$, C) interferon (IFN)-γ$^+$/IL-10$^+$, E) tumor necrosis factor (TNF)-α$^+$/IL-10$^+$, G) IL-17A$^+$/IL-10$^+$, I) IL-2$^+$/IL-17A$^+$, K) IFN-γ$^+$/IL-17A$^+$, and M) TNF-α$^+$/IL-17A$^+$ cells in the stimulated CD4$^+$ T_H cell population, as well as the intensity ratios of B) IL-2/IL-10, D) IFN-γ/IL-10, F) TNF-α/IL-10, H) IL-17A/IL-10, J) IL-2/IL-17A, L) IFN-γ/IL-17A, and N) TNF-α/IL-17A expression, represented by the median fluorescence intensity (MFI), on stimulated CD4$^+$ T_H cells of healthy controls belonging to the ≤30 (*N*=40), 31-35 (*N*=13), 36-40 (*N*=7), and >40 (*N*=15) age groups are shown. Kruskal-Wallis test performed, accompanied by the Dunn's test for multiple comparisons, median displayed. ns: non-significant, *: p≤0.05, **: p≤0.01	384
Figure 114.	**Cytokine production by stimulated Natural Killer (NK) cells of control women belonging to different age-associated subgroups.** The prevalence of A) interferon (IFN)-γ$^+$, C) tumor necrosis factor (TNF)-α$^+$, and E) interleukin (IL)-10$^+$ cells in the stimulated NK cell population, as well as the intensity of B) IFN-γ, D) TNF-α, and F) IL-10 expression, represented by the median fluorescence intensity (MFI), on stimulated NK cells of healthy controls belonging to the ≤30 (*N*=37), 31-35 (*N*=14), 36-40 (*N*=5), and >40 (*N*=14) age groups are depicted. Kruskal-Wallis test performed, accompanied by the Dunn's test for multiple comparisons, median shown. ns: non-significant, *: p≤0.05	385
Figure 115.	**Ratios of cytokine production by stimulated T helper (T_H) cells of women with recurrent pregnancy loss (RPL) belonging to different age-associated subgroups.** The	386

	prevalence ratios of A) interleukin (IL)-2$^+$/IL-10$^+$, C) interferon (IFN)-γ$^+$/IL-10$^+$, E) tumor necrosis factor (TNF)-α$^+$/IL-10$^+$, G) IL-17A$^+$/IL-10$^+$, I) IL-2$^+$/IL-17A$^+$, K) IFN-γ$^+$/IL-17A$^+$, and M) TNF-α$^+$/IL-17A$^+$ cells in the stimulated CD4$^+$ T_H cell population, as well as the intensity ratios of B) IL-2/IL-10, D) IFN-γ/IL-10, F) TNF-α/IL-10, H) IL-17A/IL-10, J) IL-2/IL-17A, L) IFN-γ/IL-17A, and N) TNF-α/IL-17A expression, represented by the median fluorescence intensity (MFI), on stimulated CD4$^+$ T_H cells of women with RPL belonging to the ≤30 (*N*=27), 31-35 (*N*=28), 36-40 (*N*=23), and >40 (*N*=4) age groups are shown. Kruskal-Wallis test performed, accompanied by the Dunn's test for multiple comparisons, median displayed. ns: non-significant	
Figure 116.	**Cytokine production by stimulated Natural Killer (NK) cells of women with recurrent pregnancy loss (RPL) belonging to different age-associated subgroups.** The prevalence of A) interferon (IFN)-γ$^+$, C) tumor necrosis factor (TNF)-α$^+$, and E) interleukin (IL)-10$^+$ cells in the stimulated NK cell population, as well as the intensity of B) IFN-γ, D) TNF-α, and F) IL-10 expression, represented by the median fluorescence intensity (MFI), on stimulated NK cells of women with RPL belonging to the ≤30 (*N*=28), 31-35 (*N*=28), 36-40 (*N*=24), and >40 (*N*=4) age groups are depicted. Kruskal-Wallis test performed, accompanied by the Dunn's test for multiple comparisons, median shown. ns: non-significant	387
Figure 117.	**Ratios of cytokine production by stimulated T helper (T_H) cells of control women belonging to different ethnic subgroups.** The prevalence ratios of A) interleukin (IL)-2$^+$/IL-10$^+$, C) interferon (IFN)-γ$^+$/IL-10$^+$, E) tumor necrosis factor (TNF)-α$^+$/IL-10$^+$, G) IL-17A$^+$/IL-10$^+$, I) IL-2$^+$/IL-17A$^+$, K) IFN-γ$^+$/IL-17A$^+$, and M) TNF-α$^+$/IL-17A$^+$ cells in the stimulated CD4$^+$ T_H cell population, as well as the intensity ratios of B) IL-2/IL-10, D) IFN-γ/IL-10, F) TNF-α/IL-10, H) IL-17A/IL-10, J) IL-2/IL-17A, L) IFN-γ/IL-17A, and N) TNF-α/IL-17A expression, represented by the median fluorescence intensity (MFI), on stimulated CD4$^+$ T_H cells of healthy controls belonging to the Asian (*N*=4), Black (*N*=8), White (*N*=57), and Mixed (*N*=6) ethnic groups are illustrated. Kruskal-Wallis test performed, accompanied by the Dunn's test for multiple comparisons, median depicted. ns: non-significant, *: p≤0.05, **: p≤0.01	389
Figure 118.	**Cytokine production by stimulated Natural Killer (NK) cells of control women belonging to different ethnic subgroups.**	390

	The prevalence of A) interferon (IFN)-γ$^+$, C) tumor necrosis factor (TNF)-α$^+$, and E) interleukin (IL)-10$^+$ cells in the stimulated NK cell population, as well as the intensity of B) IFN-γ, D) TNF-α, and F) IL-10 expression, represented by the median fluorescence intensity (MFI), on stimulated NK cells of healthy controls belonging to the Asian (*N*=5), Black (*N*=8), White (*N*=52), and Mixed (*N*=5) ethnic groups are shown. Kruskal-Wallis test performed, accompanied by the Dunn's test for multiple comparisons, median displayed. ns: non-significant	
Figure 119.	**Ratios of cytokine production by stimulated T helper (T_H) cells of women with recurrent pregnancy loss (RPL) belonging to different ethnic subgroups.** The prevalence ratios of A) interleukin (IL)-2$^+$/IL-10$^+$, C) interferon (IFN)-γ$^+$/IL-10$^+$, E) tumor necrosis factor (TNF)-α$^+$/IL-10$^+$, G) IL-17A$^+$/IL-10$^+$, I) IL-2$^+$/IL-17A$^+$, K) IFN-γ$^+$/IL-17A$^+$, and M) TNF-α$^+$/IL-17A$^+$ cells in the stimulated CD4$^+$ T_H cell population, as well as the intensity ratios of B) IL-2/IL-10, D) IFN-γ/IL-10, F) TNF-α/IL-10, H) IL-17A/IL-10, J) IL-2/IL-17A, L) IFN-γ/IL-17A, and N) TNF-α/IL-17A expression, represented by the median fluorescence intensity (MFI), on stimulated CD4$^+$ T_H cells of women with RPL belonging to the Asian (*N*=16), and White (*N*=52) ethnic groups are illustrated. Mann-Whitney test performed, median depicted. ns: non-significant	391
Figure 120.	**Cytokine production by stimulated Natural Killer (NK) cells of women with recurrent pregnancy loss (RPL) belonging to different ethnic subgroups.** The prevalence of A) interferon (IFN)-γ$^+$, C) tumor necrosis factor (TNF)-α$^+$, and E) interleukin (IL)-10$^+$ cells in the stimulated NK cell population, as well as the intensity of B) IFN-γ, D) TNF-α, and F) IL-10 expression, represented by the median fluorescence intensity (MFI), on stimulated NK cells of women with RPL belonging to the Asian (*N*=18) and White (*N*=52) ethnic groups are shown. Mann-Whitney test performed, median displayed. ns: non-significant	392
Figure 121.	**Cytokine production by T helper (T_H) cells of White women with recurrent pregnancy loss (RPL) and White controls.** The prevalence of A) tumor necrosis factor (TNF)-α$^+$ and C) interleukin (IL)-10$^+$ cells in the unstimulated CD4$^+$ T_H cell population, the intensity of B) TNF-α expression, represented by the median fluorescence intensity (MFI), on unstimulated CD4$^+$ T_H cells, the prevalence of D) IL-2$^+$, F) TNF-α$^+$, H) IL-10$^+$, and J) IL-17A$^+$ cells in the stimulated CD4$^+$ T_H cell population, as well as the intensity of E) IL-2,	394

	G) TNF-α, and I) IL-10 expression on stimulated $CD4^+$ T_H cells of healthy controls (*N*=57) and women with RPL (*N*=52) of White ethnic origin is illustrated. Normally distributed dataset without significantly different variances (F): Unpaired t test used, mean and standard deviation illustrated. Non-normally distributed datasets (A-E, G-J): Mann Whitney test performed, median depicted. ns: non-significant, **: p≤0.01, ***: p≤0.001, ****: p≤0.0001	
Figure 122.	**Ratios of cytokine production by stimulated T helper (T_H) cells of White women with recurrent pregnancy loss (RPL) and White controls.** The prevalence ratios of A) interleukin (IL)-2^+/IL-10^+, C) interferon (IFN)-γ^+/IL-10^+, E) tumor necrosis factor (TNF)-α^+/IL-10^+, G) IL-$17A^+$/IL-10^+, and J) TNF-α^+/IL-$17A^+$ cells in the stimulated $CD4^+$ T_H cell population, as well as the intensity ratios of B) IL-2/IL-10, D) IFN-γ/IL-10, F) TNF-α/IL-10, H) IL-17A/IL-10, I) IL-2/IL-17A, and K) TNF-α/IL-17A expression, represented by the median fluorescence intensity (MFI), on stimulated $CD4^+$ T_H cells of healthy controls (*N*=57) and women with RPL (*N*=52) of White ethnic origin are displayed. Mann-Whitney test performed, median depicted. ns: non-significant, *: p≤0.05, **: p≤0.01, ***: p≤0.001, ****: p≤0.0001	395
Figure 123.	**Cytokine production by Natural Killer (NK) cells of White women with recurrent pregnancy loss (RPL) and White controls.** The prevalence of A) tumor necrosis factor (TNF)-α^+ and B) interleukin (IL)-10^+ cells in the unstimulated NK cell population, the prevalence of D) TNF-α^+ and F) IL-10^+ cells in the stimulated NK cell population, the intensity of C) interferon (IFN)-γ, E) TNF-α, and G) IL-10 expression, represented by the median fluorescence intensity (MFI), on stimulated NK cells, as well as the intensity ratio of H) IFN-γ/IL-10 on stimulated NK cells of healthy controls (*N*=52) and women with RPL (*N*=52) of White ethnic origin is shown. I) The prevalence of TNF-α^+ cells in the unstimulated $CD56^{dim}CD16^+$ NK cell population, J) the intensity of TNF-α expression on unstimulated $CD56^{dim}CD16^+$ NK cells, and K) the intensity of IFN-γ expression on stimulated $CD56^{dim}CD16^+$ NK cells of healthy controls (*N*=17) and women with RPL (*N*=16) of White ethnic origin is also illustrated. Mann-Whitney test performed, median depicted. ns: non-significant, *: p≤0.05, **: p≤0.01, ****: p≤0.0001	396

Figure 124.	**Protein concentration (pg/mL) in peripheral blood mononuclear cell (PBMC) cultures derived from White women with recurrent pregnancy loss (RPL) and White controls.** The levels of A) interleukin (IL)-2, B) tumor necrosis factor (TNF)-α, C) IL-17A, D) IL-5, E) IL-8, and F) granulocyte-macrophage colony-stimulating factor (GM-CSF) secretion by unstimulated PBMCs, the levels of G) IL-5, H) IL-13, and I) IL-8 by stimulated PBMCs, and the ratios of J) TNF-α/IL-5, K) IL-2/IL-13, L) interferon (IFN)-γ/IL-13, and M) TNF-α/IL-13 secretion levels by stimulated PBMCs isolated from healthy controls (*N*=52) and women with RPL (*N*=57) of White ethnic origin is depicted. Normally distributed dataset without significantly different variances (I): Unpaired t test used, mean and standard deviation illustrated. Non-normally distributed datasets (A-H, J-M): Mann Whitney test performed, median depicted. ns: non-significant, *: p≤0.05, **: p≤0.01, ***: p≤0.001, ****: p≤0.0001	397
Figure 125.	**Cytokine production by T helper (T_H) cells of women with recurrent pregnancy loss (RPL), consuming low levels of alcohol, and controls with similar alcohol consumption habits.** The prevalence of A) tumor necrosis factor (TNF)-α^+ and C) interleukin (IL)-10^+ cells in the unstimulated $CD4^+$ T_H cell population, the intensity of B) TNF-α expression, represented by the median fluorescence intensity (MFI), on unstimulated $CD4^+$ T_H cells, the prevalence of D) IL-2^+, F) TNF-α^+, H) IL-10^+, and J) IL-$17A^+$ cells in the stimulated $CD4^+$ T_H cell population, as well as the intensity of E) IL-2, G) TNF-α, and I) IL-10 expression on stimulated $CD4^+$ T_H cells of healthy controls (*N*=27) and women with RPL (*N*=24), consuming low levels of alcohol, is illustrated. Normally distributed dataset without significantly different variances (D): Unpaired t test used, mean and standard deviation illustrated. Non-normally distributed datasets (A-C, E-J): Mann Whitney test performed, median depicted. ns: non-significant, *: p≤0.05, **: p≤0.01, ***: p≤0.001	400
Figure 126.	**Ratios of cytokine production by stimulated T helper (T_H) cells of women with recurrent pregnancy loss (RPL), consuming low levels of alcohol, and controls with similar alcohol consumption habits.** The prevalence ratios of A) interleukin (IL)-2^+/IL-10^+, C) interferon (IFN)-γ^+/IL-10^+, E) tumor necrosis factor (TNF)-α^+/IL-10^+, G) IL-$17A^+$/IL-10^+, and J) TNF-α^+/IL-$17A^+$ cells in the stimulated $CD4^+$ T_H cell population, as well as the intensity ratios of B) IL-2/IL-10,	401

	D) IFN-γ/IL-10, F) TNF-α/IL-10, H) IL-17A/IL-10, I) IL-2/IL-17A, and K) TNF-α/IL-17A expression, represented by the median fluorescence intensity (MFI), on stimulated $CD4^+$ T_H cells of healthy controls (*N*=27) and women with RPL (*N*=24), consuming low levels of alcohol, are displayed. Mann-Whitney test performed, median depicted. ns: non-significant, *: p≤0.05, **: p≤0.01	
Figure 127.	**Cytokine production by Natural Killer (NK) cells of women with recurrent pregnancy loss (RPL), consuming low levels of alcohol, and controls with similar alcohol consumption habits.** The prevalence of A) tumor necrosis factor (TNF)-α^+ and B) interleukin (IL)-10^+ cells in the unstimulated NK cell population, the prevalence of D) TNF-α^+ and F) IL-10^+ cells in the stimulated NK cell population, the intensity of C) interferon (IFN)-γ, E) TNF-α, and G) IL-10 expression, represented by the median fluorescence intensity (MFI), on stimulated NK cells, as well as the intensity ratio of H) IFN-γ/IL-10 on stimulated NK cells of healthy controls (*N*=25) and women with RPL (*N*=23), consuming low levels of alcohol, is shown. I) The prevalence of TNF-α^+ cells in the unstimulated $CD56^{dim}CD16^+$ NK cell population, J) the intensity of TNF-α expression on unstimulated $CD56^{dim}CD16^+$ NK cells, and K) the intensity of IFN-γ expression on stimulated $CD56^{dim}CD16^+$ NK cells of healthy controls (*N*=12) and women with RPL (*N*=8), consuming low levels of alcohol, is also illustrated. Mann-Whitney test performed, median depicted. ns: non-significant, ***: p≤0.001, ****: p≤0.0001	402
Figure 128.	**Protein concentration (pg/mL) in peripheral blood mononuclear cell (PBMC) cultures derived from women with recurrent pregnancy loss (RPL), consuming low levels of alcohol, and controls with similar alcohol consumption habits.** The levels of A) interleukin (IL)-2, B) tumor necrosis factor (TNF)-α, C) IL-17A, D) IL-5, E) IL-8, and F) granulocyte-macrophage colony-stimulating factor (GM-CSF) secretion by unstimulated PBMCs, the levels of G) IL-5, H) IL-13, and I) IL-8 by stimulated PBMCs, and the ratios of J) TNF-α/IL-5, K) IL-2/IL-13, L) interferon (IFN)-γ/IL-13, and M) TNF-α/IL-13 secretion levels by stimulated PBMCs isolated from healthy controls (*N*=26) and women with RPL (*N*=27), consuming low levels of alcohol, is depicted. Mann Whitney test performed, median depicted. ns: non-significant, *: p≤0.05, **: p≤0.01	403

Figure 129.	**Ratios of cytokine production by stimulated T helper (T_H) cells of women with recurrent pregnancy loss (RPL), who were either in the 3rd trimester of their subsequent pregnancy or had a live birth, and in those with a subsequent miscarriage.** The prevalence ratios of A) interleukin (IL)-2^+/IL-10^+, C) interferon (IFN)-γ^+/IL-10^+, E) tumor necrosis factor (TNF)-α^+/IL-10^+, G) IL-$17A^+$/IL-10^+, I) IL-2^+/IL-$17A^+$, K) IFN-γ^+/IL-$17A^+$, and M) TNF-α^+/IL-$17A^+$ cells in the stimulated $CD4^+$ T_H cell population, as well as the intensity ratios of B) IL-2/IL-10, D) IFN-γ/IL-10, F) TNF-α/IL-10, H) IL-17A/IL-10, J) IL-2/IL-17A, L) IFN-γ/IL-17A, and N) TNF-α/IL-17A expression, represented by the median fluorescence intensity (MFI), on stimulated $CD4^+$ T_H cells of women with RPL belonging to the 3rd trimester/Live birth subgroup (*N*=13) and of those belonging to the miscarriage subgroup (*N*=19) are displayed. Mann-Whitney test performed, median depicted. ns: non-significant	405
Figure 130.	**Cytokine production by stimulated Natural Killer (NK) cells of women with recurrent pregnancy loss (RPL), who were either in the 3rd trimester of their subsequent pregnancy or had a live birth, and in those with a subsequent miscarriage.** The prevalence of A) interferon (IFN)-γ^+, C) tumor necrosis factor (TNF)-α^+, and E) interleukin (IL)-10^+ cells in the stimulated NK cell population, as well as the intensity of B) IFN-γ, D) TNF-α, and F) IL-10 expression, represented by the median fluorescence intensity (MFI), on stimulated NK cells of women with RPL belonging to the 3rd trimester/Live birth subgroup (*N*=13) and of those belonging to the miscarriage subgroup (*N*=19) are illustrated. Normally distributed dataset without significantly different variances (B): Unpaired t test used, mean and standard deviation shown. Non-normally distributed datasets (A, C-F): Mann Whitney test performed, median depicted. ns: non-significant	406
Figure 131.	**Protein concentration (pg/mL) in unstimulated peripheral blood mononuclear cell (PBMC) cultures derived from women with recurrent pregnancy loss (RPL), who were either in the 3rd trimester of their subsequent pregnancy or had a live birth, and in those with a subsequent miscarriage.** The levels of A) interleukin (IL)-2, B) interferon (IFN)-γ, C) tumor necrosis factor (TNF)-α, D) IL-17A, E) IL-10, F) IL-4, G) IL-5, H) IL-13, I) IL-8, J) granulocyte colony-stimulating factor (G-CSF), and K) granulocyte-macrophage	407

	colony-stimulating factor (GM-CSF) secretion by PBMCs isolated from women with RPL belonging to the 3rd trimester/Live birth subgroup (*N*=13) and of those belonging to the miscarriage subgroup (*N*=23) is shown. Normally distributed dataset without significantly different variances (I): Unpaired t test used, mean and standard deviation shown. Non-normally distributed datasets (A-H, J-K): Mann Whitney test performed, median depicted. ns: non-significant, *: p≤0.05	
Figure 132.	**Protein concentration (pg/mL) in stimulated peripheral blood mononuclear cell (PBMC) cultures derived from women with recurrent pregnancy loss (RPL), who were either in the 3rd trimester of their subsequent pregnancy or had a live birth, and in those with a subsequent miscarriage.** The levels of A) interleukin (IL)-2, B) interferon (IFN)-γ, C) tumor necrosis factor (TNF)-α, D) IL-17A, E) IL-10, F) IL-4, G) IL-5, H) IL-13, I) IL-8, J) granulocyte colony-stimulating factor (G-CSF), and K) granulocyte-macrophage colony-stimulating factor (GM-CSF) secretion by PBMCs isolated from women with RPL belonging to the 3rd trimester/Live birth subgroup (*N*=13) and of those belonging to the miscarriage subgroup (*N*=23) is depicted. Mann Whitney test performed, median illustrated. ns: non-significant, *: p≤0.05, **: p≤0.01	408
Immune Biomarkers for the Identification of Women with RPL		
Figure 133.	**Elastic Net (EN) analysis results for the identification of women with recurrent pregnancy loss (RPL).** The EN algorithm was run 100 times. The number of times (frequency) each marker was selected is displayed. The 1st quartile of markers is highlighted (light blue). G-CSF: granulocyte colony stimulating factor, GM-CSF: granulocyte-macrophage colony-stimulating factor, IFN: interferon, IL: interleukin, MFI: median fluorescence intensity, NK cells: natural killer cells, T_C cells: cytotoxic T cells, T_H cells: T helper cells, TNF: tumor necrosis factor, Treg: regulatory T cell	427
Figure 134.	**Least Absolute Shrinkage and Selection Operator (LASSO) analysis results for the identification of women with recurrent pregnancy loss (RPL).** The LASSO algorithm was run 100 times. The number of times (frequency) each marker was selected is displayed. The 1st quartile of markers is highlighted (light blue). CD: cluster of differentiation, G-CSF: granulocyte colony stimulating factor,	428

	GM-CSF: granulocyte-macrophage colony-stimulating factor, IFN: interferon, IL: interleukin, MFI: median fluorescence intensity, NK cells: natural killer cells, T_C cells: cytotoxic T cells, T_H cells: T helper cells, TNF: tumor necrosis factor, Treg: regulatory T cell	
Figure 135.	**Box plots depicting the distribution of features selected through the combination of Elastic Net (EN) and Least Absolute Shrinkage and Selection Operator (LASSO) methods in the recurrent pregnancy loss (RPL) and control cohorts.** Normalised data for features including T cell and natural killer (NK) cell prevalence in lymphocytes, $CD56^{bright}CD16^-$ cell prevalence in NK cells, CD69 median fluorescence intensity (MFI) on total and $CD56^{dim}CD16^+$ NK cells, mean $CD107a^+$ alive NK cell prevalence in NK:K562 co-cultures, interferon (IFN)-γ and tumor necrosis factor (TNF)-α MFI on stimulated NK cells, TNF-α^+ cell prevalence in unstimulated and stimulated T helper (T_H) cells, interleukin (IL)-10^+ and TNF-α^+/IL-$17A^+$ cell prevalence in stimulated T_H cells, IL-17A/IL-10 and IL-2/IL-10 MFI on stimulated T_H cells, as well as IL-8, TNF-α, and IL-10 secretion by unstimulated peripheral blood mononuclear cells (PBMCs) and granzyme A secretion by stimulated PBMCs are illustrated. The Wilcoxon signed-ranked test was used and the False Discovery Rate (FDR)-corrected p values (Benjamini-Hochberg method) are displayed.	429
Figure 136.	**Box plots displaying the levels of the manually selected features in women with recurrent pregnancy loss (RPL) and controls.** The prevalence (%) of natural killer (NK) cells and T cells in lymphocytes and $CD56^{bright}CD16^-$ cells in NK cells, as well as the ratio of NK to T cells in women with RPL and controls is shown. The Wilcoxon signed-ranked test was used and the resulting p values are included.	430
Figure 137.	**Receiver operating characteristic (ROC) curve illustrating the sensitivity versus the specificity of each of the 4 markers selected for the identification of women with recurrent pregnancy loss (RPL).** Markers included represent the ratio between Natural Killer (NK) and T cell prevalence (NK_CD3), T (CD3+ in Lymphocytes) and NK (NK cells in Lymphocytes) cell prevalence in lymphocytes, and $CD56^{bright}CD16^-$ cell prevalence in NK cells (CD56brightCD16- cell in NK cells). The area under curve (AUC) value for each marker is shown as a percentage.	431

Appendices		
Supplementary Figure 1.	**Questions 1-4 of questionnaire distributed through SmartSurvey™ to recurrent pregnancy loss (RPL) clinics nationwide.** Questions included on this page were focused on obtaining information on the clinicians completing their survey and the institution in which the clinics belong to.	481
Supplementary Figure 2.	**Questions 5-8 of questionnaire distributed through SmartSurvey™ to recurrent pregnancy loss (RPL) clinics nationwide.** Questions on this page were designed to collect information in regards to the criteria used to diagnose RPL and thus recruit women in RPL clinics.	482
Supplementary Figure 3.	**Questions 9-11 of questionnaire distributed through SmartSurvey™ to recurrent pregnancy loss (RPL) clinics nationwide.** Questions on this page were designed to collect information in regards to the tests performed to identify anatomical, hypothalamic-pituitary-adrenal axis-associated, and genetic/chromosomal RPL risk factors.	483
Supplementary Figure 4.	**Question 12 of questionnaire distributed through SmartSurvey™ to recurrent pregnancy loss (RPL) clinics nationwide.** The question on this page was generated to obtain information on the tests performed to identify haematological RPL risk factors.	484
Supplementary Figure 5.	**Questions 13-16 of questionnaire distributed through SmartSurvey™ to recurrent pregnancy loss (RPL) clinics nationwide.** Questions on this page were designed to collect information on the tests performed to identify thyroid-associated, diabetes-associated, infection-associated, and other known RPL risk factors.	485
Supplementary Figure 6.	**Questions 17-19 of questionnaire distributed through SmartSurvey™ to recurrent pregnancy loss (RPL) clinics nationwide.** Questions on this page were created to collect information in regards to the use of immunological tests in RPL clinics.	486
Supplementary Figure 7.	**Questions 20-21 of questionnaire distributed through SmartSurvey™ to recurrent pregnancy loss (RPL) clinics nationwide.** Questions on this page were created to collect information in regards to the treatments used for the management of idiopathic RPL.	487
Supplementary Figure 8.	**Question 22 of questionnaire distributed through SmartSurvey™ to recurrent pregnancy loss (RPL) clinics nationwide.** The question on this page was design to collect information on the responders' opinion in regards to the	488

	effectiveness of the different treatments for idiopathic RPL and thus the likelihood to suggest them to women with this condition.	
Supplementary Figure 9.	**Basic principles of the flow and mass cytometry techniques utilised.** A) During cell examination by flow cytometry, fluorescently stained cells pass through a light source. In the BD FACSCanto™ II cell analyzer (BD Biosciences) the light source consists of three excitation lasers, a violet, a blue, and a red, which produce light beams at 405nm, 488nm, and 633nm respectively. The resulting forward scatter (FSC) signal measures light parallel to the laser beam, indicating cell size, while the side scatter (SSC) measures diffraction of light at a 90º angle from the beam, indicating structural complexity and granularity of the cell. Dichroic mirrors partition light and direct certain wavelengths to the appropriate detector. The photomultiplier detectors amplify the signal, enabling the detection and quantification of emitted light of different wavelengths. Signals are converted to a digital readout and are analysed. This set-up allows the simultaneous assessment of 8 colours and thus the examination of ≤8 parameters on each cell. B) During mass cytometry, cells labelled with heavy metals pass through a nebulizer, creating aerosol, and a plasma torch, vaporizing cells and generating an ion cloud. Low mass ions, such as biological molecules and environmental contaminants, are removed by a quadrupole mass analyser. The filtered heavy ions are accelerated and enter a time-of-flight (TOF) chamber, being separated according to their mass-to-charge ratio and reflected towards a detector. The detector measures a mass spectrum, representing each isotope's identity and quantity. This Helios Cytometry by Time-Of-Flight (Fluidigm) set-up allows the simultaneous investigation of >40 parameters on each cell.	490
Supplementary Figure 10.	**Effect of Peripheral Blood Mononuclear Cell (PBMC) isolation time on Natural Killer (NK) cells.** A) NK cell prevalence in Lymphocytes (%), B) $CD56^{dim}CD16^{+}$ cell prevalence in NK cells (%), C) $CD56^{bright}CD16^{-}$ cell prevalence in NK cells (%), and D) $CD69^{+}$ cell prevalence in NK cells (%) are displayed in two paired groups, one for PBMCs isolation 24h after blood collection and one for PBMCs isolation 48h after blood collection (*N*=11). The median value for each group is shown. Wilcoxon matched-pairs signed rank test performed. ns: non-significant	492

Supplementary Figure 11.	**Effect of peripheral blood mononuclear cell (PBMC) isolation time on T cells.** A) T cell prevalence in Lymphocytes (%), B) $CD4^+$ cell prevalence in T cells (%), C) $CD8^+$ cell prevalence in T cells (%), D) regulatory T cell (Treg) prevalence in $CD4^+$ T cells, and E) $CD45RA^+$ cell prevalence in T cells (%) are depicted in two paired groups, one for PBMCs isolation 24h after blood collection and one for PBMCs isolation 48h after blood collection (*N*=11). Normally distributed datasets (A, C, D, E): Paired t test performed, mean and standard deviation displayed. Non-normally distributed datasets (B): Wilcoxon matched-pairs signed rank test used, median illustrated. ns: non-significant, **: p≤0.01	493
Supplementary Figure 12.	**Effect of peripheral blood mononuclear cell (PBMC) isolation time on cytokine production by $CD4^+$ T helper cells.** A) IL-2^+ cell prevalence in $CD4^+$ T cells (%), B) IFN-γ^+ cell prevalence in $CD4^+$ T cells (%), C) TNF-α^+ cell prevalence in $CD4^+$ T cells (%), D) IL-10^+ cell prevalence in $CD4^+$ T cells (%), and E) IL-$17A^+$ cell prevalence in $CD4^+$ T cells (%) are displayed in two paired groups, one for PBMCs isolation 24h after blood collection and one for PBMCs isolation 48h after blood collection (*N*=11). Normally distributed datasets (A, B, C, E): Paired t test used, mean and standard deviation shown. Non-normally distributed datasets (D): Wilcoxon matched-pairs signed rank test performed, median depicted. ns: non-significant	494
Supplementary Figure 13.	**Effect of peripheral blood mononuclear cell (PBMC) isolation time on cytokine production and cytokine receptor expression by Natural Killer (NK) cells.** A) IFN-γ^+ cell prevalence in NK cells (%), B) TNF-α^+ cell prevalence in NK cells (%), C) IL-10^+ cell prevalence in NK cells (%), D) $CD25^+$ cell prevalence in NK cells (%), and E) $CD215^+$ cell prevalence in NK cells (%) are depicted in two paired groups, one for PBMCs isolation 24h after blood collection and one for PBMCs isolation 48h after blood collection (*N*=11). Normally distributed datasets (E): Paired t test performed, mean and standard deviation illustrated. Non-normally distributed datasets (A, B, C, D): Wilcoxon matched-pairs signed rank test used, median shown. ns: non-significant	495
Supplementary Figure 14.	**Percentage of lymphocytes expressing each cytokine of interest, following stimulation with 0.05µg/mL phorbol 12-myristate 13-acetate and 1µg/mL ionomycin for 4h, 6h, and 12h.** The mean prevalence of cells expressing IL-17A,	496

	IL-10, IL-2, IFN-γ, and TNF-α in the total lymphocyte population is illustrated (*N*=2), with the error bars representing standard deviation.	
Supplementary Figure 15.	**Percentage of Natural Killer (NK) cells expressing each cytokine of interest, following stimulation with 0.05μg/mL phorbol 12-myristate 13-acetate and 1μg/mL ionomycin for 4h, 6h, and 12h.** The mean prevalence of cells expressing IL-10, IFN-γ, and TNF-α in the total $CD3^{+}CD56^{-}$ NK cell population is illustrated (*N*=2), while error bars representing standard deviation are also shown.	497
Supplementary Figure 16.	**Percentage of lymphocytes expressing each cytokine of interest, following stimulation with different concentrations of phorbol 12-myristate 13-acetate (PMA) and ionomycin for 12h.** The mean prevalence of cells expressing IL-17A, IL-10, IL-2, IFN-γ, and TNF-α in the total lymphocyte population is depicted (*N*=2), with the error bars representing standard deviation.	498
Supplementary Figure 17.	**Percentage of Natural Killer (NK) cells expressing each cytokine of interest, following stimulation with different concentrations of phorbol 12-myristate 13-acetate (PMA) and ionomycin for 12h.** The mean prevalence of cells expressing IL-10, IFN-γ, and TNF-α in the total $CD3^{+}CD56^{-}$ NK cell population is illustrated (*N*=2), while error bars representing standard deviation are also depicted.	499
Supplementary Figure 18.	**Percentage of peripheral blood mononuclear cell (PBMCs) death following a 12h stimulation period with 0.025μg/mL-0.5μg/mL and 0.05μg/mL-1μg/mL phorbol 12-myristate 13-acetate (PMA)-ionomycin concentrations.** The mean cell death is displayed (*N*=2), while the standard deviation is shown in the form of error bars.	499
Supplementary Figure 19.	**Titration of antibodies used in the flow cytometry assay.** The separation indices resulting from the use of different titres of the antibodies included in the A) Natural Killer (NK) cell, B) T cell, C) T helper cell cytokine, and D) NK cell cytokine panel are displayed.	502
Supplementary Figure 20.	**Titration of the Zombie dead cell stain used in the flow cytometry assay.** The separation indices resulting from the use of various amounts of the dye solution for the staining of cells that were processed according to the protocols of the different panels are illustrated	503
Supplementary Figure 21.	**Optimization of extracellular antibody addition timing in the cytokine panels of the flow-cytometry based assay.**	504

	Average percentage of cells positive for each marker targeted by the extracellular antibodies used in the A) T helper (T_H) cell cytokine and B) Natural Killer cell cytokine panels are shown (*N*=2), in relation to the timing of their addition. Specifically, marker expression on cells stained with extracellular antibodies prior to fixation, permeabilization, and intracellular antibody addition and on cells stained with both intracellular and extracellular antibodies after the fixation and permeabilization process is depicted. Error bars representing standard deviation are included.	
Supplementary Figure 22.	**Flow cytometry assay validation.** The prevalence of A) Natural Killer (NK) and T lymphocytes, B) $CD56^{dim}CD16^{+}$, $CD56^{bright}CD16^{-}$, $CD69^{+}$ NK cell subsets, C) $CD4^{+}$, $CD8^{+}$, $CD45RA^{+}$, and regulatory (Treg) T cell subsets, D) IL-10^{+}, IL-$17A^{+}$, IFN-γ^{+}, and TNF-α^{+} T helper cells, and E) IL-10^{+}, IFN-γ^{+}, TNF-α^{+}, $CD25^{+}$, and $CD215^{+}$ NK cells is illustrated (*N*=8). The mean and standard deviation of each dataset is shown.	505
Supplementary Figure 23.	**Dead cell prevalence in the peripheral blood mononuclear cell populations stained with the different panels of the flow cytometry assay.** Samples isolated in from women with recurrent pregnancy loss and controls were stained for cell death with Zombie Green and processed according to the Natural Killer (NK) (*N*=116) and T (*N*=117) cell panel protocol, not having undergone prior stimulation, or the T (*N*=113) and NK (*N*=109) cell cytokine panel protocol, being previously stimulated with phorbol 12-myristate 13-acetate and ionomycin. Zombie $Green^{+}$ dead cell prevalence A) in each panel and B) in panels not requiring prior stimulation compared to those requiring pre-stimulation is depicted. Mann-Whitney test used, median illustrated. ns: non-significant	506
Supplementary Figure 24.	**Titrations of antibodies used in the mass cytometry assay.** The separation indices resulting from the use of different titres of the antibodies included in the mass cytometry panel are displayed. Antibodies titrated are separated into A) anti-cluster of differentiation (CD), B) anti-killer-cell immunoglobulin-like receptor (KIR), C) anti- immunoglobulin-like transcript (ILT) receptor, D) anti-chemokine receptor, E) anti-natural killer group (NKG)2 receptor, F) anti-natural cytotoxicity receptor, and G) anti-inhibitory immune checkpoint receptor antibodies, according to their target molecules.	514

Supplementary Figure 25.	**Peripheral blood mononuclear cell (PBMC) and K562 cell visualization by Giemsa staining and light microscopy.** Cells in A) PBMC-only samples, B) co-cultures containing PBMC and K562 cells at a 3:1 ratio, and C) K562-only cell cultures are displayed.	519
Supplementary Figure 26.	**Titration of dyes used in the cytotoxicity assay.** The mean separation indices, resulting from the use of different amounts of A) PKH67 or B) propidium iodide (PI) solution, in duplicated of peripheral blood mononuclear cell (PBMC):K562 cell co-cultures, including different ratios of these cells, are illustrated. An average of the results obtained by the use different ratios is also shown.	520
Supplementary Figure 27.	**Optimization of peripheral blood mononuclear cell (PBMC):K562 cell co-culture duration.** Mean specific K562 target cell death (%) in co-cultures including different PBMC:K562 cell ratios is illustrated in relation to the co-culture duration (h) (*N*=2). An average of specific target cell death in co-cultures including different cell ratios is also shown for each co-culture duration. Error bars representing standard deviation are included.	521
Supplementary Figure 28.	**Optimization of peripheral blood mononuclear cell (PBMC):K562 cell ratios used in co-cultures.** Mean specific K562 target cell death (%) in PBMC:K562 cell co-cultures, in which different ratios of these cells were used, is displayed (*N*=2). Error bars representing standard deviation are also shown.	522
Supplementary Figure 29.	**Optimization of peripheral blood mononuclear cell (PBMC):K562 cell ratios used in co-cultures, in which a constant final volume is maintained.** Mean specific K562 target cell death (%) in PBMC:K562 cell co-cultures, in which different ratios of these cells were used maintaining a constant final volume, is depicted (*N*=2). Error bars representing standard deviation are also displayed.	523
Supplementary Figure 30.	**Optimization of K562 cell staining performed during the cytotoxicity assay.** Mean specific K562 target cell death (%) in peripheral blood mononuclear cell (PBMC):K562 cell co-cultures, in which an anti-CD235 antibody or PKH67 were used for labelling K562 cells, is illustrated (*N*=2). Co-cultures used included different PBMC:K562 cell ratios and an average of specific target cell death across these co-cultures is also displayed. Error bars representing standard deviation are shown.	524

Supplementary Figure 31.	**Optimization of dead cell staining performed during the cytotoxicity assay.** Mean specific K562 target cell death (%) in peripheral blood mononuclear cell (PBMC):K562 cell co-cultures, in which Zombie red or propidium iodide (PI) were used for dead cell staining is displayed (*N*=2). Co-cultures used included different PBMC:K562 cell ratios and an average of specific target cell death across these co-cultures is also shown. Error bars representing standard deviation are included.	525
Supplementary Figure 32.	**Cytotoxicity assay optimization using a new K562 target cell line.** Mean specific K562 target cell death (%) in co-cultures including different peripheral blood mononuclear cell (PBMC):K562 cell ratios, using K562 cells derived from new or older cultures is illustrated (*N*=2). An average of specific target cell death in co-cultures including different cell ratios is also shown. Error bars representing standard deviation are depicted.	526
Supplementary Figure 33.	**Cytotoxicity assay optimization using Natural Killer (NK) cell enrichment and dead K562 cell removal.** Mean specific K562 target cell death (%) in co-cultures containing peripheral blood mononuclear cells (PBMCs) and alive K562 cells, enriched NK and total K562 cells, and enriched NK cells and alive K562 cells is shown (*N*=2). In co-cultures including PBMCs the effector:target cell ratios used were equal to 12.5:1 (Low), 25:1 (Medium), and 50:1 (High), while the average specific K562 target cell death observed in each of these conditions was calculated. In co-cultures including NK cells, 0.5:1 (Low), 1:1 (Medium), and 2:1 (High) effector:target cell ratios were used, and the average value was again included. Error bars representing standard deviation are displayed.	527
Supplementary Figure 34.	**Cytotoxicity assay optimization by interleukin (IL)-2 pre-stimulation of Natural Killer (NK) cells.** Mean specific K562 target cell death (%) in co-cultures including different NK:K562 cell ratios, following or in the absence of IL-2-mediated NK cell pre-stimulation is illustrated (*N*=2). An average of specific target cell death in co-cultures including different cell ratios is also displayed. Error bars representing standard deviation are included.	528
Supplementary Figure 35.	**Cytotoxicity assay validation.** A) Specific K562 target cell death (%), B) $CD107a^+$ cell prevalence in alive Natural Killer (NK) cells (%), and C) CD107a expression levels on alive NK cells, represented by the median fluorescence intensity (MFI),	530

	in co-cultures containing different NK:K562 cell ratios are illustrated (*N*=7). For each of these parameters of NK cell activity the average of the values obtained from the different co-culture conditions for each sample is also shown. The mean and standard deviation of each dataset is displayed.	
Supplementary Figure 36.	**Effect of Natural Killer (NK) cell:K562 cell ratios used in co-cultures for the evaluation of specific target cell death and CD107a expression.** The A) specific K562 cell death (*N*=135), B) $CD107a^+$ dead NK cell prevalence (*N*=116), C) CD107a expression intensity on dead NK cells, represented by the median fluorescence intensity (MFI) (*N*=116), D) $CD107a^+$ alive NK cell prevalence (*N*=116), and E) CD107a expression intensity on alive NK cells (*N*=116) in co-cultures including different ratios of NK cells:K562 cells are depicted. NK cells used were derived from both women with recurrent pregnancy loss (RPL) and controls. Friedman test was performed, accompanied by the Dunn's test for multiple comparisons, median displayed. ns: non-significant, *: adjusted p≤0.05, ***: adjusted p≤0.001	532
Supplementary Figure 37.	**Enzyme-linked immunosorbent assay optimization.** Mean concentration (pg/mL) of A) granulocyte colony-stimulating factor (G-CSF), B) granulocyte-macrophage colony-stimulating factor (GM-CSF), C) granzyme A, D) granzyme B, E) interferon (IFN)-γ, F) interleukin (IL)-10, G) IL-13, H) IL-17A, I) IL-2, J) IL-4, K) IL-5, L) IL-8, M) perforin, and N) tumor necrosis factor (TNF)-α as detected by the enzyme-linked immunosorbent assay, in samples diluted 1:1, 1:2, 1:8, 1:32, 1:128, 1:512, 1:2048 in cell culture medium, is illustrated. Concentration in samples obtained by women with recurrent pregnancy loss (RPL, *N*=5), healthy controls (Controls, *N*=4), total samples from women with RPL and controls (Total, *N*=9), and an unstimulated control (Unstim, *N*=1) are displayed in the form of different groups. Error bars representing standard deviation are included.	534
Supplementary Figure 38.	**Density plot of the area under curve (AUC) values of the 18 marker-based model for the identification of women with recurrent pregnancy loss (RPL), run 1000 times using permuted and non-permuted data.** The mean AUC values for each dataset is highlighted (bold). The 18 markers taken into consideration represent the 18 features selected by the Elastic Net (EN) and Least Absolute Shrinkage and Selection Operator (LASSO) methods.	537

Supplementary Figure 39.	**Receiver operating characteristic (ROC) curve of the 4 marker-based model for the identification of women with recurrent pregnancy loss (RPL).** The area under curve (AUC) and the 95% confidence interval (CI) values are displayed.	538

Table summary		page
Materials and Methods		
Table 1.	**Antibodies used in the flow cytometry-based assay.** The target molecule of each antibody, the fluorochrome, the company from which each antibody was obtained, the catalogue number, and the clone are depicted. The respective isotype used to replace each antibody in the fluorescence minus one controls, the company from which each isotype was obtained, and the catalogue numbers are also shown. CD: cluster of differentiation, FoxP3: forkhead box P3, IFN: interferon, IL: interleukin, TNF: tumor necrosis factor	138
Table 2.	**Antibodies used in the mass cytometry-based assay.** The target molecule and metal are depicted for each antibody. For each readily-conjugated antibody, the catalogue number and clone are shown. Conjugated antibodies were supplied by Fluidigm. For the unconjugated antibodies, the company supplying each antibody, the respective catalogue number, and the clone are displayed. Labelling kits for antibody conjugation were supplied by Fluidigm. CD: cluster of differentiation, CXCR: C-X-C motif chemokine receptors, ILT: immunoglobulin-like transcript, KIR: killer-cell immunoglobulin-like receptor, NKG2: natural killer group 2, PD-1: programmed cell death protein 1, TIGIT: T cell immunoreceptor with Ig and ITIM domains, TIM-3: T cell immunoglobulin and mucin domain-containing protein-3, β2m: β2 microglobulin	139
Table 3.	**Reagents used in the present study.** Additional regents used in the cytotoxicity, enzyme-linked immunosorbent, flow cytometry, mass cytometry, and T, B, and Natural Killer cell assays are depicted alongside the supplying company and catalogue number. Other reagents utilised for blood and cell isolation or used in multiple assays are also included.	140
Table 4.	**T, B, and Natural Killer (NK) cell (TBNK) assay antibody panel.** The cell markers targeted by each antibody used and the respective fluorophore are included. The rationale behind the use of each marker is also shown.	145

Table 5.	**Flow cytometry Natural Killer (NK) cell panel.** The antibody targets included to examine the NK cell population and subpopulations of interest and assess NK cell activity are depicted alongside the respective fluorophores. APC: allophycocyanin, CD: cluster of differentiation, FITC: fluorescein isothiocyanate, PE: phycoerythrin	148
Table 6.	**Flow cytometry T cell panel.** The antibody targets included to assess the T cell population and subpopulations of interest are displayed alongside the respective fluorophores. APC: allophycocyanin, BV: brilliant violet, CD: cluster of differentiation, FITC: fluorescein isothiocyanate, FoxP3: forkhead box P3, PE: phycoerythrin, PE-Cy: phycoerythrin-cyanine, PerCP: peridinin chlorophyll protein	148
Table 7.	**Flow cytometry T helper cell cytokine panel.** The antibody targets included to evaluate cytokine production by T helper cells are depicted alongside the respective fluorophores. APC: allophycocyanin, BV: brilliant violet, CD: cluster of differentiation, FITC: fluorescein isothiocyanate, IFN: interferon, IL: interleukin, PE: phycoerythrin, PE-Cy: phycoerythrin-cyanine, TNF: tumor necrosis factor	149
Table 8.	**Flow cytometry Natural Killer (NK) cell cytokine panel.** The antibody targets included to assess cytokine production and cluster of differentiation (CD)25 and CD215 expression by total and $CD56^{dim}CD16^{+}$ NK cells are displayed alongside the respective fluorophores. APC: allophycocyanin, BV: brilliant violet, FITC: fluorescein isothiocyanate, IFN: interferon, IL: interleukin, PE: phycoerythrin, PE-Cy: phycoerythrin-cyanine, PerCP-Cy: peridinin chlorophyll protein-cyanine, TNF: tumor necrosis factor	149
Table 9.	**Mass cytometry assay panel.** The antibody targets included in the mass cytometry panel to thoroughly examine Natural Killer (NK) cell populations and subpopulations of interest are depicted alongside the respective metal. Markers used to examine T and B cell subpopulations are also included. CD: cluster of differentiation, CXCR: C-X-C motif chemokine receptors, DNA: deoxyribonucleic acid, ILT: immunoglobulin-like transcript, KIR: killer-cell immunoglobulin-like receptor, NKG2: natural killer group 2, PD-1: programmed cell death protein 1, TIGIT: T cell immunoreceptor with Ig and ITIM domains, TIM-3: T cell immunoglobulin and mucin domain-containing protein-3	159

Table 10.	**Antibody cocktail generated for mass cytometry staining.** The antibodies included in the mass cytometry panel, defined by their target molecule and metal tag, are illustrated alongside the amount of each used in the cocktail to stain 100µL of peripheral blood mononuclear cell sample. The resulting total cocktail volume is also shown. CD: cluster of differentiation, CXCR: C-X-C motif chemokine receptors, ILT: immunoglobulin-like transcript, KIR: killer-cell immunoglobulin-like receptor, NKG2: natural killer group 2, PD-1: programmed cell death protein 1, TIGIT: T cell immunoreceptor with Ig and ITIM domains, TIM-3: T cell immunoglobulin and mucin domain-containing protein-3	164
Table 11.	**Cytotoxicity assay panel.** The dyes used to stain target K562 cells, dead cells, and examine the levels of Natural Killer (NK) cell degranulation, through the assessment of CD107a expression, are displayed alongside their respective fluorophore. APC: allophycocyanin, FITC: fluorescein isothiocyanate, PE: phycoerythrin	172
Table 12.	**Enzyme-linked immunosorbent assay panel.** The targets of the antibody-coated microspheres, which were used to evaluate the secretion levels of cytokines and cytolytic granule contents by peripheral blood mononuclear cells (PBMCs), are displayed alongside the respective microsphere number. G-CSF: granulocyte-colony stimulating factor, GM-CSF: granulocyte-macrophage colony-stimulating factor, IFN: interferon, IL: interleukin, TNF: tumor necrosis factor	176
National Survey Exploring the Current Practice for the Diagnosis and Management of Idiopathic RPL		
Table 13.	**Respondent job designation and healthcare sector.** Both the total number of responses (*N*) and the percentage (%) calculated based on the total responses collected for each question is displayed. NHS: National Health Service (A - Response rate=94.59%, B - Response rate=97.30%)	190
Table 14.	**Recurrent pregnancy loss service guidelines.** Both the total number of responses (*N*) and the percentage (%) calculated based on the total responses obtained for this question is shown. ESHRE: European Society of Human Reproduction and Embryology, NICE: National Institute for Health and Care Excellence, RCOG: Royal College of Obstetricians and Gynaecologists (Response rate=100.00%)	191
Table 15.	**Diagnostic tests performed for the identification of immunological recurrent pregnancy loss (RPL) risk**	201

	factors, either routinely or when clinically indicated. The use of tests assessing the levels of Natural Killer (NK), T, and B cells, examining the helper (T_H), cytotoxic (T_C), and regulatory (Treg) T cell subpopulations and the B-1 and B-2 B cell subpopulations, and evaluating NK cell cytotoxicity and T_H cell cytokine production, as well as the use of anti-Human Leukocyte Antigen (HLA), anti-HY antibody, and anti-paternal blocking antibody screening and HLA-typing were investigated. Both the total number of responses (*N*) and the percentage (%) calculated based on the total responses obtained is illustrated (*N*=32). CD: cluster of differentiation (Response rate=86.49%)	
Table 16.	**Treatments offered for the management of idiopathic recurrent pregnancy loss (RPL).** Both the total number of responses (*N*) and the percentage (%) calculated based on the total responses obtained (*N*=32) is depicted. (Response rate=86.49%)	204
Table 17.	**Estimated efficiency and likelihood to suggest non-steroidal anti-inflammatory drugs and steroids for the management of idiopathic recurrent pregnancy loss.** Both the total number of responses (*N*) and the percentage (%) calculated based on the total responses obtained for each treatment is displayed. The response rate for each treatment is also illustrated.	206
Table 18.	**Estimated efficiency and likelihood to suggest hormonal treatments for the management of idiopathic recurrent pregnancy loss.** Both the total number of responses (*N*) and the percentage (%) calculated based on the total responses obtained for each treatment is shown. The response rate for each treatment is also depicted.	207
Table 19.	**Estimated efficiency and likelihood to suggest biologic treatments for the management of idiopathic recurrent pregnancy loss.** Both the total number of responses (*N*) and the percentage (%) calculated based on the total responses obtained for each treatment is illustrated. The response rate for each treatment is also shown.	208
Table 20.	**Estimated efficiency and likelihood to suggest allogeneic cell immunization for the management of idiopathic recurrent pregnancy loss.** Both the total number of responses (*N*) and the percentage (%) calculated based on the total responses obtained for each treatment is depicted. The response rate for each treatment is also displayed.	208

Table 21.	**Estimated efficiency and likelihood to suggest vitamin supplementation for the management of idiopathic recurrent pregnancy loss.** Both the total number of responses (*N*) and the percentage (%) calculated based on the total responses obtained for each treatment is illustrated. The response rate for each treatment is also depicted.	209
Table 22.	**Estimated efficiency and likelihood to suggest other treatments for the management of idiopathic recurrent pregnancy loss.** Both the total number of responses (*N*) and the percentage (%) calculated based on the total responses obtained for each treatment is shown. The response rate for each treatment is also displayed.	210
Participant Demographics		
Table 23.	**Summary of participant demographics, including age, gravidity, parity, and body mass index (BMI), as well as time of blood collection.** The median and 95% confidence interval (CI) in the control (*N*=80) and recurrent pregnancy loss (RPL) (*N*=100) group is displayed, alongside the p value. Mann-Whitney test used, ns: non-significant, *: p≤0.05, ****: p≤0.0001	220
Table 24.	**Contingency table illustrating the ethnic background of controls and women with recurrent pregnancy loss (RPL) recruited in this study.** Women in the control (*N*=78) and RPL (*N*=82) group were split into four ethnic groups, including Asian, Black, White, and Mixed. The number of women in each subgroup is depicted, alongside the p value. Chi-square test, ***: p≤0.001	223
Table 25.	**Contingency table depicting the body mass index (BMI) group of controls and women with recurrent pregnancy loss (RPL) recruited in this study.** Women in the control (*N*=70) and RPL (*N*=88) group were split into five BMI groups, including underweight, healthy weight, overweight, obese, and severely obese. The number of women in each subgroup is illustrated, alongside the p value. Chi-square test, ns: non-significant	223
Table 26.	**Contingency table illustrating the levels of alcohol consumption of controls and women with recurrent pregnancy loss (RPL) recruited in this study.** Women in the control (*N*=79) and RPL (*N*=99) group were split into four groups, according to the average amount of alcohol they consume per week. The number of women in each	224

	subgroup is displayed, alongside the p value. Chi-square test, ****: p≤0.0001	
Table 27.	**Contingency table depicting the smoking habits of controls and women with recurrent pregnancy loss (RPL) recruited in this study.** Women in the control (*N*=79) and RPL (*N*=98) group were split into three groups, including non-smokers, ex-smokers, and smokers. The number of women in each subgroup is shown. P values for the two comparisons made by grouping ex-smokers with either the non-smoker or the smoker group are also included. Fisher's exact test, ns: non-significant	224
Table 28.	**Contingency table illustrating the use of illicit drugs by controls and women with recurrent pregnancy loss (RPL) recruited in this study.** Women in the control (*N*=79) and RPL (*N*=76) group were split into two groups, based on illicit drug use. The number of women in each subgroup is displayed, alongside the p value. Fisher's exact test, ns: non-significant	225
	Immunophenotyping	
Table 29.	**Overview of changes in lymphocyte population and subpopulation prevalence in the peripheral blood of women with recurrent pregnancy loss (RPL) compared to control women.** Alterations in Natural Killer (NK), T, and B cell levels detected by flow cytometry are depicted. Treg: regulatory T cell, ↓: decreased, ↑: increased, ns: non-significant, **: p≤0.01, ****: p≤0.0001	264
	NK cell Activation and Cytotoxicity Evaluation	
Table 30.	**Overview of changes in peripheral immune activity of women with recurrent pregnancy loss (RPL) compared to control women.** Alterations in Natural Killer (NK) cell cytotoxicity and degranulation, cytolytic molecule secretion by unstimulated (U) and stimulated (S) peripheral blood mononuclear cells (PBMCs), and NK cell population and subpopulation activation, examined via the cytotoxicity assay, utilizing CD107a as a degranulation marker, enzyme-linked immunosorbent assay (ELISA), and flow cytometry, using CD69 as an activation marker, respectively, are displayed. MFI: median fluorescence intensity, ↓: decreased, ↑: increased, ns: non-significant, *: p≤0.05, **: p≤0.01, ***: p≤0.001, ****: p≤0.0001	316
Table 31.	**Overview of major Natural Killer (NK) cell phenotypic changes in the peripheral blood of women with recurrent pregnancy loss (RPL) compared to control women.**	317

	Presence (+) or absence (-) of receptor expression on NK cell clusters reduced and increased in RPL, as detected via mass cytometry, is depicted.	
Cytokine Analysis		
Table 32.	**Overview of changes in cytokine production in the peripheral blood of women with recurrent pregnancy loss (RPL) compared to control women.** Alterations in cytokine production by unstimulated (U) and stimulated (S) T helper (T_H) cells and total and $CD56^{dim}CD16^{+}$ Natural Killer (NK) cells detected by flow cytometry are displayed. IFN: interferon, IL: interleukin, MFI: median fluorescence intensity, TNF: tumor necrosis factor, ↓: decreased, ↑: increased, ns: non-significant, *: p≤0.05, **: p≤0.01, ***: p≤0.001, ****: p≤0.0001	409
Table 33.	**Overview of changes in cytokine, chemokine, and growth factor secretion in the peripheral blood of women with recurrent pregnancy loss (RPL) compared to control women.** Alterations in protein concentration (pg/mL) in unstimulated (U) and stimulated (S) peripheral blood mononuclear cell (PBMC) cultures assessed using the enzyme-linked immunosorbent assay are shown. G-CSF: granulocyte colony stimulating factor, GM-CSF: granulocyte-macrophage colony-stimulating factor, IFN: interferon, IL: interleukin, TNF: tumor necrosis factor, ↓: decreased, ↑: increased, ns: non-significant, *: p≤0.05, **: p≤0.01, ***: p≤0.001, ****: p≤0.0001	411
Appendices		
Supplementary Table 1.	**Backbone cocktail used in antibody titrations for the mass cytometry assay.** The antibodies added in the backbone cocktail, defined by their target molecule and metal tag, are included alongside the amount of each used per 100µL of peripheral blood mononuclear cell sample. CD: cluster of differentiation	512
Supplementary Table 2.	**Markers investigated for the identification of candidate immunological biomarkers distinguishing women with RPL.** Each marker examined and the respective assay used for data collection is depicted. CD: cluster of differentiation, G-CSF: granulocyte-colony stimulating factor, GM-CSF: granulocyte-macrophage colony-stimulating factor, IFN: interferon, IL: interleukin, MFI: median fluorescence intensity, NK: Natural Killer cells, PBMC: peripheral blood mononuclear cell, T_H cells: T helper cells, TNF: tumor necrosis factors, Treg: regulatory T cell	535

1.2 Abbreviations

- AAb: asymmetric antibody
- ADCC: antibody-dependent cellular cytotoxicity
- Ang: angiopoietin
- ANOVA: analysis of variance
- APC: antigen-presenting cell
- APS: antiphospholipid syndrome
- AUC: area under curve
- BMI: body mass index
- Breg: regulatory B cell
- CCL: C-C motif chemokine ligand
- CCR: C-C motif chemokine receptor
- CD: cluster of differentiation
- CI: confidence interval
- CMV: cytomegalovirus
- CTLA: cytotoxic T-lymphocyte-associated protein
- CXCL: C-X-C motif chemokine ligand
- CXCR: C-X-C motif chemokine receptor
- CyTOF: cytometry by time-of-flight
- DC: dendritic cell
- DNA: deoxyribonucleic acid
- dNK cell: decidual natural killer cell
- ELISA: enzyme-linked immunosorbent assay
- EN: Elastic Net
- eNK cell: endometrial natural killer cell
- ESHRE: European Society of Human Reproduction and Embryology
- EVT: extravillous trophoblast
- FasL: Fas ligand
- FBS: fetal bovine serum
- FDR: False Discovery Rate
- FMO: fluorescence minus one

- FoxP3: forkhead box P3
- FSC-A: forward scatter area
- FSC-H: forward scatter height
- G-CSF: granulocyte-colony stimulating factor
- GM-CSF: granulocyte-macrophage colony-stimulating factor
- HbA1c: glycated haemoglobin
- hCG: human chorionic gonadotropin
- HLA: human leukocyte antigen
- IFN: interferon
- Ig: immunoglobulin
- IL: interleukin
- ILT: immunoglobulin-like transcript
- IQR: interquartile range
- IVIg: intravenous immunoglobulin
- KIR: killer-cell immunoglobulin-like receptor
- LASSO: Least Absolute Shrinkage and Selection Operator
- LIR: leukocyte immunoglobulin-like receptor
- LMWH: low molecular weight heparin
- logFC: log fold change
- MC: mast cell
- MDS: multi-dimensional scaling
- MFI: median fluorescence intensity
- MIC: major histocompatibility complex class I chain-related protein
- MIF: macrophage migration inhibitory factor
- MIP: macrophage inflammatory protein
- MMI: median metal intensity
- MMP: matrix metalloproteinase
- Mφ: macrophage
- NAb: natural antibody
- NCR: natural cytotoxicity receptor
- NF-κB: nuclear factor kappa-light-chain-enhancer of activated B cells

- NHS: National Health Service
- NICE: National Institute for Health and Care Excellence
- NK cell: natural killer cell
- NKG2: natural killer group 2
- NLR: neutrophil-to-lymphocyte ratio
- PBMC: peripheral blood mononuclear cell
- PBS: phosphate-buffered saline
- PD-1: programmed cell death protein 1
- PD-L1: programmed death-ligand 1
- PI: propidium iodide
- PMA: phorbol 12-myristate 13-acetate
- pNK cell: peripheral natural killer cell
- RCOG: Royal College of Obstetricians and Gynaecologists
- REC: Research Ethics Committee
- RM: recurrent miscarriage
- RNA: ribonucleic acid
- ROC: receiver operating characteristic
- RPL: recurrent pregnancy loss
- SD: standard deviation
- SP: substance P
- SSC-A: side scatter area
- TBNK assay: T, B, and NK cell assay
- T_C cell: cytotoxic T cell
- TGF: transforming growth factor beta
- T_H cell: T helper cell
- TIGIT: T cell immunoreceptor with Ig and ITIM domains
- Tim-3: T cell immunoglobulin and mucin domain-containing protein-3
- TNF: tumor necrosis factor
- Treg: regulatory T cell
- TSH: thyroid-stimulating hormone
- ULBP: UL16-binding protein

- UMAP: uniform manifold approximation and projection
- uNK cell: uterine natural killer cell
- VEGF: vascular endothelial growth factor
- β2m: β2 microglobulin

2 INTRODUCTION

Parts of this chapter have been submitted for publication as:

Bagkou Dimakou D, Lissauer D, Tamblyn J, Coomarasamy A, Richter A. Understanding human immunity in idiopathic Recurrent Pregnancy Loss. Eur J Obstet Gynecol Reprod Biol.

2.1 Definition, prevalence, and impact

Miscarriage is defined as the spontaneous loss of pregnancy prior to viability, which in the UK is specified as the 24th gestational week.[1-3] The definition of recurrent pregnancy loss (RPL), also termed recurrent miscarriage, remains heterogenic.[4] According to the Royal College of Obstetricians and Gynaecologists (RCOG) and the National Institute for Health and Care Excellence (NICE), RPL is defined as the loss of three or more consecutive pregnancies,[1, 2] while the European Society of Human Reproduction and Embryology (ESHRE) guidance recommends that RPL should be diagnosed upon the presence of two, not necessarily consecutive, miscarriages,[5] as only a minority of couples with RPL experience non-consecutive losses.[6] The terms RPL and RM are often used interchangeably, although “RM” should be reserved for cases with ultrasound and/or histological confirmation of intrauterine loss.[7, 8]

Each minute, approximately 44 pregnancy losses are thought to occur, resulting to a yearly global miscarriage rate around 23,000,000.[3] According to ESHRE the estimated RPL prevalence ranges between 1% and 3%, depending on the definition used.[9] When defined as 3 or more consecutive losses, RPL occurs in ~1% of women,[1, 3, 10-12] while the latest review reported a ~2% population prevalence of women with two miscarriages.[3]

RPL is linked to additional obstetric complications, such as future preterm birth, placental abruption, fetal growth restriction, and stillbirth, while it is also associated with long-term health issues, including venous thromboembolism, cardiovascular disease, as well as mental health conditions.[3] The significant psychological impact

of RPL for couples, including but not restricted to an increased risk of anxiety, depression, and post-traumatic stress disorder, should be highlighted.[13-17] A significant economic impact of miscarriage on both individuals and the health-care system should also be taken into account, with an estimated £471,000,000/year short-term national economic cost in the UK reported.[3]

2.2 Risk factors

RPL is a multifactorial condition with a range of predisposing factors recognised. Reproductive history and maternal age are the major independent risk factors influencing pregnancy outcome, with the risk of fetal loss significantly increased for women of higher order loss and/or advanced age.[1, 3, 4, 9, 18-25] Black ethnic background was found to be linked to an increased miscarriage risk, compared to White ethnicity, albeit the mechanisms behind such observation remain unclear.[3] A significant association between RPL and paternal age, ≥40 years, has been described, although larger, well-designed trials are required.[1, 3, 9] Maternal factors more weakly associated with RPL include obesity,[3, 26] cigarette smoking,[3, 27-30] alcohol consumption,[3, 31, 32] elevated caffeine intake,[30, 32-34] vitamin D deficiency,[35] cocaine use,[29] organic compound exposure,[3, 36] and persistent stress.[3] Although aiming for a healthy body mass index (BMI) and avoidance of potentially harmful substances during pregnancy is suggested, insufficient data have been obtained.[9]

Considering genetic predisposition to RPL, parental and fetal chromosomal abnormalities are detected in a significant percentage of cases.[5, 37] Fetal aneuploidy is the most common cause of miscarriage, in particular early 1st-trimester

loss.[18, 37, 38] Karyotypic abnormalities are most commonly present as autosomal trisomies (~60%), monosomy X (~20%), and polyploidy (~20%).[39] Although RPL prevalence among first-degree relatives of women with RPL is also elevated compared to controls, supporting the presence of a genetic predisposition,[40] the subsequent pregnancy prognosis is higher in RPL couples with an aneuploid, compared to those with an euploid miscarriage.[41-43] Consanguinity has also been linked to fetal loss, even though a genetic background of this condition has not been clearly displayed.[44] Routine parental karyotyping is not currently recommended.[1] However, in a large-cohort study, chromosomal abnormalities were detected in 7.6% of 1122 women with RPL.[45] Paternal abnormalities, such as microdeletions of the Y chromosome and DNA fragmentation may also be involved in the aetiology of RPL.[46]

Underlying maternal comorbidities, including hereditary and acquired thrombophilia, congenital and acquired uterine malformations, and endocrine conditions such as untreated thyroid disease, polycystic ovary syndrome, and diabetes mellitus are also important risk factors for RPL (Figure 1).[1, 9, 18, 45, 47-58] For women investigated for RPL, positive measurement of antiphospholipid antibodies is the most frequent and treatable risk factor identified. In a large-cohort study including women with at least three consecutive miscarriages 12.2% tested positive for these antibodies,[59] while in another large-cohort study on women with two or more miscarriages 20.8% appeared positive.[60] A recent systematic review and meta-analysis also demonstrated a positive association between antiphospholipid antibodies and RPL.[61] Albeit the exact mechanisms by which these associations arise are not fully understood, a likely pro-inflammatory and pro-thrombotic pathogenesis,

characterised by placental infarction, abnormal trophoblast invasion, and complement pathway dysregulation is anticipated.[61-65]

Transvaginal and transplacental infections, including *chlamydia trachomatis*, *herpes simplex virus*, *ureaplasma*, and *mycoplasma*, are also associated with an increased risk of recurrent and spontaneous loss.[66-73] In acute infection of the fetus, placenta, or uterus excessive local inflammation can be induced. Chronic endometritis, characterized by endometrial plasma cell infiltration, obstructing the establishment and maintenance of pregnancy, may also result from infection.[48, 74] Indeed, chronic endometritis prevalence rates of between 7% and 58% have been reported in women with otherwise unexplained RPL.[74-76] This heterogeneity in part reflects different methods of detection, with higher rates detected using hysteroscopy and/or immunohistochemistry.[74, 76-78] Further well powered studies are required to more accurately establish endometritis rates in the RPL population. Currently, the Chronic Endometritis and Recurrent Miscarriage study is investigating the effect of antibiotic treatment for endometritis on the live birth rate of women with RPL.[79]

In ~50% of RPL cases, no underlying aetiological factor can be identified, termed “idiopathic RPL”.[18, 45, 48, 49] For couples this lack of explanation and the potential difficulty in identifying an effective treatment can be extremely difficult and often frustrating. Although couples’ emotions following a miscarriage may vary, feelings of grief, fear, shock, and even guilt have been reported.[80] The absence of an explanation can result in women and couples feeling hopeless, potentially heightening their anxiety during the grief process and throughout future pregnancies.[80]

Revised concepts regarding idiopathic RPL are gradually coming to light, with immune dysregulation at the forefront of much recent research activity. Studies examining the immune system of women with RPL, commonly focus on the idiopathic subpopulation, excluding women for which a known cause has been identified. It should be however underlined that for none of the risk factors a clear causal relation with RPL has been established.[9, 81] Given the heterogeneity of recognized factors contributing to pregnancy loss, it is possible that more than one aetiology underlies recurrent losses. Hence, it is important to understand whether immune dysfunction is exclusive to women with idiopathic RPL or whether immune dysregulation may also underlie non-idiopathic cases.

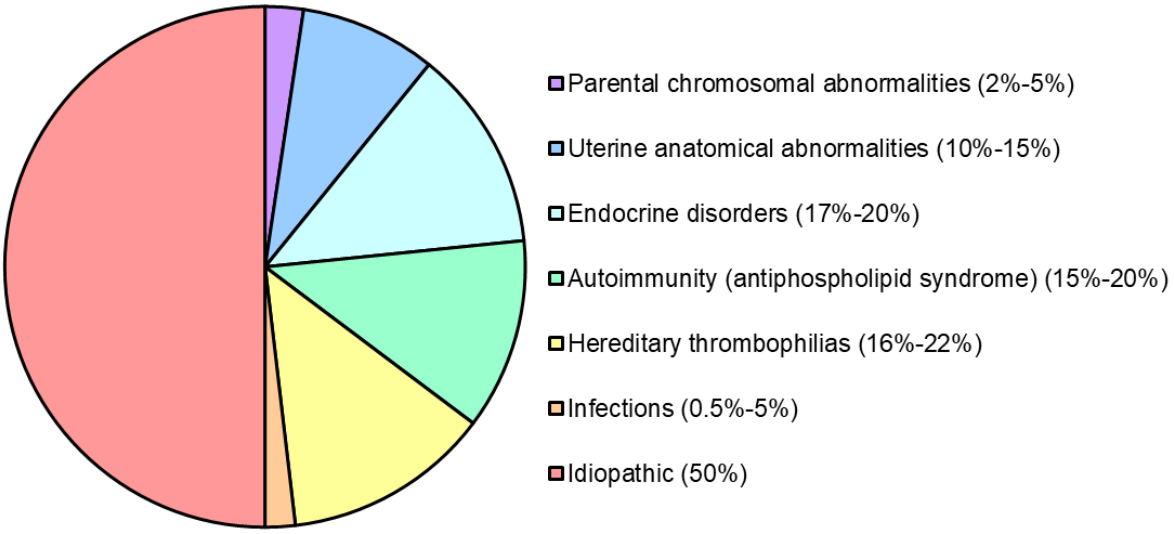


Figure 1. Risk factors associated with recurrent pregnancy loss (RPL). *The prevalence of underlying conditions in women with RPL is displayed. In around half of the cases no risk factors can be identified and the condition is termed "idiopathic".*[9, 18, 37, 48, 82, 83]

2.3 The role of the immune system in RPL

It is now over 50 years since Sir Peter Medawar kindled scientific interest in the unique problem posed by the existence of the fetal allograft within the uterus.[84, 85] Traditionally, the maternal-fetal interface was considered an inert environment with protection from maternal immunity. In fact there is a series of active immune processes to sustain balance of the maternal-fetal tolerance and anti-pathogen defence. Similar to organ transplantation, miscarriage was considered a direct consequence of immune activity against the fetal "graft".[85, 86] The concept of "graft-host" fetal-maternal interactions during pregnancy is now regarded as obsolete, with a synergistic activity of the dynamic immune system and fetal components considered central in the establishment and maintenance of human pregnancy.[86]

The immunological dialogue taking place at the fetal-maternal interface in the endometrium and decidua is fascinatingly complex involving a diverse and unique array of immune cells and molecules (Figure 2). Human decidualization is initiated during the secretory menstrual cycle phase, prior to implantation, and is characterised by uterine gland transformation, vascular remodelling, morphological stromal cell changes, and an influx of Natural Killer (NK) cells.[87] Immune cell recruitment and activity is crucial to this process, with the decidua being enriched with a unique leukocyte infiltrate; comprising 70% NK cells, 20%-30% macrophages, and 3%-10% T cells.[88-90] Decidual immune cells actively interact with fetal-derived extravillous trophoblast cells (EVTs), invading the decidua.[88] EVTs are negative for human leukocyte antigen (HLA) class II and HLA-A, HLA-B, and HLA-D, likely permitting their protection from T cell-mediated cytotoxicity. However, they express HLA-C, HLA-E, and HLA-G, thereby facilitating their protection from NK cell-

mediated responses, signalling through inhibitory killer-cell immunoglobulin-like (KIR), immunoglobulin-like transcript (ILT), and natural killer group (NKG)2 receptors.[88, 91-106] Indeed, in co-cultures, NK, cluster of differentiation (CD)4^+ T helper (T_H), and $CD8^+$ cytotoxic T (T_C) cells were shown to cluster around EVTs without inducing lysis.[91] Decidual NK (dNK) cell levels were found to be increased through the *in vitro* contact with trophoblasts, while trophoblast-conditioned medium was shown to reduce degranulation, highlighting a trophoblast-induced modification of NK cell activity in the decidua during pregnancy.[107]

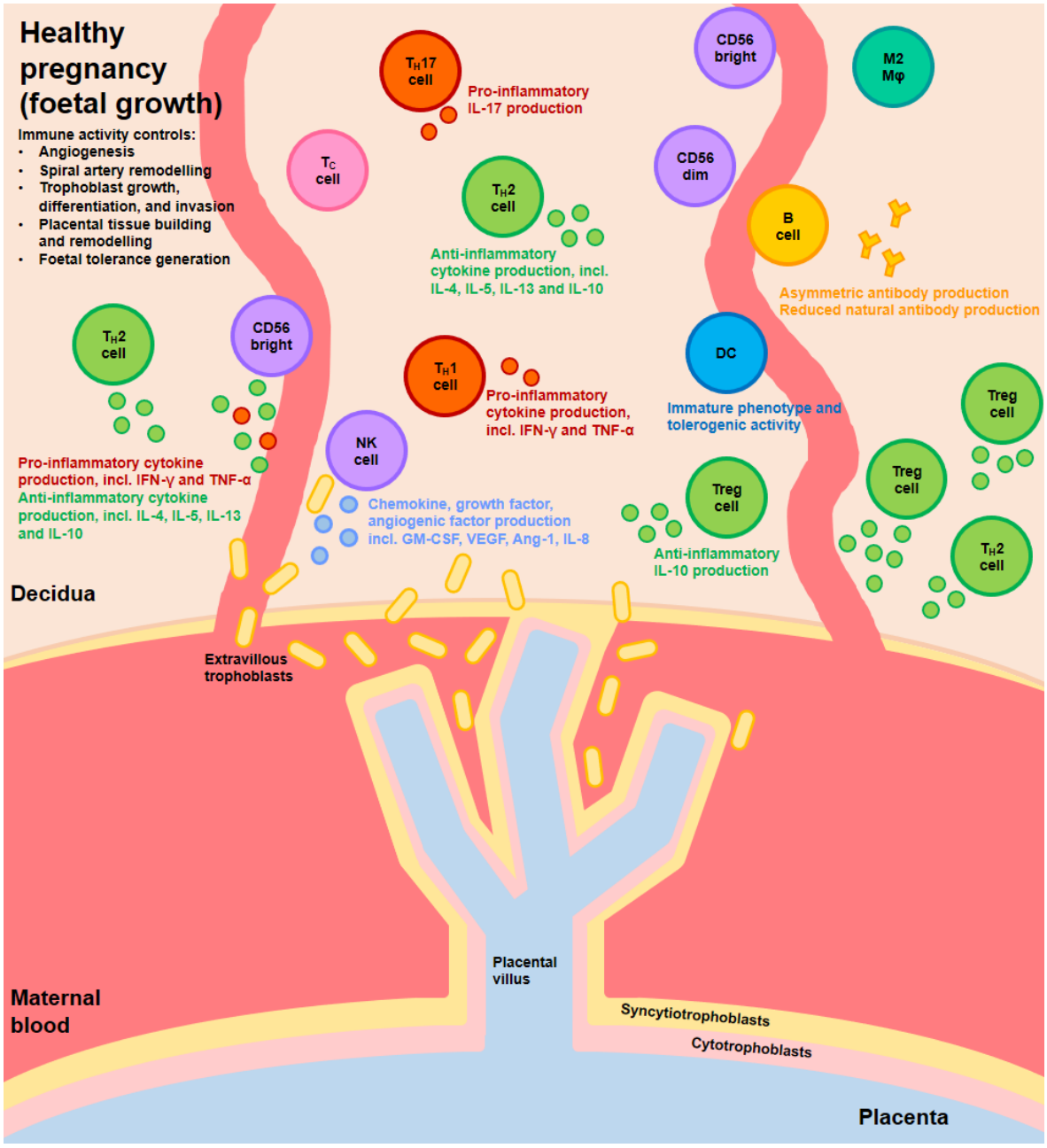


Figure 2. Overview of decidual immunity during healthy pregnancy, at the stage of fetal growth. *The contribution of decidual immune cell populations in the establishment and maintenance of pregnancy is displayed. Ang-1: angiopoietin 1, CD: cluster of differentiation, DC: dendritic cell, GM-CSF: granulocyte-macrophage colony-stimulating factor, IFN: interferon, IL: interleukin, Mφ: macrophage, NK cell: natural killer cell, T_C cell: cytotoxic T cell, T_H cell: T helper cell, TNF: tumor necrosis factor, Treg cell: regulatory T cell, VEGF: vascular endothelial growth factor*

Fetal-maternal interactions appear to extend to the peripheral blood (Figure 3). During haemochorial placentation spiral arteries are invaded by EVTs, mediating their remodelling by replacing endothelial cells, to allow low-pressure blood flow to the placenta.[106, 108-110] Thus, throughout this process, EVTs are in direct contact with the maternal blood stream.[110, 111] Additionally, villous syncytiotrophoblasts, which constitute the outer layer of the placental villi, acquiring important, endothelial, endocrine, and exchange functions, are bathed in maternal blood.[108, 109, 112] These cells are HLA^-, being protected from T cell recognition.[91, 109, 110, 112, 113] Mechanisms such as soluble HLA-G secretion could also control peripheral NK (pNK) cell-mediated responses, although these cells are thought to be subject to NK cell killing.[114-117]

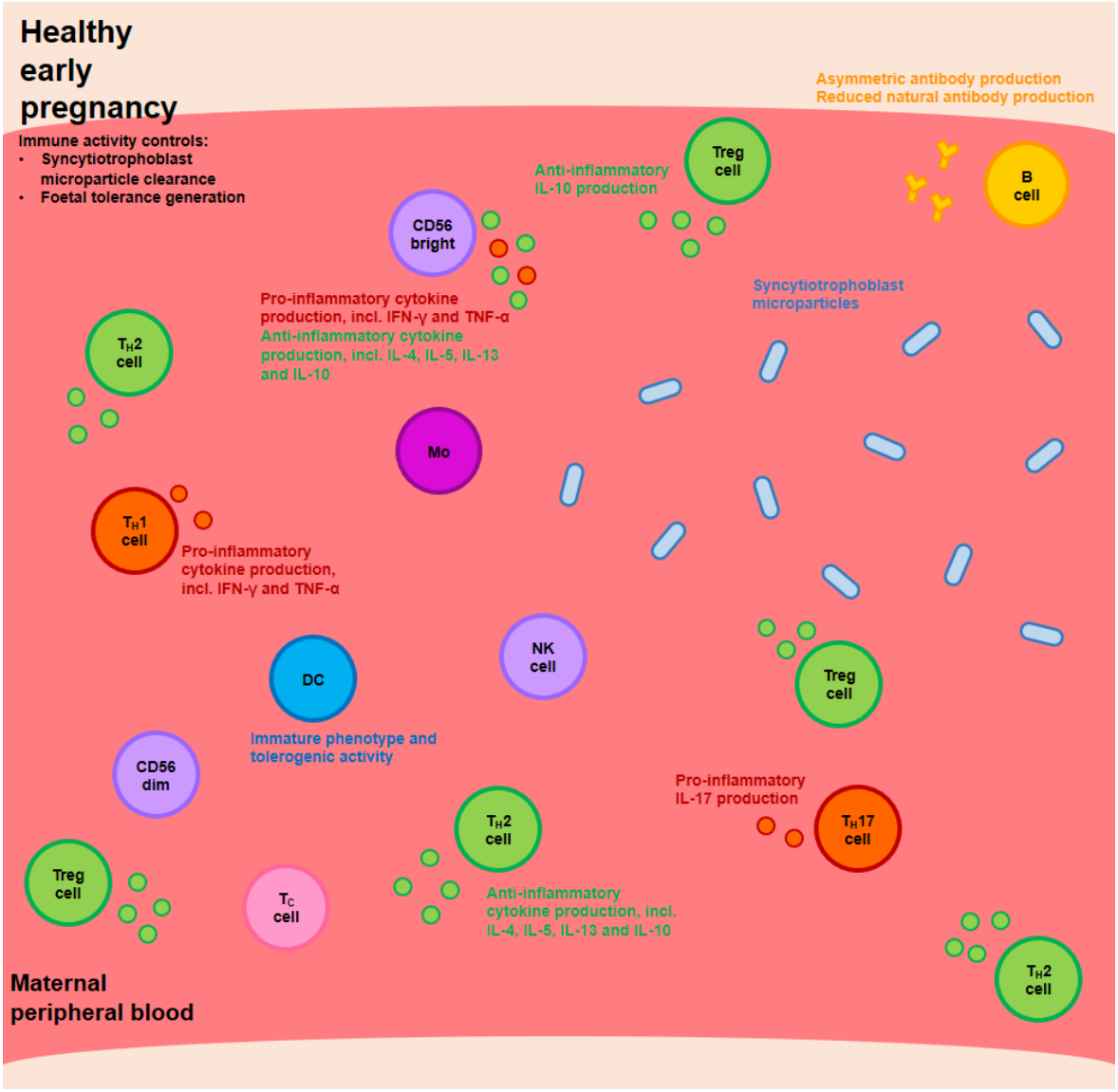


Figure 3. Overview of peripheral immunity during healthy early pregnancy. *The activity of peripheral immune cell populations during the initial pregnancy stages is illustrated. CD: cluster of differentiation, DC: dendritic cell, IFN: interferon, IL: interleukin, Mo: monocyte, NK cell: natural killer cell, T_C cell: cytotoxic T cell, T_H cell: T helper cell, TNF: tumor necrosis factor, Treg cell: regulatory T cell*

Overall, as shall be discussed in detail, immune activity in pregnancy is a double-edged sword (Figures 4, 5). For instance, endometrial NK (eNK) cell hyperactivity could promote anti-fetal responses, while defective NK cell activity could lead to insufficient senescent endometrial stromal clearance, contributing to the development of an inflammatory environment that promotes aberrant endometrial receptivity.[118] Furthermore, haemochorial placentation requires extensive remodelling of the uterine vasculature, resulting in maternal blood flow to the intervillous space, leading however to intense alterations in oxygen tension and free radical production.[81] Even though decidual cells are characterized by resistance to stress signals, excessive stress, potentially generated due to exacerbated EVT invasion, could result to miscarriage.[81] Defective EVT invasion has also been linked to RPL.[119] Furthermore, syncytiotrophoblast microparticles are released in the circulation during normal placental surface turnover and repair, interacting with the maternal peripheral immunity.[112] During healthy pregnancy, these microparticles may be recognised via Toll-like receptors on dendritic cells (DCs) and macrophages, mediating their clearance.[112] However, high microparticle prevalence, possibly due to defective clearance, and their possible modification by oxidative stress could induce pro-inflammatory cytokine secretion by NK cells, promoting systemic inflammation.[112]

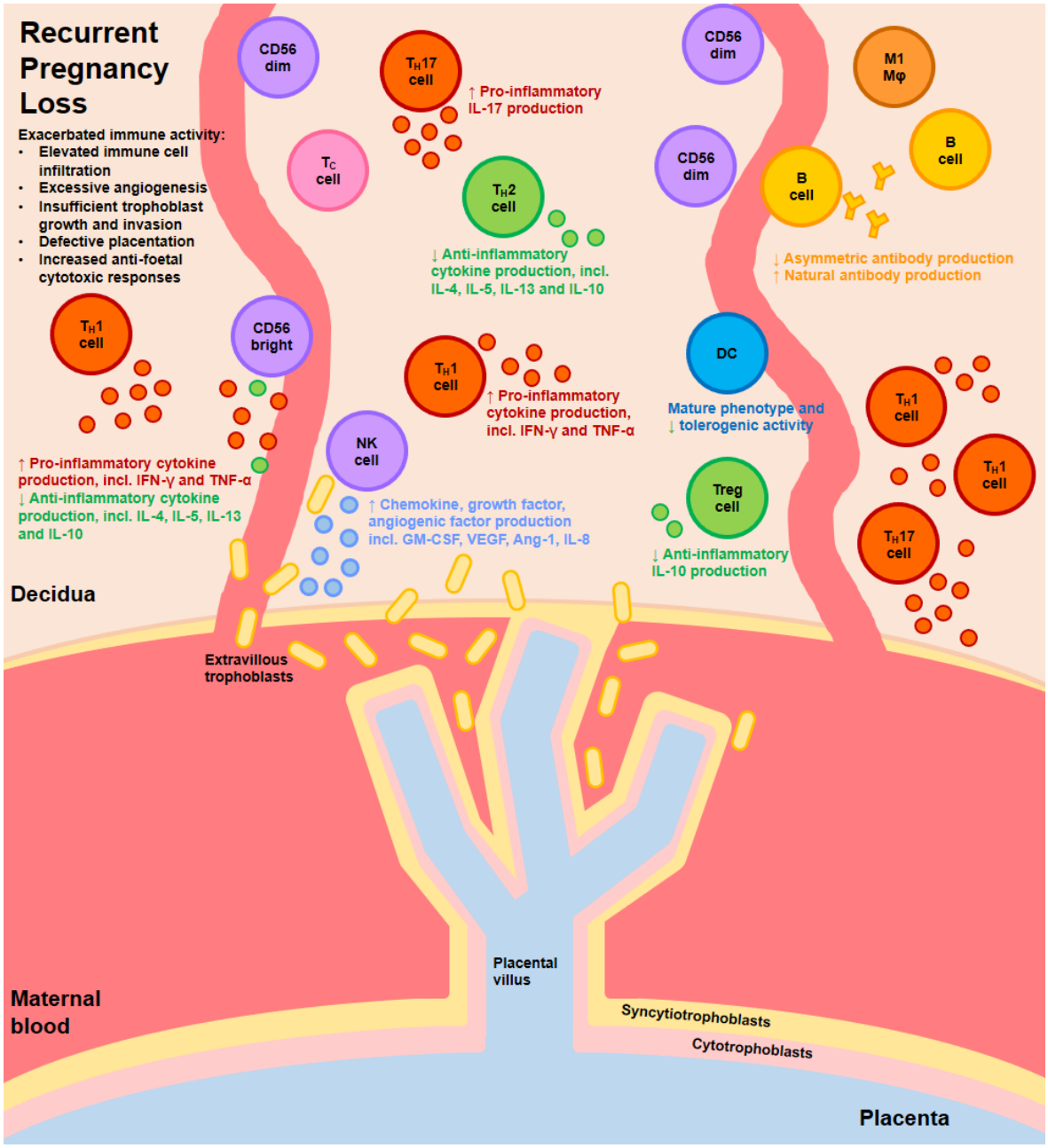


Figure 4. Overview of decidual immunity in women with recurrent pregnancy loss. *The suggested pro-inflammatory shift in the decidual immune cell activity of women with recurrent pregnancy loss is depicted. Ang-1: angiopoietin 1, CD: cluster of differentiation, DC: dendritic cell, GM-CSF: granulocyte-macrophage colony-stimulating factor, IFN: interferon, IL: interleukin, Mφ: macrophage, NK cell: natural killer cell, T_C cell: cytotoxic T cell, T_H cell: T helper cell, TNF: tumor necrosis factor, Treg cell: regulatory T cell, VEGF: vascular endothelial growth factor*

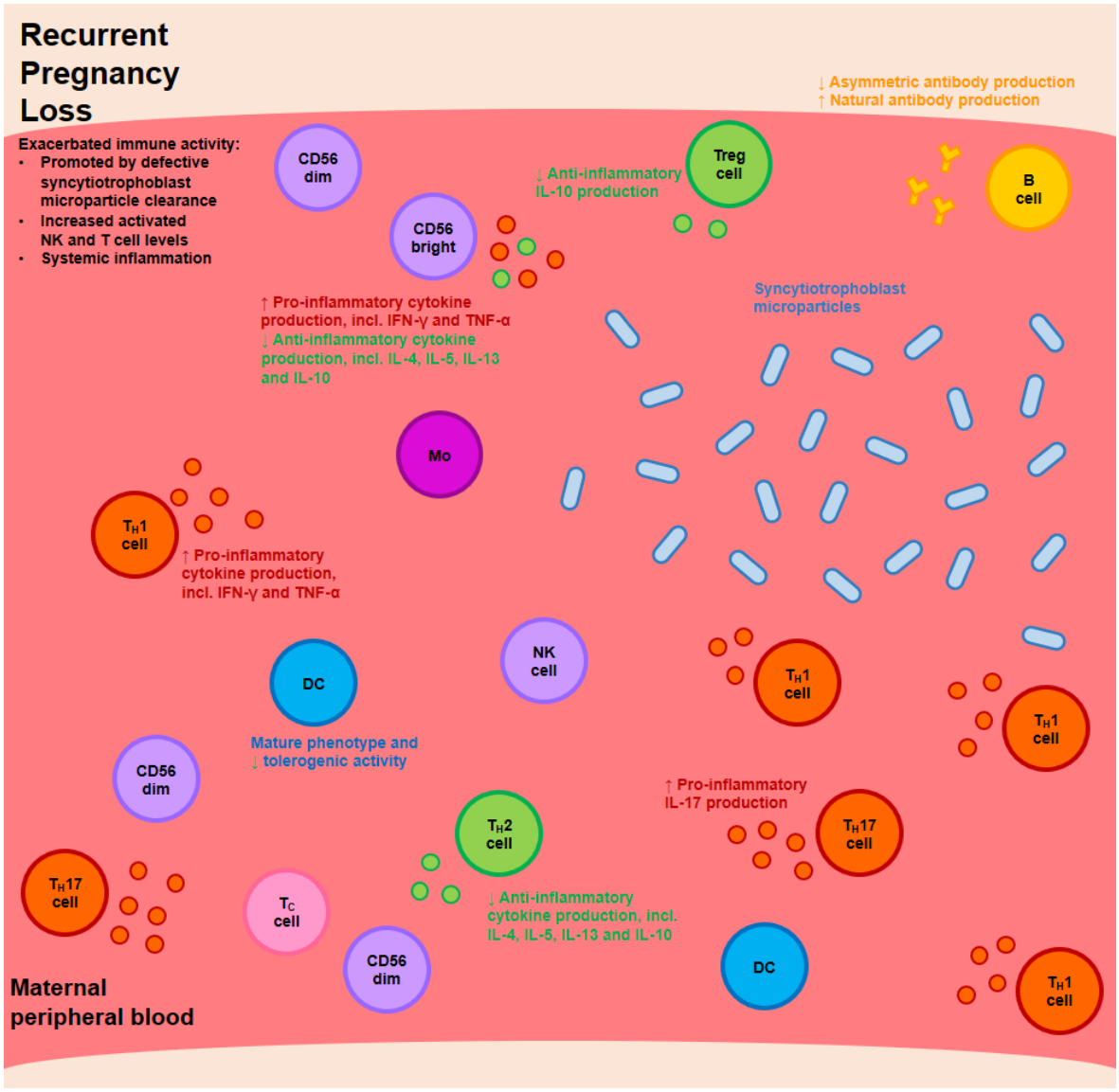


Figure 5. Overview of peripheral immunity in women with recurrent pregnancy loss. *The suggested pro-inflammatory shift in the peripheral immune cell activity of women with recurrent pregnancy loss is shown. CD: cluster of differentiation, DC: dendritic cell, IFN: interferon, IL: interleukin, Mo: monocyte, NK cell: natural killer cell, T_C cell: cytotoxic T cell, T_H cell: T helper cell, TNF: tumor necrosis factor, Treg cell: regulatory T cell*

A recent paradigm, the “implantation checkpoint hypothesis” highlights the presence of multiple checkpoints during the menstrual cycle and early pregnancy, ensuring maximum reproductive success.[81] Aberrant immune activity can interfere with these checkpoints, resulting in miscarriage. For instance, poorly controlled inflammation during the decidualization process can extend the “window of receptivity” allowing out-of-phase implantation and disabling the disposal of “low-quality” embryos, thereby permitting implantation of embryos with impaired growth and survival potential.[81, 120, 121] This suggests that pre-conceptual strategies to identify endometrial and or decidua immune cell dysfunction in high-risk women may show promise.

Hence, pregnancy appears highly dynamic with a diverse plethora of pro- and anti-inflammatory innate and adaptive immune responses contributing to essential reproductive processes, including implantation, trophoblast invasion and spiral artery remodelling, fetal growth, and parturition.[86, 122] The following sections shall discuss current evidence regarding individual cell types and their potential role in RPL.

2.4 NK cells in RPL

Due to their high levels in the uterus, reaching up to 90% of local lymphocytes, NK cells are highly anticipated as key mediators for reproductive success (Figure 6).[123] Human NK cells are characterised by their $CD56^{+}CD3^{-}$ phenotype.[124] NK cells accumulate in the endometrium during the luteal phase and in the decidua during the early stages of pregnancy, with their population being progressively diminished from mid-gestation onwards; thus indicating a greater role prior to and during implantation and early pregnancy.[88, 118, 125-129] Two main NK cell populations are present both in peripheral blood and uterus, $CD56^{dim}CD16^{+}$ ($CD56^{dim}$) and $CD56^{bright}CD16^{-}$ ($CD56^{bright}$). $CD56^{dim}$ cells are the major circulatory NK cell subpopulation and are considered primarily cytolytic whereas the $CD56^{bright}$ subset is most prevalent in the uterine tissue and is characterized by lower cytotoxic and higher cytokine-producing capacity.[130-135] This distinction in NK cell activity is mainly used to characterise cell responsiveness to different stimuli, with $CD56^{dim}$ cells responding more efficiently to receptor simulation through cell-surface ligands and $CD56^{bright}$ cells being more effective responders to cytokine stimulation.[136, 137] Furthermore, due to their CD16 expression, $CD56^{dim}$ NK cells are considered antibody-dependent cellular cytotoxicity (ADCC) mediators, inducing the lysis of antibody-coated target cells.[138, 139] During the 1^{st} pregnancy trimester, more than 90% of dNK cells display a $CD56^{bright}$ phenotype, while this phenotype is only seen in about 10% of pNK cells during early pregnancy.[140]

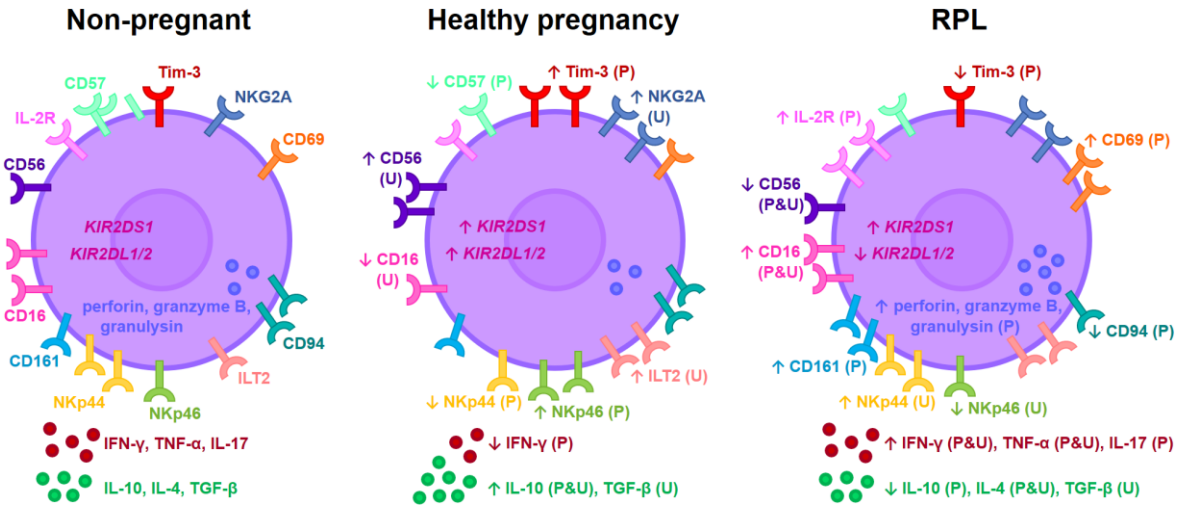


Figure 6. Natural Killer (NK) cell genetic, phenotypic, and functional changes in healthy pregnancy and recurrent pregnancy loss (RPL). *Alterations in receptor expression, killer-cell immunoglobulin-like receptor (KIR) gene frequencies, cytolytic molecule production, and cytokine secretion detected in the periphery (P) and uterus (U) of pregnant vs non-pregnant women and in RPL vs healthy pregnancy are displayed. CD: cluster of differentiation, IFN: interferon, IL: interleukin, IL-2R: IL-2 receptor, ILT: immunoglobulin-like transcript, NKG2: natural killer group 2, Tim-3: T cell immunoglobulin and mucin domain-containing protein-3, TGF: transforming growth factor, TNF: tumor necrosis factor*

Although the exact NK cell function remains unclear, a pivotal role in the control of placental trophoblast invasion and spiral artery remodelling is anticipated. From the luteal phase of the menstrual cycle, NK cells constitute 70% of the endometrial leukocyte population, being preferentially located adjacent to local arteries and glands, supporting endometrial remodelling in preparation for implantation.[141, 142] The formation of a dense uterine NK (uNK) cell infiltrate surrounding fetal trophoblasts coincides both spatially and temporally with this process.[88, 129, 143-145] NK cells do not appear capable of killing trophoblasts,[146-148] being however potent producers of cytokines, chemokines, growth and angiogenic factors, and matrix metalloproteinases (MMPs), including tumor necrosis factor (TNF)-α, interferon

(IFN)-γ, interleukin (IL)-10, macrophage migration inhibitory factor (MIF), macrophage inflammatory protein (MIP)-1α, IL-8, granulocyte-macrophage colony-stimulating factor (GM-CSF), vascular endothelial growth factor (VEGF), angiopoietin (Ang)1, MMP-7, and MMP-9 potentially contributing to angiogenesis, spiral artery and decidual tissue remodelling, trophoblast growth, differentiation, and invasion, and placental tissue building and remodelling.[88, 109, 122, 139, 141, 143, 149-158] uNK cells also exhibit immunomodulatory potential during pregnancy,[159] for example mediating extracellular adenosine triphosphate-to-adenosine conversion through the synergistic activity of CD39 with CD73, which is present on trophoblasts,[160] and secreting immunoregulatory cytokines such as IL-10 and transforming growth factor beta (TGF-β).[141]

The potential prognostic value of NK cell parameters in women at high risk of RPL has gained much interest. Increased $CD56^{+}$, $CD56^{dim}$, and $CD56^{bright}$ cell levels are measured as predictive biomarkers for a subsequent loss in women with RPL.[161-167] Consistent with this, elevated pre-conceptual pNK cell activity is suggested as a prognostic miscarriage marker for women with a history of RPL.[161, 168-170] However, the accuracy and reproducibility of these tests continues to be challenged and the data remains highly heterogeneous.[25, 129, 165, 171-175]

2.4.1 NK cell numbers

In a systematic review on the pNK and uNK cell prognostic value in regards to subsequent pregnancy outcome in women with RPL and infertility, the lack of a consensus on the “normal”/“abnormal” NK cell definition was highlighted as a primary issue leading to heterogeneous findings.[172] During pregnancy, similar to

the non-pregnant state, uNK cells are thought to mostly belong to the less cytotoxic $CD16^-$ subpopulation.[176] Some findings suggest a pregnancy-induced alteration in pNK cell counts, with a reduction in pNK cell prevalence and absolute counts throughout the different trimesters, primarily caused by alterations in the $CD56^{dim}$ subset.[177, 178] However in other reports no significant difference was detected in the total, $CD56^{bright}$, or $CD56^{dim}$ pNK cell absolute counts or the pNK cell prevalence of non-pregnant and pregnant women.[179-181]

In RPL, an increase in $CD56^+$ pNK cell frequencies both pre-conception and during pregnancy has been reported. This increase affects both $CD56^+$ pNK cell prevalence within the whole lymphocyte population and the absolute counts.[163, 164, 179, 182-190] It is postulated that this reflects an increase in the $CD56^{dim}$ subset resulting in a reduced $CD56^{bright}$-to-$CD56^{dim}$ pNK cell ratio.[164, 185, 190-192] Contradictory findings have however been obtained, with some studies reporting no change in pNK cell number or $CD56^{dim}/CD56^{bright}$ NK ratio in the peripheral blood leukocyte and lymphocyte populations of women with RPL.[193-196] A meta-analysis of studies examining NK cell levels in women with RPL reported an elevation of total and $CD56^{dim}CD16^+$ cell levels, compared to controls, even though a high heterogeneity between studies was highlighted.[197]

Elevated uNK cell numbers have also been detected in women with RPL. Specifically, in both pregnant and non-pregnant women, including those with idiopathic RPL, elevated endometrial NK cell infiltration is reported.[129, 167, 198-200] In the non-pregnant state $CD56^{dim}$ uNK cell frequencies were increased in women with miscarriages compared to controls, with reduced $CD56^{bright}$ subsets concomitantly measured.[167, 174, 201] It could be suggested by these findings that due to abnormally

elevated NK cell recruitment to the endometrium during RPL, there is an inability of the local mechanisms to support $CD56^{dim}$ cell conversion into the less cytotoxic $CD56^{bright}$ subset. It should be highlighted that although uNK cells are thought to be, at least in part, recruited from peripheral blood, the origins of these cells have not been clearly defined, with findings also supporting their development from tissue-resident progenitors.[158, 202, 203] However, the reported uNK increase has not been consistently demonstrated with others supporting dysregulation of NK function rather than frequency to be important.[173, 174, 184, 204] For instance, a recent study demonstrated reduced NK cell prevalence in the endometrium of women with RPL.[205] These inconsistencies could, at least partly, stem from differences in the cohorts or methodologies. It is also possible that elevated NK cells underlie only some RPL cases, potentially contributing to the disease pathogenesis through increased cytotoxicity towards the fetal-placental unit, but also through a more intense induction of angiogenesis and thus augmented blood flow at the peri-implantation period, leading to high oxidative stress.[206] Based on these hypotheses, anti-inflammatory medications have been used in an effort to reduce the anti-fetal NK cell activity. For instance, in a randomized controlled trial in non-pregnant women with RPL and elevated uNK cell levels, the steroid agent prednisolone induced a uNK cell reduction, although the therapeutic potential of that effect was not reported.[199]

Using single-cell RNA-sequencing Vento-Tormo et al. and following studies described three main dNK cell subsets, including $CD18^{-}CD39^{+}CD103^{-}$ dNK1, $CD18^{+}CD39^{-}CD103^{-}$ dNK2 expressing the *ANXA1* and *ITGB2* genes, and $CD160^{+}KLRB1^{+}CD18^{+}CD39^{-}CD103^{+}$ dNK3 cells.[160, 207] dNK1 cells exhibited a

higher inhibitory and activating KIR expression and was the only subset expressing ILT2, while inhibitory and activating NKG2 receptors were detected on dNK1 and dNK2 cells, indicating a particular interaction of the dNK1 subset with EVTs.[160, 192, 207, 208] In agreement to that, dNK1 cells were abundant in the decidual compacta, the site of trophoblast infiltration.[192] NKG2D expression was also detected on the $CD103^+$ dNK3 subset in a different study.[208] The $ILT2^+KIR^{high}$ dNK1 subset is the most prevalent in the decidua.[208] $CD39^+$ dNK1 cells exhibited the higher cytoplasmic granule level and elevated cytolytic molecule expression, indicating a more intense cytotoxic potential,[160] as well as an enrichment of angiogenesis associated genes.[207] On the other hand, an enriched expression of genes associated with cytokine signalling was displayed in dNK2 and dNK3 cells.[207] In another study, dNK2 and dNK3 cells appeared as more responsive to stimulation, through degranulation, cytokine, and chemokine secretion, while $ILT2^+KIR^{high}$ dNK1 cells displayed reduced responsiveness accompanied by preferential chemokine production.[208] In RPL an increase in the dNK3, accompanied by a reduction in the dNK1 subset was observe.[192, 207] Pro-inflammatory gene expression, such as CD69, was elevated on dNK3 cells, while anti-inflammatory gene expression was downregulated on dNK1 cells of women with RPL.[192] Furthermore, IFN-γ expression and secretion was augmented in all three dNK subsets of women with this condition, suggesting a contribution of all these populations in the potential excessive inflammation during RPL.[207] It is thus evident that further detailed examinations of NK cell subpopulations in the context of pregnancy and miscarriage is required to fully elucidate the involvement of these cells in RPL pathogenesis.

2.4.2 NK cell receptors

The activity of NK cells is orchestrated by an array of inhibitory and activating receptors, present on the surface of these cells (Figure 7). Heterogeneity of receptor expression within the NK cell pool results in the recognition and response to various stimuli.[139] Shifts in the balance between activating and inhibitory signalling are responsible for NK cell activation. Specifically, cross-linking of multiple activating receptors, accompanied by a lack of sufficient inhibitory signalling results in NK cell activity, possibly through signalling towards a central molecule, whose levels act as a threshold for activation.[156] Although the contribution of NK cells in RPL is a matter of debate, a recent review highlights that an increased NK cell activation stage, due to deficient signalling through inhibitory receptors could underlie the pathogenesis of this condition.[209]

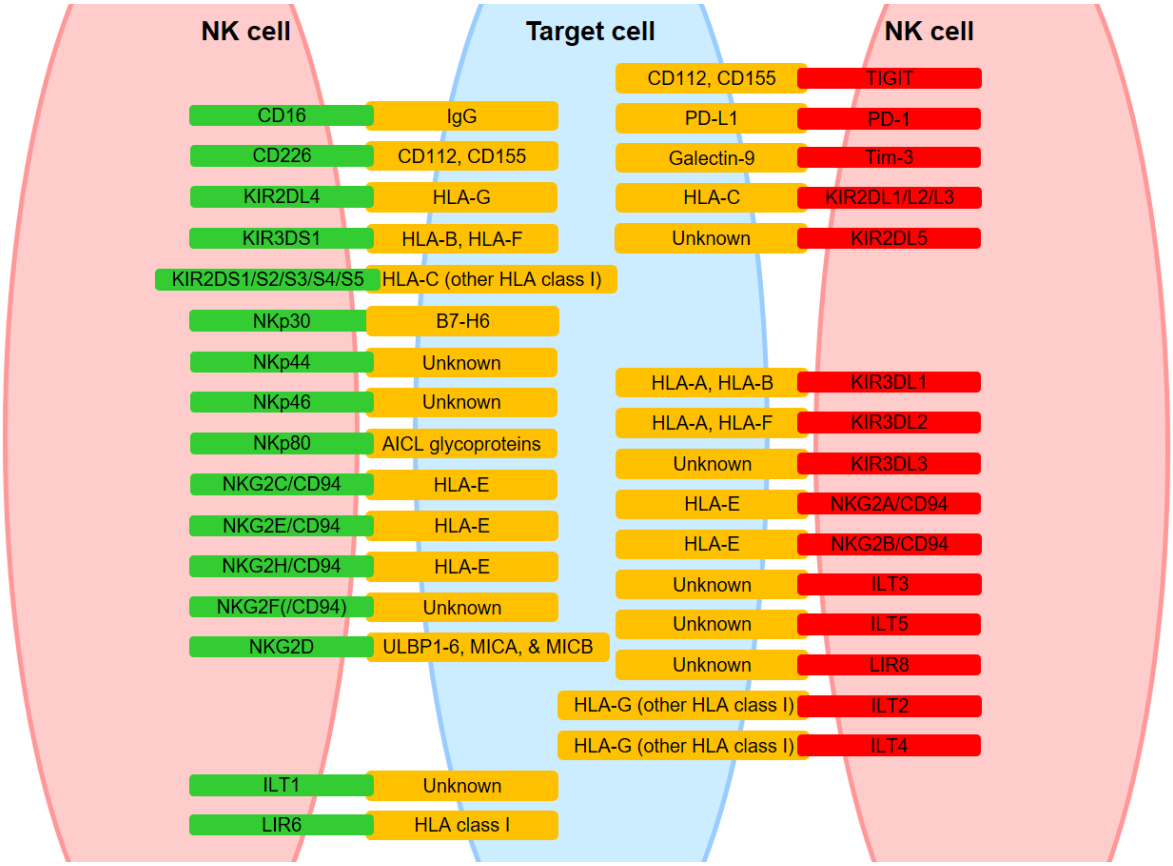


Figure 7. Natural Killer (NK) cell receptors and their cognate ligands on target cells. *Receptors transmitting activating (green) and inhibitory (red) signals on NK cells are displayed. Molecules whose interaction with the respective receptors is not fully established are shown in parentheses. CD: cluster of differentiation, HLA: human leukocyte antigen, IgG: immunoglobulin G, ILT: immunoglobulin-like transcript, KIR: killer-cell immunoglobulin-like receptor, MIC: MHC class I chain-related protein, NKG2: natural killer group 2, PD-1: programmed cell death protein 1, PD-L1: programmed death-ligand 1, TIGIT: T cell immunoreceptor with Ig and ITIM domains, Tim-3: T cell immunoglobulin and mucin domain-containing protein-3, ULBP: UL16-binding protein*

KIRs are some of the main receptors regulating NK cell function, through HLA class I recognition.[210] KIR2DL1, KIR2DL2, KIR2DL3, KIR2DL5, KIR3DL1, KIR3DL2, and KIR3DL3 are inhibitory, while KIR2DS1, KIR2DS2, KIR2DS3, KIR2DS4, KIR2DS5, and KIR3DS1 are activating.[95, 149, 203, 211, 212] KIR2DL4 is specific for HLA-G and is considered activating with inhibitory potential.[95, 213-216] HLA-C1 is recognised by

KIR2DL2/2DL3/2DS2/2DS4, HLA-C2 is the ligand of KIR2DL1/2DS1/2DS4 receptors.[95, 102, 150, 214, 217-219] HLA-Bw that is not present on trophoblasts is bound by KIR3DL1/3DS1, while KIR3DL1 is also a high-affinity HLA-A receptor.[95, 102, 217] HLA-C-specific activating and inhibitory KIR expression appears elevated on uNK, compared to pNK cells, suggesting a predisposition towards HLA-C recognition in the uterus.[102, 150, 151, 217, 220] This predisposition is thought to be particularly evident during pregnancy, potentially being directed by an elevation in stromal cell HLA-C expression due to decidualization, modifying the local NK cell population in preparation for the interaction with HLA-C^+ trophoblasts.[217] Both activating and inhibitory KIRs are expressed and appear functional on dNK cells,[151, 221] with diverse signalling combinations inducing different dNK cell responses. For instance, KIR2DL1 inhibitory signalling was shown to override activating KIR2DS1 signalling, while GM-CSF production was induced upon KIR2DS1-HLA-C2 interaction even in the presence of HLA-C2-specific inhibitory receptors.[151]

KIRs are encoded by a polygenic and highly polymorphic gene complex, constituting two KIR haplotypes.[222, 223] Different maternal KIR-fetal HLA-C combinations are thought to be associated with pregnancy failure and RPL.[88, 224-228] For instance, in women with RPL the frequency of the *KIR AA* genotype appears more common than controls, while higher *HLA-C2* frequency has been detected in products of conception following a miscarriage, linking the maternal *KIR AA* genotype and the fetal *HLA-C2* allele to an increased miscarriage risk.[218, 223, 229] Additionally, elevated *KIR2DS1* and reduced *KIR2DL1* and *KIR2DL2* frequencies were reported in women with RPL.[225, 226, 229] The increased activating and reduced inhibitory *KIR-HLA-C* combinations reported in women in RPL and the elevated prevalence of KIR

repertoires with an elevated activating KIR content are in agreement to the suggested aberrant NK cell activity in women with this condition.[212, 226] On the other hand no significant change in the *KIR* genotype, individual *KIR* gene frequencies, *HLA-C* allele frequencies, or matching *KIR-HLA-C* combinations in couples with RPL could be observed in some studies.[212, 225-228, 230-232] Due to the methodological variation in genetic studies, no rationale is yet accepted for the introduction of *KIR/HLA-C* genotyping in clinical practice.[219]

ILT receptors are also important mediators of NK cell activity. Leukocyte immunoglobulin-like receptor (LIR)8, ILT2, ILT3, ILT4, and ILT5 are inhibitory, while LIR6, ILT1, ILT7, and ILT8 transmit activating signals.[233, 234] ILT2 expression on decidual lymphocytes, $CD56^{dim}$, and $CD56^{bright}$ NK cells, was found to be increased during pregnancy,[216, 235, 236] highlighting a potential role of this receptor in reproductive success. Both ILT2 and ILT4 interact with HLA-G, which is expressed on EVTs, inhibiting anti-trophoblast NK cell activity, while the ligands of other ILTs remain undefined.[233-235, 237-240] However, the trophoblast-like choriocarcinoma cell lines, JAR and JEG3, appeared susceptible to $ILT2^+$ NK cell-mediated cytotoxicity, possibly due to activating signalling through other receptors.[241] $HLA\text{-}G^+$ target cells were also shown to induce a reduction in VEGF, placental growth factor, IL-8, and C-X-C motif chemokine ligand (CXCL)10 secretion by $ILT2^+$ dNK cells,[149] possibly controlling the extend of local remodelling during early pregnancy. ILT receptors on macrophages and DCs have exhibited a lower affinity for major HLA class I molecules, with ILT2 binding certain *HLA-A* alleles, ILT4 associating with multiple *HLA-B* alleles, and LIR6 and ILT6 preferentially binding *HLA-C* alleles.[242] Whether

these interactions occur between ILT receptors on NK cells and their HLA class I^+ targets, remains to be elucidated.

Natural cytotoxicity receptors (NCRs), including NKp30, NKp44, NKp46, and NKp80 are also involved in NK cell activation.[123, 243-245] Specifically, NKp30 and NKp46 are associated with both NK cell cytotoxicity and cytokine production, while NKp44 and NKp80 are thought to induce NK cell-mediated cytotoxicity.[244, 246-248] Interestingly, an inhibitory property of NKp44 has also been described upon binding to proliferating cell nuclear antigen and HLA class I.[249] However, this role of NKp44 requires further examination. NKp30 and NKp46 are constitutively expressed on NK cells, while NKp44 represents the first marker expressed upon NK cell activation.[123, 243, 246, 247, 250, 251] NKp46 expression on pNK cells is associated with the pregnant status, while NKp44 expression during pregnancy is thought to be reduced.[236] Moreover, NKp44, but not NKp30 or NKp46, were shown to bind ligands on human trophoblasts and trophoblast-like cell lines, while NKp44 and NKp46 were found to be involved in pNK cell-mediated trophoblast lysis.[149, 241, 252] NCR expression on uNK cells during pregnancy has also been reported.[107, 221, 245, 253, 254] On dNK cells, NKp30 engagement results to IFN-γ, TNF-α, GM-CSF, MIP1-α, and MIP1-β, secretion, while NKp44 and NKp46 binding induces cytotoxicity.[253, 255, 256] NKp80 expression on dNK cells does not appear affected by co-culture with trophoblasts.[107] In women undergoing their 1st or 2nd spontaneous miscarriage, $NKp46^+CD56^{dim}CD16^+$ dNK cell and $NKp44^+CD56^{dim}CD16^+$ and $NKp44^+CD56^{bright}CD16^-$ dNK cell prevalence was found to be elevated compared to controls undergoing elective pregnancy termination, while NKp30 expression by dNK cells appeared unaltered.[256] In women with RPL, NKp46, but not NKp30 or

NKp44, expression on pNK, eNK, and CD56^{bright} dNK cells was shown to be reduced.[243, 257, 258] However, in another study no alteration in NKp46 expression by pNK cells could be detected in non-pregnant women with RPL.[196]

NKG2 receptors, with the exception of NKG2D, form heterodimers with CD94.[211] The CD94/NKG2A and CD94/NKG2B heterodimers constitute inhibitory receptors, while CD94/NKG2C, CD94/NKG2E, CD94/NKG2F, CD94/NKG2H, and NKG2D are activating.[211, 213, 245, 251, 259-261] HLA-E, in association with an HLA-A, HLA-B, HLA-C, or HLA-G1 leader sequence peptide, is bound with high affinity by CD94/NKG2A and is also recognised by CD94/NKG2A, CD94/NKGK2B and CD94/NKG2C.[88, 92, 93, 105, 234, 238, 251] CD94/NKG2A is also an HLA-G receptor.[262, 263] Elevated NKG2A and reduced NK2C expression by NK cells was detected in the endometrium, compared to the circulation, suggesting a bias towards HLA-E-mediated inhibition of NK cell activity in the local microenvironment.[220] Both activating and inhibitory NKG2 receptor expression was also detected on dNK cells.[105, 221, 264] NKG2A expression is increased during pregnancy, with this receptor being present on almost all dNK cells,[216, 253] indicating a susceptibility of these cells to inhibitory signals. NKG2D binds multiple ligands, including MHC class I chain-related proteins (MICs) A and B and UL16-binding proteins (ULBPs).[211, 252, 265] Expression of ULBP1, but not other NKG2D ligands, was detected on trophoblast-like cell lines, while no NKG2D ligand expression was present on 1st-trimester villous and extravillous trophoblasts, highlighting a potential mechanism of immune evasion.[241, 266] Moreover, 1st-trimester trophoblast induced a reduction in NKG2D expression upon their interaction with dNK cells.[107] However, in another study NKG2D stimulation by ULBP^{+} trophoblasts was shown to result in trophoblast killing and

IFN-γ production.[252] Recently, the presence of a NKG2D single nucleotide polymorphism associated with elevated NK cell activity was found to be enhanced in women with RPL, suggesting a contribution of this receptor to pregnancy loss.[267-269]

Apart from these four major receptor groups, multiple other molecules are important in the regulation of NK cell function and thus could be involved in the potentially aberrant NK cell activity during RPL. CD57 is one of the major activating NK cell receptors, with its expression being associated with the later stages of $CD56^{dim}CD16^{+}$ NK cell maturation.[270, 271] During pregnancy $CD57^{+}$ cell levels in the peripheral blood appeared reduced,[272] potentially as a mechanism to control pNK cell activity. In contrast to that, NK cell expression of the CD38 ectoenzyme, whose engagement promotes pNK cell cytotoxicity and cytokine production,[156, 273, 274] appears elevated during pregnancy.[236, 275] CD27 is also expressed on pNK cells, with the expression of this marker being associated with reduced cytotoxicity and higher capacity for IFN-γ and TNF-α production.[276, 277] $CD27^{+}CD56^{bright}$ NK cell accumulation was detected in the 1^{st}-trimester decidua, where their IFN-γ-producing capacity is thought to be central in the inhibition of T_H17 cell expansion that could contribute to fetal loss.[140] Furthermore, CD161 expression defines an NK cell subset with enhanced proliferation in response to cytokine-mediated stimulation.[278] An elevated $CD161^{+}CD56^{+}$ prevalence in the peripheral blood was reported in non-pregnant women with RPL.[189] Other receptors central to NK cell activity are CD25 and CD215, which constitute the α chains of the IL-2 and IL-15 receptors, respectively, and CD122 that constitutes the common β chain for these receptors.[279] IL-2 and IL-15 are involved in multiple aspects of NK cell activation

including NK cell proliferation, cytotoxicity, and cytokine production, while IL-15 is also critical to NK cell maturation.[280-284] Interestingly, elevated IL-2 receptor levels were detected in the blood of women with RPL during the 1st pregnancy trimester, compared to healthy controls.[285] Finally, CD226 is an activating receptor, promoting both cytotoxicity and cytokine production.[245, 286-288] CD226-mediated pNK cell cytolytic- and cytokine-producing activity was induced upon stimulation with trophoblasts,[252] indicating a central role of this molecule in fetal-maternal interactions.

Immune checkpoint molecules are also expressed on NK cells, controlling their activity. For instance, programmed cell death protein 1 (PD-1) is expressed on a small pNK cell percentage, being associated with reduced capacity for proliferation, degranulation, and IFN-γ and TNF-α production.[289-291] Fascinatingly, high levels of the ligand of this receptor, programmed death-ligand 1 (PD-L1), were detected on EVTs by immunohistochemistry.[160] Thus, the PD-1/PD-L1 interaction could constitute one mechanism of trophoblast-mediated control of immune activity during pregnancy. Another immune checkpoint molecule involved in the control of NK cell activity is T cell immunoreceptor with Ig and ITIM domains (TIGIT). TIGIT expression by both pNK and dNK cells has been reported.[292-294] Binding to its high-affinity CD155 and low-affinity CD112 ligand, results in the inhibition of NK cell cytotoxicity, through a reduction in perforin and granzyme B production and a disruption of cytolytic granule polarization, and to the suppression of IFN-γ production, through the inhibition of nuclear factor-κB signalling.[286, 292-297] TIGIT shares its ligands with the activating CD226,[297] and thus its inhibitory effect could be enhanced through its interference with the activating CD226-CD155/CD112 interactions. Interestingly,

TIGIT mRNA expression by dNK cells was found to be significantly upregulated by progesterone in a dose-dependent manner in both mice and humans,[294] highlighting the importance of this receptor during pregnancy. PD-1$^+$ pNK cells were found to be reduced in the 2nd and 3rd pregnancy trimesters, compared to the 1st one, while TIGIT$^+$ pNK cell levels appeared increased throughout pregnancy,[293, 298] indicating a role of PD-1 and TIGIT at different gestation stages.

T cell immunoglobulin and mucin domain-containing protein-3 (Tim-3) expression on NK cells and its interaction with its ligand galectin-9, are also linked to suppression of cytotoxicity and perforin synthesis, reduced NK cell capacity for pro-inflammatory cytokine production, an increased production of anti-inflammatory cytokines, and a promotion of regulatory T cell (Treg) differentiation.[299-301] Moreover, Tim-3 is thought to be involved in the induction of NK cell exhaustion, characterised by a shift towards inhibitory receptor expression, impaired responsiveness to cytokines, and defective activity, preventing chronic inflammation.[299, 302, 303] However, NK cells' Tim-3 was also linked to an increased responsiveness to stimulation in contrast to the association of this marker with NK cell exhaustion and was characterised as a weak inhibitory receptor, whose activity can be surpassed by cytokine-mediated stimulation.[304] An activating effect of Tim-3-galectin-9 ligation on pNK cells has also been described.[305] Although the exact function of this receptor on NK cells remains to be understood, Tim-3-mediated regulation of NK cell activity was also detected in the context of pregnancy.[306, 307] During the 1st trimester Tim-3$^+$ pNK cell levels appear elevated, accompanied by increased serum galectin-9, while Tim-3$^+$ dNK cells displayed an elevated IL-4 and a decreased TNF-α and perforin production,[301, 307, 308] highlighting a potential

involvement of this receptor in both systemic and local immunosuppression during pregnancy. Moreover, galectin-9 is produced by trophoblasts, resulting in diminished anti-trophoblast Tim-3^{+} NK cell-mediated cytotoxicity.[301, 306, 308, 309] In pregnant mice, elevated galectin-9 expression was also detected on decidual Tregs,[310] suggesting a positive regulatory feedback loop between Tim-3^{+} NK cells and Tregs.

In women with RPL, reduced Tim-3 levels on pNK cells and decreased peripheral galenctin-9 production and secretion were reported, accompanied by enhanced Tim-3^{+} pNK cell activation and a failure to promote Treg development,[301, 309] suggesting an overall reduction in the immunosuppressive capacity of these cells. However, and elevation in decidual and placental Tim-3 and Galectin-9 expression has also been reported in women with RPL, undergoing miscarriage.[311] In women with miscarriage, Tim-3 expression on pNK and dNK cells appeared compromised, being accompanied by an impaired Tim-3^{+} NK cell-mediated immunosuppression.[306, 308] In agreement to that, embryo resorption is enhanced upon Tim-3 blockage.[306] Tim-3^{+}CD56^{dim} pNK cell prevalence was also found to be elevated in women that did not conceive, following embryo transfer, compared to those that did, underlining a potential predictive capacity of Tim-3 in implantation failure.[312] Thus, a contribution of this immune checkpoint molecule in reproductive success is evident.

NK cell migration is controlled by an array of receptors. For example, most CD56^{dim}CD16^{+} pNK cells are thought to display a C-X-C motif chemokine receptor (CXCR)1^{high}CX3CR1^{high}CXCR2^{+}CXCR3^{+}CXCR4^{+}CXCR6^{+} phenotype, while most CD56^{bright}CD16^{-} pNK cells appear to be C-C motif chemokine receptor

(CCR)5^{high}CCR7^{high}CXCR3^{high}CXCR4^{high}CX3CR1^{low}CXCR6^{low}CXCR1^{+}CXCR2^{+}, although variable expression patterns of these receptors have been reported in different studies.[203, 313-320] Once exposed to the uterine microenvironment, pNK cell chemokine receptor profile is thought to be altered.[318] eNK cells have displayed a CXCR3^{+}CXCR4^{+}CXCR1^{-}CXCR2^{-} phenotype,[321] while a CXCR3^{+}CXCR4^{+} CXCR6^{low}CCR1^{low}CCR5^{low} profile was detected on most dNK cells.[314, 318, 319] The expression of these receptors orchestrates NK cell migration towards different chemokines, such as IL-8, a CXCR1/CXCR2 ligand, the CXCR3 ligands CXCL10 and CXCL11, the CXCR4 ligand CXCL12, the CX3CR1 ligand CX3CL1, and the CCR7 ligands C-C motif chemokine ligand (CCL)19 and CCL21.[317, 318, 320]

Multiple chemokines binding receptors on NK cells, including IL-8, CXCL1, CXCL6, CXCL9, CXCL10, CXCL11, CXCL12, CX3CL1, and multiple C-C motif chemokine ligands, are expressed on endothelial, stromal and immune cells in the endometrium and decidua, facilitating pNK and uNK cell migration and allowing local accumulation during early pregnancy.[314, 318, 321-325] Interestingly, the uterine expression of multiple of these chemokines is promoted by progesterone and oestrogen, possibly through the induction of IFN-γ,[318, 321, 322] highlighting the complexity of immune-hormonal interactions. A variety of placental chemokines is also seen,[324, 326] potentially contributing to NK cell chemoattraction towards the fetal-placental unit. Villous cytotrophoblasts, syncytiotrophoblasts, and EVTs, express and secrete chemokines, like CXCL6, CXCL9, CXCL10, CXCL12, and CXCL16,[314, 319, 324, 327-330] attracting both pNK and dNK cells, particularly those of the CD56^{bright} subset.[319, 327, 331] Overall, chemokine signalling appears essential to NK cell migration towards the fetal-maternal interface. Hence, alterations in chemokine receptor expression

on NK cells could affect reproductive success. For instance, certain CX3CR1 and CCR5 haplotypes have been linked to reduced RPL risk,[332] while in women with this condition an elevation in CXCL5 and CCL3 plasma levels was also seen.[333] Additional research is required to establish whether alterations in NK cell migration potential are involved in the pathogenesis of reproductive conditions like RPL.

2.4.3 NK cell cytotoxicity

As it is suggested by their name, NK cells are characterised by their capacity to kill target cells through multiple mechanisms, including exocytosis of perforin- and granzyme-containing lytic granules, Fas-Fas ligand (FasL) interaction-induced caspase-dependent apoptosis, and ADCC.[139, 334] A variation in pNK cell killing capacity during the different menstrual cycle phases has been reported, with decreased cytotoxicity reported during the luteal phase,[335] although contradicting findings were obtained.[125] Similarly, the contribution of pNK cell cytolytic activity in pregnancy remains conflicting. Reduced cytotoxicity has been reported during pregnancy comparative to the non-pregnant state.[272, 336] CD69 is often used as a marker of NK cell cytotoxicity, although it is also linked to multiple aspects of NK cell activation, such as proliferation, Ca^{2+} mobilization, target cell lysis, and cytokine secretion.[259, 337-343] In normal pregnancy, a significant increase in the percentage of $CD56^{bright}$, but not $CD56^{dim}$, pNK cells expressing the CD69 activation marker has been measured from the 1st to the 3rd trimester.[178] This may reflect the general systemic immunological response mounted in pregnancy in response to increasing circulating volumes of trophoblast debris.

NK cell activity may become dysregulated in women with RPL. In pregnant and non-pregnant women with a history of RPL, increased pNK cell cytotoxicity against common cancer target K562 cells, compared to healthy fertile controls was reported.[168, 186, 187, 191, 344] Moreover, the prevalence of total, $CD56^{dim}$, and $CD56^{bright}$ pNK cells expressing CD69 was found to be increased in women with RPL compared to healthy controls, suggesting overall elevation in the cytotoxic potential of the circulating NK cell population.[189, 262] In addition, a significant reduction in CD94 expression, a marker negatively correlated with NK cell cytotoxicity,[345, 346] was measured on pNK cells isolated from women with RPL.[262] Hence, elevated pNK cytotoxic activity may result from dysregulation of mechanisms inhibiting NK cell activation. Furthermore, an increased expression of perforin by total, $CD56^{dim}$, $CD56^{bright}$, and $CD69^{+}$ pNK cells has been reported in women with RPL, as well as an elevated prevalence of granulysin$^{+}CD56^{dim}$ and granzyme $B^{+}CD56^{bright}$ pNK cells.[195, 347] Thus, an enhanced production of cytolytic molecules could also account for the heightened cytotoxic potential of pNK cells during this condition. A similar situation has been described in the decidua obtained from women with spontaneous miscarriage, including RPL, where an increased presence of CD69-expressing $CD56^{bright}$ cells was reported.[348] Increased $CD69^{+}$ activated cell prevalence in the blood could result in increased recruitment of such cells to the uterus on a monthly basis and during pregnancy, promoting local immune activity.

However, opposing results have again been obtained with regards to both pNK and uNK cytotoxic activity in women with RPL. In some studies, no significant difference in pNK activation, cytotoxicity, and cytolytic molecule release was observed between women with RPL and healthy controls,[171, 185, 188, 349] while an increase in

pNK cell CD94 expression and a reduced pNK cell cytotoxicity in these women has also been reported.[189, 195, 196, 350] Interestingly, using the K562 cytotoxicity assay, synthetic pre-implantation factor was found to induce a decrease in CD69 activation marker expression on pNK cells of non-pregnant women with RPL,[351] indicating that these cells are not resistant to trophoblast-mediated modulation of their activity. Furthermore, unaltered $CD69^+$ endometrial and decidual cell levels have been detected in women with RPL.[167, 352] An overall decreased cytotoxic capacity of decidual $CD56^+$ leukocytes has also been detected in spontaneous miscarriage, indicating a possible link between defective decidual $CD56^+$ leukocyte activity and early pregnancy loss.[353] In addition, as previously mentioned, CD94 can mediate either inhibitory or activating signalling, based on the NKG2 molecule it dimerizes with.[159, 251, 341, 346, 354] Alternative markers, more conclusively defining NK cell cytotoxicity within the context of RPL, are required to assess the validity of these findings.

2.4.4 NK cell cytokine and angiogenic factor production

Although NK cell cytotoxicity is more commonly utilised as a marker of NK cell activity, these cells are also potent cytokine producers. Based upon their cytokine secretion profile, NK cells may be categorized into NK1 cells, secreting Type-1 cytokines, like TNF-α and IFN-γ, and NK2 cells, secreting Type-2 cytokines, including IL-5 and IL-13.[248, 355-357] NKr1 and the NK3 subsets, which secrete immunosuppressive cytokines, such as IL-10 and TGF-β respectively, may also be defined.[358-360] It is important to highlight that sub-classification of NK cells according to their cytokine secretion, is just one approach to stratify uNK cell function and is not superior to more recent definitions of NK cells subsets, such as the dNK1, dNK2,

and dNK3 cell states that distinguish dNK cells according to gene expression profiling.[160, 207]

It has been shown that both $CD56^{dim}$ and $CD56^{bright}$ pNK cells in healthy non-pregnant women are mostly IFN-γ^+ NK1 cells, consistent with a pro-inflammatory pNK cell phenotype.[360] During early pregnancy, spontaneous secretion of IL-4, IL-10, and IFN-γ by both pNK and dNK cells has been reported.[361] Although contradicting findings have been obtained, it has been suggested that during healthy pregnancy pNK cells' IFN-γ production may be reduced,[362] with the prevalence of both the $CD56^{dim}$ and the $CD56^{bright}$ NKr1 cells in the peripheral blood mononuclear cell (PBMC) population significantly enhanced.[360] In the decidua uNK cells similarly demonstrate prominent regulatory cytokine production, including TGF-β and IL-10.[88, 112] A high proportion of both $CD56^{dim}$ and $CD56^{bright}$ uNK cells during pregnancy appear of NK3 origin, with fewer NK1 cells identified.[360] 1^{st} trimester miscarriage-derived uNK cell-conditioned medium was found to impede endometrial stromal cell decidualization, mainly through the activity of TNF-α,[363] highlighting a potential harmful effect of this cytokine on pregnancy success. Thus, the anti-inflammatory shift in the NK cell cytokine production may play some important roles in the maintenance of pregnancy.

Dysregulated NK cell cytokine secretion appears in women with RPL, even pre-conception. Fukui et al. describe a Type-1 pro-inflammatory shift, with peripheral blood IFN-γ^+TNF-α^+ $CD56^{bright}$ cells increased in non-pregnant women with RPL and the frequency of IL-4^+IL-10^+ $CD56^{bright}$ cells being significantly lower comparative to controls.[194] Furthermore, in the absence of stimulation, an increase in IFN-γ^+ total and $CD56^{dim}$ and IL-17^+ $CD56^{bright}$ pNK cells was detected in non-pregnant women

with RPL.[190] NKr1 cells, belonging to both the $CD56^{dim}$ and $CD56^{bright}$ subsets, were also reduced in the peripheral blood during miscarriage compared to early normal pregnancy.[360] A potential role for NK cell-derived regulatory cytokines in pregnancy success is in fact proposed. Consistent with this "pro-inflammatory" hypothesis, elevated IFN-γ and TNF-α and decreased IL-4 production by 1^{st}-trimester dNK cells was reported in women with RPL,[364] while in the decidua of women with spontaneous miscarriage increased pro-inflammatory NK1 and decreased regulatory NK3 $CD56^{dim}$ and $CD56^{bright}$ cells have been observed.[360] Interestingly, pro- and anti-inflammatory production by uNK cells was found to be induced by semen.[365] Semen-induced IL-10 and IL-4 production by $CD56^{bright}$ uNK was reported to be reduced in women with RPL compared to controls,[365] indicating an early establishment of the excessive Type-1 shift in the uterus of women with this condition.

There is however conflicting evidence, suggesting an important role of IFN-γ and TNF-α in human pregnancy. The percentage of IFN-γ^+ and/or TNF-α^+ NK cells, particularly those belonging in the $CD56^{bright}$ subset, were found to be decreased in the mid-secretory endometrium of non-pregnant women with idiopathic RPL, indicating a role of these cytokines in pregnancy maintenance.[243] IFN-γ and TNF-α are possibly important during implantation but their excessive or imbalanced production may be detrimental. Moreover, increased prevalence of IL-4^+ and TGF-β^+ pNK cells has also been detected in non-pregnant women with RPL.[190] Overall, the evidence on the use of cytokine profiling in RPL remain highly heterogeneous.

NK cell secretion of angiogenic growth factors is also considered central in decidual and placental remodelling.[366] Angiogenic growth factor secretion was reduced

upon uNK cell co-culture with EVTs and cytotrophoblasts, possibly through the activity of a soluble factor, while uNK cytokine secretion was decreased upon direct uNK cell-trophoblasts interaction,[367] highlighting a synergistic activity of these cells for the control of the local inflammation and angiogenesis. Additionally, IL-8, a chemokine with angiogenic potential, is thought to interact with EVTs, promoting MMP-2 secretion and invasion.[368] IL-8 plasma levels appeared reduced in women with RPL.[333] On the other hand, VEGFα, angiogenin, and basic fibroblast growth factor expression by eNK cells is elevated in women with this condition, possibly contributing to altered endometrial vascularity during implantation and thus to pregnancy loss.[369]

2.5 T cells in RPL

T cells represent a major component of adaptive immunity, acquiring both cytotoxic and immunomodulatory potential. T cell prevalence and absolute counts in the peripheral blood are not altered during normal pregnancy.[180, 362, 370] These cells are abundant in the human endometrium.[50, 141] Even though throughout menstruation and early pregnancy, absolute uterine T cell numbers remain constant, a relative decrease in their frequency is observed due to the surge in NK cells.[371] Throughout pregnancy the prevalence of decidual T cells increases from 5%-20% in the 1st trimester up to 80% during the last pregnancy weeks.[372] In both the peripheral blood and decidua, T cells could acquire an important role in the recognition of fetal antigens and the modulation of local immune responses. In agreement to that, peripheral T cells during pregnancy display a more prevalent activated phenotype and appear less susceptible to Fas-induced apoptosis.[180, 373] However, during healthy early pregnancy the levels of the checkpoint receptors, TIGIT and PD-1, but

not Tim-3, on peripheral T cells appeared enhanced compared to the following gestation stages,[293, 307] highlighting an immunosuppressive mechanism restricting T cell activity.[286, 374, 375] Utilizing mouse models with transgenic fetal antigen-specific T cell receptors, peripheral and uterine T cells demonstrated immune awareness towards paternally-derived fetal antigens, exhibiting a diverse range of responses, including proliferation, activation, anergy, and clonal deletion.[376]

The role of T cells in RPL has similarly gained increased attention. A reduction in peripheral T cell prevalence has been reported in non-pregnant women with RPL.[377] Conversely, T cell density appeared elevated in the luteal phase endometrium of women with this condition.[378] Using different markers, such as HLA-DR, CD25, and CD69, augmented T cell activation in the peripheral blood and decidua of women with recurrent and spontaneous pregnancy loss has been reported.[188, 379, 380] A predictive value of T cell parameters for women with RPL has also been proposed. Decreased peripheral T cell numbers have been detected in women with RPL and a following miscarriage compared to those with successful pregnancy outcomes.[182, 381] These findings have not been consistent, with others reporting no significant alterations in the T cell population in the circulation, endometrium, or decidua of women with RPL and no T cell level-associated predictive value.[167, 173, 352, 382-384] An increased $CD4^+/CD8^+$ T cell ratio has been however detected in the endometrium of women with RPL compared to healthy controls,[201] and in women with RPL whose subsequent pregnancy resulted in miscarriage.[174, 385] Thus, rather than total T cell levels, the ratio between uterine T_H and T_C cells may be useful for miscarriage diagnosis and prognosis.

2.5.1 Cytotoxic T cells

T_C cells constitute a central immune effector subset, being capable of killing malignant and infected cells through a variety of mechanisms, such as cytolytic granule formation, death receptor interactions, and cytokine secretion.[386-388] The peripheral T_C cell prevalence and absolute counts do not appear to be altered during or after pregnancy, compared to the non-pregnant state.[180, 362, 373] However, during pregnancy, activation markers are expressed by decidual T_C cells, suggesting recognition of fetal antigens.[389] Fetal antigen-specific T_C cells have also been detected in the maternal periphery.[390] The fetus can be recognized by these cells directly through its HLA-C expression on EVTs and indirectly through maternal antigen-presenting cells (APCs),[391] potentially being subject to T_C cell-mediated cytotoxicity.[141] Trophoblast antigen-specific tolerance is maybe induced through the upregulation of death receptors, including Tim-3 and PD-1, on maternal T_C cells.[391, 392] $Tim\text{-}3^+PD\text{-}1^+CD8^+$ T cells were found to be more prevalent in the decidua than peripheral blood, implying a partial suppression of local T_C cell activity.[391, 392] Trophoblast-derived secreted HLA-G1 was also shown to trigger activated T_C cell apoptosis.[115] T_C cells at the fetal-maternal interface are possibly less cytotoxic, which may reflect the unique placental tissue microenvironment. T_C lymphocytes are however thought to contribute to implantation via the release of colony-stimulating factors, like GM-CSF.[393] In pregnant mice GM-CSF administration was found to prevent trophoblast killing and fetal resorption in a T_C cell-dependent manner,[393] indicating a T_C cell self-regulating mechanism.

Heterogeneous data has been collected regarding the role of T_C cells in RPL. In women with RPL, peripheral blood T_C cells have been reported as elevated, with a

concomitant decrease in $CD4^+/CD8^+$ T cell ratio.[394] Increased T_C cell levels have also been reported in the decidua of women with this condition.[192] Conversely in other studies a reduced or unaltered peripheral blood T_C cell population of women with RPL was detected, accompanied by an unchanged $CD4^+/CD8^+$ cell ratio.[187, 377] Furthermore, the peripheral and endometrial T_C cell levels did not appear predictive of pregnancy outcome.[173, 381] The pre-conceptional activation status of T_C cells, as assessed based on the expression of the activation markers CD69 and CD154, in the peripheral blood of women with idiopathic RPL was not different from that of controls.[395] However, in another study in non-pregnant women with idiopathic RPL, circulating $HLA\text{-}DR^+CD8^+$ activated T cell prevalence was elevated.[396] Hence the value of measuring T_C cell frequencies in RPL appears limited.

2.5.2 T helper cell cytokine profiling

T_H cells acquire a critical role in shaping adaptive immunity, with the cytokine-producing activity of these cells linked to reproductive success (Figure 8).[386, 387] Peripheral T_H cell levels were not found to be significantly different between non-pregnant and pregnant women and women with idiopathic miscarriage, with these cells composing ~40% of the lymphocyte population.[180, 362, 373, 397] An increased prevalence of activated T_H cells was reported in the peripheral blood of women with idiopathic RPL, even though the $HLA\text{-}DR^+$ T cells of these women appeared to be anergic, being incapable of upregulating CD25.[395, 396] However, contradicting findings reporting an unaltered T_H cell prevalence and T_H/T_C ratio in the peripheral blood of these women have also been obtained.[187] No predictive value of peripheral T_H cell levels has been reported, either prior to or during pregnancy.[381] In the

endometrium of healthy women, T_H cells constituted ~3% of the local cellular population, while in women with RPL a $CD4^+$ shift has been reported, with these cells constituting ~11% of the endometrial cellular population.[167, 174] The decidual T_H cell prevalence appeared equal to ~5% of the local lymphocyte population during both 1st-trimester pregnancy and idiopathic miscarriage.[397]

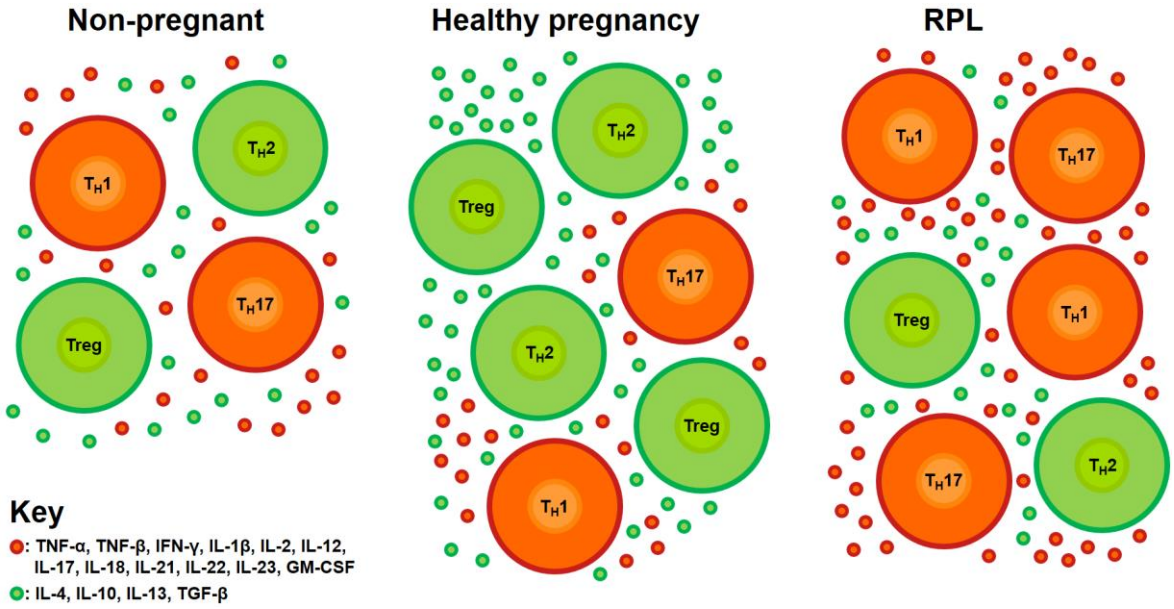


Figure 8. T helper (T_H) cell subset prevalence and cytokine secretion in non-pregnant and pregnant women and women with recurrent pregnancy loss (RPL). *Alterations in pro-inflammatory T_H1 and T_H17 and anti-inflammatory T_H2 and regulatory T cell (Treg) subpopulation levels, as well as changes in pro-inflammatory tumor necrosis factor (TNF)-α, TNF-β, interferon (IFN)-γ, interleukin (IL)-1β, IL-2, IL-12, IL-17, IL-18, IL-21, IL-22, IL-23, and granulocyte-macrophage colony-stimulating factor (GM-CSF) and anti-inflammatory IL-4, IL-10, IL-13, and transforming growth factor (TGF)-β secretion in the periphery and uterus of pregnant vs non-pregnant women and in RPL vs healthy pregnancy are depicted.*

The T_H cell population is divided into four major subsets; T_H1, T_H2, T_H17, and Tregs. The T_H1 and T_H2 cytokine balance is considered crucial in the orchestration of immune responses during pregnancy. The major pro-inflammatory T_H cell subset is composed by T_H1 cells, secreting cytokines, such as IL-1, IL-2, IFN-γ, TNF-α, and

TNF-β, stimulating cellular immunity and inflammation.[386, 398-400] Another important function of T_H cells is the activation of humoral responses that is mediated by the T_H2 subset, which is often classified as anti-inflammatory, secreting cytokines like IL-4, IL-5, IL-10, IL-12, and IL-13.[386, 398, 399] Direct T_H cell-associated cytokine effects on fetal survival and development have been described. Cytokines are mostly growth and/or differentiation factors, thus potentially act locally to encourage fetal growth.[398] The original "T_H1/T_H2 hypothesis" proposes that in healthy pregnant women a shift towards T_H2-mediated responses occurs, accompanied by a reduction in the T_H1 cell function, being reflected by a shift in the expression of the respective cytokines both in the periphery and placental tissue.[373, 398, 401-404] This hypothesis has subsequently also been linked to RPL, suggesting that in those women a failure in the establishment of the T_H2 shift results to a bias towards T_H1 responses, potentially directed against paternal trophoblast antigens.[401, 404-408] Additional T_H subsets have since been identified, including pro-inflammatory T_H17 cells, secreting IL-17, GM-CSF, IL-21, and IL-22,[386, 409, 410] and anti-inflammatory Tregs, from which IL-10 is primarily secreted.[386, 410, 411] With this discovery of novel T cell subtypes, the binary T_H1/T_H2 paradigm has been scrutinized with attention shifted towards the balance between the pro-inflammatory T_H1 and T_H17 and the anti-inflammatory T_H2 and Treg activity, referred to as "Type-1/Type-2 hypothesis".

An increase in T_H1 and T_H17 cytokine production, including TNF-α, TNF-β, IFN-γ, IL-1β, IL-12, IL-17, IL-18, and IL-23, in the peripheral blood and uterus of both pregnant and non-pregnant women with RPL has been widely suggested.[384, 401, 404, 407, 408, 412-421] In decidua basalis, the implantation site, a Type-2 T cell accumulation was detected in healthy women, but not those with RPL,[422] highlighting these cells'

importance from the early pregnancy stages. Reduced Type-2 cytokine secretion was identified in the peripheral blood and decidua of women with RPL, with low IL-10 concentrations most frequently cited.[404, 405, 407, 408, 413, 418] Consistently, PBMC expression of T_H1-associated *T-bet* was upregulated in women with RPL, while T_H2-related *GATA3* was reduced.[386, 423] RPL has also been associated with polymorphisms of the IL-10 promoter and polymorphisms linked to elevated IFN-γ and TNF-α production.[424-426] Moreover, the balance between pro- and anti-inflammatory cytokines, has been considered important; a significant pro-inflammatory skew is reported in RPL with increased T_H1-/T_H2-associated cytokine ratios reported pre-pregnancy in the peripheral blood and endometrium.[201, 427] At the 1st trimester and during miscarriage, women with RPL similarly demonstrated a significant pro-inflammatory shift in Type-1/Type-2 cytokines ratios.[407, 408] The Type-1 shift in women with RPL was also validated by single-cell RNA-sequencing.[192, 207] T_H2 bias was associated with a following normal delivery in women with RPL.[428] Indeed, decreased IFN-γ and TNF-α and elevated IL-10 levels in the circulation have been linked to pregnancy success,[429-431] highlighting potential markers for the prediction of pregnancy outcome of women with RPL.

Fascinatingly, the Type-1/Type-2 shift in women with RPL is thought to be reflected by the T_H17/Treg ratio. High plasticity between these cells has been described.[432] The T_H1/T_H17 balance is regulated by IL-6, with this cytokine promoting T_H17 differentiation alongside TGF-β, while inhibiting TGF-β-induced Treg development.[386, 433] Elevated serum IL-6 levels have been detected in women with RPL,[434] while single-nucleotide polymorphisms in the gene encoding for IL-6 have also been associated with an increased miscarriage risk.[435] The T_H17 cell/Treg

ratio, the T_H17-associated retinoic acid-related orphan receptor-γt/Treg-associated forkhead box P3 (FoxP3) transcription factor ratio, and the respective cytokine production patterns appear elevated in the peripheral blood and decidua of pregnant women with RPL.[384, 386, 434, 436-439] A similar trend was also detected in the periphery of non-pregnant women with this condition.[440] Additionally, Treg-mediated suppression of IL-17 production in T_H cell cultures, was found to be decreased when peripheral blood cells of women with idiopathic RPL were used, compared to that in cultures derived from control women undergoing elective pregnancy terminations.[441] The augmented T_H17 cell/Treg ratio in women with RPL is possibly linked to vitamin D deficiency, as it appeared reduced upon vitamin D supplementation.[438]

Increased Type-1 cytokine production may be associated with RPL through the promotion of T cell-, NK cell-, and macrophage-mediated cytotoxicity against fetal cells.[139, 399, 400, 442] Importantly, this can be restricted by Type-2 cytokine release.[399, 406] More specifically, systemic IFN-γ elevation prohibits implantation and has displayed embryotoxic effects. TNF-α was also shown to block embryonic development and induce fetal demise in murine models.[443] On the other hand, IL-10 is considered to exert protective effects during pregnancy, through its anti-inflammatory role.[444] Alongside IL-10, progesterone and estradiol were shown to suppress T_H1 cytokine production by PBMCs derived from women with RPL, which was found to be enhanced upon trophoblast stimulation.[445, 446]

However, the former “Type-1/Type-2 hypothesis” is not consistently demonstrated, with no significant alterations in IL-6, IL-12, IL-4, IL-13, TGF-β, and IFN-γ concentrations or T_H1/T_H2 ratios measured in women with RPL comparative to

healthy controls reported in other similarly powered studies.[204, 370, 373, 412, 413, 447] Contradicting findings indicating a Type-2 cytokine dominance in the circulation and decidua of women with RPL have also been obtained.[377, 448, 449] Moreover, the predictive value of peripheral and endometrial cytokine secretion in women with RPL has been challenged.[175, 421, 449] The theory suggesting an anti-inflammatory cytokine shift during pregnancy has been characterized as an oversimplification, as it is now known that depending on its stage pregnancy can be dominated by either pro- or anti-inflammatory processes.[450] Implantation, placentation and decidualization during the 1st trimester, and parturition are thought to be characterized by pro-inflammatory immune activity.[443] Furthermore, TNF-α and IFN-γ are produced during healthy pregnancy, with murine models suggesting a fundamental role in fetal development.[451-453] Specifically, IFN-γ is considered central to the remodelling of the local spiral arteries,[454, 455] while a protective role of TNF-α is displayed.[456] T_H1 cytokines may also be concerned with immunosurveillance during pregnancy and be involved in the control of trophoblast invasion.[406, 457, 458] The T_H17 population appears enriched in the human 1st-trimester decidua, compared to the peripheral blood,[459] highlighting an important role of these cells during early pregnancy. Alongside Tregs, T_H17 cells were shown to facilitate trophoblast growth, promoting proliferation and inhibiting apoptosis, and control their invasiveness, through a reduction in trophoblast production of MMP-9.[460] Overall, a dynamic balance between cytokine responses appears to be required, with the effects of individual cytokines dependent upon the gestational stage and their relative concentration.[406, 461] For instance, trophoblast proliferation is stimulated by GM-CSF, while overproduction of IFN-γ and TNF-α is thought to

induce trophoblast apoptosis and inhibit trophoblast outgrowth, obstructing fetal development.[406, 462, 463] Thus, therapies altering cytokine balance, such as progesterone, could provide a valuable tool against RPL.[464]

2.5.3 Regulatory T cells

Tregs are considered a central immunosuppressive component of adaptive immunity. It has been suggested that Tregs control excessive inflammation, inducing fetal antigen-specific tolerance from early implantation, being also involved in the regulation of vascular remodelling.[141, 391, 465] Indeed the prevalence of these cells in the peripheral blood and decidua was found to be elevated during early pregnancy, possibly as a part of the overall enhanced immune activity.[141, 397, 466-469] Interestingly, in agreement to the theory suggesting a dominant immunosuppressive state during the 2nd trimester, circulating Treg prevalence was found to be higher during that stage compared to the 1st trimester.[468] Treg recruitment in the fetal-maternal interface as well as their local differentiation is thought to be, at least partly, induced by trophoblasts, with EVTs and the HTR8/SVneo 1st-trimester trophoblast cell line shown to promote Treg development.[142, 460, 470] The observed Treg decline postpartum agrees with the withdrawal of immunological stimulation induced by the fetal-allograft.[468]

Defects in Treg numbers or activity could underlie RPL pathogenesis. In mice deficient for the enhancer for the FoxP3-encoding gene that is essential for Treg differentiation,[471] an augmented fetal resorption rate was seen,[472] underlining a key role of these cells in pregnancy maintenance. In agreement to that, Treg depletion in pregnant mice resulted in fetal rejection,[473] while adoptive transfer of

Tregs from pregnant mice to abortion-prone ones displayed a pregnancy-protective effect.[474] In humans, peripheral Treg levels appear reduced in women with RPL pre-conception, during pregnancy, and at the time of miscarriage.[383, 384, 397, 436, 440, 466, 467] Decidual Treg prevalence is also thought to be decreased during both early pregnancy and at the time of miscarriage in women with RPL.[384, 397, 466, 467] Furthermore, reduced cytotoxic T-lymphocyte-associated protein (CTLA)-4 expression by the peripheral Tregs of women with RPL was detected,[436] suggesting a possible deficiency in the immunosuppressive capacity of these cells. Treg quantification in the circulation during early pregnancy has also been suggested as predictive of reproductive outcome, with low levels of these cells being associated with miscarriage.[475] Overall, Treg deficiency, both peripherally and in the decidua micro-environment during pregnancy may lead to a failure in fetal-specific maternal tolerance, resulting in pregnancy loss.[397, 467] Although the exact implication of the Treg subtypes in reproduction requires further examination, these cells appear central to reproductive success.

2.6 B cells in RPL

During pregnancy cell-mediated autoimmunity, like rheumatoid arthritis, is ameliorated, while antibody-mediated autoimmune conditions, such as systemic lupus erythematosus, are often aggravated,[50, 476-479] suggesting a role of the humoral immune system in pregnancy. The B cell population in the endometrium and decidua represents only a small stromal cell fraction and thus the implication of these cells in pregnancy has not been extensively studied.[126, 127, 141, 371, 480-483] During pregnancy, a non-significant trend towards elevated circulating B cell levels has been observed.[180] Even though the potential B cell role in early pregnancy

remains to be elucidated, in the 3rd trimester and at the time of parturition a peripheral B cell lymphopenia is reported,[484] highlighting a lack of B cell involvement during the later pregnancy stages.

Despite the low uterine B cell levels, dysregulation of humoral immunity may be linked to RPL. In women with a history of RPL, pre-conception circulating $CD19^+$ B cell frequencies are unaltered.[379] However, endometrial $CD20^+$ B cell levels are increased in women with RPL compared to controls,[174] although this finding could be associated with elevated presence of chronic endometritis.[76, 77] A predictive value of endometrial B cell prevalence was also suggested, with its levels being augmented in women with RPL and a subsequent 1st-trimester miscarriage, compare to those who maintained a conceptus at least until the 36th gestation week.[174]

B cells have been subcategorized into three major subsets, B-1, B-2, and regulatory B cells (Bregs), in both murine models and humans,[485-488] although within the context of pregnancy and RPL they remain poorly defined. B-1 cells were initially identified in mice but were more recently defined in humans as $CD20^+CD27^+CD43^+CD70^-$ cells in the adult peripheral blood and in the umbilical cord blood.[489, 490] These cells have drawn a lot of attention in the context of autoimmunity due to their association with natural antibody (NAb) production that is going to be discussed in the following section. B-2 cells are considered as the "conventional" B cell subtype as following antigen recognition, these cells can undergo somatic hypermutation and class switch recombination, enhancing the affinity and repertoire of antibodies, and differentiate into antibody-secreting plasma

or memory cells.[491] Currently alterations in the numbers of these cells have not been associated with miscarriage.

2.6.1 Antibody production

Antibody production by B cells is the central mechanism of humoral immunity. Murine and human B-1 cells have been characterized by spontaneous production of low-affinity polyreactive, often autoreactive, NAbs in the absence of exogenous immunization.[485, 489, 490, 492-500] Due to their broad reactivity, NAbs are considered as central in the primary response against infections, but are also primary suspects in autoimmunity, including antiphospholipid syndrome.[485, 486, 499-502] It has been suggested that autoantibody production is mainly mediated by the $CD5^+$ B-1 cell subset,[494, 503-507] even though in humans $CD5^-$ NAb-producing B cells have also been detected.[508, 509] $CD5^+$ B cell prevalence in the circulation was found to be significantly reduced during human pregnancy, highlighting a possible protective mechanism through reduction in NAb production.[510, 511] Elevated $CD5^+$ B cell levels and failure to limit NAb production has subsequently been linked to pregnancy complications.[485, 486, 507]

The production of anti-HLA antibodies is also thought to be involved in the pathogenesis of RPL, with their presence linked to a reduced likelihood of a subsequent live birth.[512] Most of these antibodies detected in women with secondary RPL were reported to be complement-fixing, directed against either paternal antigens or antigens associated with their firstborn child, indicating either the presence of a direct anti-fetal immune activity or increased fetal-microchimerism, indirectly dysregulating maternal immunity.[512] Interestingly anti-HLA antibodies

were more frequently detected in women with RPL who had previously successfully delivered a male offspring, suggesting a potential association with H-Y antigens.[512]

Whether these antibodies are harmful is however unclear with others suggesting an overall protective effect of maternally-derived anti-paternal antibodies during pregnancy.[485, 513, 514] Human pregnancy-protective antibody production by term placenta-derived B cells upon *in vitro* stimulation with CD40 ligand, IL-4, and IL-10 has been reported.[485] It is possible that this protective anti-paternal antibody population is, at least partly, composed of asymmetric antibodies (AAbs). AAbs are structurally abnormal, binding antigen but lacking capacity for the activation of effector immune functions.[486, 515] A possible protective blocking role for these antibodies has been suggested.[516, 517] Consistent with this, AAbs production was found to be elevated in the placenta and maternal serum during normal pregnancy, possibly under the influence of progesterone, with lower concentrations linked to pregnancy failure, including RPL.[485, 515, 518-521] Overall, according to the ESHRE 2017 guidelines, anti-HLA antibody testing is not recommended for women with RPL due to the lack of sufficient supporting evidence.[9]

2.6.2 Regulatory B cells

B cells also acquire cytokine-secreting properties, regulating DC and T cell function.[522, 523] $CD19^{+}CD24^{high}CD38^{high}$ Bregs have been identified in humans and are thought to contribute to the maintenance of tolerance.[488, 524] In murine models, Bregs were reported to control cellular immunity, inhibiting uncontrollable tissue-specific inflammation.[486, 525] Bregs are mainly characterized by their IL-10 secretion, even though TGF-β- and IL-35-secreting B cells with regulatory capacity

have also been detected.[486, 525-528] IL-10$^+$ Bregs inhibit T_H1 activation and T_H17 differentiation, promoting T_H cell conversion into Tregs.[488, 524, 529] Interestingly, reduced circulating Breg levels were detected in pregnant abortion-prone mice compared to controls,[530] while Breg transfer from non-pregnant mice to abortion-prone ones at the starting point of pregnancy was found to prevent fetal rejection.[531] Additionally, this Breg transfer was linked to a decreased mature DC population and increased Treg presence.[531] A reduction in IL-10-producing B cell levels has also been reported in the periphery of women with RPL, compared to pregnant controls.[532] Hence, Bregs may contribute to tolerance maintenance during pregnancy.[486] Further research is however required to fully elucidate the mechanisms of action of Bregs in the context of normal human pregnancy and reproductive failure.

2.7 Other immune cells in RPL

2.7.1 Dendritic cells

Multiple immune cell subtypes, such as DCs and macrophages are involved in placental development, trophoblast invasion, and local vascular remodelling, being often localized adjacent to EVTs, and spiral arteries.[533] DCs and macrophages acquire a central role in antigen recognition and presentation, hence being key in the orchestration of lymphocyte-mediated immunity. CD83$^+$CD80/86$^+$ mature DCs are potent APCs, capable of inducing antigen-specific T cell activation and thus possibly triggering anti-fetal immune responses.[534, 535] The promotion of an immature DC state is thought to contribute to fetal tolerance. Although, elevated expression of molecules linked to the mature phenotype and activation of DCs was

displayed on the surface of these cells in pregnant compared to non-pregnant women,[536, 537] in one study, this increase was found to be accompanied by a reduction in the expression of HLA-DR, which is central to DC activity, suggesting that during pregnancy DCs are circulating in an incompletely activated state, potentially being incapable of activating T cells through antigen presentation.[537] Furthermore, human chorionic gonadotropin secretion by trophoblasts was found to restrict $CD1c^+$ DC maturation, while trophoblasts were shown to inhibit pro-inflammatory TNF and IL-12p70 production by circulating DCs.[538]

A similar trend towards tolerogenic DC activity has also been described in the uterus. DC frequencies in the endometrium and decidua during early pregnancy are low, representing approximately 1%-2% of decidual leukocytes.[141, 483, 539] Murine experiments highlighted that low DC density in the decidua, as well as the potential entrapment of these cells in tissue, could result in the lack of DC-mediated orchestration of immunogenic anti-fetal T cell responses.[540, 541] Additionally, even though no consensus has been reached in regards to the defining phenotype of human decidual DCs, it is thought that these cells adopt an immature tolerogenic profile, possessing a reduced T cell stimulatory capacity, secreting IL-10 and TGF-β, and promoting Treg differentiation.[141, 483, 542] In allogeneic-mated mice uterine APCs, including mostly DCs and ~30% macrophages, were found to suppress alloreactive lymphocyte proliferation and promote paternal antigen-specific Treg expansion.[543] 1^{st}-trimester decidua-derived myeloid DCs were also found to promote T_H2 differentiation.[534] In the fetal-maternal interface, an interplay between uNK cells and DCs has been described, with DC-mediated IL-15 production stimulating NK cell recruitment, proliferation, and activation, which in turn promotes

IFN-γ-mediated DC activation and thus DC-mediated Treg induction.[544] Moreover, HLA-G expression on DCs could contribute to the establishment of tolerance through the inhibition of NK cell cytotoxicity, while DC maturation can be blocked by NK cells, promoting the immature tolerogenic state.[544]

Even though decidual DC numbers are small, these cells could also be involved in reproductive disorders including RPL. During early pregnancy, a non-significant reduction in circulating DC levels was reported in women with RPL.[545] In the decidua during normal pregnancy a decrease in $CD83^+$ DCs was observed between the 7^{th} and 11^{th} gestational week, but no such change could be detected in the decidua of women with RPL, indicating a possible association of this condition with mature DC activity.[546] Furthermore, $ILT4^+$ DCs, which are possibly implicated in Treg induction and tolerance generation, were found to be reduced in both the endometrium and peripheral blood of women with RPL.[547] It has also been recently suggested that successful decidualization in early pregnancy may in part rely upon stromal cell differentiation into DCs, which however results in generation of senescent DCs that have to be cleared by activated uNK cells.[548] Whether defects in this process predispose to early pregnancy loss requires further validation, but uncontrollable senescence in the decidua could be associated with RPL.[548]

2.7.2 Monocytes/Macrophages

During early pregnancy, macrophages represent the second largest decidual immune cell population, comprising around 20%-30% of local leukocytes.[90, 533] The population of tissue-resident macrophages is replenished through the differentiation of circulating monocytes.[549, 550] The numbers of monocytes in the peripheral blood

are augmented in pregnant, compared to non-pregnant women,[362] indicating an important role of these cells during gestation. Monocyte/macrophage migration in response to trophoblast signals has been displayed, highlighting a possible mechanism of monocyte recruitment to the uterus during gestation, enhancing the local macrophage population.[122, 551, 552] Through experiments in mice, progesterone and oestrogen were also found to be important in the maintenance of uterine macrophage levels.[553] Macrophages appear essential for menstruation, being involved in tissue degradation, local debris clearance, and endometrial regeneration and angiogenesis, while also contributing to blastocyst implantation and embryo selection.[111, 554, 555] During early pregnancy, even prior to EVT invasion, macrophages may also cooperate with NK cells in the decidua, mediating vascular remodelling and contributing to EVT invasion and local immunomodulation, through their phagocytic ability and through MMP, fibroblast growth factor, platelet-derived growth factor, VEGF, and IL-10 secretion.[155, 556, 557]

An immunomodulatory role of macrophages in pregnancy has been suggested. Decidualized endometrial stromal cell-conditioned medium was shown to inhibit monocyte differentiation, promote IL-10 secretion, impede TNF-α and lL-12p70, and enhance the expression of tolerogenic markers, such as ILT2, while non-decidualized condition medium promoted TNF-α production,[558] indicating the promotion of an immature tolerogenic phenotype of monocyte-derived cells upon decidualization. Inhibitory ILT2 and ILT4 receptors expressed on activated monocytes/macrophages can bind to HLA-G$^+$ trophoblasts, reducing monocyte/macrophage-mediated lysis and promoting anti-inflammatory cytokine production.[559, 560] Through their IL-15 production, decidual macrophages promote

local NK cell differentiation, activation, and IFN-γ release, which induces indoleamine 2,3-dioxygenase upregulation in macrophages that in turn hinders effector T cell activity and enhances Treg differentiation.[561-564] Moreover, decidual macrophages were found to inhibit dNK cell-mediated cytotoxicity towards trophoblasts in vitro, at least partly through TGF-β secretion.[565] Macrophages have also been subcategorised into two subtypes, pro-inflammatory M1 and immunosuppressive M2.[557, 566] However, these subsets do not represent fixed macrophage states as depending on the local microenvironment they can transition between the M1 and M2 phenotype.[557] The versatility of macrophages could provide an essential tool in pregnancy-related functions.[552] In agreement to the theory suggesting the presence of multiple shifts in immune activity depending on the pregnancy stage,[86, 122] the peri-implantation period is thought to be underlined by the pro-inflammatory activity of M1 macrophages, followed by the generation of a mixed M1/M2 macrophage population, with a shift towards anti-inflammatory M2 predominance at the stage of placental development, and an M1 predominance prior to parturition.[562, 564, 566-568] The M2 macrophage recruitment and polarization may be influenced by hormones like progesterone and oestrogen,[569, 570] and is also promoted by trophoblast-derived IL-6.[571]

Contradicting findings have been obtained in regards to macrophage involvement in miscarriage, with an augmentation of the decidual macrophage population being observed in women with idiopathic spontaneous miscarriage,[572] but not in those with RPL.[352] An increase in the $CD4^+CD14^+$ endometrial macrophage numbers was however suggested by findings in women with idiopathic RPL and a miscarriage in their subsequent pregnancy.[167] Using the *Cd11b-Dtr* mouse model, macrophage

depletion was found to lead to embryo implantation arrest, while monocyte/macrophage administration alleviated implantation failure, suggesting a causative role of macrophage depletion in infertility.[573] Polarization towards the pro-inflammatory M1 phenotype was initially thought to promote the development of pregnancy complications, whilst the immunosuppressive M2 phenotype was considered essential during healthy pregnancy.[552, 557, 568, 570, 574] In agreement to that hypothesis, immunomodulatory agents like IL-10 were found to be expressed by decidual macrophages.[160] However, this dichotomy appears an oversimplification, with the pro- and anti-inflammatory macrophage balance likely dependent upon the pregnancy stage.[567] Even though alterations in their numbers or activity could contribute to immune dysregulation in RPL, the examination of myeloid leukocyte activity is beyond the scope of the present study.

2.8 Immunological testing in idiopathic RPL

Immunological testing is an expanding field, however at present no accepted diagnostic or prognostic criteria for RPL exist. Immunological testing is typically offered in cases of idiopathic RPL. However, apart from the controversy in regards to the definition of RPL,[1, 2, 5] the testing strategy for the identification of RPL-associated risk factors and thus the diagnosis of idiopathic RPL remains contentious. For instance, tests like fetal karyotyping, anti-phospholipid antibody screening, and assessment of uterine anatomical abnormalities are consistently recommended for the investigation of RPL-associated risk factors,[1, 9, 82, 575-579] while test such as diabetes investigation, prolactin assessment, thyroid screening, and parental karyotyping are recommended only by certain national and/or international guidelines.[9, 82, 575-579] Common immunological tests considered include

enumeration of circulating NK, T_C, T_H, and B cells and assays evaluating NK cell cytotoxicity and T_H cell-associated cytokine production. However, there are no clear guidelines as to which tests should be performed nor their clinical utility.

NK cell testing is available, and as outlined there are studies indicating potential benefit for women with RPL. Nonetheless, no consensus has been reached in regards to the definition of “elevated” NK cell levels. Even though, in healthy individuals, NK cell prevalence in the peripheral blood lymphocyte population was found to fluctuate between approximately 3% and 34%,[580, 581] in women with RPL high pNK cell proportions have been defined as over 12%, 15%, and 18% in different studies.[164, 166, 182, 183, 185] Accordingly, there is a lack of consensus on the definition of elevated uNK cell levels, with one study using 13.8% of the local stromal cell population as the upper limit,[129] and another defining the normal levels of these cells using a cut-off value of 5% of uterine stromal cells.[199] Hence, prospective case-control studies with sufficient power are required for the establishment of reference ranges and cut-off values in healthy controls and women with RPL prior to the introduction of immunological testing into routine clinical practice. Additionally, NK cell parameters are affected by multiple factors that should be taken into consideration, such as age, sex, body mass index, and time of day.[581-584] NK cell levels were shown to be affected by menstrual cycle phase, with the pNK cell population being increased in the luteal compared to the follicular phase and the uNK cell number and prevalence being elevated during the late luteal phase.[125, 371, 585, 586] Furthermore, the cytotoxic capacity of pNK cells was found to be reduced at the luteal phase, following ovulation,[335, 587] even though in one study no significant change could be detected.[125] NK cells are also thought to be influenced by a

sympathetic response to stressors. Specifically, physical exercise and psychological stress were shown to result in an ephemeral elevation in NK cell levels and cytotoxic activity.[588-604] Due to these factors resulting in data heterogeneity there is currently not enough evidence supporting the use of peripheral or endometrial NK cell testing in women with RPL as stated in the ESRE 2018 guidelines.[5]

In regards to T_H cell-associated cytokine testing, T_H1/T_H2 cytokine levels during normal pregnancy and RPL have displayed a wide range,[418, 430] not allowing the agreement on a clear definition of "increased" Type-1/Type-2 cytokine ratios. Cytokine networks are also outlined by high levels of complexity, with both T_H1-like and T_H2-like functions exhibited by pleiotropic cytokines, and a significant redundancy, with different cytokines exerting the same function, generating difficulties in evaluating the effects of alterations in individual cytokines and questioning the value of an absolute Type-1/Type-2 measurement.[399, 406, 412] Indeed, it has been proposed that cytokine combinations, their relative concentrations, and the timing of cytokine release during gestation are mostly important during pregnancy and miscarriage.[399, 406, 412] Similar to NK cells, leukocyte, granulocyte, monocyte, neutrophil, lymphocyte, B cell, and total, cytotoxic, and T_H cell levels in the circulation were found to be transiently augmented by physical and psychological stress, even though a decrease in B, T, and T_H cell levels and an unaltered B cell proportion were also reported.[588, 592, 594, 596-599, 601, 602, 604] As miscarriage is thought to induce significant psychological stress to the couples, possibly hindering the success of the following pregnancy,[605] this factor should be taken into consideration when comparing women with RPL to controls.

Given the innate difficulties of endometrial and decidual sampling, another key question is whether dysregulated uterine immune activity is reflected in the periphery pre-conception and/or in early pregnancy. The relationship between uNK cells and their peripheral counterparts remains contentious. Different theories regarding uNK origin have been described, including the potential recruitment of pNK cells to the decidua, where they undergo further differentiation, and the possible dNK cell development from endometrium-resident progenitors.[159, 202, 203, 606] Cumulative evidence suggest that uNK cells constitute a heterogeneous population, encompassing both terminally differentiated NK cells trafficked from the periphery and other tissues and endogenously generated cells.[203, 606] Similarly, modifications in the T_H and T_C cell populations have been reported in the uterus compared to circulation, indicating altered local activity.[607] Cytokine secretion and activity may also differ between the uterus and circulation, with significant efforts made to understand the relationship between these sites.[50, 399, 608]

Although controversial, based on the findings of immunological tests, immunomodulatory treatments may be prescribed to support conception. Multiple reviews have highlighted the lack of strong evidence supporting the use of most immunomodulatory therapies, including granulocyte-colony stimulating factor (G-CSF), TNF-α inhibitors, intralipid, aspirin, steroids, leukocyte immunization, and intravenous immunoglobulin (IVIg), for the management of RPL,[609-615] while rare but severe adverse effects have also been described.[616-620] Even though immunomodulation has not been found to be effective for the improvement of live birth rates of an unselected population of women with RPL, it could be promising for the treatment of certain subgroups, such as those with underlying immune

dysfunction.[609, 610, 621] In agreement to the effects of stress on the immune system, it has been proposed that providing psychotherapy, including supportive care, to women with RPL is highly efficient in improving success rates of following pregnancies, often resulting to a >50% increase.[58, 622-624] The high effectiveness of supportive care in improving the pregnancy outcome of women with RPL however, questions the use of immunomodulatory agents.

The rationale behind immunological testing, in particular in regards to NK cells, and immunomodulatory treatments offered to women with idiopathic RPL remains ambiguous, with more robust evidence required to recommend such an approach.[5, 625-627] Overall, immunological alterations could be implicated in RPL aetiology but further research is required to elucidate the mechanisms behind this association, assess the diagnostic and prognostic value of immunological testing, and accurately identify women who may benefit from targeted immunotherapies. Further prospective studies are required before any firm conclusions or recommendations are formulated. Moreover, advancing our understanding of immune dysregulation in RPL shall help diminish the incidence of “unexplained” loss and the psychological distress associated with this gap of knowledge.[628]

3 AIMS AND OBJECTIVES

The present research project aims to examine variation in practice in regards to the diagnosis and management of idiopathic RPL, determine whether RPL is underlined by peripheral immunological alterations, and thus assess whether immunological testing is an appropriate method for the diagnosis and/or prognosis of this condition. For the assessment of practice in RPL clinics, a survey was designed and distributed nationwide. Furthermore, pre-conception phenotypic and functional characterisation of circulating leukocytes was performed via flow cytometry, mass cytometry, enzyme-linked immunosorbent assay, and an NK cell cytotoxicity assay using peripheral blood samples of non-pregnant women with RPL and controls. RPL subpopulation analysis was also performed, to identify women subgroups more likely to display an underlying immune pathology and hence more likely to benefit from immunological testing. Women with RPL were followed-up for the identification of potential biomarkers with a predictive value in regards to the outcome of their subsequent pregnancy.

4 MATERIALS AND METHODS

Parts of this chapter have been submitted for publication as:

Bagkou Dimakou D, Tamblyn J, Chu J, Coomarasamy A, Richter A. Diagnosis and management of idiopathic recurrent pregnancy loss (RPL): Current immune testing and immunomodulatory treatment practice in the United Kingdom. J Reprod Immunol.

4.1 Ethics

Ethical approval was obtained from the Research Ethics Committee. Women with RPL were recruited through Tommy's miscarriage clinics operating at Birmingham Women's Hospital and at the University Hospital Coventry & Warwickshire (reference: 16/WM/0423, IRAS ID: 215646 and reference: 17/WM/0050, IRAS ID: 213740). Control women were recruited through the nursing team at Birmingham Women's Hospital, under the CHHIP study (reference: 14/WM/1146, IRAS ID: 155401), while blood for optimization and validation experiments was obtained from volunteers in the Clinical Immunology Service of the University of Birmingham (reference: ERN_16-1708). Written informed consent was obtained from all participants recruited.

4.2 Survey

4.2.1 Development and distribution

The survey was developed with a focus on the variation in current guidelines in regards to the tests offered in RPL clinics and the lack of a therapeutic strategy in cases with no identifiable underlying conditions. The survey consisted of 22 questions, most of which were closed-ended, to reduce time required for completion, with an open-ended section for additional information. Questions were primarily in multiple-choice format, with a Likert scale utilised to examine respondents' views on the efficacy of different treatments for women with idiopathic RPL. Likert scale use allowed the rapid collection of information, providing a reliable estimate of the respondents' opinion, and permitting further statistical analysis.[629]

Domains assessed included guideline use, criteria for assessment in RPL clinics, investigation of underlying pathologies, with subgrouping to aid completion, and therapies offered for RPL management. The main interest of the present survey was immunological testing use and management of idiopathic RPL using immunomodulatory agents, with clinicians perspectives on potential treatments evaluated.

Prior to its distribution the survey was piloted by the two Specialist Nurses who currently care for women at the Tommy's National Centre in Birmingham. This served to ensure both the validity and quality of the questionnaire in terms of content and design. A senior clinician working in the Tommy's clinic helped design the survey and ensure questionnaire accuracy and completeness.

The National questionnaire was distributed through SmartSurvey™ (©2020, Tewkesbury, Gloucestershire, United Kingdom, https://www.smartsurvey.co.uk/). This was disseminated using well-established networks formed through previous miscarriage trials performed by Prof Coomarasamy and his research team.[630, 631] NHS-associated recipients were identified using Tommy's established miscarriage network, while private clinics were contacted following self-guided online research. The survey hyperlink was circulated by email in two stages. In stage 1 (June 2020) the survey was sent to 94 recipients, associated with 60 National Health Service (NHS) centres, and 14 private reproductive medicine clinics (*N*=108 recipients). In stage 2 (July 2020) the survey was re-circulated to the 108 previous recipients and 40 additional NHS-associated recipients, newly added to the Tommy's miscarriage network (Total *N*=148 recipients). The complete questionnaire is included in the Appendices (Supplementary Figures 1-8).

4.2.2 Data analysis

Results were reported as descriptive statistics, calculated using Excel (Microsoft Office, 2016). Each question's response rate was calculated and the percentages of different answers were determined according to the total number of responders for each question. For Likert scale data, individual response rates were calculated for each sub-question, referring to a specific treatment. Accordingly, percentages for each Likert scale point were calculated based on the number of responses for the specific sub-question. Both complete and partial responses were obtained. In the case of partial responses, the complete survey was assessed to ensure interpretation accuracy. All responses were checked to avoid duplication. 2 of the partial responses were found to overlap with the completed ones, according to the Internet Protocol address and the institution name, and were thus excluded from the analysis. 5 partial responses were included in the final analysis.

4.3 Participants

Women aged ≥18 years with a minimum of 2, not necessarily consecutive, miscarriages in their reproductive history, occurring prior to the 24^{th} week of gestation were recruited in the RPL group (*N*=100). Exclusion criteria included the presence of an active systemic or a known chronic infection and use of immunomodulatory agents, such as oral steroids or biologics. Asthma inhaler, aspirin, and enoxaparin sodium use did not comprise exclusion criteria, but were recorded. A healthy non-pregnant reproductive age "control" cohort (*N*=80) was recruited for comparative analysis. It was ensured that controls had no significant underlying reproductive or medical history, in particular autoimmune disorders,

active systemic, or chronic infections. Women taking oral medications with potential immunomodulatory properties were also excluded.

A 30min rest period was required prior to sample collection, to limit the effects of physical activity on the immune system.[590, 592, 595, 598] Baseline demographic data were recorded using a standardised data proforma, with information regarding sample collection time also recorded. The subsequent pregnancy outcome of women with RPL was obtained via the Lorenzo and Badger.net databases of Birmingham Women's Hospital. Patients not included in these databases were contacted directly. Pregnancy outcome data collection was completed on 15/04/2021 at the University Hospital Coventry & Warwickshire and on 17/05/2021 at Birmingham Women's Hospital.

4.4 Reagents

Table 1. Antibodies used in the flow cytometry-based assay. *The target molecule of each antibody, the fluorochrome, the company from which each antibody was obtained, the catalogue number, and the clone are depicted. The respective isotype used to replace each antibody in the fluorescence minus one controls, the company from which each isotype was obtained, and the catalogue numbers are also shown. CD: cluster of differentiation, FoxP3: forkhead box P3, IFN: interferon, IL: interleukin, TNF: tumor necrosis factor*

Target	Fluorochrome	Company	Catalogue Number	Clone	Isotype	Company (Isotype)	Catalogue number (Isotype)
CD3	APC-H7	BD Biosciences	560176	SK7	Mouse IgG1, κ	BD Biosciences	561427
CD4	PerCP	BD Biosciences	345770	SK3	Mouse IgG1, κ	BioLegend	400148
CD8	BV510	BD Biosciences	563919	SK1	Mouse IgG1, κ	BioLegend	400172
CD16	FITC	BD Biosciences	335035	NKP15	Mouse IgG1, κ	Thermo Fisher Scientific	11-4714-42
CD25	BV510	BioLegend	302640	BC96	Mouse IgG1, κ	BioLegend	400172
CD25	FITC	BioLegend	356106	M-A251	Mouse IgG1, κ	Thermo Fisher Scientific	11-4714-42
CD45RA	PE	BioLegend	304108	HI100	Mouse IgG2b, κ	Thermo Fisher Scientific	12-4732-42
CD56	APC	BD Biosciences	341027	NCAM16.2	Mouse IgG2b, κ	Thermo Fisher Scientific	17-4732-42
CD69	PE	BD Biosciences	555531	FN50	Mouse IgG1, κ	Thermo Fisher Scientific	12-4714-42
CD127	BV421	BD Biosciences	562436	HIL-7R-M21	Mouse IgG1, κ	BioLegend	400158
CD215	PE	Thermo Fisher Scientific	12-7159-42	eBioJM7A4	Mouse IgG2b, κ	Thermo Fisher Scientific	12-4732-42
FoxP3	PE-Cyanine7	Thermo Fisher Scientific	25-4776-42	PCH101	Rat IgG2a, κ	Thermo Fisher Scientific	25-4321-82
IFN-γ	BV421	BD Biosciences	564791	4S.B3	Mouse IgG1, κ	BioLegend	400158
IL-2	PE-Cyanine7	Thermo Fisher Scientific	25-7029-42	MQ1-17H12	Rat IgG2a, κ	Thermo Fisher Scientific	25-4321-82
IL-10	PE	BioLegend	501404	JES3-9D7	Rat IgG1, κ	Thermo Fisher Scientific	12-4301-82
IL-10	PE-Cyanine7	Thermo Fisher Scientific	25-7108-42	JES3-9D7	Rat IgG1, κ	Thermo Fisher Scientific	25-4301-82
IL-17A	FITC	Miltenyi Biotec	130-120-410	CZ8-23G1	Mouse IgG1, κ	Thermo Fisher Scientific	11-4714-42
TNF-α	APC	Thermo Fisher Scientific	17-7349-82	MAb11	Mouse IgG1, κ	Thermo Fisher Scientific	17-4714-42
TNF-α	PerCP-Cyanine5.5	Thermo Fisher Scientific	45-7349-42	MAb11	Mouse IgG1, κ	Thermo Fisher Scientific	45-4714-82

Table 2. Antibodies used in the mass cytometry-based assay. *The target molecule and metal are depicted for each antibody. For each readily-conjugated antibody, the catalogue number and clone are shown. Conjugated antibodies were supplied by Fluidigm. For the unconjugated antibodies, the company supplying each antibody, the respective catalogue number, and the clone are displayed. Labelling kits for antibody conjugation were supplied by Fluidigm. CD: cluster of differentiation, CXCR: C-X-C motif chemokine receptors, ILT: immunoglobulin-like transcript, KIR: killer-cell immunoglobulin-like receptor, NKG2: natural killer group 2, PD-1: programmed cell death protein 1, TIGIT: T cell immunoreceptor with Ig and ITIM domains, TIM-3: T cell immunoglobulin and mucin domain-containing protein-3, β2m: β2 microglobulin*

Target	Metal	Conjugated		Unconjugated			
		Catalogue Number (Fluidigm)	Clone	Company (Antibody)	Catalogue number (Antibody)	Clone (Antibody)	Catalogue number (Labelling kit - Fluidigm)
CD298 and β2m (barcoding)	106Cd	-	-	BioLegend	341712	LNH-94	201106A
	110Cd	-	-				201110A
	112Cd	-	-	BioLegend	316302	2M2	201112A
	114Cd	-	-				201114A
CD3	141Pr	3141019B	UCHT1	-	-	-	-
CD4	145Nd	3145001B	RPA-T4	-	-	-	-
CD5	143Nd	3143007B	UCHT2	-	-	-	-
CD8a	116Cd	-	-	BioLegend	344702	SK1	201116A
CD14	148Nd	3148010B	RMO52	-	-	-	-
CD16	209Bi	3209002B	3G8	-	-	-	-
CD19	142Nd	3142001B	HIB19	-	-	-	-
CD25	149Sm	3149010B	2A3	-	-	-	-
CD27	150Nd	3150017B	LG.3A10	-	-	-	-
CD38	111Cd	-	-	BioLegend	303535	HIT2	201111A
CD45	89Y	3089003B	HI30	-	-	-	-
CD56	155Gd	3155008B	B159	-	-	-	-
CD57	115In	-	-	BioLegend	359602	HNK-1	201115
CD69	144Nd	3144018B	FN50	-	-	-	-
CD94	174Yb	3174015B	HP-3D9	-	-	-	-
CD122	170Er	3170004B	Tu27	-	-	-	-
CD127	168Er	3168017B	A019D5	-	-	-	-
CD161	164Dy	3164009B	HP-3G10	-	-	-	-
CD226	171Yb	3171013B	DX11	-	-	-	-
CX3CR1	172Yb	3172017B	2A9-1	-	-	-	-
CXCR1	147Sm	-	-	R&D Systems	MAB330	42705	201147A
CXCR2	147Sm	3147010B	5E8/CXCR2	-	-	-	-
CXCR3	163Dy	3163004B	G025H7	-	-	-	-
CXCR4	163Dy	-	-	BioLegend	306523	12G5	201163A
CXCR5	153Eu	3153020B	RF8B2	-	-	-	-
CXCR6	160Gd	3160016B	K041E5	-	-	-	-
ILT1	152Sm	-	-	BioLegend	337902	24	201152A
ILT2	156Gd	3156020B	GHI/75	-	-	-	-
ILT2/LIR6	158Gd	-	-	R&D Systems	MAB30851	586326	201158A
ILT3	161Dy	-	-	BioLegend	333002	ZM4.1	201161A
ILT4	161Dy	3161019B	42D1	-	-	-	-
ILT5	161Dy	-	-	R&D Systems	MAB1806	222821	201161A
KIR2DL1/S1/S3/S5	146Nd	-	-	BioLegend	339502	HP-MA4	201146A
KIR2DL1/S5	151Eu	-	-	R&D Systems	MAB1844	143211	201151A
KIR2DL2/L3	173Yb	3173010B	DX27	-	-	-	-

KIR2DL2/L3/S2/S4	198Pt	-	-	R&D Systems	MAB1848	180704	201198
KIR2DL4	176Yb	-	-	R&D Systems	MAB2238	181703	201176A
KIR2DL5	173Yb	-	-	Miltenyi Biotec	130-096-200	UP-R1	201173A
KIR2DS4	165Ho	-	-	R&D Systems	MAB1847	179315	201165A
KIR3DL1	167Er	3167013B	DX9	-	-	-	-
KIR3DL2	167Er	-	-	R&D Systems	MAB2878	539304	201167A
NKG2A	169Tm	3169013B	Z199	-	-	-	-
NKG2C	166Er	-	-	R&D Systems	MAB138	134591	201166A
NKG2D	166Er	3166016B	ON72	-	-	-	-
NKp30	159Tb	3159017B	Z25	-	-	-	-
NKp44	162Dy	-	-	BioLegend	325102	P44-8	201162A
NKp46	162Dy	3162021B	BAB281	-	-	-	-
NKp80	159Tb	-	-	R&D Systems	MAB1900	239127	201159A
PD-1	175Lu	3175008B	EH12.2H7	-	-	-	-
TIGIT	154Sm	3154016B	MBSA43	-	-	-	-
TIM-3	154Sm	3154010B	F38-2E2	-	-	-	-

Table 3. Reagents used in the present study. *Additional regents used in the cytotoxicity, enzyme-linked immunosorbent, flow cytometry, mass cytometry, and T, B, and Natural Killer cell assays are depicted alongside the supplying company and catalogue number. Other reagents utilised for blood and cell isolation or used in multiple assays are also included.*

Reagent	Company	Catalogue number
Cytotoxicity assay		
APC anti-human CD107a (LAMP-1) Antibody	BioLegend	328620
BV421 Mouse Anti-Human HLA-ABC Clone G46-2.6	BD Biosciences	565332
CD235a (Glycophorin A) Monoclonal Antibody (10F7MN), FITC, eBioscience™	Thermo Fisher Scientific	11-9886-42
Coverquick 2000 Q Path® Mounting Media	VWR	5547530
Dead Cell Removal Kit	Miltenyi Biotec	130-090-101
EasySep™ Buffer	STEMCELL Technologies	20144
EasySep™ Human NK Cell Isolation Kit	STEMCELL Technologies	17955
EasySep™ Magnet	STEMCELL Technologies	18000
Fisherbrand™ Borosilicate Glass Rectangular Coverslips	Fisher Scientific	12363128
Fisherbrand™ Microscopic Slides with Ground Edges, Twin Frost	Fisher Scientific	11572203
Hematology Reagent B Thiazin Stain	ELITechGroup	SS-071B-EU
Hematology Reagent C Eosin Stain	ELITechGroup	SS-071C-EU
Interleukin-2, human (hIL-2) recombinant (E. coli)	Sigma-Aldrich	10799068001
K562 Cell line human	Sigma-Aldrich	89121407-1VL
LS Columns	Miltenyi Biotec	130-042-401
PKH67 Green Fluorescent Cell Linker Midi Kit for General Cell Membrane Labeling	Sigma-Aldrich	MIDI67-1KT
Propidium iodide solution - 1.0 mg/mL Solution in Water	Sigma-Aldrich	P4864
Shandon™ Cytoclip™ Stainless-Steel Slide Clip	Thermo Fisher Scientific	12608036
Shandon™ Single Cytofunnel™	Thermo Fisher Scientific	13127963
Shandon™ White Filter Cards	Thermo Fisher Scientific	5991022
Zombie Red™ Fixable Viability Kit	BioLegend	423109
Enzyme-linked immunosorbent assay		
Bio-Plex Calibration Kit	Bio-Rad	171203060
Invitrogen™ Hand-Held Magnetic Plate Washer	Thermo Fisher Scientific	EPX-55555-000
PROCARTAPLEX 14 PLEX, 1PLATE, 14-PLEX	Thermo Fisher Scientific	PPX-14
Flow cytometry assay		
Cell Staining Buffer	BioLegend	420201
eBioscience™ Foxp3 / Transcription Factor Staining Buffer Set	Thermo Fisher Scientific	00-5523-00
Fixation/Permeabilization Solution Kit with BD GolgiStop™	BD Biosciences	554715
Ionomycin from Streptomyces conglobatus	Sigma-Aldrich	I9657
Phorbol 12-myristate 13-acetate	Sigma-Aldrich	P8139
OneComp eBeads™ Compensation Beads	Thermo Fisher Scientific	01-1111-41
Zombie Green™ Fixable Viability Kit	BioLegend	423112

Mass cytometry		
2.0 mL Graduated Skirted Tube, Natural Standard Screw Cap (Sterile)	STARLAB	E1420-2341
Amicon Ultra-0.5 Centrifugal Filter Unit (Ultracel-3 regenerated cellulose membrane, 0.5 mL)	Merck Millipore	UFC500324
Amicon Ultra-0.5 Centrifugal Filter Unit (Ultracel-50 regenerated cellulose membrane, 0.5 mL)	Merck Millipore	UFC505096
Amicon Ultra-0.5 Centrifugal Filter Unit (Ultracel-100 regenerated cellulose membrane, 0.5 mL)	Merck Millipore	UFC510024
Antibody Stabilizer PBS 50 mL	Candor	131 050
Benzonase® Nuclease, Purity > 99%10 ku	Merck Millipore	70664-3
Bond-Breaker™ TCEP Solution	Thermo Fisher Scientific	77720
Cell-ID™ Cisplatin-194Pt	Fluidigm	201194
Cell-ID™ Intercalator-Rh	Fluidigm	201103A
EQ™ Four Element Calibration Beads	Fluidigm	201078
HRP Protector™	Candor	222 050
Maxpar® Cell Staining Buffer	Fluidigm	201068
Maxpar® Fix and Perm Buffer	Fluidigm	201067
PBS, 10x Concentrate	BioLegend	926201
Pierce™ 16% Formaldehyde (w/v), Methanol-free	Thermo Fisher Scientific	28906
Sodium azide, BioUltra, ≥99.5% (T)	Merck Millipore	71289-5G
Ultrafree®-MC Centrifugal Filter, 0.1 µm pore size, hydrophilic PVDF	Merck Millipore	UFC30VV00
T, B, and Natural Killer cell assay		
6-color TBNK Reagent with BD Trucount™ Tubes	BD Biosciences	337166
7-Color Setup Beads	BD Biosciences	335775
CD-Chex Plus®	Streck	213369
Other		
BD Vacutainer CPT™ Mononuclear Cell Preparation Tube - Sodium Heparin	BD Biosciences	362753
BD Vacutainer Tube EDTA (K3) 4mL	Medisave	368860
CellWASH	BD Biosciences	349524
Dimethyl sulfoxide	Sigma-Aldrich	D2650
Falcon™ Round-Bottom Polystyrene Test Tubes	Fisher Scientific	10579511
Fetal Bovine Serum, qualified, heat inactivated, Brazil	Thermo Fisher Scientific	10500064
Fisherbrand™ Premium Microcentrifuge Tubes: 1.5mL	Thermo Fisher Scientific	12330343
Fisherbrand™ Premium Microcentrifuge Tubes: 0.6mL	Thermo Fisher Scientific	11916955
Gibco™ Trypan Blue Solution, 0.4%	Thermo Fisher Scientific	15250061
Human TruStain FcX™ (Fc Receptor Blocking Solution)	BioLegend	422302
Lysing Solution 10X Concentrate	BD Biosciences	349202
Mr. Frosty™ Freezing Container	Thermo Fisher Scientific	5100-0001
Nunc™ 15mL Conical Sterile Polypropylene Centrifuge Tubes	Thermo Fisher Scientific	339650
Nunc™ 50mL Conical Sterile Polypropylene Centrifuge Tubes	Thermo Fisher Scientific	339652
Nunc™ Biobanking and Cell Culture Cryogenic Tubes	Thermo Fisher Scientific	377267PK
Nunc™ Non-treated T25 EasYFlask, Filter Cap	Thermo Fisher Scientific	169900
Penicillin-Streptomycin (10,000 U/mL)	Thermo Fisher Scientific	15140122
RPMI 1640 Medium	Thermo Fisher Scientific	21875091
SAFETY Blood Collection Set + Holder 21G x 3/4" tubing length 7 1/2" (19 cm), sterile	Greiner Bio-One	450085

4.5 Peripheral blood sample collection, storage, and peripheral blood mononuclear cell isolation

For each participant, approximately 24mL of blood was obtained in Vacutainer® CPT™ tubes with sodium heparin (BD Biosciences) and 2mL were collected in EDTA tubes (Medisave). The EDTA tubes were included to permit assessment of T, B, and NK cell levels by flow cytometry via the T, B, and NK cell (TBNK) assay, as described in Chapter 4.8. EDTA tubes were stored at room temperature for a maximum of 3 days. The CPT™ tube samples were used for the isolation of PBMCs, which were utilised for thorough immune assessment, as detailed in Chapters 4.9-4.12. Following blood collection, CPT™ tubes were inverted 20-30 times and were stored upright at room temperature and protected from light, for a maximum of 48h (PBMC isolation time optimization detailed in Appendices, Chapter 13.4).

Prior to PBMC isolation, tubes were re-inverted 10 times and centrifuged at 1500g for 30min. The platelet/PBMC layer formed during centrifugation was transferred to a 15mL centrifuge tube (Thermo Fisher Scientific). To reduce platelet quantity, the tube was inverted 10 times and cells were washed by one 15min centrifugation at 300g with 15mL CellWash (BD Biosciences). The tube was again inverted 10 times and re-washed with 10mL CellWash via 10min centrifugation at 300g. Isolated PBMCs were counted by light microscopy, after dead cell staining using 0.1% Trypan blue (Thermo Fisher Scientific), and were resuspended in Roswell Park Memorial Institute (RPMI) 1640 medium (ThermoFisher Scientific), supplemented with 10% Fetal Bovine Serum (FBS) (ThermoFisher Scientific) and 1% penicillin/streptomycin (ThermoFisher Scientific). No samples were excluded on the

basis of cell death at this stage. Alive cell counts were utilised to calculate sample amount allocated to each experiment.

4.6 Peripheral blood mononuclear cell storage at -80^{o}C

Following isolation 2x10^{6}-5x10^{6} PBMCs were frozen down to be later used in the mass cytometry assay. Cells were washed with 50mL complete RMPI by 10min centrifugation and the pellet was retained on ice for 10min. The freezing solution, composed of 90% sterile FBS and 10% Dimethyl sulfoxide (Sigma-Aldrich) was simultaneously prepared and retained on ice together with the cryogenic tubes (Thermo Fisher Scientific). 1mL of freezing solution was then added drop-by-drop to the cell pellet and the resuspended PBMCs were transferred into cryogenic tubes and were stored overnight at -80^{o}C in Mr. Frosty™ freezing container (Thermo Fisher Scientific). The tubes were then stored at -80^{o}C.

4.7 Peripheral blood mononuclear cell stimulation

To examine cytokine production and secretion patterns, freshly isolated PBMCs were stimulated (PBMC stimulation optimization detailed in Appendices, Chapter 13.5). PBMCs were resuspended in complete RPMI medium, including 10% FBS and 1% penicillin/streptomycin at a 10^{6} cells/mL concentration. Two cultures were generated per sample, one to be used in the flow assay and one to be used for the enzyme-linked immunosorbent assay (ELISA) (Figure 9). Unstimulated controls were set-up for each assay. PBMC stimulation was induced by the addition of 0.025µg/mL phorbol 12-myristate 13-acetate (PMA) (Sigma-Aldrich) and 0.5µg/mL ionomycin (Sigma-Aldrich) (Figure 9A). The cell suspension was incubated for 30min at 37^{o}C and 5% CO_2. After incubation 0.7µL/mL GolgiStop™ (BD

Biosciences), a monensin-based protein transport inhibitor, inducing protein accumulation in the Golgi complex, was added in cultures later used for flow cytometry. All cultures were incubated at 37°C and 5% CO_2 for 12h, and were then centrifuged for 10min at 500g. The pellets of cultures containing GolgiStop™ were used for the assessment of cytokine production by T and NK cells and to investigate NK cells' CD25 and CD215 expression patterns. Non-GolgiStop™ culture supernatants were stored in -80°C to be later used for the examination of cytokine secretion by PBMCs.

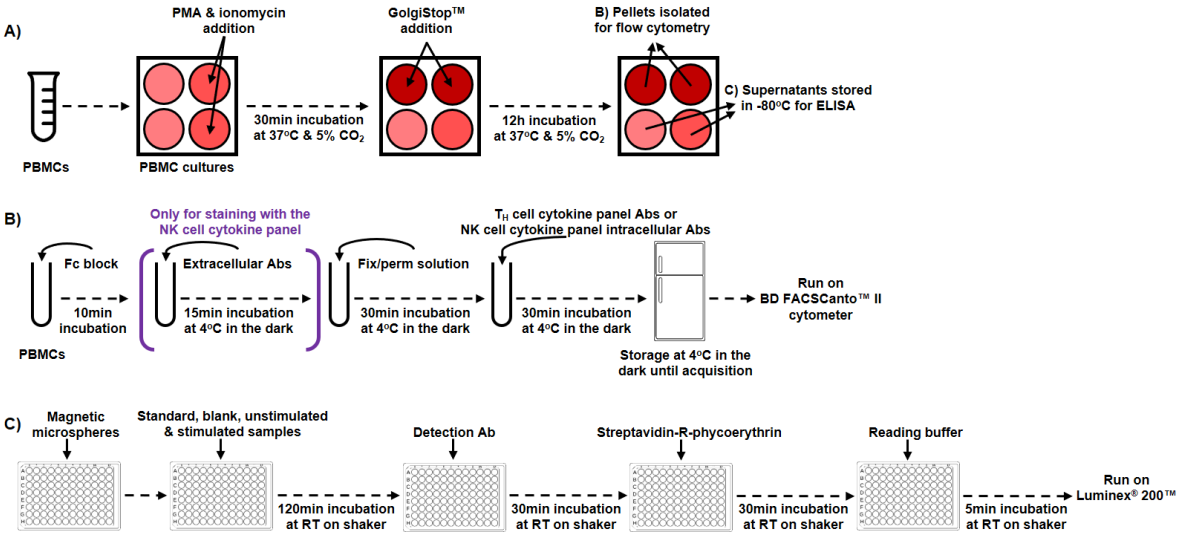


Figure 9. Summary of the experimental pipeline for cytokine assessment. *The major steps of the protocols followed for A) peripheral blood mononuclear cell (PBMC) stimulation, B) examination of cytokine production by flow cytometry, and C) cytokine, chemokine, and colony-stimulating factor secretion quantification by enzyme-linked immunosorbent assay (ELISA) are outlined. Wash steps are not included. Ab: antibody, Fc block: Fc receptor blocking solution, Fix/perm: fixation/permeabilization, NK cell: natural killer cell, RT: room temperature, T_H cell: T helper cell*

4.8 T, B, and NK cell assay

The whole-blood TBNK assay, which is routinely used in the Clinical Immunology service of the University of Birmingham for the investigation and management of cellular immunodeficiency disorders, was used to measure T, B, and NK cell prevalence. A lyse/no wash method was performed to prevent bead and cell loss. Specifically, 20µL of BD Multitest™ 6-color TBNK Reagent (BD Biosciences) was added into BD Trucount™ tubes (BD Biosciences) (Table 4). Samples were thoroughly mixed and 50µL were added to the tubes, which were then gently vortexed and incubated at room temperature in the dark for 15min. 450µL 1X Lysing solution (BD Biosciences), diluted in deionized water, was added and the tubes were gently vortexed and incubated at room temperature in the dark for 15min. Samples were run on the BD FACSCanto™ II (BD Biosciences) cytometer, with the number of positive cells for each marker determined by the BD FACSCanto™ Software (BD Biosciences).

Table 4. T, B, and Natural Killer (NK) cell (TBNK) assay antibody panel. *The cell markers targeted by each antibody used and the respective fluorophore are included. The rationale behind the use of each marker is also shown.*

Marker	Fluorophore	Rationale
CD3	FITC	T cell identification
CD4	PE-Cy7	T helper cell identification
CD8	APC-Cy7	Cytotoxic T cell identification
CD16	PE	NK cell identification
CD56		
CD19	APC	B cell identification
CD45	PerCP-Cy5.5	Leukocyte identification

Leukocyte clusters were gated according to side scatter and CD45 expression, with $CD3^+$ T cells, $CD3^+CD4^+CD8^-$ T helper cells, $CD3^+CD4^-CD8^+$ cytotoxic T cells, $CD3^-CD19^+CD56/CD16^-$ B cells, and $CD3^-CD19^-CD56/CD16^+$ NK cell levels subsequently assessed (Figure 10). The TBNK assay was performed as part of routine Clinical Immunology Service work, by Mr Steven Dix, Ms Genevieve Panaro, and Ms Kamila Silverio Fernadez.

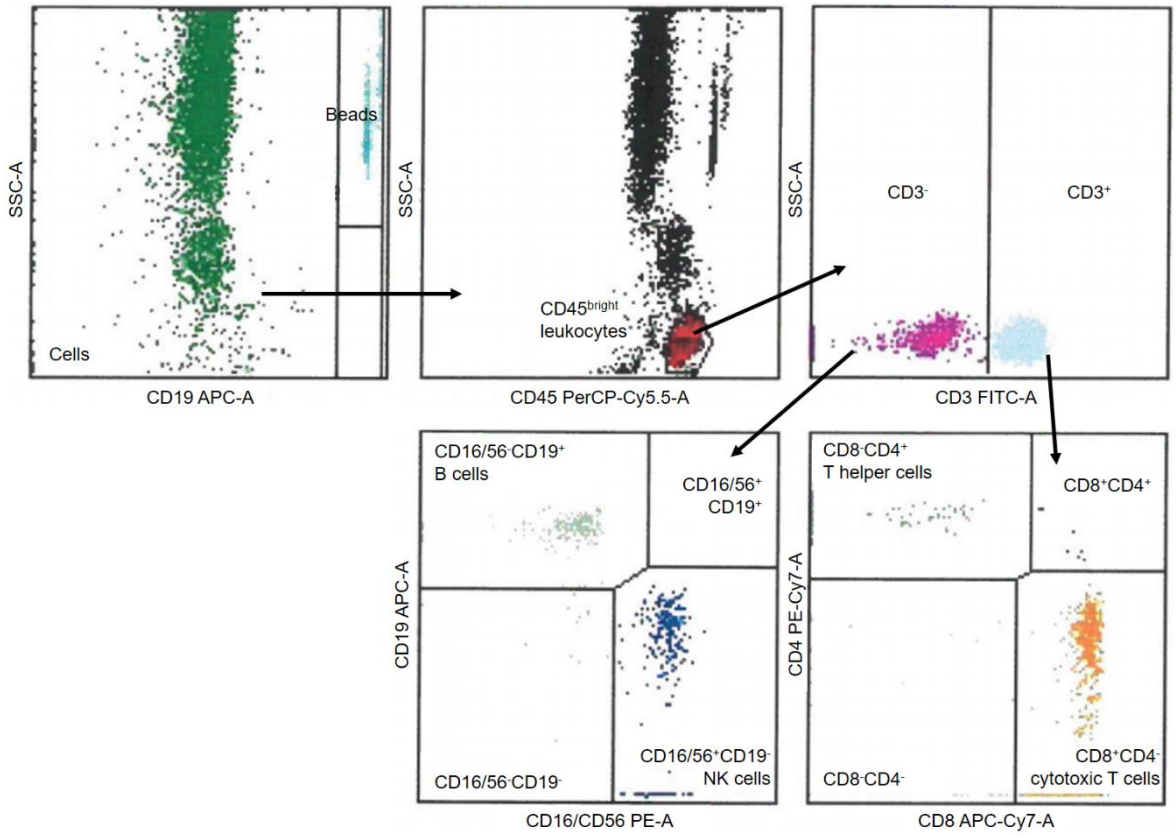


Figure 10. T, B, and Natural Killer (NK) cell (TBNK) assay gating strategy. *Following bead exclusion the leukocyte population was gated on based on their CD45 (PerCP-Cy5.5) expression and side scatter (SSC) properties. The CD3 (FITC) expression of leukocytes was examined and the $CD3^-$ cells were assessed for their CD16/CD56 (PE) and CD19 (APC) expression to measure $CD16/CD56^+CD19^-$ NK and $CD16/CD56^-CD19^+$ B cell levels. The CD4 (PE-Cy7) and CD8 (APC-Cy7) expression of the $CD3^+$ T cell population was further investigated to determine the levels of the $CD8^-CD4^+$ helper and $CD8^+CD4^-$ cytotoxic subpopulations.*

4.9 Flow cytometry

4.9.1 Panel design

Four antibody panels were generated (Flow cytometry optimization and validation detailed in Appendices, Chapters 13.6-13.7). The NK cell panel was used to examine total, $CD56^{dim}CD16^{+}$, and $CD56^{bright}CD16^{-}$ NK cell prevalence as well as the presence of activated cells within these populations (Table 5). The T cell panel was designed to assess total, helper, cytotoxic, naïve, and regulatory T cell prevalence (Table 6). IL-2, IL-10, IL-17A, IFN-γ, and TNF-α cytokine production by T_H cells was assessed via the T helper cell cytokine panel (Table 7), while IL-10, IFN-γ, and TNF-α production as well as CD25 and CD215 cytokine receptor expression by total and $CD56^{dim}CD16^{+}$ NK cells was examined using the NK cell cytokine panel (Table 8). One sample tube was generated per panel, as described in the following sections, alongside an unstained control and one tube containing Zombie Green™ dye (BioLegend) for the evaluation of cell death. Furthermore, for each antibody used, a fluorescence minus one (FMO) control was created, containing every antibody in the panel except for the one of interest, which was replaced by an isotype. For each of the cytokine panels an additional control tube containing stained unstimulated cells was also generated, reflecting the *in vivo* cytokine production.[333]

Table 5. Flow cytometry Natural Killer (NK) cell panel. *The antibody targets included to examine the NK cell population and subpopulations of interest and assess NK cell activity are depicted alongside the respective fluorophores. APC: allophycocyanin, CD: cluster of differentiation, FITC: fluorescein isothiocyanate, PE: phycoerythrin*

NK cell panel		
Antibody target	**Fluorophore**	**Rationale**
CD3	APC-H7	T cell exclusion
CD56	APC	NK cell identification
CD16	FITC	NK cell subset identification
CD69	PE	NK cell activity evaluation

Table 6. Flow cytometry T cell panel. *The antibody targets included to assess the T cell population and subpopulations of interest are displayed alongside the respective fluorophores. APC: allophycocyanin, BV: brilliant violet, CD: cluster of differentiation, FITC: fluorescein isothiocyanate, FoxP3: forkhead box P3, PE: phycoerythrin, PE-Cy: phycoerythrin-cyanine, PerCP: peridinin chlorophyll protein*

T cell panel		
Antibody target	**Fluorophore**	**Rationale**
CD3	APC-H7	T cell identification
CD4	PerCP	T helper cell identification
CD8	BV510	Cytotoxic T cell identification
CD45RA	PE	Naïve T cell identification
CD25	FITC	Regulatory T cell identification
CD127	BV421	
FoxP3	PE-Cy7	

Table 7. Flow cytometry T helper cell cytokine panel. *The antibody targets included to evaluate cytokine production by T helper cells are depicted alongside the respective fluorophores. APC: allophycocyanin, BV: brilliant violet, CD: cluster of differentiation, FITC: fluorescein isothiocyanate, IFN: interferon, IL: interleukin, PE: phycoerythrin, PE-Cy: phycoerythrin-cyanine, TNF: tumor necrosis factor*

T helper cell cytokine panel		
Antibody target	**Fluorophore**	**Rationale**
CD3	APC-H7	T cell identification
CD8	BV510	Cytotoxic T cell exclusion
IL-2	PE-Cy7	Cytokine expression evaluation
IL-10	PE	
IL-17A	FITC	
IFN-γ	BV421	
TNF-α	APC	

Table 8. Flow cytometry Natural Killer (NK) cell cytokine panel. *The antibody targets included to assess cytokine production and cluster of differentiation (CD)25 and CD215 expression by total and $CD56^{dim}CD16^{+}$ NK cells are displayed alongside the respective fluorophores. APC: allophycocyanin, BV: brilliant violet, FITC: fluorescein isothiocyanate, IFN: interferon, IL: interleukin, PE: phycoerythrin, PE-Cy: phycoerythrin-cyanine, PerCP-Cy: peridinin chlorophyll protein-cyanine, TNF: tumor necrosis factor*

NK cell cytokine panel		
Antibody target	**Fluorophore**	**Rationale**
CD3	APC-H7	T cell exclusion
CD56	APC	NK cell identification
CD16	FITC	NK cell subset identification
CD25	BV510	Cytokine receptor expression evaluation
CD215	PE	
IL-10	PE-Cy7	Cytokine expression evaluation
IFN-γ	BV421	
TNF-α	PerCP-Cy5.5	

4.9.2 NK cell panel staining

To assess NK cell population and subpopulation prevalence the expression of CD3, CD56, CD16, and the CD69 cytotoxicity marker were measured.[340] For this, 10^6 freshly isolated PBMCs were added in the sample tube and $0.25x10^6$ cells were added in each control tube. 5µL Human TruStain FcX™ Fc Receptor Blocking Solution (BioLegend) was added to limit unspecific staining. The tubes were incubated for 10min, extracellular antibodies and 5µL of isotype dyes were, added and the cells were incubated for 15min at 4°C protected from light. 5 drops of 1X Lysing Solution (BD Biosciences), diluted in deionized water were also added. The tubes were incubated protected from light for 10min at 4°C and were washed with 2mL CellWash buffer (BD Biosciences) by 5min centrifugation at 500g. The fixed cells were resuspended in 0.5mL CellWash buffer and were stored at 4°C protected from light until acquisition.

4.9.3 T cell panel staining

The T cell panel was designed for the quantification of total, helper, and cytotoxic, and $FoxP3^+CD25^+CD127^{low/-}$ regulatory T cells,[632, 633] as well as the identification of $CD45RA^+$ naïve T_H and T_C cells.[634] Sample preparation and extracellular antibody staining for the T cell panel was identical to that performed for the NK cell panel. However, as intracellular FoxP3 was included in the T cell panel, after the 15min incubation at 4°C the cells were washed with 1mL CellWash buffer by a 5min centrifugation at 500g. For the fixation and permeabilization of cells the eBioscience™ Foxp3/Transcription Factor Staining Buffer Set (Thermo Fisher Scientific) was used. 1mL FoxP3 Fixation/Permeabilization working solution,

consisting of 0.25mL Fixation/Permeabilization Concentrate (Thermo Fisher Scientific) and 0.75mL Fixation/Permeabilization Diluent (Thermo Fisher Scientific), was added to the tubes, which were then incubated at 4^{o}C for 30min protected from light. Cells were washed twice with 2mL 1X Permeabilization Buffer (Thermo Fisher Scientific), diluted in ddH_2O, by 5min centrifugation at 500g. The pellet was resuspended in 100μL 1X Permeabilization Buffer and the intracellular anti-FoxP3 antibody was added. The tubes were then incubated at 4^{o}C, protected from light, for 30min. Lastly, the stained cells were washed twice with 2mL 1X Permeabilization Buffer by 5min centrifugation at 500g, and the pellet was resuspended in 0.5mL CellWash buffer and stored at 4^{o}C protected from light until acquisition.

4.9.4 Cytokine panel staining

PBMCs stimulated with PMA and ionomycin, and unstimulated controls, were used to investigate cytokine production by T_H and NK cells (Figure 9B). The expression of CD25, the IL-2 receptor alpha chain, and CD215, the IL-15 receptor alpha chain, were also examined as both IL-2 and IL-15 are considered potent NK cell activators.[635] The staining protocol followed was similar for both cytokine panels. However, only the intracellular staining steps were followed for T_H cell cytokine staining. Specifically, 10^6 PBMCs were added in each sample tube and $0.25x10^6$ were added in each control tube, alongside 5μL Fc block. Cells were incubated for 10min. The extracellular antibodies of the NK cell cytokine panel were added to the tubes, which were then incubated for 15min at 4^{o}C in the dark. Cells were then washed with 1mL CellWash buffer by centrifugation at 500g for 5min. The following parts of the protocol were identical for both the T_H and NK cell cytokine tubes. For cell fixation and permeabilization the Fixation/Permeabilization Solution Kit with BD

GolgiStop™ (BD Biosciences) was used. 250µL Fixation/Permeabilization solution (BD Biosciences) were added and the tubes were incubated for 30min at 4ºC. Cells were washed twice with 1mL 1X BD Perm/Wash™ Buffer (BD Biosciences), diluted in ddH_2O, and the pellet was resuspended in 50µL 1X BD Perm/Wash™ Buffer. The intracellular antibodies were added in the NK cell cytokine panel tubes and both intracellular and extracellular antibodies were added in the T_H cell cytokine panel tubes. All tubes were incubated, protected from light for 30min at 4ºC and were then washed two times with 1X BD Perm/Wash™ Buffer by 5min centrifugations at 500g. Pellets were resuspended in 0.5mL CellWash buffer and were stored at 4ºC, protected from light, until acquisition.

4.9.5 Dead cell staining

One additional tube was generated per panel to assess dead cell levels. $0.25x10^6$ PBMCs were added per tube and were washed with phosphate-buffered saline (PBS). The Zombie Green™ dye was diluted 1:100 in PBS and 12.5µL were added to the cells, which were then incubated for 15min in the dark. Following the incubation period the cells were washed with 2mL Cell staining buffer (BioLegend) and were then processed according to the protocol of the respective panel. Samples with PBMC death higher than 40% were excluded from statistical analysis.

4.9.6 Data analysis

All sample and control tubes were analysed by flow cytometry using the BD FACSCanto™ II (BD Biosciences) cytometer. Data acquisition was performed using the BD FACSCanto™ Software (BD Biosciences) and the uncompensated .fcs files produced were processed on FlowJo v10.6.2.[636] Sample quality evaluation and

data clean-up was performed using the FlowAI 2.0 plugin,[637] eliminating anomalies due to unwanted events. The “GoodEvents” subpopulation produced was used for further analysis. A panel-specific compensation matrix was generated, based on compensation tubes generated for each antibody included in the panel (Compensation tube preparation detailed in Appendices, Chapter 13.9). The positive signal produced by each antibody, as well as the negative signal produced by the unstained control were used to calculate the matrix, which was applied to all samples and controls of the respective panel.

A standardized gating strategy was used adjusting for sample variation (Figures 11-14). In all panels the singlet population was initially identified and the lymphocyte population was selected. All gates were set according to the FMO tubes, ensuring that the positive population for the marker of interest was not higher than 2% in the respective FMO control. For the sample and control tubes stained with the NK cell panel (Figure 11), the $CD3^{-}CD56^{+}$ NK cell population was selected, within which the $CD56^{dim}CD16^{+}$ and $CD56^{bright}CD16^{-}$ subpopulations were identified. In total, $CD56^{dim}CD16^{+}$, and $CD56^{bright}CD16^{-}$ NK cells CD69 expression was assessed. The frequency of CD69-expressing cells and the expression levels of CD69 on individual cells, quantified according to the median fluorescence intensity (MFI) of this marker, were measured.

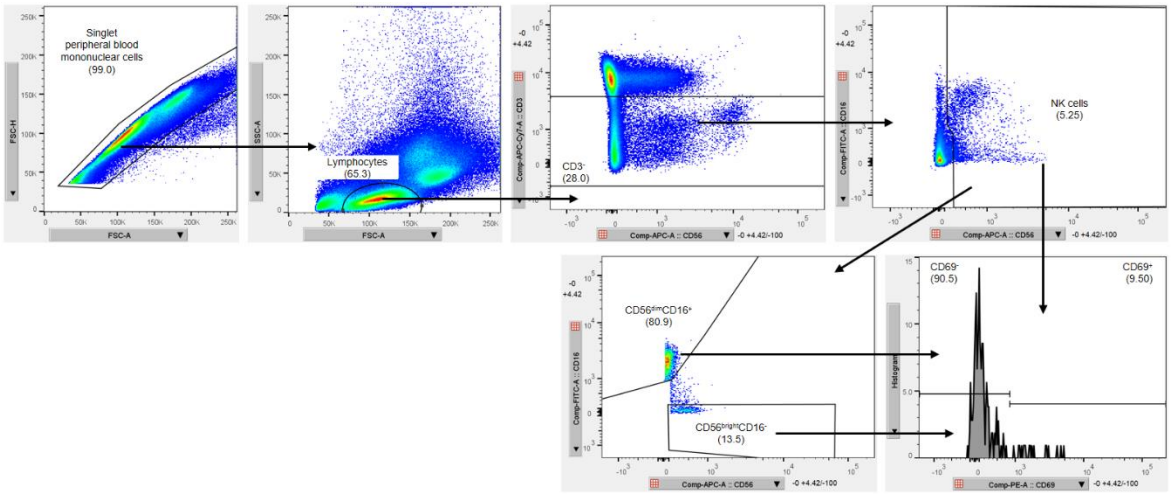


Figure 11. Flow cytometry assay Natural Killer (NK) cell panel gating strategy. *The singlet population was selected based on the forward scatter height (FSC-H) and forward scatter area (FSC-A). In that gate lymphocytes were selected according to their side (SSC-A) and forward scatter area (FSC-A). In the lymphocyte gate the $CD3^-$ population was gated on and in that gate $CD56^+$ NK cells were identified. In the NK cell population the $CD56^{dim}CD16^+$ and $CD56^{bright}CD16^-$ subsets were selected. CD69 expression on total $CD3^-CD56^+$, $CD3^-CD56^{dim}CD16^+$, and $CD3^-CD56^{bright}CD16^-$ NK cells was evaluated.*

To assess T cell subsets, the following gating strategy was utilised (Figure 12). In the lymphocyte gate the $CD3^+$ T cell population was gated on and its $CD4^+CD8^-$ and $CD4^-CD8^+$ subsets were identified. The frequency of $CD45RA^+$ cells in these subsets was assessed. Furthermore, in the $CD4^+CD8^-$ T cell gate the $FoxP3^+$ population was selected, inside which $CD25^+CD127^{low/-}$ Tregs were detected.

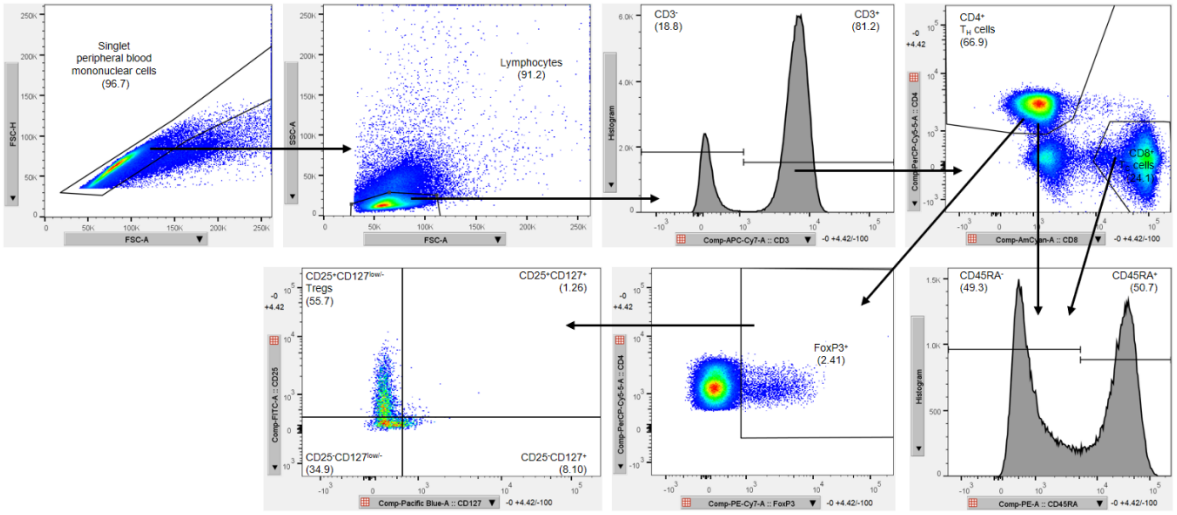


Figure 12. Flow cytometry assay T cell panel gating strategy. *The singlet population was selected based on the forward scatter height (FSC-H) and forward scatter area (FSC-A). In that gate lymphocytes were selected according to their side (SSC-A) and forward scatter area (FSC-A). In the lymphocyte gate the $CD3^+$ T cell population was gated on and in that gate the helper $CD4^+CD8^-$ (T_H) and cytotoxic $CD4^-CD8^+$ (T_C) subsets were identified. In both these subsets the expression of CD45RA was assessed. In the $CD4^+CD8^-$ gate the $FoxP3^+$ population was also selected. The $CD25^+CD127^{low/-}$ regulatory (Treg) subpopulation in the $FoxP3^+$ cell gate was examined.*

Similar gating strategies were followed for cytokine panel analysis. For T_H cell cytokine panel tubes (Figure 13), the $CD3^+CD8^-$ T_H lymphocyte population was selected, its IL-2^+, IL-10^+, IL-$17A^+$, IFN-γ^+, and TNF-α^+ subsets were identified, and the MFI produced by each cytokine in was recorded.

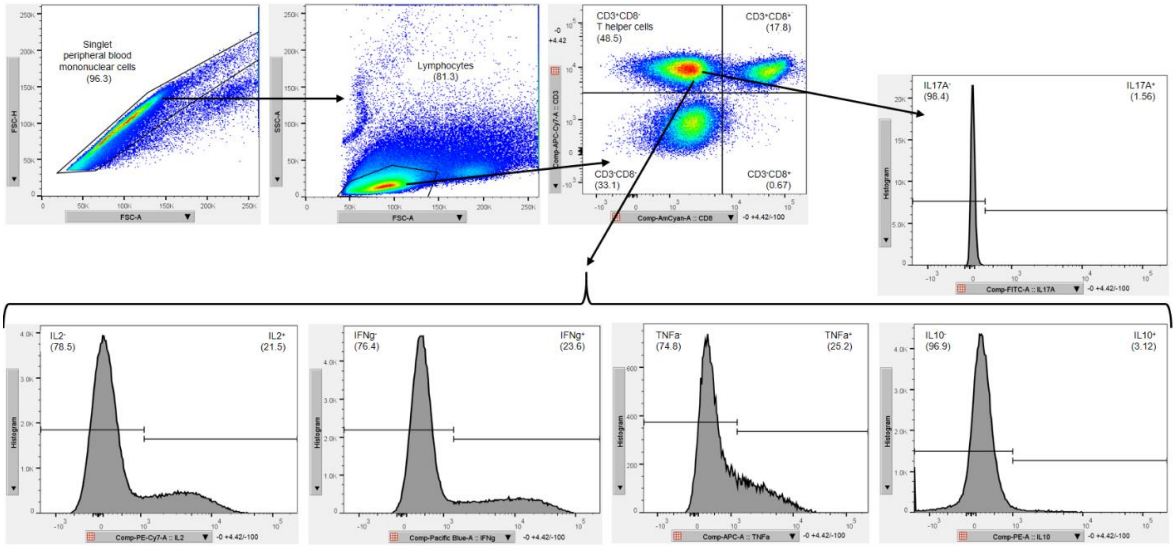


Figure 13. Flow cytometry assay T helper cell cytokine panel gating strategy. *The singlet population was selected based on the forward scatter height (FSC-H) and forward scatter area (FSC-A). In that gate lymphocytes were selected according to their side (SSC-A) and forward scatter area (FSC-A). In the lymphocyte gate the $CD3^{+}CD8^{-}$ T helper cell population was gated on and in that gate the expression of the IL-2, IFN-γ, TNF-α, IL-10, and IL-17A cytokines was assessed.*

For the NK cell cytokine panel (Figure 14), $CD3^{-}$ lymphocytes were selected and in that gate $CD56^{-}CD16^{-}$ cells were excluded. The $CD56^{bright}CD16^{-}$ population was undetectable, and thus in the CD56/$CD16^{+}$ gate the total $CD56^{+}$ NK cell population and the $CD56^{dim}CD16^{+}$ NK cell subpopulation were selected. The presence of IL-10^{+}, IFN-γ^{+}, TNF-α^{+}, $CD25^{+}$, and $CD215^{+}$ cells in each of these populations and the MFI produced by each of these markers were assessed. These parameters were only assessed in the $CD56^{dim}CD16^{+}$ population when a sufficient number of cells was present to ensure result accuracy.

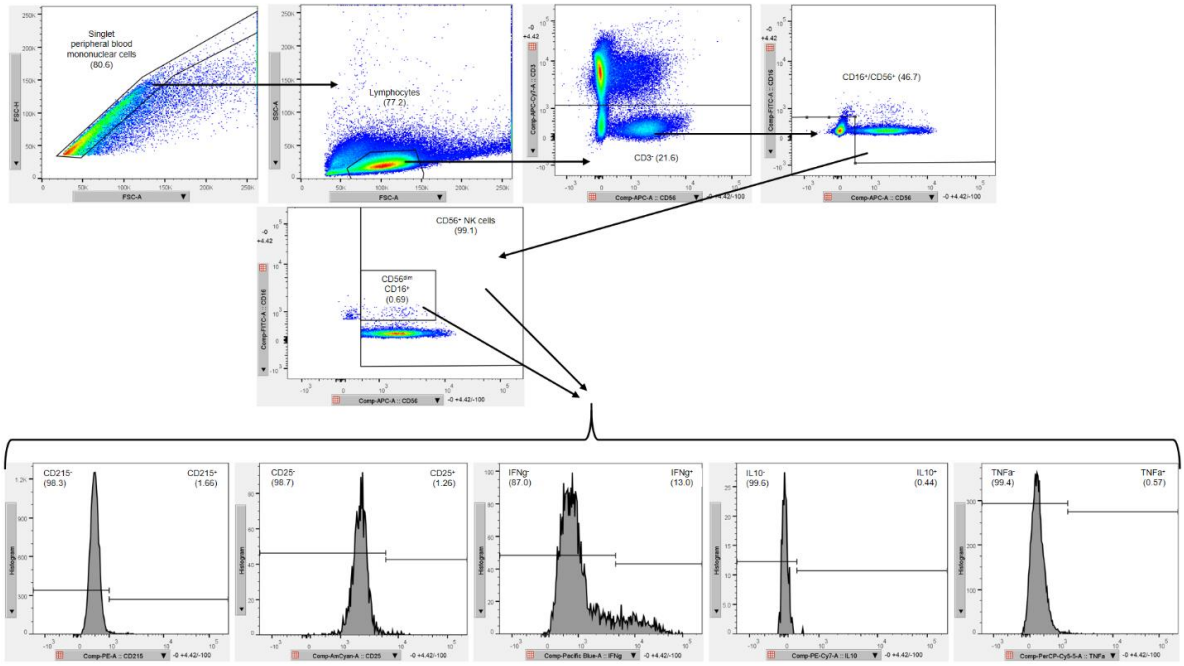


Figure 14. Flow cytometry assay Natural Killer (NK) cell cytokine panel gating strategy. *The singlet population was selected based on the forward scatter height (FSC-H) and forward scatter area (FSC-A). In that gate lymphocytes were selected according to their side (SSC-A) and forward scatter area (FSC-A). In the lymphocyte gate the CD3$^-$ cell population was gated on and in that gate the CD16$^+$ and/or CD56$^+$ population was selected. In that CD16$^+$/CD56$^+$ population, the CD56$^+$ NK cells and the CD56^{dim}CD16$^+$ NK cell subpopulation were gated on and in these gates the CD215, CD25, IFN-γ, IL-10, and TNF-α expression was examined.*

Data recorded, including the frequency of the populations of interest and the MFIs of certain markers were exported to Excel 2016.[638] The ratios between T_H1 and T_H2 cytokine production rather than the absolute values are often considered as a potential diagnostic marker for immunological PRL,[370, 423, 475] and thus such ratios were calculated. More specifically, using the T_H cell cytokine panel the percentage of IL-2$^+$/IL-10$^+$, IFN-γ$^+$/IL-10$^+$, TNF-α$^+$/IL-10$^+$, as well as the percentage of IL-17A$^+$/IL-10$^+$, IL-2$^+$/IL-17A$^+$, IFN-γ/IL-17A$^+$, and TNF-α$^+$/IL-17A$^+$ T_H cells and the respective MFI ratios were calculated. The IFN-γ$^+$/IL-10$^+$ and TNF-α$^+$/IL-10$^+$ NK cell and CD56^{dim}CD16$^+$ NK cell ratios and the respective MFIs were also calculated

using data derived from the NK cell cytokine panel. All findings were statistically evaluated in GraphPad Prism 6.[639]

4.10 Mass cytometry

4.10.1 Panel design

Mass cytometry was used to perform more detailed NK cell analysis and identify potential alterations in functional activity markers for women with RPL.[640] The mass cytometry panel generated (Table 9) focused upon the differential expression of multiple activating and inhibitory receptors, in particular those belonging to the KIR, NKG2, NCR, and ILT families (Mass cytometry antibody conjugations and titrations detailed in Appendices, Chapter 13.10-13.11). Exploratory inhibitory immune checkpoint receptors and chemokine receptors were also included in the panel. The expression of certain T and B cell markers was also assessed, given the existing evidence regarding their role in the pathogenesis of RPL.[383, 423, 485, 486, 532]

Table 9. Mass cytometry assay panel. *The antibody targets included in the mass cytometry panel to thoroughly examine Natural Killer (NK) cell populations and subpopulations of interest are depicted alongside the respective metal. Markers used to examine T and B cell subpopulations are also included. CD: cluster of differentiation, CXCR: C-X-C motif chemokine receptors, DNA: deoxyribonucleic acid, ILT: immunoglobulin-like transcript, KIR: killer-cell immunoglobulin-like receptor, NKG2: natural killer group 2, PD-1: programmed cell death protein 1, TIGIT: T cell immunoreceptor with Ig and ITIM domains, TIM-3: T cell immunoglobulin and mucin domain-containing protein-3*

Antibody target	Metal	Rationale
DNA	103Rh	Single cell identification
CD298 and β2 microglobulin	106Cd	Sample identification (Barcoding)
	110Cd	
	112Cd	
	114Cd	
Dead cells	194Pt	Dead cell exclusion
CD45	89Y	Leukocyte identification
CD3	141Pr	T cell identification
CD14	148Nd	Monocyte/macrophage exclusion
CD19	142Nd	B cell identification
CD56	155Gd	NK cell identification
CD16	209Bi	NK cell subset identification
ILT1	152Sm	Examination of immunoglobulin-like transcript receptor expression on NK cells
ILT2	156Gd	
ILT2/LIR6	158Gd	
ILT3	161Dy	
ILT4	161Dy	
ILT5	161Dy	
KIR2DL1/S1/S3/S5	146Nd	Examination of killer-cell immunoglobulin-like receptor expression on NK cells
KIR2DL1/S5	151Eu	
KIR2DL2/L3	173Yb	
KIR2DL2/L3/S2/S4	198Pt	
KIR2DL4	176Yb	
KIR2DL5	173Yb	
KIR2DS4	165Ho	
KIR3DL1	167Er	
KIR3DL2	167Er	
NKG2A	169Tm	Examination of natural killer group 2 receptor expression on NK cells
NKG2C	166Er	
NKG2D	166Er	
NKp30	159Tb	Examination of natural cytotoxicity receptor expression on NK cells
NKp44	162Dy	
NKp46	162Dy	
NKp80	159Tb	

CX3CR1	172Yb	Examination of chemokine receptor expression on NK cells
CXCR1	147Sm	
CXCR2	147Sm	
CXCR3	163Dy	
CXCR4	163Dy	
CXCR5	153Eu	
CXCR6	160Gd	
PD-1	175Lu	Examination of immune checkpoint receptor expression on NK, T, and B cells
TIGIT	154Sm	
TIM-3	154Sm	
CD57	115In	Examination of receptor expression on NK cells
CD69	144Nd	
CD94	174Yb	
CD122	170Er	
CD161	164Dy	
CD4	145Nd	Examination of receptor expression on NK and T cells
CD8a	116Cd	
CD127	168Er	
CD226	171Yb	
CD5	143Nd	Examination of additional receptor expression on NK and B cells
CD27	150Nd	
CD38	111Cd	
CD25	149Sm	Examination of receptor expression on NK, T, and B cells

4.10.2 Mass cytometry panel staining

To perform the mass cytometry assay (Figure 15), isolated PBMCs stored at -80^{o}C were utilised. Cryogenic tubes (Thermo Fisher Scientific) were retrieved and incubated at 37^{o}C until thawed. PBMCs were then transferred into a 50mL conical sterile centrifuge tube (Thermo Fisher Scientific) and washed with 50mL warm complete RPMI by 30min centrifugation at 300g. Following supernatant disposal, PBMCs were resuspended in 2mL warmed complete RPMI. To reduce clump formation, 25U of Benzonase® (Merck Millipore) was added for every 10^6 frozen PBMCs and the cells were incubated for 1h at 37^{o}C and 5% CO_2. The PBMCs were washed with 50mL warm complete RPMI by 30min centrifugation at 300g, counted using Trypan blue (Thermo Fisher Scientific) for dead cell exclusion, and then re-washed in the same manner. Finally PBMCs were resuspended in Maxpar® cell

staining buffer (Fluidigm) at a concentration equal to $3x10^6$ cells/100µL (Mass cytometry validation detailed in Appendices, Chapter 13.12).

To accommodate multiple samples in one tube, barcoding technology was utilised, with anti-CD298 and anti-β2 microglobulin (β2m) barcoding antibodies generated. Each barcode was composed of 0.8µL anti-CD298 and 0.5µL anti-β2m antibodies, labelled with the same metal tag. These targets were used to ensure total immune cell labelling.[641] Barcoding antibodies were added in each of the sample tubes, which were then incubated for 20min at room temperature. PBMCs were then washed with 3-4mL staining buffer by 5min centrifugation at 300g. The supernatant was discarded, with the barcoded samples pooled and re-centrifuged at 300g for 5min. Following supernatant removal, 5µL per 100µL of PBMCs Fc receptor blocking solution (BioLegend) was added and the mixture was incubated for 10min at room temperature.

Prior to each round of staining an antibody cocktail was generated according to the total sample volume (Table 10). To remove clumps, the antibody cocktail was added in 0.1µm Ultrafree® centrifugal filters (Merck Millipore) placed on a collection tube, centrifuged for 7min at 12000g, and flow-through was collected. The antibody cocktail was added to barcoded PBMCs that were then incubated for 30min at room temperature. 10µL of 5% Cisplatin-194Pt dead cell stain (Fluidigm) diluted in PBS were added and cells were re-incubated at room temperature for 3min. Cells were then washed with 4mL staining buffer by 5min centrifugation at 300g and fixed with 200µL PBS and 300µL 3.2% paraformaldehyde, prepared using 16% formaldehyde (Thermo Fisher Scientific) and PBS. The tube was vortexed thoroughly and was incubated for 15min at room temperature in the dark. Following incubation, cells

were washed with 3-3.5mL staining buffer by 5min centrifugation at 800g. 2µL Rh103 DNA intercalator (Fluidigm) was mixed with 0.5mL Maxpar® Fix and Perm Buffer (Fluidigm) with the solution added to the pellet to allow single nucleated cell identification. Stained cells were vortexed and incubated overnight at 4ºC, prior to acquisition.

On the acquisition day, samples were processed and run by Dr Shahram Golbabapour. The stained cells were vortexed and washed with 3mL staining buffer by centrifugation at 800g for 5min. Supernatant was removed and the pellet was resuspended and washed twice with 4mL Milli-Q® ultrapure water (Merck Millipore) by centrifugations at 800g for 5min. Immediately prior to the run the pellet was resuspended in ultrapure water, containing 10% EQ™ Four Element Calibration Beads (Fluidigm), at a $0.05x10^6$-10^6 cells/mL concentration. Samples were run using the Helios Cytometry by Time-Of-Flight (CyTOF) system (Fluidigm) and the CyTOF® Software v7.0 (Fluidigm, 2019), aiming for an optimal acquisition rate of 250-500 events/s. A minimum of 420,000 events/tube was acquired, resulting in approximately 210,000 events/sample.

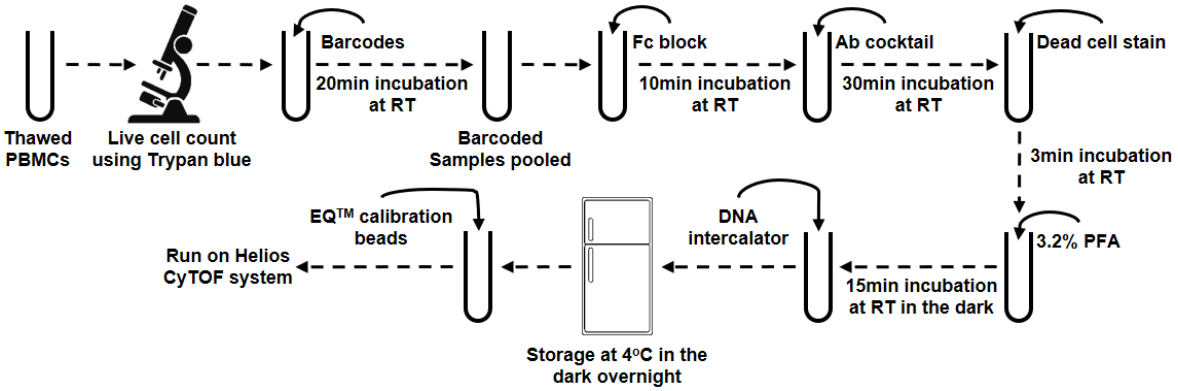


Figure 15. Summary of the experimental pipeline for detailed lymphocyte phenotypic assessment. *The major steps of the protocol followed for the examination of natural killer (NK), T, and B cells by mass cytometry are displayed. Peripheral blood mononuclear cell (PBMC) thawing steps and wash steps are not included. Ab: antibody, CyTOF: cytometry by time-of-flight, Fc block: Fc receptor blocking solution, PFA: paraformaldehyde, RT: room temperature*

Table 10. Antibody cocktail generated for mass cytometry staining. *The antibodies included in the mass cytometry panel, defined by their target molecule and metal tag, are illustrated alongside the amount of each used in the cocktail to stain 100µL of peripheral blood mononuclear cell sample. The resulting total cocktail volume is also shown. CD: cluster of differentiation, CXCR: C-X-C motif chemokine receptors, ILT: immunoglobulin-like transcript, KIR: killer-cell immunoglobulin-like receptor, NKG2: natural killer group 2, PD-1: programmed cell death protein 1, TIGIT: T cell immunoreceptor with Ig and ITIM domains, TIM-3: T cell immunoglobulin and mucin domain-containing protein-3*

Antibody	µL	Antibody	µL
CD38 - 111Cd	0.75	CXCR6 - 160Gd	1.00
CD94 - 174Yb	0.75	CXCR3 - 163Dy	0.50
KIR2DL1/2DS5 - 151Eu	0.75	CD19 - 142Nd	0.20
KIR2DS4 - 165Ho	1.00	CD27 - 150Nd	0.20
KIR3DL2 - 167Er	1.00	ILT5 - 161Dy	0.20
KIR2DL4 - 176Yb	1.00	CD127 - 168Er	0.50
KIR2DL1/S1/S3/S5 - 146Nd	0.75	CX3CR1 - 172Yb	0.75
ILT1 - 152Sm	0.50	KIR2DL2/L3/S2/S4 - 198Pt	0.50
ILT2/LIR6 - 158Gd	0.50	CD69 - 144Nd	0.50
ILT3 - 161Dy	0.50	NKp30 - 159Tb	0.75
CD161 - 164Dy	0.20	NKp44 - 162Dy	0.50
CD25 - 149Sm	0.50	NKG2A - 169Tm	0.75
KIR3DL1 - 167Er	0.20	PD1 - 175Lu	0.75
CD122 - 170Er	0.50	CXCR1 - 147Sm	0.50
KIR2DL2/L3 - 173Yb	1.00	CXCR5 - 153Eu	0.50
CD16 - 209Bi	0.20	NKp80 - 159Tb	0.20
CD5 - 143Nd	0.50	NKp46 - 162Dy	0.50
CD56 - 155Gd	0.75	NKG2C - 166Er	0.50
CD45 - 89Y	0.75	KIR2DL5 - 173Yb	0.75
CD14 - 148Nd	0.20	CD57 - 115In	0.20
TIGIT - 154Sm	0.75	CXCR2 - 147Sm	0.20
CXCR4 - 163Dy	0.20	ILT2 - 156Gd	0.75
CD8a - 116Cd	0.50	ILT4 - 161Dy	1.00
CD3 - 141Pr	0.50	NKG2D - 166Er	0.75
CD4 - 145Nd	0.20	CD226 - 171Yb	0.50
TIM3 - 154Sm	0.75	Total	28.65

4.10.3 Data analysis

Raw data, in the form of .fcs files, was normalised using the CyTOF® Software v7.0 (Fluidigm, 2019) according to the EQ™ Four Element Calibration Beads (Fluidigm).[642] The .fcs files were then uploaded to Cytobank (Beckman Coulter), where data clean-up and debarcoding were performed (Figure 16). EQ™ beads were gated out. 103Rh DNA staining was used for single-cell identification and in that gate the $^{194}Pt^-$ live cell population was identified. Debarcoding was performed on the live population (Figure 16).

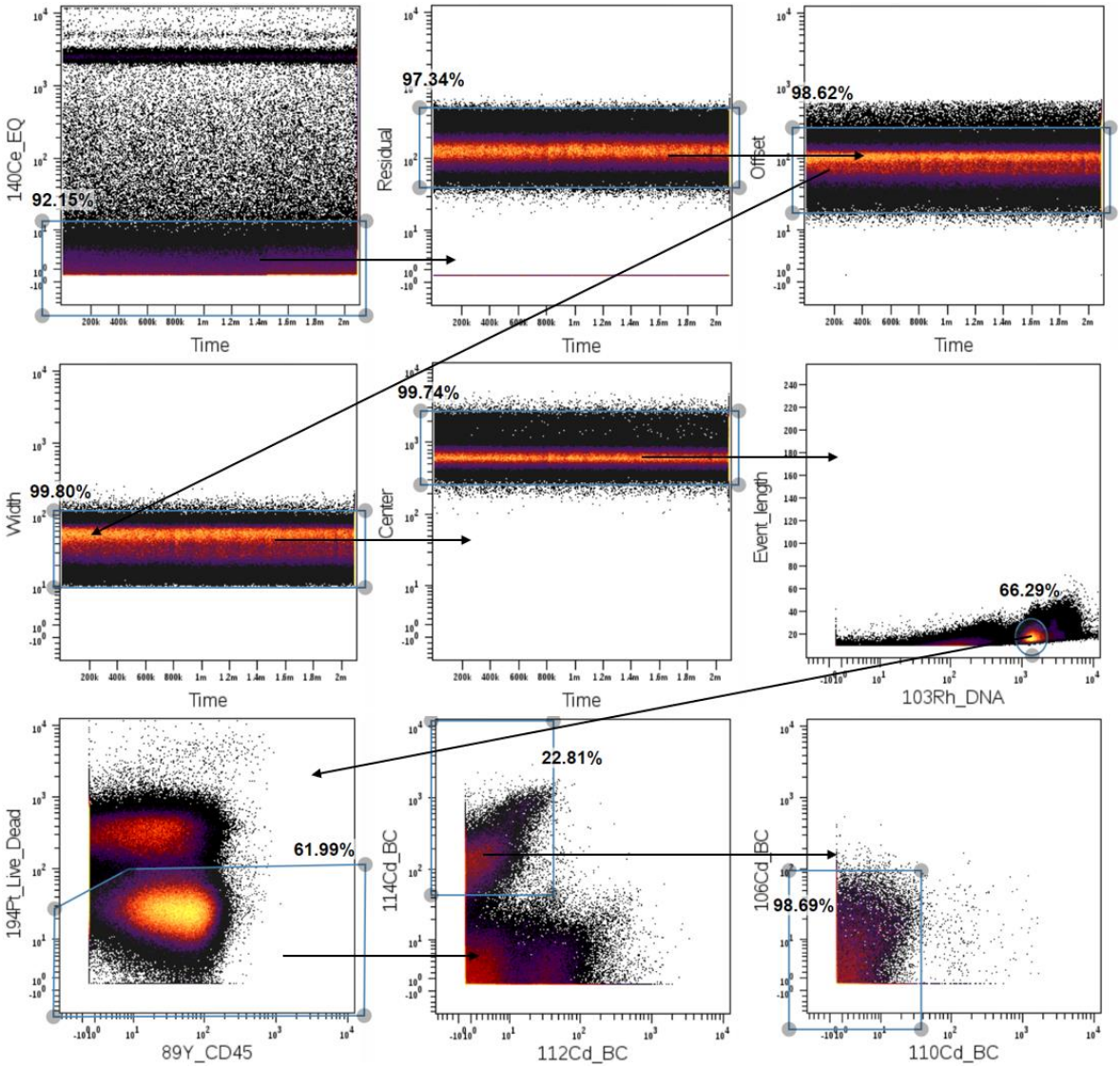


Figure 16. Mass cytometry data clean-up and debarcoding. *Calibration beads were initially excluded and outliers were then removed according to the residual, offset, width, and center parameters. The singlet population was gated on according to DNA staining. In the singlet population the live cells were gated on. To debarcode data, in the live cell gate the population positive for the barcode of interest was selected, while populations positive for the other barcodes were excluded.*

Following debarcoding, the resulting .fcs file for each sample was analysed on Cytobank (Beckman Coulter). $CD3^{-}CD45^{+}CD14^{-}CD19^{-}CD56^{+}$ NK cells, $CD3^{+}CD45^{+}CD14^{-}CD19^{-}CD56^{-}$ T cells, and $CD3^{-}CD45^{+}CD14^{-}CD19^{+}CD56^{-}$ B cells were selected (Figure 17). Cells belonging in each of these lymphocyte subpopulations were exported as different .fcs files and were analysed separately.

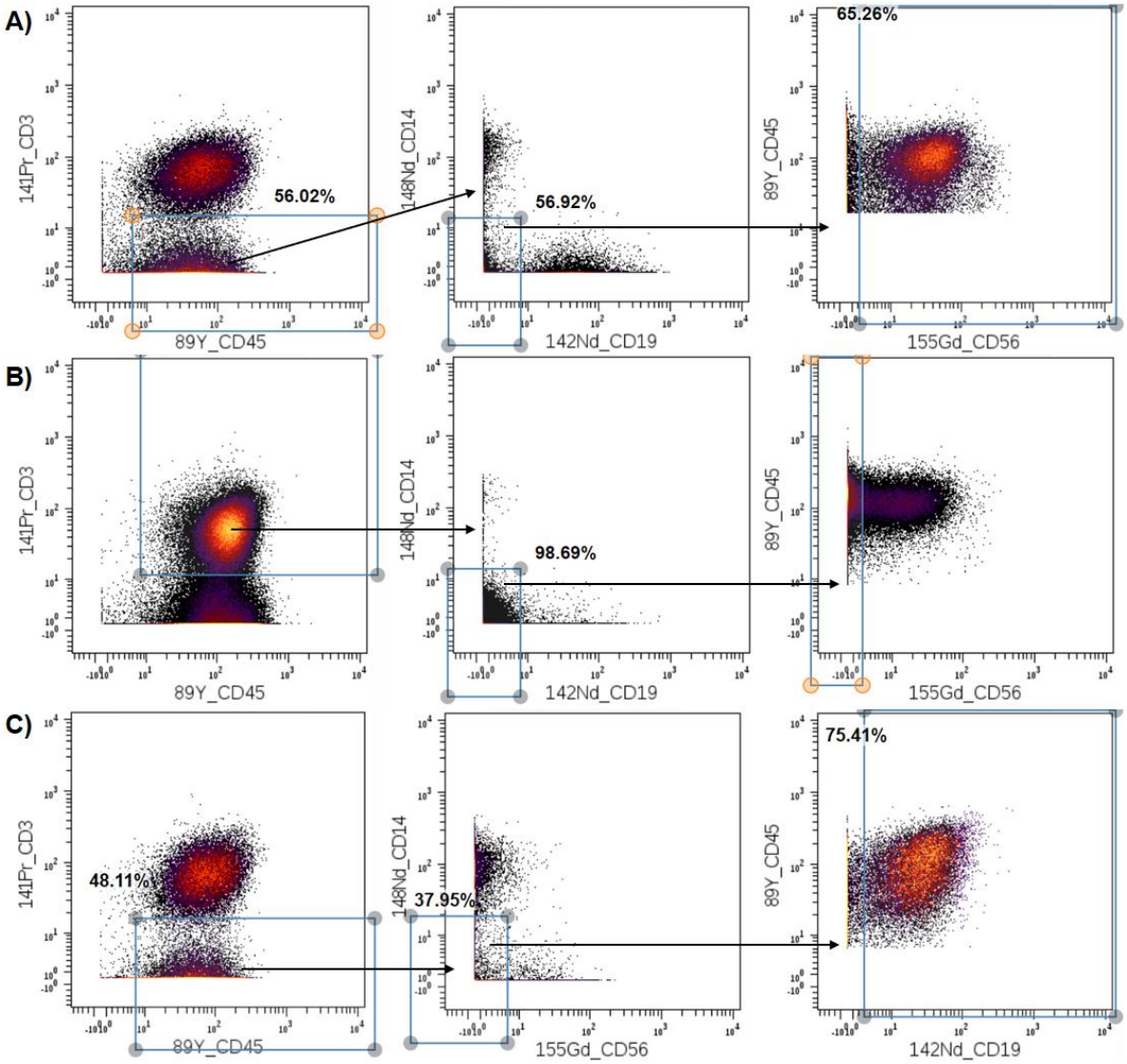


Figure 17. Mass cytometry assay lymphocyte gating strategy. *The gating strategies used for the identification of the A) Natural Killer, B) T, and C) B cell subpopulations in the cleaned-up and debarcoded mass cytometry data are illustrated. More specifically, NK cells were identified through gating on $CD3^{-}CD45^{+}$ cells, followed by gating on $CD14^{-}CD19^{-}$ cells, and $CD56^{+}$ cell identification. T cells were detected through $CD3^{+}CD45^{+}$ cell gating, followed by $CD14^{-}CD19^{-}$ cell identification, and gating on the $CD56^{-}$ cell population. The B cell population was identified through gating on $CD3^{-}CD45^{+}$ cells, followed by $CD14^{-}CD56^{-}$ cell gating, and selection of $CD19^{+}$ cells.*

4.11 Cytotoxicity assay

To evaluate the cytotoxic capacity of NK cells in women with RPL and controls, HLA^- K562 cells were used as targets (Figure 18A).[643] K562 cells (Sigma-Aldrich), were maintained at a $0.25x10^6$-$1x10^6$ cell density in RPMI 1640 medium (Thermo Fisher Scientific), supplemented with 10% FBS (Thermo Fisher Scientific) and 1% penicillin/streptomycin (Thermo Fisher Scientific). Cells were incubated in T25 flasks (Thermo Fisher Scientific) at 5% CO_2 and 37ºC. Passaging was performed, every 48h-72h, to maintain cell density or when the medium become acidic. Subcultures were created the day prior to the assay to minimize spontaneous cell death.

Alive K562 cells, isolated using the Dead Cell Removal Kit (Miltenyi Biotec), were used in the cytotoxicity assay (Cytotoxicity assay optimization, troubleshooting, and validation detailed in Appendices, Chapters 13.14-13.15). $1x10^7$ K562 cells were isolated from cultures and centrifuged at 300g for 10min to remove the supernatant. The pellet was resuspended in 100µL Dead Cell Removal MicroBeads (Miltenyi Biotec) and incubated for 15min at room temperature. Alongside, an LS column (Miltenyi Biotec) was placed on a MidiMACS™ Separator (Miltenyi Biotec) and washed with 3mL 1X Binding Buffer, composed by 20X Binding Buffer Stock Solution (Miltenyi Biotec) diluted in sterile ddH_2O. The cell suspension was then added to the column, alongside 3mL 1X Binding Buffer. Cells were allowed to pass through the column, which was then washed four times with 3mL 1X Binding Buffer. The effluent was collected and live cells counted.

To accurately distinguish them from NK cells, a PKH67 membrane dye (Sigma-Aldrich) was used to label K562 cells. Prior to labelling K562 cells were washed with

serum-free RPMI medium by 5min centrifugation at 400g. The supernatant was removed and the cell suspension was prepared by the addition of 0.25mL Diluent C to the pellet. Immediately prior to staining, 1µL of the PKH67 ethanolic dye solution was added to 0.25mL Diluent C. The cell suspension was mixed with the dye solution and incubated for 3min at room temperature in the dark, being periodically mixed. To stop staining 2.5mL complete medium was added and the mixture was incubated for 1min. The supernatant was removed after a 10min centrifugation at 400g and the stained cells were washed three times with 10mL complete medium by 5min centrifugations at 400g.

NK cells required for the cytotoxicity assay were isolated from fresh PBMCs by negative selection, using the EasySep™ Human NK Cell Isolation Kit (STEMCELL Technologies) (Figure 18B). PBMCs were resuspended in EasySep™ Buffer (STEMCELL Technologies) at a $5x10^7$ cells/mL concentration. The cells were added to a 5mL Falcon™ tube (Fisher Scientific) alongside 50µL of EasySep™ Human NK Cell Isolation Cocktail per mL of suspension. The tube was gently vortexed and incubated at room temperature for 5min. EasySep™ Dextran RapidSpheres™ were vortexed for 30s and 50µL were added per mL of cell suspension. The tube was immediately topped-up with 2.5mL EasySep™ Buffer and was placed into the EasySep™ magnet (STEMCELL Technologies), where it was incubated for 3min at room temperature. The tube-magnet assembly was inverted for 3s, to allow pouring of enriched NK cells into a new tube.

Cultures composed of enriched NK cells and alive K562 cells were generated, with the cells added at a 0.5:1, 1:1, and 2:1 ratio (Figure 18C). K562 cell number remained constant between cultures at $5x10^4$ cells/well. The final volume of the co-

cultures was also maintained at 2mL. Duplicates of cultures were generated when an adequate NK cell number was available. Cells were co-cultured in complete RPMI medium for 2h, at 37ºC, and 5% CO_2. Control stained K562-only cultures, unstained K562 cultures, and unstained K562/NK cell co-cultures were also set up. After the 2h incubation, cells were washed with 2mL CellWash buffer (BD Biosciences) by 5min centrifugation at 400g. The pellet was resuspended in 1mL CellWash buffer. ~10^6 cells were added in Falcon™ tubes and were stained with 5μL anti-CD107a antibody (BioLegend), to assess degranulation.(644) The mixture was vortexed and was incubated for 20min on ice protected from light. Cells were washed with 2mL CellWash buffer by 5min centrifugation at 400g and the pellet was resuspended in 1mL CellWash buffer. Immediately prior to the flow cytometric analysis a 0.5mg/mL propidium iodide (PI) solution was prepared using 1mg/mL PI (Sigma-Aldrich) diluted in CellWash buffer. 25μL of solution were added to 1mL cell suspension, which was then incubated on ice, in the dark for 15min. Thus, a three colour panel was used (Table 11). Apart from the stained sample tubes and K562-only control, an unstained tube containing both K562 and NK cells was generated per sample. Although NK cells were examined for their degranulation levels, the main outcome of interest was K562 cell death, and thus these cells were used for compensation. Specifically, tubes containing single-stained K562 cells, with either PKH67, PI, or the anti-CD107a antibody and an unstained K562 cell control were generated for compensation. The samples and controls were examined by flow cytometry using the BD FACSCanto™ II (BD Biosciences) cytometer.

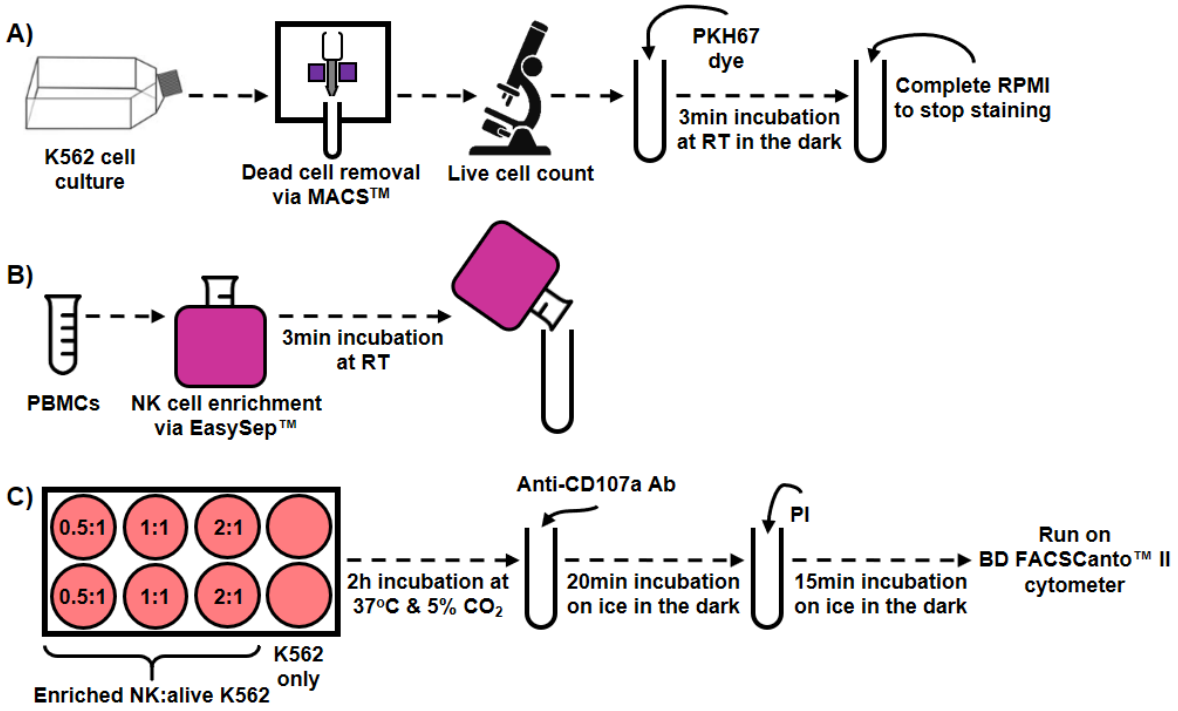


Figure 18. Summary of the experimental pipeline for Natural Killer (NK) cell cytotoxicity assessment. *The major steps of the protocols followed for A) alive K562 isolation and staining, B) NK cell enrichment, and C) NK-K562 co-culture for the evaluation of NK cell degranulation, using CD107a as a degranulation marker, and the examination K562 cell death, using propidium iodide (PI), are illustrated. Wash steps are not included. Ab: antibody, CD: cluster of differentiation, complete RPMI: Roswell Park Memorial Institute 1640 medium containing 10% FBS and 1% penicillin/streptomycin, PBMCs: peripheral blood mononuclear cells, RT: room temperature*

Table 11. Cytotoxicity assay panel. *The dyes used to stain target K562 cells, dead cells, and examine the levels of Natural Killer (NK) cell degranulation, through the assessment of CD107a expression, are displayed alongside their respective fluorophore. APC: allophycocyanin, FITC: fluorescein isothiocyanate, PE: phycoerythrin*

Dye	Fluorophore	Rationale
PKH67	FITC	K562 cell staining
Propidium iodide	PE	Dead cell staining
Anti-CD107a antibody	APC	NK cell degranulation assessment

4.11.1 Data analysis

Data was acquired using the BD FACSCanto™ Software (BD Biosciences) and the resulting uncompensated .fcs files were processed using FlowJo v10.6.2.[636] Similar to the flow-based assay, sample quality was assessed and data was cleaned up using FlowAI 2.0.[637] All further analysis was performed on the "GoodEvents" subset.

To correct for fluorescence spillover compensation was performed. A compensation matrix was generated using the single-stained K562 cell data and a universal unstained K562 control. The singlet population was gated on and single-stained K562 cells were used to detect a positive signal for each dye, while unstained K562 cells were used for negative signal detection. The resulting matrix was applied to all samples.

A standardize gating strategy was pursued (Figure 19), with single cells detected followed by alive $PI^{-}PKH67^{+}$ and dead $PI^{+}PKH67^{+}$ K562 cells, as well as alive $PI^{-}PKH67^{-}$ and dead $PI^{+}PKH67^{-}$ NK cells identification. In both the alive and dead NK cell gates the percentage of cells expressing CD107a and the median intensity of this marker's expression were examined.

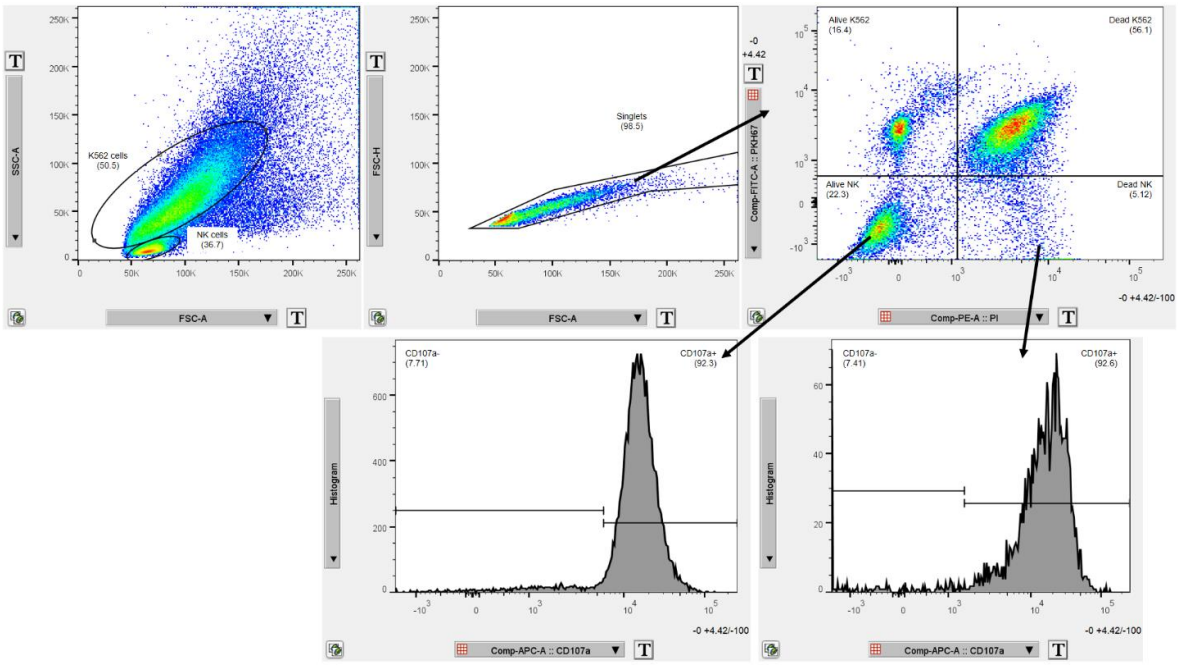


Figure 19. Natural Killer (NK) cell cytotoxicity assay gating strategy. *The NK and K562 populations are displayed according to their side (SSC-A) and forward scatter (FSC-A) area. In the "FlowAIGoodEvent" population the singlet population was gated on, according to the forward scatter height (FSC-H) and FSC-A. In that gate the alive and dead NK and K562 cell populations were detected, according to the PKH67 membrane dye staining of K562 cells and the propidium iodide (PI) staining of dead cells. In the alive and dead NK cell gates the expression of CD107a was examined.*

Data were exported to Excel 2016.[638] For duplicate cultures, median values were calculated. Specific target cell death was calculated according to the following equations:[645, 646]

K562 death (%)=100xdead K562/(dead K562+alive K562)

Specific target cell death (%)=100xNK cell cytotoxicity/(Maximum death–K562 death in control)=100xNK cell cytotoxicity/[100–100xdead $K562_{control}$/(dead $K562_{control}$+alive $K562_{control}$)], where NK cell cytotoxicity=K562 death in co-cultures

(%)–K562 death in K562-only control (%)=100xdead $K562_{co\text{-}cultures}$/(dead $K562_{co\text{-}cultures}$+alive $K562_{co\text{-}cultures}$)–100xdead $K562_{control}$/(dead $K562_{control}$+alive $K562_{control}$)

Data from cultures were different NK:K562 cell ratios were used, were examined separately, but the average value for each sample was also calculated on Excel 2016 and was entered into GraphPad Prism 6.[639] The effect of the different culture ratios on these parameters of NK cell activity was also statistically evaluated using GraphPad Prism 6.[639]

4.12 Enzyme-linked immunosorbent assay

For the examination of cytokine and cytolytic molecule secretion by PBMCs the ProcartaPlex™ Multiplex Immunoassay (ThermoFisher Scientific) was used (Figure 9C, Table 12). The assay targeted G-CSF, GM-CSF, IFN-γ, TNF-α, IL-2, IL-4, IL-5, IL-8, IL-10, IL-13, IL-17A, granzyme A, granzyme B, and perforin, using magnetic microspheres of different sizes (ELISA optimization and validation detailed in Appendices, Chapter 13.17).

Table 12. Enzyme-linked immunosorbent assay panel. *The targets of the antibody-coated microspheres, which were used to evaluate the secretion levels of cytokines and cytolytic granule contents by peripheral blood mononuclear cells (PBMCs), are displayed alongside the respective microsphere number. G-CSF: granulocyte-colony stimulating factor, GM-CSF: granulocyte-macrophage colony-stimulating factor, IFN: interferon, IL: interleukin, TNF: tumor necrosis factor*

Target	Microsphere number	Rationale
G-CSF	42	Evaluation of cytokine secretion by PBMCs
GM-CSF	44	
IFN-γ	43	
IL-10	28	
IL-13	35	
IL-17A	36	
IL-2	19	
IL-4	20	
IL-5	21	
IL-8	27	
TNF-α	45	
Granzyme A	74	Evaluation of cytolytic molecule secretion by PBMCs
Granzyme B	72	
Perforin	53	

Due to the inclusion of multiple cytokine-targets, six standard solutions were utilised. The antigen standard vials were centrifuged for 10s at 2000g. 50µL cell culture medium, composed by RPMI (Thermo Fisher Scientific) supplemented with 10% heat-inactivated FBS (Thermo Fisher Scientific) and 1% penicillin/streptomycin (Thermo Fisher Scientific), was added in five of the standard vials. The vials were gently vortexed for 30s, were centrifuged at 2000g for 10s, and were incubated on ice for 10min to allow full reconstitution. The contents of one of the reconstituted vials were transferred to the remaining standard vial, which was also vortexed for 30s, centrifuged at 2000g for 10s, and incubated on ice for 10min. After all standards were reconstituted the contents of each vial were pooled into one. This vial was

gently vortexed for 30s and centrifuged for 10s at 2000g. The ProcartaPlex™ Multiplex Immunoassay User Guide [Publication Number MAN0017081 Revision G.0 (38)] (ThermoFisher Scientific) was then followed. 4-fold serial standard dilutions were performed and were retained on ice.

PBMC culture supernatants stored in -80ºC were thawed on ice, vortexed, and centrifuged at 10000g for 10min to remove particulates and avoid generation of microsphere aggregates. Simultaneously, the 10X Wash Buffer Concentrate was brought to room temperature and was vortexed for 15s. 20mL of Wash Buffer Concentrate were then mixed with 180mL ddH_2O, with the 1X dilution used in the assay. To prepare the plate, Magnetic Microsphere solution was vortexed for 30s, with 50µL added per well of a 96-well Flat Bottom Plate. The plate was inserted into a Hand-Held Magnetic Plate Washer (ThermoFisher Scientific) and incubated at room temperature for 2min to allow microsphere accumulation at the bottom. Following incubation, liquid was removed and 150µL 1X Wash Buffer was added to each well. The plate was again incubated on the washer for 2min. The Wash Buffer was removed and the plate was removed from the washer. 50µL of the standard dilutions, blank, stimulated, and unstimulated samples were added into dedicated wells. The standard dilutions and blank were added in duplicates. The plate was sealed with Plate Seal, covered with a Black Microplate Lid, and was incubated for 120min at room temperature on a plate shaker at 700rpm. The plate was then placed on the washer, incubated for 2min, and the liquid was removed. The plate was washed twice with 150µL 1X Wash Buffer. 25µL of 1X Detection Antibody Mixture were added in each well and the plate was sealed, covered, and incubated for 30min at room temperature, being shaken at 700rpm. The plate was incubated for 2min on

the washer, the liquid was removed, and the plate was washed twice. 50µL of streptavidin-R-phycoerythrin were then added in each well, the plate was sealed and covered, and it was incubated for 30min at room temperature on a plate shaker at 700rpm. Liquid was removed and the plate was washed twice. Lastly, 120µL Reading Buffer was added to each well and the plate was sealed, covered, and incubated at room temperature for 5min, shaken at 700rpm. The plate was run on Luminex® 200™ Instrument System (Thermo Fisher Scientific), using the Bio-Plex Manager Software 6.1 (Bio-Rad). Prior to each run the instrument was calibrated using the Bio-Plex Calibration Kit (Bio-Rad).

4.12.1 Data analysis

Raw data was exported from the Bio-Plex Manager Software 6.1 (Bio-Rad) to Excel 2016,[638] where it was reviewed to ensure that microsphere counts were higher than 50 per sample and microsphere aggregates were lower than 30%. The coefficient of variation of the duplicates of each standard dilution for each marker of interest was examined. This value was calculated by dividing the standard deviation of each duplicate set by the respective mean. Values lower than 20% were accepted. The recovery rate for the observed versus the expected concentrations for each standard was also examined to ensure values were between 70 and 130. Recovery rate was calculated by dividing the observed value by the expected one and multiplying the result by 100. If the coefficient of variation value was higher than 20% or the recovery rate was outside the accepted range, the standard curve for the respective marker was adjusted through the removal of outliers from the automatically optimized standard curve. The observed concentration (pg/mL) for each of the samples and unstimulated controls was recorded. Values reported to be

out of range were replaced with the highest or lowest values of the respective standard. Pro- to anti-inflammatory cytokine secretion ratios were also calculated. The resulting data were statistically analysed in GraphPad Prism 6.[639]

4.13 Statistical analysis and data presentation

4.13.1 Survey

Most survey data were presented in the form of descriptive statistics, using tables generated via Excel (Microsoft Office, 2016). Responses collected using a Likert scale were assigned numerical values (1=Not effective/Would not suggest, 2=Rarely effective/Would probably not suggest, 3=Somewhat effective/Could suggest depending on the case, 4=Often effective/Would probably suggest, 5=Very effective/Would definitely suggest) and were analysed and using GraphPad Prism 6.[639] Due to the ordinal nature of the data no normality test was performed. Responses referring to “other” treatments were excluded from the analysis as no further information was provided. Data was paired, with information from the same responder recorded for the various therapies, and hence the Friedman non-parametric test ($\alpha=0.05$) was used. However, this required the exclusion of incomplete responses with data missing for any of the included therapies, resulting in the analysis of $N=17$ responses. Dunn’s post-hoc test (Family-wise $\alpha=0.05$) was also used to perform pairwise comparisons of the therapies. The family-wise threshold of significance was set to 0.05 and the multiplicity adjusted p values were reported. Results were presented using GraphPad Prism 6.

4.13.2 Participant demographics

Participants' demographic characteristics were examined using GraphPad Prism 6 to investigate the presence of potential differences, possibly affecting immune activity. The distribution of continuous quantitative datasets, including age, BMI, and time of blood collection was initially assessed using the D'Agostino-Pearson omnibus normality test (α=0.05). If both the RPL and control datasets followed normal distribution an unpaired t test (α=0.05) was used. In that case an F test was performed to examine the variances of the populations. If significant difference between variances was detected ($p<0.05$) the Welch's correction was applied to the unpaired t test. If one or both datasets was found not to follow normal distribution, the Mann-Whitney test (α=0.05) was performed. The Mann-Whitney test was also performed to evaluate the potential differences in discrete quantitative datasets, including gravidity and parity. The Median and 95% Confidence Interval (CI) were used for the description of non-normally distributed quantitative data. Categorical data was analysed in the form of contingency tables in GraphPad Prism 6 using Chi-square (α=0.05) or, when a 2x2 contingency table was examined, Fisher's exact test (α=0.05). Data were presented via graphs generated on Excel.

4.13.3 TBNK, flow, cytotoxicity assay, and ELISA

Processed TBNK, flow, cytotoxicity, and ELISA data was entered into GraphPad Prism 6 for further statistical analysis.[639] As previously described, data distribution was assessed via the D'Agostino-Pearson omnibus normality test and according to the distribution an unpaired t test, with or without the Welch's correction, or a Mann-Whitney test was performed. For paired data, when normal distribution was detected

a paired t test (α=0.05) was used. When at least one of the datasets was found not to follow normal distribution the Wilcoxon matched-pairs signed rank test (α=0.05) was utilised. For comparisons between more than two paired datasets, in the case of non-normally distributed data, the Friedman test was used, accompanied by the Dunn's test for multiple comparisons. P values adjusted for multiple comparisons were reported.

Data were presented using GraphPad Prism 6, with the Mean and Standard Deviation displayed when all datasets were normally distributed and the Median displayed when at least one dataset did not follow normal distribution. In text, the Mean and Standard Deviation (SD) or Median and 95% Confidence Interval (CI) was reported. In certain cases, the interquartile range (IQR) was reported as a measure of variability.

4.13.4 Subpopulation analysis

Women with idiopathic or non-idiopathic RPL were separately examined to investigate whether immune dysregulation constitutes a universal miscarriage mechanism. The subpopulation of women with at least five losses in their reproductive history was also examined to assess the potential impact of higher order losses. Both the RPL and control populations were also split into age- and ethnicity-related subpopulations to assess the impact of potential age- and ethnicity-associated immune alterations in RPL. To control for ethnic diversity and alcohol intake, parameters found to be significantly different between the total RPL and control populations, were compared between the White and low alcohol-consuming subpopulations, respectively. These subgroups were chosen due to their overall

power and the similar distribution of women between the RPL and control subpopulations. Lastly, to evaluate the predictive potential of immune biomarkers in regards to the subsequent pregnancy outcome of women with RPL, the RPL group was split into two subgroups, one including both women undergoing the 3rd trimester of their subsequent pregnancy and those who had a live birth following their recruitment and a one including women with a following miscarriage. Comparisons between subpopulations and controls were performed in GraphPad Prism 6 utilizing the statistical analysis strategy described. When more than two unpaired datasets were analysed, the parametric one-way analysis of variance (ANOVA) (α=0.05) or the non-parametric Kruskal-Wallis test (α=0.05) was used, accompanied by a Dunn's multiple comparisons test.

4.13.5 Mass cytometry

High-dimensional data was analysed and presented using 64-bit R 4.0.3 and RStudio.[647, 648] The CATALYST pipeline, and the *CATALYST*, *cowplot*, *flowCore*, *diffcyt*, *scatter*, *SingleCellExperiment*, *umap*, and *uwot* packages were used (Appendices, Chapter 13.13).[649-658] All markers included in the mass cytometry panel were entered in R 4.0.3, excluding the lineage markers based on which NK, T, and B cells were identified. Markers included in our panel were chosen as relatively stable cell features that can be used to define the cells' identity and were thus characterised as cell "type" markers.[659] Data and metadata were entered in a *SingleCellExperiment* format. High-resolution clustering was performed via *FlowSOM* and metaclustering via *ConsensusClusterPlus*. 20 clusters were generated to maximize stability, as is displayed in the Delta area plot (Figure 20). Total cell counts in each cluster were reported.

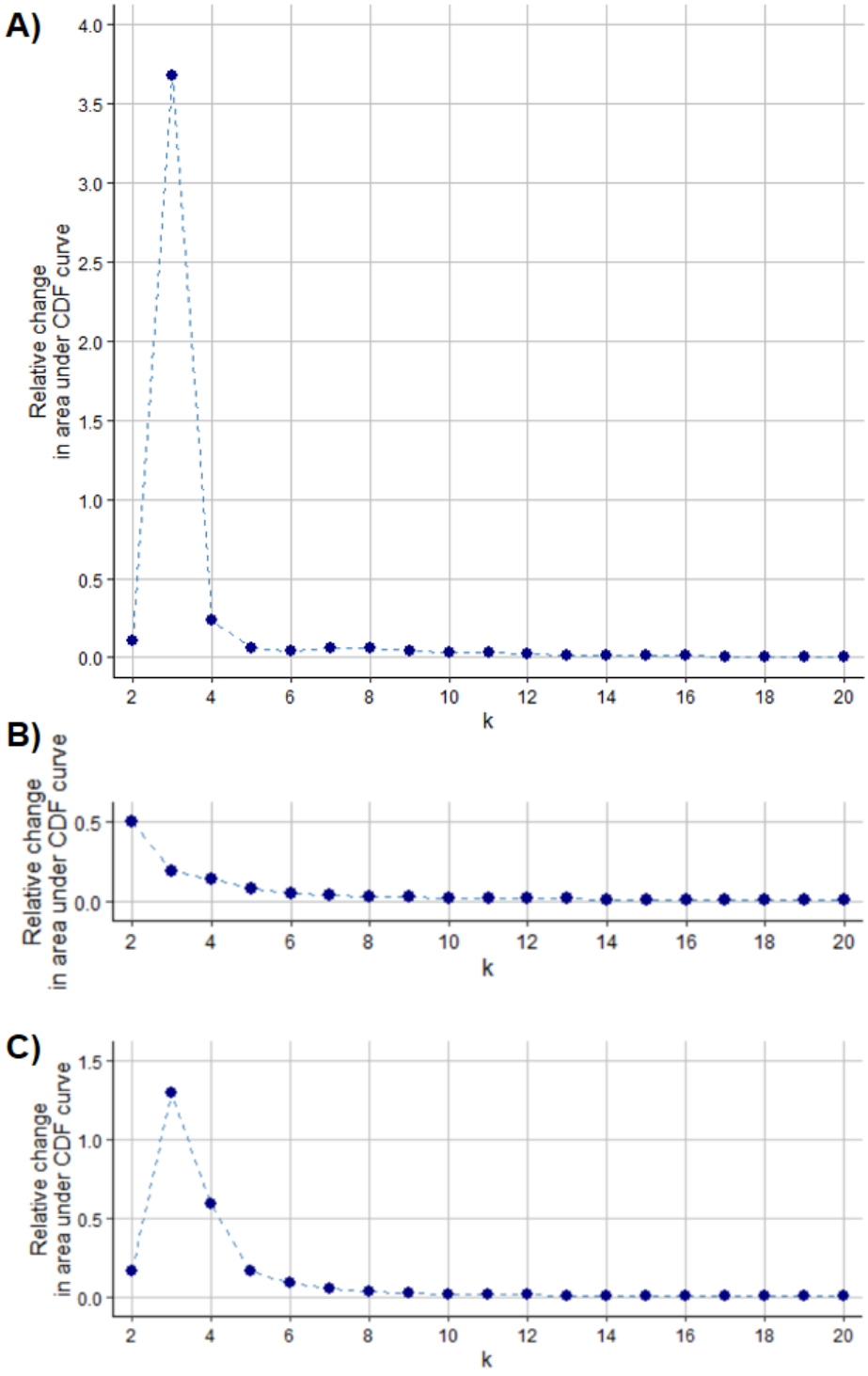


Figure 20. Delta area plot generated following FlowSOM clustering and ConsensusClusterPlus metaclustering. *The delta score, represented by the relative change in the area under the CDF curve, indicates the relative amount of additional cluster stability obtained when clustering into k groups, compared to clustering into k-1 groups, in each of the A) Natural Killer, B) T, and C) B cell datasets.*

CATALYST was used for dimensionality reduction, taking into account 1000 randomly selected cells per sample.[651] Differential abundance testing was then performed using *diffcyt*.[659] Randomized ion counts generated by mass cytometry are expected to follow a log-normal distribution and thus an inverse hyperbolic sine transformation was used for normalisation. The method performed to examine the differential abundance of cell population was *diffcyt-DA-edgeR*, calculating cluster abundance based on cell counts, with clusters with low counts being excluded.[659] To correct for multiple comparisons, adjusted p values were reported. The threshold of significance for adjusted p values was set at 0.05.

4.14 Statistical analysis for biomarker identification

Immune markers that could identify women with RPL in the clinical setting were investigated. RPL (*N*=100) and control (*N*=80) data for 111 markers, obtained via flow cytometry, cytotoxicity assay, and ELISA was utilised (Supplementary Table 2). All following analysis was performed by Dr Animesh Acharjee and Prof Georgios Gkoutos.

Statistical analysis was performed using R 4.1.0 and multiple packages, including *randomForest*, *ggplot2*, *caret*, and *metaboanalyst*.[648, 660-663] Markers with >50% missing data were excluded from the analysis. In the case of markers missing ≤50% of data, missing values were imputed with the mean value of the respective marker. Outliers were defined as values with higher than 5xfold change. No outliers were detected. As variables were measured on different scales, an auto-scaled standardized normalisation was performed to provide each of the markers equal weights, according to the following equation:

Normalised $x=(x- \bar{x})/\sigma_x$, where $\bar{x}$ represents the mean and σ the standard deviation of the variable of interest.

A combination of both univariate and multivariate approaches was utilised for biomarker analysis. Univariate analysis for each marker was performed via the Wilcoxon signed-ranked test and the False Discovery Rate (FDR)-corrected p values were obtained, via the Benjamini-Hochberg procedure. The FDR-adjusted p values were then ranked from lowest to highest, with 0.05 being set as the threshold for statistical significance. Multivariate analysis was also performed using two methods: Least Absolute Shrinkage and Selection Operator (LASSO) and Elastic Net (EN).[664, 665] Both methods are based on the random forest classification algorithm and are used for selecting important features. The two methods differ on the interpretation of strongly associated markers, with LASSO do not taking into consideration the correlation factor and EN capturing the clusters of correlating markers. 10-fold cross-validation was performed to optimise the penalty. Both methods were run 100 times, with markers contributing to the variation between the RPL and control cohort being selected and markers not contributing being removed. Markers were then ranked based on the frequency that they were selected. Finally, the first quartile of markers was selected. The overlap between chosen markers was considered.

Code utilised is published and made available by Dr Animesh Acharjee and Prof Georgios Gkoutos on their GitHub repositories: https://github.com/jaw-bioinf/Biomarker_Identification/ and github/InFlamUOB/NSDTraumaMODS.[664, 665]

Taking into consideration the biological relevance and clinical application of each of the highest-ranking markers, 4 potential markers were selected for additional analysis. The Wilcoxon signed-ranked test was again utilised, alongside the Benjamini-Hochberg procedure.

5 NATIONAL SURVEY EXPLORING THE CURRENT PRACTICE FOR THE DIAGNOSIS AND MANAGEMENT OF IDIOPATHIC RPL

Parts of this chapter have been submitted for publication as:

Bagkou Dimakou D, Tamblyn J, Chu J, Coomarasamy A, Richter A. Diagnosis and management of idiopathic recurrent pregnancy loss (RPL): Current immune testing and immunomodulatory treatment practice in the United Kingdom. J Reprod Immunol.

5.1 Results

5.1.1 Respondent/institution demographics

Survey responses from England and Scotland were collected (Figure 21). Overall, 37/148 responses were received (Total response rate=25.00%). Of these, 5 were partially completed. The respondent group consisted of 25 (71.43%) Obstetrics and Gynaecology Consultants, 6 (17.14%) Specialist Nurses, including 1 Research Nurse, 2 (5.71%) Associate Specialists, 1 (2.86%) Professor in Obstetrics and Gynaecology, and 1 (2.86%) Clinical Manager (Table 13A). 35 (97.22%) of the respondents worked in NHS clinics, including 1 NHS-research, and 1 (2.78%) belonged to the private sector (Table 13B).

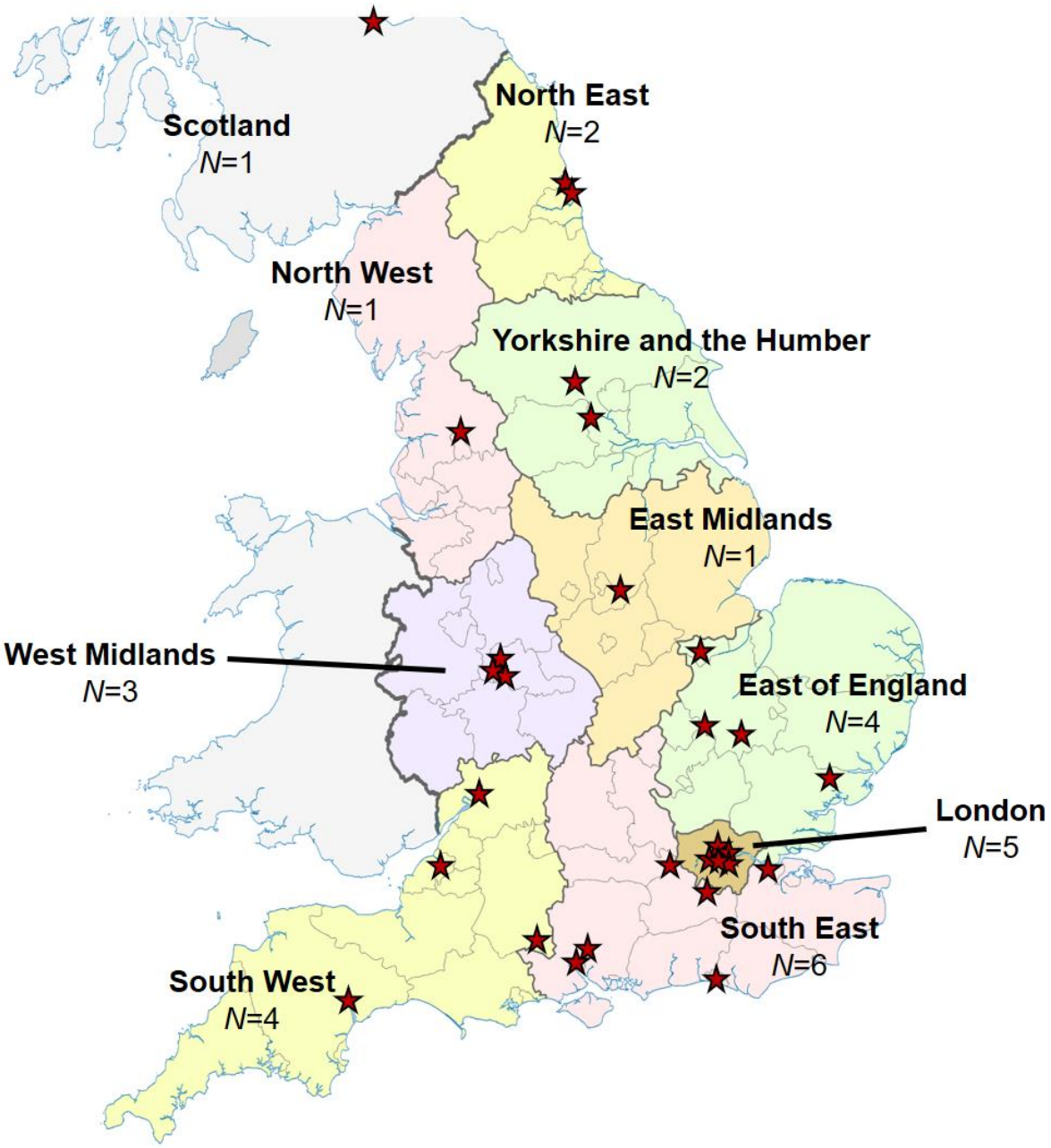


Figure 21. Respondent geographical location. *The number of responses collected from clinics in different regions of England and Scotland is illustrated, alongside the clinics' approximate geographical location (stars). (Response rate=78.38%) Picture adapted from Wikipedia (https://en.wikipedia.org/wiki/File:English_regions_2009.svg)*

Table 13. Respondent job designation and healthcare sector. *Both the total number of responses (N) and the percentage (%) calculated based on the total responses collected for each question is displayed. NHS: National Health Service (A - Response rate=94.59%, B - Response rate=97.30%)*

Respondent/institution information	*N* (%)
A) Respondent specialization/position	
Consultant Obstetrician and Gynaecologist	25 (71.43%)
Nurse	6 (17.14%)
Associate Specialist	2 (5.71%)
Professor in Obstetrics and Gynaecology	1 (2.86%)
Clinical Manager	1 (2.86%)
B) Sector	
NHS	35 (97.22%)
Private	1 (2.78%)

Overall, 25 (67.57%) of respondents confirmed that a specific protocol is followed in their clinics for the diagnosis and management of RPL, whilst the remaining 12 (32.43%) reported that no such protocol exists in their clinics (Table 14). Wide variance in guideline use was observed: 9 (36.00%) respondents followed RCOG guidelines, 4 (16.00%) ESHRE guidance, 1 (4.00%) NICE guidelines, while 5 (20.00%) clinics followed local protocols. 1 (4.00%) clinic reported using RCOG and ESHRE guidelines and 1 (4.00%) using a combination of local and ESHRE guidance. For respondents not following a protocol, the reason behind such a decision was not provided.

Table 14. Recurrent pregnancy loss service guidelines. *Both the total number of responses (N) and the percentage (%) calculated based on the total responses obtained for this question is shown. ESHRE: European Society of Human Reproduction and Embryology, NICE: National Institute for Health and Care Excellence, RCOG: Royal College of Obstetricians and Gynaecologists (Response rate=100.00%)*

Official guidelines followed	*N* (%)
Yes	25 (67.57%)
No	12 (32.43%)
Of "Yes"	
RCOG	9 (36.00%)
ESHRE	4 (16.00%)
NICE	1 (4.00%)
Local	5 (20.00%)
RCOG/ESHRE combination	1 (4.00%)
Local/ESHRE combination	1 (4.00%)
Did not specify	4 (16.00%)

5.1.2 RPL diagnosis

With regards to referral criteria, in 17 (54.84%) clinics women were reviewed after 3 previous losses and in 13 (41.94%) clinics after 2 losses (Figure 22A). Within these 13 clinics, 8 respondents specified that review after 2 pregnancy losses is offered to older women, with a 38 (*N*=1) and 40 (*N*=1) year limit specified. In the private sector (*N*=1), women were able to self-refer with no pre-specified referral criteria. In 20 (54.05%) clinics consecutive losses were required for women to be reviewed, while in 17 (45.95%) no such requirement was in place (Figure 22B). 33 (91.67%) of the clinics reviewed women with biochemical losses, while 3 (8.33%) did not take these losses into consideration when determining eligibility (Figure 22C). Additional pre-specified investigations were required in some NHS centres, including antiphospholipid antibody screening (*N*=1), thrombophilia testing (*N*=1), and 3D scanning (*N*=1), prior to review.

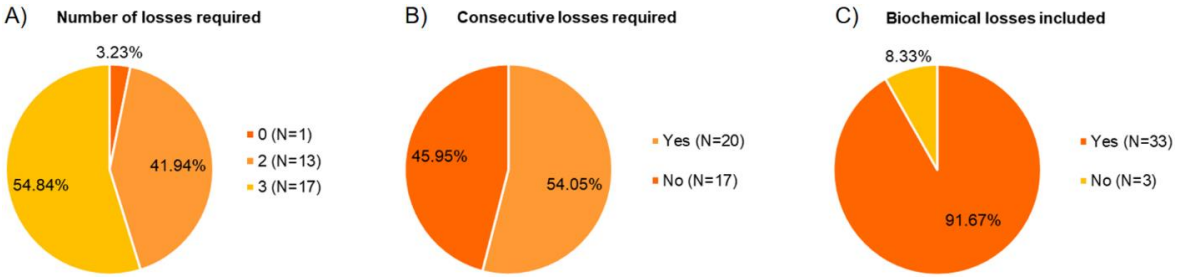


Figure 22. Diagnostic criteria for women review in recurrent pregnancy loss clinics. *Clinical criteria in regards to A) number of losses, B) presence of consecutive losses, and C) biochemical losses are illustrated. Both the number of responses (N) and percentage (%) calculated based on total responses obtained for each question is depicted. (A - Response rate=83.78%, B - Response rate=100.00%, C - Response rate=97.30%)*

5.1.3 Investigation of RPL risk factors

Information on the tests performed for the identification of risk factors associated with RPL was provided by 32 respondents (Figures 23-30). Pelvic ultrasonography (routinely: *N*=26, 81.25%; clinically indicated: *N*=6, 18.75%), fetal karyotyping (routinely: *N*=25, 78.13%; clinically indicated: *N*=7, 21.88%), anti-cardiolipin antibodies (routinely: *N*=30, 93.75%; clinically indicated: *N*=2, 6.25%), and lupus anticoagulant (routinely: *N*=30, 93.75%; clinically indicated: *N*=2, 6.25%) testing were performed in all clinics either routinely or when clinically indicated. These tests, as well as thyroid-stimulating hormone (TSH) level assessment (*N*=25, 78.13), were the tests most commonly routinely used for the detection of RPL risk factors (Figures 23-25, 27). The most common tests utilised when clinically indicated were hysteroscopy (*N*=26, 81.25%), maternal and paternal karyotyping (*N*=22, 68.75%), and hysterosalpingography (*N*=21, 65.63%) (Figures 23, 24). Other tests performed, but not routinely, included anti-Müllerian hormone (*N*=12, 37.50%), inhibin B (*N*=9, 28.13%), anti-smooth muscle (*N*=7, 21.88%), maternal (*N*=4, 12.50%) and paternal

(*N*=4, 12.50%) anti-sperm antibodies, and sperm DNA fragmentation (*N*=5, 15.63%) (Figures 26, 30).

Concerning haematological investigations, as summarised in Figure 25, the most common tests included lupus anticoagulant (routinely: *N*=30, 93.75%; clinically indicated: *N*=2, 6.25%), anti-cardiolipin antibodies (routinely: *N*=30, 93.75%; clinically indicated: *N*=2, 6.25%), Factor V Leiden (routinely: *N*=15, 46.88%; clinically indicated: *N*=10, 31.25%), Protein S deficiency (routinely: *N*=15, 46.88%; clinically indicated: *N*=10, 31.25%), and Protein C deficiency (routinely: *N*=15, 46.88%; clinically indicated: *N*=10, 31.25%).

The most commonly used tests evaluating the hypothalamic-pituitary-adrenal axis included the assessment of follicle-stimulating hormone (routinely: *N*=6, 18.75%; clinically indicated: *N*=14, 43.75%), luteinizing hormone (routinely: *N*=6, 18.75%; clinically indicated: *N*=14, 43.75%), and sex hormone binding globulin (routinely: *N*=3, 9.38%; clinically indicated: *N*=16, 50%) (Figure 26). A wide variation in thyroid- and diabetes-associated investigations was also displayed, with TSH (routinely: *N*=25, 78.13%; clinically indicated: *N*=5, 15.63%) and T4 (routinely: *N*=15, 46.88%; clinically indicated: *N*=9, 28.13%) thyroid testing being most commonly utilised and glycated haemoglobin (HbA1c) (routinely: *N*=8, 25%; clinically indicated: *N*=11, 34.38%) and random venous glucose (routinely: *N*=1, 3.13%; clinically indicated: *N*=15, 46.88%) diabetes testing being used either routinely or when clinically indicated (Figures 27, 28).

Infection-associated RPL investigations, including high vaginal ectocervical (routinely: *N*=3, 9.38%; clinically indicated: *N*=14, 43.75%) and endocervical swab

(routinely: *N*=3, 9.38%; clinically indicated: *N*=13, 40.63%) and low vaginal microbiology swab (routinely: *N*=1, 3.13%; clinically indicated: *N*=17, 53.13%) were found to be most commonly performed when clinically indicated, rather than routinely (Figure 29). Other diagnostic tests offered either routinely or clinically indicated included the assessment of homocysteine (routinely: *N*=1, 3.13%; clinically indicated: *N*=5, 15.63%), vitamin D (25OHD3) (routinely: *N*=3, 9.38%; clinically indicated: *N*=6, 18.75%), and anti-nuclear antibodies (routinely: *N*=5, 15.63%; clinically indicated: *N*=6, 18.75%) (Figure 30). In addition to the tests included in our survey, 2 (6.25%) of the respondents specified that magnetic resonance imaging scans were performed in the clinics for the identification of anatomical RPL risk factors.

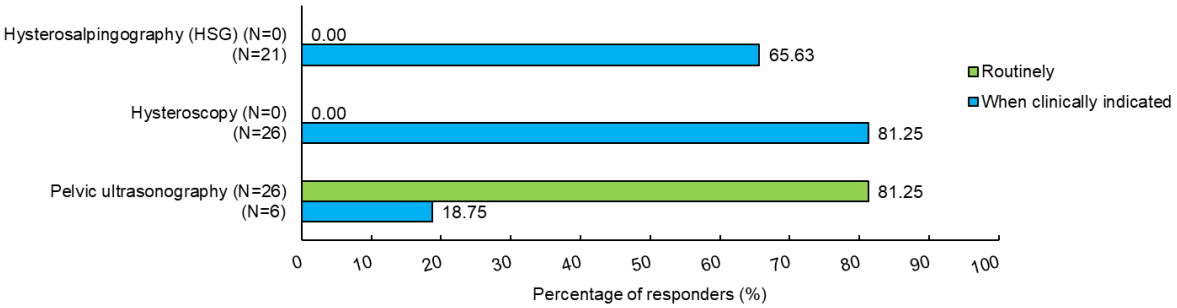


Figure 23. Summary of diagnostic tests performed for the investigation of anatomical risk factors potentially associated with recurrent pregnancy loss. *Both routine and clinically indicated investigations are included, with both the number of responses (N) and the percentage (%), calculated according to the total number of responses for the respective question (N=32). (Response rate=86.49%)*

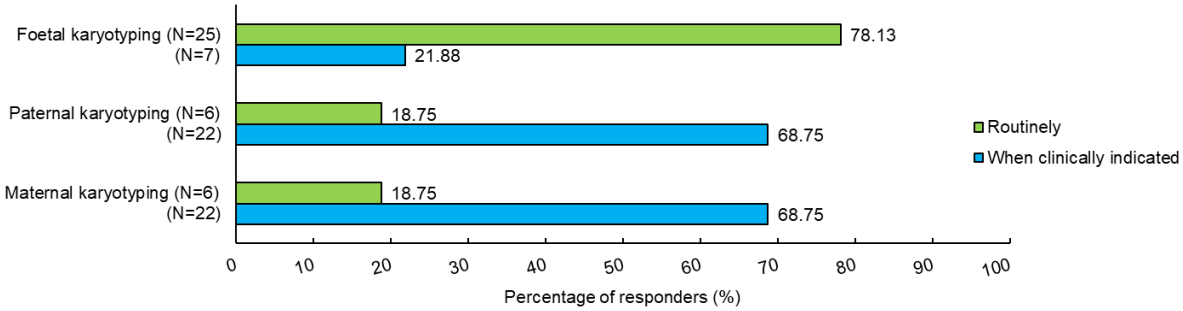


Figure 24. Summary of diagnostic tests performed for the investigation of genetic/chromosomal risk factors potentially associated with recurrent pregnancy loss. *Both routine and clinically indicated investigations are included, with both the number of responses (N) and the percentage (%), calculated according to the total number of responses for the respective question (N=32). (Response rate=86.49%)*

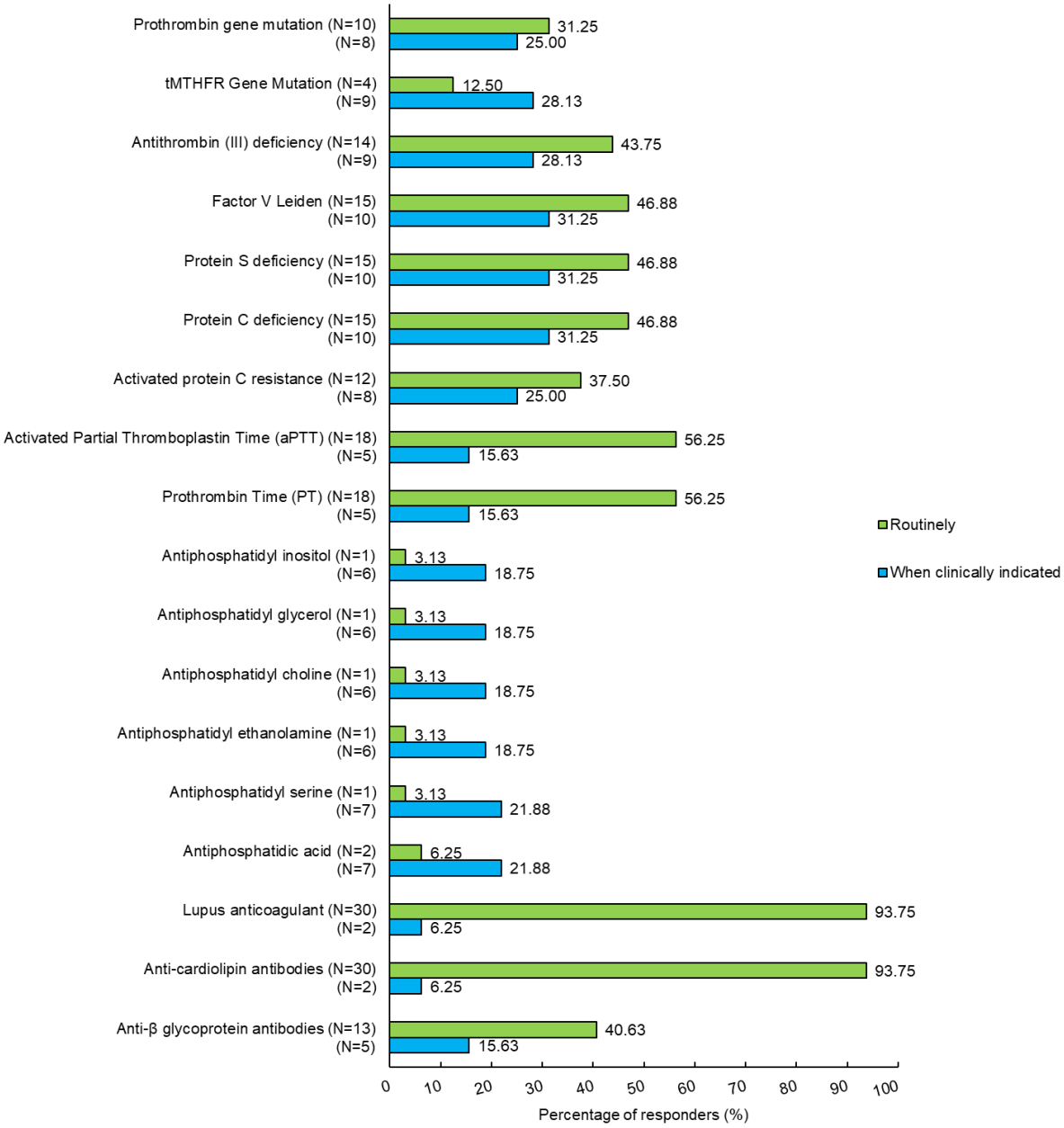


Figure 25. Summary of diagnostic tests performed for the investigation of haematological risk factors potentially associated with recurrent pregnancy loss. *Both routine and clinically indicated investigations are included, with both the number of responses (N) and the percentage (%), calculated according to the total number of responses for the respective question (N=32). (Response rate=86.49%)*

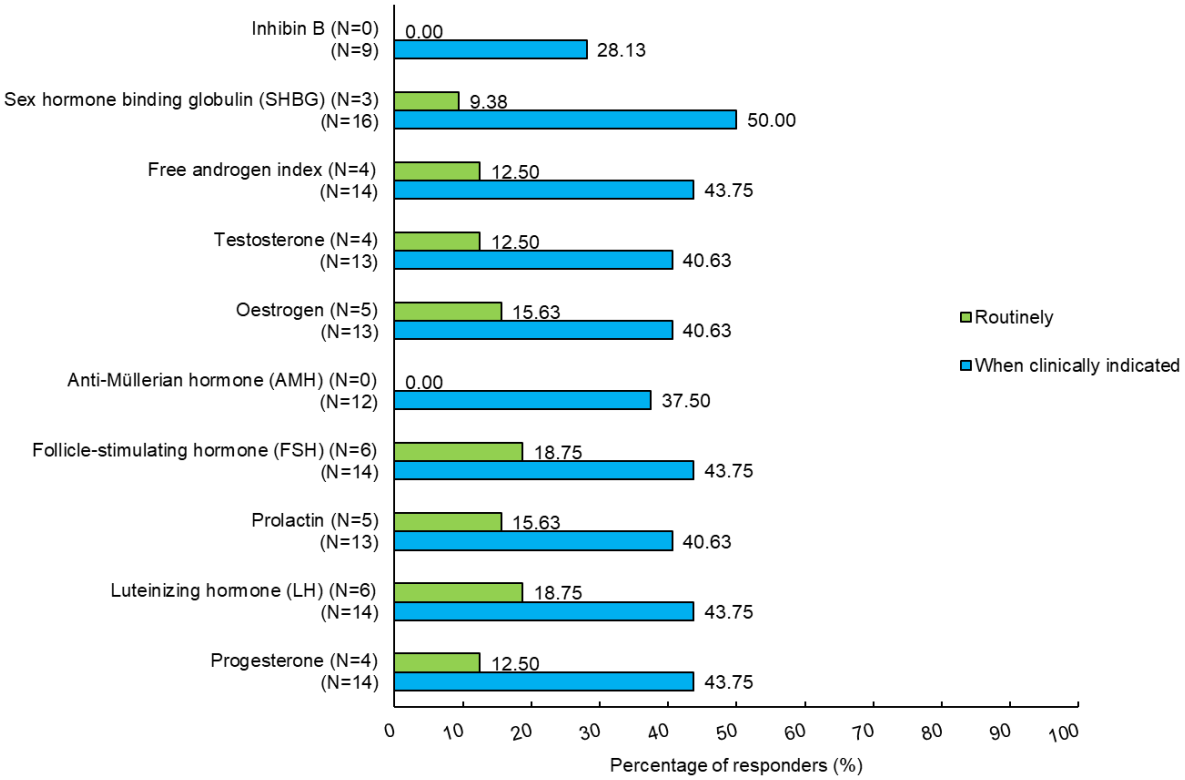


Figure 26. Summary of diagnostic tests performed for the investigation of hypothalamic-pituitary-adrenal axis-associated risk factors potentially linked to recurrent pregnancy loss. *Both routine and clinically indicated investigations are included, with both the number of responses (N) and the percentage (%), calculated according to the total number of responses for the respective question (N=32). (Response rate=86.49%)*

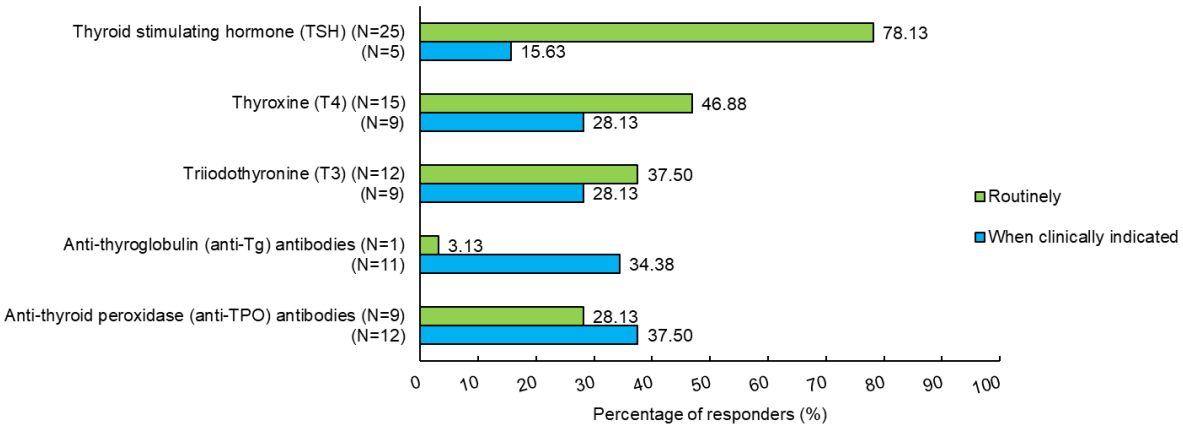


Figure 27. Summary of diagnostic tests performed for the investigation of thyroid-associated risk factors potentially linked to recurrent pregnancy loss. *Both routine and clinically indicated investigations are included, with both the number of responses (N) and the percentage (%), calculated according to the total number of responses for the respective question (N=32). (Response rate=86.49%)*

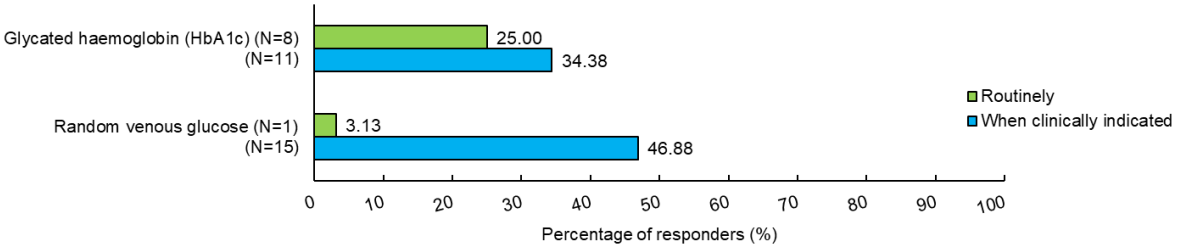


Figure 28. Summary of diagnostic tests performed for the investigation of diabetes-associated risk factors potentially linked to recurrent pregnancy loss. *Both routine and clinically indicated investigations are included, with both the number of responses (N) and the percentage (%), calculated according to the total number of responses for the respective question (N=32). (Response rate=86.49%)*

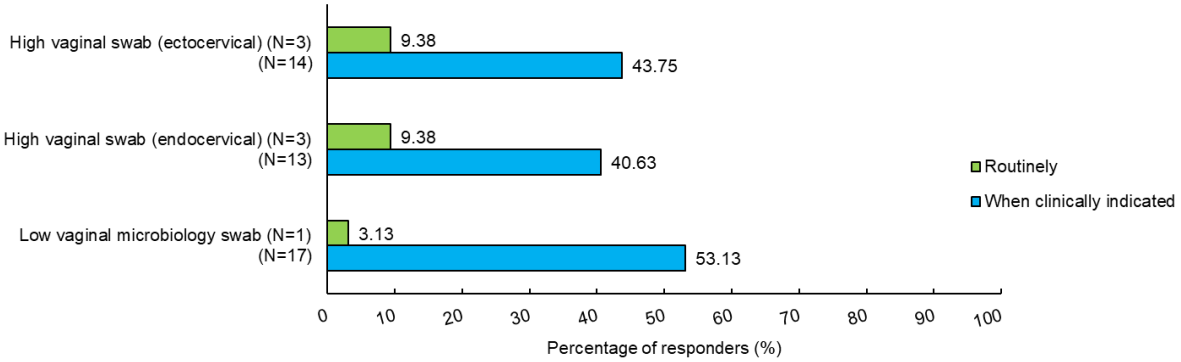


Figure 29. Summary of diagnostic tests performed for the investigation of infection-associated risk factors potentially linked to recurrent pregnancy loss. *Both routine and clinically indicated investigations are included, with both the number of responses (N) and the percentage (%), calculated according to the total number of responses for the respective question (N=32). (Response rate=86.49%)*

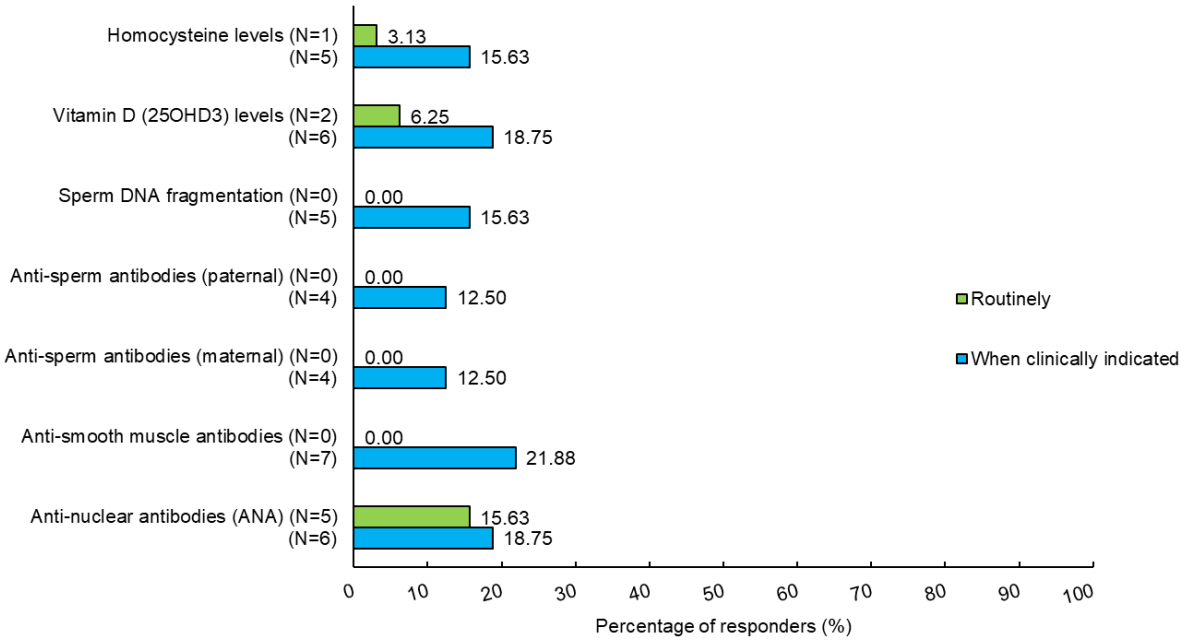


Figure 30. Summary of diagnostic tests performed for the investigation of additional risk factors potentially associated with recurrent pregnancy loss. *Both routine and clinically indicated investigations are included, with both the number of responses (N) and the percentage (%), calculated according to the total number of responses for the respective question (N=32). (Response rate=86.49%)*

5.1.4 Immunological investigations for RPL

Of particular interest in this survey was whether clinics were offering routine or clinically-focussed assessments of potential immunological RPL causes. As summarized in Table 15, immune-based tests were found not to be routinely offered by any of the responding clinics. However, in 3 (9.38%) clinics, NK, T, and B cell immunophenotyping, assessment of NK cell cytotoxicity, $CD4^+/CD8^+$ T cell immunophenotyping, and examination of T helper cell cytokine production was offered when clinically indicated. The 3 respondents were based at 1 private and 2 NHS-associated clinics. Treg and B-1/B-2 B cell immunophenotyping, as well as anti-HLA, anti-HY, and paternal blocking antibody screening, and HLA-typing were also offered when clinically indicated in the 2 (6.25%) NHS-affiliated clinics. Endometrial testing was performed in 1 (3.13%) NHS clinic, although this was reported to be part of a research trial. The use of immunological testing did not appear associated with the clinics' geographical location; the private clinic was based in the South East of England and the NHS clinics were located in the East of England and East Midlands.

Table 15. Diagnostic tests performed for the identification of immunological recurrent pregnancy loss (RPL) risk factors, either routinely or when clinically indicated. *The use of tests assessing the levels of Natural Killer (NK), T, and B cells, examining the helper (T_H), cytotoxic (T_C), and regulatory (Treg) T cell subpopulations and the B-1 and B-2 B cell subpopulations, and evaluating NK cell cytotoxicity and T_H cell cytokine production, as well as the use of anti-Human Leukocyte Antigen (HLA), anti-HY antibody, and anti-paternal blocking antibody screening and HLA-typing were investigated. Both the total number of responses (N) and the percentage (%) calculated based on the total responses obtained is illustrated (N=32). CD: cluster of differentiation (Response rate=86.49%)*

Investigation of immunological RPL risk factors	Routinely *N* (%)	When clinically indicated *N* (%)
NK, T, and B cell immunophenotyping	0 (0.00%)	3 (9.38%)
Assessment of NK cell cytotoxicity	0 (0.00%)	3 (9.38%)
$CD4^+$ T_H and $CD8^+$ T_C cell immunophenotyping	0 (0.00%)	3 (9.38%)
Treg immunophenotyping	0 (0.00%)	2 (6.25%)
Examination of T_H cell cytokine production	0 (0.00%)	3 (9.38%)
$CD5^+$ (B-1) and $CD5^-$ (B-2) B cell immunophenotyping	0 (0.00%)	2 (6.25%)
Anti-HLA antibody screening	0 (0.00%)	2 (6.25%)
Anti-HY antibody screening	0 (0.00%)	2 (6.25%)
Anti-paternal blocking antibody screening	0 (0.00%)	2 (6.25%)
HLA-typing (DQα sharing)	0 (0.00%)	2 (6.25%)

5.1.5 Idiopathic RPL management

With regards to treatment, the survey was focused on the management of idiopathic RPL (Table 16). The most common therapies were found to be supportive care and lifestyle changes, each of which was offered by 28 (87.50%) clinics. Folic acid was offered in 25 (78.13%) clinics, while progesterone was offered in 22 (68.75%). 10 respondents provided additional information about progesterone administration. In 6 clinics progesterone was initiated upon pregnancy confirmation. In 5 clinics 400mg progesterone were given, 2 of which specified that this dose was administered twice a day. Furthermore, in 2 clinics, progesterone were administered from the 14th day of the cycle until the 14th week of gestation. However, in 1 clinic, treatment was continued until the 16th gestation week. In the private clinic progesterone was initiated during the cycle in the form of pessaries, with progesterone injections utilised when required.

Aspirin was offered in 21 (65.63%) clinics and heparin in 15 (46.88%). More specifically, in 1 clinic aspirin was commenced prior to pregnancy, while in others (*N*=7) it was initiated after a positive pregnancy test or after viable intrauterine pregnancy confirmation by ultrasound scan at 7-8 gestation weeks. In different clinics, 75mg (*N*=5) or 150mg (*N*=3) of aspirin per day were prescribed to women. Based on information provided by 1 clinic, 75mg aspirin were administered when combined with low molecular weight heparin (LMWH), while 150mg were given when no heparin was prescribed. In 4 clinics aspirin was given in combination with LMWH, while 3 respondents specified that a combination of aspirin, heparin, and progesterone was administered. LMWH was commenced upon a positive pregnancy test, with a standard dose of 5000 units being utilised, adjusted for weight

(*N*=3). In 1 clinic, 75mg aspirin were administered peri-conception until the 34th pregnancy week, in combination with folic acid.

Anti-TNF-α agents, and more specifically adalimumab, and intralipid infusion were offered by the only private clinic included in the study. Adalimumab was administered to women prior to any fertility treatment. Prednisolone (*N*=5), prednisone (*N*=1), and IVIg (*N*=2) were also offered in some clinics. 1 respondent stated that upon a positive pregnancy test, 40mg prednisolone were used daily, being reduced to 5mg, while another specified that 20mg were administered only to selected cases, being gradually decreased. In the private clinic, steroids and intralipids or intravenous immunoglobulin were administered during the fertility treatment cycle and every 4 weeks during pregnancy until the 12th-16th week.

In the private clinic G-CSF and tacrolimus were also offered to some women with idiopathic RPL. It was noted that in private practice, prescription of immunomodulatory drugs to women with RPL was prohibited by the regulatory body, but prior to this regulation immunomodulators were only recommended when indicated. However, no further information in regards to the criteria guiding this decision were provided. Paternal cell and third-party donor leukocyte immunization, and trophoblast membrane infusion were not offered by any of the clinics responding to the survey.

Table 16. Treatments offered for the management of idiopathic recurrent pregnancy loss (RPL). *Both the total number of responses (N) and the percentage (%) calculated based on the total responses obtained (N=32) is depicted. (Response rate=86.49%)*

Idiopathic RPL management	*N* (%)
Aspirin	21 (65.63%)
Prednisone	1 (3.13%)
Prednisolone	5 (15.63%)
Progesterone	22 (68.75%)
Human chorionic gonadotropin (hCG)	1 (3.13%)
Anti-Tumour Necrosis Factor (TNF)-α agents	1 (3.13%)
Granulocyte-colony stimulating factor (G-CSF)	1 (3.13%)
Hydroxychloroquine	3 (9.38%)
Heparin	15 (46.88%)
Intravenous immunoglobulin (IVIg)	2 (6.25%)
Paternal cell immunization	0 (0.00%)
Third-party donor leukocyte immunization	0 (0.00%)
Trophoblast membrane infusion	0 (0.00%)
Intralipid infusion	1 (3.13%)
Endometrial scratching	3 (9.38%)
Folic acid	25 (78.13%)
Vitamin D supplementation	17 (53.13%)
Multivitamin supplementation	10 (31.25%)
Psychotherapy	8 (25.00%)
Supportive care	28 (87.50%)
Lifestyle changes (e.g. in case of obesity, high alcohol intake, illicit drug use, smoking)	28 (87.50%)

In regards to the efficiency and likelihood to suggest different treatments for the management of idiopathic RPL, most of the therapies were rated by the respondents as “not effective/would not suggest” (Tables 17-22). This included prednisone, other steroids and non-steroidal anti-inflammatory drugs, human chorionic gonadotropin (hCG) and other hormonal treatments, anti-TNF-α agents, G-CSF, hydroxychloroquine, IVIg, paternal cell and third-party donor leukocyte immunization, trophoblast membrane and intralipid infusion, and endometrial

scratching, with 79.17% to 100.00% of respondents stating that they are ineffective and they would not suggest them to women with RPL. On the other hand, based on the respondents' experience progesterone and folic acid appear more effective than hCG, anti-TNF-α agents, G-CSF, IVIg, paternal cell and third-party donor leukocyte immunization, trophoblast membrane and intralipid infusion, and endometrial scratching and hence they are more likely to be suggested for the treatment of RPL (Figure 31, Dunn's post-hoc test, $p<0.05$).

Table 17. Estimated efficiency and likelihood to suggest non-steroidal anti-inflammatory drugs and steroids for the management of idiopathic recurrent pregnancy loss. *Both the total number of responses (N) and the percentage (%) calculated based on the total responses obtained for each treatment is displayed. The response rate for each treatment is also illustrated.*

Treatment	Treatment efficiency/ Likelihood to suggest	*N* (%)	Response rate *N* (%)
Aspirin	Not effective/Would not suggest	11 (37.93%)	29 (90.63%)
	Rarely effective/Would probably not suggest	1 (3.45%)	
	Somewhat effective/Could suggest depending on the case	7 (24.14%)	
	Often effective/Would probably suggest	4 (13.79%)	
	Very effective/Would definitely suggest	6 (20.69%)	
Other non-steroidal anti-inflammatory drugs	Not effective/Would not suggest	23 (92.00%)	25 (78.13%)
	Rarely effective/Would probably not suggest	1 (4.00%)	
	Somewhat effective/Could suggest depending on the case	1 (4.00%)	
	Often effective/Would probably suggest	0 (0.00%)	
	Very effective/Would definitely suggest	0 (0.00%)	
Prednisone	Not effective/Would not suggest	19 (79.17%)	24 (75.00%)
	Rarely effective/Would probably not suggest	3 (12.50%)	
	Somewhat effective/Could suggest depending on the case	2 (8.33%)	
	Often effective / Would probably suggest	0 (0.00%)	
	Very effective/Would definitely suggest	0 (0.00%)	
Prednisolone	Not effective/Would not suggest	14 (60.87%)	23 (71.88%)
	Rarely effective/Would probably not suggest	5 (21.74%)	
	Somewhat effective/Could suggest depending on the case	3 (13.04%)	
	Often effective/Would probably suggest	0 (0.00%)	
	Very effective/Would definitely suggest	1 (4.35%)	
Other steroids	Not effective/Would not suggest	18 (85.71%)	21 (65.63%)
	Rarely effective/Would probably not suggest	1 (4.76%)	
	Somewhat effective/Could suggest depending on the case	1 (4.76%)	
	Often effective/Would probably suggest	1 (4.76%)	
	Very effective/Would definitely suggest	0 (0.00%)	

Table 18. Estimated efficiency and likelihood to suggest hormonal treatments for the management of idiopathic recurrent pregnancy loss. *Both the total number of responses (N) and the percentage (%) calculated based on the total responses obtained for each treatment is shown. The response rate for each treatment is also depicted.*

Treatment	Treatment efficiency/ Likelihood to suggest	*N* (%)	Response rate *N* (%)
Progesterone	Not effective/Would not suggest	4 (13.33%)	30 (93.75%)
	Rarely effective/Would probably not suggest	2 (6.67%)	
	Somewhat effective/Could suggest depending on the case	12 (40.00%)	
	Often effective/Would probably suggest	8 (26.67%)	
	Very effective/Would definitely suggest	4 (13.33%)	
Human Chorionic Gonadotropin (hCG)	Not effective/Would not suggest	19 (86.36%)	22 (68.75%)
	Rarely effective/Would probably not suggest	3 (13.64%)	
	Somewhat effective / Could suggest depending on the case	0 (0.00%)	
	Often effective/Would probably suggest	0 (0.00%)	
	Very effective/Would definitely suggest	0 (0.00%)	
Other hormonal treatment	Not effective/Would not suggest	19 (90.48%)	21 (65.63%)
	Rarely effective/Would probably not suggest	2 (9.52%)	
	Somewhat effective/Could suggest depending on the case	0 (0.00%)	
	Often effective/Would probably suggest	0 (0.00%)	
	Very effective/Would definitely suggest	0 (0.00%)	

Table 19. Estimated efficiency and likelihood to suggest biologic treatments for the management of idiopathic recurrent pregnancy loss. *Both the total number of responses (N) and the percentage (%) calculated based on the total responses obtained for each treatment is illustrated. The response rate for each treatment is also shown.*

Treatment	Treatment efficiency/ Likelihood to suggest	*N* (%)	Response rate *N* (%)
Anti-Tumour Necrosis Factor (TNF)-α agents	Not effective/Would not suggest	21 (100.00%)	21 (65.63%)
	Rarely effective/Would probably not suggest	0 (0.00%)	
	Somewhat effective/Could suggest depending on the case	0 (0.00%)	
	Often effective/Would probably suggest	0 (0.00%)	
	Very effective/Would definitely suggest	0 (0.00%)	
Granulocyte-Colony Stimulating factor (G-CSF)	Not effective/Would not suggest	19 (90.48%)	21 (65.63%)
	Rarely effective/Would probably not suggest	1 (4.76%)	
	Somewhat effective/Could suggest depending on the case	0 (0.00%)	
	Often effective/Would probably suggest	1 (4.76%)	
	Very effective/Would definitely suggest	0 (0.00%)	

Table 20. Estimated efficiency and likelihood to suggest allogeneic cell immunization for the management of idiopathic recurrent pregnancy loss. *Both the total number of responses (N) and the percentage (%) calculated based on the total responses obtained for each treatment is depicted. The response rate for each treatment is also displayed.*

Treatment	Treatment efficiency/ Likelihood to suggest	*N* (%)	Response rate *N* (%)
Paternal cell immunization	Not effective/Would not suggest	20 (100.00%)	20 (62.50%)
	Rarely effective/Would probably not suggest	0 (0.00%)	
	Somewhat effective/Could suggest depending on the case	0 (0.00%)	
	Often effective/Would probably suggest	0 (0.00%)	
	Very effective/Would definitely suggest	0 (0.00%)	
Third-party donor leukocyte immunization	Not effective/Would not suggest	20 (100.00%)	20 (62.50%)
	Rarely effective/Would probably not suggest	0 (0.00%)	
	Somewhat effective/Could suggest depending on the case	0 (0.00%)	
	Often effective/Would probably suggest	0 (0.00%)	
	Very effective/Would definitely suggest	0 (0.00%)	

Table 21. Estimated efficiency and likelihood to suggest vitamin supplementation for the management of idiopathic recurrent pregnancy loss. *Both the total number of responses (N) and the percentage (%) calculated based on the total responses obtained for each treatment is illustrated. The response rate for each treatment is also depicted.*

Treatment	Treatment efficiency/ Likelihood to suggest	*N* (%)	Response rate *N* (%)
Vitamin D supplementation	Not effective/Would not suggest	7 (26.92%)	26 (81.25%)
	Rarely effective/Would probably not suggest	0 (0.00%)	
	Somewhat effective/Could suggest depending on the case	3 (11.54%)	
	Often effective/Would probably suggest	6 (23.08%)	
	Very effective/Would definitely suggest	10 (38.46%)	
Multivitamin supplementation	Not effective/Would not suggest	9 (40.91%)	22 (68.75%)
	Rarely effective/Would probably not suggest	0 (0.00%)	
	Somewhat effective/Could suggest depending on the case	3 (13.64%)	
	Often effective/Would probably suggest	1 (4.55%)	
	Very effective/Would definitely suggest	9 (40.91%)	
Folic acid	Not effective/Would not suggest	5 (17.86%)	28 (87.50%)
	Rarely effective/Would probably not suggest	0 (0.00%)	
	Somewhat effective/Could suggest depending on the case	2 (7.14%)	
	Often effective/Would probably suggest	4 (14.29%)	
	Very effective/Would definitely suggest	17 (60.71%)	

Table 22. Estimated efficiency and likelihood to suggest other treatments for the management of idiopathic recurrent pregnancy loss. *Both the total number of responses (N) and the percentage (%) calculated based on the total responses obtained for each treatment is shown. The response rate for each treatment is also displayed.*

Treatment	Treatment efficiency/ Likelihood to suggest	*N* (%)	Response rate *N* (%)
Hydroxychloroquine	Not effective/Would not suggest	17 (85.00%)	20 (62.50%)
	Rarely effective/Would probably not suggest	0 (0.00%)	
	Somewhat effective/Could suggest depending on the case	2 (10.00%)	
	Often effective/Would probably suggest	0 (0.00%)	
	Very effective/Would definitely suggest	1 (5.00%)	
Heparin	Not effective/Would not suggest	11 (40.74%)	27 (84.38%)
	Rarely effective/Would probably not suggest	0 (0.00%)	
	Somewhat effective/Could suggest depending on the case	7 (25.93%)	
	Often effective/Would probably suggest	3 (11.11%)	
	Very effective/Would definitely suggest	6 (22.22%)	
Intravenous Immunoglobulin (IVIg)	Not effective/Would not suggest	20 (95.24%)	21 (65.63%)
	Rarely effective/Would probably not suggest	0 (0.00%)	
	Somewhat effective/Could suggest depending on the case	0 (0.00%)	
	Often effective/Would probably suggest	1 (4.76%)	
	Very effective/Would definitely suggest	0 (0.00%)	
Trophoblast membrane infusion	Not effective/Would not suggest	20 (100.00%)	20 (62.50%)
	Rarely effective/Would probably not suggest	0 (0.00%)	
	Somewhat effective/Could suggest depending on the case	0 (0.00%)	
	Often effective/Would probably suggest	0 (0.00%)	
	Very effective/Would definitely suggest	0 (0.00%)	
Intralipid infusion	Not effective/Would not suggest	19 (90.48%)	21 (65.63%)
	Rarely effective/Would probably not suggest	0 (0.00%)	
	Somewhat effective/Could suggest depending on the case	0 (0.00%)	
	Often effective/Would probably suggest	1 (4.76%)	
	Very effective/Would definitely suggest	1 (4.76%)	
Endometrial scratching	Not effective/Would not suggest	17 (85.00%)	20 (62.50%)
	Rarely effective/Would probably not suggest	2 (10.00%)	

	Somewhat effective/Could suggest depending on the case	1 (5.00%)	
	Often effective/Would probably suggest	0 (0.00%)	
	Very effective/Would definitely suggest	0 (0.00%)	

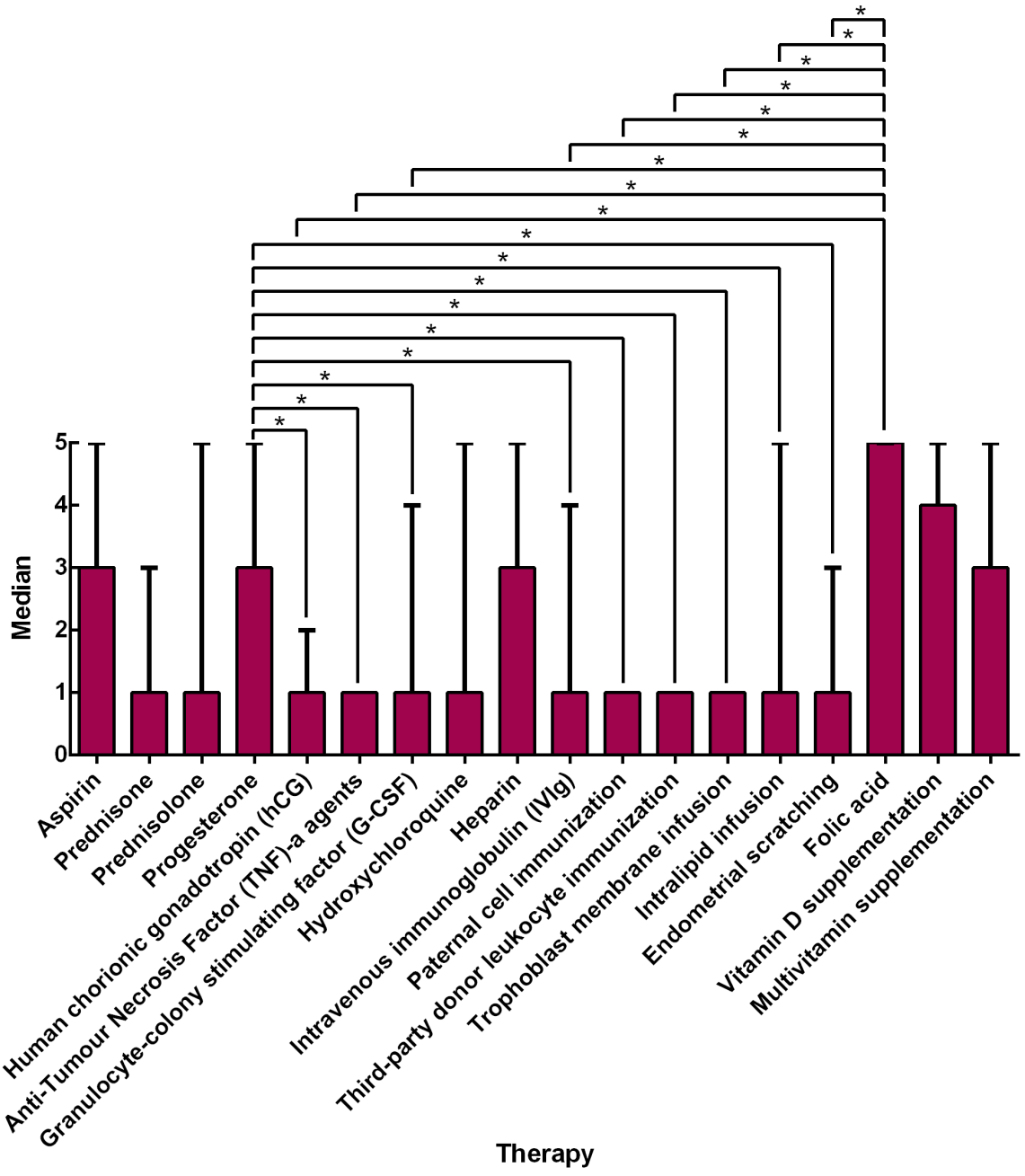


Figure 31. Median effectiveness/likelihood to suggest different treatments for the management of idiopathic recurrent pregnancy loss. *Medians were calculated based on responses obtained using a five-point Likert scale. Friedman test was used, accompanied by the Dunn's test for multiple comparisons, *: p≤0.05*

Clinical practice did not always align with the rating of different treatments. For example, 2 clinics using aspirin rated it as “not effective” and one rated it as “rarely effective”. Similarly, although prednisone was offered in 1 clinic it was rated as “not effective”. Prednisolone was rated as “rarely effective” by 2 respondents and “not effective” by 1 respondent, representing clinics utilising this treatment. 1 of the clinics utilising endometrial scratching rated it as “rarely effective”, while 3 clinics using folic acid rated it as “not effective”. Moreover, vitamin D and multivitamin supplementation were offered in 1 clinic each, being however described as “not effective”. On the other hand, progesterone was rated as at least “somewhat effective” by all respondents representing clinics that administered it, but was also rated as “often effective” by 2 clinics not utilising this treatment. Intralipid was also rated as “often effective” by 1 clinic not utilising it. Accordingly, vitamin D was rated as “very” and “often effective” by 2 clinics that however do not offer such treatment, while multivitamin supplementation was rated as “very effective” by 3 clinics not offering it.

5.2 Discussion

We successfully performed a National online survey evaluating current practice offered to couples with RPL. Importantly, we identified wide variation in the diagnosis, investigation, and management of RPL. Our findings primarily reflect NHS practice, with only one private clinic represented (Table 13B). Respondents represented RPL care across English regions, while one response from a Scottish clinic was also collected (Figure 21).

Even though a specific protocol is followed in most clinics, the guidelines used were highly varied (Table 14). Hence, the 2011 RCOG guidelines, which appeared as the most widely used, could be perceived as outdated,[1] with the newest guidelines being under review, potentially providing more up-to-date guidance.[666] Concerning eligibility for RPL specialist review, in more than half of the clinics women were assessed after 3 losses (Figure 22A). While clinics following RCOG guidance appear to adhere to the definition of RPL as the loss of at least 3 consecutive pregnancies,[1] in two of the four clinics following ESHRE guidance a 3 loss threshold was set in contrast to the ESHRE definition of RPL as at least 2, not necessarily consecutive, losses.[5] Interestingly, no previous loss threshold appear to be in place in the private clinic, even though more responses would be required to draw a meaningful conclusion about private practice. The requirement for consecutive miscarriages was one of the most controversial with ~54% of the respondents considering this parameter (Figure 22B). This highlights the inequality of miscarriage care between clinics. Miscarriage is a devastating condition for couples and thus standardized care is required to ensure an equitable approach. It has been shown that the miscarriage risk increases with each additional miscarriage, with women with RPL now shown to have a significant long-term reproductive and obstetric risk.[3, 24] As highlighted by a participant in Meaney et al. (2017),[667] requiring another loss after enduring 2 miscarriages can be particularly frustrating for women, especially those of advanced age. With new evidence arising, highlighting the need for earlier intervention,[668, 669] it is important to re-define the criteria for RPL investigations.

Similarly, high variability was detected in regards to the tests performed for the examination of RPL risk factors (Figures 23-30). However, tests such as pelvic ultrasonography, fetal karyotyping, antiphospholipid antibody screening, and TSH measurement were found to be used routinely in 78.13%-93.75% of the clinics included in our survey, in agreement to the ESHRE recommendations.[5] Even though routine immunological testing is not performed, in 9.38% of the clinics NK cell, $CD4^+/CD8^+$ T cell, and B cell immunophenotyping, as well as assessment of NK cell cytotoxicity and T helper cell cytokine production is offered (Table 15). According to another 2020 survey, routine NK cell level assessment is performed in 2.90% of the respondents' clinics.[670] Such tests are not recommended by ESRE or RCOG.[1, 5] The need for further research to illuminate the potential association of peripheral immune activity with RPL pathogenesis prior to the introduction of immunological testing to clinical practice has been highlighted in the official guidelines. Although the lack of a potential explanation can be devastating for couples and thus there is an increasing pressure to incorporate such testing in routine screening, the diagnostic value of immunological testing needs to be assessed and the potential tests offered need to be standardized through large cohort studies.

Idiopathic RPL is generally defined by the lack of identifiable RPL-associated pathology, although due to the variation in RPL investigations, cases treated as idiopathic are expected to differ between clinics. Supportive care and lifestyle changes were found to be the most utilised tools for the management of idiopathic RPL (Table 16), in agreement to ESHRE guidance.[9] Folic acid and progesterone were overall rated as significantly more effective than other treatments and more

likely to be suggested to women with idiopathic RPL (Figure 31). Indeed, latest meta-analyses highlight the beneficial effect of progesterone in women with idiopathic RPL.[612, 671] Furthermore, multivitamin and vitamin D supplementation, whose use is encouraged by ESHRE,[9] were rated by a high percentage of respondents as “very effective” (Table 21). Interestingly, aspirin, was found to be particularly popular for the management of idiopathic RPL (Table 17), although its use is not recommended by ESHRE.[5] A systematic review reported a lack of a therapeutic effect of anticoagulants in idiopathic RPL, with a non-significant reduction in live birth rates seen upon the use of aspirin.[672] This underlines the potentially severe impact of the lack of universal guidance. Most immunomodulatory therapies included in our survey did not appear to be widely used and were rated as ineffective. In agreement to these findings, immunological treatments for idiopathic RPL are not suggested by ESHRE or RCOG due to the lack of adequate scientific support.[1, 5]

In a systematic review and meta-analysis it was concluded that there is no significant therapeutic benefit of LMWH, lymphocyte immunization, and IVIg in regards to RPL, while the absence of randomized controlled trials investigating the efficacy of corticosteroids and intralipid infusion was highlighted.[612] The potential adverse effects associated with some of these treatments should also be underlined. For instance, neurological and renal damage, anaphylactic reactions, and thrombotic events have been linked to IVIg,[610, 616] while transfusion reactions and viral infections have been detected in women undergoing allogenic leukocyte immunotherapy for RPL.[617] Additionally, glucocorticoid use is linked to a range of side-effects, including, but not restricted to, hypertension, hyperglycaemia, and

osteoporosis.[618] Anti-TNF-α-associated congestive heart failure, upper respiratory tract infections, and lymphoma have also been reported.[1, 620] Moreover, the rating that was assigned to different treatments did not always match clinical practice in the respective clinics. This phenomenon is potentially an effect of the lack of a standardized treatment approach. Hence, further randomized control trials are required to establish the efficacy and safety of such therapies in the treatment of idiopathic RPL and determine the optimal dose and timing.

5.2.1 Limitations and future research

The results of this survey were heavily focused on the clinical practice in NHS-associated RPL clinics. A relatively low overall response rate was achieved, potentially due to the COVID-19 pandemic as the survey was distributed during the summer of 2020. Further distribution of the questionnaire, particularly to NHS-research and private clinics, would allow us to make valuable comparisons as immunological tests and potentially treatments are expected to be more prevalent in the private setting. No official list of private UK RPL clinics was available and thus these clinics were reached using their contact emails after self-guided research. The response rate of private clinics may have thus been affected by the identification and communication strategy. Additionally, NHS-research clinics could be involved in assessing the quality of novel diagnostic tests and immunotherapies. Hence, further information from private and NHS-research clinics would be beneficial to assess the availability and effectiveness of these tests and treatments.

A significant number of respondents reported the lack of an established protocol in their clinics. The reason behind such a phenomenon should be further examined to

determine whether the presence of multiple guidelines or the lack of a strong scientific basis behind the existing recommendations strongly influence clinical practice. At the same time, further research is required to fully elucidate the potential role of the immune system in RPL and particularly in its idiopathic form. This could lead to the identification of novel diagnostic and even prognostic biomarkers that would potentially provide an explanation for pregnancy loss and would also facilitate the detection of patients likely to benefit from the different immunomodulatory treatments. However, as previously mentioned the diagnostic assays used should be standardized across laboratories to allow the formation of meaningful conclusions in regards to the women's health status. Lastly, the need for adequately powered randomized placebo-controlled trials examining the efficacy and safety of novel immunoregulators, such as G-CSF and anti-TNF-α agents, should be again underlined. As immune dysregulation could underlie up to half of RPL cases it is important to develop appropriate diagnostic and therapeutic tools to meet the clinical needs of the couples affected.

6 PARTICIPANT DEMOGRAPHICS

6.1 Demographic data

Overall, 100 women with RPL and 80 controls were recruited in this study. Gravidity [Controls: 0.00, 95% CI (0.81, 1.52), RPL: 3.50, 95% CI (3.56, 4.38), p<0.0001] of women with RPL appeared elevated compared to that of controls, while parity [Controls: 0, 95% CI (0.60, 1.16), RPL: 0, 95% CI (0.40, 0.76)] was not significantly different between groups, although more women within the RPL cohort displayed lower live birth rates (Table 23, Figures 32, 33). Most women with RPL had 2 (*N*=43) or 3 (*N*=31) miscarriages prior to their recruitment, while women with high order losses, such as 11 (*N*=1) and 12 (*N*=1) previous miscarriages, were also recruited (Figure 34). Most participants underwent consecutive miscarriages (*N*=77), mostly occurring during the 1st pregnancy trimester, with 11 women reporting both 1st- and 2nd-trimester losses. The most common underlying RPL-associated conditions observed appeared to be uterine anatomical abnormalities (*N*=13), endocrine disorders (*N*=13), and autoimmunity (*N*=13), including antiphospholipid syndrome (Figure 35). In 5 women in the RPL group fetal genetic abnormalities were detected in at least one of their previous miscarriages, while hereditary thrombophilias were seen in 2 women with RPL (Figure 35). Other pregnancy complications detected in women with RPL included ectopic pregnancy (*N*=4), preeclampsia (*N*=3), preterm delivery (*N*=1), and stillbirth (*N*=1). Pregnancy complications, such as 1st-trimester miscarriage (*N*=9), ectopic pregnancy (*N*=1), and preterm delivery (*N*=3), were also reported by women in the control group.

Differences in the demographic characteristics of women with RPL and controls, which could affect immune activity were assessed. The median age of women in the RPL group was increased compared to controls [Controls: 30, 95% CI (30.08,

33.67), RPL: 33, 95% CI (31.99, 34.19), p=0.0447] (Table 23). Significant ethnic diversity was also detected, with more Black women and women of a mixed ethnic background recruited in the control group and more Asian women included in the RPL cohort (p=0.0007) (Table 24). In the control group, 1 woman of mixed Asian-White and 5 of mixed Black-White ethnic backgrounds were included, while the RPL group included 1 woman of mixed Black-White background. Median BMI and BMI group distribution were not found to be significantly different between controls and women with RPL (Tables 23, 25). Alcohol consumption by women in the RPL group appeared reduced compared to that of controls (p<0.0001) (Table 26), while smoking habits and illicit drug use did not appear significantly altered (Tables 27, 28). The time of blood collection was also found to be significantly different between the control and RPL group [Controls: 14.53, 95% CI (13.98, 15.03), RPL: 12.25, 95% CI (12.16, 13.18), p<0.0001] (Table 23).

Table 23. Summary of participant demographics, including age, gravidity, parity, and body mass index (BMI), as well as time of blood collection. *The median and 95% confidence interval (CI) in the control (N=80) and recurrent pregnancy loss (RPL) (N=100) group is displayed, alongside the p value. Mann-Whitney test used, ns: non-significant, *: p≤0.05, ****: p≤0.0001*

	Control women Median (95% CI)	Women with RPL Median (95% CI)	P value	Significance
Age (yrs)	30 (30.08, 33.67)	33 (31.99, 34.19)	0.0447	*
Gravidity	0 (0.81, 1.52)	3.50 (3.56, 4.38)	<0.0001	****
Parity	0 (0.60, 1.16)	0 (0.40, 0.76)	0.3021	ns
BMI (kg/m^2)	26.47 (25.75, 28.57)	25.32 (25.37, 27.80)	0.5392	ns
Time of blood collection (h)	14.53 (13.98, 15.03)	12.25 (12.16, 13.18)	<0.0001	****

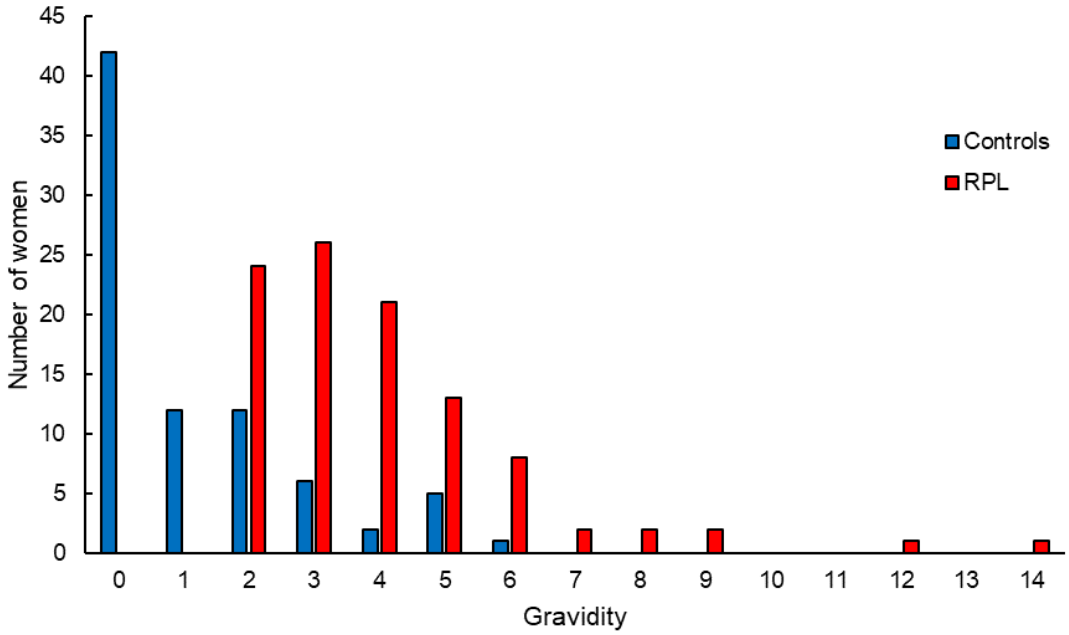


Figure 32. Number of controls and women with recurrent pregnancy loss (RPL) in relation to their gravidity. *The number of control women and women with RPL, subcategorised according to their past pregnancies is depicted.*

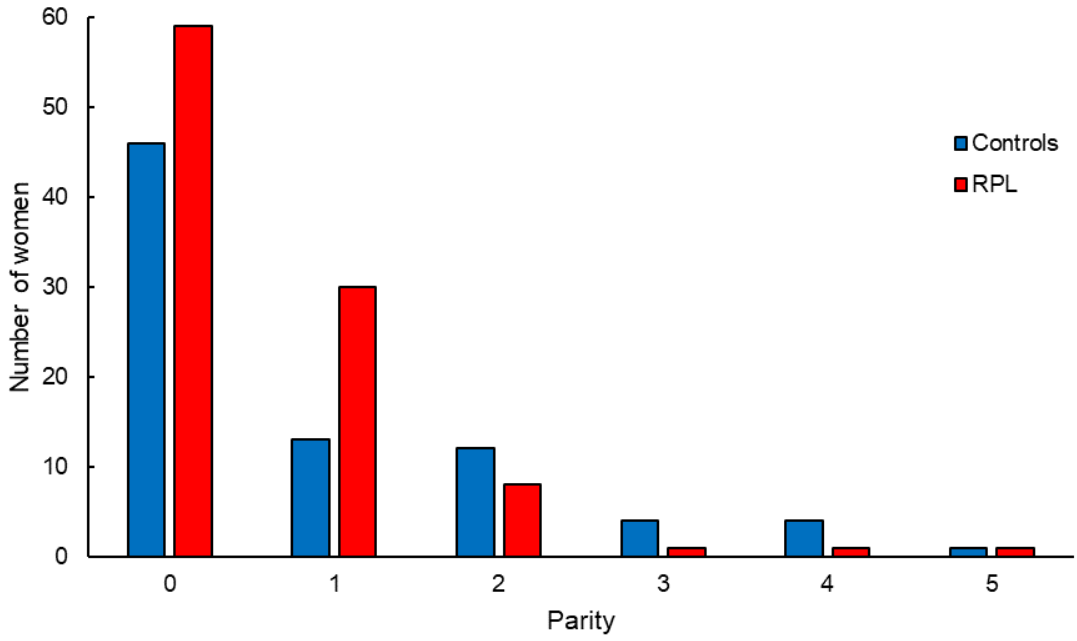


Figure 33. Number of controls and women with recurrent pregnancy loss (RPL) in relation to their parity. *The number of control women and women with RPL, subcategorised according to their past live births is depicted.*

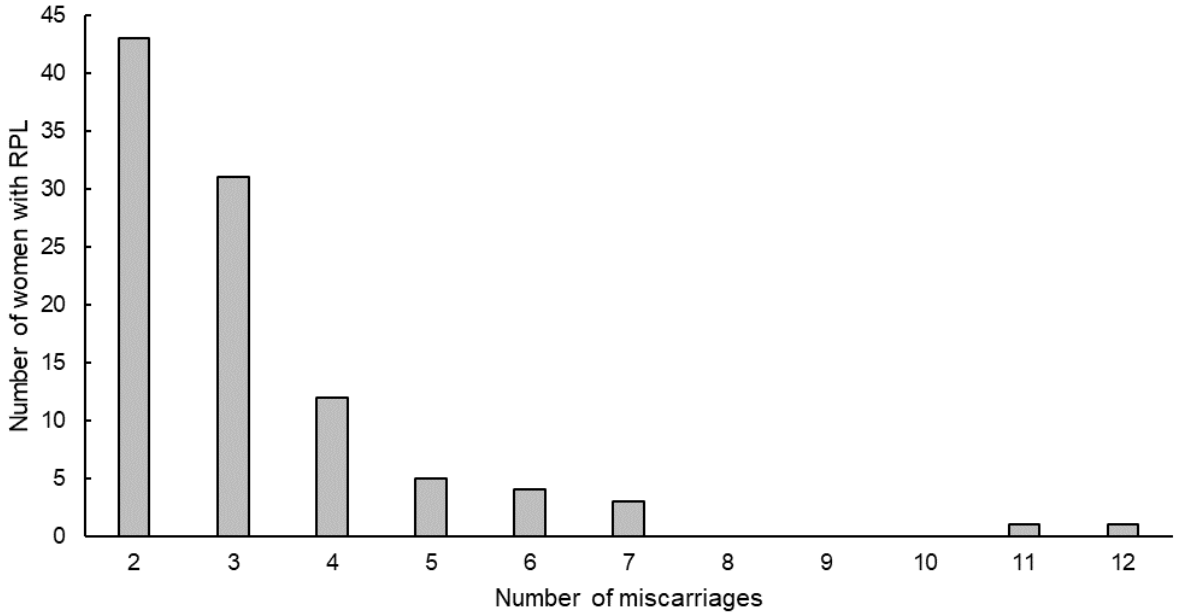


Figure 34. Number of women with recurrent pregnancy loss (RPL) in relation to the number of miscarriages in their reproductive history. *The number of women with RPL, subcategorised according to their past miscarriages is illustrated.*

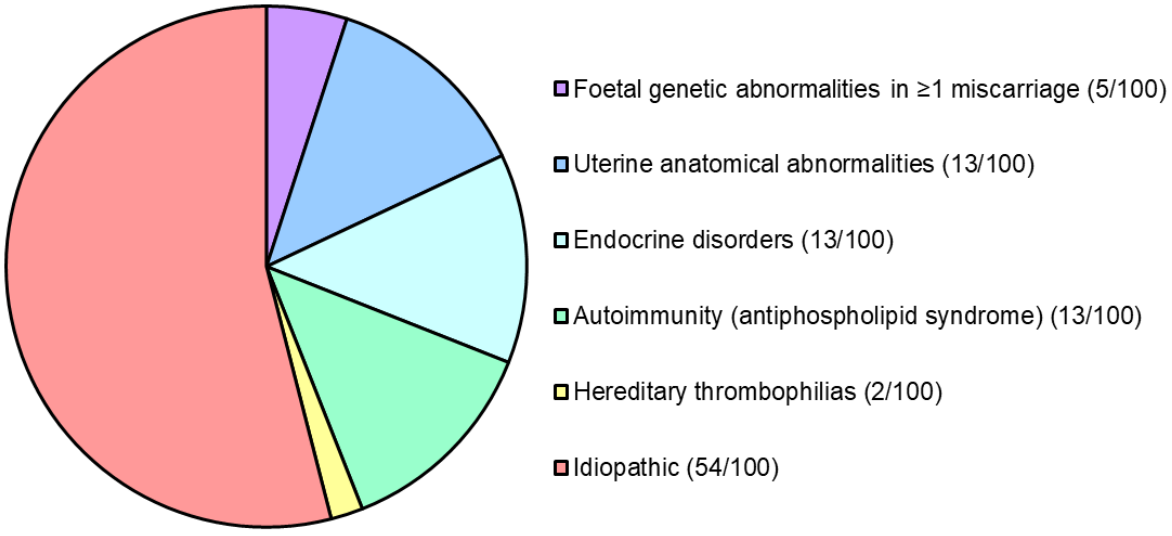


Figure 35. Underlying risk factors detected in women with recurrent pregnancy loss RPL. *The number of women in the RPL cohort (N=100) exhibiting each of the underlying conditions potentially associated with RPL is displayed. The number of women with idiopathic RPL, in whom no underlying condition could be detected is also shown.*

Table 24. Contingency table illustrating the ethnic background of controls and women with recurrent pregnancy loss (RPL) recruited in this study. *Women in the control (N=78) and RPL (N=82) group were split into four ethnic groups, including Asian, Black, White, and Mixed. The number of women in each subgroup is depicted, alongside the p value. Chi-square test, ***: p≤0.001*

	Number of control women	Number of women with RPL	P value	Significance
Asian	5	21	0.0007	***
Black	8	2		
White	59	58		
Mixed	6	1		

Table 25. Contingency table depicting the body mass index (BMI) group of controls and women with recurrent pregnancy loss (RPL) recruited in this study. *Women in the control (N=70) and RPL (N=88) group were split into five BMI groups, including underweight, healthy weight, overweight, obese, and severely obese. The number of women in each subgroup is illustrated, alongside the p value. Chi-square test, ns: non-significant*

	Number of control women	Number of women with RPL	P value	Significance
Underweight (BMI<18.5)	3	1	0.4898	ns
Healthy weight (BMI=18.5-24.9)	28	42		
Overweight (BMI=25-29.9)	17	24		
Obese (BMI=30-39.9)	21	19		
Severely Obese (BMI≥40)	1	2		

Table 26. Contingency table illustrating the levels of alcohol consumption of controls and women with recurrent pregnancy loss (RPL) recruited in this study. *Women in the control (N=79) and RPL (N=99) group were split into four groups, according to the average amount of alcohol they consume per week. The number of women in each subgroup is displayed, alongside the p value. Chi-square test, ****: p≤0.0001*

	Number of control women	Number of women with RPL	P value	Significance
No	31	70	<0.0001	****
Low (1-7 units/week)	29	27		
Moderate (8-14 units/week)	16	1		
High (>14 units/week)	3	1		

Table 27. Contingency table depicting the smoking habits of controls and women with recurrent pregnancy loss (RPL) recruited in this study. *Women in the control (N=79) and RPL (N=98) group were split into three groups, including non-smokers, ex-smokers, and smokers. The number of women in each subgroup is shown. P values for the two comparisons made by grouping ex-smokers with either the non-smoker or the smoker group are also included. Fisher's exact test, ns: non-significant*

	Number of control women	Number of women with RPL	P value	Significance
Non-smokers	72	82	0.5680 (non- & ex-smokers vs smokers) 0.1791 (non-smokers vs ex-smokers & smokers)	ns
Ex-smokers	0	10		
Smokers	7	6		

Table 28. Contingency table illustrating the use of illicit drugs by controls and women with recurrent pregnancy loss (RPL) recruited in this study. *Women in the control (N=79) and RPL (N=76) group were split into two groups, based on illicit drug use. The number of women in each subgroup is displayed, alongside the p value. Fisher's exact test, ns: non-significant*

	Number of control women	Number of women with RPL	P value	Significance
No	79	76	1	ns
Yes	0	0		

The following pregnancy outcome of women with RPL was also recorded. At the time of follow-up women in the 1st (*N*=8), 2nd (*N*=11), or 3rd (*N*=4) trimester of their subsequent pregnancy, women with a successful delivery (*N*=9), and women with a 1st-trimester (*N*=20) or 2nd-trimester (*N*=3) miscarriage were identified (Figure 36). 44 women have not gotten pregnant after their recruitment, while 1 woman could not be reached for follow-up.

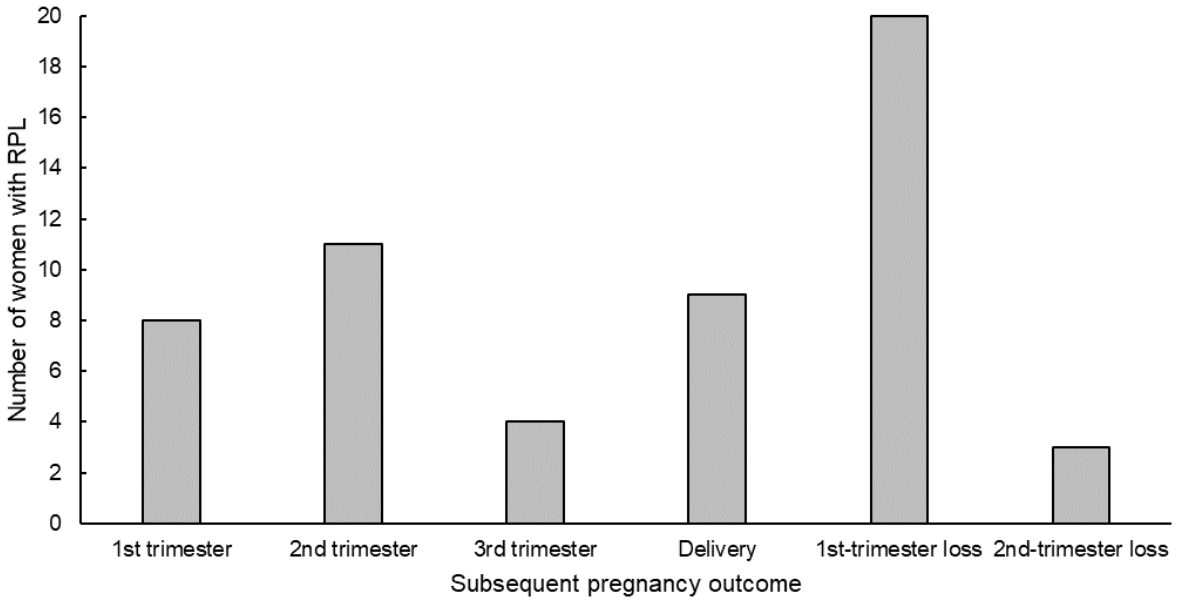


Figure 36. Subsequent pregnancy outcome of women with recurrent pregnancy loss (RPL). *The number of women with RPL, sub-categorised according to the outcome of their following pregnancy is illustrated. Women in the RPL group who have not conceived since their recruitment or who could not be reached during follow-up are not included.*

6.2 Discussion

Women in the RPL group displayed a broad range in regards to the previous miscarriage number, although most belonged in the lower order loss subgroups, having 2 or 3 miscarriages in their reproductive history (Figure 34). Additional reproductive complications were detected in both women with RPL and controls. However, only a small percentage of women appear affected, with no clear link between these conditions and aberrant immune activity having been reported. In 46.00% of women with RPL an underlying pathology associated with this condition was detected (Figure 35). No women with RPL-associated infections or couples with diagnosed chromosomal abnormalities were recruited. Additionally, hereditary thrombophilia was seen in only 2.00% of women in the RPL group (Figure 35), although in 16.00%-22.00% of women with RPL genetic thrombophilia markers were

detected in other studies.[37, 83] Thus, even though the RPL cohort was underlined by a relative variability in regards to reproductive and relevant medical history, further recruitment of women with high order losses and additional RPL-associated pathologies could allow the examination of the effect of those factors on the immunology of RPL.

The demographic characteristics of women with RPL and controls were examined to assess whether potential differences could influence experimental findings. The age and gravidity of women in the RPL group was augmented compared to controls (Table 23, Figure 32), which is expected as a minimum of two losses is required for inclusion in the RPL cohort. Circulating NK cell prevalence is thought to be elevated with increasing age, while NK cell-mediated cytotoxicity and cytokine reduction are reduced.[582, 673] Hence, the findings of this study could be affected by the age difference between groups. As expected, women with RPL displayed lower numbers of previous live births, although no significant difference in parity was seen (Table 23, Figure 33). Ethnic variation was also seen (Table 24). Although uncertain, immune alterations have been reported between individuals of different ethnic groups,[674, 675] indicating a potential influence of ethnic differences on the immunological variation between women with RPL and controls. A significant difference in the levels of alcohol consumption between women with RPL and controls was detected, with most women with RPL reporting an abstinence from alcohol (Table 26). This difference was expected as most women recruited through RPL clinics were actively trying to conceive. Even though the relationship between alcohol and immune activity has not been fully elucidated, high consumption has been linked to immune suppression, while moderate consumption appears

beneficial for immune activity.[676] Lastly, the time of blood collection, which appeared significantly different between controls and women with RPL (Table 23), could also influence the significance of experimental findings, due to a suggested circadian control of immune activity.[584, 677]

6.2.1 Limitations and future research

The present research aims to identify potential alterations in immune activity of women with RPL and thus analysis was focused on comparisons between the total RPL population and controls. As a direct link between the underlying conditions and RPL has not been definitely shown, the investigation of potential immune biomarkers could be extended to risk factor-associated RPL subpopulations. High-powered studies, with sufficient numbers of women with different underlying conditions are thus required. Moreover, no women with only 2nd-trimester losses were recruited in the RPL cohort. Immune phenotyping of women with 1st- vs those with 2nd-trimester losses could be beneficial, as immune activity is thought to shift from primarily pro- to anti-inflammatory throughout the first two trimesters.

Differences in the demographic characteristics of the RPL and control group were detected, potentially influencing the significance of the experimental findings. Hence, age- and ethnicity-associated subpopulation analysis was performed. However, as only one woman of Mixed ethnic background was recruited in the RPL group, the subgroup was excluded from analysis in the RPL population. Similarly, data on cytokine production and NK cell cytotoxicity were obtained from only one Black woman with RPL and thus this subgroup was only examined for the assessment of NK and T cell population and subpopulation prevalence. Overall,

ethnic variation in the RPL cohort was limited. This issue could be partly alleviated by the use of age-matched and ethnically-matched controls in future studies. As the miscarriage risk is significantly elevated in women with a Black ethnic background,[3] evaluation of the immune activity in this subpopulation could provide a valuable insight in the influence of ethnicity on pregnancy loss. In regards to smoking habits, vaping was included in the non-smoking group, as it is currently considered significantly less harmful than smoking during pregnancy.[678] However, sufficient data is not yet available, with additional research required to elucidate the impact of vaping on reproductive success. Due to limited time available for data collection and analysis a high percentage of women with RPL have not gotten pregnant by the time of follow-up and thus were excluded from the following pregnancy outcome sub-analysis. Hence, additional examination of predictive biomarkers through large-cohort studies is desirable.

Although not assessed in the present study, the potential influence of cytomegalovirus (CMV) seropositivity on study outcomes should also be taken into consideration. CMV has been shown to modulate NK cell activity, interfering with receptor expression and stimulation.[679] When assessing dNK cell receptor repertoire, a reduction in activating NKp46 and KIR2DL4 and inhibitory ILT2 and KIR2DL1 were shown to accompany CMV infection.[680] Upon infection, increased cytotoxic factor release by dNK cells was observed, alongside cytotoxicity against autologous decidual fibroblasts,[680] underlining a potential mechanism amplifying inflammation during early pregnancy in affected individuals. Moreover, CMV status could potentially influence the development of pregnancy-specific NK cell memory induction, with ILT2 expression on pregnancy-trained $NKG2C^+$ eNK cells being

restricted to CMV^+ women.[681] Foetal development may also be directly affected by CMV, with infection shown to diminish EVT proliferation and invasion.[682] In a trophoblast villi model, CMV infection appeared to promote dNK cell invasion in the villous space,[680] potentially exacerbating anti-trophoblast responses. Hence, CMV could be involved in alterations in foetal-maternal interactions. If possible, participant CMV status should be assessed in future studies to examine its influence on the immune activity of women with RPL.

Another limitation is that the use of hormonal contraception was not assessed in the present study. However, this factor is expected to differ between cohorts, as most women with RPL recruited were trying to conceive. NK cell fluctuation during the menstrual cycle suggests a hormonal influence on immune activity.[125] Indeed, significantly reduced levels of cytokines and chemokines, such as GM-CSF, IFN-α, IL-12p40, IL-15, CX3CL1, and CXCL10 have been detected in the reproductive tract of women using hormonal contraception, compared to controls.[683, 684] The type of contraception could also influence immune activity, with cervical T_H17 levels appearing diminished but cervicovaginal inflammatory cytokine concentration, including IFN-γ, TNF-α, and IL-1β, being enhanced in women using combined contraceptive vaginal rings, compared to those using combined oral contraceptive pills or injectable norethisterone oenanthate.[685]

The effects of hormonal contraceptives do not appear restricted to reproductive organs. A link between combined oral contraceptive use and increased incidence of autoimmunity, such as multiple sclerosis, inflammatory bowel disease, and systemic lupus erythematosus has been observed,[686] associating contraceptives with systemic immune dysregulation. In addition, contraceptive use has been linked to

increased T_C, and reduced NK cell levels, decreased TNF-α and IFN-α production by plasmacytoid DCs, as well as non-significantly reduced NK cell activity in the circulation.[125, 683, 687] Hence, the potential influence of hormonal contraception on the experimental findings of the present study should be taken into consideration.

7 IMMUNOPHENOTYPING

7.1 Results

7.1.1 TBNK assay

The prevalence of multiple immune cell populations and subpopulations in peripheral blood $CD45^+$ leukocytes was initially examined via the Trucount™ TBNK assay, which quantifies lymphocyte subsets (Controls *N*=79, RPL *N*=96). $CD3^+$ T cell levels were found to be decreased in women with RPL compared to healthy controls (Figure 37A). Specifically, in healthy controls T cells were found to constitute 77.79% (SD: 5.55) of leukocytes, while in participants with RPL this prevalence was decreased to 75.78% (SD: 5.45) (p=0.018). However, the prevalence of the $CD4^+$ [Controls: 48.70% (6.07), RPL: 48.03% (6.67)], $CD8^+$ [Controls: 25.21%, 95% CI (23.86%, 27.20%), RPL: 23.73%, 95% CI (22.69%, 24.94%)], and $CD4^+CD8^+$ [Controls: 0.42%, 95% CI (0.33%, 0.47%), RPL: 0.38%, 95% CI (0.33%, 0.44%)] T cell subsets was not significantly altered (Figures 37B-37D). The levels of $CD3^-CD56/CD16^+$ NK cells [Controls: 7.91%, 95% CI (7.03%, 9.48%), RPL: 9.61%, 95% CI (8.40, 10.60)] and $CD3^-CD19^+$ B cells [Controls: 11.86%, 95% CI (10.69%, 13.00%), RPL: 12.12%, 95% CI (10.92%, 13.93%)] in the leukocyte population were also found not to differ between women with RPL and healthy participants (Figures 37E, 37F).

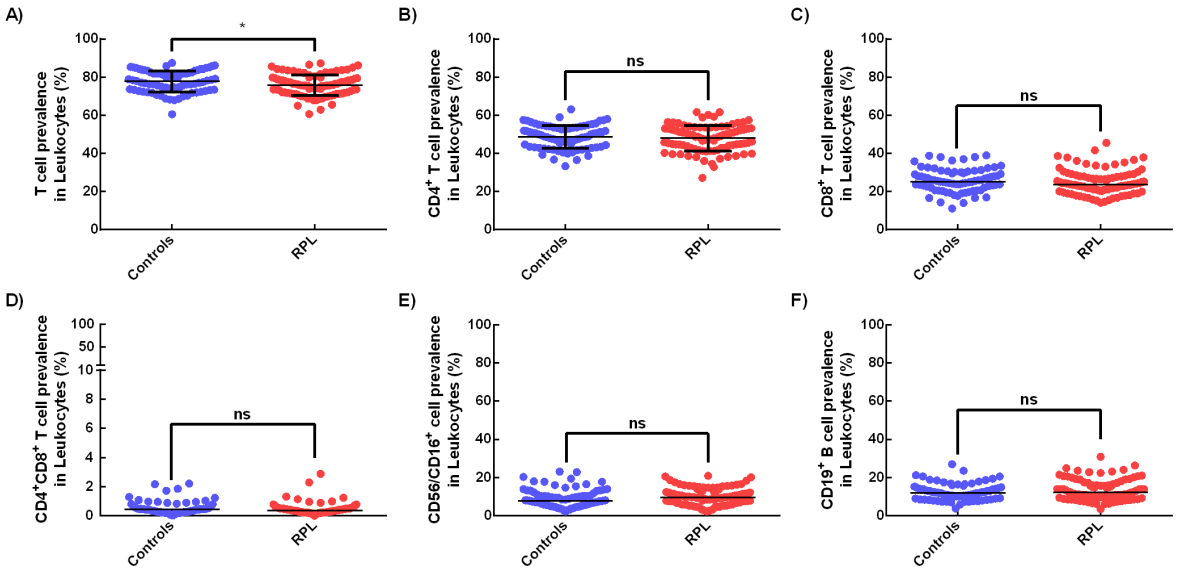


Figure 37. TBNK assay results regarding lymphocyte subpopulation prevalence. *The prevalence of A) $CD3^+$, B) $CD3^+CD4^+CD8^-$ helper, C) $CD3^+CD4^-CD8^+$ cytotoxic, and D) $CD3^+CD4^+CD8^+$ T cells in the $CD45^+$ leukocyte population, as well as E) $CD3^-CD19^-CD56/CD16^+$ Natural Killer cell and F) $CD3^-CD19^+CD56/CD16^-$ B cell prevalence in the $CD45^+$ leukocyte population of healthy controls (N=79) and women with recurrent pregnancy loss (RPL) (N=96) is illustrated. Normally distributed datasets (A, B): Unpaired t test performed, mean and standard deviation displayed. Non-normally distributed datasets (C-F): Mann-Whitney test used, median illustrated. ns: non-significant, *: p≤0.05*

When assessing absolute counts through the TBNK assay, the numbers of total [Controls: 1747.00, 95% CI (1682.00, 1881.00), RPL: 1564.00, 95% CI (1464.00, 1641.00), p=0.0031], $CD4^+$ [Controls: 1126.00, 95% CI (1051.00, 1198.00), RPL: 1003.00, 95% CI (880.20, 1078.00), p=0.0090], and $CD8^+$ [Controls: 558.00, 95% CI (523.60, 642.70), RPL: 488.60, 95% CI (447.60, 528.30), p=0.0037] T cells appeared reduced in women with RPL (Figures 38A-38C), resulting to an unaltered $CD4^+/CD8^+$ T cell ratio [Controls: 1.89, 95% CI (1.72, 2.10), RPL: 2.06, 95% CI (1.88, 2.17)] (Figure 38E). The absolute counts of $CD4^+CD8^+$ T cells [Controls: 8.70, 95% CI (7.19, 10.87), RPL: 6.93, 95% CI (6.03, 9.07)], $CD3^-CD56/CD16^+$ NK cells [Controls: 189.50, 95% CI (150.20, 219.70), RPL: 189.50, 95% CI (176.80, 216.30)] and $CD3^-CD19^+$ B cells [Controls: 267.00, 95% CI (235.80, 307.40), RPL: 252.70,

95% CI (204.90, 300.90)] were unaltered in women with RPL, compared to controls (Figures 38D, 38F, 38G).

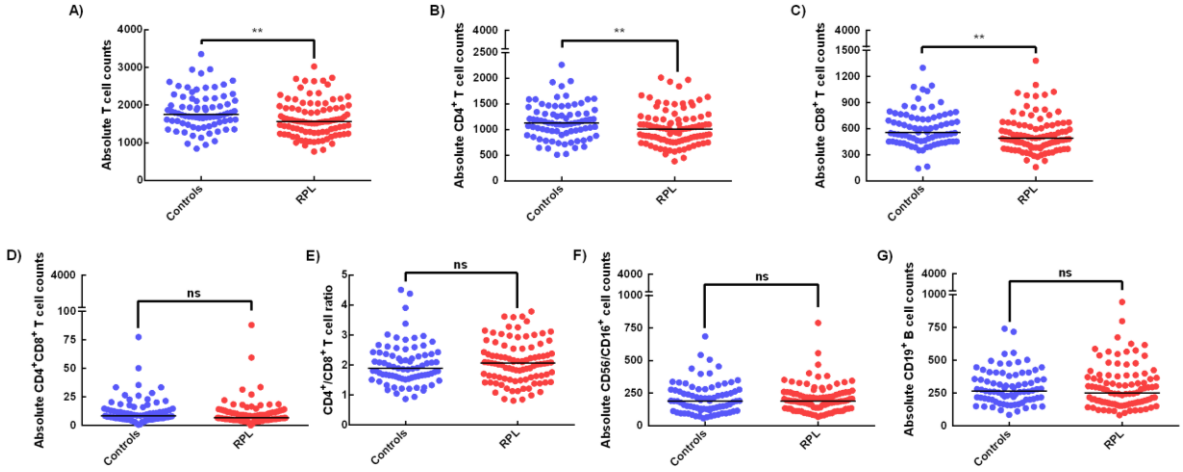


Figure 38. TBNK assay results regarding lymphocyte subpopulation absolute counts. *The absolute counts of A) $CD3^+$, B) $CD3^+CD4^+CD8^-$ helper, C) $CD3^+CD4^-CD8^+$ cytotoxic, and D) $CD3^+CD4^+CD8^+$ T cells, E) the ratio between $CD4^+$ and $CD8^+$ T leukocytes, as well as the absolute counts of F) $CD3^-CD19^-CD56/CD16^+$ Natural Killer cells and G) $CD3^-CD19^+CD56/CD16^-$ B cells in healthy controls (N=79) and women with recurrent pregnancy loss (RPL) (N=96) is shown. Mann-Whitney test utilised, median displayed. ns: non-significant, **: p≤0.01*

7.1.2 Flow cytometry assay – NK cells

More detailed investigation of the peripheral blood NK cell population and subpopulation prevalence in women with RPL (*N*=90) and controls (*N*=77) was performed using the NK cell panel of the flow cytometry assay. The prevalence of $CD3^-CD56^+$ NK cells in the PBMC [Controls: 1.12%, 95% CI (0.53%, 2.45%), RPL: 5.41%, 95% CI (3.80%, 6.34%), p<0.0001] and the lymphocyte [Controls: 1.58%, 95% CI (0.76%, 3.03%), RPL: 9.11%, 95% CI (7.75%, 10.60%), p<0.0001] populations was found to be significantly augmented in women with RPL, compared to controls (Figures 39A, 39B). The percentage of the NK cell population consisting

of the $CD56^{dim}CD16^{+}$ and $CD56^{bright}CD16^{-}$ subsets was also examined. The prevalence of the $CD56^{dim}CD16^{+}$ subset was non-significantly augmented in participants with RPL [Controls: 58.80%, 95% CI (37.10%, 70.30%), RPL: 70.05%, 95% CI (63.80%, 75.90%)], displaying a great variation in both the control and RPL groups (Figure 39C). On the other hand, $CD56^{bright}CD16^{-}$ NK cell prevalence was significantly reduced in women with RPL, compared to controls [Controls: 9.47%, 95% CI (5.76%, 13.00%), RPL: 4.92%, 95% CI (4.21%, 6.11%), p=0.0011] (Figure 39D), resulting to a reduced $CD56^{bright}CD16^{-}$-to-$CD56^{dim}CD16^{+}$ NK cell ratio [Controls: 0.20, 95% CI (0.11, 0.29), RPL: 0.09, 95% CI (0.08, 0.11), p=0.0013] (Figure 39E).

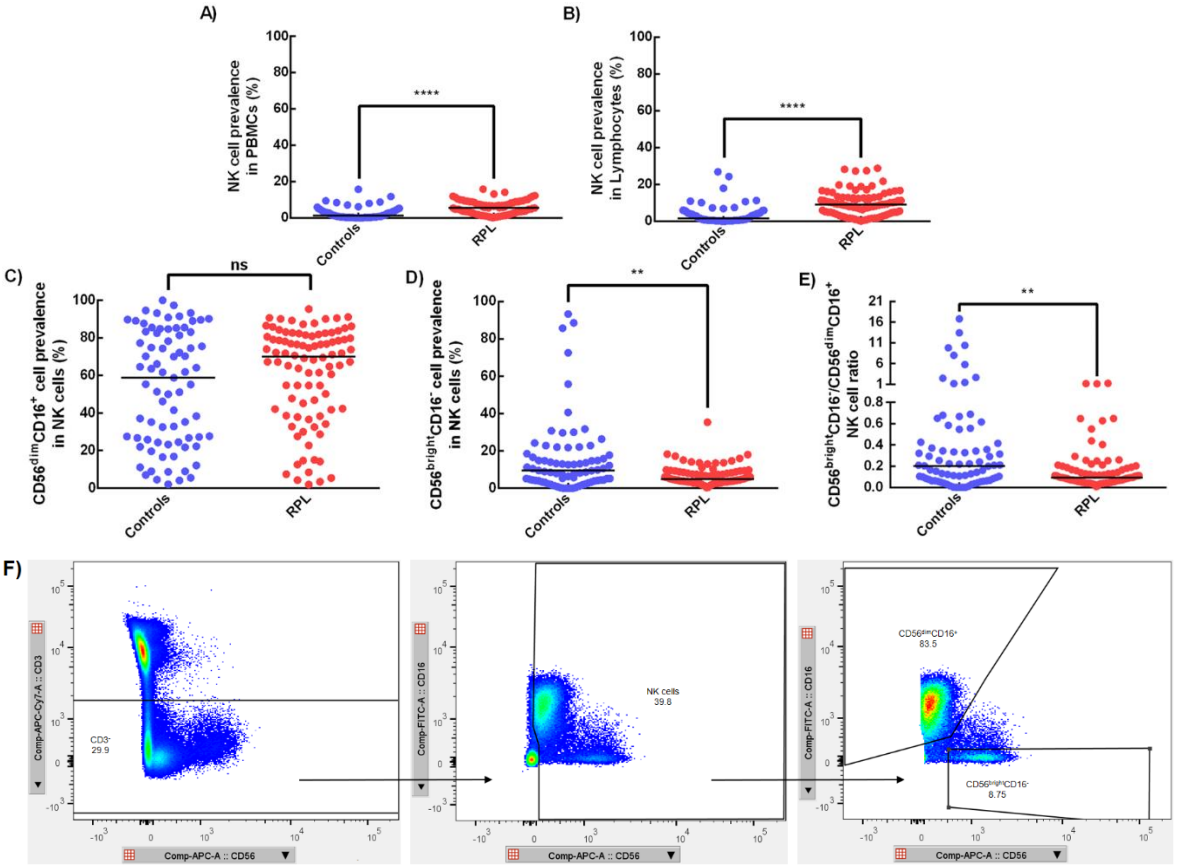


Figure 39. Natural Killer (NK) cell and NK cell subset prevalence in women with recurrent pregnancy loss (RPL) and controls. *The prevalence of $CD3^{-}CD56^{+}$ NK cells in the A) peripheral blood mononuclear cell (PBMC) and B) lymphocyte population, and the percentage of C) $CD56^{dim}CD16^{+}$ and D) $CD56^{bright}CD16^{-}$ cells in the NK cell population of healthy controls (N=77) and women with RPL (N=90) is displayed. E) The $CD56^{bright}CD16^{-}$ to $CD56^{dim}CD16^{+}$ NK cell ratio is also shown. F) Example gating summarizing the strategy used to identify NK cell population and subpopulations is included. Mann-Whitney test used, median illustrated. ns: non-significant, **: p≤0.01, ****: p≤0.0001*

7.1.3 Flow cytometry assay – T cells

Similarly, using the T cell panel of the flow cytometry assay, the levels of T cells and T cell subpopulations in the peripheral blood of women with RPL (*N*=89) and controls (*N*=80) were further assessed. $CD3^{+}$ T cell prevalence in the PBMC [Controls: 64.30%, 95% CI (60.70%, 67.50%), RPL: 46.70%, 95% CI (42.00%,

52.50%), p<0.0001] and lymphocyte [Controls: 77.50%, 95% CI (73.70%, 80.50%), RPL: 69.20%, 95% CI (64.50%, 73.00%), p<0.0001] population of women with RPL was found to be reduced compared to that of controls (Figures 40A, 40B). However, the percentages of $CD4^+$ helper [Controls: 58.45%, 95% CI (53.70%, 62.60%), RPL: 56.70%, 95% CI (54.30%, 60.20%)] and $CD8^+$ cytotoxic [Controls: 28.82% (8.57), RPL: 27.80% (8.42)] T cells were not significantly different between control participants and those with RPL (Figures 40C, 40D). In addition, the $CD45RA^+$ cell prevalence in the $CD4^+$ [Controls: 56.98% (15.36), RPL: 60.48% (19.42)] and $CD8^+$ [Controls: 88.50%, 95% CI (85.60%, 90.70%), RPL: 88.40%, 95% CI (86.10%, 89.80%)] T cell subpopulations was found to be unaltered in RPL (Figures 40E, 40F). Lastly, the $FoxP3^+CD25^+CD127^{low/-}$ Treg prevalence in the $CD4^+$ helper T cell population was also similar between controls and women with RPL [Controls: 1.09%, 95% CI (0.70%, 1.51%), RPL: 1.03%, 95% CI (0.72%, 1.44%)] (Figure 40G).

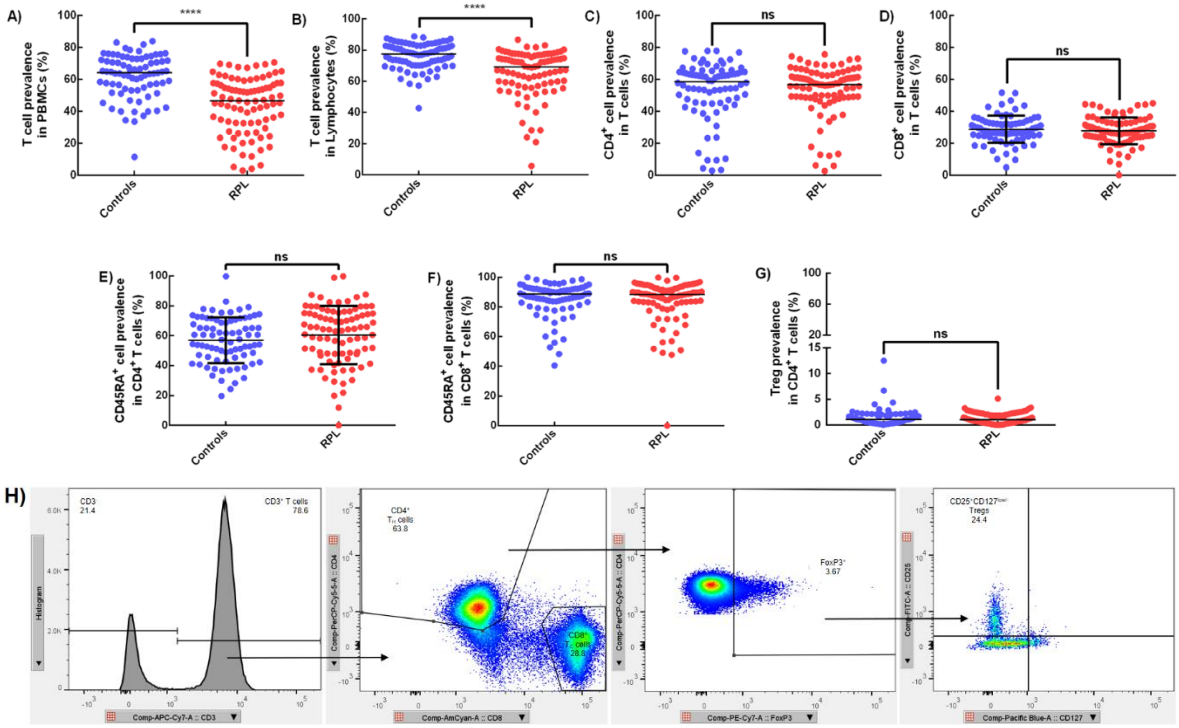


Figure 40. T cell and T cell subset prevalence in women with recurrent pregnancy loss (RPL) and controls. *The prevalence of $CD3^+$ T cells in the A) peripheral blood mononuclear cell (PBMC) and B) lymphocyte population, the percentage of C) $CD4^+CD8^-$ helper (T_H) and D) $CD4^-CD8^+$ cytotoxic (T_C) cells in the T cell population, the prevalence of $CD45RA^+$ cells in E) $CD4^+CD8^-$ and the F) $CD4^-CD8^+$ T cells, and G) the regulatory T cell (Treg) prevalence in the $CD4^+CD8^-$ T cell subpopulation of healthy controls (N=80) and women with RPL (N=89) is illustrated. H) Example gating summarizing the strategy used to identify T cell population and subpopulations is included. Normally distributed dataset without significantly different variances (D): Unpaired t test used, mean and standard deviation displayed. Normally distributed dataset with significantly different variances (E): Unpaired t test with Welch's correction utilised, mean and standard deviation shown. Non-normally distributed datasets (A-C, F, G): Mann-Whitney test performed, median illustrated. ns: non-significant, ****: p≤0.0001*

7.1.4 Mass cytometry assay – T cells

To further examine the phenotype of T and B cells in RPL (*N*=100) and control (*N*=80) cases the mass cytometry assay was utilised (Figure 41). The expression levels of 8 markers, including CD4, CD8, CD25, CD127, CD226, TIGIT/Tim-3, and PD-1, in the $CD3^+$ T cell population were examined. Although, according to the expression levels of these markers some separation between RPL and control samples could be seen in the multi-dimensional scaling (MDS) plot, it was only evident at a low level not indicating a clear distinction of the two conditions according to the T cell marker expression (Figure 42). 20 clusters were generated, based on the expression of the 8 markers of interest (Figures 43A, 43B). As it can be seen in Figure 43A clusters 4, 5, 6, 7, 9, 13, 19, and 20, which represent $CD4^+CD8^-$ cells were clearly separated from clusters 1, 2, 10, 11, 12, 15, 16, and 17, representing $C4^-CD8^+$ cells. Clusters 3, 8, and 14, located adjacent to $CD4^+CD8^-$ clusters were characterised as $CD4^-CD8^-$, while cluster 18, displaying higher similarity to $CD4^-CD8^+$ clusters, was described as $CD4^+CD8^+$ (Figure 43). $CD4^+CD8^-$ clusters appeared to be separated into two groups according to their CD127 expression, with clusters 4, 5, 6, and 7 being $CD127^{low/-}$ and clusters 9, 13, 19, and 20 being $CD127^{high/+}$ (Figure 43). Similarly, according to the levels of CD127 expression $CD4^-CD8^+$ cells were split into two subgroups, one consisting of clusters 1, 2, 10, 11, and 12, and one consisting of clusters 15, 16, and 17 (Figure 43). CD25 was expressed on the 5, 6, and 20 $CD4^+$ clusters, with low expression levels also being detected on $CD4^+CD8^+$ cluster 18 (Figure 43B). Low to medium CD226 expression was observed on the $CD4^+CD8^-$ 7, 13, and 19 clusters, as well as on the $CD4^+CD8^+$ cluster 18. Medium to high expression of this marker was observed on $CD4^-CD8^-$

cluster 8, on $CD4^{-}CD8^{+}$ cluster 11, and on $CD4^{+}CD8^{-}$ cluster 20 (Figure 43B). In regards to inhibitory immune checkpoint receptor expression, both TIGIT and/or Tim-3 and PD-1 were expressed on $CD4^{+}CD8^{-}$ clusters 7, 13, and 19, on $CD4^{-}CD8^{+}$ clusters 1 and 16, and on $CD4^{-}CD8^{-}$ cluster 3, with PD-1 expression on clusters 3 and 13 being quite low (Figure 43B). TIGIT and/or Tim-3 were also expressed on $CD4^{+}CD8^{-}$ cluster 6 and on $CD4^{-}CD8^{+}$ clusters 2 and 17 that did not expressed PD-1, while PD-1 expression in the absence of TIGIT/Tim-3 expression was not observed on any cluster (Figure 43B).

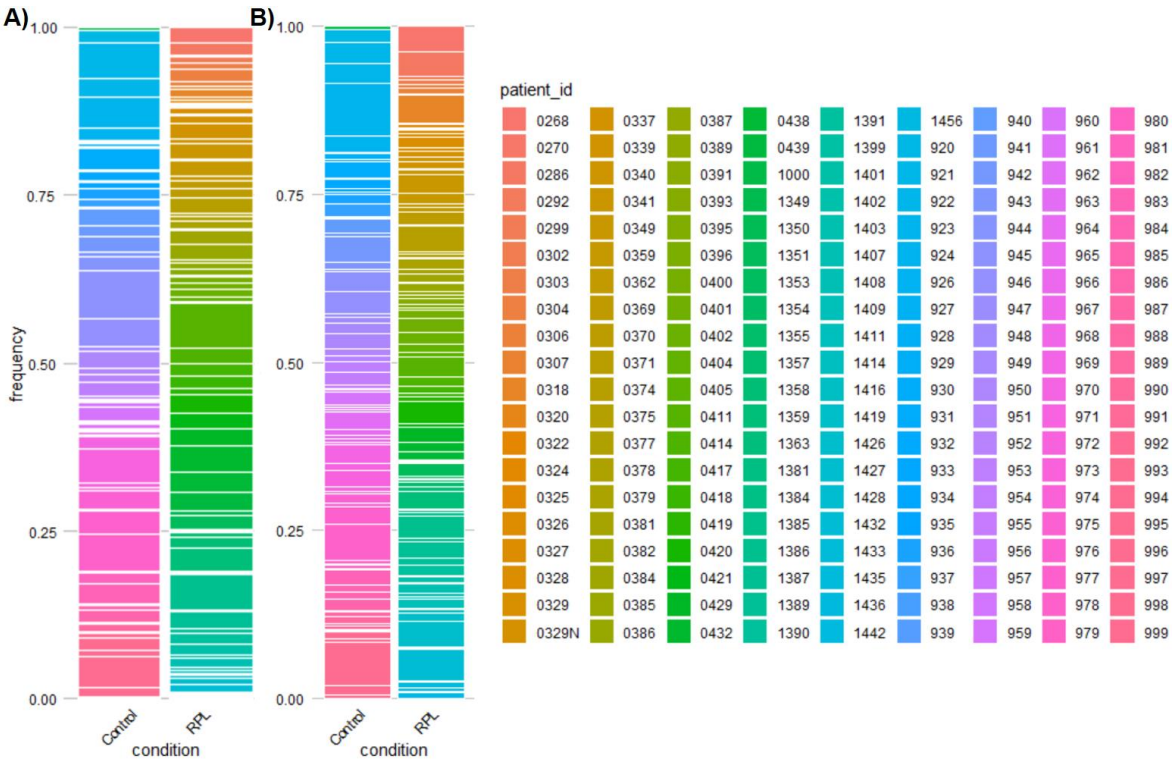


Figure 41. Relative abundance of each sample in the mass cytometry datasets used to analyse T and B cell marker expression in control women and women with recurrent pregnancy loss (RPL). *The relative frequency of each sample, calculated according to cell counts, in the total A) T cell and B) B cell populations of the control (N=80) and RPL (N=100) cohorts is depicted. Individual samples are represented by different colours, with patient_id also displayed (RPL: 0268-0439 and 1349-1456, Control: 920-1000).*

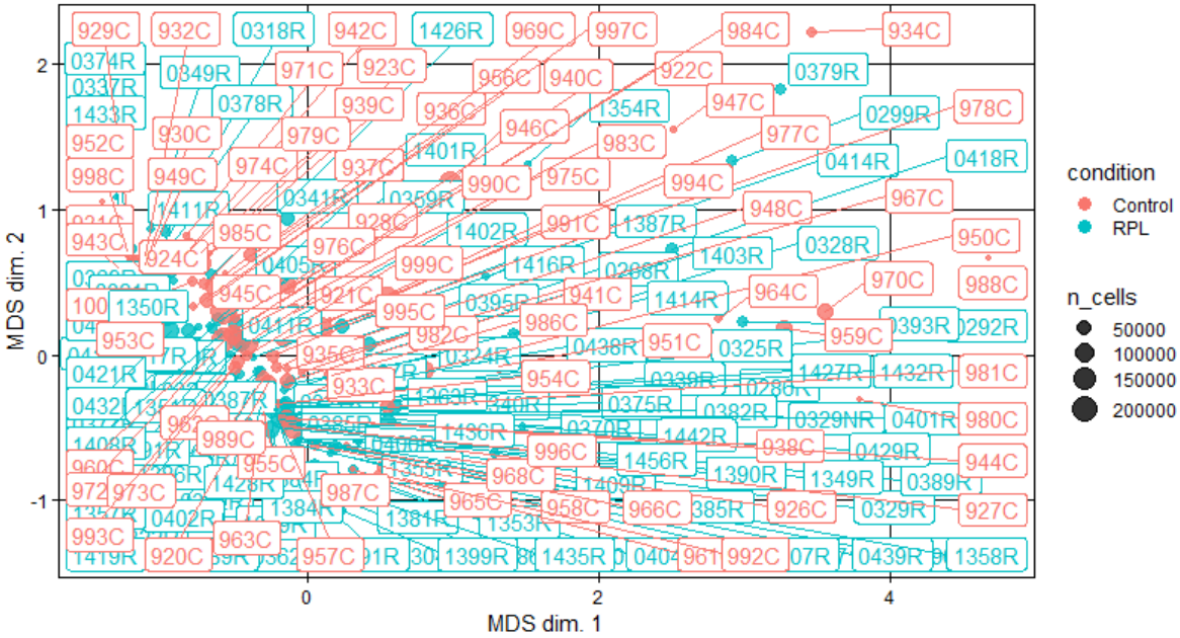


Figure 42. Multi-dimensional scaling (MDS) plot of the control and recurrent pregnancy loss (RPL) T cell samples, summarizing the level of similarity between cohorts. *The distances between samples approximate the difference in median expression of all markers examined, including CD4, CD8, CD25, CD127, CD226, T-cell immunoreceptor with Ig and ITIM domains/T cell immunoglobulin and mucin domain-containing protein 3 (TIGIT/Tim-3), and programmed cell death protein 1 (PD-1), translating multi-dimensional data into a two-dimensional scatter plot. Labels displaying the sample identity are included.*

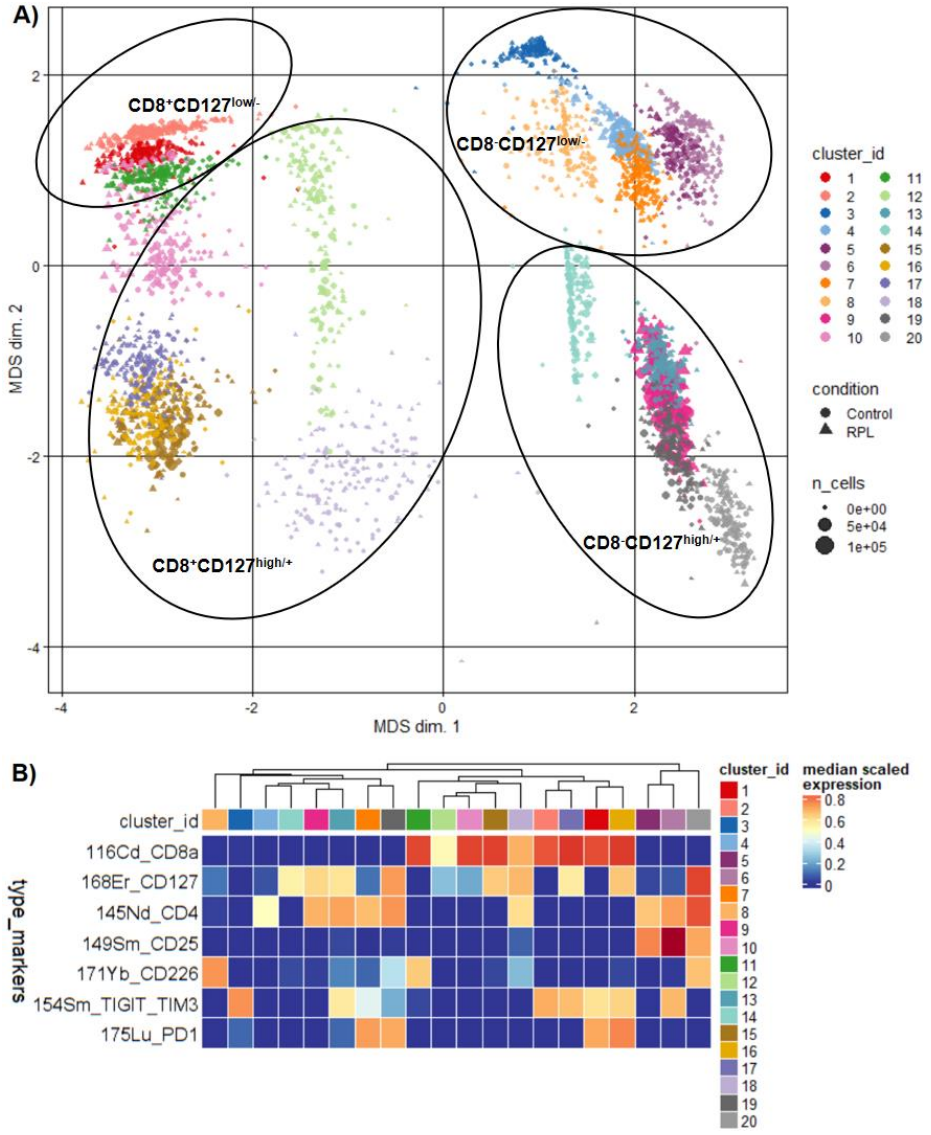


Figure 43. Multi-dimensional scaling and phenotyping of 20 T cell clusters identified by mass cytometry. *A) Multi-dimensional scaling (MDS) plot of pseudobulks generated, with each point on the plot representing a cluster-sample instance, coloured according to the cluster, shaped based on the condition, and with a size proportional to the number of cells it represents. Distances between instances indicate relative phenotypic differences between clusters and samples, taking into consideration all markers assessed. The major phenotypic subgroups are demonstrated. B) Heatmap of median cluster of differentiation (CD)4, CD8, CD25, CD127, CD226, T-cell immunoreceptor with Ig and ITIM domains/T cell immunoglobulin and mucin domain-containing protein 3 (TIGIT/Tim-3), and programmed cell death protein 1 (PD-1) expression intensity across the different T cell clusters, ranging from high (red) to low (blue).*

Using differential abundance testing, mass cytometry T cell data from participants with RPL was compared to that of healthy controls. Frequency of the $CD4^{+}CD8^{-}CD25^{-}CD127^{-}CD226^{-}$TIGIT/Tim-$3^{-}PD\text{-}1^{-}$ cluster 4 (Control counts: 21846, RPL counts: 39082) and the $CD4^{-}CD8^{+}CD25^{-}CD127^{+}CD226^{-}$TIGIT/Tim-$3^{-}PD\text{-}1^{-}$ cluster 10 (Control counts: 168868, RPL counts: 183744) was found to be elevated in the peripheral blood of women with RPL, while the prevalence of the $CD4^{-}CD8^{+}CD25^{-}CD127^{-}CD226^{-}$TIGIT/Tim-$3^{+}PD\text{-}1^{+}$ cluster 1 (Control counts: 85158, RPL counts: 34528), $CD4^{+}CD8^{-}CD25^{high}CD127^{-}CD226^{-}$TIGIT/Tim-$3^{+}PD\text{-}1^{-}$ cluster 6 (Control counts: 42602, RPL counts: 29256), $CD4^{-}CD8^{+}CD25^{-}CD127^{+}CD226^{-}$TIGIT/Tim-$3^{-}PD\text{-}1^{-}$ cluster 15 (Control counts: 582922, RPL counts: 306239), $CD4^{-}CD8^{+}CD25^{-}CD127^{+}CD226^{-}$TIGIT/Tim-$3^{+}PD\text{-}1^{+}$ cluster 16 (Control counts: 45195, RPL counts: 14856), and the $CD4^{+}CD8^{-}CD25^{-}CD127^{high}CD226^{+}$TIGIT/Tim-$3^{+}PD\text{-}1^{+}$ cluster 19 (Control counts: 108754, RPL counts: 35499) was found to be reduced in participants with this condition, compared to healthy controls (Figure 44). The frequency of clusters 3 (Control counts: 29782, RPL counts: 16323), 12 (Control counts: 39075, RPL counts: 14393), 18 (Control counts: 11704, RPL counts: 5407), 13 (Control counts: 100792, RPL counts: 82017), 9 (Control counts: 1189935, RPL counts: 749569), 20 (Control counts: 259711, RPL counts: 153154), 17 (Control counts: 51639, RPL counts: 22355), 11 (Control counts: 59262, RPL counts: 29067), 2 (Control counts: 135865, RPL counts: 84303), 5 (Control counts: 176321, RPL counts: 148937), 7 (Control counts: 41160, RPL counts: 25546), 8 (Control counts: 24287, RPL counts: 16934), 14 (Control counts: 177021, RPL counts: 114617) appeared unaltered between women with RPL and controls (Figure 44).

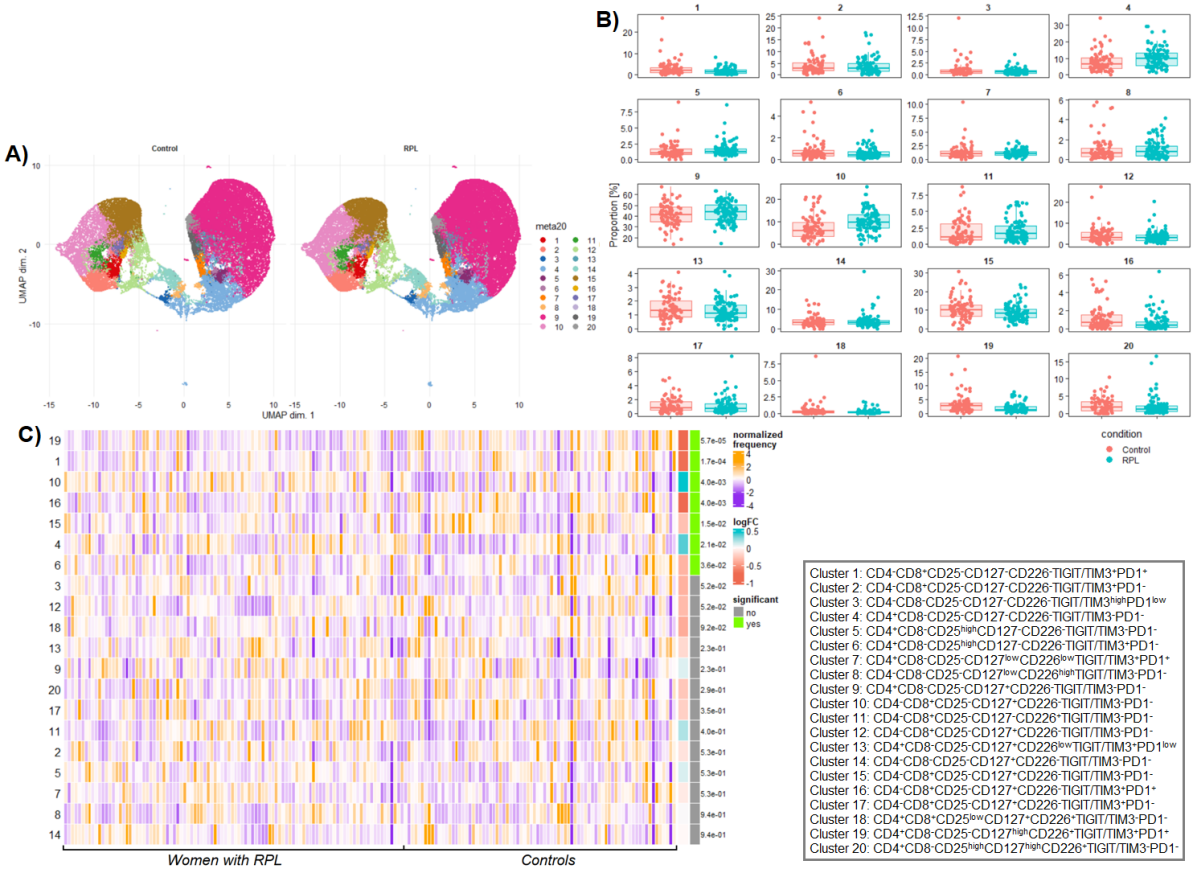


Figure 44. Visualization of T cell cluster prevalence in women with recurrent pregnancy loss (RPL) as detected by mass cytometry. *The 20 clusters of interest in women with RPL and controls are illustrated using a A) uniform manifold approximation and projection (UMAP) plot, with cells coloured according to the respective clusters, a B) relative abundance box plot, depicting cluster proportion in each sample of the control (orange) and RPL (blue) groups, and a C) differential analysis heatmap, displaying the normalised proportion of each cluster in each sample. The heatmap colour varies from purple, suggesting relative under-representation, to orange, suggesting relative over-representation. The green/grey bar indicates significantly (green) or non-significantly (grey) differentially abundant clusters, accompanied by the adjusted p values. A bar representing the log fold change (logFC), indicating over-representation in RPL (blue) or controls (orange) is also included. Cluster phenotypes according to the expression of the CD4, CD8, CD25, CD127, CD226, T-cell immunoreceptor with Ig and ITIM domains/T cell immunoglobulin and mucin domain-containing protein 3 (TIGIT/Tim-3), and programmed cell death protein 1 (PD-1) markers of interest are depicted.*

7.1.5 Mass cytometry assay – B cells

The same assay was performed on the $CD19^+$ B cell dataset. The expression of 7 markers, including CD5, CD25, CD27, CD38, TIGIT/Tim-3, and PD-1, was investigated. Based on these markers' expression, no clear separation pattern between the RPL and control samples was detected (Figure 45). 20 B cell clusters were identified according to their marker expression (Figures 46A, 46B). Clusters 15, 16, 17, 18, and 20 were found to be separated from the other clusters due to their lack of CD38 expression (Figure 46). On the other hand, clusters 1, 7, 11, and 14 displayed a similar expression pattern of the markers of interest, being negative for CD25 and CD27, but expressing CD38 (Figure 46). Moreover, clusters CD7 and CD14 were also found to express CD5 (Figure 46). Clusters 2 and 8 were separated, due to their lack of CD27 expression, from clusters 3, 4, 5, 10, 17, and 18, expressing low to medium levels of CD27, and clusters 6, 9, 12, 13, 15, 16, 19, and 20, displaying medium to high CD27 expression (Figure 46). High CD25 expression was detected on clusters 3 and 12, while expression of this marker was also detected on clusters 2, 4, 8, 9, 13, 15, 16, and 17 (Figure 46B). The inhibitory immune checkpoint receptors TIGIT, Tim-3, and PD-1 were found not to be expressed by any B cell subpopulation (Figure 46B).

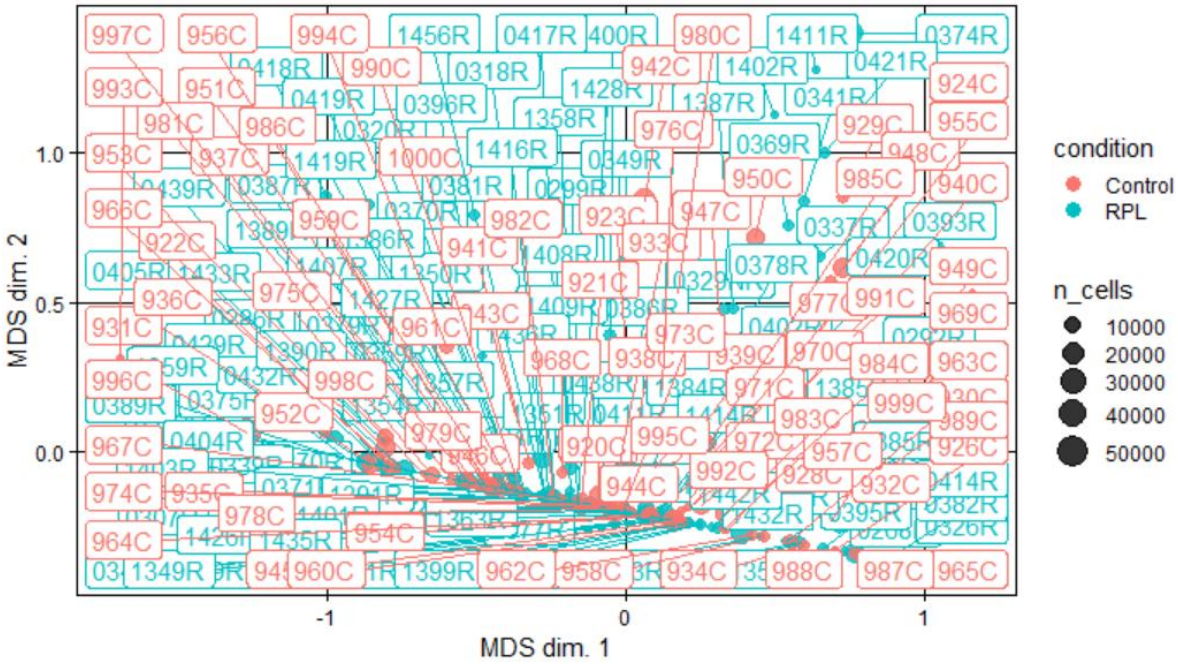


Figure 45. Multi-dimensional scaling (MDS) plot of the control and recurrent pregnancy loss (RPL) B cell samples, summarizing the level of similarity between cohorts. *The distances between samples approximate the difference in median expression of all markers examined, including CD5, CD25, CD27, CD38, T-cell immunoreceptor with Ig and ITIM domains/T cell immunoglobulin and mucin domain-containing protein 3 (TIGIT/Tim-3), and programmed cell death protein 1 (PD-1), translating multi-dimensional data into a two-dimensional scatter plot. Labels displaying the sample identity are included.*

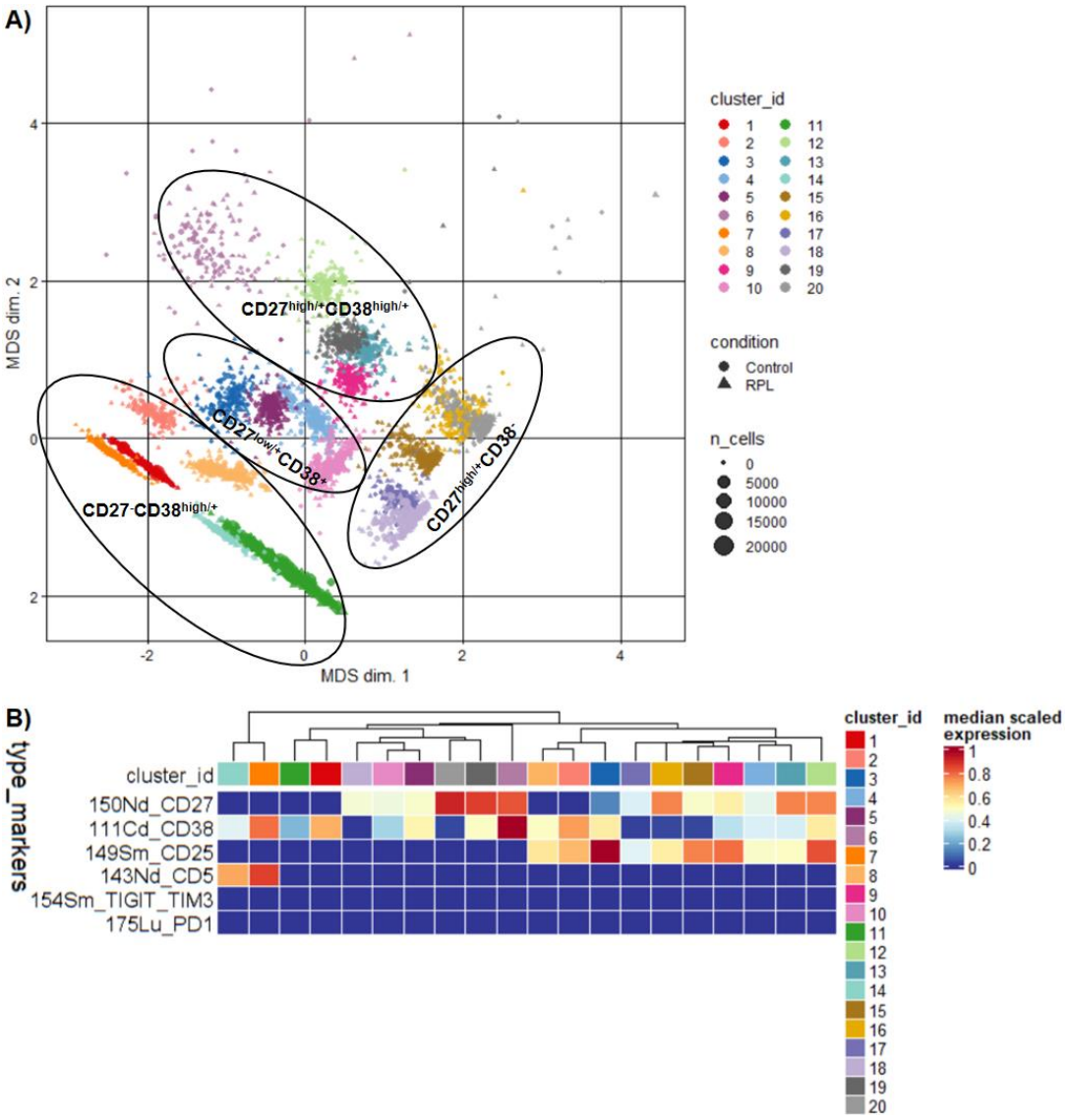


Figure 46. Multi-dimensional scaling and phenotyping of 20 B cell clusters identified by mass cytometry. *A) Multi-dimensional scaling (MDS) plot of pseudobulks generated, with each point on the plot representing a cluster-sample instance, coloured according to the cluster, shaped based on the condition, and with a size proportional to the number of cells it represents. Distances between instances indicate relative phenotypic differences between clusters and samples, taking into consideration all markers assessed. The major phenotypic subgroups are demonstrated. B) Heatmap of median cluster of differentiation (CD)5, CD25, CD27, CD38, T-cell immunoreceptor with Ig and ITIM domains/T cell immunoglobulin and mucin domain-containing protein 3 (TIGIT/Tim-3), and programmed cell death protein 1 (PD-1) expression intensity across the different B cell clusters, ranging from high (red) to low (blue).*

B cell cluster frequencies between RPL and control cases were compared using differential abundance testing. The $CD5^{-}CD25^{-}CD27^{high}CD38^{+}$TIGIT/Tim-$3^{-}PD\text{-}1^{-}$ cluster 19 (Control counts: 11843, RPL counts: 14516) was found to be increased in women with RPL, while the $CD5^{-}CD25^{+}CD27^{-}CD38^{+}$TIGIT/Tim-$3^{-}PD\text{-}1^{-}$ cluster 2 (Control counts: 8763, RPL counts: 3249), $CD5^{-}CD25^{high}CD27^{low}CD38^{+}$ TIGIT/Tim-$3^{-}PD\text{-}1^{-}$ cluster 3 (Control counts: 8665, RPL counts: 2351), $CD5^{-}CD25^{+}CD27^{-}CD38^{+}$TIGIT/Tim-$3^{-}PD\text{-}1^{-}$ cluster 8 (Control counts: 25400, RPL counts: 12047), $CD5^{-}CD25^{+}CD27^{+}CD38^{+}$TIGIT/Tim-$3^{-}PD\text{-}1^{-}$ cluster 9 (Control counts: 10518, RPL counts: 4586), and $CD5^{-}CD25^{+}CD27^{+}CD38^{-}$TIGIT/Tim-$3^{-}PD\text{-}1^{-}$ cluster 15 (Control counts: 21113, RPL counts: 12081) were reduced in women with this condition compared to controls (Figure 47). The frequency of clusters 14 (Control counts: 5763, RPL counts: 4297), 17 (Control counts: 28622, RPL counts: 14922), 6 (Control counts: 2414, RPL counts: 2070), 5 (Control counts: 14045, RPL counts: 11219), 4 (Control counts: 14113, RPL counts: 7740), 11 (Control counts: 171624, RPL counts: 129587), 18 (Control counts: 88364, RPL counts: 58974), 10 (Control counts: 145664, RPL counts: 110230), 12 (Control counts: 7539, RPL counts: 4865), 13 (Control counts: 11881, RPL counts: 7635), 16 (Control counts: 18613, RPL counts: 12665), 20 (Control counts: 358, RPL counts: 966), 7 (Control counts: 8548, RPL counts: 5447), 1 (Control counts: 69322, RPL counts: 41156) was not different between the RPL and control cohorts (Figure 47).

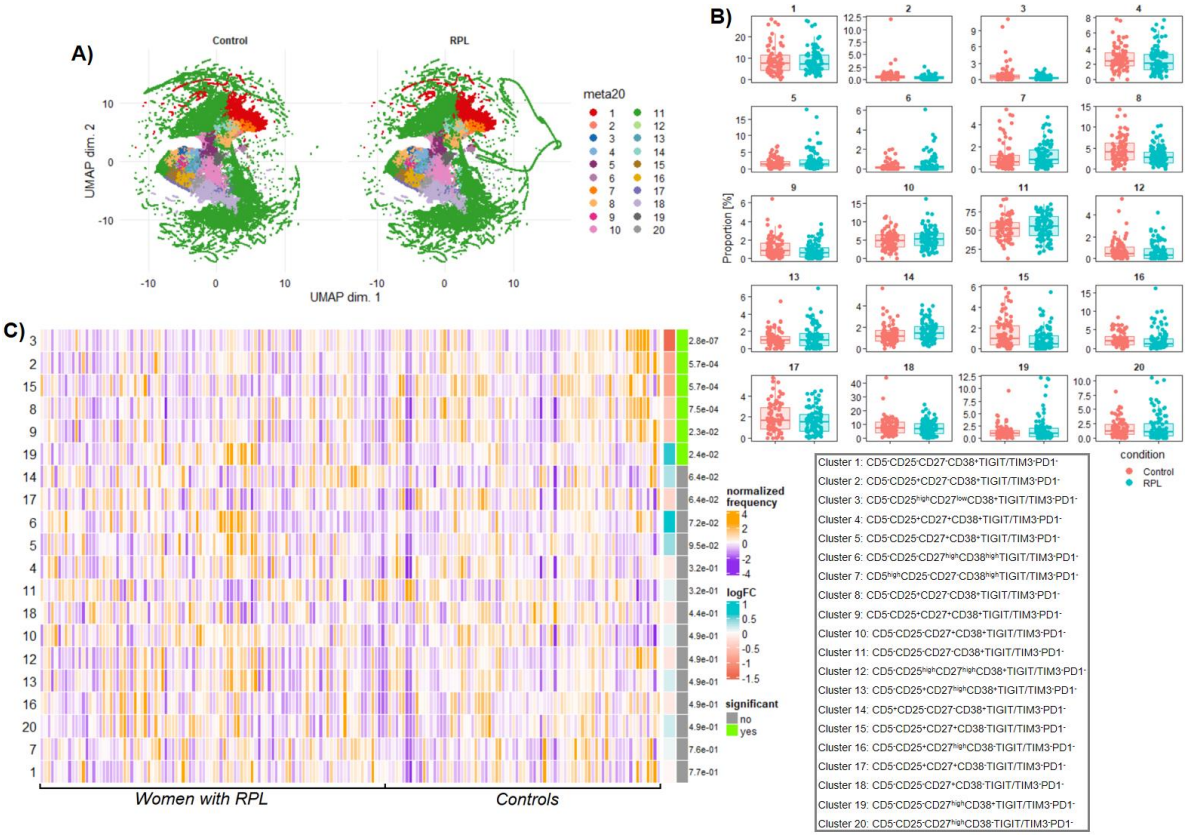


Figure 47. Visualization of B cell cluster prevalence in women with recurrent pregnancy loss (RPL) as detected by mass cytometry. *The 20 clusters of interest in women with RPL and controls are illustrated using a A) uniform manifold approximation and projection (UMAP) plot, with cells coloured according to the respective clusters, a B) relative abundance box plot, depicting cluster proportion in each sample of the control (orange) and RPL (blue) groups, and a C) differential analysis heatmap, displaying the normalised proportion of each cluster in each sample. The heatmap colour varies from purple, suggesting relative under-representation, to orange, suggesting relative over-representation. The green/grey bar indicates significantly (green) or non-significantly (grey) differentially abundant clusters, accompanied by the adjusted p values. A bar representing the log fold change (logFC), indicating over-representation in RPL (blue) or controls (orange) is also included. Cluster phenotypes according to the expression of the CD5, CD25, CD27, CD38, T-cell immunoreceptor with Ig and ITIM domains/T cell immunoglobulin and mucin domain-containing protein 3 (TIGIT/Tim-3), and programmed cell death protein 1 (PD-1) markers of interest are depicted.*

7.1.6 Immune cell subsets in RPL and control subpopulations

Comparing women with idiopathic RPL to the total control population, an increase in circulating NK cell prevalence in lymphocytes ($p<0.0001$) was detected, accompanied by unaltered $CD56^{dim}CD16^{+}$ and reduced $CD56^{bright}CD16^{-}$ cell levels ($p=0.0008$) (Figures 48A-48C). T cell prevalence in the peripheral blood appeared decreased in women with idiopathic RPL compared to controls ($p<0.0001$), while T_H, T_C, and Treg levels were unaltered (Figures 48D-48G). The same findings were observed when comparing women with non-idiopathic RPL to the total control cohort, with elevated NK cell prevalence ($p<0.0001$), reduced $CD56^{bright}CD16^{-}$ NK cell subset levels ($p=0.0499$), and decreased T cell prevalence ($p<0.0001$) detected (Figures 49A-49G). Furthermore, the elevation in NK cell percentage ($p=0.0004$) and the reduction in T cells ($p=0.0370$) was also seen in women with RPL and at least five losses in their reproductive history compared to controls, with both NK and T cell subset prevalence being unaltered (Figures 50A-50G).

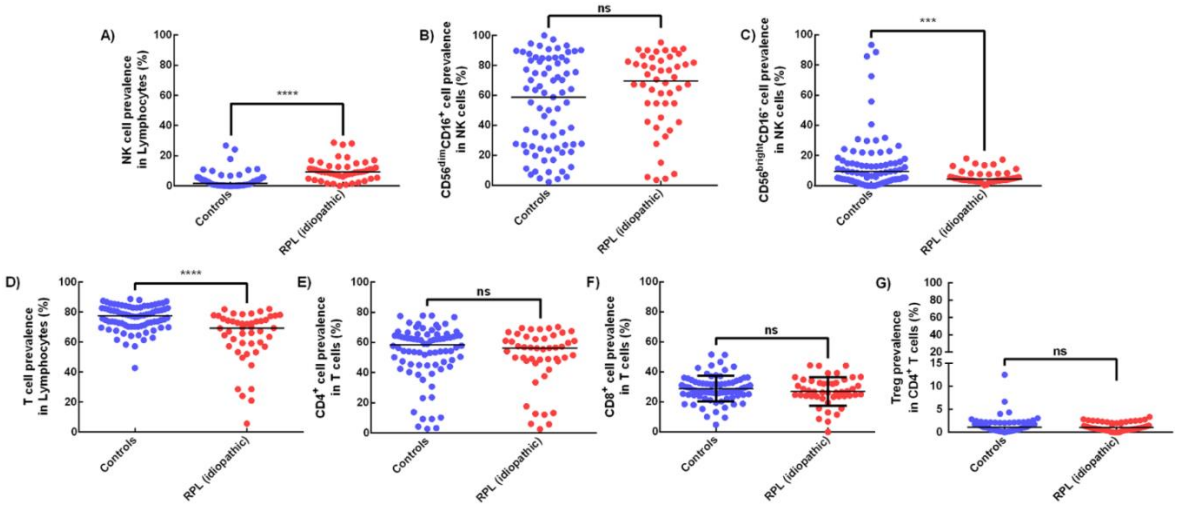


Figure 48. Natural Killer (NK) and T cell population and subpopulation prevalence in women with idiopathic recurrent pregnancy loss (RPL) and controls. *The prevalence of A) $CD3^{-}CD56^{+}$ NK cells in the lymphocyte population and B) $CD56^{dim}CD16^{+}$ and C) $CD56^{bright}CD16^{-}$ cells in the NK cell population of healthy controls (N=77) and women with idiopathic RPL (N=48) is illustrated. The percentage of D) $CD3^{+}$ T cells in the lymphocyte population, E) $CD4^{+}CD8^{-}$ and F) $CD4^{-}CD8^{+}$ cells in the T cell population, and G) regulatory T cells (Tregs) in the $CD4^{+}CD8^{-}$ T cell subpopulation of healthy controls (N=80) and women with idiopathic RPL (N=47) is also displayed. Normally distributed dataset without significantly different variances (F): Unpaired t test used, mean and standard deviation shown. Non-normally distributed datasets (A-E, G): Mann-Whitney test performed, median illustrated. ns: non-significant, ***: p≤0.001, ****: p≤0.0001*

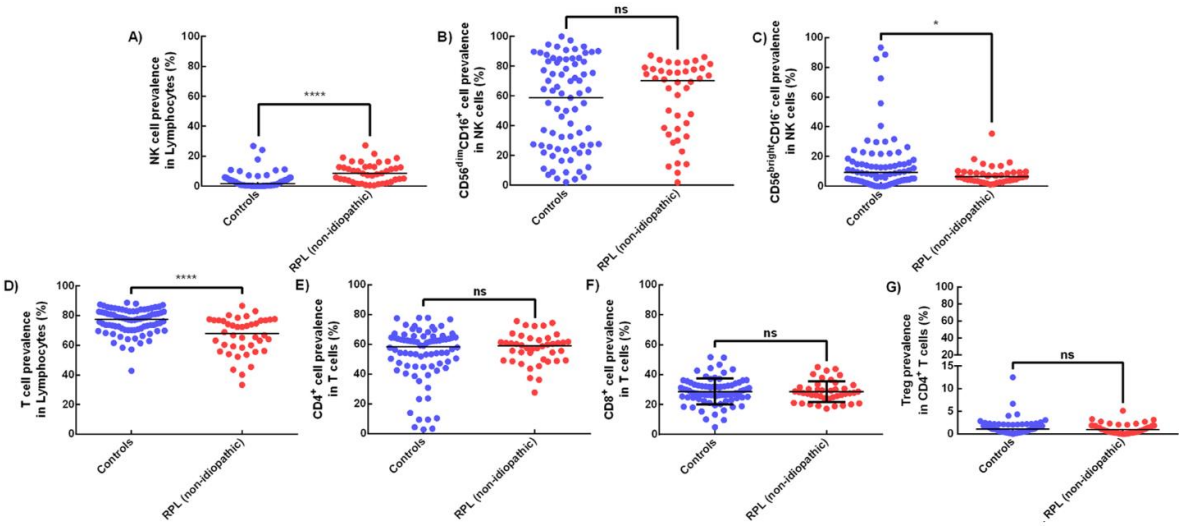


Figure 49. Natural Killer (NK) and T cell population and subpopulation prevalence in women with non-idiopathic recurrent pregnancy loss (RPL) and controls. *The prevalence of A) $CD3^{-}CD56^{+}$ NK cells in the lymphocyte population and B) $CD56^{dim}CD16^{+}$ and C) $CD56^{bright}CD16^{-}$ cells in the NK cell population of healthy controls (N=77) and women with non-idiopathic RPL (N=42) is shown. The percentage of D) $CD3^{+}$ T cells in the lymphocyte population, E) $CD4^{+}CD8^{-}$ and F) $CD4^{-}CD8^{+}$ cells in the T cell population, and G) regulatory T cells (Tregs) in the $CD4^{+}CD8^{-}$ T cell subpopulation of healthy controls (N=80) and women with non-idiopathic RPL (N=42) is also depicted. Normally distributed dataset without significantly different variances (F): Unpaired t test used, mean and standard deviation displayed. Non-normally distributed datasets (A-E, G): Mann-Whitney test performed, median illustrated. ns: non-significant, *: p≤0.05, ****: p≤0.0001*

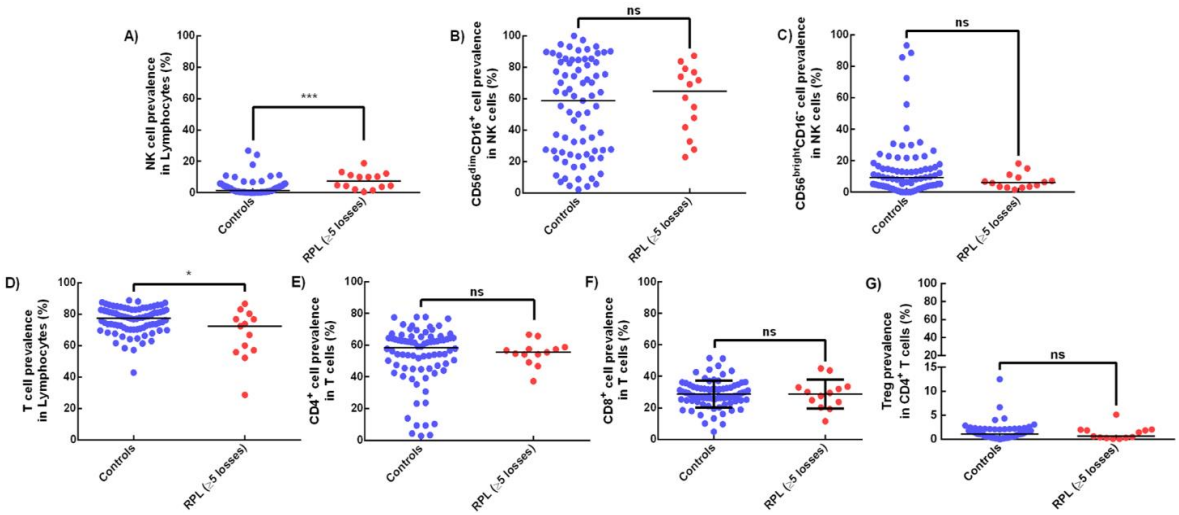


Figure 50. Natural Killer (NK) and T cell population and subpopulation prevalence in women with recurrent pregnancy loss (RPL) with at least 5 past losses and controls. *The prevalence of A) $CD3^{-}CD56^{+}$ NK cells in the lymphocyte population and B) $CD56^{dim}CD16^{+}$ and C) $CD56^{bright}CD16^{-}$ cells in the NK cell population of healthy controls (N=77) and women with RPL with a minimum of 5 losses (N=14) is depicted. The percentage of D) $CD3^{+}$ T cells in the lymphocyte population, E) $CD4^{+}CD8^{-}$ and F) $CD4^{-}CD8^{+}$ cells in the T cell population, and G) regulatory T cells (Tregs) in the $CD4^{+}CD8^{-}$ T cell subpopulation of healthy controls (N=80) and women with RPL with a minimum of 5 losses (N=13) is also displayed. Normally distributed dataset without significantly different variances (F): Unpaired t test used, mean and standard deviation illustrated. Non-normally distributed datasets (A-E, G): Mann-Whitney test performed, median shown. ns: non-significant, *: p≤0.05, ***: p≤0.001*

NK and T cell prevalence in circulating lymphocytes and the levels of $CD56^{dim}CD16^{+}$ and $CD56^{bright}CD16^{-}$ NK cell and T_H, T_C, and Treg T cell subsets were not altered in either controls or in women with RPL belonging to different age subgroups (Figures 51A-51G, 52A-52G). Similarly, these immune cell populations and subpopulations did not appear altered between control women of Asian, Black, White, or Mixed ethnic origin or between Asian, Black, and White women with RPL (Figures 53A-53G, 54A-54G). It should be highlighted that although Treg prevalence in the T_H cell population appeared different between the ethnic subgroups of the control population using the Kruskal-Wallis test ($p=0.0339$), no significant difference was identified by the post-hoc Dunn's tests for multiple comparisons (Figure 53).

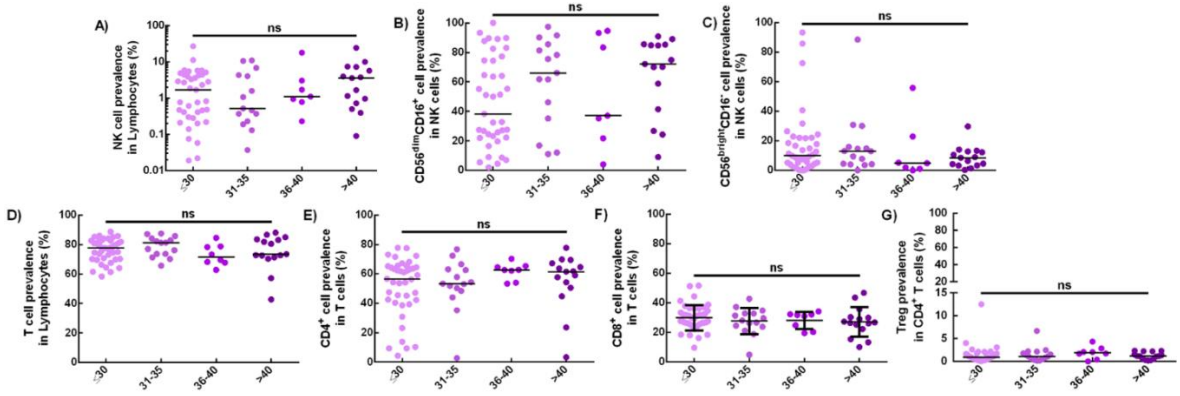


Figure 51. Natural Killer (NK) and T cell population and subpopulation prevalence in control women belonging to different age-associated subgroups. *The prevalence of A) $CD3^{-}CD56^{+}$ NK cells in the lymphocyte population and B) $CD56^{dim}CD16^{+}$ and C) $CD56^{bright}CD16^{-}$ cells in the NK cell population of healthy controls belonging to the ≤30 (N=39), 31-35 (N=15), 36-40 (N=7), and >40 (N=15) age groups is shown. The percentage of D) $CD3^{+}$ T cells in the lymphocyte population, E) $CD4^{+}CD8^{-}$ and F) $CD4^{-}CD8^{+}$ cells in the T cell population, and G) regulatory T cells (Tregs) in the $CD4^{+}CD8^{-}$ T cell subpopulation of healthy controls belonging to the ≤30 (N=41), 31-35 (N=15), 36-40 (N=8), and >40 (N=15) age groups is also depicted. Normally distributed dataset (F): One-way ANOVA test used, accompanied by the Dunn's test for multiple comparisons, mean and standard deviation illustrated. Non-normally distributed datasets (A-E, G): Kruskal-Wallis test performed, accompanied by the Dunn's test for multiple comparisons, median displayed. ns: non-significant*

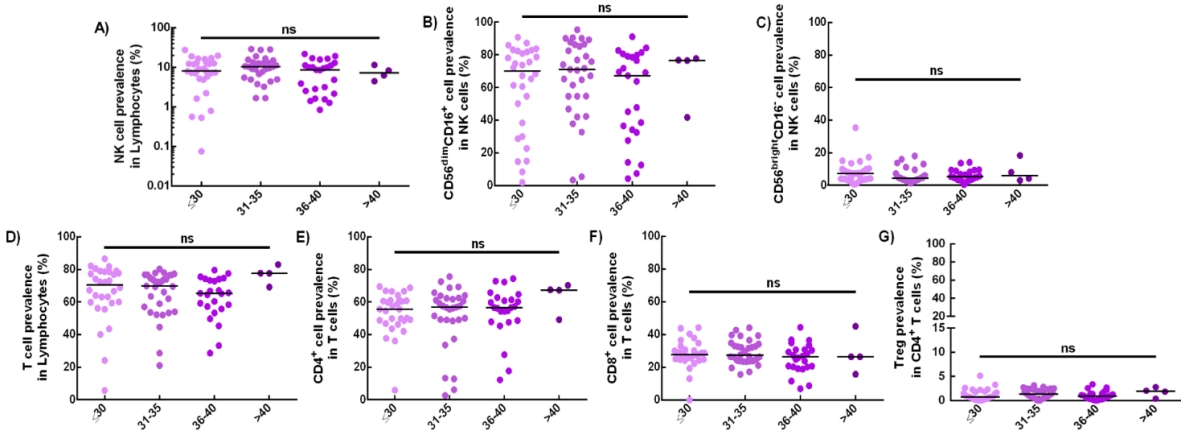


Figure 52. Natural Killer (NK) and T cell population and subpopulation prevalence in women with recurrent pregnancy loss (RPL) belonging to different age-associated subgroups. *The prevalence of A) $CD3^{-}CD56^{+}$ NK cells in the lymphocyte population and B) $CD56^{dim}CD16^{+}$ and C) $CD56^{bright}CD16^{-}$ cells in the NK cell population of women with RPL belonging to the ≤30 (N=30), 31-35 (N=31), 36-40 (N=25), and >40 (N=4) age groups is depicted. The percentage of D) $CD3^{+}$ T cells in the lymphocyte population, E) $CD4^{+}CD8^{-}$ and F) $CD4^{-}CD8^{+}$ cells in the T cell population, and G) regulatory T cells (Tregs) in the $CD4^{+}CD8^{-}$ T cell subpopulation of women with RPL belonging to the ≤30 (N=30), 31-35 (N=31), 36-40 (N=24), and >40 (N=4) age groups is also illustrated. Kruskal-Wallis test performed, accompanied by the Dunn's test for multiple comparisons, median displayed. ns: non-significant*

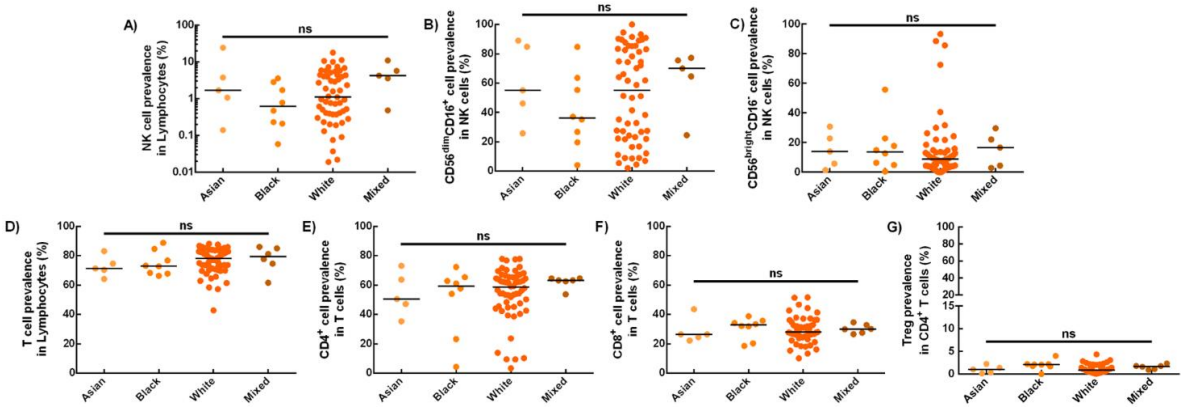


Figure 53. Natural Killer (NK) and T cell population and subpopulation prevalence in control women belonging to different ethnic subgroups. *The prevalence of A) $CD3^{-}CD56^{+}$ NK cells in the lymphocyte population and B) $CD56^{dim}CD16^{+}$ and C) $CD56^{bright}CD16^{-}$ cells in the NK cell population of healthy controls belonging to the Asian (N=5), Black (N=8), White (N=56), and Mixed (N=5) ethnic groups is illustrated. The percentage of D) $CD3^{+}$ T cells in the lymphocyte population, E) $CD4^{+}CD8^{-}$ and F) $CD4^{-}CD8^{+}$ cells in the T cell population, and G) regulatory T cells (Tregs) in the $CD4^{+}CD8^{-}$ T cell subpopulation of healthy controls belonging to the Asian (N=5), Black (N=8), White (N=58), and Mixed (N=6) ethnic groups is also depicted. Kruskal-Wallis test performed, accompanied by the Dunn's test for multiple comparisons, median displayed. ns: non-significant*

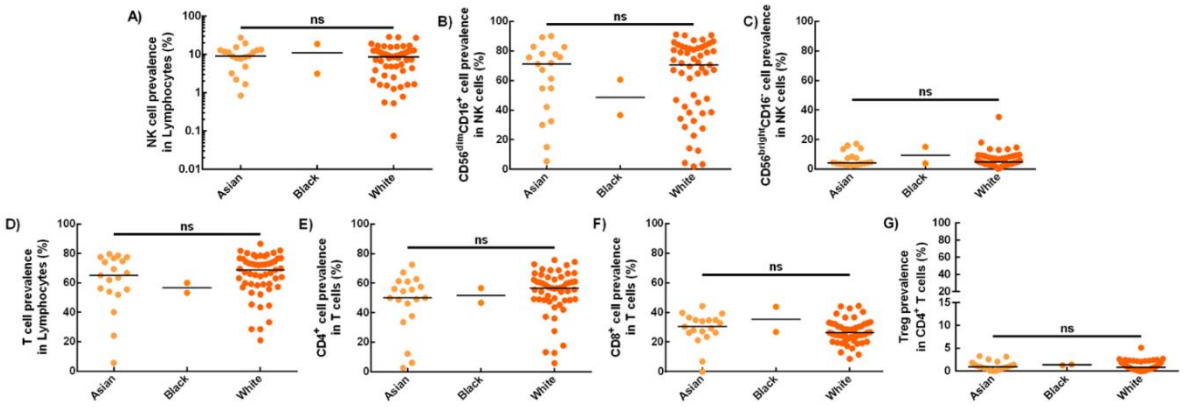


Figure 54. Natural Killer (NK) and T cell population and subpopulation prevalence in women with recurrent pregnancy loss (RPL) belonging to different ethnic subgroups. *The prevalence of A) $CD3^{-}CD56^{+}$ NK cells in the lymphocyte population and B) $CD56^{dim}CD16^{+}$ and C) $CD56^{bright}CD16^{-}$ cells in the NK cell population of women with RPL belonging to the Asian (N=19), Black (N=2), and White (N=53) ethnic groups is shown. The percentage of D) $CD3^{+}$ T cells in the lymphocyte population, E) $CD4^{+}CD8^{-}$ and F) $CD4^{-}CD8^{+}$ cells in the T cell population, and G) regulatory T cells (Tregs) in the $CD4^{+}CD8^{-}$ T cell subpopulation of women with RPL belonging to the Asian (N=19), Black (N=2), and White (N=53) ethnic groups is also illustrated. Kruskal-Wallis test performed, accompanied by the Dunn's test for multiple comparisons, median displayed. ns: non-significant*

To control for ethnic variation between groups, parameters found to be significantly different between the total RPL and control cohorts were evaluated in White-only participants. NK cell percentage in the PBMC ($p<0.0001$) and lymphocyte ($p<0.0001$) populations appeared elevated in White women with RPL compared to White controls, accompanied by a reduced $CD56^{bright}CD16^{-}$ NK cell prevalence ($p=0.0110$) and thus a decreased $CD56^{bright}CD16^{-}/CD56^{dim}CD16^{+}$ NK cell ratio ($p=0.0064$) (Figures 55A-55D). T cell prevalence in leukocytes ($p=0.0377$), PBMCs ($p<0.0001$), and lymphocytes ($p<0.0001$) appeared reduced in White women with RPL compared to White control women (Figures 55E-55G). Similar findings were obtained when controlling for variation in alcohol intake. Specifically, elevated NK cell prevalence in PBMCs ($p=0.0071$) and lymphocytes ($p=0.0010$) and decreased $CD56^{bright}CD16^{-}$ NK cell prevalence ($p=0.0367$) was seen in women with RPL consuming low alcohol amounts, compared to controls with similar alcohol consumption habits (Figures 56A-56C). However the $CD56^{bright}CD16^{-}/CD56^{dim}CD16^{+}$ NK cell ratio appeared unaltered between these two subpopulations (Figure 56D). Moreover, although T cell levels in PBMCs ($p<0.0001$) and lymphocytes ($p=0.0034$) were reduced in women with RPL consuming low alcohol amounts, the difference in T cell prevalence in leukocytes failed to reach statistical significance (Figures 56E-56G).

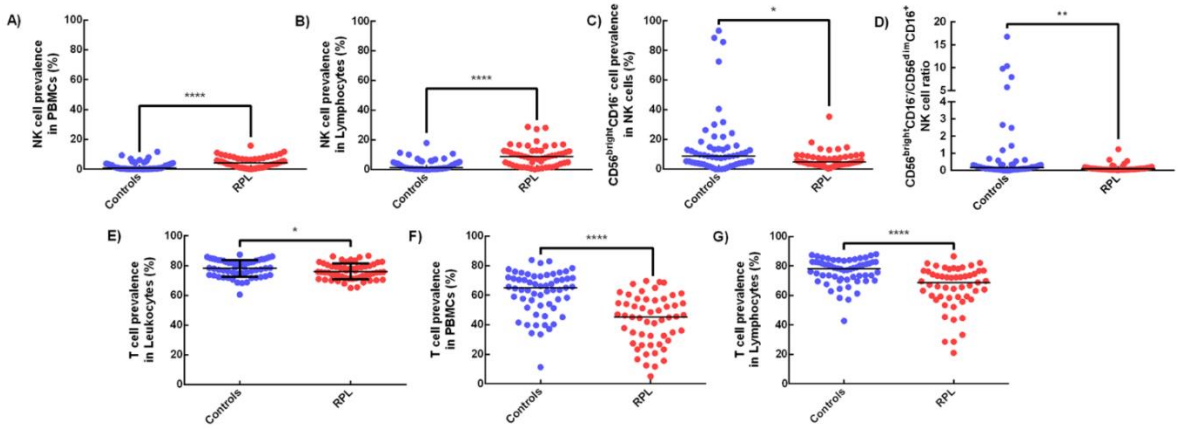


Figure 55. Natural Killer (NK) cell population and subpopulation prevalence and T cell levels in White women with recurrent pregnancy loss (RPL) and White controls. *The prevalence of $CD3^{-}CD56^{+}$ NK cells in A) the peripheral blood mononuclear cell (PBMC) and B) the lymphocyte population, C) the percentage of $CD56^{bright}CD16^{-}$ cells in the NK cell population, and D) the ratio of $CD56^{bright}CD16^{-}$ to $CD56^{dim}CD16^{+}$ NK cell prevalence in healthy controls (N=57) and women with RPL (N=53) of White ethnic origin is displayed. The percentage of $CD3^{+}$ T cells in the E) leukocyte, F) PBMC, and G) lymphocyte population of healthy controls (N=59) and women with RPL (N=56) of White ethnic origin is also shown. Normally distributed dataset without significantly different variances (E): Unpaired t test used, mean and standard deviation illustrated. Non-normally distributed datasets (A-D, F, G): Mann Whitney test performed, median depicted. *: p≤0.05, **: p≤0.01, ****: p≤0.0001*

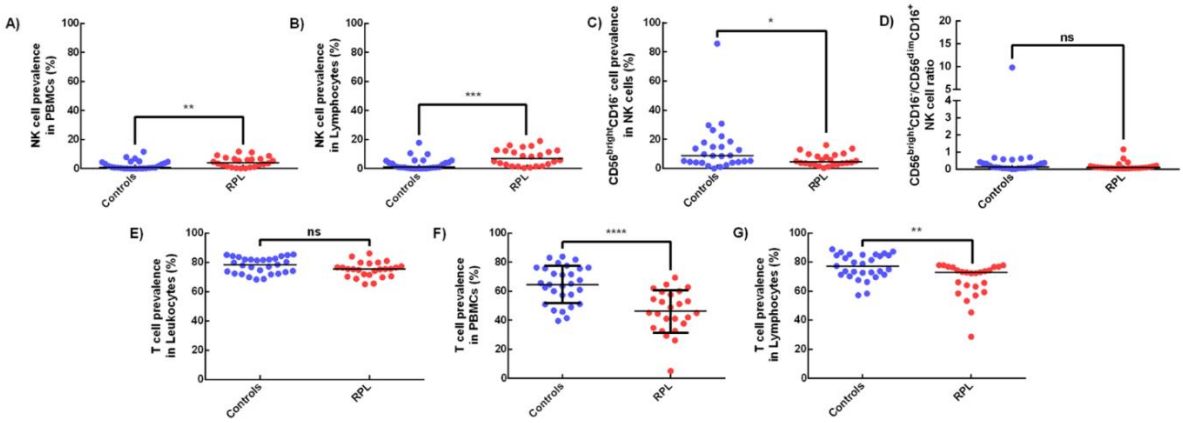


Figure 56. Natural Killer (NK) cell population and subpopulation prevalence and T cell levels in women with recurrent pregnancy loss (RPL), consuming low levels of alcohol, and controls with similar alcohol consumption habits. *The prevalence of $CD3^{-}CD56^{+}$ NK cells in A) the peripheral blood mononuclear cell (PBMC) and B) the lymphocyte population, C) the percentage of $CD56^{bright}CD16^{-}$ cells in the NK cell population, and D) the ratio of $CD56^{bright}CD16^{-}$ to $CD56^{dim}CD16^{+}$ NK cell prevalence in healthy controls (N=27) and women with RPL (N=24), consuming low levels of alcohol, is depicted. The percentage of $CD3^{+}$ T cells in the E) leukocyte, F) PBMC, and G) lymphocyte population of healthy controls (N=29) and women with RPL (N=25), consuming low levels of alcohol, is also illustrated. Normally distributed dataset without significantly different variances (F): Unpaired t test used, mean and standard deviation shown. Non-normally distributed datasets (A-E, G): Mann-Whitney test performed, median displayed. ns: non-significant, *: p≤0.05, **: p≤0.01, ***: p≤0.001, ****: p≤0.0001*

In regards to the potential prognostic capacity of immune cell markers in women with RPL, NK cell and NK cell subset prevalence appeared unaltered between women with RPL who are currently undergoing the 3rd trimester of their subsequent pregnancy or had a live birth and women with RPL and a subsequent miscarriage (Figures 57A-57D). Accordingly, no significant change in total, helper, cytotoxic, or regulatory T cell prevalence could be observed between these subpopulations of women with RPL (Figures 57E-57H).

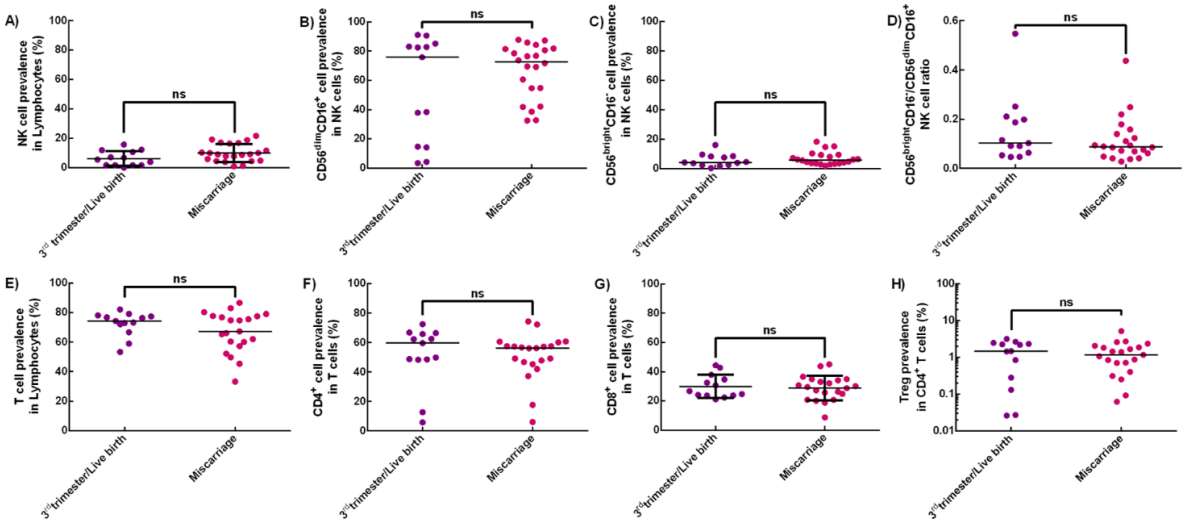


Figure 57. Natural Killer (NK) and T cell population and subpopulation prevalence in women with recurrent pregnancy loss (RPL), who were either in the 3rd trimester of their subsequent pregnancy or had a live birth, and in those with a subsequent miscarriage. *The prevalence of A) $CD3^{-}CD56^{+}$ NK cells in the lymphocyte population and B) $CD56^{dim}CD16^{+}$ and C) $CD56^{bright}CD16^{-}$ cells in the NK cell population and D) the ratio of $CD56^{bright}CD16^{-}$ to $CD56^{dim}CD16^{+}$ NK cell prevalence in women with RPL belonging to the 3rd trimester/Live birth subgroup (N=13) and in those belonging to the miscarriage subgroup (N=22) is depicted. The percentage of E) $CD3^{+}$ T cells in the lymphocyte population, F) $CD4^{+}CD8^{-}$ and G) $CD4^{-}CD8^{+}$ cells in the T cell population, and H) regulatory T cells (Tregs) in the $CD4^{+}CD8^{-}$ T cell subpopulation of women with RPL belonging to the 3rd trimester/Live birth subgroup (N=13) and of those belonging to the miscarriage subgroup (N=21) is also shown. Normally distributed datasets without significantly different variances (A, G): Unpaired t test used, mean and standard deviation illustrated. Non-normally distributed datasets (B-F, H): Mann-Whitney test performed, median displayed. ns: non-significant*

7.1.7 Summary

Table 29. Overview of changes in lymphocyte population and subpopulation prevalence in the peripheral blood of women with recurrent pregnancy loss (RPL) compared to control women. *Alterations in Natural Killer (NK), T, and B cell levels detected by flow cytometry are depicted. Treg: regulatory T cell, ↓: decreased, ↑: increased, ns: non-significant, **: p≤0.01, ****: p≤0.0001*

Cell type	Marker	Change in RPL compared to control group (significance)
NK cells	Total prevalence (%)	↑ (****)
	$CD56^{dim}CD16^{+}$ prevalence (%)	ns
	$CD56^{bright}CD16^{-}$ prevalence (%)	↓ (**)
	$CD56^{bright}CD16^{-}/CD56^{dim}CD16^{+}$ ratio	↓ (**)
T cells	Total prevalence (%)	↓ (****)
	$CD4^{+}$ prevalence (%)	ns
	$CD8^{+}$ prevalence (%)	ns
	$CD4^{+}/CD8^{+}$ ratio	ns
	$CD4^{+}CD8^{+}$ prevalence (%)	ns
	$CD45RA^{+}CD4^{+}$ prevalence (%)	ns
	$CD45RA^{+}CD8^{+}$ prevalence (%)	ns
	Treg prevalence (%)	ns
B cells	Total prevalence (%)	ns

7.2 Discussion

Due to their high prevalence in uterine tissue during pregnancy, reaching up to 90.00%, NK cells are the immune cells most closely associated with reproductive success.[123] Hence, the prevalence of these cells and their subpopulations in the peripheral blood were initially examined. The TBNK assay was utilised as it is routinely employed for the evaluation of immune cell subsets in the clinical setting. However, in the TBNK cell assay NK cells are defined as $CD3^{-}CD56^{+}$ and/or $CD3^{-}CD16^{+}$ leukocytes. Thus, the flow assay was also developed to allow identification and enumeration of $CD3^{-}CD56^{+}$ pNK cells. Using the TBNK assay, the pNK cell population of women with RPL appeared unaltered compared to controls (Figures

37E, 38F), but in the flow assay a significant increase in NK cell prevalence was detected (Figures 39A, 39B). This variation in experimental findings between assays could stem from the difference in gating strategies or from the different methodologies used. The unaltered NK cell absolute counts detected via the TBNK assay indicate that changes in this population's prevalence in women with RPL are driven by shifts in other immune subsets, such as T cells (Figure 38A). The flow assay findings come in agreement with previous studies on non-pregnant women with RPL, highlighting an increase in pNK cell prevalence in the lymphocyte population.[164, 183-185, 187] On the other hand, studies reporting an unaltered $CD56^+$ NK cell prevalence in the peripheral blood of these women have also been published.[171, 194, 347]

Furthermore, an important issue to consider is the high pNK cell level variation in both the RPL and the control populations. NK cells are thought to constitute approximately 15.00% of the circulating lymphocyte population.[251] In one study on healthy adults, NK cells, defined as $CD3^-CD56^+CD16^+$ cells, were found to represent 12.00±1.00% of lymphocytes, ranging between 2.00% and 31.00%,[688] while in another study $CD3^-CD56^+CD16^+$ cells were shown to constitute 9.80% [95% CI (5.33%-20.25%)] of lymphocytes in females, displaying significant gender-related fluctuation.[689] Mean pNK cell prevalence in women with RPL has been reported to be 11.40%, ranging between 3.08% and 27.50%.[185] In our study, the median $CD3^-CD56^+$ NK cell prevalence in the lymphocyte population was equal to 1.58% in the control group, varying from 0.02% to 26.80%, and was equal to 9.11% in the RPL group, with a minimum of 0.08% and a maximum of 28.70% (Figure 39B). Hence, the pNK cell levels detected in our study appeared to be lower than previous reports,

particularly in regards to the control group, possibly due to the PBMC isolation and staining protocol followed or as a result of a stricter gating strategy employed. Although both the RPL and control cohorts recruited are expected to reflect the national population to a great extent, the decreased levels observed could also indicate reduced development or elevated death of NK cells or increased recruitment to tissue due to undetermined factors. The absence of a clear definition for “elevated” pNK cell numbers has been underlined in a systematic review and meta-analysis, where definitions of ≥10.00%, ≥12.00%, and ≥18.00% were observed.[184] In another study 12.00%-18.00% pNK cell prevalence in lymphocytes was described as “elevated” and ≥18.00% as highly elevated.[164] According to that study however, almost half of the RPL cases displayed pNK cell levels within the “normal” range.[164] Thus, the establishment of unequivocal reference ranges is of outmost importance.

High variation in pNK cell subpopulation prevalence was also detected in our study, particularly in regards to the $CD56^{dim}CD16^{+}$ subset, whose median percentage in the NK cell population was equal to 58.80% in the control group and 70.05% in the RPL one, varying however from 2.12% to 100.00% (IQR: 58.05%) in controls and from 1.95% to 95.40% (IQR: 39.02%) in women with RPL. The levels of this subset did not appear significantly altered in participants with RPL, possibly due to the high degree of variability between cases (Figure 39C). The $CD56^{bright}CD16^{-}$ NK cell subset was reduced in participants with RPL, compared to controls, with a median prevalence equal to 4.92% and 9.47% respectively (Figure 39D). Even though the $CD56^{bright}CD16^{-}$ prevalence values also displayed a wide range, between 0.00% and 93.30% (IQR: 13.12%) in control and between 0.39% and 35.40% (IQR: 5.10%)

in RPL cases the variability detected was lower than that of the $CD56^{dim}CD16^{+}$ subset. In a study on healthy adults, including participants with reproductive conditions, a 96.00±0.90% $CD56^{dim}$ NK cell prevalence, varying between 90.00% and 99.00%, and a 4.00±0.90% $CD56^{bright}$ NK cell prevalence, ranging from 1.00% to 10.00%, was reported.[688] This difference between findings could be a result of cohort differences and use of CD16 as an additional marker for subset identification in the present study. Furthermore, an increase in the $CD56^{dim}CD16^{+}$ subset of non-pregnant women with RPL, has been reported to result in a reduced $CD56^{bright}CD16^{-}$ to $CD56^{dim}CD16^{+}$ pNK cell ratio.[185] Although in our study a $CD56^{dim}CD16^{+}$ increase was not observed, the reduction of $CD56^{bright}CD16^{-}$ cells was found to induce the same outcome (Figure 39E). In contradicting studies however, no change in the $CD56^{bright}/CD56^{dim}$ NK ratio was reported in these women.[191, 193, 194]

T cells also constitute a major decidual component and thus have been linked to the pathogenesis of RPL.[89] Using both the TBNK and flow cytometry assays, a reduction in circulating $CD3^{+}$ T cell prevalence and absolute counts in women with RPL was observed, in agreement to previous findings (Figures 37A, 38A, 40A, 40B).[377] It should be acknowledged that in clinical practice, this represents a small change in T cell proportions and the clinical significance remains to be determined. Specifically, T cell prevalence was found to be equal to 77.50% [95% CI (73.70%, 80.50%)] in controls and 69.20% in women with RPL [95% CI (64.50%, 73.00%)]. Although similar T cell ranges have been previously reported, no significant difference in regards to T cell prevalence was detected in multiple studies examining non-pregnant women with RPL.[182, 382, 383] T_H and T_C absolute counts appeared reduced in women with RPL (Figures 38B, 38C). However, both total and $CD45RA^{+}$

T_H and T_C cell prevalence was unaltered (Figures 37B, 37C, 40C-40F), in agreement to previous findings.[383, 690, 691] Contradicting findings have again been obtained with reports of decreased T_H and T_C cells in women with RPL but also findings indicating an elevation in peripheral blood T_C cells in these women.[187, 382, 394] Overall, total, $CD4^+$, and $CD8^+$ T cell levels in the peripheral blood are not thought to be altered during pregnancy compared to the non-pregnant state and throughout the different trimesters,[307, 382, 397] indicating that their activity rather than their numbers could be more closely associated with reproductive success.

Even though Tregs are considered as greatly important to reproduction and the mediation of fetal tolerance,[391] in the present study their prevalence appeared similar between the RPL and control groups (Figure 40G). However, a reduction in pre-conception Treg levels in the circulation has been previously reported.[383, 466] As peripheral Treg prevalence is drastically increased during pregnancy, and particularly during the second trimester,[397, 466, 468] it is possible that in a subpopulation of women with RPL alterations in Treg prevalence are evident during but not before pregnancy. Two $CD4^+CD25^{high}CD127^-$ Treg-like populations were also detected by mass cytometry (Figure 43B). One of these populations was found to express TIGIT and/or Tim-3 and was reduced in the RPL group (Figures 43B, 44). Unfortunately, Tim-3 and TIGIT expression could not be examined separately. In the T_H cell population, Tim-3 expression is thought to be primarily detected on T_H1 cells.[692] Although the $CD25^{high}CD127^{low/-}$ phenotype is thought to mainly include Tregs,[632, 693] CD25 expression can also be detected on activated effector T cells.[694] On the other hand, TIGIT expression has been linked to the stability and suppressive capacity of Tregs and was found to be increased upon activation.[695]

Thus, it is possible that both these subsets represent Treg subpopulations, with the activated one being reduced in women with RPL. However, independent examination of these markers is required for the validation of this hypothesis. Interestingly, none of the two Treg-like populations was found to express PD-1 (Figure 43B). PD-1 is thought to be central in the development and maintenance of the Treg population,[696, 697] thus being potentially central in reproductive success. PD-1 expression was shown to be enhanced upon stimulation,[383] which could offer a potential explanation for its absence on unstimulated Treg-like cells.

Apart from the Treg-like population an additional T_H cell cluster was found to be reduced in women with RPL, displaying a $CD25^-CD127^{high}CD226^+$TIGIT/Tim-$3^+$PD-$1^+$ phenotype (Figure 44). This cluster was the only cluster whose expression was altered in the RPL group, on which CD226 expression was observed (Figure 43B). Although CD226 is primarily linked to T_C cytotoxicity,[286, 288, 698] on T_H cells it is thought to be involved in T_H1 development,[699] indicating that this population, which is reduced in RPL cases, could be predisposed towards pro-inflammatory T_H1 activity. The $CD25^-CD127^-CD226^-$TIGIT/Tim-3^+PD-1^+, $CD25^-CD127^+CD226^-$TIGIT/Tim-3^-PD-1^-, and $CD25^-CD127^+CD226^-$TIGIT/Tim-3^+PD-1^+ T_C subpopulation levels were also decreased in RPL (Figure 44). The $CD25^-CD127^-$ phenotype is thought to be associated with a perforin- and IFN-γ-secreting effector activity, while the $CD25^{low/-}CD127^+$ one has been linked to IL-2-secreting naïve and central memory cells.[693] Using mass cytometry, elevation of the $CD25^-CD127^-CD226^-$TIGIT/Tim-3^-PD-1^- T_H and the $CD25^-CD127^+CD226^-$TIGIT/Tim-3^-PD-1^- T_C subset was detected in RPL participants (Figure 44). Intriguingly, most subsets decreased in RPL were found to be TIGIT/Tim-3^+PD-1^+, while both subsets augmented were

TIGIT/Tim-3^{-}PD-1^{-} (Figures 43B, 44), indicating an overall deficiency in the control of T cell activity in RPL. In agreement to our findings PD-1-expressing peripheral blood T_H1 and T_H17 cells were found to be less prevalent in women with idiopathic RPL than controls.[383] Additionally, in a study on women with RPL and immunological abnormalities, a reduced frequency of PD-1^{+} and Tim-3^{+} exhausted T_C cells compared to healthy controls was reported,[423] while in another study on idiopathic RPL no change in TIGIT or PD-1 expression by peripheral T_C cells was detected.[690]

B cell prevalence and absolute counts were also examined, with no difference detected between non-pregnant women with RPL and controls, in agreement to previous studies (Figures 37F, 38G).[379] Due to the small uterine B cell numbers, these cells have not been examined in detail in the context of RPL and the phenotypes associated with pregnancy have not been defined. Thus, the expression of certain B cell markers was examined by mass cytometry. No pre-conception alterations in the levels of two CD5^{+} B cell subsets were detected in the RPL compared to the control group (Figures 46B, 47). Although these cells have been linked to polyreactive natural antibody (NAb) production,[503-506] they are now thought to represent only ~75%, of the CD27^{+}CD43^{+} NAb-secreting B cell population, with NAb secretion by CD5^{-} cells also reported.[489, 508, 509] Hence, our findings indicate an absence of alteration in this subset pre-conception. However, as NAbs have been linked to pregnancy failure,[485, 486, 510] further research is required for the evaluation of total NAb-producing B cell levels in the peripheral blood of women with RPL. Another subset of interest in RPL is the CD19^{+}CD24^{high}CD38^{high} Bregs, which are thought to contribute to the maintenance

of tolerance through the production of cytokines, like IL-10.[488, 524] IL-10^{+} Bregs are thought to express high CD27 levels and CD25.[700] High CD38 levels were not detected on any population expressing CD25 and CD27 (Figure 46B). However, three populations were found to express these markers, including a CD25^{+}CD27^{+}CD38^{+}, a CD25^{high}CD27^{high}CD38^{+}, and a CD25^{+}CD27^{high}CD38^{+} one, the first of which was found to be decreased in RPL (Figures 46B, 47). Investigation using additional markers, such as IL-10 and CD24, is required to accurately determine whether Bregs are indeed reduced in non-pregnant women with this condition. CD38 and high CD27 expression can be also used for plasma cell identification.[701, 702] CD25^{+} B cells have been found to produce very low immunoglobulin amounts,[703] indicating that plasma cells most likely belong to a CD25^{-} subset. Two CD25^{-}CD27^{high}CD38$^{high/+}$ subsets were detected, one of which was found to be increased in RPL (Figures 46B, 47), highlighting a possible elevation of plasma cells. However, markers like CD78 and CD138 could be utilised to confirm the identity of these cells.[702]

Moreover, three CD25$^{high/+}$CD27$^{low/-}$CD38^{+} B cell subpopulations were found to be reduced in the RPL group (Figure 47). Although the nature and activity of these cells is unclear, the absence of CD27 expression indicates that these subsets represent naïve B cell populations,[702] while the presence for CD25 suggest a significant involvement of these cells in antigen presentation.[703] A CD25^{+}CD27^{+}CD38^{-} B cell subset was also found to be reduced in women with RPL (Figure 47), possibly representing a B cell memory subset with the ability to shape and control immune responses through antigen presentation and IL-10 secretion.[702-704] Finally, the expression of the TIGIT, Tim-3, and PD-1 immune checkpoint receptors was

examined on B cells of women with RPL and controls. These receptors were not found to be expressed by any B cell subpopulation (Figure 46B). In previous studies on pregnant and non-pregnant women Tim-3 expression on peripheral blood B cells was not detected,[705] while in a hepatitis C virus-related hepatocellular carcinoma study very low Tim-3 levels were detected on B cells of healthy controls.[706] Two subpopulations of $TIGIT^+$ marginal zone and memory Bregs have been described in humans,[707] but the expression of this receptor by circulating B cells remains to be elucidated. PD-1 expression on peripheral blood B cells has been reported and was found to increase upon activation.[706, 708] Hence, although in our study PD-1 was not expressed on detectable levels, differences in PD-1 expression between women with RPL and controls could be possibly seen after B cell activation.

Changes in circulating NK and T cell populations and subpopulations detected when comparing the total RPL cohort to controls were also observed when separately examining the idiopathic and the non-idiopathic RPL subgroups in relation to the control group (Figures 48, 49). This indicates that changes in lymphocyte numbers potentially influence the development of RPL irrespective of the presence of underlying pathologies. In agreement to these findings, $CD16^-$ and $CD16^+$ pNK cell subset prevalence in women with RPL was found not to be influenced by the presence of different potential miscarriage-associated risk factors.[169, 709] On the other hand, elevated uNK cell levels have been detected in women with idiopathic RPL compared to those with the non-idiopathic form of this condition.[710] Hence, findings in the periphery might not reflect the *in utero* situation, with further studies required for the examination of immune activity in idiopathic and non-idiopathic cases.

In women with RPL and at least five losses in their reproductive history, NK cell prevalence in the lymphocyte population appeared augmented, while T cell prevalence was reduced, as it was observed when comparing the total RPL and control groups (Figures 50A, 50D). However, the difference between women with RPL and controls did not appear exacerbated when only women with at least five losses were taken into consideration. Moreover, in these women all NK and T cell subpopulations examined were not significantly altered compared to controls (Figures 50B, 50C, 50E-50G), including the $CD56^{bright}CD16^{-}$ NK cell subset that appeared reduced in the total RPL cohort (Figure 39D). Hence, alterations in peripheral lymphocyte levels of women with RPL did not appear affected by higher order loss.

Examining the different age- and ethnicity-associated subgroups no significant change in the NK and T cell population and subpopulation prevalence was detected in either the RPL or the control group (Figures 51-54). Thus, the prevalence of these immune subsets did not appear to be influenced by age and ethnicity, in contrast to findings suggesting a potential involvement of these factors in NK and T cell distribution.[674, 711-713] In agreement to that, significant changes in the total and $CD56^{bright}CD16^{-}$/$CD56^{dim}CD16^{+}$ NK cell and T cell levels observed when comparing the total RPL and control groups were also observed when comparing only White women in these groups (Figure 55). However, when comparing women with RPL consuming low levels of alcohol to controls with similar habits, significant changes observed in regards to total and $CD56^{bright}CD16^{-}$ NK cell prevalence were in agreement to those detected when examining the original cohorts, but the $CD56^{bright}CD16^{-}$/$CD56^{dim}CD16^{+}$ NK cell ratio appeared unaltered (Figures 56A-

56D). Similarly, although T cell prevalence in the PBMC and lymphocyte population was reduced in both the total and the low-alcohol RPL populations, compared to the respective controls, the difference in T cell prevalence in leukocytes was lost when comparing the low-alcohol subgroups (Figures 56E-56G). It is thus possible that alterations in NK cell subset ratio and T cell prevalence detected in women with RPL compared to controls, were influenced by the differences in alcohol intake.

No prognostic capacity of circulating NK and T cell population and subpopulation assessment was displayed in regards to the following pregnancy outcome of women with RPL (Figure 57). In contrast to these findings, elevated pNK cell levels pre-conception have been linked to subsequent miscarriage,[161, 162, 164, 165, 171, 475] with two studies defining elevated pNK cell levels in the lymphocyte population using a threshold of 12% and another using an 18% threshold.[162, 164, 171] However, in other studies circulating NK cell and NK cell subset prevalence was found not to be significantly different between women with successful following pregnancies, subsequent miscarriages with chromosomally normal fetuses, and subsequent miscarriages with chromosomally abnormal fetuses.[169, 170, 175, 197] Furthermore, elevated circulating T cell levels pre-conception were associated with a following live birth, with no prognostic capacity of T_H and T_C cells reported.[381] Circulating Treg quantification during early pregnancy has also displayed a predictive capacity in regards to pregnancy outcome, with low Treg levels being linked to miscarriage occurrence.[475, 545] Although beyond the scope of this study, a potential prognostic capacity of B cell antibody production post-conception has also been suggested, with the presence of anti-HLA antibodies and the reduced prevalence of serum asymmetric antibodies being linked to subsequent pregnancy failure.[512, 521]

The prognostic value of uterine lymphocyte assessment also remains contentious. In a small study, increased eNK cell numbers have been reported in women with RPL whose following pregnancy resulted in miscarriage compared to those who proceeded to have a live birth.[167] In multiple other studies no predictive capacity of eNK cell prevalence was detected.[129, 172-174, 714] Furthermore, endometrial T, T_H and T_C cell prevalence did not appear to be altered in women with idiopathic RPL and a following live birth compared to those with a following failed pregnancy in some studies.[173, 174] However, elevated endometrial T_H and T_C percentages and an increased T_H/T_C ratio in women with idiopathic RPL have been associated with a following miscarriage in other studies.[167, 174] A predictive value of endometrial B cell prevalence was also suggested, being augmented in women with RPL and a following 1st-trimester miscarriage compare to those maintaining an intact conceptus until at least the 36th week of their following pregnancy.[174] However, in another study endometrial $CD20^+$ cell levels were not found to be significantly different in women with idiopathic RPL, with or without a following successful pregnancy.[173] Hence, the predictive capacity of lymphocyte examination in RPL warrants further investigation.

In conclusion, elevated pNK cell prevalence and a shift towards the primarily cytotoxic $CD56^{dim}CD16^+$ subset was detected in women with RPL, in agreement with the rationale behind immunological testing addition to miscarriage investigations. On the other hand, T cell levels appeared reduced in these women, accompanied by unaltered subset prevalence. Such findings could indicate an enhanced contribution of more aggressive NK cells to the pre-conception and potentially post-conception immune responses in women with RPL. In agreement to

this “inflammatory” hypothesis, through mass cytometry a reduction in a Treg-like and a Breg-like subset was detected in women with RPL, alongside an increase in plasma-like cells. Checkpoint receptor expression patterns on T cell subsets were also consistent with this hypothesis, highlighting a potential defect in the regulation of T cell-mediated responses in RPL.

7.2.1 Limitations and future research

NK cells could provide a valuable tool for the identification of immunological RPL but through the present study the importance of establishing a universal NK cell definition and standardising the methodology prior to the possible introduction of testing in any clinical setting was highlighted. As multiple studies have now examined pNK cell levels in control and RPL cases, a meta-analysis of the published data could facilitate reference range establishment. A similar need has arisen in regards to T cells as significant variation in the levels of both these immune cell populations and their subpopulations is seen in the peripheral blood of women with RPL and controls.

Although 100 women with RPL and 80 controls were recruited, not all samples were utilized for lymphocyte enumeration via flow cytometry due to insufficient blood volume collection and high cell death >40% in certain samples (*N*=6). The levels of cell death per sample were assessed using one additional tube per flow cytometry panel (Supplementary Figure 23). As cell death evaluation was added to the experimental plan at a later stage, it was not performed for all samples (*N*=54 control and *N*=65 RPL).

The mass cytometry panel was primarily designed for the examination of NK cell subpopulations, explained in detail later in this report. Thus, the detailed examination of T and B cell subsets was not permitted due to the limited number of metals available. However, the generation of similar phenotyping panels for T and B cells could contribute to the elucidation of pre-conceptional peripheral immune activity in women with RPL. Moreover, as a result of their limited uterine levels, the investigation of B cells in the context of pregnancy and reproductive failure remains significantly limited. Hence, further studies are required to determine whether these cells are involved in the establishment and maintenance of healthy pregnancies and in the pathogenesis of reproductive conditions, like RPL.

8 NK CELL ACTIVATION AND CYTOTOXICITY EVALUATION

8.1 Results

8.1.1 Cytotoxicity assay

NK cells are characterised by their cytotoxic capacity; hence their ability to kill target K562 cancer cells was examined in cultures containing 0.5:1 (Controls *N*=71, RPL *N*=71), 1:1 (Controls *N*=69, RPL *N*=72), and 2:1 (Controls *N*=72, RPL *N*=72) NK cell:K562 cell concentrations. Average specific target cell death in these cultures was also calculated (Controls *N*=76, RPL *N*=72). CD107a expression on alive and dead NK cells following their co-incubation with K562 cells was assessed as a marker of degranulation in the 0.5:1 (Controls *N*=71, RPL *N*=52), 1:1 (Controls *N*=69, RPL *N*=53), and 2:1 (Controls *N*=72, RPL *N*=53) NK cell:K562 cell co-cultures, with the average expression also determined (Controls *N*=76, RPL *N*=53).

Specific target cell death was not found to be induced at a different rate by NK cells isolated from women with RPL, compared to those of controls [Average controls: 4.19%, 95% CI (1.92%, 12.42%), Average RPL: 4.00%, 95% CI (1.67%, 9.13%)] (Figures 58A-58D). Moreover, no significant alterations in $CD107a^{+}$ dead NK cell prevalence [Average controls: 75.33%, 95% CI (66.27%, 79.53%), Average RPL: 76.83%, 95% CI (53.60%, 84.70%)] or CD107a expression intensity on dead NK cells [Average controls: 15823.00, 95% CI (14246.00, 17353.00), Average RPL: 15261.00, 95% CI (11957.00, 18683.00)] could be detected between the RPL and control groups, in any of the co-cultures (Figures 59A-59D, 60A-60D). CD107a expression intensity on alive NK cells in co-cultures containing different NK cell amounts and the average expression intensity in these co-cultures also appeared to be similar between RPL and control participants [Average controls: 2950.00, 95%

CI (2399.00, 3912.00), Average RPL: 5860.00, 95% CI (2101.00, 8192.00)] (Figures 60E-60H). However, the prevalence of CD107a-expressing alive NK cells in the 1:1 [Controls: 64.55%, 95% CI (50.30%, 74.90%), RPL: 77.80%, 95% CI (73.10%, 83.60%), p=0.0102] and 2:1 [Controls: 65.35%, 95% CI (49.30%, 71.40%), RPL: 75.40%, 95% CI (64.40%, 84.20%), p=0.0183], but not 0.5:1 [Controls: 70.55%, 95% CI (49.10%, 78.10%), RPL: 78.45%, 95% CI (73.50%, 82.20%)], NK cell:K562 cell co-cultures and the average $CD107a^{+}$ alive NK cell prevalence [Controls: 67.35%, 95% CI (49.57%, 75.40%), RPL: 78.05%, 95% CI (71.87%, 83.17%), p=0.0236] appeared elevated in women with RPL (Figures 59E-59H).

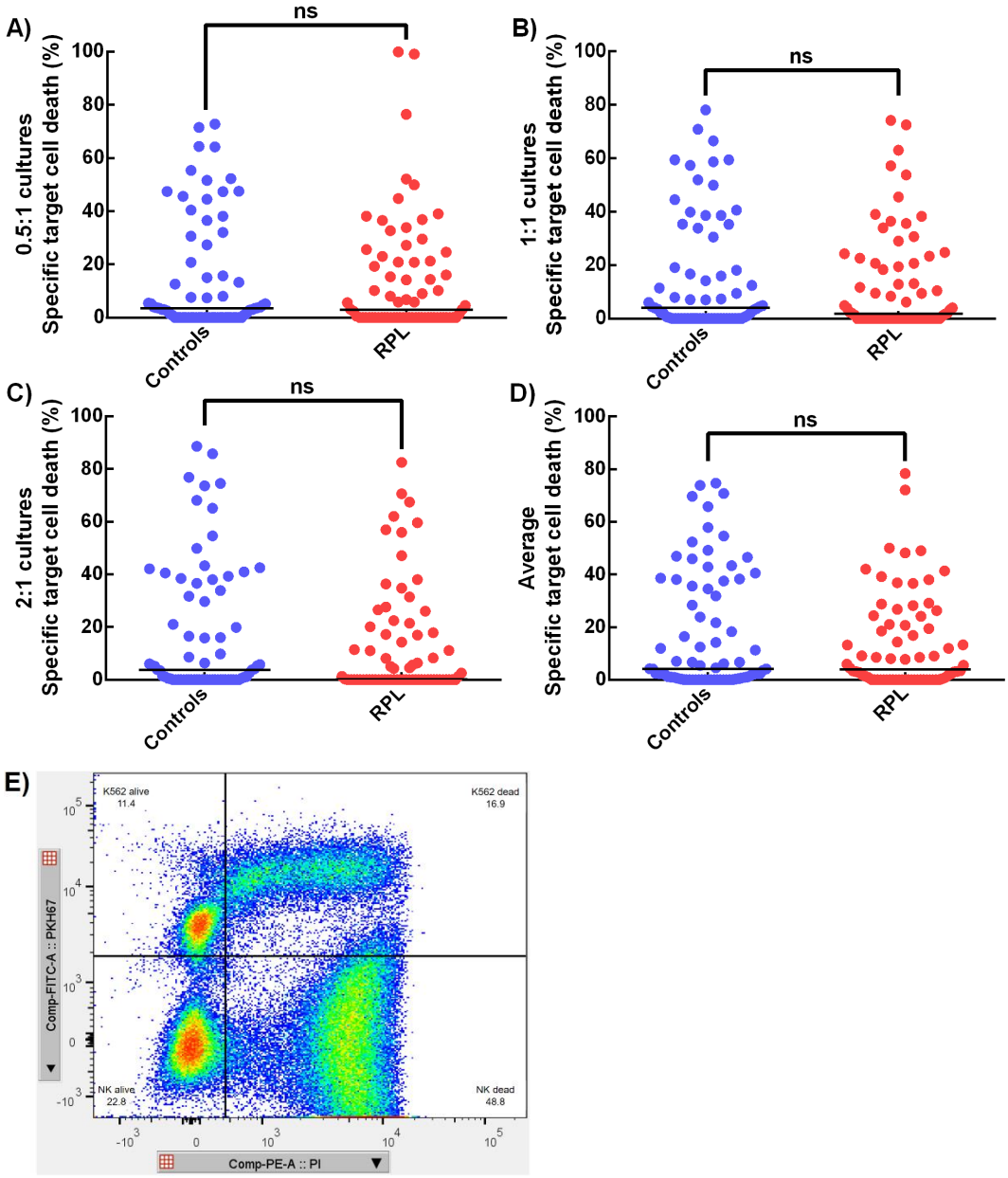


Figure 58. Specific target cell death in Natural Killer (NK) cell:K562 cell co-cultures, derived from women with recurrent pregnancy loss (RPL) and controls. *The specific K562 cell death detected in co-cultures including A) 0.5:1, B) 1:1, and C) 2:1 NK cell:K562 cell ratios is illustrated, alongside the D) average target cell death in 0.5:1, 1:1, and 2:1 cultures. NK cells isolated from healthy controls (0.5:1 cultures: N=71, 1:1 cultures: N=69, 2:1 cultures: N=72, Average of cultures: N=76) and women with RPL (0.5:1 cultures: N=71, 1:1 cultures: N=72, 2:1 cultures: N=72, Average of cultures: N=72) were used. E) Example gating used to identify dead and alive K652 and NK cell populations is displayed. Mann-Whitney test performed, median shown. ns: non-significant*

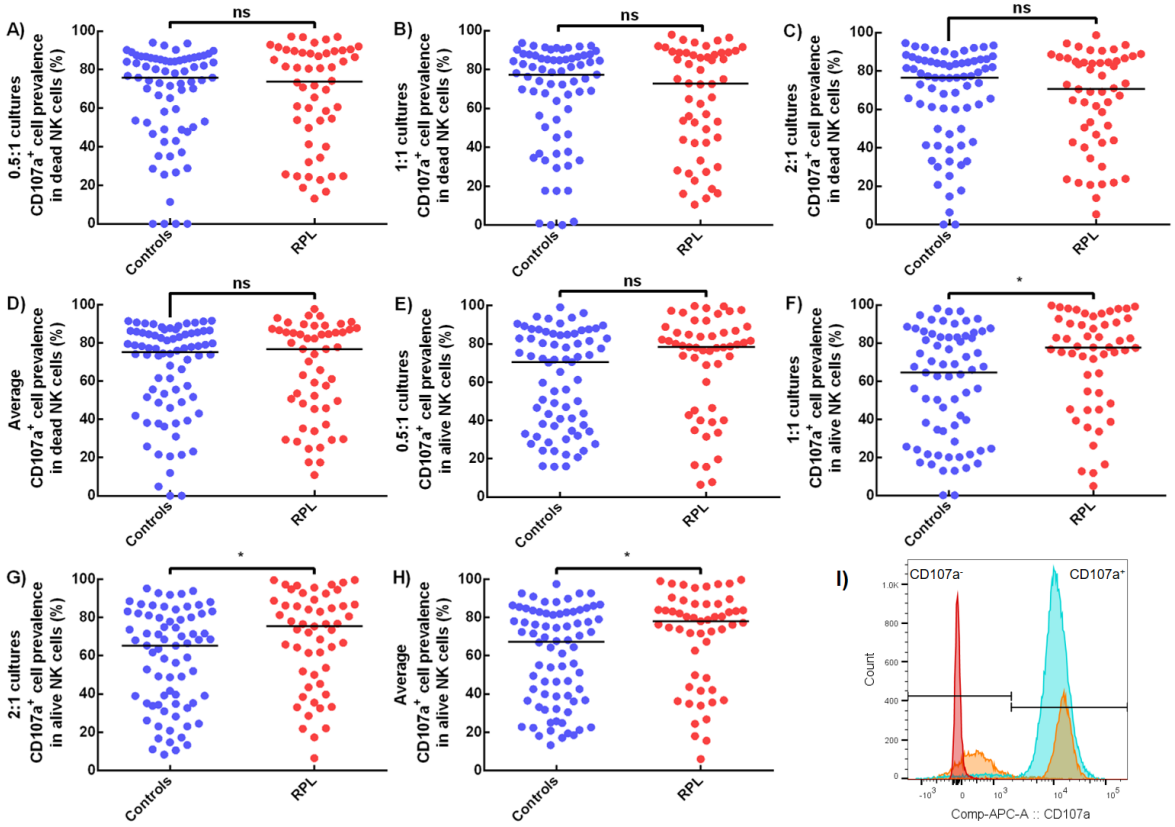


Figure 59. CD107a-expressing Natural Killer (NK) cell prevalence in NK cell:K562 cell co-cultures, derived from women with recurrent pregnancy loss (RPL) and controls. *The prevalence of A-D) dead and E-H) alive NK cells expressing CD107a in co-cultures including A, E) 0.5:1, B, F) 1:1, and C, G) 2:1 NK cell:K562 cell ratios is depicted, alongside the D, H) average prevalence of these cells in 0.5:1, 1:1, and 2:1 cultures. NK cells isolated from healthy controls (0.5:1 cultures: N=71, 1:1 cultures: N=69, 2:1 cultures: N=72, Average of cultures: N=76) and women with RPL (0.5:1 cultures: N=52, 1:1 cultures: N=53, 2:1 cultures: N=53, Average of cultures: N=53) were used. I) Example gating used to identify the CD107⁺ degranulating population is displayed, using a control (orange) and an RPL (blue) sample and a CD107a-negative control (red). Mann-Whitney test performed, median included. ns: non-significant, *: p≤0.05*

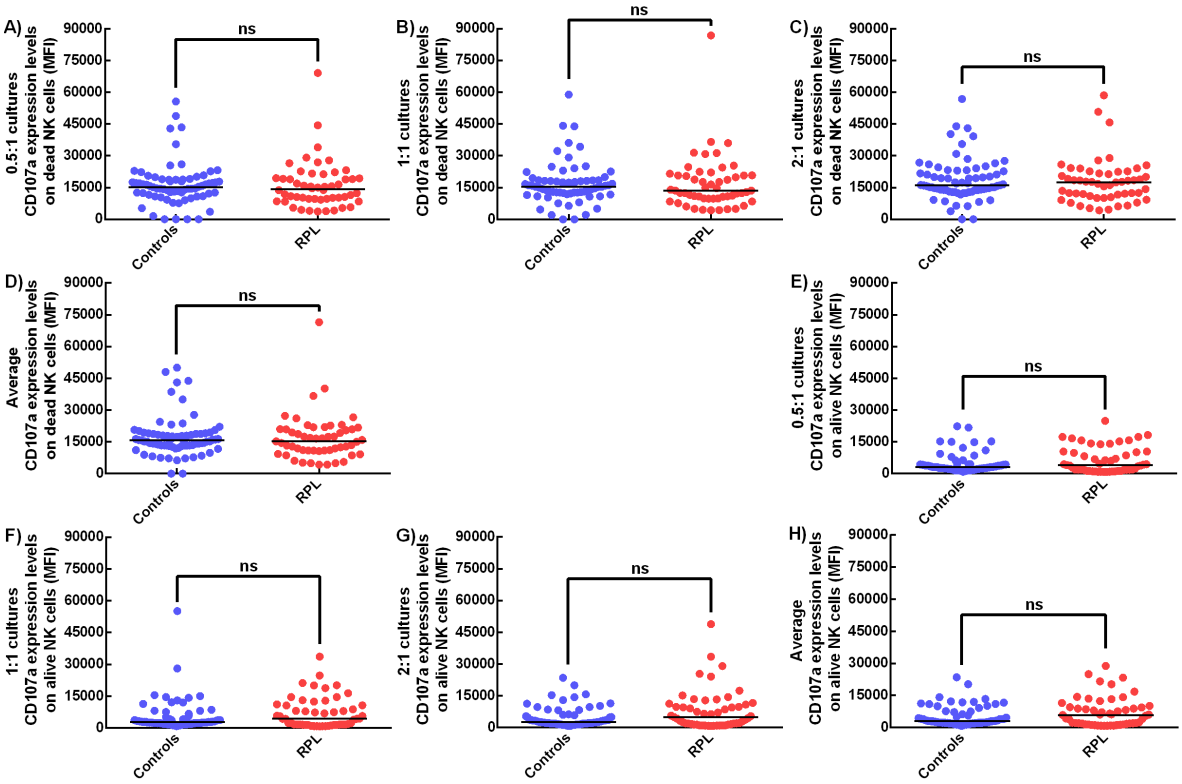


Figure 60. CD107a expression intensity on Natural Killer (NK) cells in NK cell:K562 cell co-cultures, derived from women with recurrent pregnancy loss (RPL) and controls. *The intensity of CD107a expression, represented by the median fluorescence intensity (MFI), on A-D) dead and E-H) alive NK cells in co-cultures including A, E) 0.5:1, B, F) 1:1, and C, G) 2:1 NK cell:K562 cell ratios is displayed, alongside the D, H) average expression intensity on these cells in 0.5:1, 1:1, and 2:1 cultures. NK cells isolated from healthy controls (0.5:1 cultures: N=71, 1:1 cultures: N=69, 2:1 cultures: N=72, Average of cultures: N=76) and women with RPL (0.5:1 cultures: N=52, 1:1 cultures: N=53, 2:1 cultures: N=53, Average of cultures: N=53) were used. Mann-Whitney test performed, median illustrated. ns: non-significant*

8.1.2 ELISA – Perforin and granzyme secretion

To further examine cytotoxic activity in the periphery of women with RPL, the secretion of granzymes A and B and perforin by unstimulated and stimulated PBMCs was assessed (Controls *N*=72, RPL *N*=99). In the absence of stimulation, a reduction in granzyme A levels was observed in PBMC cultures derived from women with RPL compared to those derived from control women [Controls: 10.00pg/mL, 95% CI (7.46pg/mL, 14.84pg/mL), RPL: 5.42pg/mL, 95% CI (5.42pg/mL, 6.49pg/mL), p=0.0017], while no difference in granzyme B [Controls: 6.20pg/mL, 95% CI (6.20pg/mL, 12.56pg/mL), RPL: 6.20pg/mL, 95% CI (6.20pg/mL, 6.20pg/mL)] and perforin [Controls: 415.10pg/mL, 95% CI (293.10pg/mL, 652.80pg/mL), RPL: 210.40pg/mL, 95% CI (93.97pg/mL, 418.60pg/mL)] concentration could be detected (Figures 61A-61C). PBMCs stimulation with PMA and ionomycin was found to significantly enhance granzyme A and B and perforin secretion in both women with RPL and controls (Figures 62A-62I). Following stimulation, a reduction in granzyme A [Controls: 118.60pg/mL, 95% CI (92.09pg/mL, 156.40pg/mL), RPL: 34.81pg/mL, 95% CI (25.30pg/mL, 47.73pg/mL), p<0.0001] and B [Controls: 299.70pg/mL, 95% CI (207.60pg/mL, 375.80pg/mL), RPL: 116.80pg/mL, 95% CI (76.77pg/mL, 204.80pg/mL), p=0.0013] as well as perforin [Controls: 2712pg/mL, 95% CI (2069pg/mL, 3962pg/mL), RPL: 954.20pg/mL, 95% CI (617pg/mL, 1713pg/mL), p=0.0008] concentration in RPL-derived PBMC cultures was detected, compared to controls (Figures 63A-63C).

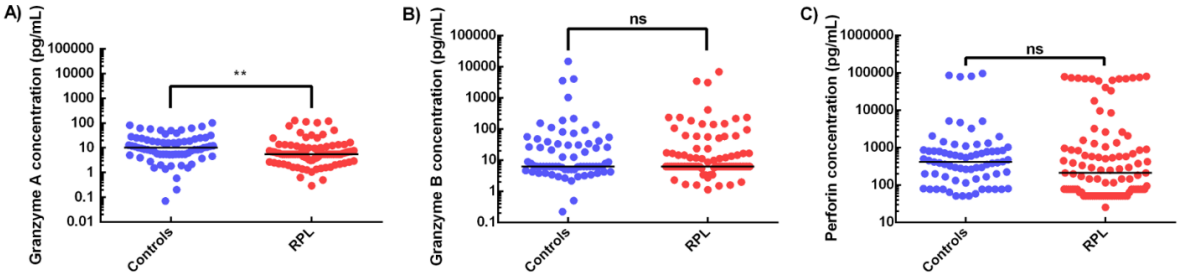


Figure 61. Granzyme and perforin concentration (pg/mL) in unstimulated peripheral blood mononuclear cell (PBMC) cultures derived from women with recurrent pregnancy loss (RPL) and controls. *The levels of A) granzyme A, B) granzyme B, and C) perforin secretion by PBMCs isolated from healthy controls (N=72) and women with RPL (N=99) is depicted. Mann-Whitney test performed, median illustrated. ns: non-significant, **: p≤0.01*

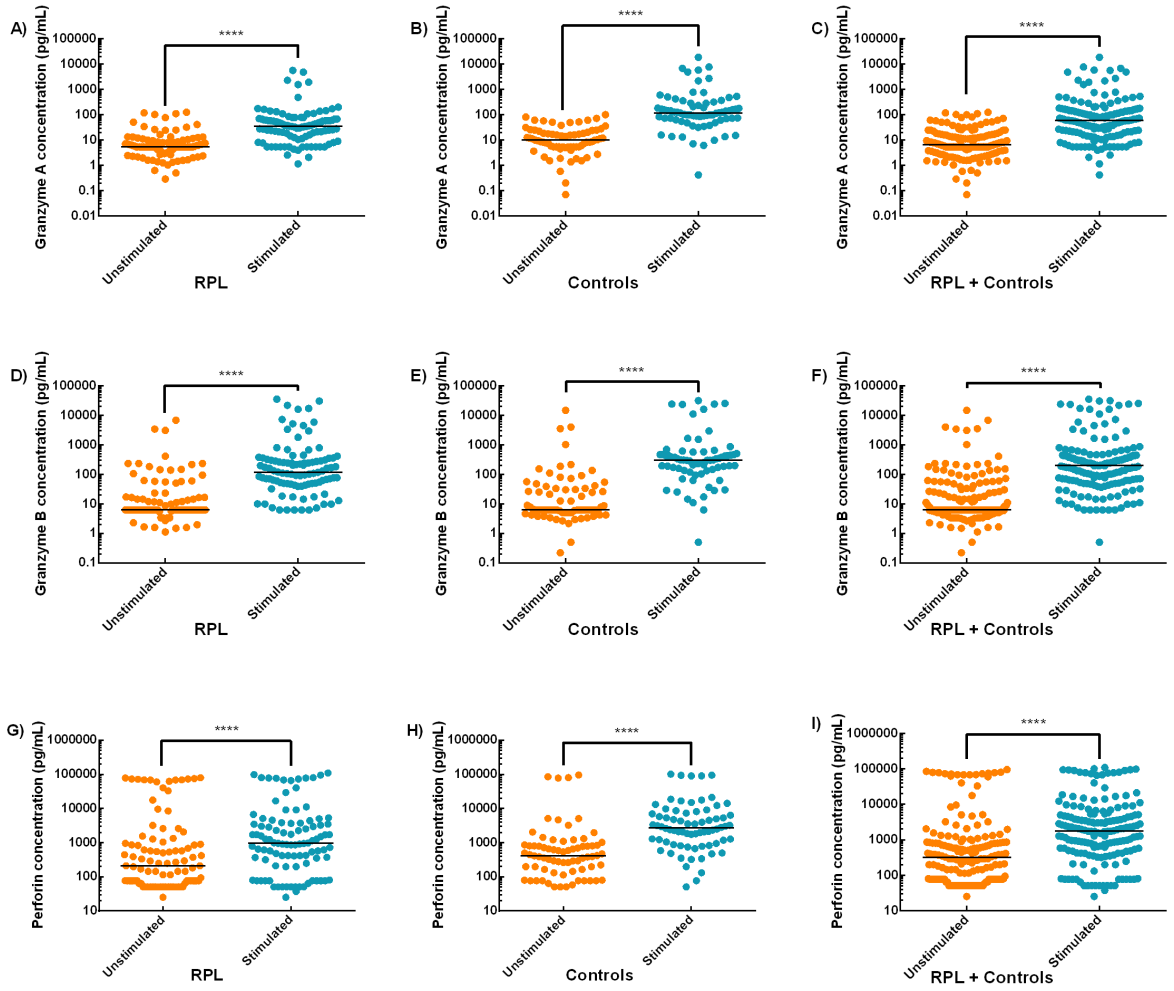


Figure 62. Granzyme and perforin concentration (pg/mL) in unstimulated and simulated peripheral blood mononuclear cell (PBMC) cultures derived from women with recurrent pregnancy loss (RPL), controls, and total participants. *The levels of A-C) granzyme A, D-F) granzyme B, and G-I) perforin secretion by PBMCs isolated from women with RPL (N=99) (A, D, G), healthy controls (N=72) (B, E, H), and total participants (N=171) (C, F, I) in the absence and following stimulation with phorbol 12-myristate 13-acetate and ionomycin, is shown. Wilcoxon matched-pairs signed rank test used, median included. ****: p≤0.0001*

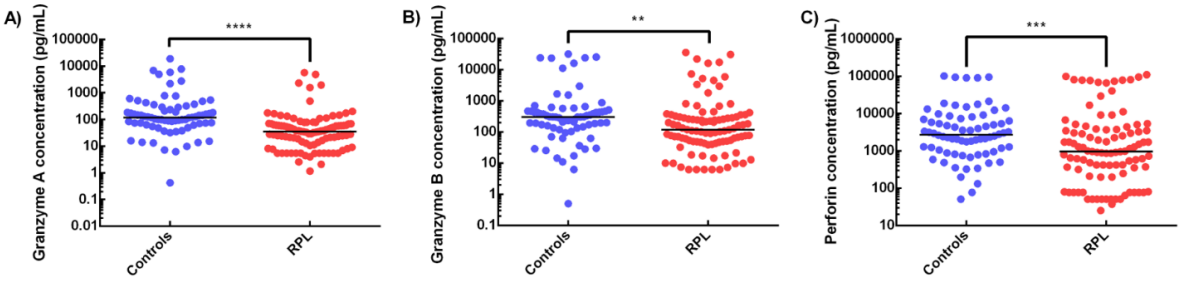


Figure 63. Granzyme and perforin concentration (pg/mL) in stimulated peripheral blood mononuclear cell (PBMC) cultures derived from women with recurrent pregnancy loss (RPL) and controls. *The levels of A) granzyme A, B) granzyme B, and C) perforin secretion by PBMCs isolated from healthy controls (N=72) and women with RPL (N=99) is illustrated. Mann-Whitney test used, median depicted. **: p≤0.01, ***: p≤0.001, ****: p≤0.0001*

8.1.3 Flow cytometry assay – NK cell activation and cytokine receptor expression

The NK cell and NK cell cytokine panels of the flow cytometry assay were also utilised to assess aspects of NK cell activity. Specifically, the expression of the CD69 activation marker was examined on unstimulated total, $CD56^{dim}CD16^{+}$, and $CD56^{bright}CD16^{-}$ NK cells (Controls *N*=77, RPL *N*=90) and the expression of CD25 and CD215, constituting the alpha chains of the IL-2 and IL-15 activating receptors respectively, was investigated on unstimulated and stimulated total (Controls *N*=71, RPL *N*=84) and $CD56^{dim}CD16^{+}$ (Controls *N*=22, RPL *N*=26) NK cells. $CD69^{+}$ cell prevalence appeared elevated in $CD56^{bright}CD16^{-}$ [Controls: 1.59%, 95% CI (0.83%, 2.85%), RPL: 3.33%, 95% CI (2.29%, 4.20%), p=0.0112], but not total [Controls: 2.70%, 95% CI (1.73%, 5.26%), RPL: 3.86%, 95% CI (2.65%, 6.42%)] or $CD56^{dim}CD16^{+}$ [Controls: 4.17%, 95% CI (2.33%, 8.05%), RPL: 3.82%, 95% CI (2.18%, 5.75%)] NK cells of women with RPL (Figures 64A-64C). On the other hand, the expression intensity of CD69 on total [Controls: 1913.00, 95% CI (1567.00, 2132.00), RPL: 982.00, 95% CI (855.00, 1106.00), p<0.0001] and $CD56^{dim}CD16^{+}$

[Controls: 1712.00, 95% CI (1448.00, 2076.00), RPL: 1015.00, 95% CI (925.00, 1204.00), p=0.001], but not CD56^{bright}CD16^{-} [Controls: 897.00, 95% CI (470.00, 1283.00), RPL: 757.00, 95% CI (665.00, 857.00)] NK cells of women with RPL was found to be decreased (Figures 64D-64F).

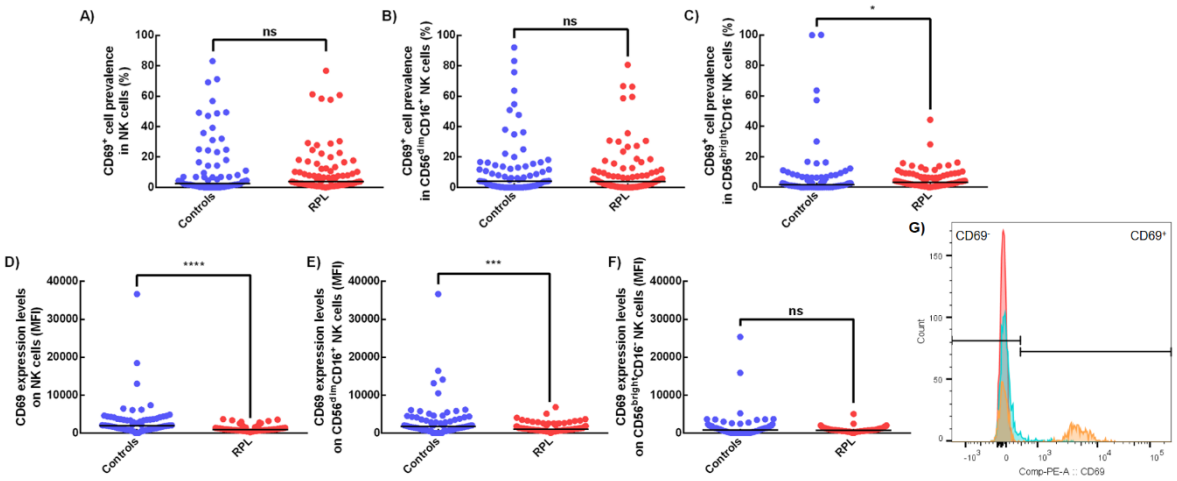


Figure 64. CD69 expression by Natural Killer (NK) cells in women with recurrent pregnancy loss (RPL) and controls. *The prevalence of A) total, B) CD56^{dim}CD16^{+}, and C) CD56^{bright}CD16^{-} NK cells expressing CD69 and the expression intensity of this marker, represented by the median fluorescence intensity (MFI), on D) total, E) CD56^{dim}CD16^{+}, and F) CD56^{bright}CD16^{-} NK cells of healthy controls (N=77) and women with RPL (N=90) is displayed. G) Example gating used to identify the CD69^{+} activated population is depicted, using two samples (orange, blue) and a CD69-negative control (red). Mann-Whitney test used, median included. ns: non-significant, *: p≤0.05, ***: p≤0.001, ****: p≤0.0001*

In the absence of stimulation, neither $CD25^+$ [Controls: 2.17%, 95% CI (1.18%, 4.21%), RPL: 1.85%, 95% CI (1.27%, 3.29%)] or $CD215^+$ [Controls: 0.39%, 95% CI (0.08%, 0.96%), RPL: 0.37%, 95% CI (0.10%, 0.88%)] NK cell prevalence, nor CD25 [Controls: 8244.00, 95% CI (5018.00, 9817.00), RPL: 7127.00, 95% CI (6418.00, 8697.00)] or CD215 [Controls: 1429.00, 95% CI (1188.00, 1777.00), RPL: 1827.00, 95% CI (1636.00, 2029.00)] expression levels on these cells were found to be significantly different between participants with RPL and controls (Figures 65A, 65B, 66A, 66B). Similarly, $CD25^+$ [Controls: 0.66%, 95% CI (0.00%, 7.14%), RPL: 0.00%, 95% CI (0.00%, 0.24%)] and $CD215^+$ [Controls: 0.00%, 95% CI (0.00%, 14.80%), RPL: 0.00%, 95% CI (0.00%, 0.08%)] $CD56^{dim}CD16^+$ NK cell prevalence and CD25 [Controls: 13149.00, 95% CI (0.00, 29730.00), RPL: 0.00, 95% CI (0.00, 21820.00)] and CD215 [Controls: 0.00, 95% CI (0.00, 2283.00), RPL: 0.00, 95% CI (0.00, 3132.00)] expression levels on $CD56^{dim}CD16^+$ NK cells were not significantly altered in the RPL, compared to the control group (Figures 65C, 65D, 66C, 66D).

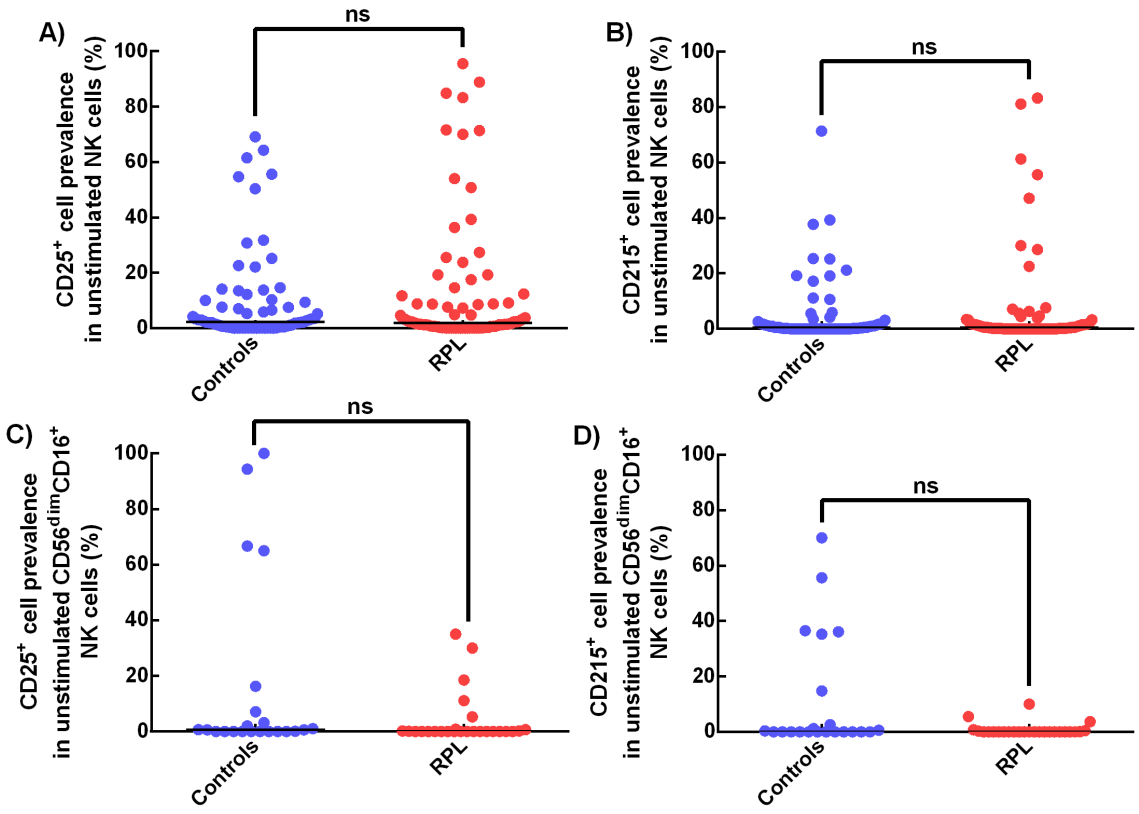


Figure 65. CD25- and CD215-expressing cell prevalence in the unstimulated total and CD56^{dim}CD16^{+} Natural Killer (NK) cell population of women with recurrent pregnancy loss (RPL) and controls. *The prevalence of A) CD25^{+} and B) CD215^{+} cells in the NK cell population, as well as the percentage of C) CD25^{+} and D) CD215^{+} cells in the CD56^{dim}CD16^{+} NK cell subpopulation of healthy controls (total NK cells: N=71, CD56^{dim}CD16^{+} NK cells: N=22) and women with RPL (total NK cells: N=84, CD56^{dim}CD16^{+} NK cells: N=26) is depicted. Mann-Whitney test used, median included. ns: non-significant*

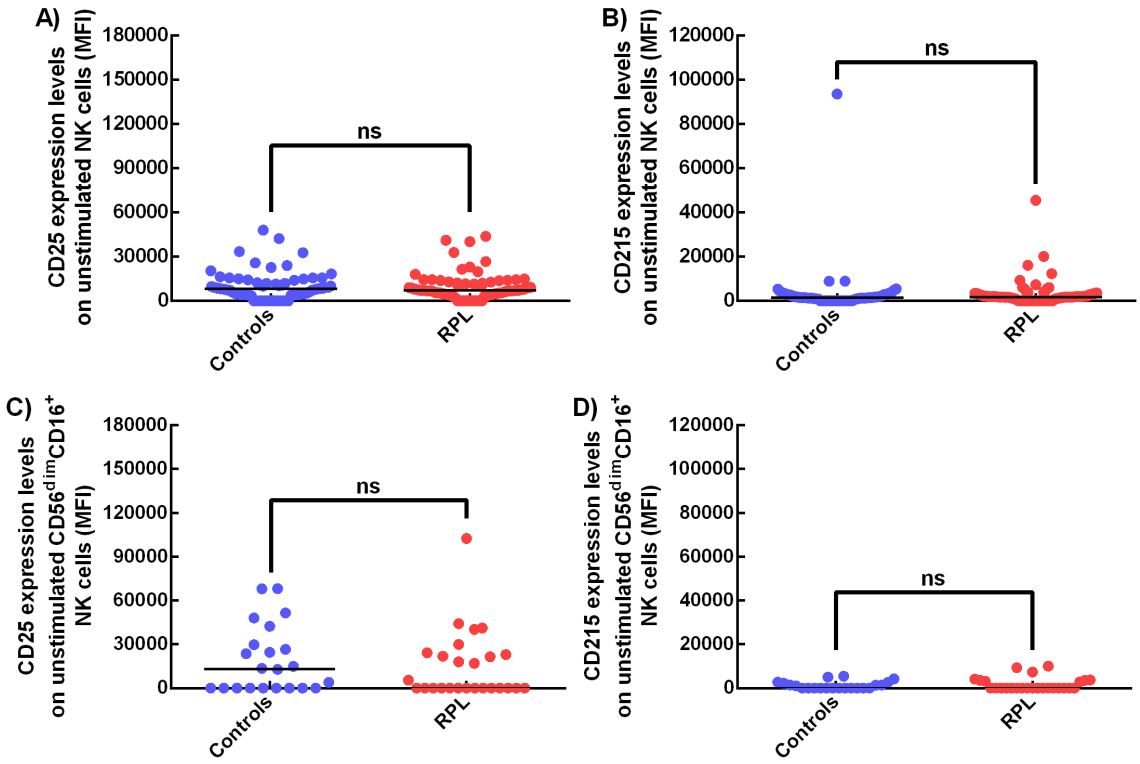


Figure 66. CD25 and CD215 expression intensity on unstimulated total and CD56^{dim}CD16^{+} Natural Killer (NK) cells of women with recurrent pregnancy loss (RPL) and controls. *The intensity of A) CD25 and B) CD215 expression on individual NK cells, represented by the median fluorescence intensity (MFI), as well as the intensity of C) CD25 and D) CD215 expression on the CD56^{dim}CD16^{+} NK cell subpopulation of healthy controls (total NK cells: N=71, CD56^{dim}CD16^{+} NK cells: N=22) and women with RPL (total NK cells: N=84, CD56^{dim}CD16^{+} NK cells: N=26) is illustrated. Mann-Whitney test performed, median depicted. ns: non-significant*

Upon stimulation, $CD25^+$ NK cell prevalence was found to be reduced in both the RPL and control groups, with no alteration in $CD215^+$ NK cell prevalence observed in either group or total participants (Figures 67A-67C, 67G-67I). The intensity of CD25 expression on NK cells was found to be significantly elevated upon stimulation in control and total participants, but not women with RPL, with CD215 expression intensity being unaltered in all participant groups (Figures 68A-68C, 68G-68I). In contrast to the total NK cell population, both $CD25^+$ cell prevalence and expression intensity in the $CD56^{dim}CD16^+$ NK cell subset appeared augmented upon stimulation in the RPL and total participant group, but not in controls (Figures 67D-67F, 68D-68F). A similar trend was detected in regards to CD215 expression, with increased $CD215^+$ cell prevalence and CD215 expression levels in the $CD56^{dim}CD16^+$ NK cell subpopulation being detected following stimulation in women with RPL and total participants, but not in control women (Figures 67J-67L, 68J-68L).

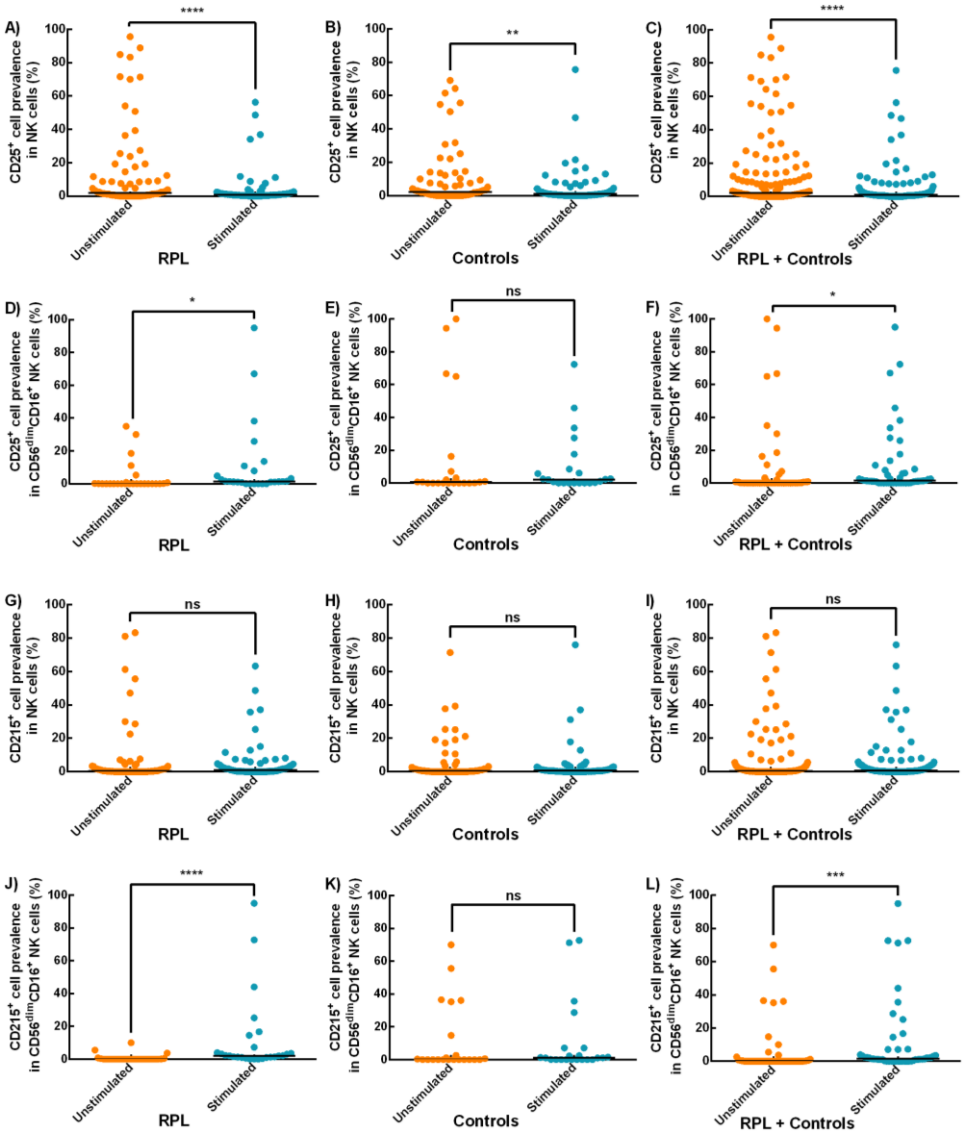


Figure 67. CD25- and CD215-expressing cell prevalence in the unstimulated and the stimulated total and CD56^{dim}CD16^{+} Natural Killer (NK) cell population of women with recurrent pregnancy loss (RPL), controls, and total participants. *The prevalence of A-C) CD25^{+} and G-I) CD215^{+} cells in the NK cell population, as well as the percentage of D-F) CD25^{+} and J-L) CD215^{+} cells in the CD56^{dim}CD16^{+} NK cell subpopulation of women with RPL (total NK cells: N=84, CD56^{dim}CD16^{+} NK cells: N=26) (A, D, G, J), controls (total NK cells: N=71, CD56^{dim}CD16^{+} NK cells: N=22) (B, E, H, K), and total participants (total NK cells: N=155, CD56^{dim}CD16^{+} NK cells: N=48) (C, F, I, L) in the absence and following stimulation with phorbol 12-myristate 13-acetate and ionomycin is depicted. Wilcoxon matched-pairs signed rank test performed, median shown. ns: non-significant, *: p≤0.05, **: p≤0.01, ***: p≤0.001, ****: p≤0.0001*

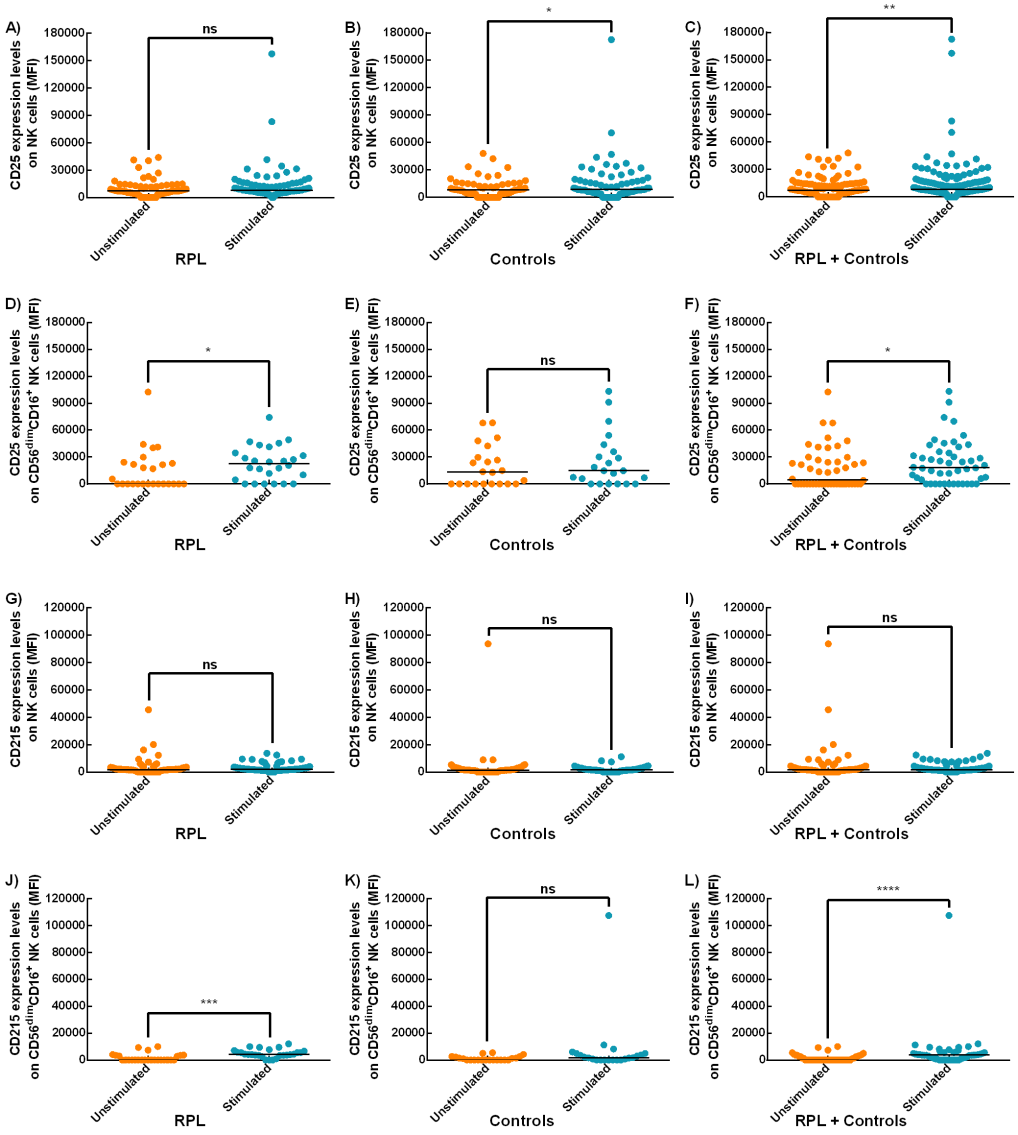


Figure 68. CD25 and CD215 expression intensity on unstimulated and stimulated total and CD56^{dim}CD16^{+} Natural Killer (NK) cells of women with recurrent pregnancy loss (RPL), controls, and total participants. *The intensity of A-C) CD25 and G-I) CD215 expression, represented by the median fluorescence intensity (MFI), on individual NK cells, as well as the intensity of D-F) CD25 and J-L) CD215 expression on the CD56^{dim}CD16^{+} NK cell subpopulation of women with RPL (total NK cells: N=84, CD56^{dim}CD16^{+} NK cells: N=26) (A, D, G, J), controls (total NK cells: N=71, CD56^{dim}CD16^{+} NK cells: N=22) (B, E, H, K), and total participants (total NK cells: N=155, CD56^{dim}CD16^{+} NK cells: N=48) (C, F, I, L) in the absence and following stimulation with phorbol 12-myristate 13-acetate and ionomycin is displayed. Wilcoxon matched-pairs signed rank test used, median illustrated. ns: non-significant, *: p≤0.05, **: p≤0.01, ***: p≤0.001, ****: p≤0.0001*

Comparing CD25 and CD215 expression on stimulated NK cells of women with RPL and controls, no significant difference in $CD25^{+}$ [Controls: 0.93%, 95% CI (0.55%, 1.52%), RPL: 0.84%, 95% CI (0.55%, 1.20%)] or $CD215^{+}$ [Controls: 0.56%, 95% CI (0.23%, 0.94%), RPL: 0.94%, 95% CI (0.37%, 1.79%)] NK cell prevalence could be detected (Figures 69A, 69B). However, elevated CD215 [Controls: 1535.00, 95% CI (1300.00, 1867.00), RPL: 2035.00, 95% CI (1738.00, 2471.00), p=0.0115], but not CD25 [Controls: 8794.00, 95% CI (7731.00, 11963.00), RPL: 8090.00, 95% CI (7301.00, 9951.00)] expression levels on stimulated NK cells of women with RPL were seen (Figures 70A, 70B). Accordingly, $CD25^{+}$ [Controls: 2.20%, 95% CI (0.00%, 8.57%), RPL: 1.38%, 95% CI (1.02%, 4.88%)] and $CD215^{+}$ [Controls: 1.09%, 95% CI (0.00%, 7.14%), RPL: 2.11%, 95% CI (1.26%, 3.95%)] cell prevalence in the $CD56^{dim}CD16^{+}$ NK cell population and CD25 expression intensity [Controls: 14737.00, 95% CI (0.00, 35850.00), RPL: 22665.00, 95% CI (10179.00, 31565.00)] on these cells appeared unaltered in women with RPL, but an increase in CD215 expression levels [Controls: 1693.00, 95% CI (0.00, 4913.00), RPL: 4251.00, 95% CI (3583.00, 5762.00), p=0.0222] on $CD56^{dim}CD16^{+}$ NK cells of women with RPL was observed (Figures 69C, 69D, 70C, 70D).

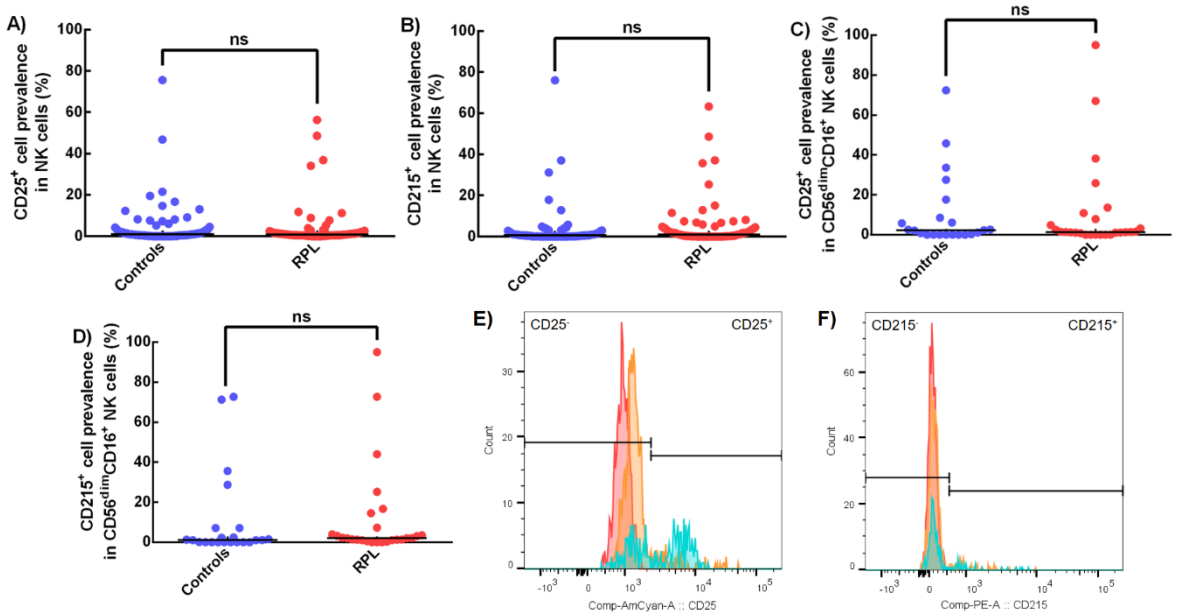


Figure 69. CD25- and CD215-expressing cell prevalence in the stimulated total and CD56^{dim}CD16^{+} Natural Killer (NK) cell population of women with recurrent pregnancy loss (RPL) and controls. *The prevalence of A) CD25^{+} and B) CD215^{+} cells in the NK cell population, as well as the percentage of C) CD25^{+} and D) CD215^{+} cells in the CD56^{dim}CD16^{+} NK cell subpopulation, following stimulation with phorbol 12-myristate 13-acetate and ionomycin, of healthy controls (total NK cells: N=71, CD56^{dim}CD16^{+} NK cells: N=22) and women with RPL (total NK cells: N=84, CD56^{dim}CD16^{+} NK cells: N=26) is illustrated. Example gating used to identify the E) CD25^{+} and F) CD215^{+} population is depicted, using two samples (orange, blue) and a control negative for the marker of interest (red). Mann-Whitney test performed, median depicted. ns: non-significant*

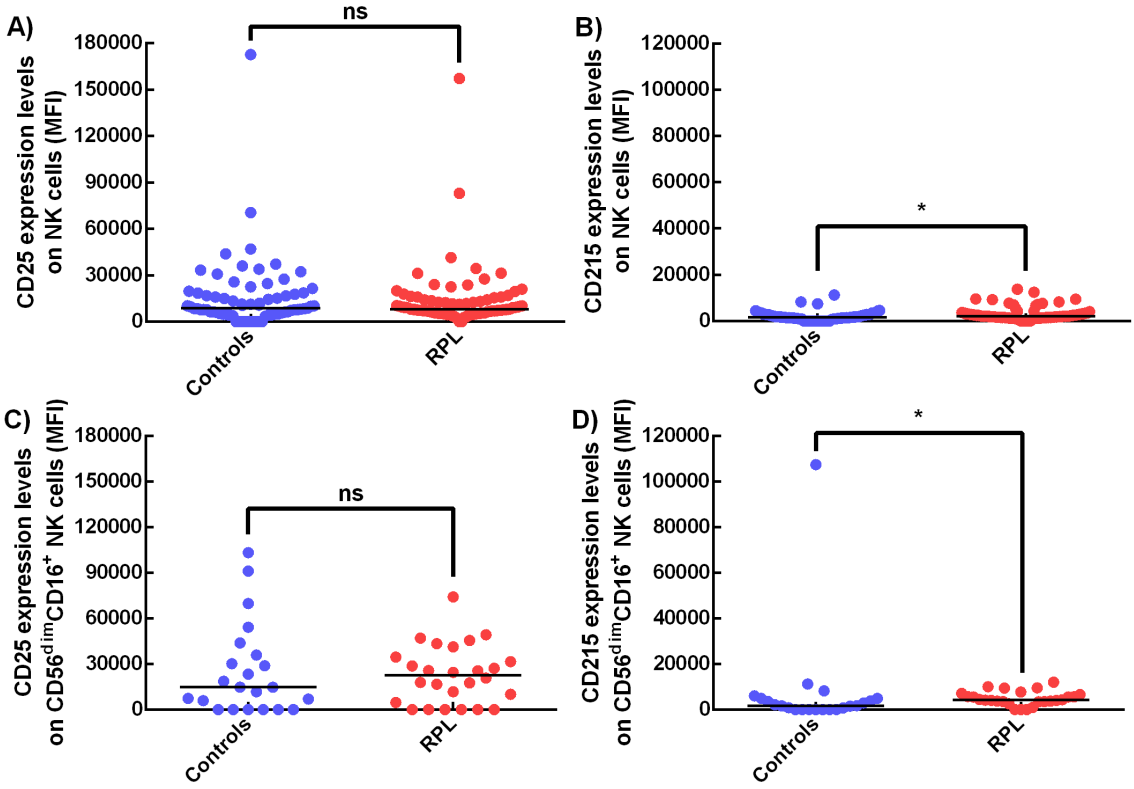


Figure 70. CD25 and CD215 expression intensity on stimulated total and CD56^{dim}CD16^{+} Natural Killer (NK) cells of women with recurrent pregnancy loss (RPL) and controls. *The intensity of A) CD25 and B) CD215 expression on individual NK cells, represented by the median fluorescence intensity (MFI), as well as the intensity of C) CD25 and D) CD215 expression on the CD56^{dim}CD16^{+} NK cell subpopulation, following stimulation with phorbol 12-myristate 13-acetate and ionomycin, of healthy controls (total NK cells: N=71, CD56^{dim}CD16^{+} NK cells: N=22) and women with RPL (total NK cells: N=84, CD56^{dim}CD16^{+} NK cells: N=26) is depicted. Mann-Whitney test used, median displayed. ns: non-significant, *: p≤0.05*

8.1.4 Mass cytometry assay – NK cells

To investigate in further depth potential alterations in the peripheral NK cell repertoire of women with RPL, mass cytometry was performed on control (*N*=80) and RPL (*N*=100) samples (Figure 71). The expression of 50 markers, including CD56, CD16, CD57, CD69, CD94, CD4, CD5, CD8α, CD25, CD27, CD38, CD122, CD127, CD161, CD226, KIR2DL1/2DS1/2DS3/2DS5, KIR2DL1/2DS5,

KIR2DL2/2DL3/2DS2/2DS4, KIR2DS4, KIR2DL2/2DL3/2DL5, KIR2DL4, KIR3DL1/3DL2, ILT1, ILT2, ILT2/LIR6, ILT3/ILT4/ILT5, NKp30/NKp80, NKp44/NKp46, NKG2A, NKG2C/NKG2D, CXCR1/CXCR2, CXCR3/CXCR4, CXCR5, CXCR6, CX3CR1, TIGIT/Tim-3, and PD-1 on $CD3^{-}CD56^{+}$ NK cells was assessed. According to these markers a low level of separation between NK cells isolated from control participants and those isolated from participants with RPL was observed (Figure 72).

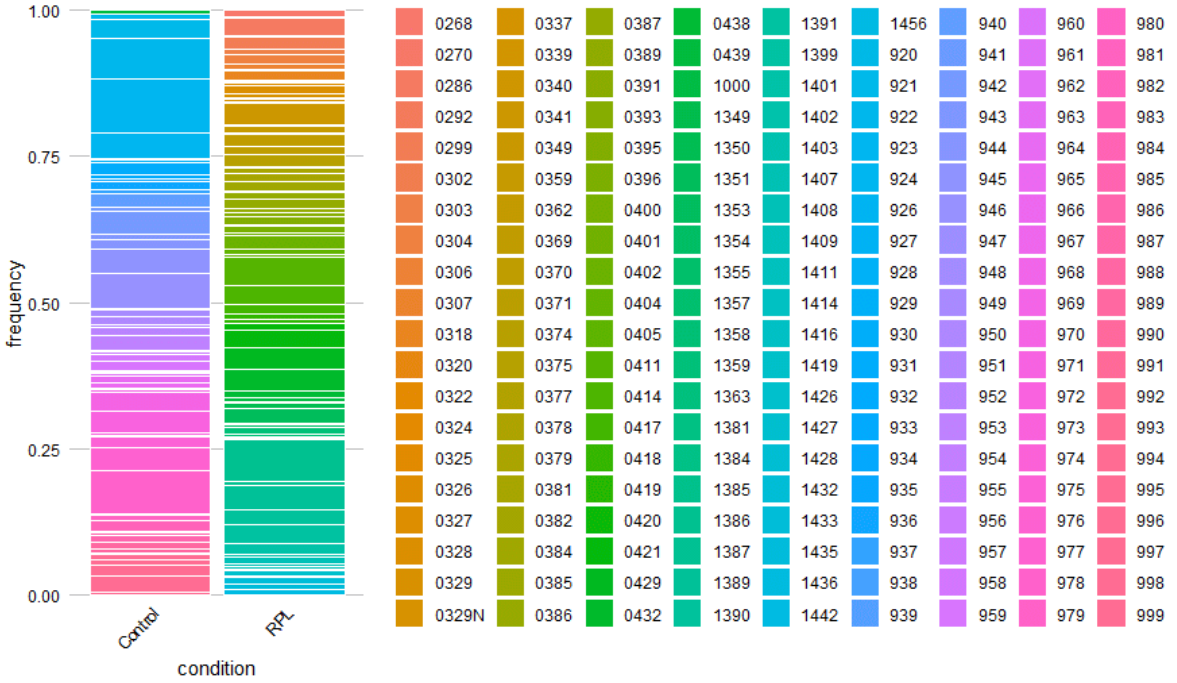


Figure 71. Relative abundance of each sample in the mass cytometry datasets used to analyse Natural Killer (NK) cell marker expression in control women and women with recurrent pregnancy loss (RPL). *The relative frequency of each sample, calculated according to cell counts, in the total NK cell population of the control (N=80) and RPL (N=100) cohorts is displayed. Individual samples are represented by different colours, with patient_id also depicted (RPL: 0268-0439 and 1349-1456, Control: 920-1000).*

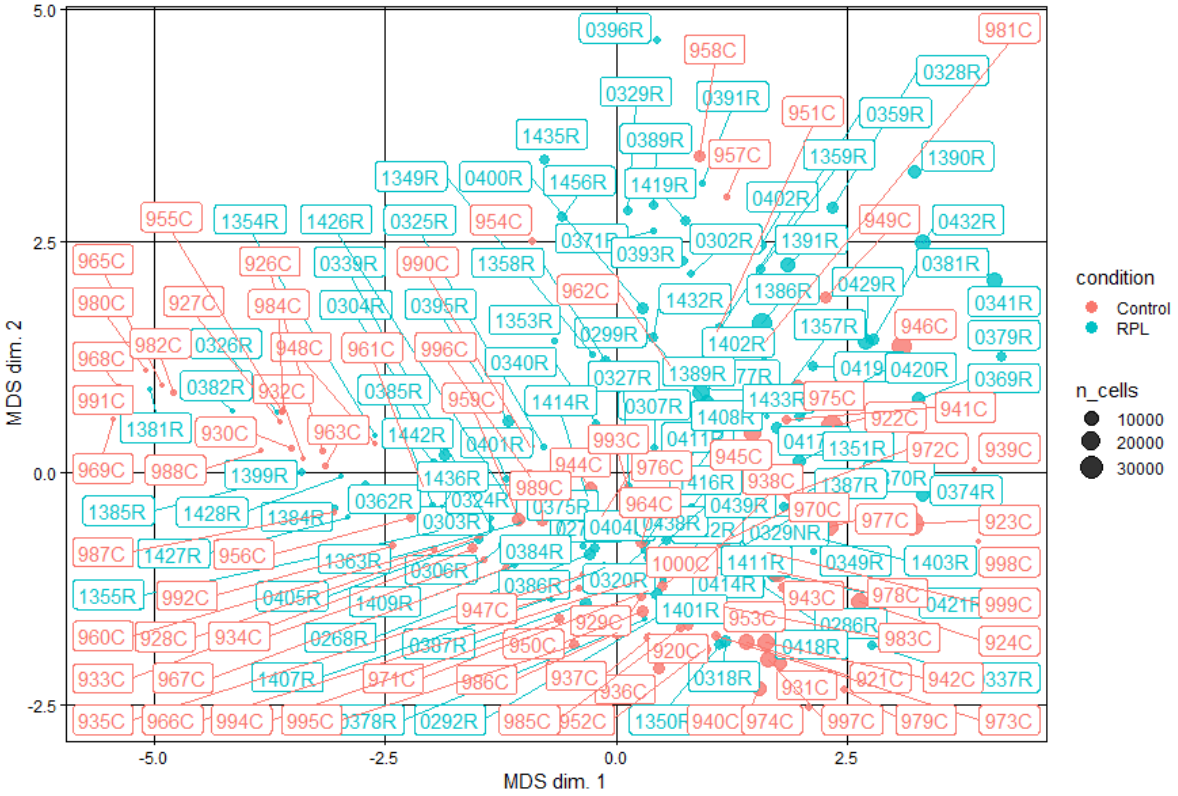


Figure 72. Multi-dimensional scaling (MDS) plot of the control and recurrent pregnancy loss (RPL) Natural Killer cell samples, summarizing the level of similarity between cohorts. *The distances between samples approximate the difference in median expression of all markers examined, including CD56, CD16, CD57, CD69, CD94, CD4, CD5, CD8α, CD25, CD27, CD38, CD122, CD127, CD161, CD226, killer-cell immunoglobulin-like receptor (KIR)2DL1/2DS1/2DS3/2DS5, KIR2DL1/2DS5, KIR2DL2/2DL3/2DS2/2DS4, KIR2DS4, KIR2DL2/2DL3/2DL5, KIR2DL4, KIR3DL1/3DL2, immunoglobulin-like transcript (ILT)1, ILT2, ILT2/LIR6, ILT3/ILT4/ILT5, NKp30/NKp80, NKp44/NKp46, natural killer group (NKG)2A, NKG2C/NKG2D, C-X-C motif chemokine receptors (CXCR)1/CXCR2, CXCR3/CXCR4, CXCR5, CXCR6, CX3CR1, T-cell immunoreceptor with Ig and ITIM domains/T cell immunoglobulin and mucin domain-containing protein 3 (TIGIT/Tim-3), and programmed cell death protein 1 (PD-1), translating multi-dimensional data into a two-dimensional scatter plot. Labels displaying the sample identity are included.*

NK cells were clustered into 20 subtypes according to the 50 markers' expression (Figures 73A, 73B). Interestingly, the strict $CD56^{dim}CD16^{+}$/$CD56^{bright}CD16^{-}$ dichotomy was not evident upon subtype examination. The $CD56^{bright}CD16^{-}$ phenotype was only detected on cluster 17 (Figure 73B). Lower CD56 expression was detected on multiple clusters, including 1-16, of whom most displayed medium to high levels of CD16 (Figure 73B). An absence of CD16 expression was observed on clusters 7 and 13, with low levels of this marker present on clusters 4, 6, and 12 (Figure 73B). Although subtype analysis was performed on $CD56^{+}$ cells, clusters 18-20 displayed extremely low CD56 expression and a lack of CD16 (Figure 73B). However, separation of clusters into two groups according to their CD57 expression was evident, with clusters 1-7 expressing high levels of this marker, and clusters 8-20 lacking CD57 (Figure 73).

The expression of multiple receptors associated with NK cell activity was examined on the 20 subtypes generated. No significant expression of KIR2DL1, KIR2DL2, KIR2DL3, KIR2DL4, KIR2DL5, KIR2DS4, KIR2DS5, PD-1, CXCR5, CXCR6, CD5, or CD25 could be detected on any of the clusters (Figure 73B). However, cluster 9 displayed high KIR3DL1 and/or KIR3DL2 expression, while clusters 2 and 11 exhibited high KR2DS1 and/or KIR2DS3 levels. Additionally clusters 1, 4, 5, 7, 9, and 11 were found to be $KIR2DS2^{+}$ (Figure 73B). In regards to ILT receptors, high ILT2 and ILT3/ILT4/ILT5, low ILT1, and possibly LIR6 expression was only detected on the $CD56^{extremely\text{-}low}CD16^{-}$ cluster 20, with ILT3, ILT4, and/or ILT5 also being present on the $CD56^{extremely\text{-}low}CD16^{-}$ cluster 18 and low ILT2 expression detected on cluster 1 (Figure 73B). On the other hand NKp30 and/or NKp80 and NKp44 and/or NKp46 expression was quite common among clusters, with only

$CD56^{extremely\text{-}low}CD16^-$ clusters 18-20 being $NKp30^-NKp80^-$ and clusters 1, 4, 5, 6, 7, 12, 13, 18, and 19 being $NKp44^-NKp46^-$ (Figure 73B). Clusters 18-20 were also found to be $NKG2A^-NKG2C^-NKG2D^-$, with most clusters being $NKG2A^-$, expressing NKG2C and/or NKG2D. However, clusters 3, 8, 14, 15, and 17 displayed both NKG2A and NKG2C and/or NKG2D expression (Figure 73B). TIGIT and/or Tim-3 immune checkpoint receptor expression was also prevalent among NK cell clusters, with only clusters 4, 6, 12, and 18-20 displaying a $TIGIT^-Tim\text{-}3^-$ phenotype (Figure 73B). CD69 was only detected on clusters 6, 15, and 18. CD4 was only present on cluster 20 and CD127 on cluster 19, while CD27 expression could only be detected at low levels on the $CD56^{bright}CD16^-$ cluster 17. On the other hand, CD8α, CD38, CD94, CD161, CD122, and CD226 expression was detected on multiple subsets. Most clusters expressed low levels of CD8α, with an absence of CD8α shown on clusters 12, 17, 19, and 20 and high CD8α levels present on clusters 7 and 13. CD38 was expressed on almost all clusters, apart from 13 and 19, while CD94 was found to be present in medium to high amounts in all NK cells, apart from subsets 18-20. CD122 was also expressed on most subsets, apart from clusters 7, 13, and 18-20, which alongside cluster 1 were also found to be $CD161^-$. Most NK cell clusters displayed low to medium levels of CD226, with clusters 10, 12, 13, 19, and 20 being $CD226^-$ and cluster 18 being $CD226^{high}$ (Figure 73B). Finally, chemokine receptor expression was evaluated: CXCR1 and/or CXCR2 expression was detected on most clusters, apart from 7, 12, 13, 14, 17, and 18-20, while CXCR3 and/or CXCR4 were also present on most NK cell subtypes, apart from cluster 2, 4, 5, 10, and 11. CX3CR1 expression was only detected on cluster 18 (Figure 73B). To highlight the key findings, inhibitory KIR, ILT, or NKG2A receptor expression was

detected on 9 clusters, with activating KIR, ILT, NCR, or NKG2 receptor expression being present on 18 clusters. While PD-1 expression was absent, TIGIT/Tim-3 was detected on 14 clusters. Furthermore, although CXCR1/CXCR2 and CXCR3/CXCR4 were prevalent, CX3CR1 was expressed on only one NK cluster, while CXCR5 and CXCR6 expression were absent.

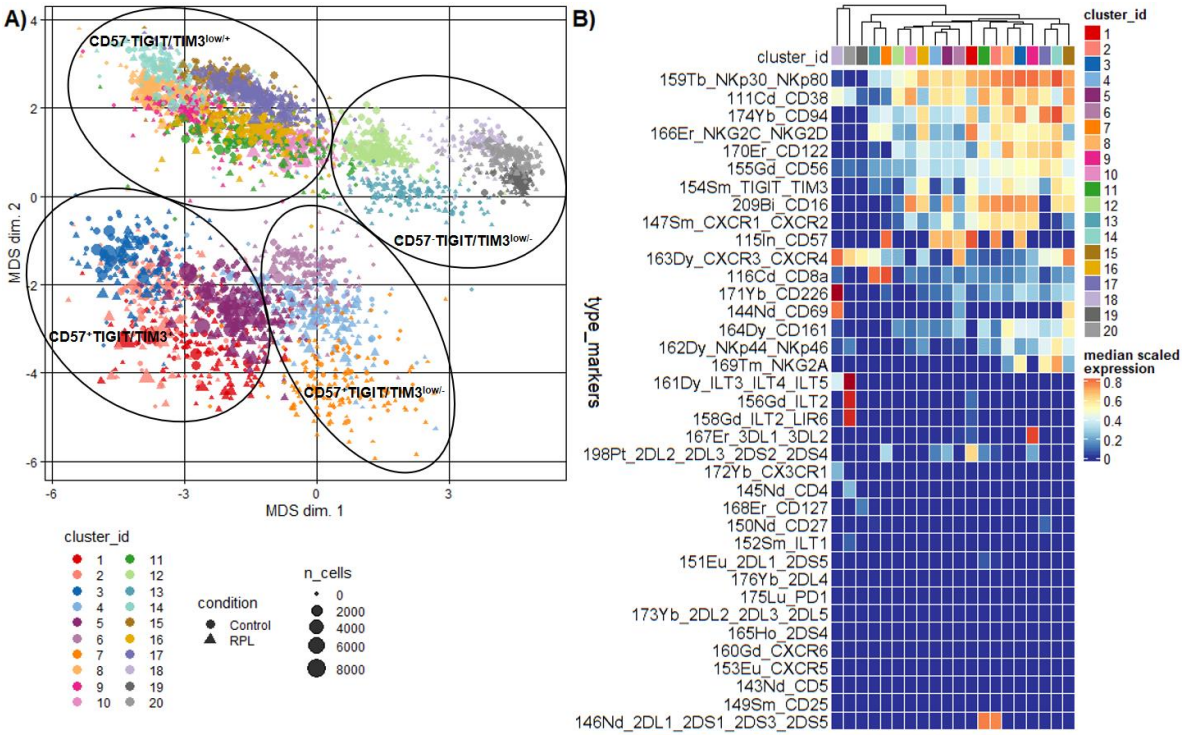


Figure 73. Multi-dimensional scaling and phenotyping of 20 Natural Killer cell clusters identified by mass cytometry. *A) Multi-dimensional scaling (MDS) plot of pseudobulks generated, with each point on the plot representing a cluster-sample instance, coloured according to the cluster, shaped based on the condition, and with a size proportional to the number of cells it represents. Distances between instances indicate relative phenotypic differences between clusters and samples, taking into consideration all markers assessed. The major phenotypic subgroups are demonstrated. B) Heatmap of median cluster of differentiation (CD)56, CD16, CD57, CD69, CD94, CD4, CD5, CD8α, CD25, CD27, CD38, CD122, CD127, CD161, CD226, killer-cell immunoglobulin-like receptor (KIR)2DL1/2DS1/2DS3/2DS5, KIR2DL1/2DS5, KIR2DL2/2DL3/2DS2/2DS4, KIR2DS4, KIR2DL2/2DL3/2DL5, KIR2DL4, KIR3DL1/3DL2, immunoglobulin-like transcript (ILT)1, ILT2, ILT2/LIR6, ILT3/ILT4/ILT5, NKp30/NKp80, NKp44/NKp46, natural killer group (NKG)2A, NKG2C/NKG2D, C-X-C motif chemokine receptors (CXCR)1/CXCR2, CXCR3/CXCR4, CXCR5, CXCR6, CX3CR1, T-cell immunoreceptor with Ig and ITIM domains/T cell immunoglobulin and mucin domain-containing protein 3 (TIGIT/Tim-3), and programmed cell death protein 1 (PD-1) expression intensity across the different Natural Killer cell clusters, ranging from high (red) to low (blue).*

Through differential abundance analysis, changes in the NK cell repertoire of women with RPL compared to that of controls were discovered. Specifically, $CD56^{dim}CD16^{high}CD57^{high}CD69^{-}CD94^{high}CD4^{-}CD8\alpha^{low}CD27^{-}CD38^{+}CD122^{+}CD127^{-}CD161^{+}CD226^{+}CXCR1/CXCR2^{+}CXCR3/CXCR4^{low}CX3CR1^{-}TIGIT/Tim\text{-}3^{+}$ cluster 3 (Control counts: 29084, RPL counts: 15045), $CD56^{dim}CD16^{+}CD57^{-}CD69^{-}CD94^{high}CD4^{-}CD8\alpha^{low}CD27^{-}CD38^{+}CD122^{high}CD127^{-}CD161^{+}CD226^{+}CXCR1/CXCR2^{-}CXCR3/CXCR4^{+}CX3CR1^{-}TIGIT/Tim\text{-}3^{+}$ cluster 14 (Control counts: 13232, RPL counts: 6461), $CD56^{dim}CD16^{+}CD57^{-}CD69^{+}CD94^{+}CD4^{-}CD8\alpha^{low}CD27^{-}CD38^{high}CD122^{+}CD127^{-}CD161^{+}CD226^{+}CXCR1/CXCR2^{+}CXCR3/CXCR4^{high}CX3CR1^{-}TIGIT/Tim\text{-}3^{+}$ cluster 15 (Control counts: 7497, RPL counts: 3851), and $CD56^{extremely\text{-}low}CD16^{-}CD57^{-}CD69^{-}CD94^{-}CD4^{+}CD8\alpha^{-}CD27^{-}CD38^{+}CD122^{-}CD127^{-}CD161^{-}CD226^{-}CXCR1/CXCR2^{-}CXCR3/CXCR4^{+}CX3CR1^{-}TIGIT/Tim\text{-}3^{-}$ cluster 20 (Control counts: 7722, RPL counts: 4821) appeared reduced in women with RPL (Figure 74). In regards to inhibitory receptor expression on these subtypes, NKG2A was detected on clusters 3, 14, 15, while cluster 20 was found to be $ILT2^{high}ILT3/ILT4/ILT5^{high}$. All of the clusters reduced in women with RPL were $NKp44/NKp46^{low/+}$, while NKp30/NKp80 and NKG2C/NKG2D activating receptor expression was also detected on clusters 3, 14, and 15 and low ILT1 expression was present on cluster 20.

On the other hand, $CD56^{dim}CD16^{high}CD57^{high}CD69^{-}CD94^{+}CD4^{-}CD8\alpha^{low}CD27^{-}CD38^{+}CD122^{+}CD127^{-}CD161^{low}CD226^{low}CXCR1/CXCR2^{+}CXCR3/CXCR4^{-}CX3CR1^{-}TIGIT/Tim\text{-}3^{+}$ cluster 2 (Control counts: 18115, RPL counts: 23522), $CD56^{dim}CD16^{low}CD57^{high}CD69^{-}CD94^{+}CD4^{-}CD8\alpha^{low}CD27^{-}CD38^{+}CD122^{+}CD127^{-}CD161^{low}CD226^{low}CXCR1/CXCR2^{+}CXCR3/CXCR4^{-}CX3CR1^{-}TIGIT/Tim\text{-}3^{-}$ cluster

4 (Control counts: 23754, RPL counts: 24859), $CD56^{dim}CD16^{high}CD57^{high}CD69^{-}CD94^{+}CD4^{-}CD8\alpha^{low}CD27^{-}CD38^{+}CD122^{+}CD127^{-}CD161^{low}CD226^{low}CXCR1/CXCR2^{+}CXCR3/CXCR4^{-}CX3CR1^{-}TIGIT/Tim\text{-}3^{+}$ cluster 5 (Control counts: 59853, RPL counts: 59864), $CD56^{dim}CD16^{-}CD57^{high}CD69^{-}CD94^{+}CD4^{-}CD8\alpha^{high}CD27^{-}CD38^{low}CD122^{-}CD127^{-}CD161^{-}CD226^{low}CXCR1/CXCR2^{-}CXCR3/CXCR4^{+}CX3CR1^{-}TIGIT/Tim\text{-}3^{low}$ cluster 7 (Control counts: 1227, RPL counts: 2282), and $CD56^{dim}CD16^{high}CD57^{-}CD69^{-}CD94^{+}CD4^{-}CD8\alpha^{low}CD27^{-}CD38^{high}CD122^{+}CD127^{-}CD161^{low}CD226^{-}CXCR1/CXCR2^{+}CXCR3/CXCR4^{-}CX3CR1^{-}TIGIT/Tim\text{-}3^{+}$ cluster 10 (Control counts: 20843, RPL counts: 25137) were augmented in women with RPL (Figure 74). Clusters elevated in RPL participants were not found to express any inhibitory receptors, while activating NKp30/NKp80 and NKG2C/NKG2D were detected on all these clusters, accompanied by activating KIR2DS1/2DS3 and NKp44/NKp46 on cluster 2, KIR2DS2 on clusters 4, 5, and 7, and NKp44/NKp46 on cluster 10.

Clusters 8 (Control counts: 53427, RPL counts: 23752), 17 (Control counts: 48721, RPL counts: 31568), 18 (Control counts: 1458, RPL counts: 1150), 6 (Control counts: 10232, RPL counts: 8023), 12 (Control counts: 31084, RPL counts: 29366), 9 (Control counts: 5837, RPL counts: 6978), 1 (Control counts: 14739, RPL counts: 18979), 19 (Control counts: 5547, RPL counts: 3846), 13 (Control counts: 1463, RPL counts: 1734), 16 (Control counts: 14269, RPL counts: 11931), 11 (Control counts: 15721, RPL counts: 10079) appeared unaltered in women with RPL (Figure 74).



Figure 74. Visualization of Natural Killer cell cluster prevalence in women with recurrent pregnancy loss (RPL) as detected by mass cytometry. *The 20 clusters of interest in women with RPL and controls are illustrated using a A) uniform manifold approximation and projection (UMAP) plot, in which cells are coloured according to the respective clusters, showing the relative cluster size, and distances representing the degree of phenotypic differences between clusters, a B) relative abundance box plot, depicting cluster proportion in each sample of the control (orange) and RPL (blue) groups, and a C) differential analysis heatmap, displaying the normalised proportion of each cluster in each sample [z score normalisation per cluster: z=(observation-mean observation)/standard deviation]. The heatmap colour varies from purple, suggesting relative under-representation, to orange, suggesting relative over-representation. The green/grey bar indicates significantly (green) or*

non-significantly (grey) differentially abundant clusters, accompanied by the adjusted p values. A bar representing the log fold change (logFC), indicating over-representation in RPL (blue) or controls (orange) is also included. Cluster phenotypes according to the expression of the CD56, CD16, CD57, CD69, CD94, CD4, CD5, CD8α, CD25, CD27, CD38, CD122, CD127, CD161, CD226, killer-cell immunoglobulin-like receptor (KIR)2DL1/2DS1/2DS3/2DS5, KIR2DL1/2DS5, KIR2DL2/2DL3/2DS2/2DS4, KIR2DS4, KIR2DL2/2DL3/2DL5, KIR2DL4, KIR3DL1/3DL2, immunoglobulin-like transcript (ILT)1, ILT2, ILT2/LIR6, ILT3/ILT4/ILT5, NKp30/NKp80, NKp44/NKp46, natural killer group (NKG)2A, NKG2C/NKG2D, C-X-C motif chemokine receptors (CXCR)1/CXCR2, CXCR3/CXCR4, CXCR5, CXCR6, CX3CR1, T-cell immunoreceptor with Ig and ITIM domains/T cell immunoglobulin and mucin domain-containing protein 3 (TIGIT/Tim-3), and programmed cell death protein 1 (PD-1) markers of interest are depicted.

8.1.5 NK cell activity in RPL and control subpopulations

NK cell cytotoxicity, evaluated through average cell death in NK cell-K562 cell co-cultures did not appear altered in either women with idiopathic RPL or those with non-idiopathic RPL, compared to the total control cohort (Figures 75A, 75B). Accordingly, NK cell cytotoxicity was not significantly different between women with RPL, with at least five previous losses, and control women (Figure 75C). Additionally, the average specific target cell death was unaltered between the age-related and ethnic subgroups in both the control and RPL populations (Figures 76A, 76B, 77A, 77B).

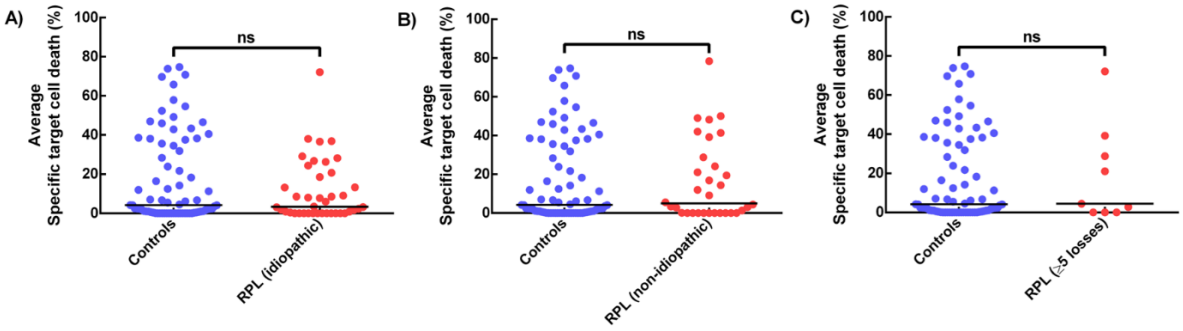


Figure 75. Specific target cell death in Natural Killer (NK) cell:K562 cell co-cultures, derived from women with idiopathic and non-idiopathic recurrent pregnancy loss (RPL), women with RPL and at least 5 past losses, and controls. *The average specific K562 target cell death in co-cultures including 0.5:1, 1:1, and 2:1 NK cell:K562 cell ratios is depicted. NK cells isolated from healthy controls (N=76) and A) women with idiopathic RPL (N=40), B) women with non-idiopathic RPL (N=32), and C) women with RPL with a minimum of 5 losses (N=9) were used. Mann-Whitney test performed, median illustrated. ns: non-significant*

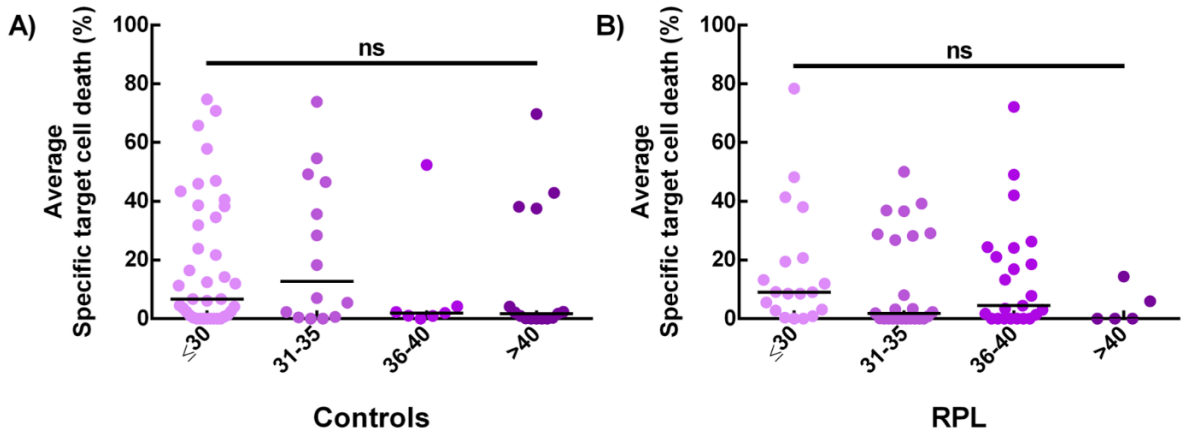


Figure 76. Specific target cell death in Natural Killer (NK) cell:K562 cell co-cultures, derived from women with recurrent pregnancy loss (RPL) and controls belonging to different age-associated subgroups. *The average specific K562 target cell death in co-cultures including 0.5:1, 1:1, and 2:1 NK cell:K562 cell ratios is shown. NK cells isolated from A) healthy controls belonging to the ≤30 (N=39), 31-35 (N=14), 36-40 (N=7), and >40 (N=15) age groups and B) women with RPL belonging to the ≤30 (N=19), 31-35 (N=25), 36-40 (N=23), and >40 (N=5) age groups were used. Kruskal-Wallis test performed, accompanied by the Dunn's test for multiple comparisons, median displayed. ns: non-significant*

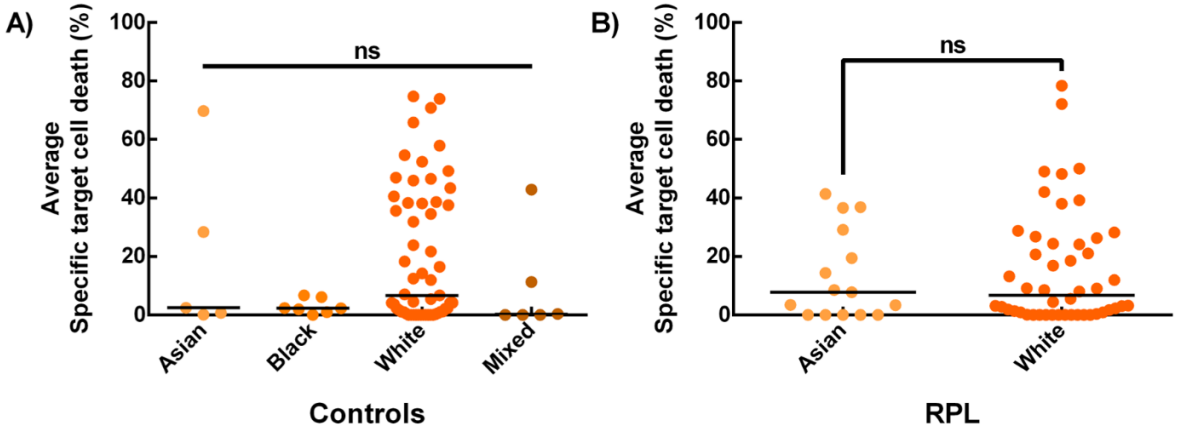


Figure 77. Specific target cell death in Natural Killer (NK) cell:K562 cell co-cultures, derived from women with recurrent pregnancy loss (RPL) and controls belonging in different ethnic subgroups. *The average specific K562 target cell death in co-cultures including 0.5:1, 1:1, and 2:1 NK cell:K562 cell ratios is depicted. NK cells isolated from A) healthy controls belonging to the Asian (N=5), Black (N=7), White (N=57), and Mixed (N=6) ethnic groups and B) women with RPL belonging to the Asian (N=15) and White (N=48) ethnic groups were used. A) Kruskal-Wallis test performed, accompanied by the Dunn's test for multiple comparisons, median illustrated, B) Mann-Whitney test used, median shown. ns: non-significant*

To control for ethnic variation and differences in alcohol intake between cohorts, average $CD107a^+$ cell prevalence in alive NK cells in NK cell-K562 cell co-cultures, which was found to be significantly different between women with RPL and controls, was assessed. No significant differences in the average $CD107a^+$ alive NK cell prevalence could be detected between White women with RPL and White controls or between women with RPL consuming low alcohol amounts and controls with similar alcohol consumption habits (Figures 78A, 79A). In regards to cytolytic molecule secretion, granzyme A secretion by unstimulated PBMCs ($p=0.0150$) and granzyme A ($p<0.0001$), B ($p=0.0007$), and perforin ($p=0.0004$) secretion by stimulated PBMCs were significantly decreased in White women with RPL (Figures

78B-78E). However, in women consuming low alcohol amounts granzyme A secretion by unstimulated PBMCs appeared unaltered compared to the respective control subgroup, while granzyme A (p=0.0005), B (p=0.0109), and perforin (p=0.0111) secretion by stimulated PBMCs was reduced (Figures 79B-79E).

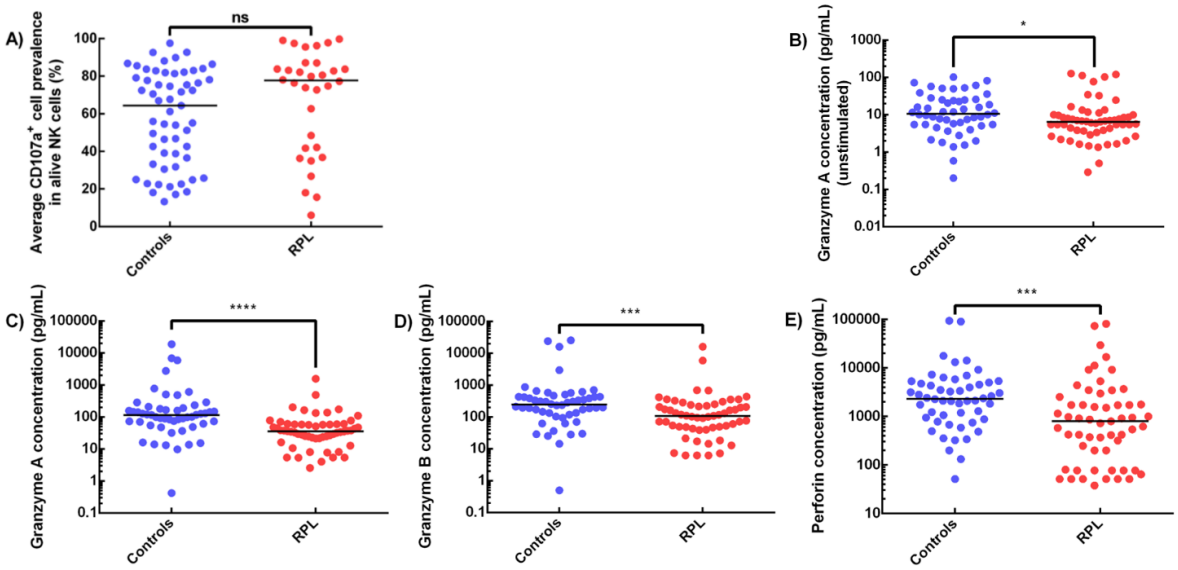


Figure 78. Natural Killer (NK) cell degranulation capacity in NK cell:K562 cell co-cultures and granzyme and perforin concentration (pg/mL) in peripheral blood mononuclear cell (PBMC) cultures derived from White women with recurrent pregnancy loss (RPL) and White controls. *A) The average prevalence of alive NK cells expressing CD107a in co-cultures including 0.5:1, 1:1, and 2:1 NK cell:K562 cell ratios is illustrated. NK cells isolated from healthy controls (N=57) and women with RPL (N=32) of White ethnic origin were used. The levels of B) granzyme A in unstimulated PBMC cultures and C) granzyme A, D) granzyme B, and E) perforin in stimulated PBMC cultures are also shown. PBMCs isolated from healthy controls (N=52) and women with RPL (N=57) of White ethnic origin were utilised. Mann-Whitney test used, median depicted. ns: non-significant, *: p≤0.05, ***: p≤0.001, ****: p≤0.0001*

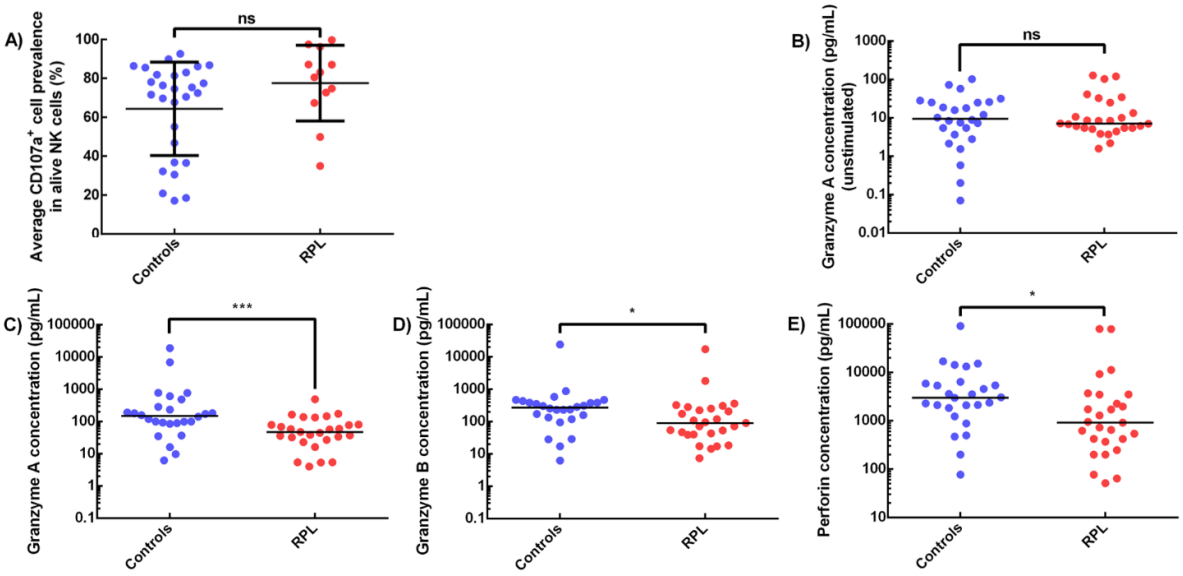


Figure 79. Natural Killer (NK) cell degranulation capacity in NK cell:K562 cell co-cultures and granzyme and perforin concentration (pg/mL) in peripheral blood mononuclear cell (PBMC) cultures derived from women with recurrent pregnancy loss (RPL), consuming low levels of alcohol, and controls with similar alcohol consumption habits. *A) The average prevalence of alive NK cells expressing CD107a in co-cultures including 0.5:1, 1:1, and 2:1 NK cell:K562 cell ratios is shown. NK cells isolated from healthy controls (N=28) and women with RPL (N=12), consuming low levels of alcohol, were used. The levels of B) granzyme A in unstimulated PBMC cultures and C) granzyme A, D) granzyme B, and E) perforin in stimulated PBMC cultures are also illustrated. PBMCs isolated from healthy controls (N=26) and women with RPL (N=27), consuming low levels of alcohol, were utilised. Normally distributed dataset without significantly different variances (A): Unpaired t test used, mean and standard deviation shown. Non-normally distributed datasets (B-E): Mann-Whitney test performed, median displayed. ns: non-significant, *: p≤0.05, ***: p≤0.001*

Moreover, CD69 expression levels on total and $CD56^{dim}CD16^{+}$ NK cells and the prevalence of $CD69^{+}$ cells in $CD56^{bright}CD16^{-}$ NK cells, which were also significantly different between women with RPL and controls, were examined in these subgroups. CD69 expression intensity on total ($p<0.0001$) and $CD56^{dim}CD16^{+}$ ($p=0.0012$) NK cells was reduced in White women with RPL, compared to controls with the same ethnic background, while $CD69^{+}CD56^{bright}CD16^{-}$ NK cell prevalence appeared unaltered (Figures 80A-80C). NK cells' CD69 expression intensity also appeared decreased in women with RPL, reporting low alcohol consumption levels, compared to the respective control subgroup ($p=0.0097$), with no significant difference detected in CD69 expression levels on $CD56^{dim}CD16^{+}$ NK cells and $CD69^{+}$ cell prevalence in $CD56^{bright}CD16^{-}$ NK cells (Figures 81A-81C). CD215 expression levels on stimulated total ($p=0.0150$) and $CD56^{dim}CD16^{+}$ ($p=0.0292$) NK cells appeared elevated in White women with RPL compared to White controls (Figures 80D, 80E), while they appeared unaltered between women with RPL and controls in the low alcohol intake subgroups (Figures 81D, 81E).

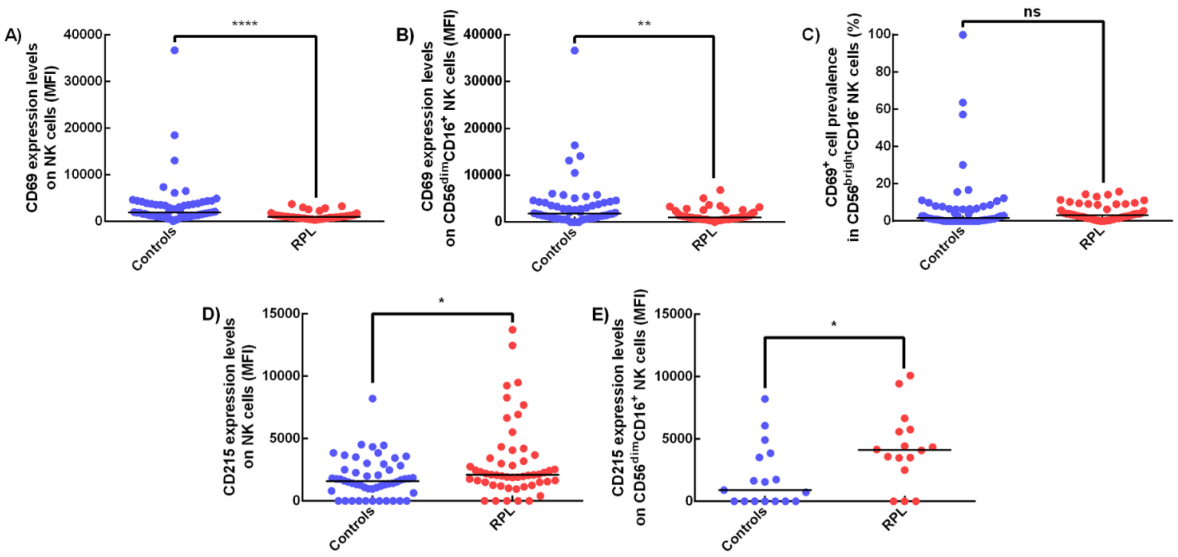


Figure 80. CD69 and CD215 expression by Natural Killer (NK) cells in White women with recurrent pregnancy loss (RPL) and White controls. *The expression intensity of CD69, represented by the median fluorescence intensity (MFI), on A) total and B) $CD56^{dim}CD16^{+}$ NK cells and C) the prevalence CD69-expressing $CD56^{bright}CD16^{-}$ NK cells of healthy controls (N=57) and women with RPL (N=53) of White ethnic origin is displayed. The expression intensity of CD215 on stimulated D) NK cells of healthy controls (N=52) and women with RPL (N=52) and E) $CD56^{dim}CD16^{+}$ NK cells of healthy controls (N=17) and women with RPL (N=16) of White ethnic origin is also shown. Mann-Whitney test used, median included. ns: non-significant, *: p≤0.05, **: p≤0.01, ****: p≤0.0001*

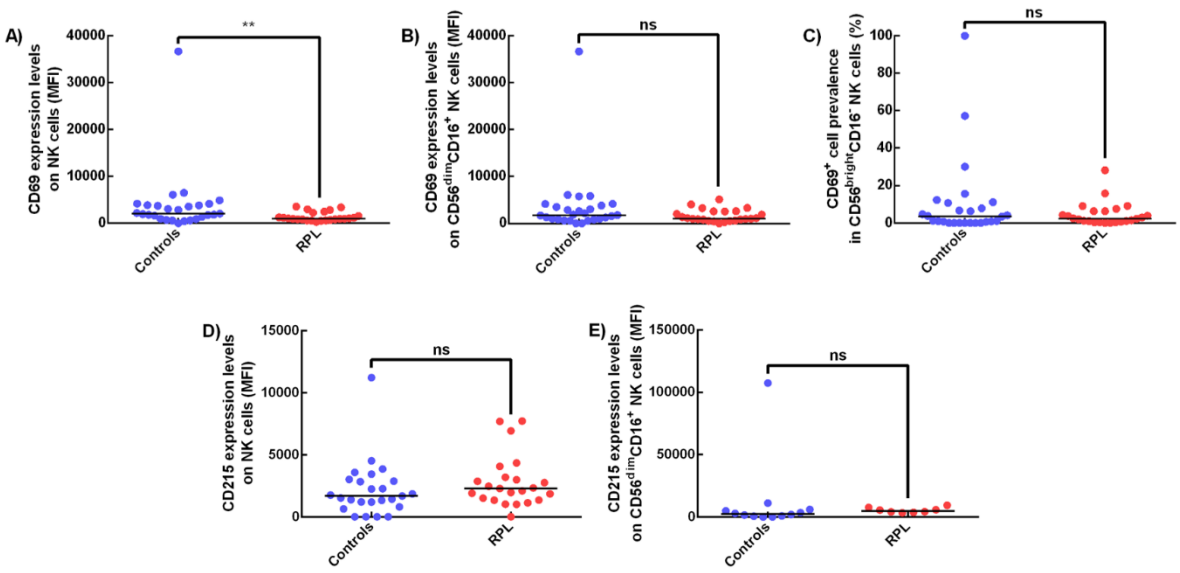


***Figure 81. CD69 and CD215 expression by Natural Killer (NK) cells in women with recurrent pregnancy loss (RPL)**, **consuming low levels of alcohol, and controls with similar alcohol consumption habits.** The expression intensity of CD69, represented by the median fluorescence intensity (MFI), on A) total and B) $CD56^{dim}CD16^{+}$ NK cells and C) the prevalence CD69-expressing $CD56^{bright}CD16^{-}$ NK cells of healthy controls (N=27) and women with RPL (N=24), consuming low levels of alcohol, is shown. The expression intensity of CD215 on stimulated D) NK cells of healthy controls (N=25) and women with RPL (N=23) and E) $CD56^{dim}CD16^{+}$ NK cells of healthy controls (N=12) and women with RPL (N=8), consuming low levels of alcohol, is also illustrated. Mann-Whitney test used, median depicted. ns: non-significant, **: p≤0.01*

The average specific target cell death did not appear predictive of following pregnancy outcome in women with RPL (Figure 82A). Similarly, granzyme A and B and perforin secretion by unstimulated and stimulated PBMCs was not significantly different between women with RPL that were either in the 3rd trimester of their subsequent pregnancy or had a live birth and those that had a miscarriage following their recruitment (Figures 82B-82G).

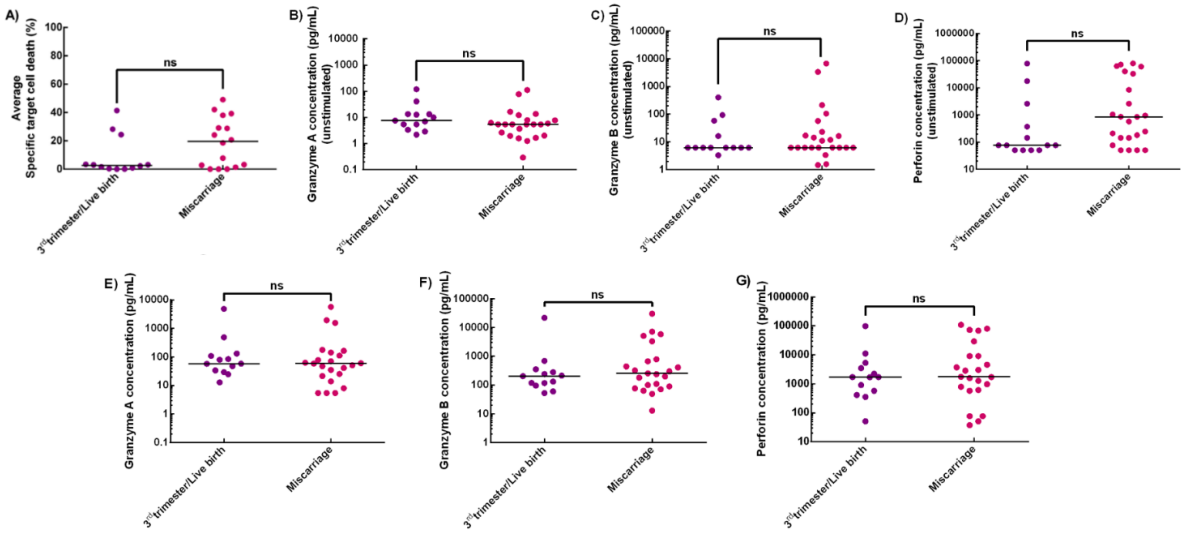


Figure 82. Specific target cell death in Natural Killer (NK) cell:K562 cell co-cultures and granzyme and perforin concentration (pg/mL) in peripheral blood mononuclear cell (PBMC) cultures derived from women with recurrent pregnancy loss (RPL), who were either in the 3rd trimester of their subsequent pregnancy or had a live birth, and from those with a subsequent miscarriage. *A) The average specific K562 target cell death in co-cultures including 0.5:1, 1:1, and 2:1 NK cell:K562 cell ratios is depicted. NK cells isolated from women with RPL belonging to the 3rd trimester/Live birth subgroup (N=12) and from those belonging to the miscarriage subgroup (N=16) were used. The levels of B) granzyme A, C) granzyme B, and D) perforin in unstimulated PBMC cultures and the levels of E) granzyme A, F) granzyme B, and G) perforin in stimulated PBMC cultures are also illustrated. PBMCs isolated from women with RPL belonging to the 3rd trimester/Live birth subgroup (N=13) and from those belonging to the miscarriage subgroup (N=23) were utilised. Mann-Whitney test performed, median displayed. ns: non-significant*

8.1.6 Summary

Table 30. Overview of changes in peripheral immune activity of women with recurrent pregnancy loss (RPL) compared to control women. *Alterations in Natural Killer (NK) cell cytotoxicity and degranulation, cytolytic molecule secretion by unstimulated (U) and stimulated (S) peripheral blood mononuclear cells (PBMCs), and NK cell population and subpopulation activation, examined via the cytotoxicity assay, utilizing CD107a as a degranulation marker, enzyme-linked immunosorbent assay (ELISA), and flow cytometry, using CD69 as an activation marker, respectively, are displayed. MFI: median fluorescence intensity, ↓: decreased, ↑: increased, ns: non-significant, *: p≤0.05, **: p≤0.01, ***: p≤0.001, ****: p≤0.0001*

Assay type	Marker	Change in RPL compared to control group (significance)
Cytotoxicity	Average specific target cell death (%)	ns
	Average $CD107a^+$ degranulating alive NK cell prevalence (%)	↑ (*)
	Average CD107a expression levels on degranulating alive NK cells (MFI)	ns
ELISA PBMCs (U)	Granzyme A concentration (pg/mL)	↓ (**)
	Granzyme B concentration (pg/mL)	ns
	Perforin concentration (pg/mL)	ns
ELISA PBMCs (S)	Granzyme A concentration (pg/mL)	↓ (****)
	Granzyme B concentration (pg/mL)	↓ (**)
	Perforin concentration (pg/mL)	↓ (***)
Flow cytometry	$CD69^+$ activated NK cell prevalence (%)	ns
	$CD69^+$ activated $CD56^{dim}CD16^+$ NK cell prevalence (%)	ns
	$CD69^+$ activated $CD56^{bright}CD16^-$ NK cell prevalence (%)	↑ (*)
	CD69 expression levels on activated NK cells (MFI)	↓ (****)
	CD69 expression levels on activated $CD56^{dim}CD16^+$ NK cells (MFI)	↓ (***)
	CD69 expression levels on activated $CD56^{bright}CD16^-$ NK cells (MFI)	ns

Table 31. Overview of major Natural Killer (NK) cell phenotypic changes in the peripheral blood of women with recurrent pregnancy loss (RPL) compared to control women. *Presence (+) or absence (-) of receptor expression on NK cell clusters reduced and increased in RPL, as detected via mass cytometry, is depicted.*

Receptor type	Receptor	4 clusters reduced in RPL				5 clusters increased in RPL				
		3	14	15	20	2	4	5	7	10
Inhibitory	NKG2A	+	+	+	-	-	-	-	-	-
Inhibitory	ILT2	-	-	-	+	-	-	-	-	-
Inhibitory	ILT3/ILT4/ILT5	-	-	-	+	-	-	-	-	-
Activating	NKG2C/NKG2D	+	+	+	-	+	+	+	+	+
Activating	ILT1	-	-	-	+	-	-	-	-	-
Activating	KIR2DS1/2DS3	-	-	-	-	+	-	-	-	-
Activating	KIR2DS2	-	-	-	-	-	+	+	+	-
Activating	CD57	+	-	-	-	+	+	+	+	-
Chemokine	CXCR3/CXCR4	+	+	+	+	-	-	-	+	-

8.2 Discussion

As suggested by their name, NK cells are characterised by their capacity to kill target cells, potentially including fetal cells. Previous studies have reported both an increase and a reduction in the cytotoxic potential of NK cells in the peripheral blood of non-pregnant women with RPL.[168, 187, 191, 196, 350] However, an unaltered NK cell cytotoxic potential in these women has also been reported.[171] In agreement to the later finding, no significant difference in the cytotoxic activity of pNK cells could be detected between the RPL and control groups in the present study (Figure 58). This variability between studies could be associated with differences in menstrual cycle phase at the point of PBMC isolation, as pNK cell cytotoxicity is thought to vary significantly throughout the menstrual cycle.[587] In this study, participant recruitment was not able to be controlled in regards to the menstrual cycle phase, as much higher numbers would be needed and the study was aiming to provide a representation of the general population.

To evaluate NK cell capacity for degranulation, CD107a expression was also examined upon co-incubation of pNK cells with their targets.[644] Interestingly, in the 1:1 and 2:1 NK:K562 cell cultures, the prevalence of alive NK cells expressing this marker was elevated when pNK cells derived from women with RPL were used (Figures 59F, 59G). These findings suggest that pNK cells of women with RPL acquire an enhanced degranulation capacity upon interaction with target cells, without however being capable of more effective target cell lysis. Surprisingly, $CD107a^+$ dead and alive pNK cell prevalence was found to be increased in cultures containing the smallest NK cell amounts, while the expression intensity of this marker on dead pNK cells was elevated in cultures with the highest effector:target cell ratio (Supplementary Figures 36B-36E). It is possible that in cultures with higher NK cell concentration, there is a reduced K562 cell availability, resulting in the degranulation of a smaller percentage of NK cells. However, in contrast to previous reports,[196] the levels of specific target cell death were not found to be affected by the different effector:target cell ratios used (Supplementary Figure 36A).

As increased pNK degranulation in women with RPL was not found to result in augmented target cell killing, perforin and granzyme secretion by PBMCs in the absence and following stimulation was evaluated. These molecules are stored in cytolytic T_C and NK cell granules and are released as a death-inducing mechanism.[715] Reduced granzyme A, but not granzyme B or perforin, secretion was detected in the absence of stimulation in RPL-derived PBMC cultures (Figure 61). Unaltered granzyme B^+ and $perforin^+$ pNK cell levels have also been previously reported in non-pregnant women with RPL in the absence of stimulation, being however accompanied by reduced granzyme B expression intensity.[196] Upon

stimulation, granzyme A and B and perforin secretion were all found to be reduced in the RPL cohort (Figure 63). Even though perforin and granzyme secretion by pNK cells was not separately examined, it can be speculated that increased pNK cell degranulation in women with RPL is counterbalanced by reduced production of cytolytic molecules, resulting to an unaltered cytolytic capacity compared to non-pregnant controls. In contrast to these findings, using a cytotoxicity assay with K562 target cells, NK cells from patients with RPL displayed strong perforin and granzyme release, which was not significantly different than that of healthy controls.[349] NK cells are key players in anti-viral immunity and tumour surveillance and thus the impact of reduced granular secretion should be examined. Primary RPL has displayed a borderline significant association to subsequent cancer development.[716] Hence, this functional work supports a wider understanding of NK cell activity.

Two markers commonly used to assess NK cell activation potential are CD69 and CD94. CD69 is considered a marker for NK cell activation, with a positive correlation reported between its expression and NK cell cytotoxicity.[339, 340] Through flow cytometry, $CD69^{+}CD56^{bright}CD16^{-}$, but not $CD69^{+}CD56^{dim}CD16^{+}$, pNK cell prevalence appeared elevated in women with RPL, while the expression intensity of this marker on total and $CD56^{dim}CD16^{+}$ pNK cells was reduced (Figure 64). In agreement to these findings, unaltered $CD69^{+}CD56^{dim}$ pNK cell concentration was previously reported in non-pregnant women with RPL.[185] However, an elevated $CD69^{+}$ pNK cell prevalence, affecting both the $CD56^{dim}$ and the $CD56^{bright}$ subset has also been reported in these women.[189, 262] The $CD56^{dim}CD16^{+}$ subset is considered the primary mediator of NK cell cytotoxicity, while the $CD56^{bright}CD16^{-}$

subset is characterised by a lower cytolytic and a higher cytokine-producing ability.[131-133, 137] Hence, a reduction in the pNK cell cytotoxic potential in participants with RPL is suggested. However, as this effect was not detected using the cytotoxicity assay, it is possible that changes in NK cell activation, illustrated through the altered CD69 expression pattern in women with RPL, are mostly linked to alterations in the cytokine-producing capacity of these cells that is explored later in this study.

Mass cytometry was used to identify pNK cell populations, focusing on their inhibitory and activating receptor expression. Although the term populations is used for the description of the clusters identified, this does not infer that these phenotypes represent fixed subsets. Of the 20 NK cell clusters detected by mass cytometry, only one cluster exhibited the $CD56^{bright}CD16^{-}$ phenotype (Figure 73B). Interestingly the prevalence of this population was not found to be altered in women with RPL (Figure 74), in contrast to the findings of the flow cytometry-based assay (Figure 39D). However, most clusters appeared to be $CD56^{dim}$, expressing low, medium, or high levels of CD16 (Figure 73B). Although these expression patterns are partially in agreement with previous findings, indicating a 90% prevalence of $CD56^{dim}CD16^{high/+}$ cells in the pNK cell population and a 10% prevalence of $CD56^{bright}CD16^{low/-}$ pNK cells,[133] the absolute $CD56^{dim}CD16^{+}$/$CD56^{bright}CD16^{-}$ dichotomy was not seen. Specifically, two $CD56^{dim}CD16^{-}$ pNK cell populations were identified, alongside three $CD56^{extremely\text{-}low}CD16^{-}$ populations (Figure 73B). CD69 expression was only detected on one of the $CD56^{extremely\text{-}low}CD16^{-}$ populations and on two $CD56^{dim}$ clusters (Figure 73B), one of which was found to be reduced in women with RPL in agreement to the findings of the flow cytometry-based assay (Figures 64, 74). Using

mass cytometry no CD69 expression was detected on $CD56^{bright}CD16^{-}$ pNK cells (Figure 73B). Although in both the flow and the mass cytometry assay unstimulated NK cells were used, it is possible that some activation was induced during cell staining and preparation, resulting to CD69 expression by $CD56^{bright}CD16^{-}$ pNK cells in the flow cytometry-based but not in the mass cytometry assay. On the other hand, CD94 expression is thought to negatively correlate with the cytotoxic activity of NK cells.[345] Contradicting findings have been obtained in regards to the expression of this marker on pNK cells of non-pregnant women with RPL with both an elevation and a reduction of CD94 expression reported.[189, 262] Medium to high CD94 expression was detected on all $CD56^{dim}$ and $CD56^{bright}$ pNK cell clusters (Figure 73B). Even though this receptor is considered inhibitory, its effect on NK cell function is actually dependent on its association with NKG2 receptors as it is going to be discussed later.

Alongside the mass cytometry assay, the cytokine panel of the flow cytometry-based assay was utilised to assess the expression of the alpha chain of two NK cell receptors, CD25 and CD215, binding the IL-2 and IL-15 cytokines, respectively, which are considered central to NK cell activation.[282, 635, 717] In the absence of stimulation CD25 and CD215 expression on total and $CD56^{dim}CD16^{+}$ pNK cells was not significantly different between non-pregnant women with RPL and controls (Figures 65, 66), in agreement to previous findings.[262] CD25 expression on total and $CD56^{dim}CD16^{+}$ pNK cells also appeared unaltered between the RPL and control groups following stimulation (Figures 69A, 69C, 70A, 70C). CD25 expression on NK cells has been associated with the proliferative potential, the cytotoxicity, and cytokine-producing activity of NK cells.[340, 718, 719] Thus, the lack of an altered pNK

cell cytotoxic potential in women with RPL could be associated with the unaltered CD25 expression profile of these cells. CD25 could not be detected on NK cells by mass cytometry (Figure 73B), possibly due to the small prevalence of unstimulated pNK cells expressing this subunit.

On the other hand, upon stimulation CD215 expression levels were found to be elevated on both total and $CD56^{dim}CD16^{+}$ pNK cells of participants with RPL compared to controls (Figures 70B, 70D). Although CD215 was not examined by mass cytometry, the expression of CD122, which constitutes the beta chain of the IL-2 and IL-15 receptors,[279] was assessed. CD122 was detected on most $CD56^{dim}$ cells and on the $CD56^{bright}$ cluster (Figure 73B). CD122 is associated with commitment to the NK cell lineage, as IL-15 responsiveness is considered essential to NK cell maturation.[284, 720] Absence of CD122 was observed on the two $CD56^{dim}CD16^{-}$ and the three $CD56^{extremely\text{-}low}CD16^{-}$ clusters (Figure 73B), indicating an immature identity. CD122 did not exhibit a preferential expression on clusters whose prevalence was increased or reduced in women with RPL (Figure 74), in agreement to a previous study reporting no alteration in CD122 expression by pNK cells between non-pregnant women with RPL and controls.[262] NK cells primarily respond to IL-15 stimulation either through *trans*-presentation, involving membrane-bound or soluble IL-15/CD215 complex interaction with CD122/CD132 on NK cells.[721, 722] However, through their CD215 expression, stimulated NK cells may facilitate IL-15-CD122/CD132 interaction through a *cis*-presentation mechanism.[717, 722] Although the extent in which the *cis*-presentation mechanism operates remains unclear, according to the present findings this mechanism could constitute a secondary reaction to NK cell stimulation, amplifying the immune response,

particularly in women with RPL, thus underlining CD215 as a potential therapeutic target.

Mass cytometry facilitated the generation of a detailed pNK cell phenotype map, allowing the simultaneous examination of 50 markers. CD57 emerged as a marker of primary importance, separating the 20 pNK cell clusters into two groups, one $CD57^{high}$ and one $CD57^{-}$ (Figure 73). CD57 expression is thought to define a mature NK cell subset, and thus it is not commonly detected on $CD56^{bright}$ cells, which are thought to represent a less mature subset.[270, 271] In agreement to that, the $CD56^{bright}CD16^{-}$ cluster, as well as the $CD56^{extremely\text{-}low}CD16^{-}$ clusters, appeared as $CD57^{-}$ (Figure 73B). Furthermore, KIR^{+} NK cell subtypes were more prevalent among the $CD57^{+}$ populations, with at least one KIR being expressed in 5/7 $CD57^{+}$ and 2/13 $CD57^{-}$ clusters (Figure 73B), in parallel with previous findings.[271] Interestingly, 3/4 clusters reduced in women with RPL displayed a $CD57^{-}$ phenotype, while 4/5 clusters increased were $CD57^{high}$ (Figure 74). $CD57^{+}$ NK cells are considered more potent mediators of cytotoxicity, expressing higher perforin and granzyme B levels and being more sensitive to CD16 stimulation than $CD57^{-}$ cells, possibly due to the higher prevalence of $CD16^{+}$ cells.[271] Thus, increased prevalence of $CD57^{high}$ NK cells in the peripheral blood of non-pregnant women with RPL could indicate an increased pre-disposition towards cytotoxic activation. This finding is in agreement with the increased NK cell degranulation observed, although the overall reduction in cytolytic molecule release suggests a defect in cytotoxic immune activity of women with RPL. However, as it is going to be later discussed, NK cell inflammatory activity is not restricted to cytotoxic granule release but also

involves pro-inflammatory cytokine production, triggered by activating receptor signalling.

To investigate that in more detail KIR expression was assessed. KIRs are considered the primary mediators of NK cell activity, binding HLA-A, HLA-B, and HLA-C molecules.[211] These receptors can be sub-categorised into inhibitory, including KIR2DL1, KIR2DL2, KIR2DL3, KIR2DL5, KIR3DL1, and KIR3DL2, and activating ones such as KIR2DS1, KIR2DS2, KIR2DS3, KIR2DS4, and KIR2DS5.[211, 212] KIR2DL4 is considered as an activating receptor, triggering NK cell cytotoxicity, acquiring however a weak inhibitory capacity.[215] Due to their high similarity, antibodies binding multiple KIRs are usually produced and thus these receptors are often examined in groups. Using a custom panel we aimed to distinguish between inhibitory and activating KIR groups. Most KIRs, including KIR2DL1, KIR2DL2, KIR2DL3, KIR2DL4, KIR2DL5, KIR2DS4, and KIR2DS5 were not expressed by any pNK cell subset (Figure 73B). However, previous studies have reported an increase in both the numbers of $KIR2DL1^{+}$ and $KIR2DL2/L3^{+}$ pNK cells and expression intensity of these receptors in women with RPL.[190, 196] On the other hand, in genotyping studies significantly less women with RPL were found to acquire the inhibitory KIR2DL1, KIR2DL2, and KIR2DL3 and the KIR2DS4 activating gene.[723, 724] Findings highlighting an unaltered KIR2DL1 and KIR2DL2/L3 expression on $CD56^{dim}CD16^{+}$ and $CD56^{bright}CD16^{-}$ pNK cells of non-pregnant women with RPL compared to the controls have also been reported.[725] Hence, further examination of these receptors utilizing higher NK cell amounts is warranted.

High levels of inhibitory KIR3DL1 and/or KIR3DL2 were detected on one $CD56^{dim}CD16^{high}$ cluster (Figure 73B). No alteration in the prevalence of the

KIR3DL1- and/or KIR3DL2-expressing cluster could be detected between women with RPL and controls (Figure 74), even though KR3DL1^{+} pNK cell numbers have been reported to be increased in non-pregnant women with RPL.[190] This contradiction could possibly stem from the simultaneous investigation of KIR3DL1 and KIR3DL2. KIR2DS1 and/or KIR2DS3 were detected on two CD56^{dim}CD16^{high} clusters, while KIR2DS2 was the most common KIR detected, present on 6/20 clusters, including five CD16-expressing CD56^{dim} ones and one CD56^{dim}CD16^{-} cluster (Figure 73B). One of the KIR2DS1/KIR2DS3^{+} clusters and 3/6 KIR2DS2^{+} clusters were found to be elevated in women with RPL, while none were found to be reduced (Figure 74), indicating a promotion of an activating KIR repertoire in the periphery of those women. In agreement to these findings, genotypes with a high content of activating KIR genes appeared to be enhanced in women with a history of RPL.[212, 724]

The expression of inhibitory ILT2, ILT3, ILT4, and ILT5 and activating ILT1 and LIR6 on pNK cells was also assessed.[234] ILT2, ILT4, and LIR6 are known to recognise and bind MHC class I molecules, while the ligands of other ILTs remain undefined.[237, 242] Inhibitory ILT receptor expression was detected on clusters whose frequency was unaltered in RPL, while both activating and inhibitory ILTs were detected on a CD56$^{extremely\text{-}low}$CD16^{-} cluster, whose frequency was found to be reduced in women with RPL (Figures 73B, 74). Thus, inhibitory/activating ILT balance does not appear to be involved in RPL pathogenesis.

In addition, activating NCRs, including NKp46, NKp30, NKp44, and NKp80, were examined.[244, 245] NCR ligands remain largely unidentified. NKp30 and/or NKp80 expression appeared particularly prevalent among pNK cell subsets, with only the

$CD56^{extremely\text{-}low}CD16^{-}$ clusters lacking their expression. NKp44 and/or NKp46 were also quite common, being present on 11/20 subsets (Figure 73B). Interestingly, all clusters reduced in women with RPL were NKp44/NKp46^{+}, while 3/4 also expressed NKp30/NKp80. Similarly, all clusters augmented in RPL were NKp30/NKp80^{+}, while 2/5 were also NKp44/NKp46^{+} (Figure 74). Thus, although aberrant cytokine production in RPL has been associated with NCR activity,[726] no clear link between NCR expression patterns on NK cells and RPL could be observed, in agreement to previous findings reporting an absence of significant differences in NCR expression between non-pregnant women with RPL and fertile controls.[196]

NKG2 receptors are also considered primary mediators of NK cell activity and hence the expression of NKG2A, NKG2C, and NKG2D was also examined. NKG2A and NKG2C mediate NK cell activity in the form of CD94 heterodimers, with NKG2A/CD94 recognising HLA-G and HLA-E, resulting to inhibition of NK cell activity, and NKG2C/CD94 binding HLA-G, promoting NK cell activation.[92, 93, 211, 263] On the other hand, activating NKG2D binds multiple ligands, including MHC class I chain-related proteins (MIC) A and B, independently of CD94.[211, 245] All clusters expressing NKG2C/NKG2D or NKG2A were CD94^{+} (Figure 73B). Only $CD94^{-}CD56^{extremely\text{-}low}CD16^{-}$ subsets, one of which was reduced in women with RPL, displayed a NKG2C/NKG2D^{-} phenotype (Figures 73B, 74). Fascinatingly, 3 $NKG2A^{+}CD56^{dim}CD16^{high/+}$ pNK cell clusters were found to be reduced in women with RPL, while none of the NKG2A^{+} pNK cell subsets was elevated in these women compared to controls (Figure 74). In contrast to these findings, elevated NKG2A^{+} and NKG2D^{+} total and $CD56^{dim}CD16^{+}$ pNK cell numbers have been detected in women with RPL,[190] while in other studies unaltered NKG2D expression and an

unaffected NKG2A and NKG2D genetic repertoire has been reported in women with RPL.[196, 723]

Taken together, activating receptor expression was detected on the clusters whose frequency was elevated in women with RPL and those whose frequency was decreased. However, no inhibitory KIR, ILT, NCR, or NKG2 receptor expression was detected on pNK cell clusters augmented in the RPL group, while clusters that were reduced in women with RPL were found to express inhibitory NKG2A or ILTs (Figure 74). Hence, the present findings indicate that in non-pregnant women with RPL there is a potential predisposition of pNK cells towards response to activating signals, possibly not counterbalanced by sufficient inhibitory signalling. However, this observation and hypothesis contradict previous reports, suggesting a NKG2A and inhibitory KIR upregulation in women with RPL.[190]

Immune checkpoint receptor levels on pNK cells were also investigated. PD-1 expression, which is associated with reduced proliferative, cytokine-producing, and cytotoxic NK cell capacity, was not observed on any NK cell subset (Figure 73B).[291] Although PD-1^{+} pNK cells have been previously detected in about 1/4 of healthy individuals, the expression of this receptor was found to be restricted to CMV seropositive individuals.[291] On the other hand, TIGIT and/or Tim-3 were prevalent among pNK cell subsets, being expressed on 14/20 NK cell clusters, including the CD56^{bright}CD16^{-} subpopulation (Figure 73B). Even though CD56^{bright}CD16^{-} pNK cells are thought to be separated according to their Tim-3 expression,[304] Tim-3^{+} and Tim-3^{-} CD56^{bright}CD16^{-} subsets were not distinguished, possibly due to the limited number of clusters generated. Tim-3 activity on pNK cells remains to be elucidated, but its stimulation has been shown to inhibit pNK cell cytotoxicity.[304, 309]

TIGIT expression has been associated with reduced pNK cell cytotoxic and pro-inflammatory IFN-γ-producing capacity, possibly through the inhibition of nuclear factor kappa-light-chain-enhancer of activated B cells (NF-κB) signalling.[292, 296] 3/4 clusters reduced and 4/5 clusters increased in women with RPL were found to be TIGIT/Tim-3^{+} (Figure 74). Thus, no clear association between the expression of these receptors and RPL could be detected.

TIGIT binds CD155 and CD112, with high and low affinity, respectively, resulting in an inhibition of NK cell mediated-cytotoxicity.[297] However, these ligands are also recognised by the activating CD226.[245, 297, 727] CD226^{+} pNK cells are characterised by enhanced proliferative potential, motility, cytotoxicity, and capacity for IFN-γ- and GM-CSF production.[728] Hence, TIGIT and CD226 are thought to compete for ligand binding, resulting in either inhibition or promotion of cytotoxicity.[286] CD226 was found to be expressed on most pNK cell clusters, including CD56^{dim}, CD56^{bright}, and CD56$^{extremely\text{-}low}$ subsets (Figure 73B). In 3/4 subsets reduced in RPL medium CD226 expression was detected and in 4/5 subsets increased in women with this condition low CD226 levels were observed. CD226^{+} clusters reduced in RPL were also TIGIT/Tim-3^{+}, while 3/5 clusters increased were CD226^{+}TIGIT/Tim-3^{+} (Figures 73B, 74). As TIGIT was examined alongside Tim-3, its possible correlation with CD226 expression on pNK cells could not be assessed. Further research is required to examine the relative expression of these receptors in women with RPL, and identify whether changes in CD226 and TIGIT levels are associated with an alteration of NK cell activation potential in the periphery of women with this condition.

Additional receptors were also examined by mass cytometry. CD5 could not be identified on any pNK cell subsets (Figure 73B). CD5^{low} NK cells have only been

detected in pulmonary tuberculosis and patients with multiple myeloma and plasmacytoma.[729, 730] As these cells have displayed cytotoxic capacity against K562 targets,[729, 730] additional research about their prevalence in healthy individuals could provide a useful insight into this NK cell subset. Similarly, CD4 expression was only detected in one of the $CD56^{extremely\text{-}low}CD16^{-}$ subsets that was found to be reduced in women with RPL (Figures 73B, 74). A role of CD4 in IFN-γ and TNF-α production by NK cells has been suggested,[731] even though the exact properties of this subset have not yet been fully elucidated. CD127 expression was also restricted to one $CD56^{extremely\text{-}low}CD16^{-}$ cluster, whose frequency did not appear to be different between the RPL and control groups (Figures 73B, 74). According to their CD127 expression, these cells are thought to be in an early stage of maturation, not being committed to the NK lineage.[732] In agreement to that, the $CD127^{+}$ subset, appeared to be $CD57^{-}CD122^{-}$, also lacking KIR expression (Figure 73B), which is associated with later pNK cell maturation stages.[210] In regards to CD27, in contrast to previous findings,[276] low expression was detected only on the $CD56^{bright}CD16^{-}$ subset (Figure 73B). $CD27^{+}$ NK cells are thought to be more potent IFN-γ producers than $CD27^{-}$ ones, but are characterised by a lower cytotoxic capacity.[277] The prevalence of the $CD27^{+}$ pNK cell cluster was not found to be significantly different between women with RPL and controls (Figure 74).

Furthermore, CD8α expression was detected most clusters, apart from one $CD56^{dim}CD16^{low}$, two $CD56^{extremely\text{-}low}$CD16-, and the $CD56^{bright}CD16^{-}$ subset (Figure 73B). NK cells are thought to express CD8 in the form of CD8α/α homodimers, whose activity is not yet fully understood.[733, 734] However, $CD8^{+}$ NK cells are considered more cytolytic, although CD8α ligation was shown to promote NK cell

activity, without inducing cytotoxicity.[735, 736] CD8α/α is also thought to be involved in the stabilization of KIR3DL1 binding to its ligands, promoting KIR3DL1 clustering and enhancing its inhibitory effect.[737] Additionally, CD8 ligation by class I HLA molecules was found to trigger NK cell apoptosis,[738] highlighting a potential role of this receptor on the establishment of fetal tolerance. However, CD8α expression was observed in almost all clusters reduced and increased in women with RPL (Figure 74). Thus, further experiments are required to evaluate potential alterations in $CD8\alpha^{+}$ NK cell levels and activity in RPL. CD38, who is thought to promote NK cell activity, being involved in cytoplasmic calcium regulation,[273, 274] was expressed on almost all pNK cell clusters, apart from one $CD56^{dim}CD16^{-}$ and one $CD56^{extremely\text{-}low}CD16^{-}$ subset that were not found to be significantly altered in RPL compared to control participants (Figures 73B, 74).

CD161 also was detected on most pNK cell subsets, apart from one $CD56^{dim}CD16^{+}$, the two $CD56^{dim}CD16^{-}$, and the three $CD56^{extremely\text{-}low}CD16^{-}$ clusters. Except from the $CD56^{dim}CD16^{+}$ subset, all the $CD161^{-}$ clusters were also found to be negative for CD122, suggesting that CD161 is mostly present on cells committed to the NK lineage (Figure 73B). $CD161^{+}$ NK cells have displayed an enhanced responsiveness to cytokine stimulation, characterised by an increased proliferative ability and an enhanced capacity for IFN-γ production.[278] pNK cell clusters increased in RPL appeared to be $CD161^{low}$, while medium CD161 expression levels were detected in clusters whose frequency was decreased in the RPL, with an exception of two $CD161^{-}$ clusters, one elevated and one reduced in the RPL group (Figure 74). This suggests an overall reduction in CD161 expression by peripheral NK cells in non-pregnant participants with RPL. However, in one study activating CD161 expression

by $CD56^{dim}CD16^{+}$ and $CD56^{bright}CD16^{-}$ pNK cells was not found to be different between non-pregnant women with RPL and controls.[725] Hence, further studies are required to elucidate the role of CD161 expression in NK cell activity during RPL.

Lastly, mass cytometry was used to examine chemokine receptor expression on the surface of pNK cells. The $CX3CR1^{+}$ pNK cell subset frequency was not found to be altered between RPL and control cases (Figure 74). However, specific CX3CR1 genotypes have been associated with RPL,[332] suggesting an involvement of this cytokine receptor in the pathogenesis of this condition. CX3CR1 expression was only detected on a $CD56^{extremely\text{-}low}CD16^{-}$ cluster (Figure 73B), in contrast to previous studies detecting this receptor on both $CD16^{+}$ and $CD16^{-}$ NK cells.[313, 314] All pNK cell subsets were found to express CXCR1/CXCR2 and/or CXCR3/CXCR4. In agreement to previous findings, CXCR1/CXCR2 expression was observed on $CD56^{dim}$ but not $CD56^{bright}$ pNK cell subsets, while CXCR3/CXCR4 was present in detectable levels on both these subsets (Figure 73B).[315] CXCR1 or CXCR2 were expressed on 2/4 subsets reduced and 4/5 subsets increased in women with RPL (Figure 74). CXCR1 is involved in lymphocyte migration towards sites of inflammation, while CXCR2 is thought to acquire a role in angiogenesis.[739, 740] Thus, both chemokines receptors could be involved in recruitment of pNK cells to the uterus during early pregnancy, facilitating local remodelling. However, further research is required to determine the potential involvement of CXCR1 and CXCR2 in RPL. On the other hand, CXCR3 and CXCR4 expression is considered central to NK cell uterine migration, with their ligands also being present in the decidua during pregnancy.[314, 321, 739] This requires further consideration as at least one of these receptors was present on all pNK cell subsets that were reduced in women with

RPL, while 4/5 subsets elevated in this participant group were $CXCR3^{-}CXCR4^{-}$ (Figure 74), indicating a possible deficiency in NK cell uterine migration in RPL in agreement to latest findings highlighting a reduction in eNK cell levels.[205]

Overall, the use of mass cytometry for the assessment of NK cells has been limited. In a study examining the pNK cell repertoire diversity in healthy individuals, a predominance of $CD56^{dim}$ subpopulations was detected, with only 1/50 most abundant clusters being $CD56^{bright}$,[741] similar to present data revealing 1/20 $CD56^{bright}$ cluster. These findings reflect the highest prevalence of the $CD56^{dim}$ subset but could also indicate a higher phenotypic diversity of the $CD56^{dim}$ population. Contradictory mass cytometry findings have been obtained regarding CD57 expression, with one study presenting CD57 as the primary marker separating the pNK cell population into two major subsets,[208] consistent with present data, and another reporting expression of this receptor on only 2/50 most prevalent clusters.[741]

In line with the present study, a high abundance of $CD94^{+}$ and $NKG2D^{+}$ subpopulations and an absence of KIR2DL1 and KIR2DL5 have been detected in healthy adults.[741] However, while present findings suggest that NKG2A and NKp46 expression is not highly prevalent among NK cells, these receptors were previously detected on 40/50 and 25/50 most abundant clusters in adults, respectively.[741] Inconsistencies between mass cytometry findings could stem from the different analysis pipelines employed, the various number of clusters generated, and also the different cohort characteristics, such as age, gender, and underlying health issues, such as reproductive conditions. Mass cytometry has also revealed pNK cell phenotypic changes during pregnancy, including elevated CD38, NKp46, ILT2,

KIR2DL3, NKG2A, and NKG2C on both the $CD56^{dim}$ and $CD56^{bright}$ subsets.[236] Hence, detailed phenotyping facilitated by mass cytometry can be a useful tool in elucidating immune cell involvement in the pathogenic mechanism underlying RPL.

Similarly to when examining the total RPL and control cohorts, the cytotoxic capacity of circulating NK cells was not different between controls and the idiopathic, non-idiopathic, and ≥5 loss RPL subgroups (Figure 75). These findings indicate that the cytotoxic activity of NK cell is not influenced by either the presence of underlying RPL-associated risk factors or the number of previous losses. Accordingly, in a previous report no association between pNK cell cytotoxicity and the presence of different potential miscarriage causes could be detected.[169] Moreover, pNK cell cytotoxic activity was found not to be significantly altered between patients with different numbers of spontaneous miscarriages in their reproductive history.[169]

NK cell cytotoxicity was not altered between the age- and ethnicity-related subgroups of women with RPL and controls (Figures 76, 77). However, in contrast to the comparison between the total RPL and control populations (Figure 59H), no significant difference in the degranulation capacity of NK cells could be detected between RPL and control subpopulations controlled for ethnicity and alcohol intake (Figures 78A, 79A). Variation in those factors could thus impact the difference in NK degranulation observed between women with RPL and controls. Alterations in cytolytic molecule secretion by PBMCs detected in RPL did not appear affected by ethnic variation (Figures 78B-78E), but granzyme A secretion by unstimulated PBMCs appeared to be influenced by alcohol intake (Figure 79B). Furthermore, changes in the activation state of $CD56^{bright}CD16^{-}$ NK cells, could have been influenced by ethnic differences between the RPL and control groups as no

significant alteration could be detected between the White subgroups (Figure 80C). Differences in $CD56^{dim}CD16^{+}$ and $CD56^{bright}CD16^{-}$ NK cell activation could also be affected by variation in alcohol intake, with no changes detected between the low-alcohol subgroups (Figures 81B, 81C). Similarly, the significant difference in CD215 expression intensity on total and $CD56^{dim}CD16^{+}$ NK cells could be influenced by variation in alcohol intake, but not ethnicity, according to the subpopulation analysis (Figures 80D, 80E, 81D, 81E).

No clear prognostic capacity of peripheral NK cell cytotoxicity or cytolytic molecule secretion by PBMCs could be detected in regards to the following pregnancy outcome of women with RPL (Figure 82), in agreement to previous findings.[171, 475] It is has been however demonstrated that women with RPL in whom the pre-conception pNK cell activity is elevated acquire an increased risk for subsequent miscarriage, particularly in pregnancies with a karyotypically normal fetus.[161, 168, 170, 742] Interestingly, in another study an elevated miscarriage rate was detected in women with RPL in who low pNK cell activity was detected,[25] highlighting the need for further research using standardized methods. Additionally, eNK cell activity was not significantly altered in women with RPL and a following miscarriage, compared to those with a subsequent live birth,[175] while $CD57^{+}$ and $CD69^{+}$ endometrial leukocyte prevalence also appeared unaltered.[167] Overall, in a 2011 systematic review no association between the pNK and uNK cell activity and subsequent pregnancy outcome of women with RPL was reported,[172] in agreement to the present findings.

In summary, pNK cell cytotoxicity appeared unaltered in women with RPL, challenging the use of such test in miscarriage clinics. Elevated NK cell

degranulation capacity was detected, possibly being counterbalanced by reduced cytolytic molecule production, as indicated by the reduced granzyme A, B, and perforin levels in PBMC cultures. Utilizing CD69 as a marker, increased levels of activated $CD56^{bright}CD16^{-}$ pNK cells were seen in women with RPL, indicating a contribution of NK cell cytokine production to RPL pathogenesis. On the other hand, the elevated $CD57^{high}$ pNK cell subset prevalence observed by mass cytometry, highlighted the presence of a mature, highly cytotoxic NK cell population in the circulation of women with RPL. The mass cytometry panel was heavily focused on the expression of activating and inhibitory receptors on NK cells, in particular HLA-specific KIR, ILT, and NKG2 receptors that are thought to orchestrate fetal-maternal immune interactions. An over-representation of subsets lacking inhibitory receptor expression was evident in women with RPL, underlining a potential defect in the regulation of anti-fetal NK cell activity. Importantly, an increase in $CXCR3^{-}CXCR4^{-}$ pNK cell subsets was detected in women with RPL, highlighting a possible dysregulation in the uterine migration of these cells and thus in the inflammatory processes medicating decidualization and placentation.

8.2.1 Limitations and future research

The aim of this study was to evaluate assays used for the diagnosis of “immunological” RPL and further examine the role of immune cells, and particularly NK cells in this condition. While the cytotoxicity assay employed is commonly used to evaluate the killing activity of NK cells, extensive optimization was required and in a lot of cases no specific target cell death was detected. Apart from K562 cells, different targets could be utilised, including trophoblast cells, to obtain a more accurate representation of pNK cell-mediated cytotoxic events during early

pregnancy. Moreover, due to the limited cell number available, perforin and granzyme secretion was evaluated using total PBMC cultures. Separate examination of the secretion of these molecules by NK cells is required to fully understand the role of NK cells in RPL.

Due to the high blood volume required for the cytotoxicity assay, samples investigated did not represent the entirety of the RPL and control cohorts recruited. The number of samples assessed by flow cytometry to examine NK cell activation and cytokine receptor expression was also limited by lack of an adequate blood amount and in some cases by increased levels of cell death (>40%).

Through our mass cytometry panel we were able to generate a detailed map of pNK cell phenotypes in women with RPL. This technique allows the simultaneous assessment of a large number of molecules. However, due to the lack of antibodies binding to individual receptors, certain markers, mostly KIRs but also ILT2/LIR6, were examined together. Additionally, due to the limited number of metals, some markers with similar activity, such as TIGIT and Tim-3, ILT3, ILT4, and ILT5, and CXCR3 and CXCR4, were assigned to the same metal and were examined together. Thus, the present panel could help guide a more focused examination of different NK cell receptor subsets in the peripheral blood, but also in the uterus of women with RPL.

In conclusion, certain aspects of NK cell activity did appear dysregulated in women with RPL, although not displaying a clear pro- or anti-inflammatory pattern. Hence, upon further evaluation NK cell assays may provide a useful research tool. However, currently no obvious NK cell activity-associated biomarker for RPL has been

identified and thus the introduction of such tests into routine clinical practice is not recommended.

9 CYTOKINE ANALYSIS

9.1 Results

9.1.1 Flow cytometry assay – T_H cell cytokine production

Peripheral T_H cell cytokine production is often assessed in non-pregnant women with RPL as a measure of pro- and anti-inflammatory immune activity. Hence, IL-2, IFN-γ, TNF-α, IL-10, and IL-17A production by these cells was measured by flow cytometry (Controls *N*=76, RPL *N*=84). In the absence of exogenous stimulation, IL-2^+ [Controls: 0.02%, 95% CI (0.01%, 0.03%), RPL: 0.02%, 95% CI (0.01%, 0.02%)], IFN-γ^+ [Controls: 0.32%, 95% CI (0.20%, 0.61%), RPL: 0.36%, 95% CI (0.14%, 0.50%)], and IL-$17A^+$ [Controls: 0.18%, 95% CI (0.11%, 0.29%), RPL: 0.11%, 95% CI (0.07%, 0.20%)] T_H cell prevalence and IL-2 [Controls: 2554.00, 95% CI (2076.00, 3448.00), RPL: 2544.00, 95% CI (1976.00, 3095.00)], IFN-γ [Controls: 1161.00, 95% CI (895.00, 1400.00), RPL: 1409.00, 95% CI (1232.00, 1576.00)], and IL-17A [Controls: 313.00, 95% CI (286.00, 367.00), RPL: 368.50, 95% CI (322.00, 394.00)] expression levels, represented by the MFI, were not found to be significantly different between the RPL and control groups (Figures 83A, 83B, 83E, 84A, 84B, 84E). Baseline prevalence of TNF-α^+ cells in the T_H cell population appeared decreased in participants with RPL [Controls: 13.40%, 95% CI (9.52%, 16.40%), RPL: 3.56%, 95% CI (1.91%, 5.76%), $p<0.0001$], while the intensity of TNF-α expression on these cells was augmented [Controls: 248.00, 95% CI (229.00, 266.00), RPL: 491.50, 95% CI (394.00, 642.00), $p<0.0001$] (Figures 83C, 84C). Similarly, IL-10^+ T_H cell prevalence was reduced in women with RPL [Controls: 0.82%, 95% CI (0.24%, 1.89%), RPL: 0.01%, 95% CI (0.00%, 0.04%), $p<0.0001$], but the expression levels of this cytokine on unstimulated T_H cells appeared

unaltered [Controls: 828.00, 95% CI (665.00, 950.00), RPL: 832.50, 95% CI (531.00, 1297.00)] (Figures 83D, 84D).

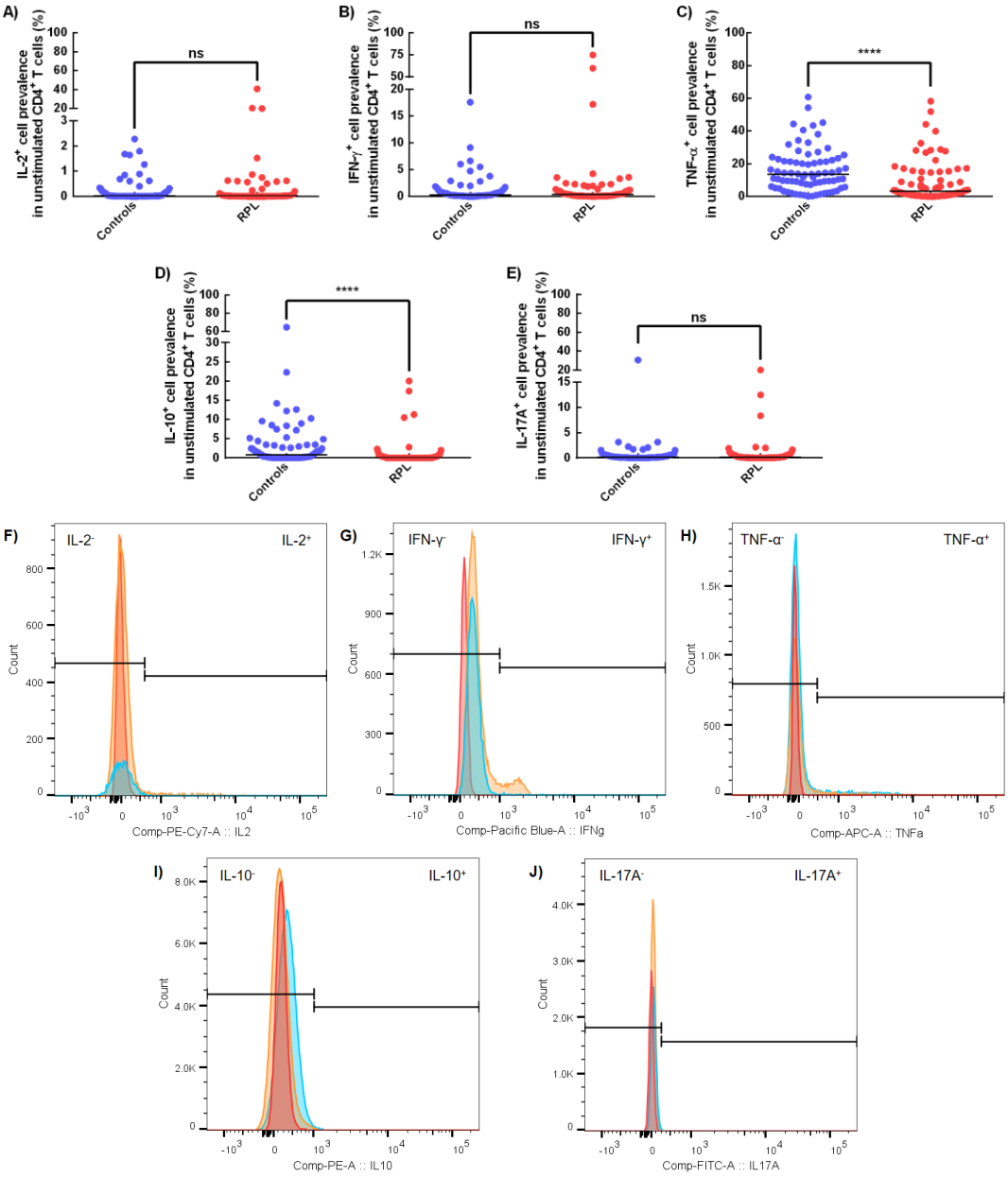


Figure 83. Cytokine-expressing cell prevalence in the unstimulated T helper (T_H) cell population of women with recurrent pregnancy loss (RPL) and controls. *The prevalence of A) interleukin (IL)-2$^+$, B) interferon (IFN)-γ$^+$, C) tumor necrosis factor (TNF)-α$^+$, D) IL-10$^+$, and E) IL-17A$^+$ cells in the CD4$^+$ T_H cell population of healthy controls (N=76) and women with RPL (N=82) is illustrated. Due to low T_H cell number (<10), N=2 RPL samples were excluded. Example gating used to identify F) IL-2$^+$, G) IFN-γ$^+$, H) TNF-α$^+$, I) IL-10$^+$, and J) IL-17A$^+$ T_H cells using two samples (orange, blue) and a control negative for the marker of interest (red) is included. Mann-Whitney test used, median illustrated. ns: non-significant, ****: p≤0.0001*

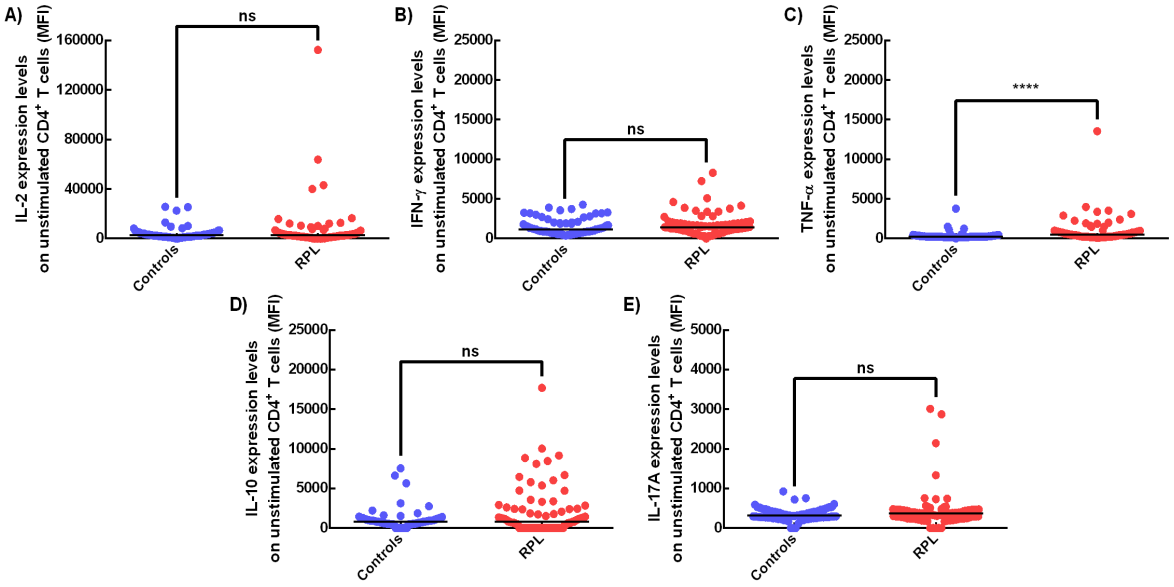


Figure 84. Cytokine expression intensity on unstimulated T helper (T_H) cells of women with recurrent pregnancy loss (RPL) and controls. *The intensity of A) interleukin (IL)-2, B) interferon (IFN)-γ, C) tumor necrosis factor (TNF)-α, D) IL-10, and E) IL-17A expression on individual CD4⁺ T_H cells, represented by the median fluorescence intensity (MFI), of healthy controls (N=76) and women with RPL (N=82) is depicted. Due to low T_H cell number (<10), N=2 RPL samples were excluded. Mann-Whitney test used, median illustrated. ns: non-significant, ****: p≤0.0001*

The effect of PMA- and ionomycin-mediated stimulation on T_H cell cytokine production in the RPL and control cohorts, as well as the total population recruited was examined. Stimulation was found to greatly promote production of all cytokines of interest by T_H cells in both women with RPL and controls (Figures 85, 86), without inducing increased cell death (Supplementary Figure 23). Similar to the unstimulated state, the levels of IFN-γ⁺ stimulated T_H cells [Controls: 9.37%, 95% CI (6.75%, 12.60%), RPL: 6.73, 95% CI (5.95%, 9.97%)] and the expression intensity of this cytokine [Controls: 2078.00, 95% CI (1674.00, 3064.00), RPL: 2637.00, 95% CI (1877.00, 3420.00)] were not found to be significantly different between participants with and without RPL (Figures 87B, 88B). IL-2⁺ [Controls:

19.25%, 95% CI (13.80%, 25.60%), RPL: 12.45%, 95% CI (8.49%, 17.90%), p=0.0084] and TNF-α^+ [Controls: 50.87% (20.40), RPL: 33.44% (21.17), p<0.0001] cell prevalence was however found to be reduced in the RPL group (Figures 87A, 87C). Although IL-2 expression levels were also decreased in RPL [Controls: 6169.00, 95% CI (5082.00, 8543.00), RPL: 5109.00, 95% CI (4352.00, 5862.00), p=0.0121], TNF-α levels appeared increased [Controls: 562.50, 95% CI (434.00, 720.00), RPL: 896.50, 95% CI (694.00, 1237.00), p=0.0016] (Figures 88A, 88C). The percentage of IL-10-expressing T_H cells was lower in RPL cases [Controls: 6.70%, 95% CI (3.57%, 11.90%), RPL: 0.43%, 95% CI (0.24%, 0.80%), p<0.0001] but IL-10 expression levels on these cells were augmented [Controls: 1073.00, 95% CI (868.00, 1371.00), RPL: 3466.00, 95% CI (2144.00, 4801.00), p<0.0001] (Figures 87D, 88D). IL-17A was also found to be expressed in a lower percentage of T_H cells in women with RPL [Controls: 0.67%, 95% CI (0.51%, 0.88%), RPL: 0.46%, 95% CI (0.37%, 0.59%), p=0.0362], with the expression levels of this cytokine appearing unaltered [Controls: 416.00, 95% CI (329.00, 593.00), RPL: 433.00, 95% CI (362.00, 493.00)] (Figures 87E, 88E).

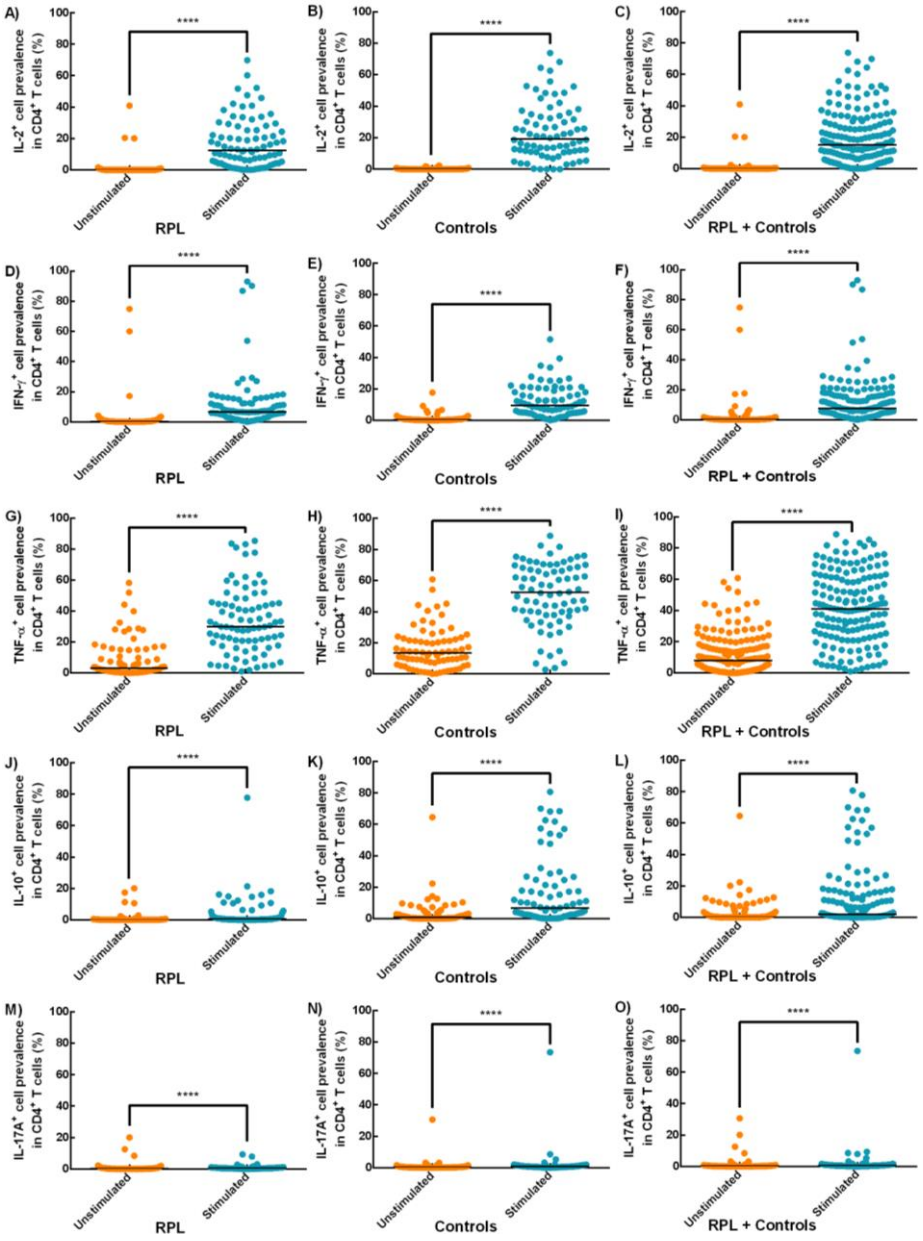


Figure 85. Cytokine-expressing cell prevalence in the unstimulated and the stimulated T helper (T_H) cell population of women with recurrent pregnancy loss (RPL), controls, and total participants. *The prevalence of A-C) interleukin (IL)-2$^+$, D-F) interferon (IFN)-γ$^+$, G-I) tumor necrosis factor (TNF)-α$^+$, J-L) IL-10$^+$, and M-O) IL-17A$^+$ cells in the CD4$^+$ T_H cell population of women with RPL (N=82) (A, D, G, J, M), controls (N=76) (B, E, H, K, N), and total participants (N=158) (C, F, I, L, O) in the absence and following stimulation with phorbol 12-myristate 13-acetate and ionomycin is depicted. Due to low T_H cell number (<10), N=2 RPL samples were excluded. Wilcoxon matched-pairs signed rank test used, median illustrated. ****: p≤0.0001*

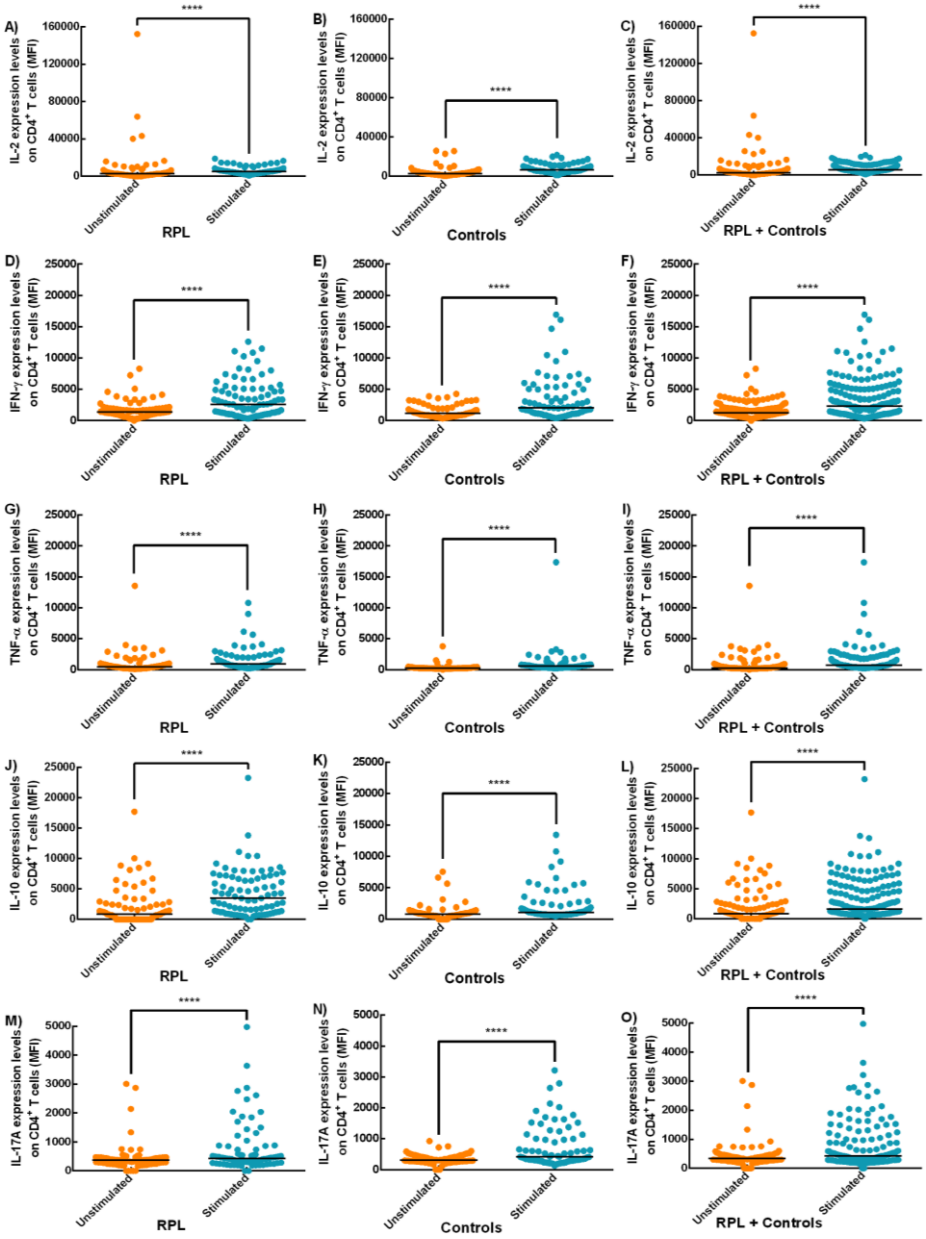


Figure 86. Cytokine expression intensity on unstimulated and stimulated T helper (T_H) cells of women with recurrent pregnancy loss (RPL), controls, and total participants. *The intensity of A-C) interleukin (IL)-2, D-F) interferon (IFN)-γ, G-I) tumor necrosis factor (TNF)-α, J-L) IL-10, and M-O) IL-17A expression, represented by the median fluorescence intensity (MFI), on individual $CD4^+$ T_H cells of women with RPL (N=82) (A, D, G, J, M), controls (N=76) (B, E, H, K, N), and total participants (N=158) (C, F, I, L, O) in the absence and following stimulation with phorbol 12-myristate 13-acetate and ionomycin is shown. Due to low T_H cell number (<10), N=2 RPL samples were excluded. Wilcoxon matched-pairs signed rank test used, median included. ****: p≤0.0001*

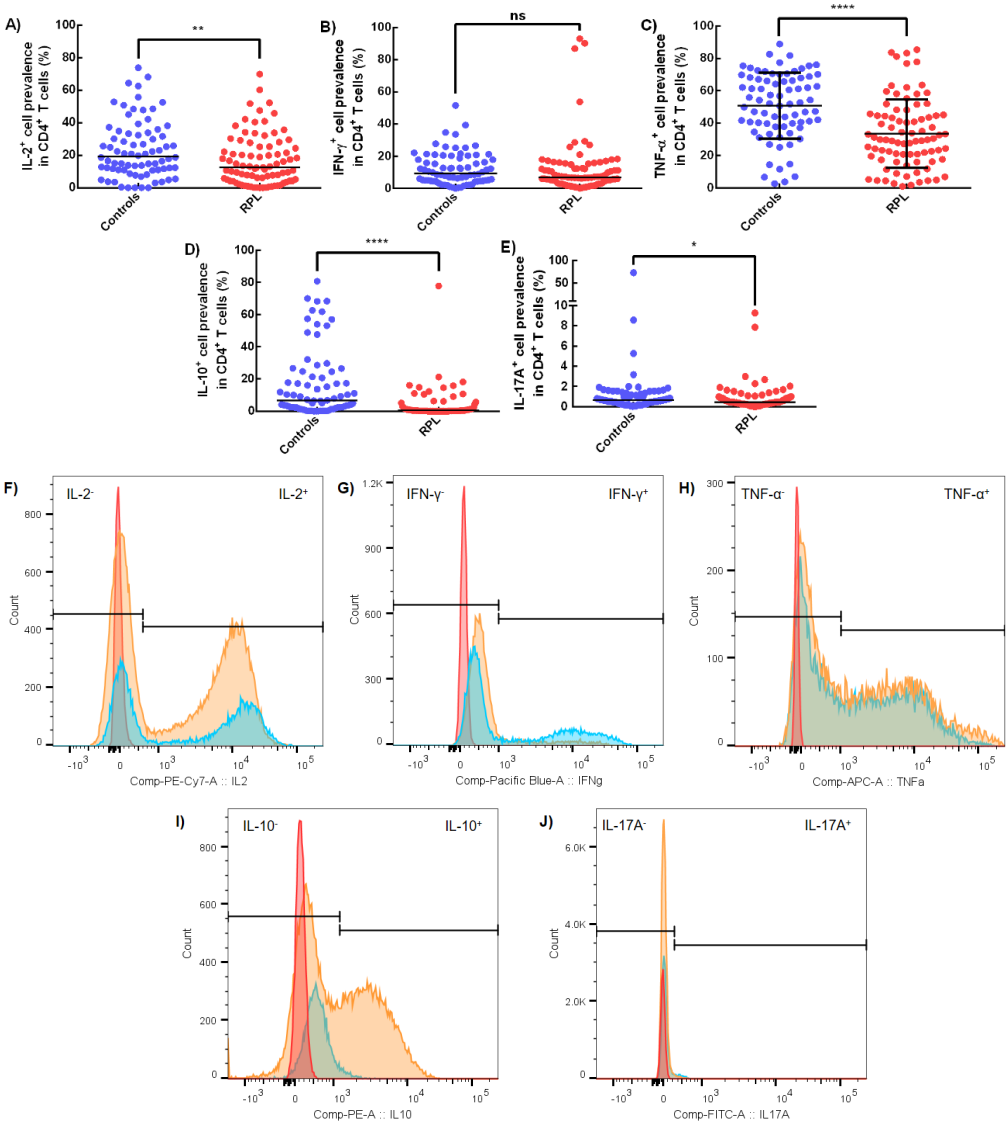


Figure 87. Cytokine-expressing cell prevalence in the stimulated T helper (T_H) cell population of women with recurrent pregnancy loss (RPL) and controls. *The prevalence of A) interleukin (IL)-2$^+$, B) interferon (IFN)-γ$^+$, C) tumor necrosis factor (TNF)-α$^+$, D) IL-10$^+$, and E) IL-17A$^+$ cells in the CD4$^+$ T_H cell population, following stimulation with phorbol 12-myristate 13-acetate and ionomycin, of healthy controls (N=76) and women with RPL (N=84) is displayed. Example gating used to identify F) IL-2$^+$, G) IFN-γ$^+$, H) TNF-α$^+$, I) IL-10$^+$, and J) IL-17A$^+$ T_H cells using two samples (orange, blue) and a control negative for the marker of interest (red) is included. Normally distributed datasets (C): Unpaired t test performed, mean and standard deviation depicted. Non-normally distributed datasets (A, B, D, E): Mann-Whitney test used, median illustrated. ns: non-significant, *: p≤0.05, **: p≤0.01, ****: p≤0.0001*

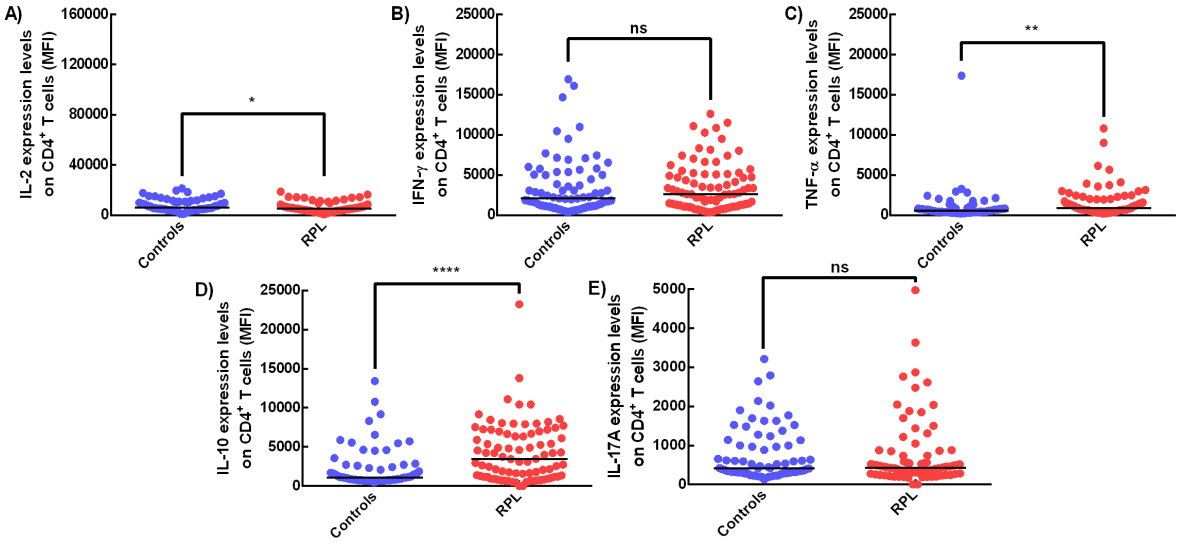


Figure 88. Cytokine expression intensity on stimulated T helper (T_H) cells of women with recurrent pregnancy loss (RPL) and controls. *The intensity of A) interleukin (IL)-2, B) interferon (IFN)-γ, C) tumor necrosis factor (TNF)-α, D) IL-10, and E) IL-17A expression on individual $CD4^+$ T_H cells, represented by the median fluorescence intensity (MFI), following stimulation with phorbol 12-myristate 13-acetate and ionomycin, of healthy controls (N=76) and women with RPL (N=84) is shown. Mann-Whitney test performed, median included. ns: non-significant, *: p≤0.05, **: p≤0.01, ****: p≤0.0001*

Instead of the absolute cytokine levels, the ratios between pro- and anti-inflammatory cytokine production following T_H cell stimulation are often examined in RPL clinics. The ratios of pro-inflammatory IL-2-, IFN-γ-, TNF-α-, or IL-17A-expressing T_H cells to anti-inflammatory $IL\text{-}10^+$ T_H cell prevalence were all increased in RPL ($p<0.0001$) (Figures 89A-89D), while the respective expression level ratios were found to be reduced (IL-2/IL-10: $p<0.0001$, IFN-γ/IL-10: $p<0.0001$, TNF-α/IL-10: $p=0.0136$, IL-17A/IL-10: $p<0.0001$) (Figures 90A-90D). The T_H1- to T_H17-associated cytokine production ratios were also assessed. The prevalence of $IL\text{-}2^+/IL\text{-}17A^+$ and $IFN\text{-}\gamma^+/IL\text{-}17A^+$ T_H cells was not found to be significantly different between women with RPL and controls, while the $TNF\text{-}\alpha^+/IL\text{-}17A^+$ T_H cell ratio was

decreased in the RPL group (p=0.0434) (Figures 89E-89G). Regarding cytokine expression levels on T_H cells, the IL-2/IL-17A ratio was reduced (p=0.0087), the IFN-γ/IL-17A ratio was unaltered, and the TNF-α/IL-17A ratio was elevated (p=0.0031) in participants with RPL (Figures 90E-90G).

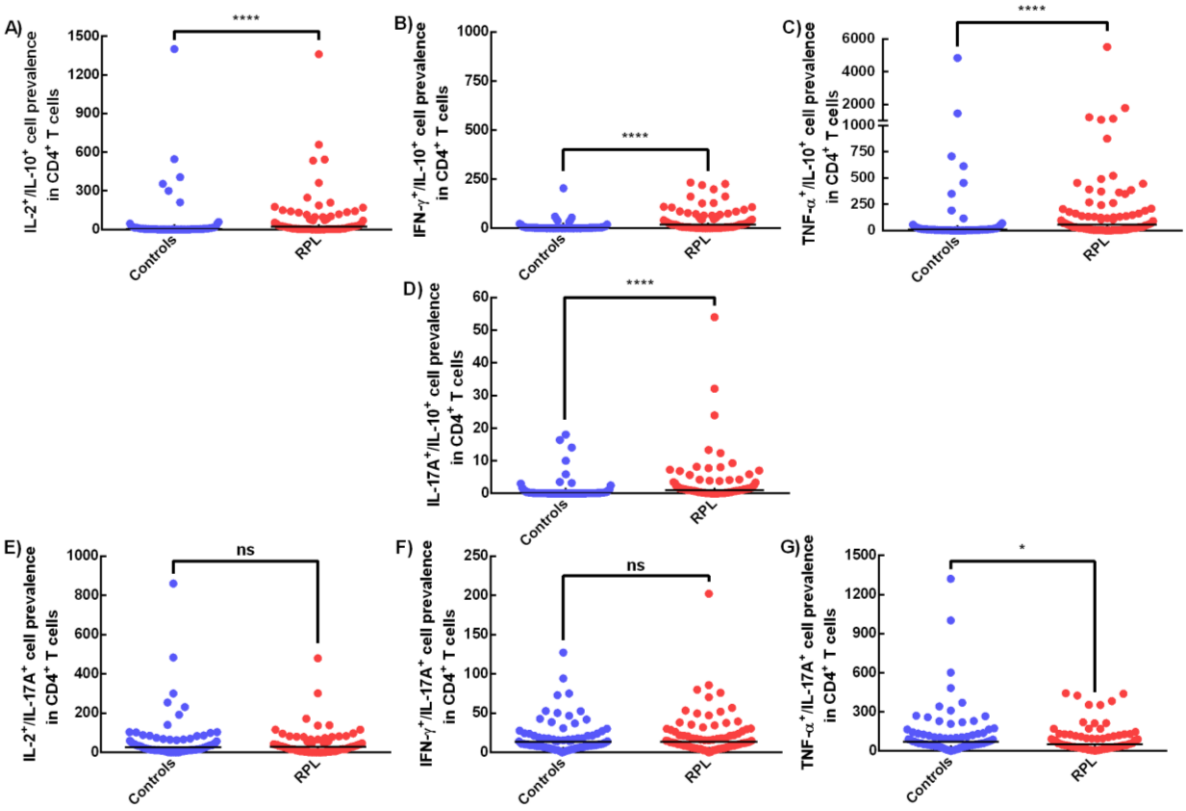


Figure 89. Cytokine-expressing cell prevalence ratios in the stimulated T helper (T_H) cell population of women with recurrent pregnancy loss (RPL) and controls. *The prevalence ratios of A) interleukin (IL)-2$^+$/IL-10$^+$, B) interferon (IFN)-γ$^+$/IL-10$^+$, C) tumor necrosis factor (TNF)-α$^+$/IL-10$^+$, D) IL-17A$^+$/IL-10$^+$, E) IL-2$^+$/IL-17A$^+$, F) IFN-γ$^+$/IL-17A$^+$, and G) TNF-α$^+$/IL-17A$^+$ cells in the CD4$^+$ T_H cell population, following stimulation with phorbol 12-myristate 13-acetate and ionomycin, of healthy controls (N=76) and women with RPL (N=82) are illustrated. Mann-Whitney test performed, median depicted. ns: non-significant, *: p≤0.05, ****: p≤0.0001*

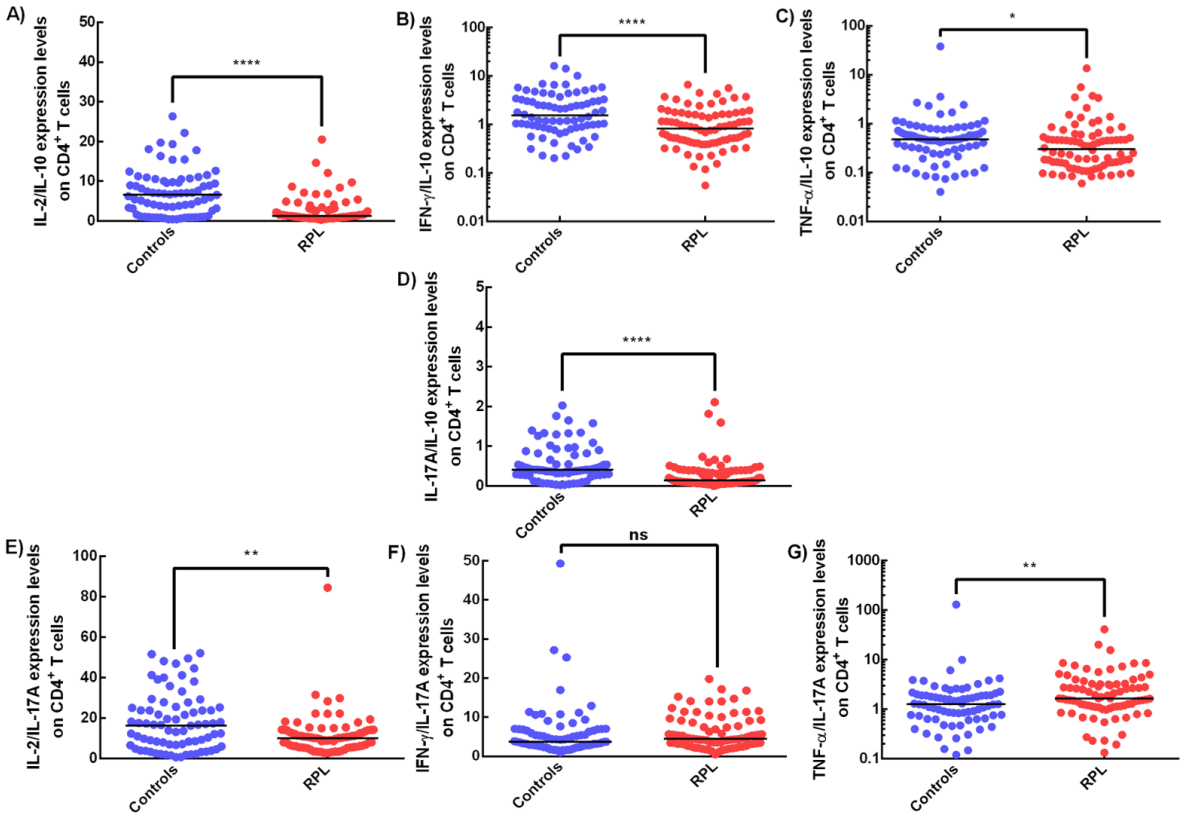


Figure 90. Cytokine expression intensity ratios on stimulated T helper (T_H) cells of women with recurrent pregnancy loss (RPL) and controls. *The intensity ratios of A) interleukin (IL)-2/IL-10, B) interferon (IFN)-γ/IL-10, C) tumor necrosis factor (TNF)-α/IL-10, D) IL-17A/IL-10, E) IL-2/IL-17A, F) IFN-γ/IL-17A, and G) TNF-α/IL-17A expression on individual CD4⁺ T_H cells, represented by the median fluorescence intensity (MFI), following stimulation with phorbol 12-myristate 13-acetate and ionomycin, of healthy controls (N=76) and women with RPL (N=82) are displayed. Mann-Whitney test used, median included. ns: non-significant, *: p≤0.05, **: p≤0.01, ****: p≤0.0001*

9.1.2 Flow cytometry assay – NK cell cytokine production

Cytokine production by total (Controls *N*=71, RPL *N*=84) and $CD56^{dim}CD16^{+}$ (Controls *N*=22, RPL *N*=26) NK cells was also assessed to fully elucidate these cells' contribution to the peripheral immune activity of non-pregnant women with RPL. In the absence of stimulation, IFN-γ⁺ NK cell prevalence [Controls: 0.91%, 95% CI (0.61%, 1.54%), RPL: 1.29%, 95% CI (0.63%, 2.58%)] and IFN-γ expression

levels [Controls: 2529.00, 95% CI (2087.00, 3058.00), RPL: 2676.00, 95% CI (2091.00, 2946.00)] on these cells did not appear altered in women with RPL (Figures 91A, 92A). TNF-α^+ [Controls: 1.50%, 95% CI (0.43%, 2.78%), RPL: 0.11%, 95% CI (0.03%, 0.22%), p<0.0001] and IL-10^+ [Controls: 0.05%, 95% CI (0.00%, 0.23%), RPL: 0.00%, 95% CI (0.00%, 0.02%), p=0.0468] NK cell prevalence, but not TNF-α [Controls: 1121.00, 95% CI (950.00, 1270.00), RPL: 1274.00, 95% CI (892.00, 1670.00)] or IL-10 [Controls: 336.00, 95% CI (0.00, 433.00), RPL: 0.00, 95% CI (0.00, 240.00)] expression intensity were reduced in the RPL group (Figures 91B, 91C, 92B, 92C). In regards to unstimulated $CD56^{dim}CD16^+$ NK cell cytokine production, no significant alteration in IFN-γ^+ [Controls: 0.38%, 95% CI (0.00%, 10.00%), RPL: 0.25%, 95% CI (0.00%, 3.41%)] and IL-10^+ [Controls: 0.00%, 95% CI (0.00%, 0.13%), RPL: 0.00%, 95% CI (0.00%, 0.79%)] cell prevalence or IFN-γ [Controls: 2608.00, 95% CI (0.00, 4852.00), RPL: 2421.00, 95% CI (0.00, 5799.00)] and IL-10 [Controls: 0.00, 95% CI (0.00, 369.00), RPL: 0.00, 95% CI (0.00, 406.00)] expression levels could be detected in women with RPL (Figures 91D, 91F, 92D, 92F). However, both the prevalence of TNF-α^+ $CD56^{dim}CD16^+$ NK cells [Controls: 0.85%, 95% CI (0.00%, 8.72%), RPL: 0.00%, 95% CI (0.00%, 0.07%), p=0.0061] and the respective expression intensity [Controls: 1470.00, 95% CI (0.00, 3227.00), RPL: 0.00, 95% CI (0.00, 819.00), p=0.0080] were reduced in RPL compared to control cases (Figures 91E, 92E).

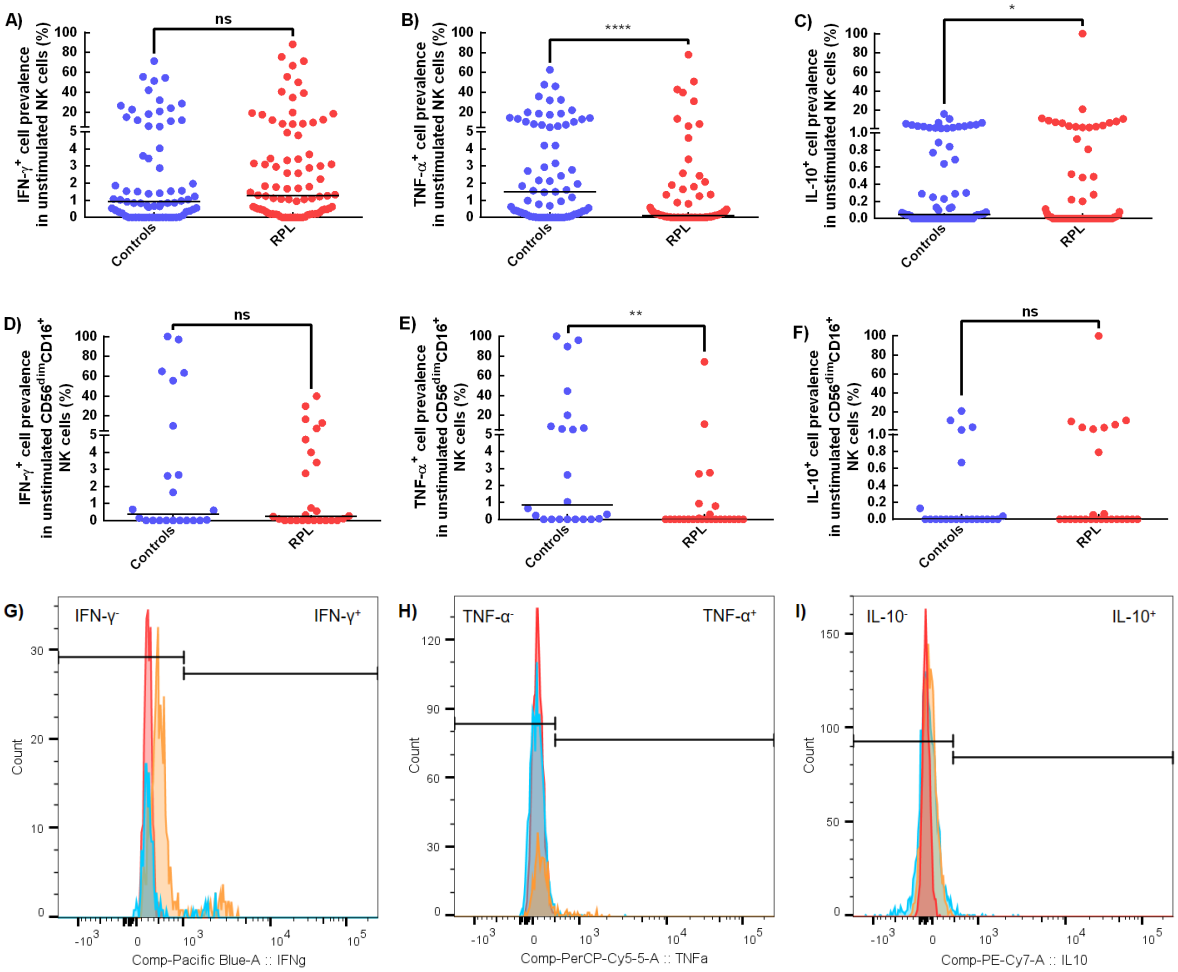


Figure 91. Cytokine-expressing cell prevalence in the unstimulated total and CD56^{dim}CD16^{+} Natural Killer (NK) cell population of women with recurrent pregnancy loss (RPL) and controls. *The prevalence of A) interferon (IFN)-γ^{+}, B) tumor necrosis factor (TNF)-α^{+}, and C) interleukin (IL)-10^{+} cells in the NK cell population, as well as the percentage of D) IFN-γ^{+}, E) TNF-α^{+}, and F) IL-10^{+} cells in the CD56^{dim}CD16^{+} NK cell subpopulation of healthy controls (total NK cells: N=71, CD56^{dim}CD16^{+} NK cells: N=22) and women with RPL (total NK cells: N=84, CD56^{dim}CD16^{+} NK cells: N=26) is shown. Example gating used to identify G) IFN-γ^{+}, H) TNF-α^{+}, and I) IL-10^{+} NK cells using two samples (orange, blue) and a control negative for the marker of interest (red) is included. Mann-Whitney test used, median depicted. ns: non-significant, *: p≤0.05, **: p≤0.01, ****: p≤0.0001*

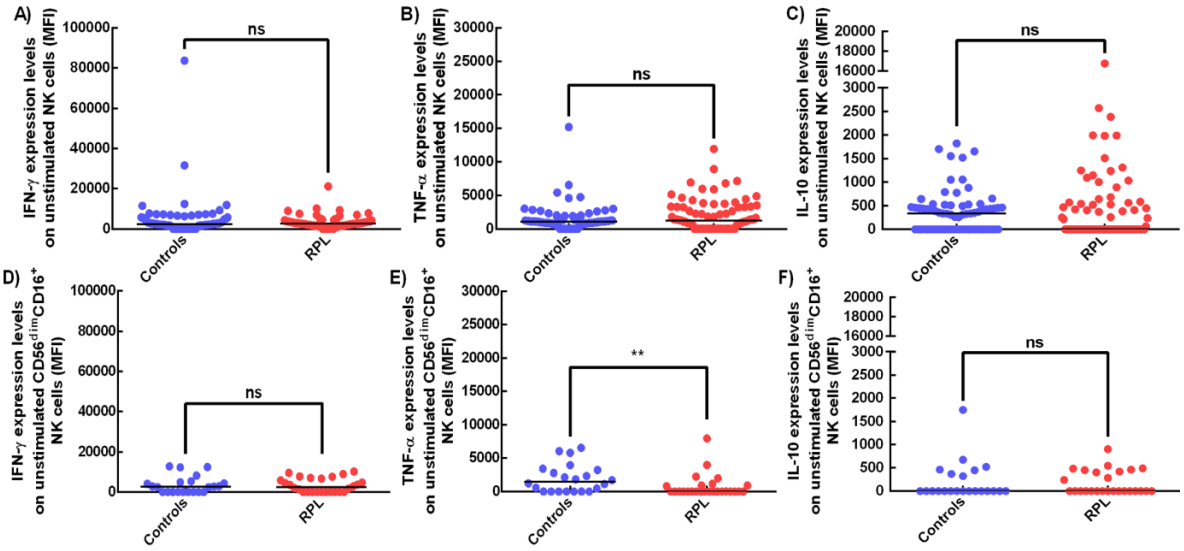


Figure 92. Cytokine expression intensity on unstimulated total and CD56^{dim}CD16^{+} Natural Killer (NK) cells of women with recurrent pregnancy loss (RPL) and controls. *The intensity of A) interferon (IFN)-γ, B) tumor necrosis factor (TNF)-α, and C) interleukin (IL)-10 expression on individual NK cells, represented by the median fluorescence intensity (MFI), as well as the intensity of A) IFN-γ, B) TNF-α, and C) IL-10 expression on the CD56^{dim}CD16^{+} NK cell subpopulation of healthy controls (total NK cells: N=71, CD56^{dim}CD16^{+} NK cells: N=22) and women with RPL (total NK cells: N=84, CD56^{dim}CD16^{+} NK cells: N=26) is displayed. Mann-Whitney test used, median illustrated. ns: non-significant, **: p≤0.01*

Following PMA- and ionomycin-mediated stimulation, IFN-γ and TNF-α production by NK cells was found to be elevated in both the RPL and control groups (Figures 93A-93F, 94A-94F). An alteration in IL-10^{+} NK cell prevalence was not seen after stimulation in either the RPL or the control groups, although a significant increase was detected when both groups were taken into consideration (Figures 93G-93I). IL-10 expression intensity on total NK cells was found to be significantly increased in control and total cases, but not participants with RPL, after stimulation (Figures 94G-94I). In regards to the CD56^{dim}CD16^{+} NK cell subset, IFN-γ^{+} cell prevalence was increased in RPL and total, but not control, cases following stimulation but the

expression levels of this cytokine were elevated in the control and total, but not RPL, cases (Figures 95A-95C, 96A-96C). Both TNF-α^+ cell prevalence and the expression intensity of this cytokine in the $CD56^{dim}CD16^+$ population were increased upon stimulation in women in RPL and in the total participant group, but not in controls (Figures 95D-95F, 96D-96F). Lastly, the prevalence of IL-10^+ $CD56^{dim}CD16^+$ NK cells did not appeared altered following stimulation, while an augmentation in the intensity of IL-10 expression on these cells was only detected in the control and total participant groups (Figures 95G-95I, 96G-96I).

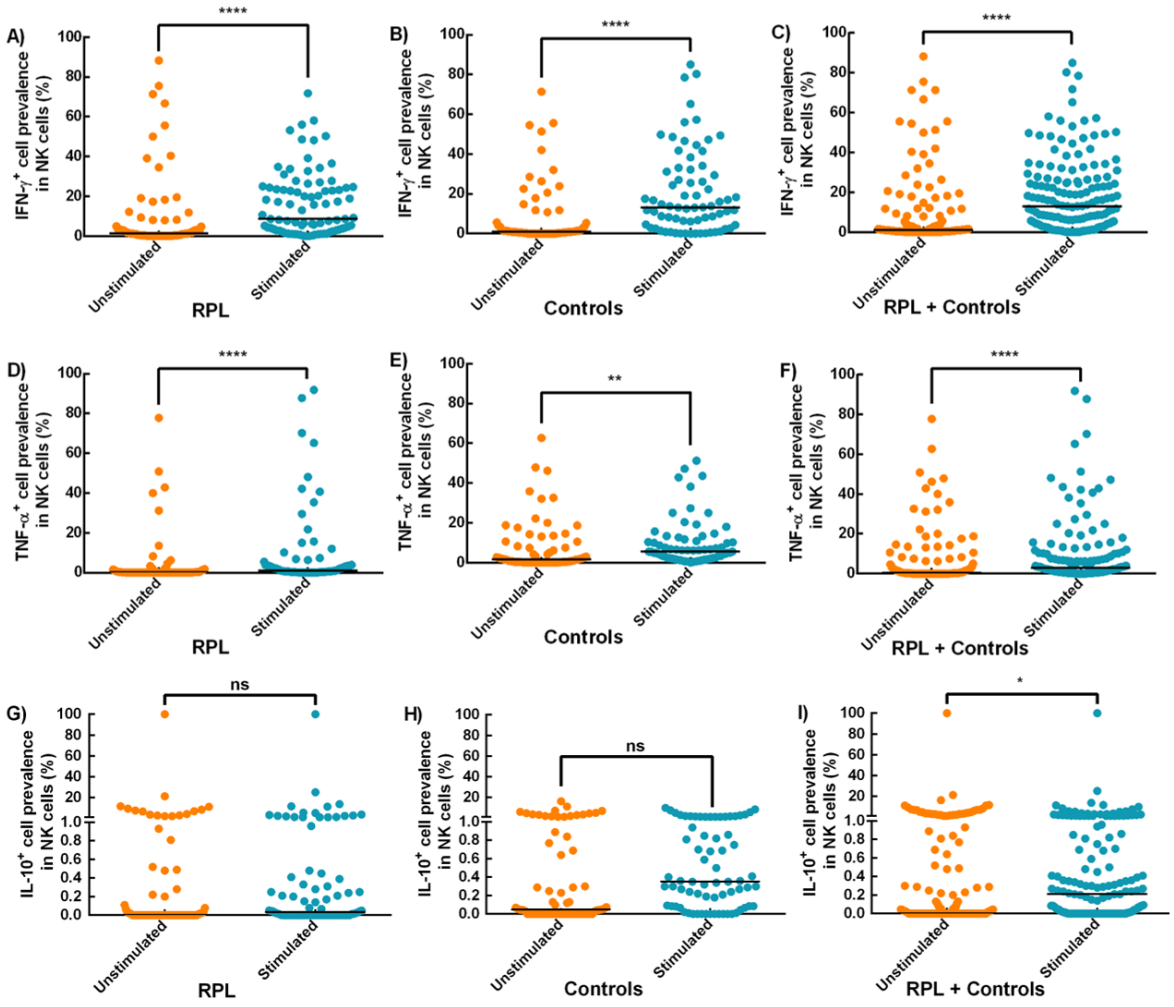


Figure 93. Cytokine-expressing cell prevalence in the unstimulated and the stimulated Natural Killer (NK) cell population of women with recurrent pregnancy loss (RPL), controls, and total participants. *The prevalence of A-C) interferon (IFN)-γ⁺, D-F) tumor necrosis factor (TNF)-α⁺, and G-I) interleukin (IL)-10⁺ cells in the NK cell population of women with RPL (N=84) (A, D, G), controls (N=71) (B, E, H), and total participants (N=155) (C, F, I) in the absence and following stimulation with phorbol 12-myristate 13-acetate and ionomycin is illustrated. Wilcoxon matched-pairs signed rank test used, median included. ns: non-significant, *: p≤0.05, **: p≤0.01, ****: p≤0.0001*

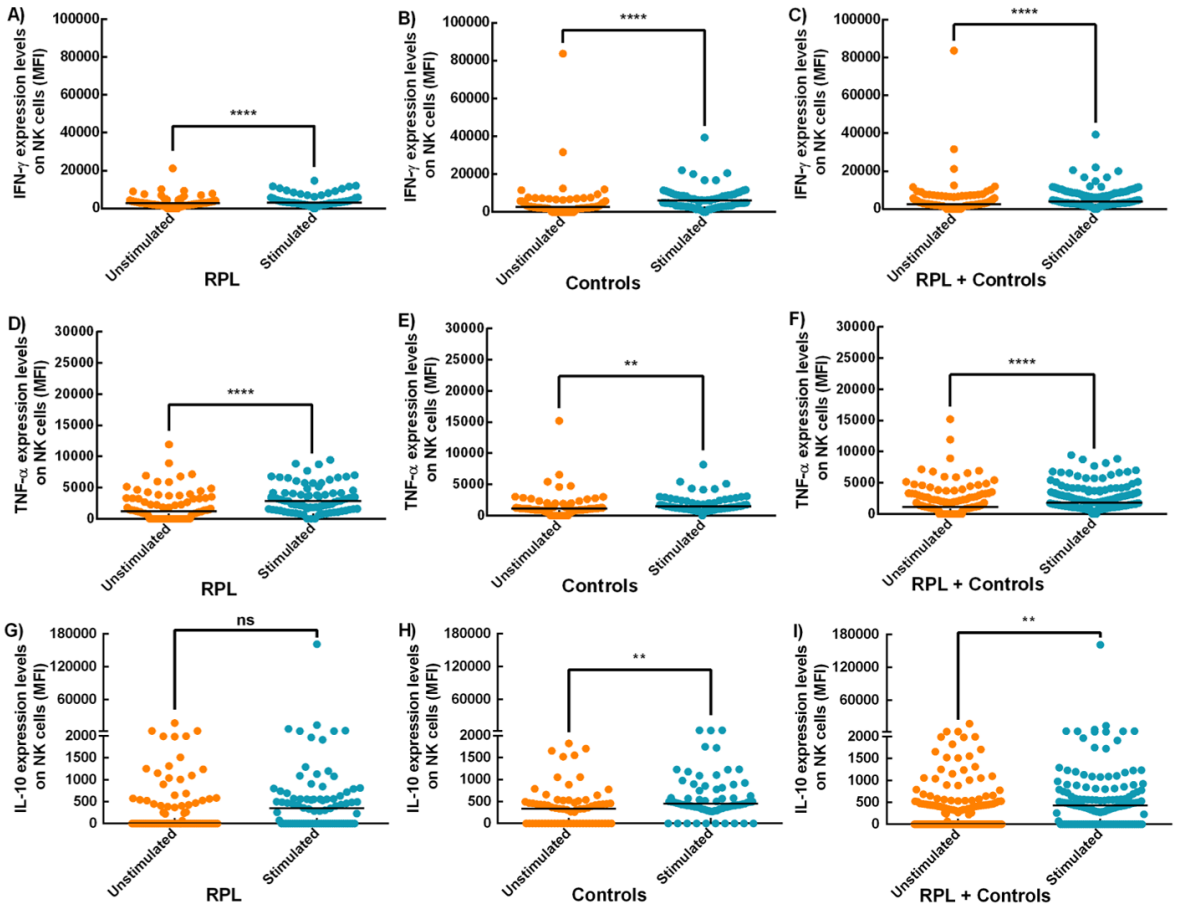


Figure 94. Cytokine expression intensity on unstimulated and stimulated Natural Killer (NK) cells of women with recurrent pregnancy loss (RPL), controls, and total participants. *The intensity of A-C) interferon (IFN)-γ, D-F) tumor necrosis factor (TNF)-α, and G-I) interleukin (IL)-10 expression, represented by the median fluorescence intensity (MFI), on individual NK cells of women with RPL (N=84) (A, D, G), controls (N=71) (B, E, H), and total participants (N=155) (C, F, I) in the absence and following stimulation with phorbol 12-myristate 13-acetate and ionomycin is shown. Wilcoxon matched-pairs signed rank test performed, median depicted. ns: non-significant, **: p≤0.01, ****: p≤0.0001*

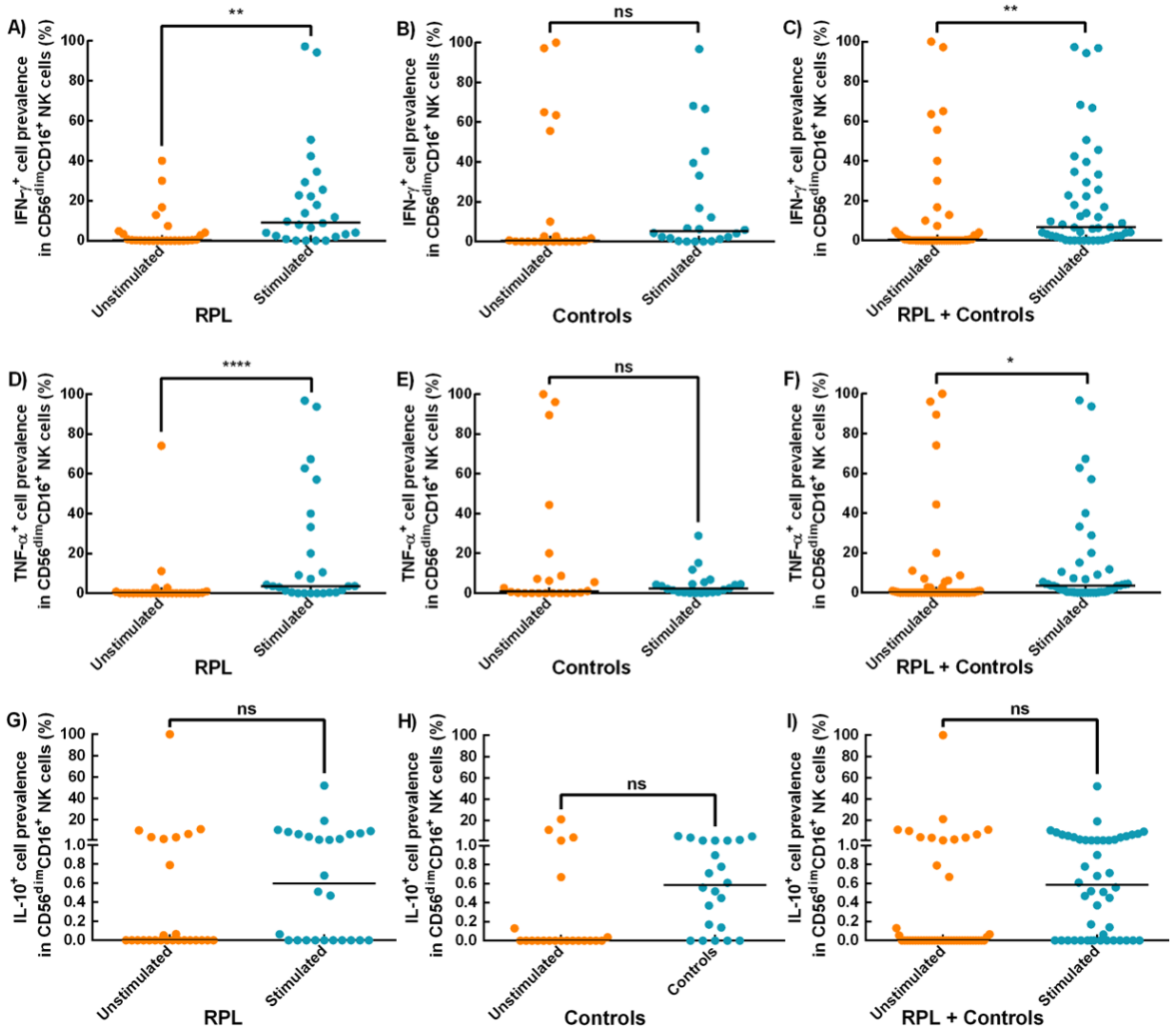


Figure 95. Cytokine-expressing cell prevalence in the unstimulated and the stimulated CD56^{dim}CD16^{+} Natural Killer (NK) cell population of women with recurrent pregnancy loss (RPL), controls, and total participants. *The prevalence of A-C) interferon (IFN)-γ^{+}, D-F) tumor necrosis factor (TNF)-α^{+}, and G-I) interleukin (IL)-10^{+} cells in the CD56^{dim}CD16^{+} NK cell population of women with RPL (N=26) (A, D, G), controls (N=22) (B, E, H), and total participants (N=48) (C, F, I) in the absence and following stimulation with phorbol 12-myristate 13-acetate and ionomycin is displayed. Wilcoxon matched-pairs signed rank test used, median shown. ns: non-significant, *: p≤0.05, **: p≤0.01, ****: p≤0.0001*

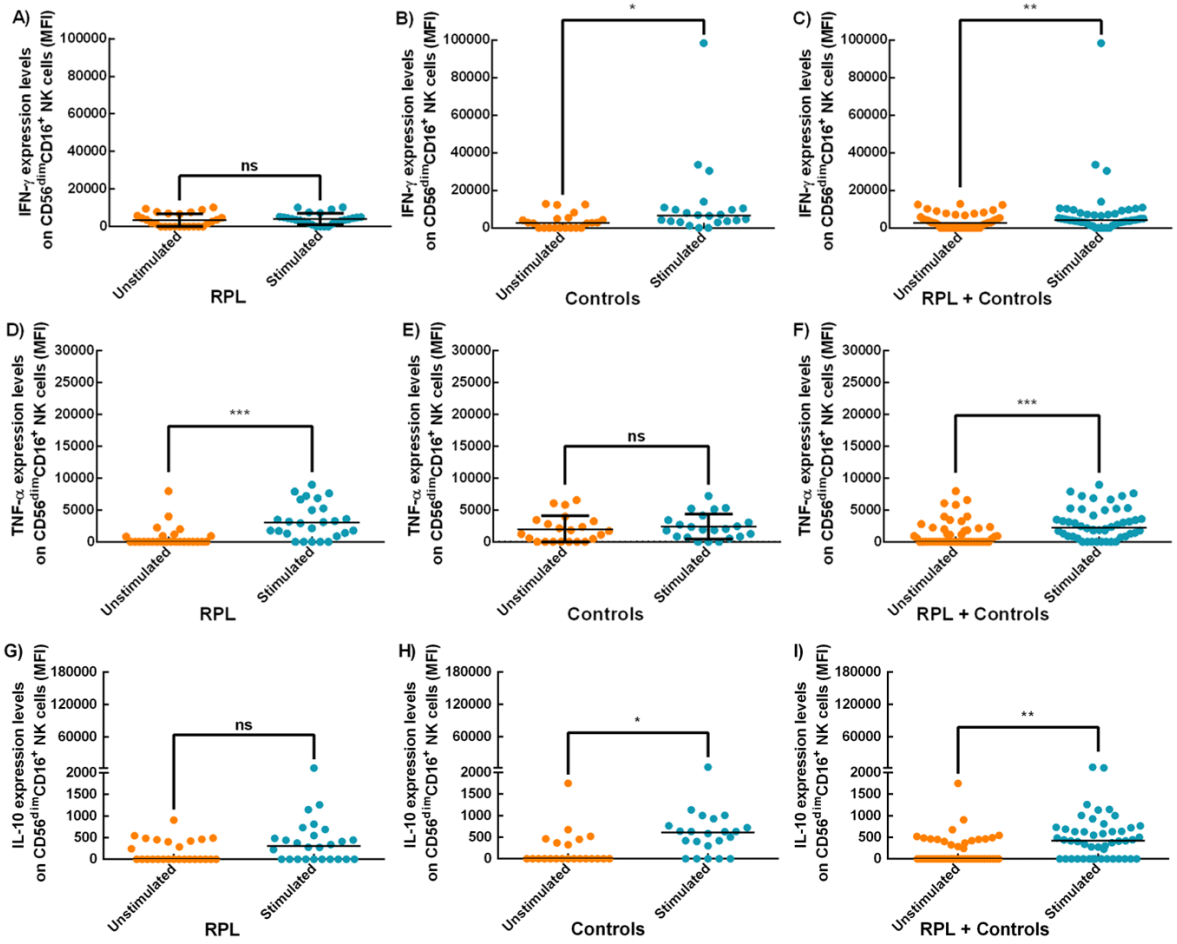


Figure 96. Cytokine expression intensity on unstimulated and stimulated CD56^{dim}CD16^{+} Natural Killer (NK) cells of women with recurrent pregnancy loss (RPL), controls, and total participants. *The intensity of A-C) interferon (IFN)-γ, D-F) tumor necrosis factor (TNF)-α, and G-I) interleukin (IL)-10 expression, represented by the median fluorescence intensity (MFI), on individual CD56^{dim}CD16^{+} NK cells of women with RPL (N=26) (A, D, G), controls (N=22) (B, E, H), and total participants (N=48) (C, F, I) in the absence and following stimulation with phorbol 12-myristate 13-acetate and ionomycin is depicted. Normally distributed datasets (A, D): Paired t test used, mean and standard deviation illustrated. Non-normally distributed datasets (B-D, F-I): Wilcoxon matched-pairs signed rank test performed, median shown. ns: non-significant, *: p≤0.05, **: p≤0.01, ***: p≤0.001*

Furthermore, NK cell cytokine production upon stimulation was compared between women with RPL and controls. The percentage of TNF-α^+ [Controls: 5.56%, 95% CI (3.96%, 6.80%), RPL: 1.11%, 95% CI (0.65%, 2.33%), p<0.0001] and IL-10^+ [Controls: 0.35%, 95% CI (0.24%, 0.69%), RPL: 0.04%, 95% CI (0.00%, 0.17%), p=0.0006], but not IFN-γ^+ [Controls: 13.30%, 95% CI (8.76%, 19.10%), RPL: 8.91%, 95% CI (6.09%, 18.90%)] cells was reduced in women with RPL (Figures 97A-97C). The expression levels of IFN-γ [Controls: 5976.00, 95% CI (4509.00, 7205.00), RPL: 3205.00, 95% CI (2928.00, 3777.00), p=0.0002] and IL-10 [Controls: 453.00, 95% CI (406.00, 504.00), RPL: 352.50, 95% CI (0.00, 497.00), p=0.0452] were decreased in women with this condition but the levels of TNF-α [Controls: 1445.00, 95% CI (1232.00, 1735.00), RPL: 2832.00, 95% CI (2132.00, 3345.00), p<0.0001] were elevated (Figures 98A-98C). Regarding the $CD56^{dim}CD16^+$ subpopulation, a reduction was detected in IFN-γ expression levels [Controls: 6627.00, 95% CI (3597.00, 10483.00), RPL: 3754.00, 95% CI (2391.00, 4965.00), p=0.0283] but not prevalence of IFN-γ^+ cells [Controls: 5.09%, 95% CI (1.25%, 33.20%), RPL: 9.23%, 95% CI (3.23%, 22.70%)] in women with RPL, while the TNF-α [Controls: 2398.00 (1981.00), RPL: 3311.00 (2787.00)] and IL-10 [Controls: 607.50, 95% CI (301.00, 765.00), RPL: 309.50, 95% CI (0.00, 483.00)] expression levels and the prevalence of TNF-α^+ [Controls: 2.28%, 95% CI (0.44%, 4.55%), RPL: 3.61%, 95% CI (0.46%, 20.00%)] and IL-10^+ [Controls: 0.59%, 95% CI (0.14%, 1.06%), RPL: 0.60%, 95% CI (0.00%, 6.45%)] $CD56^{dim}CD16^+$ NK cells appeared unaltered (Figures 97D-97F, 98D-98F).

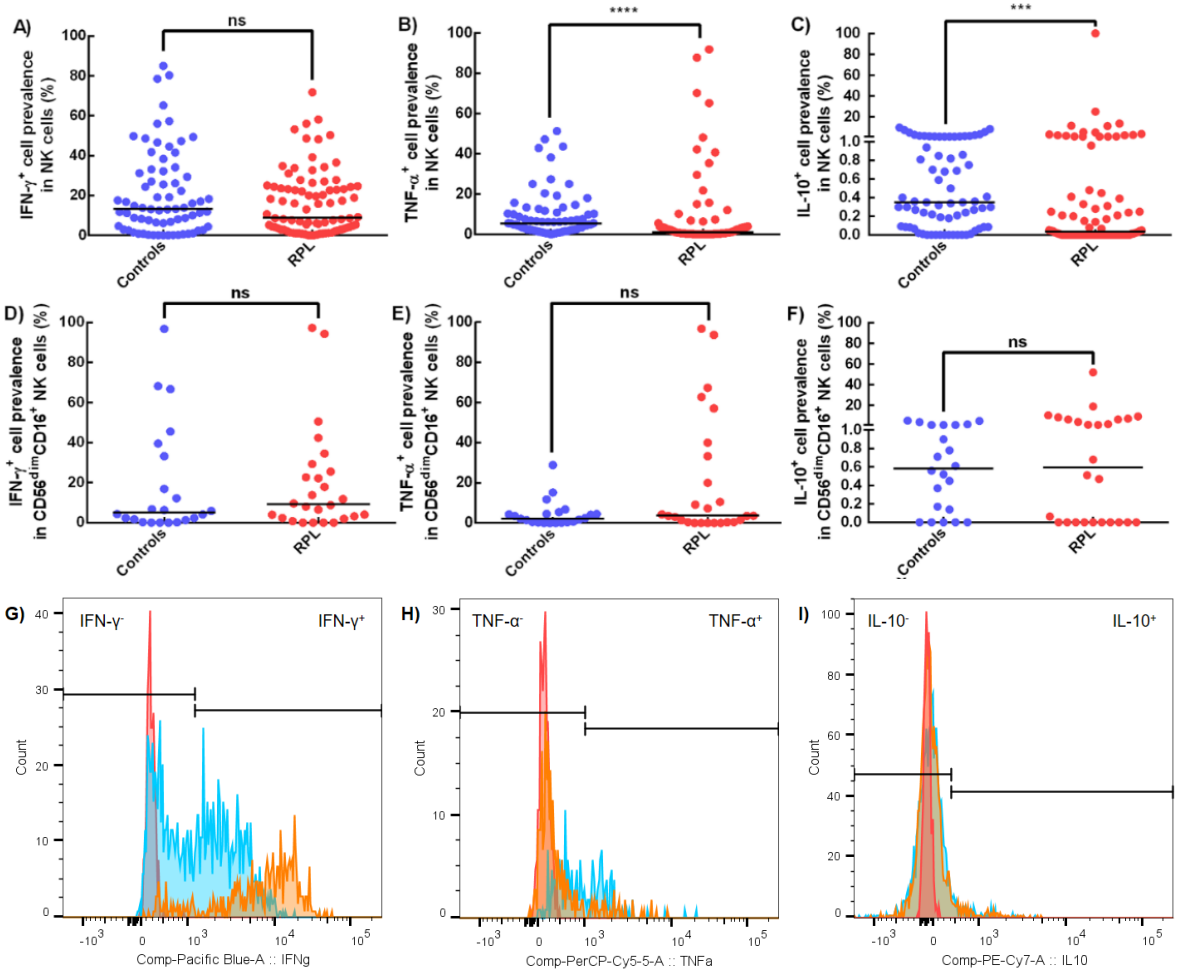


Figure 97. Cytokine-expressing cell prevalence in the stimulated total and CD56^{dim}CD16^{+} Natural Killer (NK) cell population of women with recurrent pregnancy loss (RPL) and controls. *The prevalence of A) interferon (IFN)-γ^{+}, B) tumor necrosis factor (TNF)-α^{+}, and C) interleukin (IL)-10^{+} cells in the NK cell population, as well as the percentage of D) IFN-γ^{+}, E) TNF-α^{+}, and F) IL-10^{+} cells in the CD56^{dim}CD16^{+} NK cell subpopulation, following stimulation with phorbol 12-myristate 13-acetate and ionomycin, of healthy controls (total NK cells: N=71, CD56^{dim}CD16^{+} NK cells: N=22) and women with RPL (total NK cells: N=84, CD56^{dim}CD16^{+} NK cells: N=26) is illustrated. Example gating used to identify G) IFN-γ^{+}, H) TNF-α^{+}, and I) IL-10^{+} NK cells using two samples (orange, blue) and a control negative for the marker of interest (red) is included. Mann-Whitney test used, median included. ns: non-significant, ***: p≤0.001, ****: p≤0.0001*

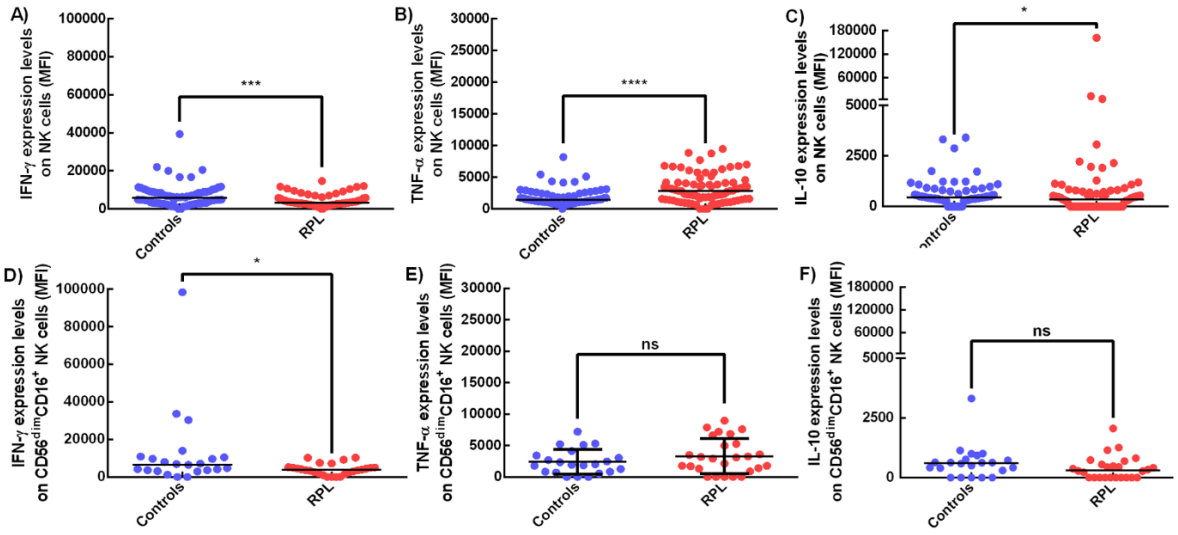


Figure 98. Cytokine expression intensity on stimulated total and CD56^{dim}CD16^{+} Natural Killer (NK) cells of women with recurrent pregnancy loss (RPL) and controls. *The intensity of A) interferon (IFN)-γ, B) tumor necrosis factor (TNF)-α, and C) interleukin (IL)-10 expression on individual NK cells, represented by the median fluorescence intensity (MFI), as well as the intensity of A) IFN-γ, B) TNF-α, and C) IL-10 expression on the CD56^{dim}CD16^{+} NK cell subpopulation, following stimulation with phorbol 12-myristate 13-acetate and ionomycin, of healthy controls (total NK cells: N=71, CD56^{dim}CD16^{+} NK cells: N=22) and women with RPL (total NK cells: N=84, CD56^{dim}CD16^{+} NK cells: N=26) is depicted. Normally distributed datasets (E): Unpaired t test performed, mean and standard deviation shown. Non-normally distributed datasets (A-D, F): Mann-Whitney test used, median illustrated. ns: non-significant, *: p≤0.05, ***: p≤0.001, ****: p≤0.0001*

The ratios between pro- and anti-inflammatory cytokine production by stimulated total and CD56^{dim}CD16^{+} NK cells were also investigated. IFN-γ^{+}/IL-10^{+} and TNF-α^{+}/IL-10^{+} total and CD56^{dim}CD16^{+} NK cell ratios appeared unaltered in women with RPL compared to controls (Figures 99A-99D). Similarly the IFN-γ/IL-10 expression levels on CD56^{dim}CD16^{+} NK cells and the TNF-α/IL-10 expression levels on both total and CD56^{dim}CD16^{+} NK cells were not found to be significantly different between the RPL and control groups (Figures 100B-100D). However, the IFN-γ-to-IL-10

expression intensity ratio on NK cells was reduced in participants with RPL (p=0.0061) (Figure 100A).

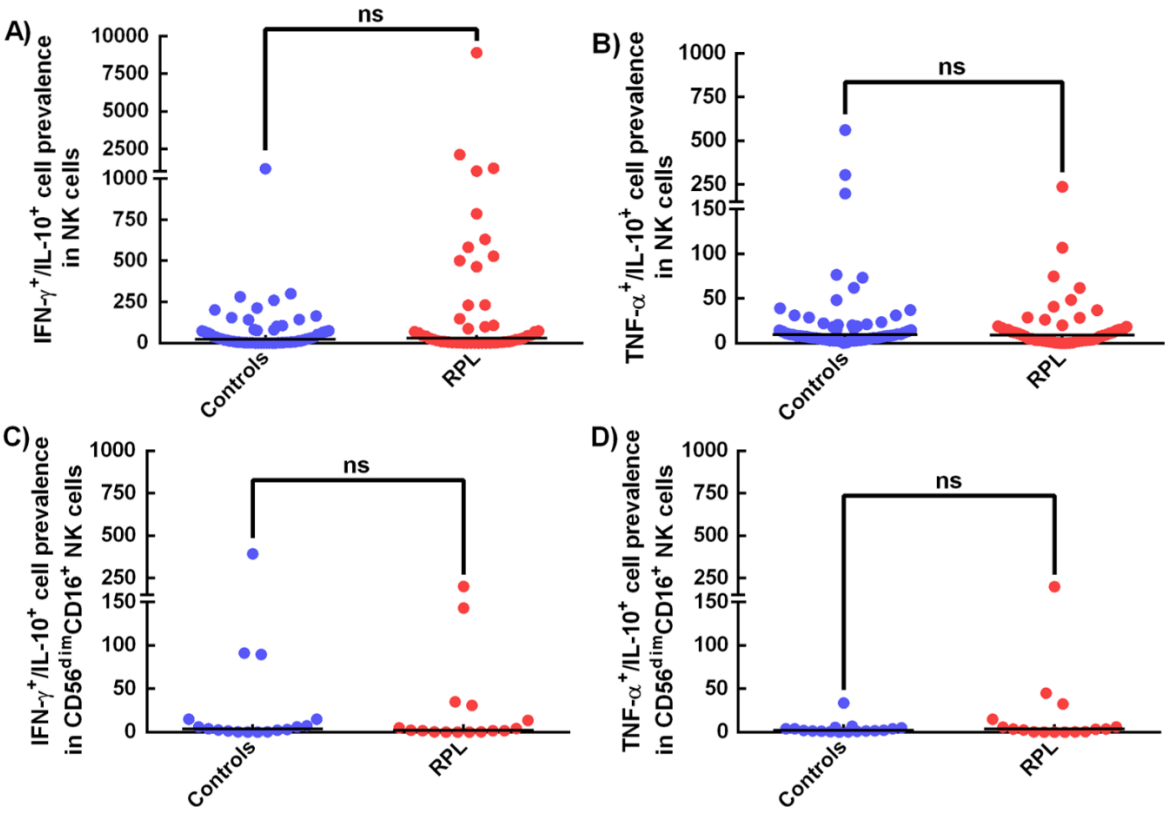


Figure 99. Cytokine-expressing cell prevalence ratios in the stimulated total and CD56^{dim}CD16^{+} Natural Killer (NK) cell population of women with recurrent pregnancy loss (RPL) and controls. *The prevalence ratios of A) interferon (IFN)-γ^{+}/interleukin (IL)-10^{+} and B) tumor necrosis factor (TNF)-α^{+}/IL-10^{+} cells in the NK cell population, as well as the C) IFN-γ^{+}/IL-10^{+} and D) TNF-α^{+}/IL-10^{+} cell ratios in the CD56^{dim}CD16^{+} NK cell subpopulation, following stimulation with phorbol 12-myristate 13-acetate and ionomycin, in healthy controls (total NK cells: N=61, CD56^{dim}CD16^{+} NK cells: N=17) and women with RPL (total NK cells: N=50, CD56^{dim}CD16^{+} NK cells: N=16) is depicted. Mann-Whitney test performed, median shown. ns: non-significant*

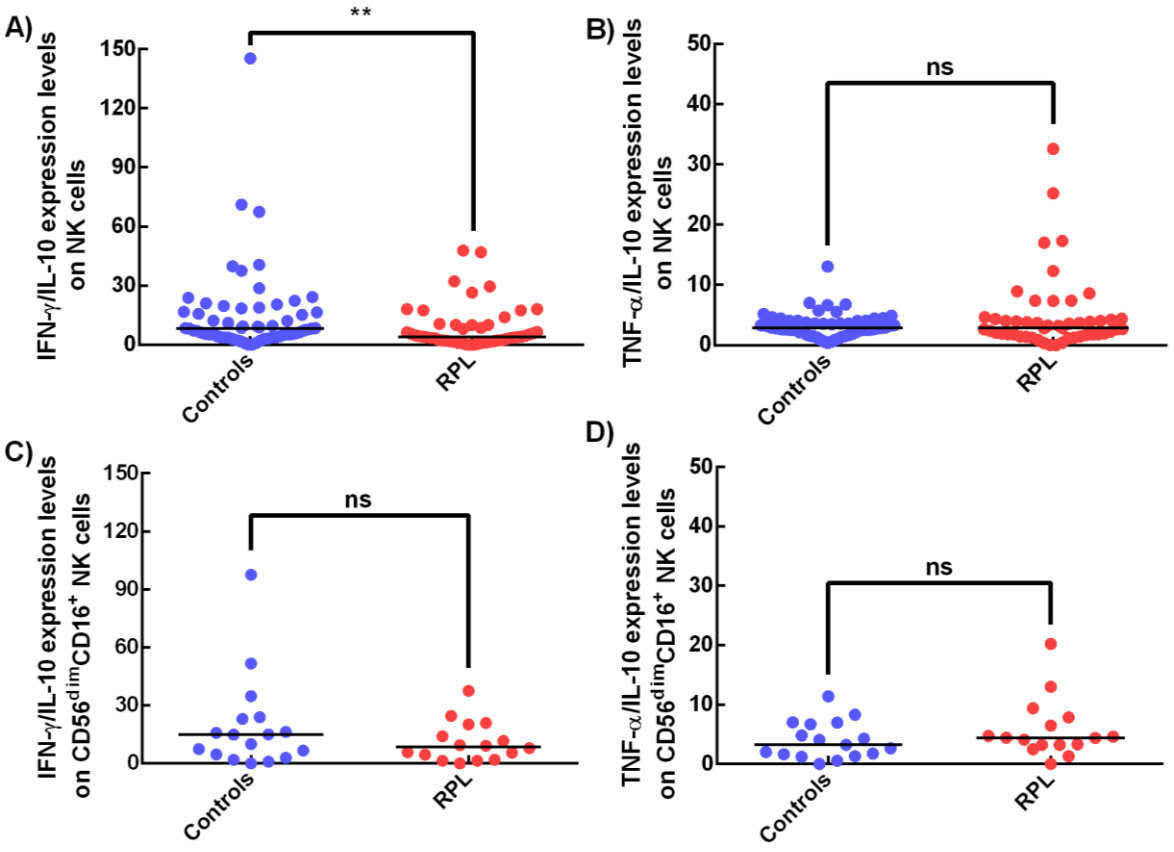


Figure 100. Cytokine expression intensity ratios on stimulated total and CD56^{dim}CD16^{+} Natural Killer (NK) cells of women with recurrent pregnancy loss (RPL) and controls. *The intensity ratios of A) interferon (IFN)-γ/interleukin (IL)-10 and B) tumor necrosis factor (TNF)-α/IL-10 expression on individual NK cells, represented by the median fluorescence intensity (MFI), as well as the intensity of C) IFN-γ/IL-10 and D) TNF-α/IL-10 expression on the CD56^{dim}CD16^{+} NK cell subpopulation, following stimulation with phorbol 12-myristate 13-acetate and ionomycin, in healthy controls (total NK cells: N=61, CD56^{dim}CD16^{+} NK cells: N=17) and women with RPL (total NK cells: N=50, CD56^{dim}CD16^{+} NK cells: N=16) is displayed. Mann-Whitney test used, median illustrated. ns: non-significant, **: p≤0.01*

9.1.3 ELISA – Cytokine, chemokine, and colony-stimulating factor secretion

ELISAs were used to detect whether changes in cellular cytokine expression translated into changes in their secretion patterns. Thus, cytokine secretion by the total PBMC population was evaluated. Alongside IL-2, IFN-γ, TNF-α, IL-10, and IL-17A, the secretion levels of the IL-4, IL-5, and IL-13 cytokines, the IL-8 chemokine, and the G-CSF and GM-CSF colony-stimulating factors were also assessed (Controls *N*=72, RPL *N*=99). In the absence of stimulation, IFN-γ [Controls: 12.18pg/mL, 95% CI (12.18pg/mL, 12.18pg/mL), RPL: 12.18pg/mL, 95% CI (12.18pg/mL, 12.18pg/mL)], IL-10 [Controls: 74.84pg/mL, 95% CI (4.17pg/mL, 823.00pg/mL), RPL: 263.10pg/mL, 95% CI (121.00pg/mL, 623.40pg/mL)], IL-4 [Controls: 5.99pg/mL, 95% CI (4.20pg/mL, 7.57pg/mL), RPL: 12.65pg/mL, 95% CI (4.37pg/mL, 12.65pg/mL)], IL-13 [Controls: 4.39pg/mL, 95% CI (4.39pg/mL, 4.39pg/mL), RPL: 4.39pg/mL, 95% CI (4.39pg/mL, 4.39pg/mL)], and G-CSF [Controls: 85.91pg/mL, 95% CI (16.80pg/mL, 401.00pg/mL), RPL: 303.00pg/mL, 95% CI (101.60pg/mL, 618.80pg/mL)] secretion levels in PBMC cultures appeared similar between women with RPL and controls, while TNF-α [Controls: 523.80pg/mL, 95% CI (53.04pg/mL, 2966.00pg/mL), RPL: 3332.00pg/mL, 95% CI (1908.00pg/mL, 6506.00pg/mL), p=0.0313], IL-17A [Controls: 2.81pg/mL, 95% CI (1.93pg/mL, 2.81pg/mL), RPL: 2.81pg/mL, 95% CI (2.81pg/mL, 2.81pg/mL), p<0.0001], IL-8 [Controls: 3553.00pg/mL, 95% CI (2128.00pg/mL, 5060.00pg/mL), RPL: 7405.00pg/mL, 95% CI (5943.00pg/mL, 12669.00pg/mL), p=0.0006], and GM-CSF [Controls: 56.94pg/mL, 95% CI (18.43pg/mL, 104.60pg/mL), RPL: 146.90pg/mL, 95% CI (72.67pg/mL, 299.10pg/mL), p=0.0022] levels were increased and IL-2 [Controls: 9.16pg/mL, 95% CI (7.74pg/mL, 11.55pg/mL), RPL:

7.42pg/mL, 95% CI (6.37pg/mL, 8.79pg/mL), p=0.0080] and IL-5 [Controls: 21.80pg/mL, 95% CI (17.40pg/mL, 27.75pg/mL), RPL: 15.84pg/mL, 95% CI (11.31pg/mL, 15.84pg/mL), p<0.0001] levels were reduced in participants with RPL (Figures 101A-101K).

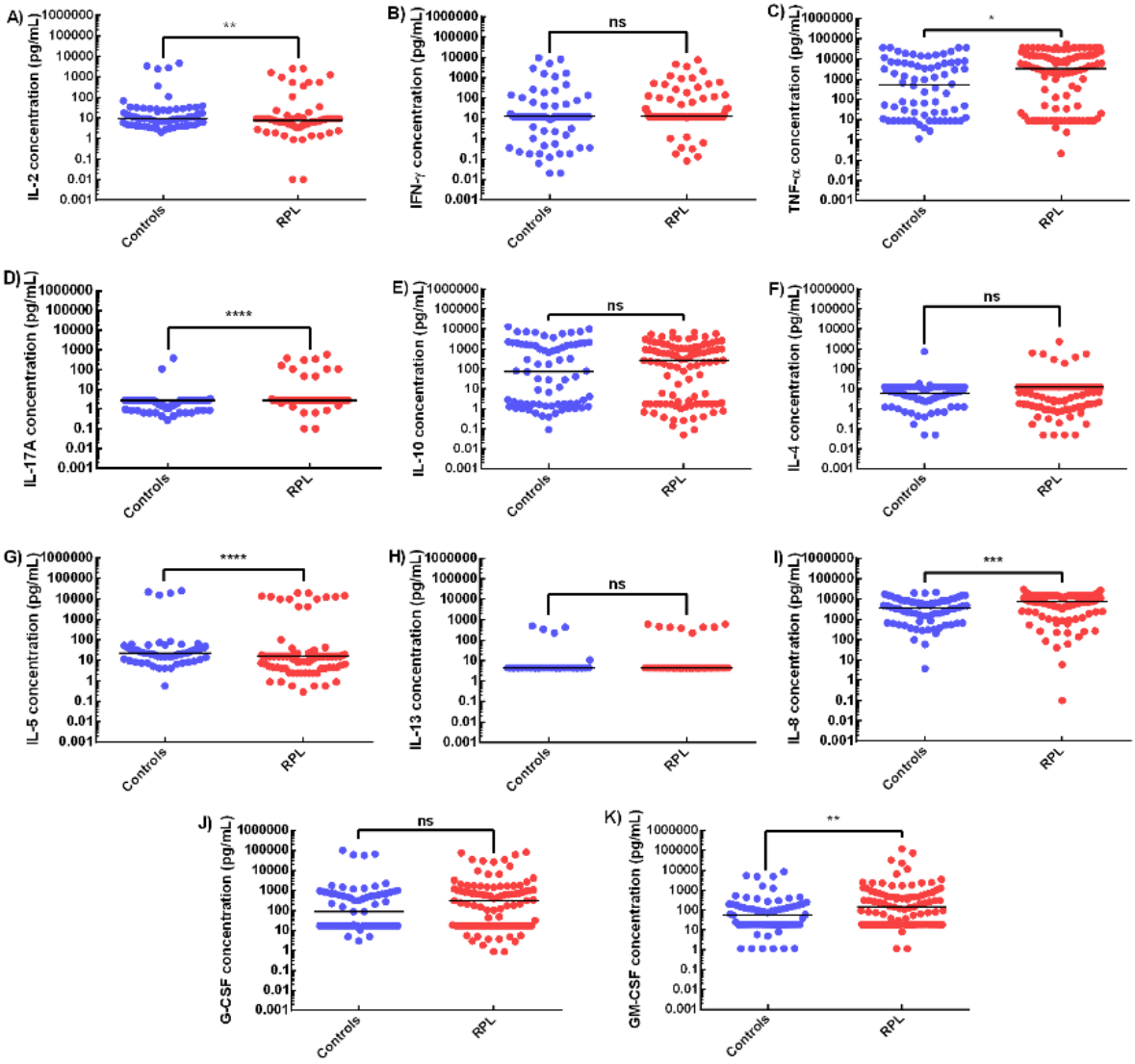


Figure 101. Protein concentration (pg/mL) in unstimulated peripheral blood mononuclear cell (PBMC) cultures derived from women with recurrent pregnancy loss (RPL) and controls. *The levels of A) interleukin (IL)-2, B) interferon (IFN)-γ, C) tumor necrosis factor (TNF)-α, D) IL-17A, E) IL-10, F) IL-4, G) IL-5, H) IL-13, I) IL-8, J) granulocyte colony-stimulating factor (G-CSF), and K) granulocyte-macrophage colony-stimulating factor (GM-CSF) secretion by PBMCs isolated from healthy controls (N=72) and women with RPL (N=99) is depicted. Mann-Whitney test performed, median illustrated. ns: non-significant, *: p≤0.05, **: p≤0.01, ***: p≤0.001, ****: p≤0.0001*

Secretion of IL-2, IFN-γ, IL-17A, IL-4, IL-5, IL-13, and GM-CSF was increased upon stimulation in both the RPL and control groups (Figures 102A-102F, 102J-102L, 103D-103L, 104G-104I). On the other hand, G-CSF secretion appeared reduced upon stimulation in women with RPL and controls (Figures 104D-104F). Secreted IL-10 levels were also decreased following stimulation, but only in the RPL and total participant groups (Figures 103A-103C). Conversely, TNF-α and IL-8 secretion was elevated upon stimulation in the control and total participant groups, but not in women with RPL (Figures 102G-102I, 104A-104C).

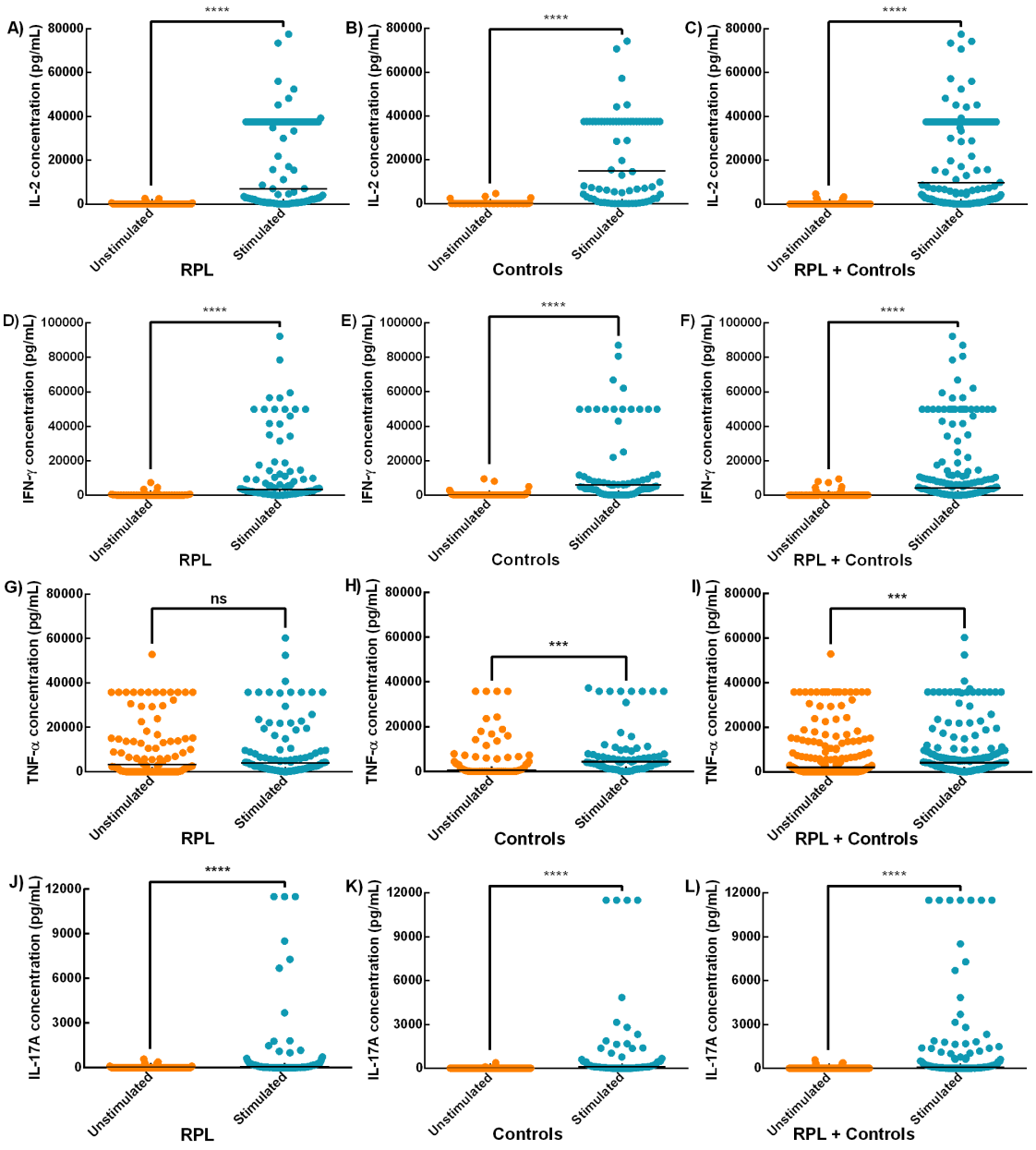


Figure 102. Pro-inflammatory cytokine concentration (pg/mL) in unstimulated and stimulated peripheral blood mononuclear cell (PBMC) cultures derived from women with recurrent pregnancy loss (RPL), controls, and total participants. *The levels of A-C) interleukin (IL)-2, D-F) interferon (IFN)-γ, G-I) tumor necrosis factor (TNF)-α, and J-L) IL-17A secretion by PBMCs isolated from women with RPL (N=99) (A, D, G, J), healthy controls (N=72) (B, E, H, K), and total participants (N=171) (C, F, I, L) in the absence and following stimulation with phorbol 12-myristate 13-acetate and ionomycin, is displayed. Wilcoxon matched-pairs signed rank test performed, median shown. ns: non-significant, ***: p≤0.001, ****: p≤0.0001*

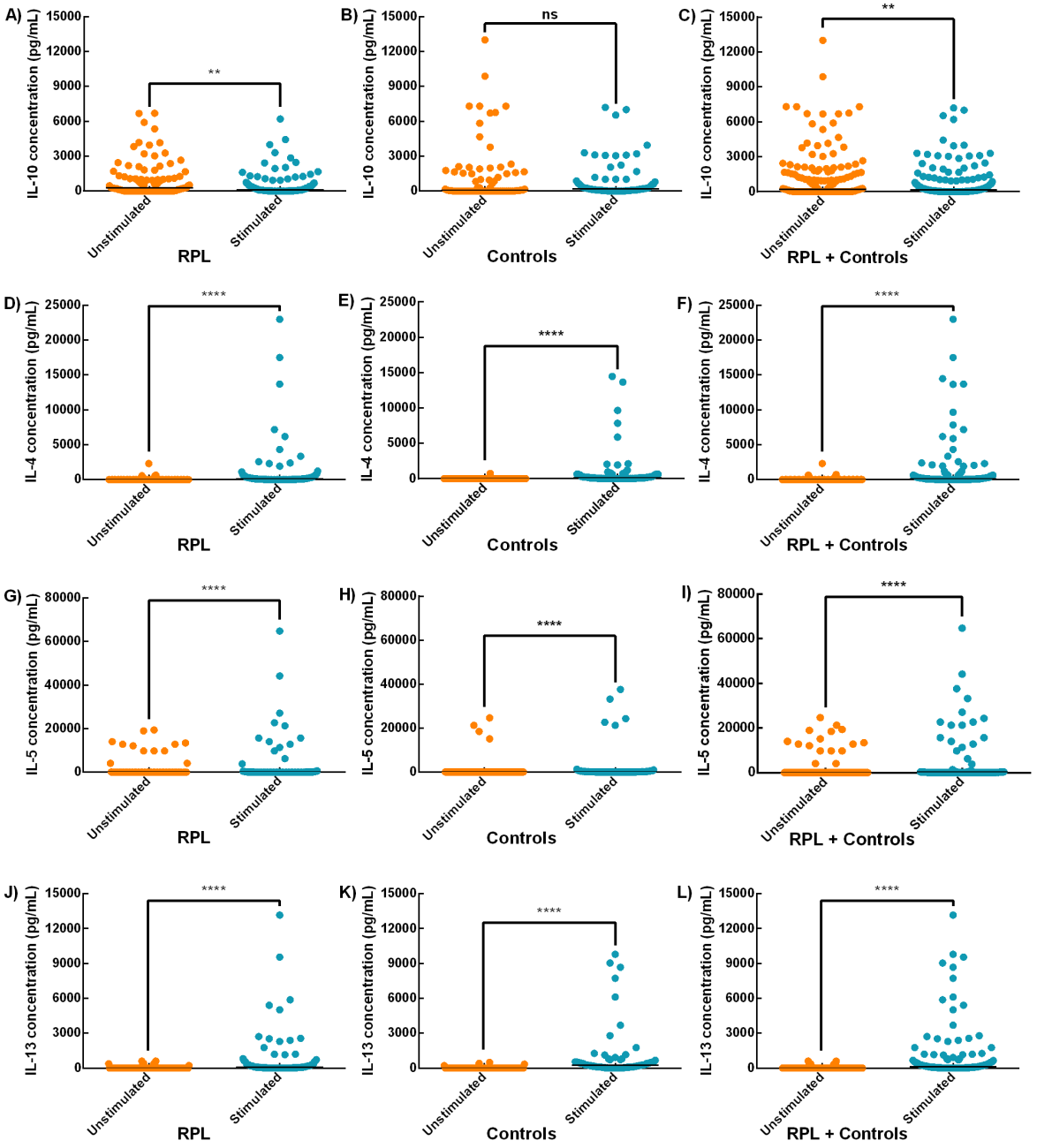


Figure 103. Anti-inflammatory cytokine concentration (pg/mL) in unstimulated and stimulated peripheral blood mononuclear cell (PBMC) cultures derived from women with recurrent pregnancy loss (RPL), controls, and total participants. *The levels of A-C) interleukin (IL)-10, D-F) IL-4, G-I) IL-5, and J-L) IL-13 secretion by PBMCs isolated from women with RPL (N=99) (A, D, G, J), healthy controls (N=72) (B, E, H, K), and total participants (N=171) (C, F, I, L) in the absence and following stimulation with phorbol 12-myristate 13-acetate and ionomycin, is illustrated. Wilcoxon matched-pairs signed rank test used, median depicted. ns: non-significant, **: p≤0.01, ****: p≤0.0001*

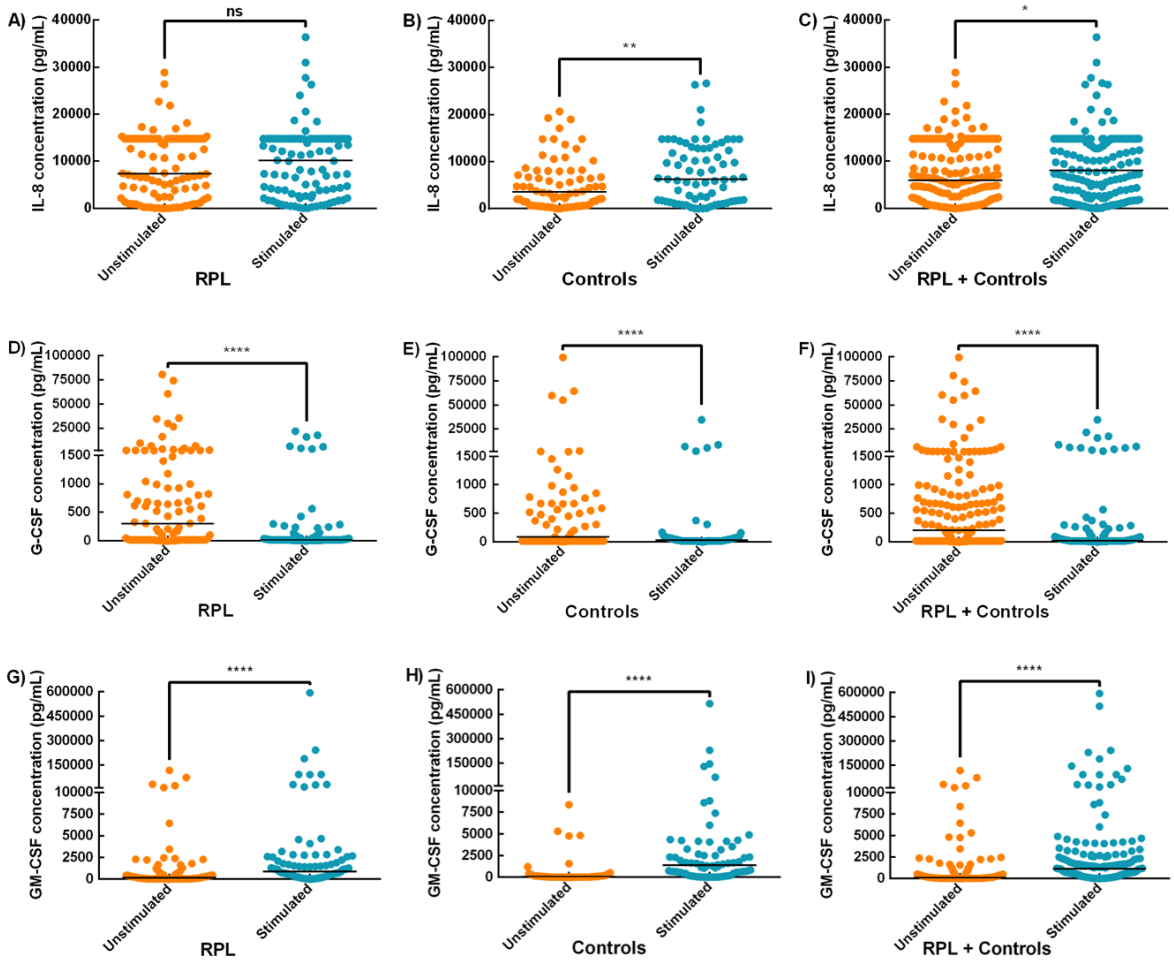


Figure 104. Chemokine and colony-stimulating factor concentration (pg/mL) in unstimulated and stimulated peripheral blood mononuclear cell (PBMC) cultures derived from women with recurrent pregnancy loss (RPL), controls, and total participants. *The levels of A-C) interleukin (IL)-8, D-F) granulocyte colony-stimulating factor (G-CSF), and G-I) granulocyte-macrophage colony-stimulating factor (GM-CSF) secretion by PBMCs isolated from women with RPL (N=99) (A, D, G), healthy controls (N=72) (B, E, H), and total participants (N=171) (C, F, I) in the absence and following stimulation with phorbol 12-myristate 13-acetate and ionomycin, is shown. Wilcoxon matched-pairs signed rank test used, median included. ns: non-significant, *: p≤0.05, **: p≤0.01, ****: p≤0.0001*

The secretion levels of these molecules following stimulation were also compared between women with RPL and controls. No significant difference in IL-2 [Controls: 15039.00pg/mL, 95% CI (6681.00pg/mL, 37500.00pg/mL), RPL: 6986.00pg/mL, 95% CI (2705.00pg/mL, 34854.00pg/mL)], IFN-γ [Controls: 5850.00pg/mL, 95% CI (3775.00pg/mL, 7441.00pg/mL), RPL: 3237.00pg/mL, 95% CI (2335.00pg/mL, 4626.00pg/mL)], TNF-α [Controls: 4363.00pg/mL, 95% CI (3657.00pg/mL, 5871.00pg/mL), RPL: 4038.00pg/mL, 95% CI (2477.00pg/mL, 5329.00pg/mL)], IL-17A [Controls: 104.50pg/mL, 95% CI (63.02pg/mL, 209.30pg/mL), RPL: 57.02pg/mL, 95% CI (30.50pg/mL, 114.80pg/mL)], IL-10 [Controls: 183.30pg/mL, 95% CI (95.91pg/mL, 288.30pg/mL), RPL: 100.60pg/mL, 95% CI (61.99pg/mL, 267.60pg/mL)], IL-4 [Controls: 121.10pg/mL, 95% CI (69.98pg/mL, 246.20pg/mL), RPL: 83.12pg/mL, 95% CI (44.55pg/mL, 129.20pg/mL)], G-CSF [Controls: 25.16pg/mL, 95% CI (16.80pg/mL, 40.29pg/mL), RPL: 16.80pg/mL, 95% CI (16.80pg/mL, 21.81pg/mL)], or GM-CSF [Controls: 1384.00pg/mL, 95% CI (745.90pg/mL, 1794.00pg/mL), RPL: 869.90pg/mL, 95% CI (657.50pg/mL, 1200.00pg/mL)] secretion was detected between the RPL and control groups (Figures 105A-105F, 105J-105K). However, participants with RPL displayed reduced IL-5 [Controls: 130.80pg/mL, 95% CI (93.87pg/mL, 200.80pg/mL), RPL: 53.86pg/mL, 95% CI (36.42pg/mL, 68.84pg/mL), p=0.0016] and IL-13 [Controls: 244.70pg/mL, 95% CI (142.10pg/mL, 407.00pg/mL), RPL: 72.35pg/mL, 95% CI (38.19pg/mL, 128.30pg/mL), p=0.0030] secretion by stimulated PBMCs and increased secretion of IL-8 [Controls: 6287.00pg/mL, 95% CI (3889.00pg/mL, 9725.00pg/mL), RPL: 10219.00pg/mL, 95% CI (6968.00pg/mL, 13477.00pg/mL), p=0.0276] (Figures 105G-105I). The ratios of pro- to anti-inflammatory cytokine

secretion were also examined. The ratios of IL-2, IFN-γ, TNF-α, and IL-17A to IL-10 and IL-4 secretion were not altered in women with RPL (Figures 106A-106H). Additionally, the IL-2/IL-5, IFN-γ/IL-5, and IL-17A/IL-5 secretion were also unaltered in the RPL compared to the control group, but the TNF-α/IL-5 ratio was augmented in women with RPL ($p=0.0120$) (Figures 106I-106L). The IL-2/IL-13 ($p=0.0105$), IFN-γ/IL-13 ($p=0.0040$), and TNF-α/IL-13 ($p<0.0001$) ratios were also elevated in women with RPL compared to controls, but the IL-17A/IL-13 appeared unaltered (Figures 106M-106P).

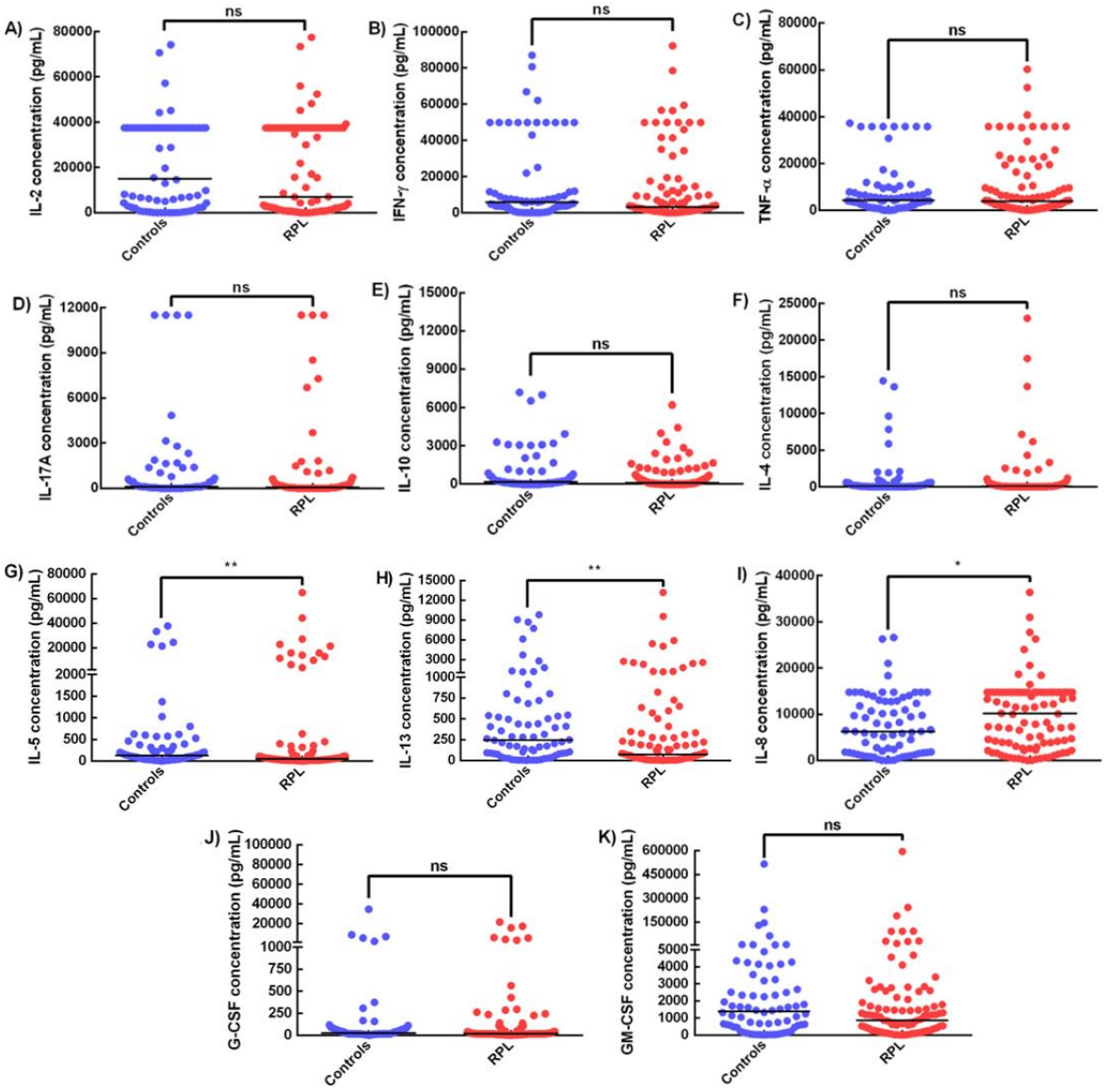


Figure 105. Protein concentration (pg/mL) in stimulated peripheral blood mononuclear cell (PBMC) cultures derived from women with recurrent pregnancy loss (RPL) and controls. *The levels of A) interleukin (IL)-2, B) interferon (IFN)-γ, C) tumor necrosis factor (TNF)-α, D) IL-17A, E) IL-10, F) IL-4, G) IL-5, H) IL-13, I) IL-8, J) granulocyte colony-stimulating factor (G-CSF), and K) granulocyte-macrophage colony-stimulating factor (GM-CSF) secretion by PBMCs isolated from healthy controls (N=72) and women with RPL (N=99), following stimulation with phorbol 12-myristate 13-acetate and ionomycin, is illustrated. Mann-Whitney test used, median displayed. ns: non-significant, *: p≤0.05, **: p≤0.01*

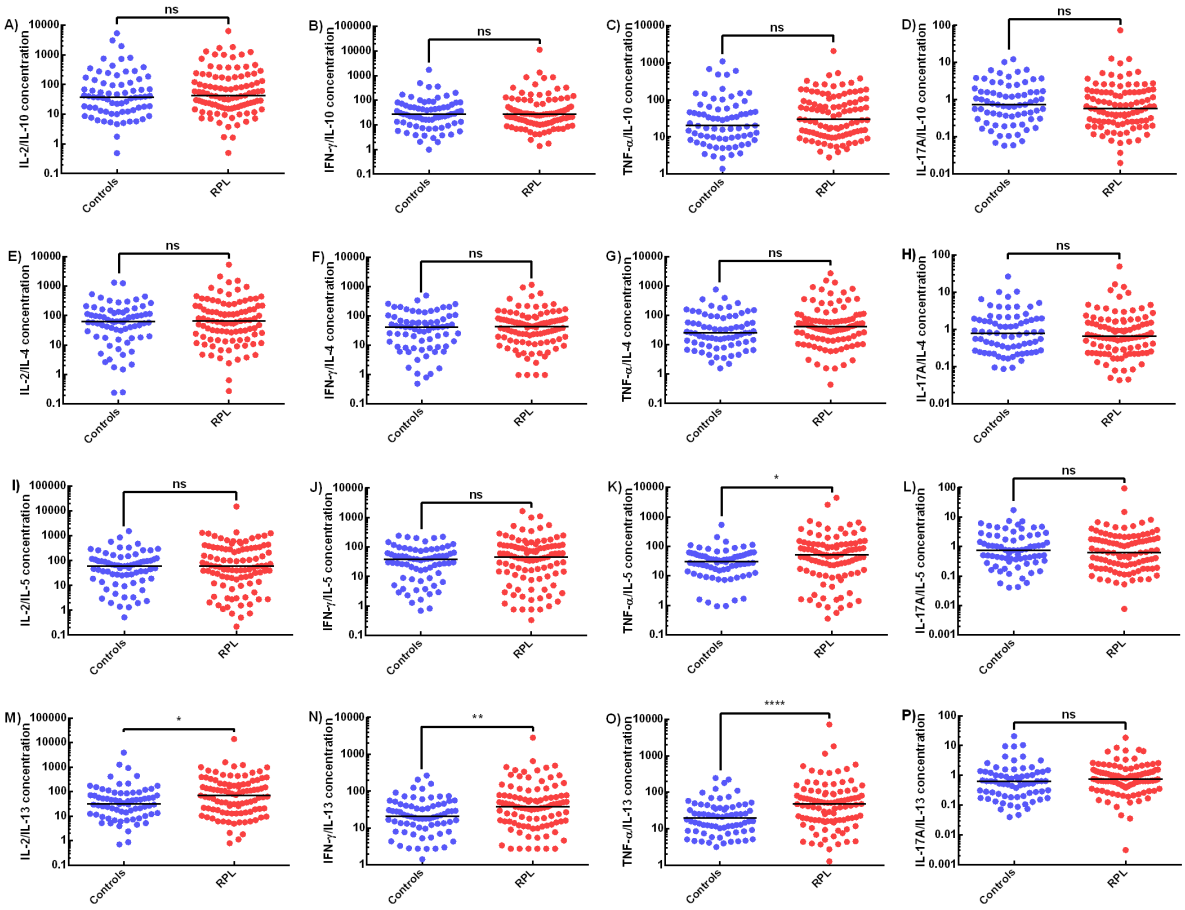


Figure 106. Protein concentration ratios in stimulated peripheral blood mononuclear cell (PBMC) cultures derived from women with recurrent pregnancy loss (RPL) and controls. *The ratios of A) interleukin (IL)-2/IL-10, B) interferon (IFN)-γ/IL-10, C) tumor necrosis factor (TNF)-α/IL-10, D) IL-17A/IL-10, E) IL-2/IL-4, F) IFN-γ/IL-4, G) TNF-α/IL-4, H) IL-17A/IL-4, I) IL-2/IL-5, J) IFN-γ/IL-5, K) TNF-α/IL-5, L) IL-17A/IL-5, M) IL-2/IL-13, N) IFN-γ/IL-13, O) TNF-α/IL-13, and P) IL-17A/IL-13 secretion levels by PBMCs isolated from healthy controls (N=72) and women with RPL (N=99) is displayed. Mann-Whitney test performed, median illustrated. ns: non-significant, *: p≤0.05, **: p≤0.01, ****: p≤0.0001*

9.1.4 Cytokine balance in RPL and control subpopulations

In women with idiopathic RPL an increase in IL-2$^+$/IL-10$^+$ ($p<0.0001$), IFN-γ$^+$/IL-10$^+$ ($p<0.0001$), TNF-α$^+$/IL-10$^+$ ($p<0.0001$), and IL-17A$^+$/IL-10$^+$ ($p<0.0001$) T_H cell prevalence was detected, compared to the total control population, accompanied by a reduction in IL-2/IL-10 ($p<0.0001$), IFN-γ/IL-10 ($p<0.0001$), TNF-α/IL-10 ($p=0.0223$), and IL-17A/IL-10 ($p<0.0001$) cytokine expression intensity on these cells (Figures 107A-107H). IL-2$^+$/IL-17A$^+$, IFN-γ$^+$/IL-17A$^+$, and TNF-α$^+$/IL-17A$^+$ T_H cell prevalence appeared unaltered between women with idiopathic RPL and controls (Figures 107I, 107K, 107M). However, IL-2/IL-17A expression levels on T_H cells were found to be reduced in women with idiopathic RPL ($p=0.0307$), with IFN-γ/IL-17A levels being unaltered, and TNF-α/IL-17A levels being elevated ($p=0.0107$) (Figures 107J, 107L, 107N). The prevalence of TNF-α$^+$ ($p<0.0001$) and IL-10$^+$ ($p<0.0001$), but not IFN-γ$^+$ NK cells appeared reduced in women with idiopathic RPL, with the expression levels of IFN-γ on these cells being reduced ($p<0.0001$), TNF-α levels being increased ($p<0.0001$), and IL-10 levels being unaltered (Figures 108A-108F).

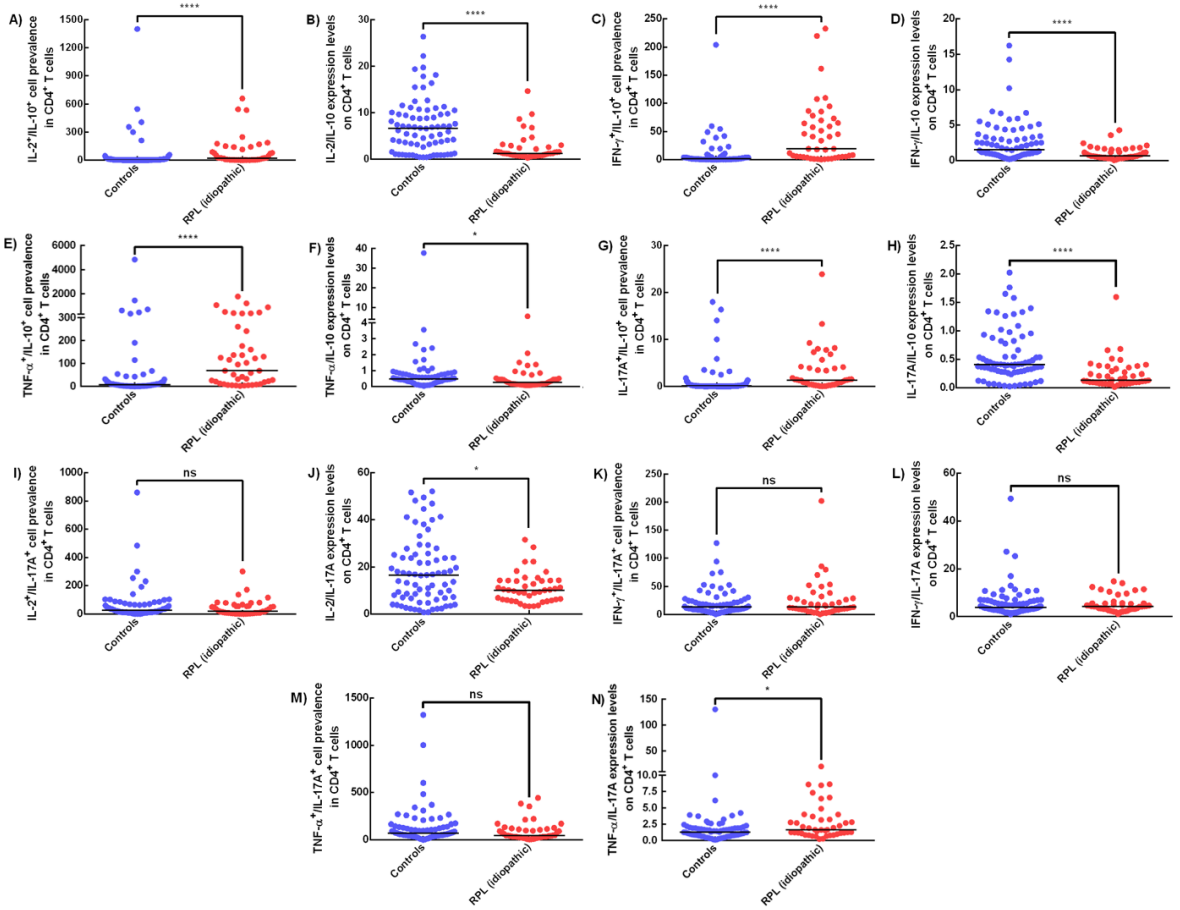


Figure 107. Ratios of cytokine production by stimulated T helper (T_H) cells of women with idiopathic recurrent pregnancy loss (RPL) and controls. *The prevalence ratios of A) interleukin (IL)-2$^+$/IL-10$^+$, C) interferon (IFN)-γ$^+$/IL-10$^+$, E) tumor necrosis factor (TNF)-α$^+$/IL-10$^+$, G) IL-17A$^+$/IL-10$^+$, I) IL-2$^+$/IL-17A$^+$, K) IFN-γ$^+$/IL-17A$^+$, and M) TNF-α$^+$/IL-17A$^+$ cells in the stimulated CD4$^+$ T_H cell population, as well as the intensity ratios of B) IL-2/IL-10, D) IFN-γ/IL-10, F) TNF-α/IL-10, H) IL-17A/IL-10, J) IL-2/IL-17A, L) IFN-γ/IL-17A, and N) TNF-α/IL-17A expression, represented by the median fluorescence intensity (MFI), on stimulated CD4$^+$ T_H cells of healthy controls (N=76) and women with idiopathic RPL (N=44) are displayed. Mann-Whitney test performed, median depicted. ns: non-significant, *: p≤0.05, ****: p≤0.0001*

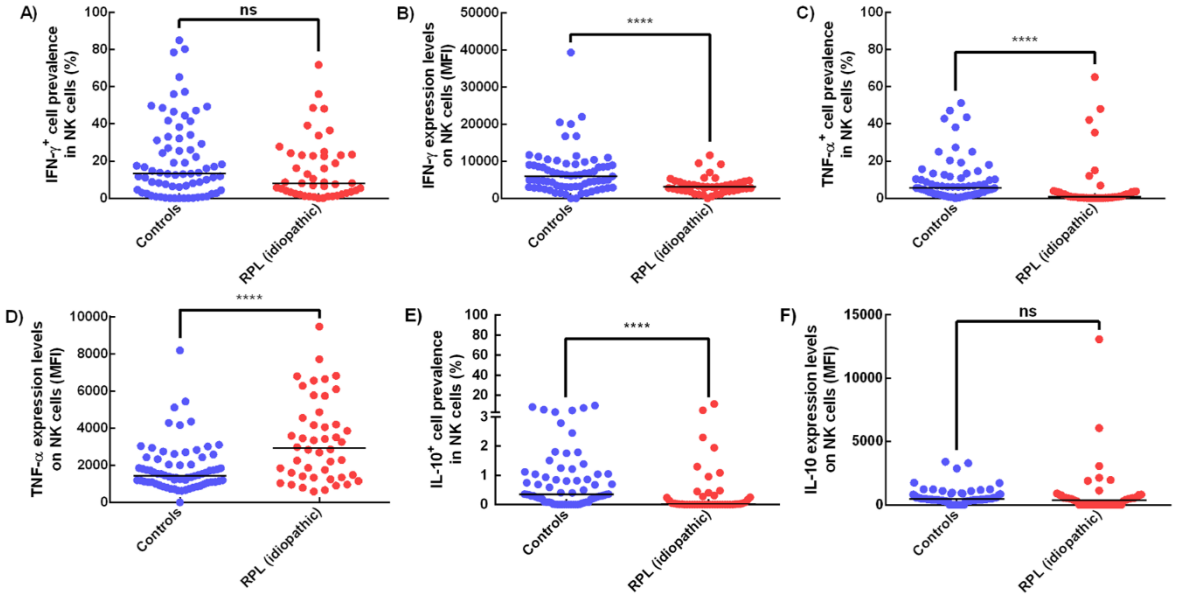


Figure 108. Cytokine production by stimulated Natural Killer (NK) cells of women with idiopathic recurrent pregnancy loss (RPL) and controls. *The prevalence of A) interferon (IFN)-γ⁺, C) tumor necrosis factor (TNF)-α⁺, and E) interleukin (IL)-10⁺ cells in the stimulated NK cell population, as well as the intensity of B) IFN-γ, D) TNF-α, and F) IL-10 expression, represented by the median fluorescence intensity (MFI), on stimulated NK cells of healthy controls (N=71) and women with idiopathic RPL (N=46) are illustrated. Mann-Whitney test performed, median shown. ns: non-significant, ****: p≤0.0001*

The increase in IL-2^+/IL-10^+ (p=0.0002), IFN-γ^+/IL-10^+ (p<0.0001), TNF-α^+/IL-10^+ (p=0.0003), and IL-$17A^+$/IL-10^+ (p=0.0001) T_H cell prevalence was also seen in women with non-idiopathic RPL compared to controls, accompanied by reduced IL-2/IL-10 (p<0.0001), IFN-γ/IL-10 (p=0.0135), and IL-17A/IL-10 (p=0.0006) and unaltered TNF-α/IL-10 expression levels on T_H cells (Figures 109A-109H). Furthermore, IL-2^+/IL-$17A^+$, IFN-γ^+/IL-$17A^+$, and TNF-α^+/IL-$17A^+$ T_H cell levels appeared unaltered in women with non-idiopathic RPL (Figures 109I, 109K, 109M). IL-2/IL-17A expression levels on T_H cells were reduced in these women compared to controls (p=0.0325), while IFN-γ/IL-17A levels were unaltered and TNF-α/IL-17A levels were elevated (p=0.0224) (Figures 109J, 109L, 109N). Decreased TNF-α^+ (p=0.0024), but not IFN-γ^+ or IL-10^+ NK cell levels were detected in women with non-idiopathic RPL, accompanied by elevated TNF-α (p=0.0008), but not IFN-γ or IL-10 expression intensity (Figures 110A-110F).

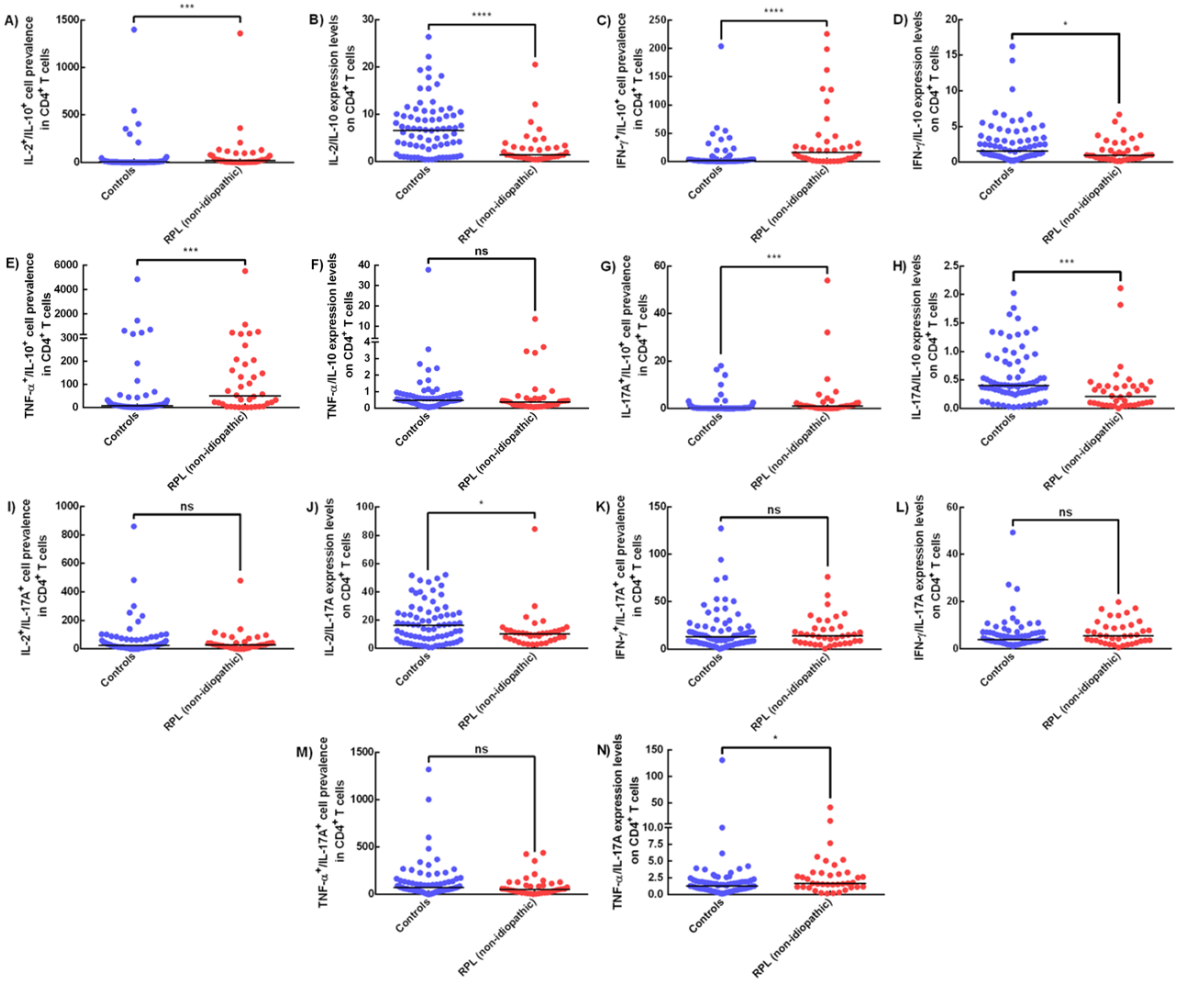


Figure 109. Ratios of cytokine production by stimulated T helper (T_H) cells of women with non-idiopathic recurrent pregnancy loss (RPL) and controls. *The prevalence ratios of A) interleukin (IL)-2$^+$/IL-10$^+$, C) interferon (IFN)-γ$^+$/IL-10$^+$, E) tumor necrosis factor (TNF)-α$^+$/IL-10$^+$, G) IL-17A$^+$/IL-10$^+$, I) IL-2$^+$/IL-17A$^+$, K) IFN-γ$^+$/IL-17A$^+$, and M) TNF-α$^+$/IL-17A$^+$ cells in the stimulated CD4$^+$ T_H cell population, as well as the intensity ratios of B) IL-2/IL-10, D) IFN-γ/IL-10, F) TNF-α/IL-10, H) IL-17A/IL-10, J) IL-2/IL-17A, L) IFN-γ/IL-17A, and N) TNF-α/IL-17A expression, represented by the median fluorescence intensity (MFI), on stimulated CD4$^+$ T_H cells of healthy controls (N=76) and women with non-idiopathic RPL (N=38) are depicted. Mann-Whitney test performed, median shown. ns: non-significant, *: p≤0.05, ***: p≤0.001, ****: p≤0.0001*

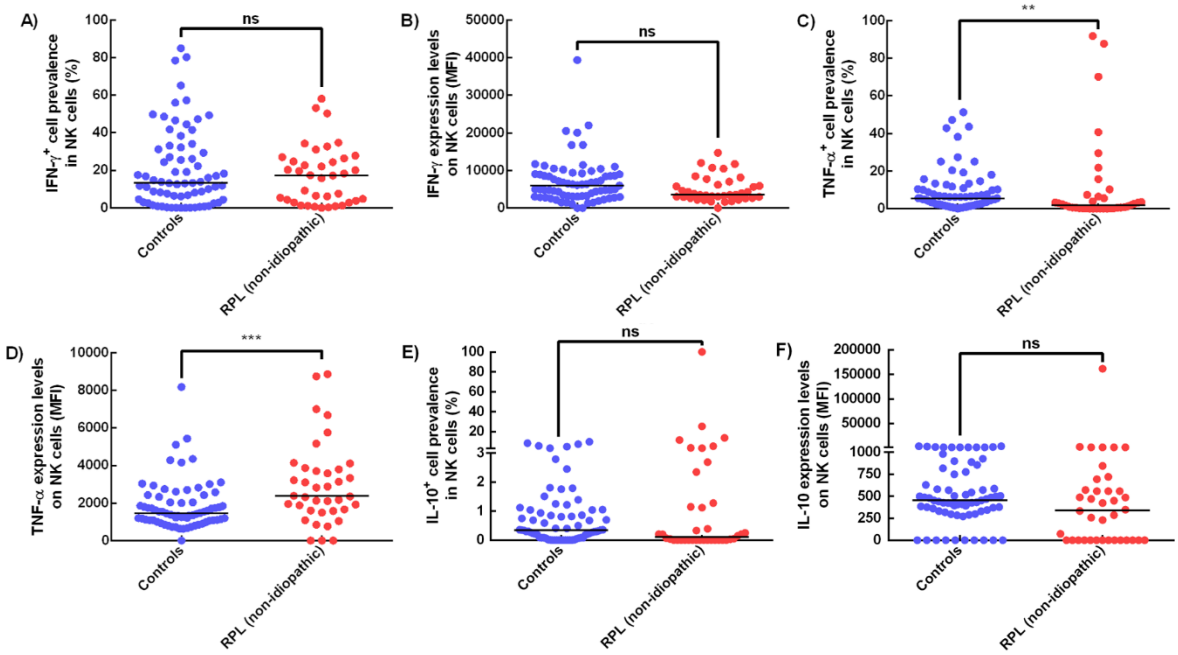


Figure 110. Cytokine production by stimulated Natural Killer (NK) cells of women with non-idiopathic recurrent pregnancy loss (RPL) and controls. *The prevalence of A) interferon (IFN)-γ⁺, C) tumor necrosis factor (TNF)-α⁺, and E) interleukin (IL)-10⁺ cells in the stimulated NK cell population, as well as the intensity of B) IFN-γ, D) TNF-α, and F) IL-10 expression, represented by the median fluorescence intensity (MFI), on stimulated NK cells of healthy controls (N=71) and women with non-idiopathic RPL (N=38) are displayed. Mann-Whitney test performed, median illustrated. ns: non-significant, ****: p≤0.0001*

In women with RPL and at least five losses in their reproductive history, augmented IL-2^+/IL-10^+ (p=0.0014), IFN-γ^+/IL-10^+ (p=0.0002), TNF-α^+/IL-10^+ (p=0.0005), and IL-$17A^+$/IL-10^+ (p=0.0100) T_H cell levels were detected compared to controls (Figures 111A, 111C, 111E, 111G). Reduced IL-2/IL-10 expression levels on T_H cells were also seen in these women (p=0.0147), while IFN-γ/IL-10, TNF-α/IL-10, and IL-17A/IL-10 levels were not significantly altered (Figures 111B, 111D, 111F, 111H). Unaltered IL-2^+/IL-$17A^+$, IFN-γ^+/IL-$17A^+$, and TNF-α^+/IL-$17A^+$ T_H cell prevalence was seen in women with RPL and at least five losses, compared to the total control cohort, while IL-2/IL-17A (p=0.0495), but not IFN-γ/IL-17A or TNF-α/IL-17A expression intensity on these cells was reduced (Figures 111I-111N). Moreover, IFN-γ^+, TNF-α^+, and IL-10^+ NK cell prevalence was not significantly different between this RPL subgroup and controls, while TNF-α (p=0.0012), but not IFN-γ or IL-10 expression levels were elevated on NK cells of women with RPL and higher order losses (Figures 112A-112F).

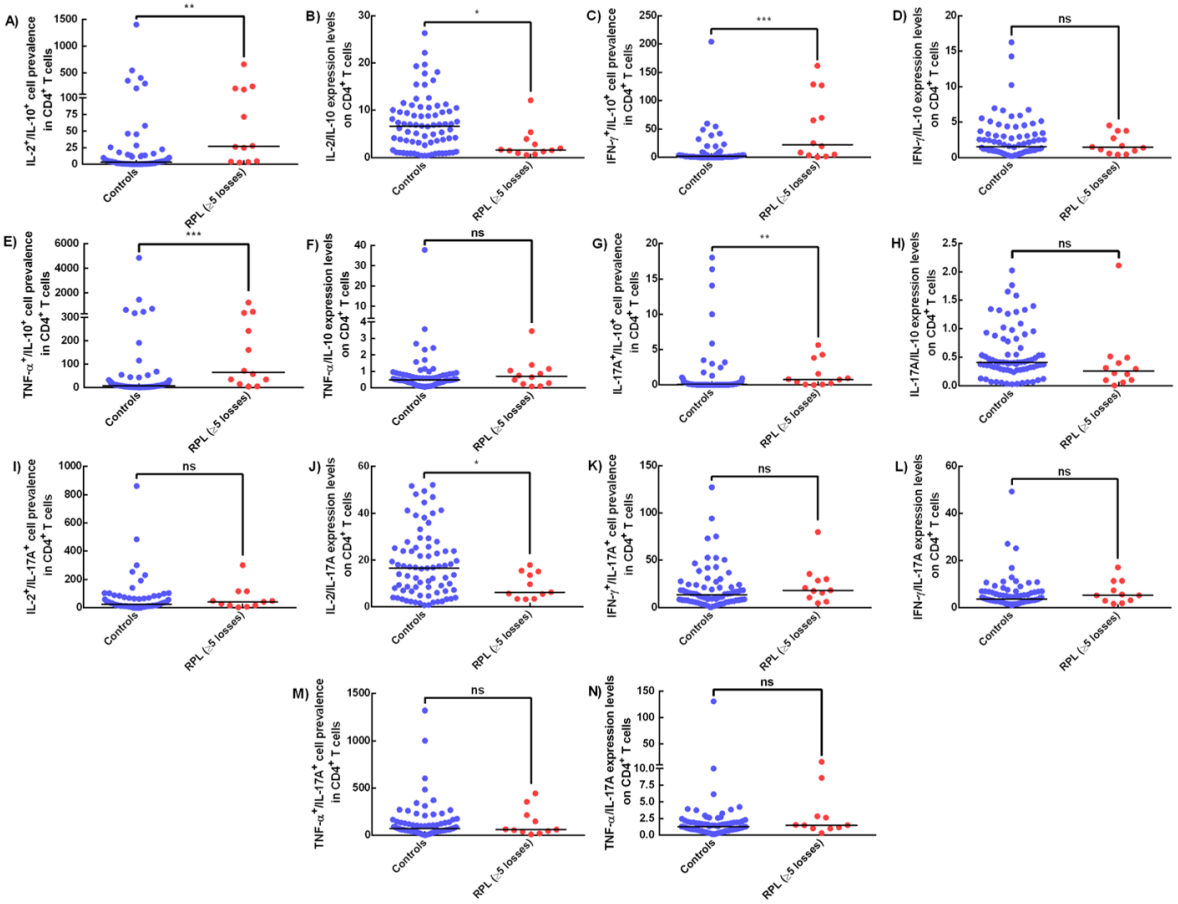


Figure 111. Ratios of cytokine production by stimulated T helper (T_H) cells of women with recurrent pregnancy loss (RPL) with at least 5 past losses and controls. *The prevalence ratios of A) interleukin (IL)-2$^+$/IL-10$^+$, C) interferon (IFN)-γ$^+$/IL-10$^+$, E) tumor necrosis factor (TNF)-α$^+$/IL-10$^+$, G) IL-17A$^+$/IL-10$^+$, I) IL-2$^+$/IL-17A$^+$, K) IFN-γ$^+$/IL-17A$^+$, and M) TNF-α$^+$/IL-17A$^+$ cells in the stimulated CD4$^+$ T_H cell population, as well as the intensity ratios of B) IL-2/IL-10, D) IFN-γ/IL-10, F) TNF-α/IL-10, H) IL-17A/IL-10, J) IL-2/IL-17A, L) IFN-γ/IL-17A, and N) TNF-α/IL-17A expression, represented by the median fluorescence intensity (MFI), on stimulated CD4$^+$ T_H cells of healthy controls (N=76) and women with RPL with a minimum of 5 losses (N=12) are displayed. Mann-Whitney test performed, median depicted. ns: non-significant, *: p≤0.05, **: p≤0.01, ***: p≤0.001*

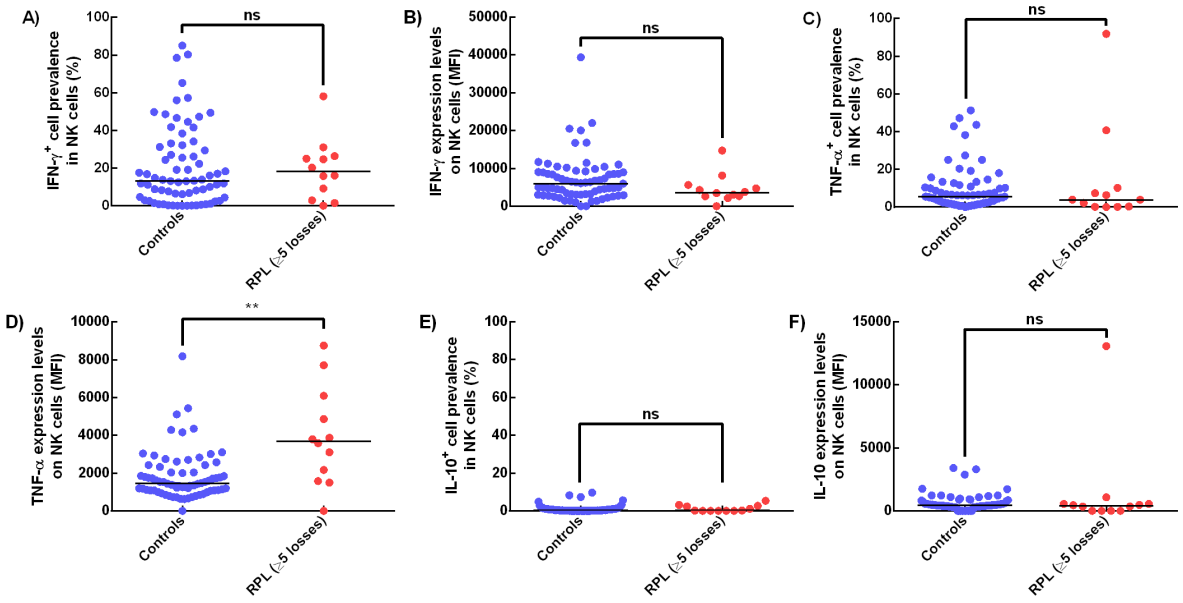


Figure 112. Cytokine production by stimulated Natural Killer (NK) cells of women with recurrent pregnancy loss (RPL) with at least 5 past losses and controls. *The prevalence of A) interferon (IFN)-γ⁺, C) tumor necrosis factor (TNF)-α⁺, and E) interleukin (IL)-10⁺ cells in the stimulated NK cell population, as well as the intensity of B) IFN-γ, D) TNF-α, and F) IL-10 expression, represented by the median fluorescence intensity (MFI), on stimulated NK cells of healthy controls (N=71) and women with RPL with a minimum of 5 losses (N=12) are illustrated. Mann-Whitney test performed, median shown. ns: non-significant, **: p≤0.01*

Within the control population, IL-2^+/IL-10^+, IFN-γ^+/IL-10^+, TNF-α^+/IL-10^+, IL-$17A^+$/IL-10^+, and TNF-α^+/IL-$17A^+$ T_H cell prevalence did not appeared altered between the different age-related subgroups (Figures 113A, 113C, 113E, 113G, 113M). However, IL-2^+/IL-$17A^+$ ($p=0.0022$) and IFN-γ^+/IL-$17A^+$ ($p=0.0156$) T_H cell prevalence was elevated in control women over 40, compared to control women up to 30 years of age (Figures 113I, 113K). Additionally, IL-2/IL-10, IFN-γ/IL-10, IL-17A/IL-10, IL-2/IL-17A, and IFN-γ/IL-17A expression levels on T_H cells were unaltered in control women of different age groups, while TNF-α/IL-10 expression levels on these cells were elevated in control women between 31 and 35, compared to those up to 30 years of age ($p=0.0032$) (Figures 113B, 113D, 113F, 113H, 113J, 113L). TNF-α/IL-17A expression intensity on T_H cells appeared significantly altered through the Kruskal-Wallis test ($p=0.0478$) but no significant difference between two subgroups could be identified through the Dunn's test for multiple comparisons (Figure 113N). TNF-α^+ ($p=0.0146$), but not IFN-γ^+ or IL-10^+ NK cell prevalence was increased in control women between 31 and 35 years of age, compared to those up to 30 ($p=0.0146$), while the expression levels of these cytokines on NK cells appeared unaltered (Figures 114A-114F). However, none of these age-related differences in T_H and NK cell cytokine production could be detected in the RPL population (Figures 115-116).

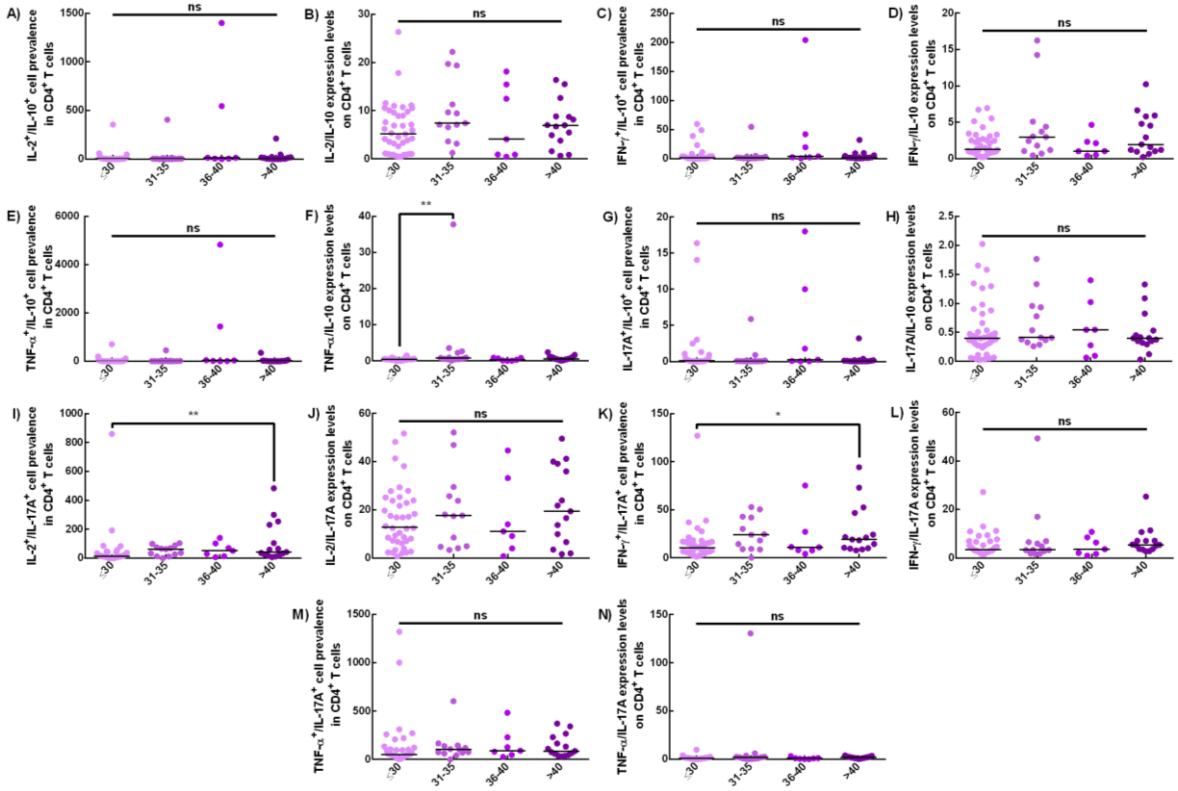


Figure 113. Ratios of cytokine production by stimulated T helper (T_H) cells of control women belonging to different age-associated subgroups. *The prevalence ratios of A) interleukin (IL)-2$^+$/IL-10$^+$, C) interferon (IFN)-γ$^+$/IL-10$^+$, E) tumor necrosis factor (TNF)-α$^+$/IL-10$^+$, G) IL-17A$^+$/IL-10$^+$, I) IL-2$^+$/IL-17A$^+$, K) IFN-γ$^+$/IL-17A$^+$, and M) TNF-α$^+$/IL-17A$^+$ cells in the stimulated CD4$^+$ T_H cell population, as well as the intensity ratios of B) IL-2/IL-10, D) IFN-γ/IL-10, F) TNF-α/IL-10, H) IL-17A/IL-10, J) IL-2/IL-17A, L) IFN-γ/IL-17A, and N) TNF-α/IL-17A expression, represented by the median fluorescence intensity (MFI), on stimulated CD4$^+$ T_H cells of healthy controls belonging to the ≤30 (N=40), 31-35 (N=13), 36-40 (N=7), and >40 (N=15) age groups are shown. Kruskal-Wallis test performed, accompanied by the Dunn's test for multiple comparisons, median displayed. ns: non-significant, *: p≤0.05, **: p≤0.01*

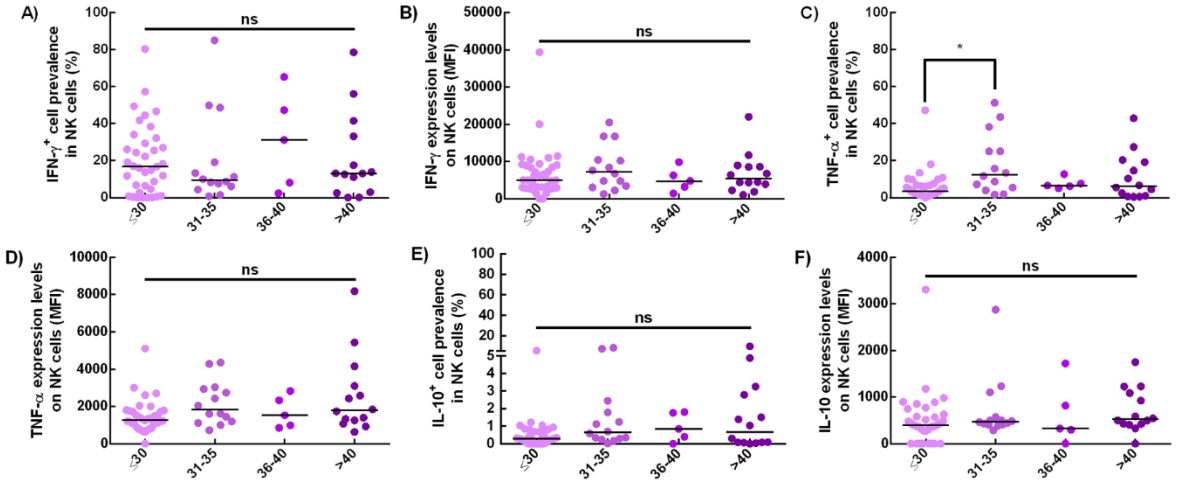


Figure 114. Cytokine production by stimulated Natural Killer (NK) cells of control women belonging to different age-associated subgroups. *The prevalence of A) interferon (IFN)-γ⁺, C) tumor necrosis factor (TNF)-α⁺, and E) interleukin (IL)-10⁺ cells in the stimulated NK cell population, as well as the intensity of B) IFN-γ, D) TNF-α, and F) IL-10 expression, represented by the median fluorescence intensity (MFI), on stimulated NK cells of healthy controls belonging to the ≤30 (N=37), 31-35 (N=14), 36-40 (N=5), and >40 (N=14) age groups are depicted. Kruskal-Wallis test performed, accompanied by the Dunn's test for multiple comparisons, median shown. ns: non-significant, *: p≤0.05*

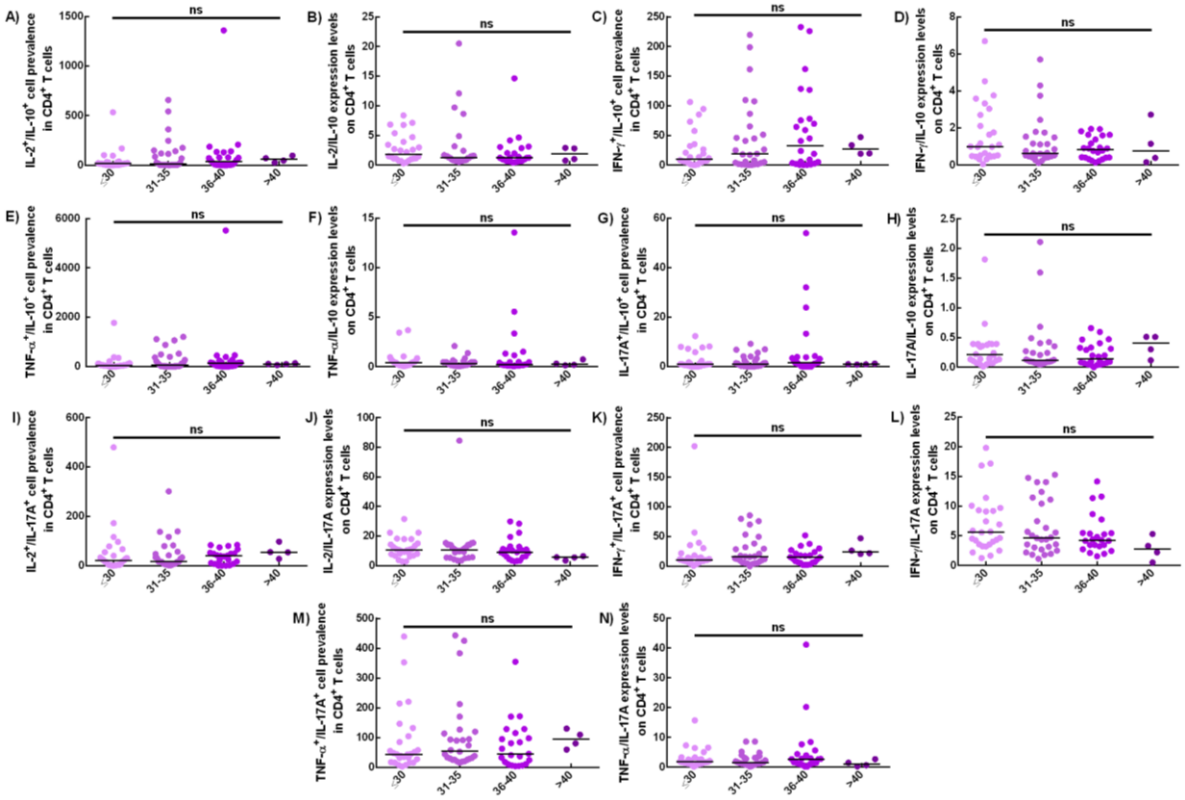


Figure 115. Ratios of cytokine production by stimulated T helper (T_H) cells of women with recurrent pregnancy loss (RPL) belonging to different age-associated subgroups. *The prevalence ratios of A) interleukin (IL)-2$^+$/IL-10$^+$, C) interferon (IFN)-γ$^+$/IL-10$^+$, E) tumor necrosis factor (TNF)-α$^+$/IL-10$^+$, G) IL-17A$^+$/IL-10$^+$, I) IL-2$^+$/IL-17A$^+$, K) IFN-γ$^+$/IL-17A$^+$, and M) TNF-α$^+$/IL-17A$^+$ cells in the stimulated CD4$^+$ T_H cell population, as well as the intensity ratios of B) IL-2/IL-10, D) IFN-γ/IL-10, F) TNF-α/IL-10, H) IL-17A/IL-10, J) IL-2/IL-17A, L) IFN-γ/IL-17A, and N) TNF-α/IL-17A expression, represented by the median fluorescence intensity (MFI), on stimulated CD4$^+$ T_H cells of women with RPL belonging to the ≤30 (N=27), 31-35 (N=28), 36-40 (N=23), and >40 (N=4) age groups are shown. Kruskal-Wallis test performed, accompanied by the Dunn's test for multiple comparisons, median displayed. ns: non-significant*

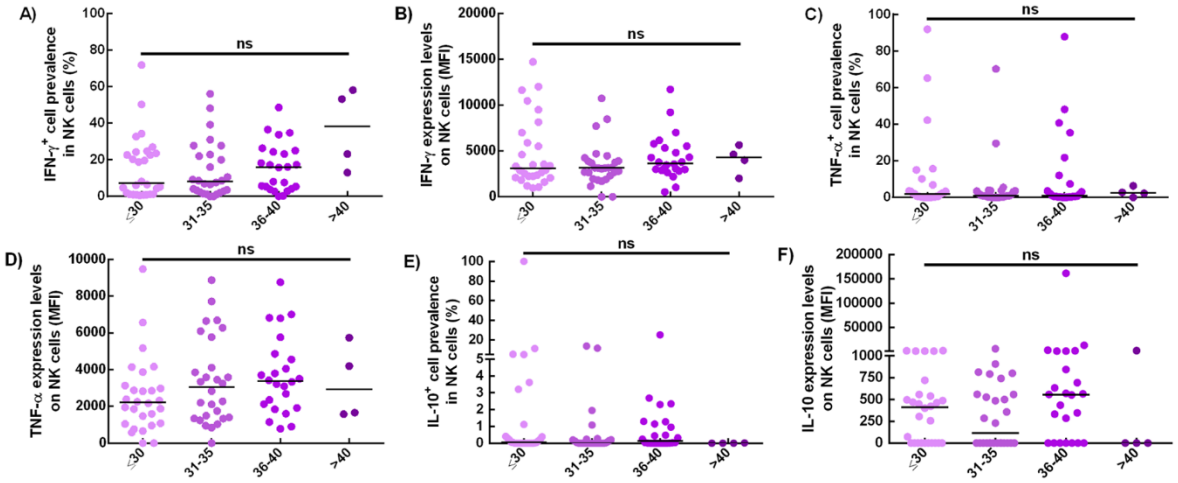


Figure 116. Cytokine production by stimulated Natural Killer (NK) cells of women with recurrent pregnancy loss (RPL) belonging to different age-associated subgroups. *The prevalence of A) interferon (IFN)-γ$^+$, C) tumor necrosis factor (TNF)-α$^+$, and E) interleukin (IL)-10$^+$ cells in the stimulated NK cell population, as well as the intensity of B) IFN-γ, D) TNF-α, and F) IL-10 expression, represented by the median fluorescence intensity (MFI), on stimulated NK cells of women with RPL belonging to the ≤30 (N=28), 31-35 (N=28), 36-40 (N=24), and >40 (N=4) age groups are depicted. Kruskal-Wallis test performed, accompanied by the Dunn's test for multiple comparisons, median shown. ns: non-significant*

Similarly, ethnicity-associated variation in cytokine production was evaluated in the control and RPL cohorts. IL-2$^+$/IL-10$^+$, IFN-γ$^+$/IL-10$^+$, TNF-α$^+$/IL-10$^+$, IL-17A$^+$/IL-10$^+$, IL-2$^+$/IL-17A$^+$, IFN-γ$^+$/IL-17A$^+$, and TNF-α$^+$/IL-17A$^+$ T_H cell levels did not appear different between control women of different ethnic backgrounds (Figures 117A, 117C, 117E, 117G, 117I, 117K, 117M). Although IL-2/IL-10, IL-17A/IL-10, IL-2/IL-17A, and TNF-α/IL-17A expression levels on T_H cells of control women also appeared unaltered between ethnic groups, IFN-γ/IL-10 levels were reduced in women of Mixed ethnicity, compared to Asian and White controls (p=0.0095), TNF-α/IL-10 levels were decreased in women of Mixed ethnicity, compared to Asian, Black, and White women (p=0.0061), and IFN-γ/IL-17A levels on these cells were elevated in White compared to Black control women (p=0.0307) (Figures 117B, 117D, 117F, 117H, 117J, 117L, 117N). IFN-γ, TNF-α, and IL-10 production by NK cells did not appear significantly different between the ethnic subgroups of the control population (Figures 118A-118F). Comparing the Asian and White subgroups of the RPL cohort, no significant difference in T_H and NK cell cytokine production could be detected (Figures 119-120).

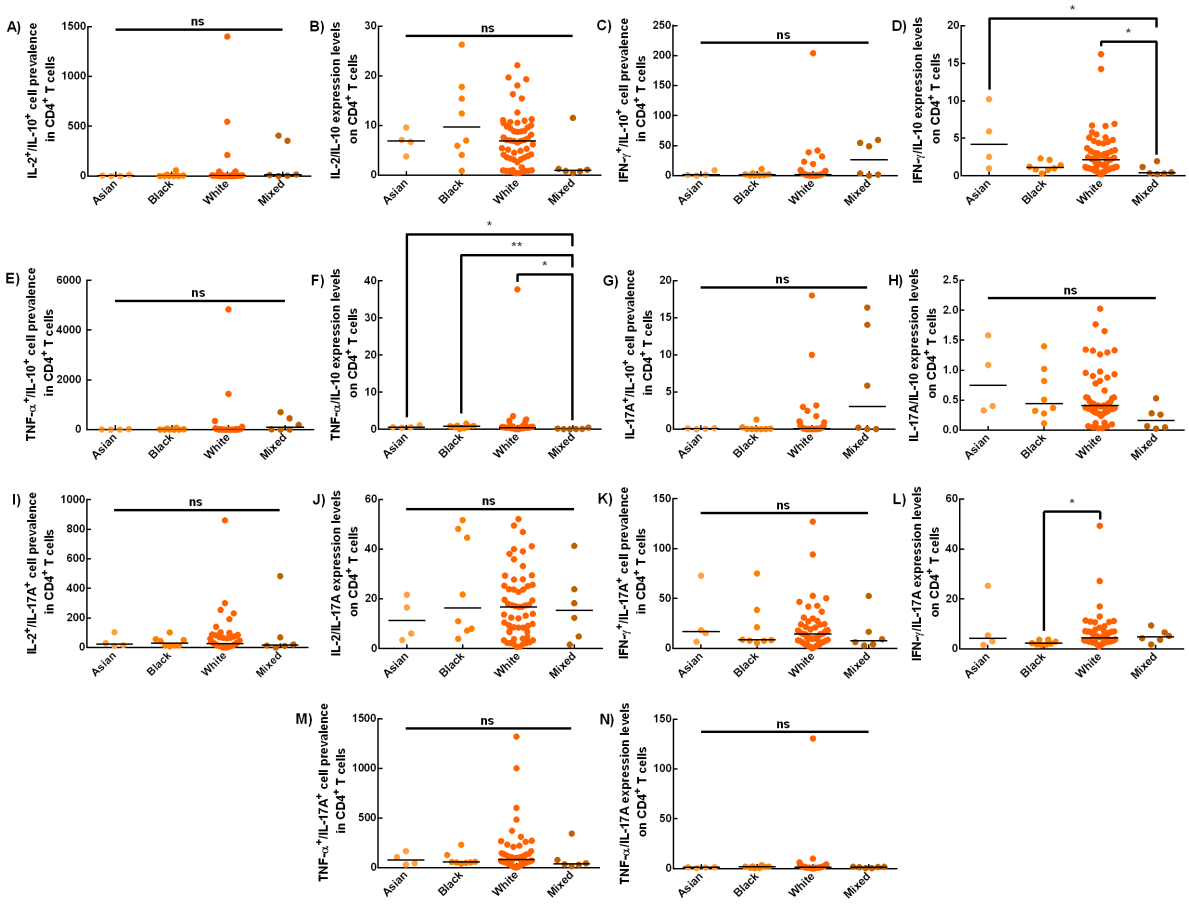


Figure 117. Ratios of cytokine production by stimulated T helper (T_H) cells of control women belonging to different ethnic subgroups. *The prevalence ratios of A) interleukin (IL)-2$^+$/IL-10$^+$, C) interferon (IFN)-γ$^+$/IL-10$^+$, E) tumor necrosis factor (TNF)-α$^+$/IL-10$^+$, G) IL-17A$^+$/IL-10$^+$, I) IL-2$^+$/IL-17A$^+$, K) IFN-γ$^+$/IL-17A$^+$, and M) TNF-α$^+$/IL-17A$^+$ cells in the stimulated CD4$^+$ T_H cell population, as well as the intensity ratios of B) IL-2/IL-10, D) IFN-γ/IL-10, F) TNF-α/IL-10, H) IL-17A/IL-10, J) IL-2/IL-17A, L) IFN-γ/IL-17A, and N) TNF-α/IL-17A expression, represented by the median fluorescence intensity (MFI), on stimulated CD4$^+$ T_H cells of healthy controls belonging to the Asian (N=4), Black (N=8), White (N=57), and Mixed (N=6) ethnic groups are illustrated. Kruskal-Wallis test performed, accompanied by the Dunn's test for multiple comparisons, median depicted. ns: non-significant, *: p≤0.05, **: p≤0.01*

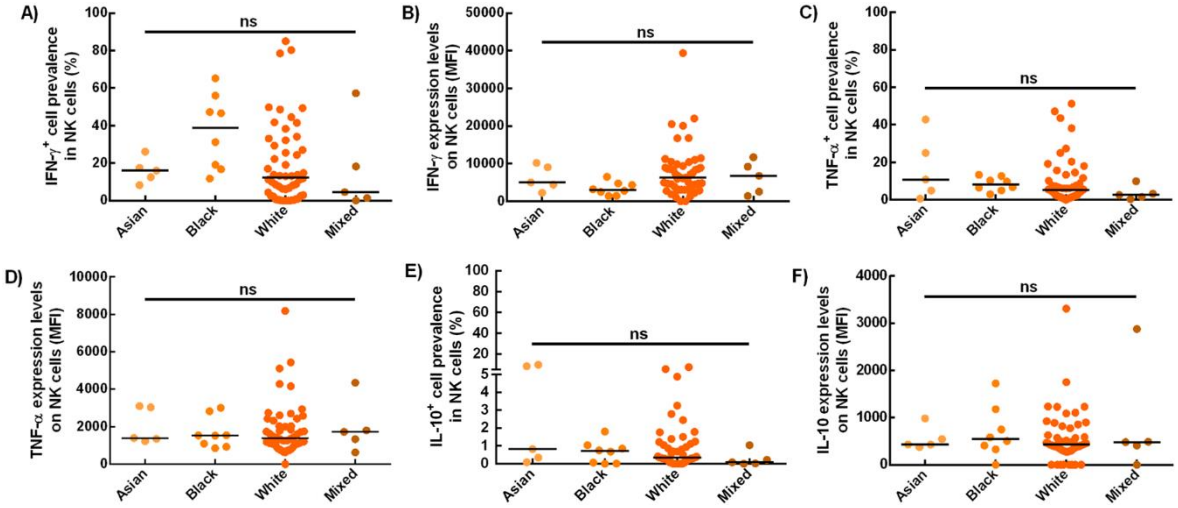


Figure 118. Cytokine production by stimulated Natural Killer (NK) cells of control women belonging to different ethnic subgroups. *The prevalence of A) interferon (IFN)-γ⁺, C) tumor necrosis factor (TNF)-α⁺, and E) interleukin (IL)-10⁺ cells in the stimulated NK cell population, as well as the intensity of B) IFN-γ, D) TNF-α, and F) IL-10 expression, represented by the median fluorescence intensity (MFI), on stimulated NK cells of healthy controls belonging to the Asian (N=5), Black (N=8), White (N=52), and Mixed (N=5) ethnic groups are shown. Kruskal-Wallis test performed, accompanied by the Dunn's test for multiple comparisons, median displayed. ns: non-significant*

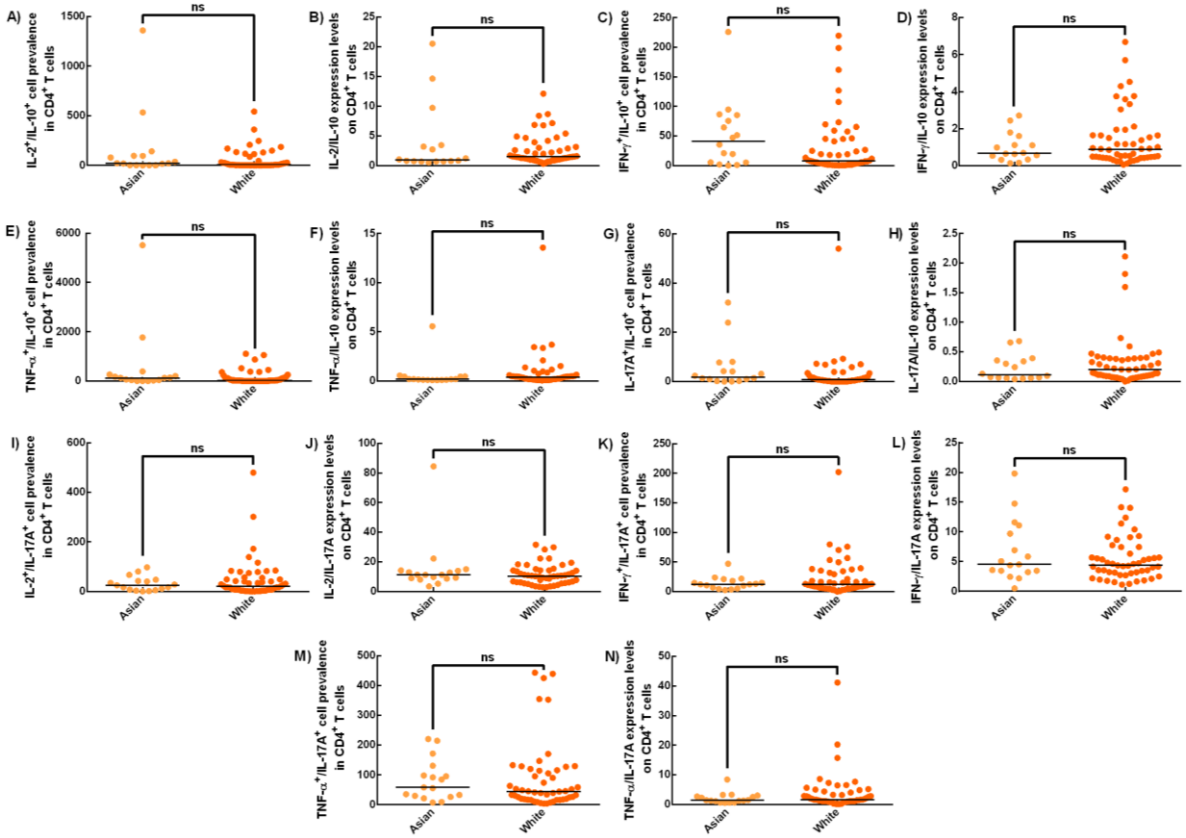


Figure 119. Ratios of cytokine production by stimulated T helper (T_H) cells of women with recurrent pregnancy loss (RPL) belonging to different ethnic subgroups. *The prevalence ratios of A) interleukin (IL)-2$^+$/IL-10$^+$, C) interferon (IFN)-γ$^+$/IL-10$^+$, E) tumor necrosis factor (TNF)-α$^+$/IL-10$^+$, G) IL-17A$^+$/IL-10$^+$, I) IL-2$^+$/IL-17A$^+$, K) IFN-γ$^+$/IL-17A$^+$, and M) TNF-α$^+$/IL-17A$^+$ cells in the stimulated CD4$^+$ T_H cell population, as well as the intensity ratios of B) IL-2/IL-10, D) IFN-γ/IL-10, F) TNF-α/IL-10, H) IL-17A/IL-10, J) IL-2/IL-17A, L) IFN-γ/IL-17A, and N) TNF-α/IL-17A expression, represented by the median fluorescence intensity (MFI), on stimulated CD4$^+$ T_H cells of women with RPL belonging to the Asian (N=16), and White (N=52) ethnic groups are illustrated. Mann-Whitney test performed, median depicted. ns: non-significant*

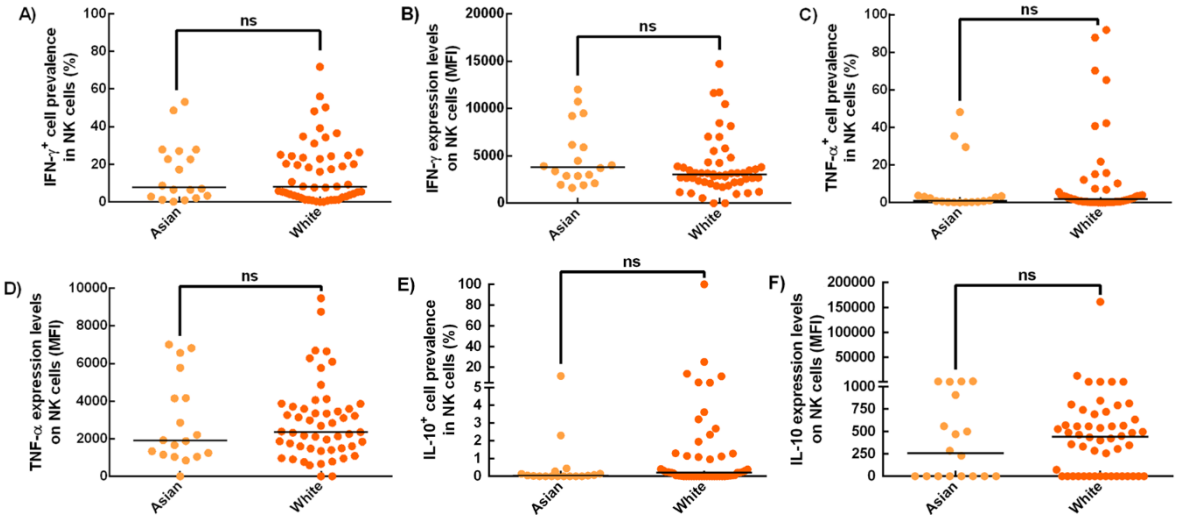


Figure 120. Cytokine production by stimulated Natural Killer (NK) cells of women with recurrent pregnancy loss (RPL) belonging to different ethnic subgroups. *The prevalence of A) interferon (IFN)-γ⁺, C) tumor necrosis factor (TNF)-α⁺, and E) interleukin (IL)-10⁺ cells in the stimulated NK cell population, as well as the intensity of B) IFN-γ, D) TNF-α, and F) IL-10 expression, represented by the median fluorescence intensity (MFI), on stimulated NK cells of women with RPL belonging to the Asian (N=18) and White (N=52) ethnic groups are shown. Mann-Whitney test performed, median displayed. ns: non-significant*

To control for ethnic variation between the RPL and control cohorts, cytokine markers displaying a significant change between the total RPL and control groups were also compared between White women with RPL and White controls. In White women with RPL reduced unstimulated TNF-α⁺ ($p<0.0001$) and IL-10⁺ ($p<0.0001$) and stimulated TNF-α⁺ ($p<0.0001$) and IL-10⁺ ($p<0.0001$) T_H cell levels were seen, while IL-2⁺ and IL-17A⁺ T_H cell prevalence upon stimulation appeared unaltered (Figures 121A, 121C, 121D, 121F, 121H, 121J). TNF-α expression levels on unstimulated T_H cells ($p=0.0078$) and IL-10 expression levels on stimulated T_H cells ($p=0.0004$) appeared elevated in White women with RPL, while IL-2 levels on stimulated T_H cells were reduced ($p=0.0056$) and TNF-α levels on these cells were unaltered (Figures 121B, 121E, 121G, 121I). Upon stimulation in the T_H cell

population of White women with RPL, augmented IL-2^+/IL-10^+ ($p=0.0025$), IFN-γ^+/IL-10^+ ($p<0.0001$), TNF-α^+/IL-10^+ ($p=0.0001$), and IL-$17A^+$/IL-10^+ ($p<0.0001$) and reduced TNF-α^+/IL-$17A^+$ ($p=0.0179$) cell prevalence was detected compared to controls of a White ethnic background (Figures 122A, 122C, 122E, 122G, 122J). Conversely, in White women with RPL decreased IL-2/IL-10 ($p<0.0001$), IFN-γ/IL-10 ($p<0.0001$), IL-17A/IL-10 ($p<0.0001$), and IL-2/IL-17A ($p=0.0492$), elevated TNF-α/IL-17A ($p=0.0118$), and unaltered TNF-α/IL-10 expression levels on stimulated NK cells were seen (Figures 122B, 122D, 122F, 122H, 122I, 122K). Furthermore, reduced TNF-α^+ unstimulated ($p<0.0001$) and stimulated ($p=0.0031$) NK cell levels, unaltered IL-10^+ unstimulated and stimulated NK cell prevalence, and decreased TNF-α^+ unstimulated $CD56^{dim}CD16^+$ NK cell subset levels ($p=0.0187$) were displayed when comparing White women with RPL to White controls (Figures 123A, 123B, 123D, 123F, 123I). IFN-γ expression levels on stimulated NK cells of White women with RPL appeared decreased ($p<0.0001$), accompanied by elevated TNF-α ($p=0.0011$), unaltered IL-10, and a reduced ratio of IFN-γ/IL-10 ($p=0.0140$) expression levels on these cells (Figures 123C, 123E, 123G, 123H). On the $CD56^{dim}CD16^+$ NK cell subpopulation of these women unaltered TNF-α expression intensity was detected in the absence of stimulation, while IFN-γ expression levels upon stimulation also appeared similar to that of White control women (Figures 123J, 123K). In regards to protein secretion in the White women subpopulation, in the absence of stimulation reduced IL-2 ($p=0.0007$) and IL-5 ($p<0.0001$), elevated IL-17A ($p=0.0001$) and IL-8 ($p=0.0414$), and unaltered TNF-α and GM-CSF secretion by PBMCs of women with RPL was seen, while upon PBMC stimulation unaltered IL-8 and reduced IL-5 ($p<0.0001$) and IL-13 ($p=0.0002$) secretion was

detected in these women, resulting to elevated TNF-α/IL-5 (p=0.0019), IL-2/IL-13 (p=0.0215), IFN-γ/IL-13 (p=0.0039), and TNF-α/IL-13 (p<0.0001) ratios (Figures 124A-124M).

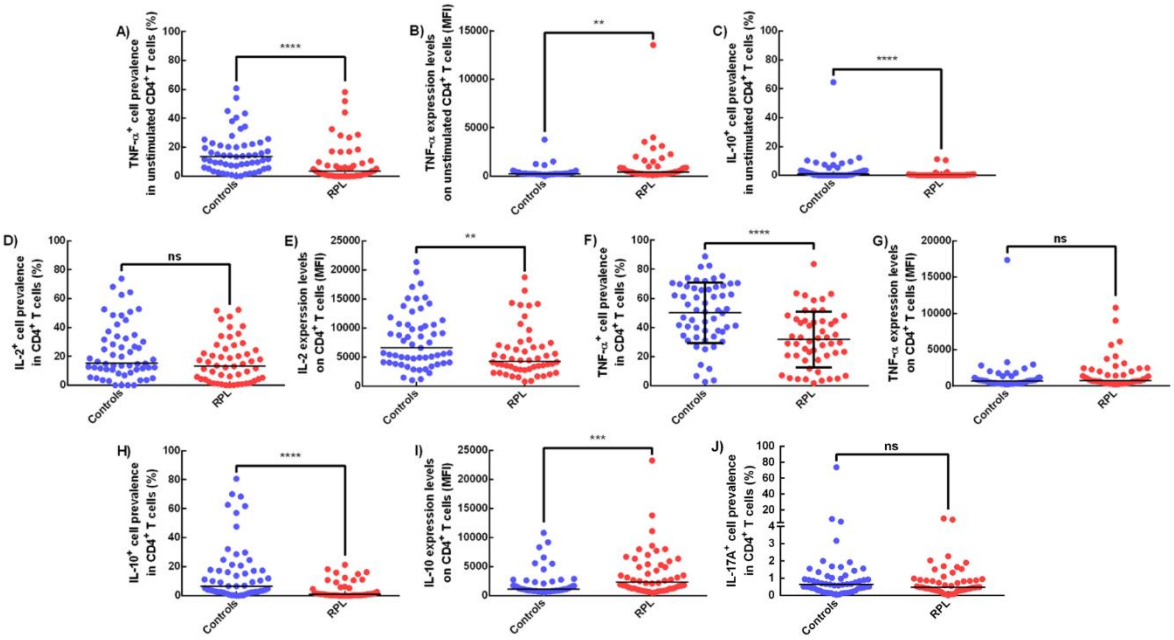


Figure 121. Cytokine production by T helper (T_H) cells of White women with recurrent pregnancy loss (RPL) and White controls. *The prevalence of A) tumor necrosis factor (TNF)-α⁺ and C) interleukin (IL)-10⁺ cells in the unstimulated CD4⁺ T_H cell population, the intensity of B) TNF-α expression, represented by the median fluorescence intensity (MFI), on unstimulated CD4⁺ T_H cells, the prevalence of D) IL-2⁺, F) TNF-α⁺, H) IL-10⁺, and J) IL-17A⁺ cells in the stimulated CD4⁺ T_H cell population, as well as the intensity of E) IL-2, G) TNF-α, and I) IL-10 expression on stimulated CD4⁺ T_H cells of healthy controls (N=57) and women with RPL (N=52) of White ethnic origin is illustrated. Normally distributed dataset without significantly different variances (F): Unpaired t test used, mean and standard deviation illustrated. Non-normally distributed datasets (A-E, G-J): Mann Whitney test performed, median depicted. ns: non-significant, **: p≤0.01, ***: p≤0.001, ****: p≤0.0001*

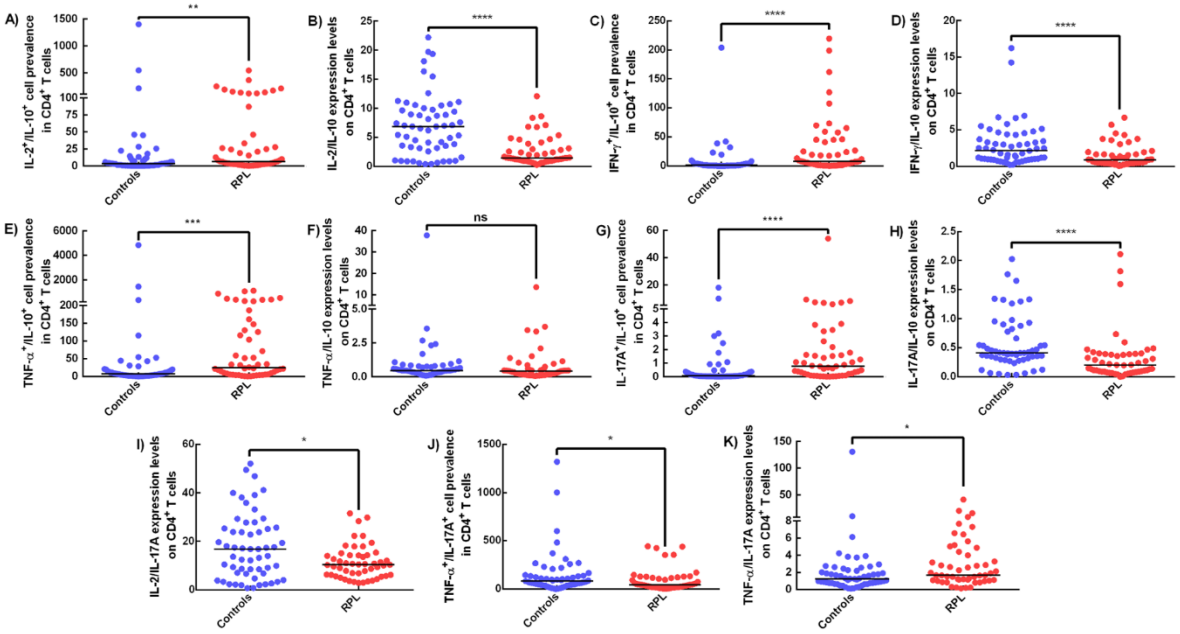


Figure 122. Ratios of cytokine production by stimulated T helper (T_H) cells of White women with recurrent pregnancy loss (RPL) and White controls. *The prevalence ratios of A) interleukin (IL)-2$^+$/IL-10$^+$, C) interferon (IFN)-γ$^+$/IL-10$^+$, E) tumor necrosis factor (TNF)-α$^+$/IL-10$^+$, G) IL-17A$^+$/IL-10$^+$, and J) TNF-α$^+$/IL-17A$^+$ cells in the stimulated CD4$^+$ T_H cell population, as well as the intensity ratios of B) IL-2/IL-10, D) IFN-γ/IL-10, F) TNF-α/IL-10, H) IL-17A/IL-10, I) IL-2/IL-17A, and K) TNF-α/IL-17A expression, represented by the median fluorescence intensity (MFI), on stimulated CD4$^+$ T_H cells of healthy controls (N=57) and women with RPL (N=52) of White ethnic origin are displayed. Mann-Whitney test performed, median depicted. ns: non-significant, *: p≤0.05, **: p≤0.01, ***: p≤0.001, ****: p≤0.0001*

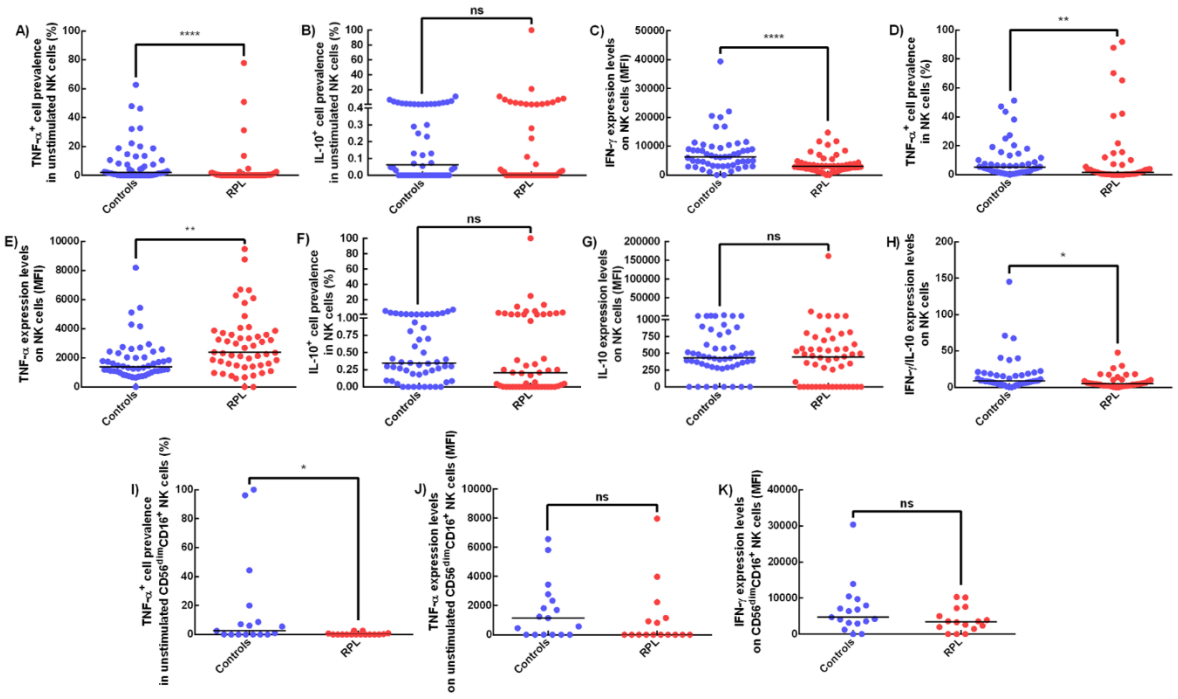


Figure 123. Cytokine production by Natural Killer (NK) cells of White women with recurrent pregnancy loss (RPL) and White controls. *The prevalence of A) tumor necrosis factor (TNF)-α$^+$ and B) interleukin (IL)-10$^+$ cells in the unstimulated NK cell population, the prevalence of D) TNF-α$^+$ and F) IL-10$^+$ cells in the stimulated NK cell population, the intensity of C) interferon (IFN)-γ, E) TNF-α, and G) IL-10 expression, represented by the median fluorescence intensity (MFI), on stimulated NK cells, as well as the intensity ratio of H) IFN-γ/IL-10 on stimulated NK cells of healthy controls (N=52) and women with RPL (N=52) of White ethnic origin is shown. I) The prevalence of TNF-α$^+$ cells in the unstimulated CD56^{dim}CD16$^+$ NK cell population, J) the intensity of TNF-α expression on unstimulated CD56^{dim}CD16$^+$ NK cells, and K) the intensity of IFN-γ expression on stimulated CD56^{dim}CD16$^+$ NK cells of healthy controls (N=17) and women with RPL (N=16) of White ethnic origin is also illustrated. Mann-Whitney test performed, median depicted. ns: non-significant, *: p≤0.05, **: p≤0.01, ****: p≤0.0001*

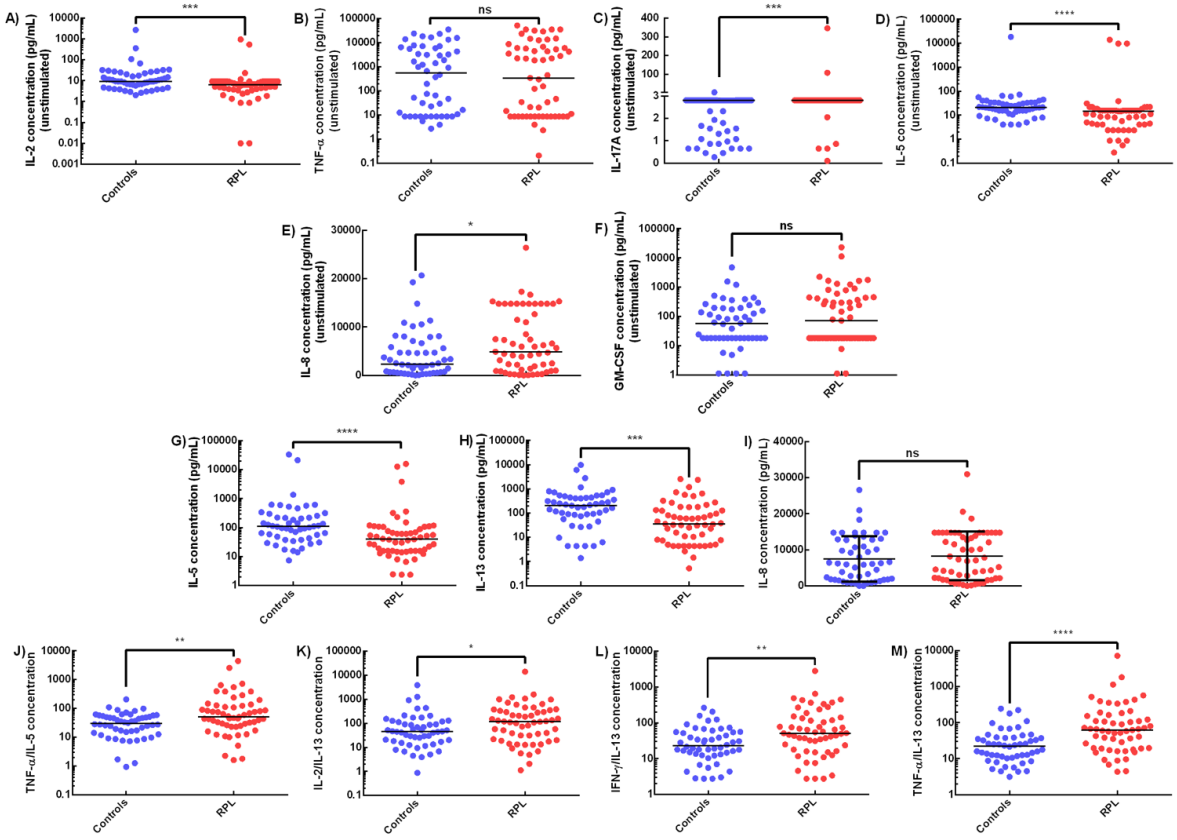


Figure 124. Protein concentration (pg/mL) in peripheral blood mononuclear cell (PBMC) cultures derived from White women with recurrent pregnancy loss (RPL) and White controls. *The levels of A) interleukin (IL)-2, B) tumor necrosis factor (TNF)-α, C) IL-17A, D) IL-5, E) IL-8, and F) granulocyte-macrophage colony-stimulating factor (GM-CSF) secretion by unstimulated PBMCs, the levels of G) IL-5, H) IL-13, and I) IL-8 by stimulated PBMCs, and the ratios of J) TNF-α/IL-5, K) IL-2/IL-13, L) interferon (IFN)-γ/IL-13, and M) TNF-α/IL-13 secretion levels by stimulated PBMCs isolated from healthy controls (N=52) and women with RPL (N=57) of White ethnic origin is depicted. Normally distributed dataset without significantly different variances (I): Unpaired t test used, mean and standard deviation illustrated. Non-normally distributed datasets (A-H, J-M): Mann Whitney test performed, median depicted. ns: non-significant, *: p≤0.05, **: p≤0.01, ***: p≤0.001, ****: p≤0.0001*

The same cytokine markers were compared between women with RPL and controls consuming low levels of alcohol, controlling for variation in alcohol intake. IL-10$^+$ cell prevalence in the unstimulated T_H cell population appeared unaltered between controls and women with RPL consuming low levels of alcohol, while TNF-α$^+$ cell prevalence was reduced in this subpopulation of women with RPL (p=0.0006), accompanied however by elevated TNF-α expression levels (p=0.0027) (Figures 125A-125C). Upon stimulation, in women with RPL consuming low levels of alcohol a decrease in TNF-α$^+$ (p=0.0002) and IL-10$^+$ (p=0.0178) T_H cell prevalence was seen, with IL-2$^+$ and IL-17A$^+$ T_H cell levels being unaltered (Figures 125D, 125F, 125H, 125J). Augmented TNF-α (p=0.0281) and unaltered IL-2 and IL-10 expression levels were also detected on stimulated T_H cells of women with RPL with low levels of alcohol intake, compared to controls with similar alcohol consumption habits (Figures 125E, 125G, 125I). Furthermore, upon stimulation elevated IFN-γ$^+$/IL-10$^+$ (p=0.0269) and IL-17A$^+$/IL-10$^+$ (p=0.0297) T_H cell prevalence, reduced IL-17A/IL-10 (p=0.0435) and increased TNF-α/IL-17A (p=0.0020) expression levels, and unaltered IL-2$^+$/IL-10$^+$, TNF-α$^+$/IL-10$^+$, and TNF-α$^+$/IL-17A$^+$ T_H cell prevalence and IL-2/IL-10, IFN-γ/IL-10, TNF-α/IL-10, and IL-2/IL-17A expression levels were detected in this RPL subpopulation (Figures 126A-126K). In regards to NK cells, TNF-α$^+$ cell prevalence in the unstimulated NK cell population appeared reduced in women with RPL consuming low levels of alcohol (p=0.0005), while IL-10$^+$ NK cell prevalence was unaltered (Figures 127A, 127B). Upon stimulation, TNF-α$^+$ and IL-10$^+$ NK cell prevalence did not appear to be significantly different between women with RPL and controls with low alcohol intake, but elevated TNF-α expression levels (p<0.0001) and unaltered levels of IFN-γ, IL-10, and IFN-γ/IL-10 were detected in

women with RPL (Figures 127C-127H). TNF-α^+ unstimulated $CD56^{dim}CD16^+$ NK cell levels, TNF-α expression intensity on these cells, and IFN-γ intensity on stimulated $CD56^{dim}CD16^+$ NK cells did not appear significantly different between women with RPL and controls in the low alcohol intake subpopulation (Figures 127I-127K). Most proteins secreted by unstimulated PBMCs, including IL-5, IL-8, IL-17A, TNF-α, and GM-CSF, did not displayed significantly different levels between the subpopulations characterised by low alcohol consumption, with the exception of IL-2 whose levels were reduced in this subpopulation of women with RPL (p=0.0266) (Figures 128A-128F). On the other hand, IL-5 (p=0.0092) and IL-13 (p=0.0191), but not IL-8, secretion by stimulated PBMCs appeared reduced in women with RPL reporting low alcohol consumption rates, resulting to elevated TNF-α/IL-13 (p=0.0390), but unaltered IL-2/IL-13, IFN-γ/IL-13, and TNF-α/IL-13 ratios (Figures 128G-128M).

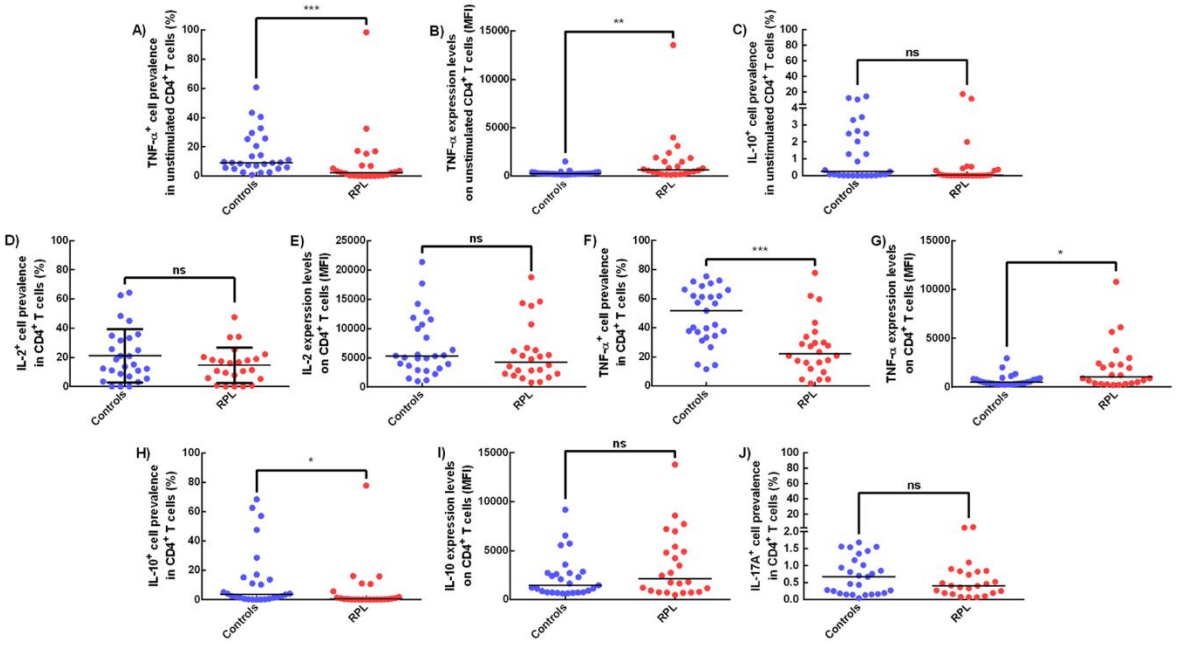


Figure 125. Cytokine production by T helper (T_H) cells of women with recurrent pregnancy loss (RPL), consuming low levels of alcohol, and controls with similar alcohol consumption habits. *The prevalence of A) tumor necrosis factor (TNF)-α$^+$ and C) interleukin (IL)-10$^+$ cells in the unstimulated CD4$^+$ T_H cell population, the intensity of B) TNF-α expression, represented by the median fluorescence intensity (MFI), on unstimulated CD4$^+$ T_H cells, the prevalence of D) IL-2$^+$, F) TNF-α$^+$, H) IL-10$^+$, and J) IL-17A$^+$ cells in the stimulated CD4$^+$ T_H cell population, as well as the intensity of E) IL-2, G) TNF-α, and I) IL-10 expression on stimulated CD4$^+$ T_H cells of healthy controls (N=27) and women with RPL (N=24), consuming low levels of alcohol, is illustrated. Normally distributed dataset without significantly different variances (D): Unpaired t test used, mean and standard deviation illustrated. Non-normally distributed datasets (A-C, E-J): Mann Whitney test performed, median depicted. ns: non-significant, *: p≤0.05, **: p≤0.01, ***: p≤0.001*

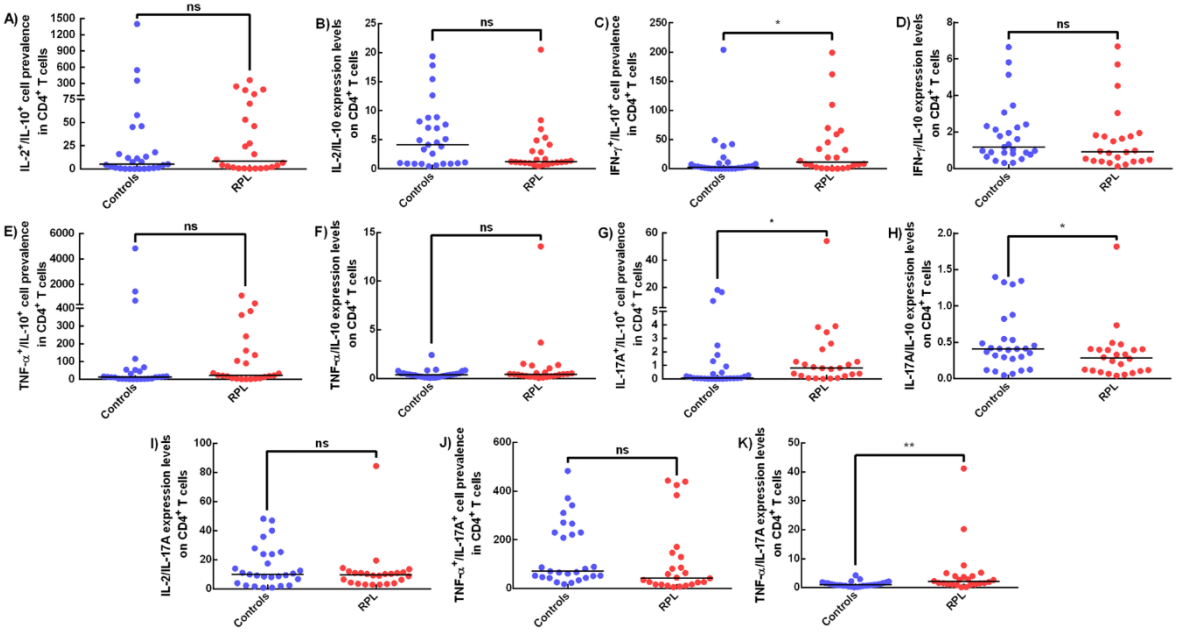


Figure 126. Ratios of cytokine production by stimulated T helper (T_H) cells of women with recurrent pregnancy loss (RPL), consuming low levels of alcohol, and controls with similar alcohol consumption habits. *The prevalence ratios of A) interleukin (IL)-2$^+$/IL-10$^+$, C) interferon (IFN)-γ$^+$/IL-10$^+$, E) tumor necrosis factor (TNF)-α$^+$/IL-10$^+$, G) IL-17A$^+$/IL-10$^+$, and J) TNF-α$^+$/IL-17A$^+$ cells in the stimulated CD4$^+$ T_H cell population, as well as the intensity ratios of B) IL-2/IL-10, D) IFN-γ/IL-10, F) TNF-α/IL-10, H) IL-17A/IL-10, I) IL-2/IL-17A, and K) TNF-α/IL-17A expression, represented by the median fluorescence intensity (MFI), on stimulated CD4$^+$ T_H cells of healthy controls (N=27) and women with RPL (N=24), consuming low levels of alcohol, are displayed. Mann-Whitney test performed, median depicted. ns: non-significant, *: p≤0.05, **: p≤0.01*

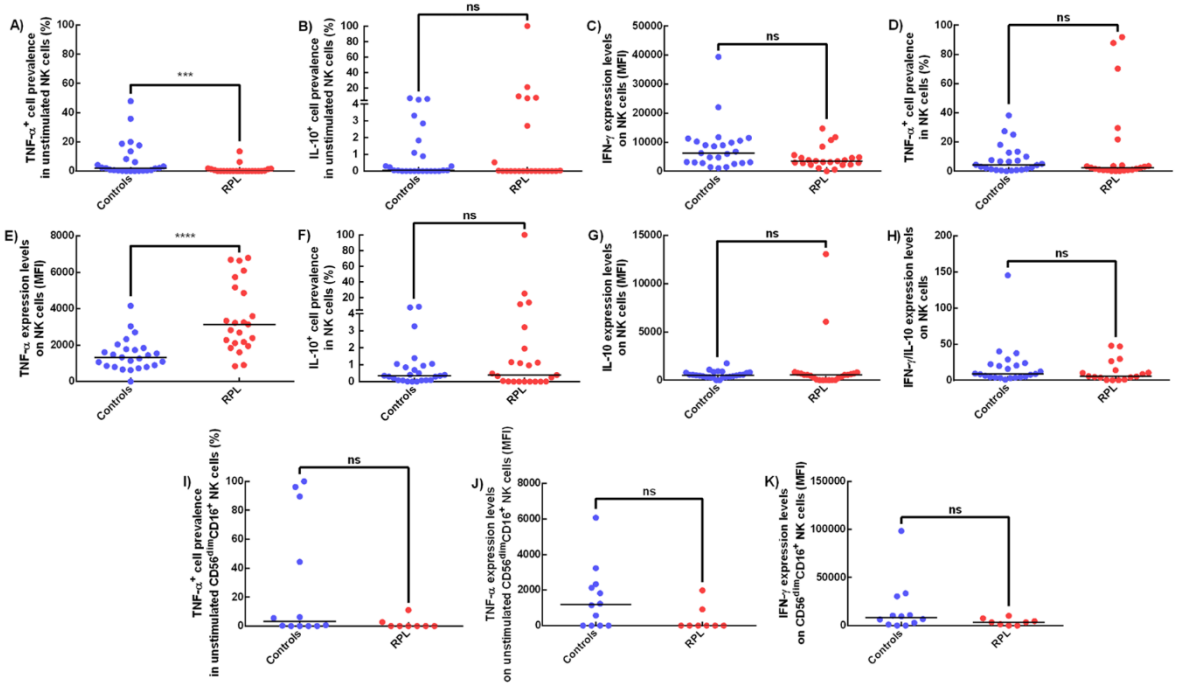


Figure 127. Cytokine production by Natural Killer (NK) cells of women with recurrent pregnancy loss (RPL), consuming low levels of alcohol, and controls with similar alcohol consumption habits. *The prevalence of A) tumor necrosis factor (TNF)-α^{+} and B) interleukin (IL)-10^{+} cells in the unstimulated NK cell population, the prevalence of D) TNF-α^{+} and F) IL-10^{+} cells in the stimulated NK cell population, the intensity of C) interferon (IFN)-γ, E) TNF-α, and G) IL-10 expression, represented by the median fluorescence intensity (MFI), on stimulated NK cells, as well as the intensity ratio of H) IFN-γ/IL-10 on stimulated NK cells of healthy controls (N=25) and women with RPL (N=23), consuming low levels of alcohol, is shown. I) The prevalence of TNF-α^{+} cells in the unstimulated CD56^{dim}CD16^{+} NK cell population, J) the intensity of TNF-α expression on unstimulated CD56^{dim}CD16^{+} NK cells, and K) the intensity of IFN-γ expression on stimulated CD56^{dim}CD16^{+} NK cells of healthy controls (N=12) and women with RPL (N=8), consuming low levels of alcohol, is also illustrated. Mann-Whitney test performed, median depicted. ns: non-significant, ***: p≤0.001, ****: p≤0.0001*

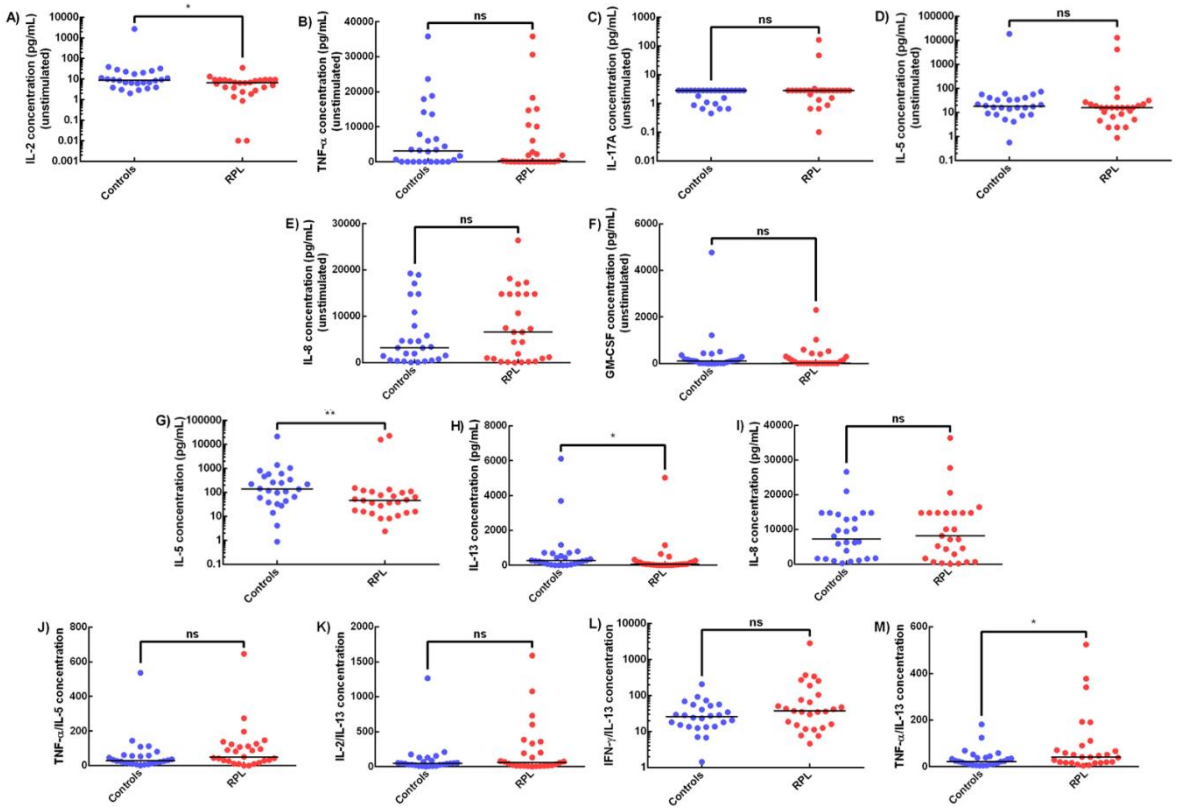


Figure 128. Protein concentration (pg/mL) in peripheral blood mononuclear cell (PBMC) cultures derived from women with recurrent pregnancy loss (RPL), consuming low levels of alcohol, and controls with similar alcohol consumption habits. *The levels of A) interleukin (IL)-2, B) tumor necrosis factor (TNF)-α, C) IL-17A, D) IL-5, E) IL-8, and F) granulocyte-macrophage colony-stimulating factor (GM-CSF) secretion by unstimulated PBMCs, the levels of G) IL-5, H) IL-13, and I) IL-8 by stimulated PBMCs, and the ratios of J) TNF-α/IL-5, K) IL-2/IL-13, L) interferon (IFN)-γ/IL-13, and M) TNF-α/IL-13 secretion levels by stimulated PBMCs isolated from healthy controls (N=26) and women with RPL (N=27), consuming low levels of alcohol, is depicted. Mann Whitney test performed, median depicted. ns: non-significant, *: p≤0.05, **: p≤0.01*

Examining the prognostic value of cytokine-associated immune markers, the IL-2^+/IL-10^+, IFN-γ^+/IL-10^+, TNF-α^+/IL-10^+, IL-$17A^+$/IL-10^+, IL-2^+/IL-$17A^+$, IFN-γ^+/IL-$17A^+$, and TNF-α^+/IL-$17A^+$ stimulated T_H cell ratios and the respective ratios of cytokine expression intensity on these cells did not appear significantly different between the RPL subgroup including women during the 3rd trimester of their following pregnancy and those with a live birth after their recruitment and the RPL subgroup of women with a subsequent miscarriage (Figures 129A-129N). Similarly, IFN-γ, TNF-α, and IL-10 production by stimulated NK cells did not appear to be altered according to the subsequent pregnancy outcome of women with RPL (Figures 130A-130F). In regards to cytokine secretion, the levels of TNF-α release ($p=0.0358$), but not the secretion of other cytokines, chemokines, or growth factors by unstimulated PBMCs appeared elevated in women with a following miscarriage (Figures 131A-131K). However, IL-2 ($p=0.0312$), IFN-γ ($p=0.0315$), IL-17A ($p=0.0287$), IL-10 ($p=0.0279$), IL-4 ($p=0.0032$), IL-5 ($p=0.0200$), IL-13 ($p=0.0305$), and GM-CSF ($p=0.0213$), but not TNF-α, IL-8, or G-CSF secretion by stimulated PBMCs was enhanced in these women (Figures 132A-132K).

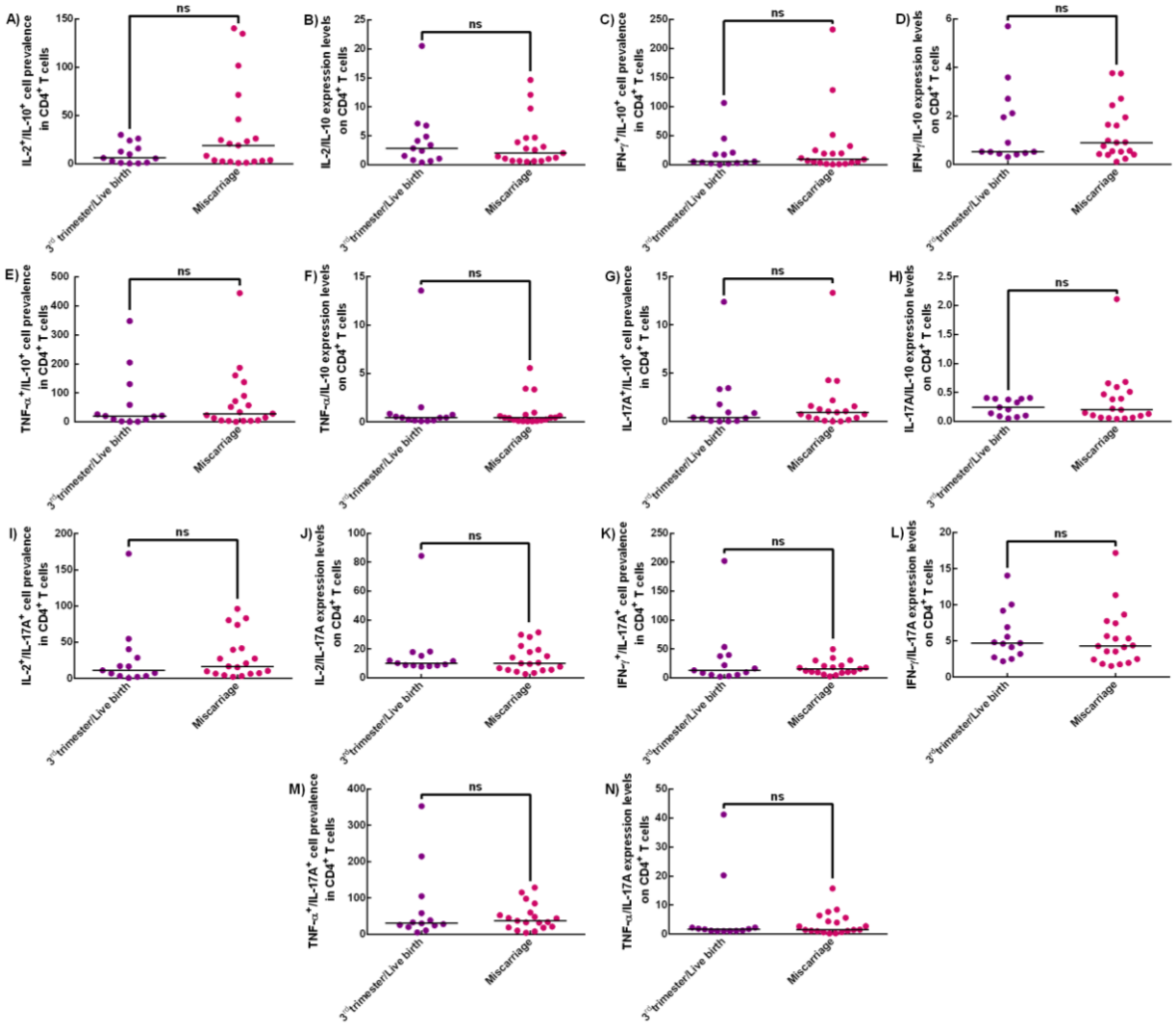


Figure 129. Ratios of cytokine production by stimulated T helper (T_H) cells of women with recurrent pregnancy loss (RPL), who were either in the 3rd trimester of their subsequent pregnancy or had a live birth, and in those with a subsequent miscarriage. *The prevalence ratios of A) interleukin (IL)-2$^+$/IL-10$^+$, C) interferon (IFN)-γ$^+$/IL-10$^+$, E) tumor necrosis factor (TNF)-α$^+$/IL-10$^+$, G) IL-17A$^+$/IL-10$^+$, I) IL-2$^+$/IL-17A$^+$, K) IFN-γ$^+$/IL-17A$^+$, and M) TNF-α$^+$/IL-17A$^+$ cells in the stimulated CD4$^+$ T_H cell population, as well as the intensity ratios of B) IL-2/IL-10, D) IFN-γ/IL-10, F) TNF-α/IL-10, H) IL-17A/IL-10, J) IL-2/IL-17A, L) IFN-γ/IL-17A, and N) TNF-α/IL-17A expression, represented by the median fluorescence intensity (MFI), on stimulated CD4$^+$ T_H cells of women with RPL belonging to the 3rd trimester/Live birth subgroup (N=13) and of those belonging to the miscarriage subgroup (N=19) are displayed. Mann-Whitney test performed, median depicted. ns: non-significant*

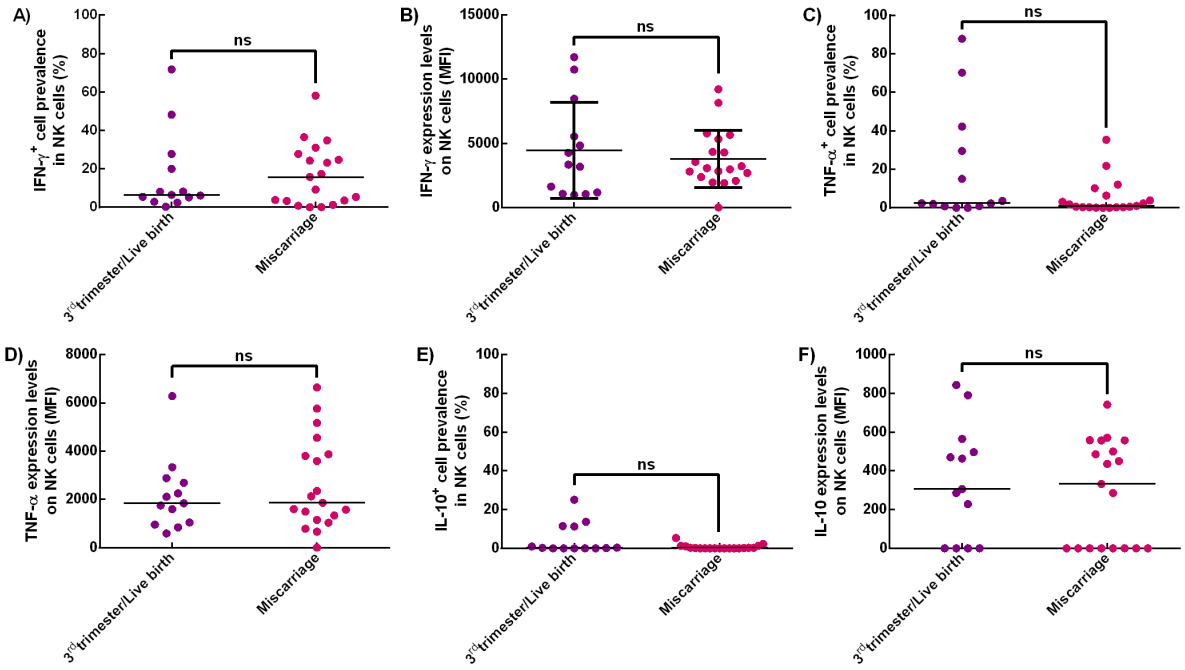


Figure 130. Cytokine production by stimulated Natural Killer (NK) cells of women with recurrent pregnancy loss (RPL), who were either in the 3rd trimester of their subsequent pregnancy or had a live birth, and in those with a subsequent miscarriage. *The prevalence of A) interferon (IFN)-γ+, C) tumor necrosis factor (TNF)-α+, and E) interleukin (IL)-10+ cells in the stimulated NK cell population, as well as the intensity of B) IFN-γ, D) TNF-α, and F) IL-10 expression, represented by the median fluorescence intensity (MFI), on stimulated NK cells of women with RPL belonging to the 3rd trimester/Live birth subgroup (N=13) and of those belonging to the miscarriage subgroup (N=19) are illustrated. Normally distributed dataset without significantly different variances (B): Unpaired t test used, mean and standard deviation shown. Non-normally distributed datasets (A, C-F): Mann Whitney test performed, median depicted. ns: non-significant*

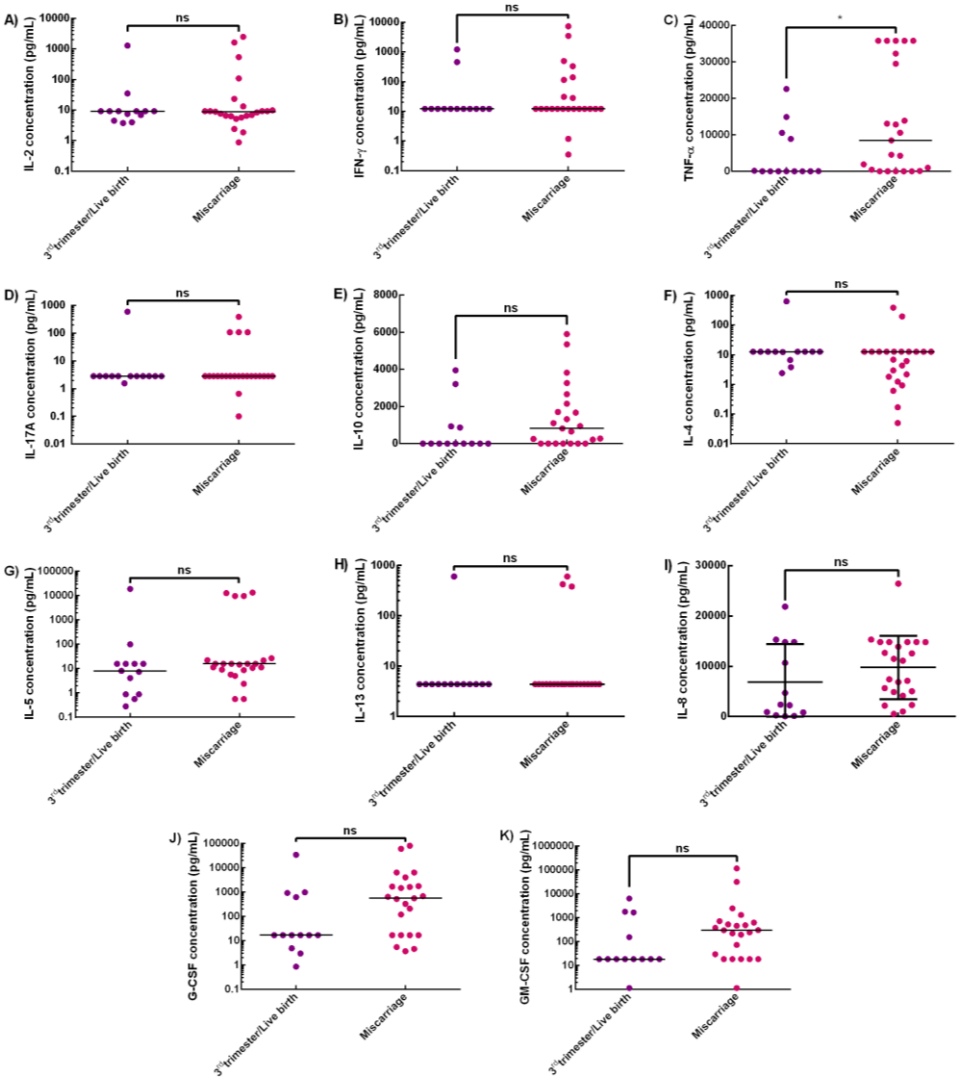


Figure 131. Protein concentration (pg/mL) in unstimulated peripheral blood mononuclear cell (PBMC) cultures derived from women with recurrent pregnancy loss (RPL), who were either in the 3rd trimester of their subsequent pregnancy or had a live birth, and in those with a subsequent miscarriage. *The levels of A) interleukin (IL)-2, B) interferon (IFN)-γ, C) tumor necrosis factor (TNF)-α, D) IL-17A, E) IL-10, F) IL-4, G) IL-5, H) IL-13, I) IL-8, J) granulocyte colony-stimulating factor (G-CSF), and K) granulocyte-macrophage colony-stimulating factor (GM-CSF) secretion by PBMCs isolated from women with RPL belonging to the 3rd trimester/Live birth subgroup (N=13) and of those belonging to the miscarriage subgroup (N=23) is shown. Normally distributed dataset without significantly different variances (I): Unpaired t test used, mean and standard deviation shown. Non-normally distributed datasets (A-H, J-K): Mann Whitney test performed, median depicted. ns: non-significant, *: p≤0.05*

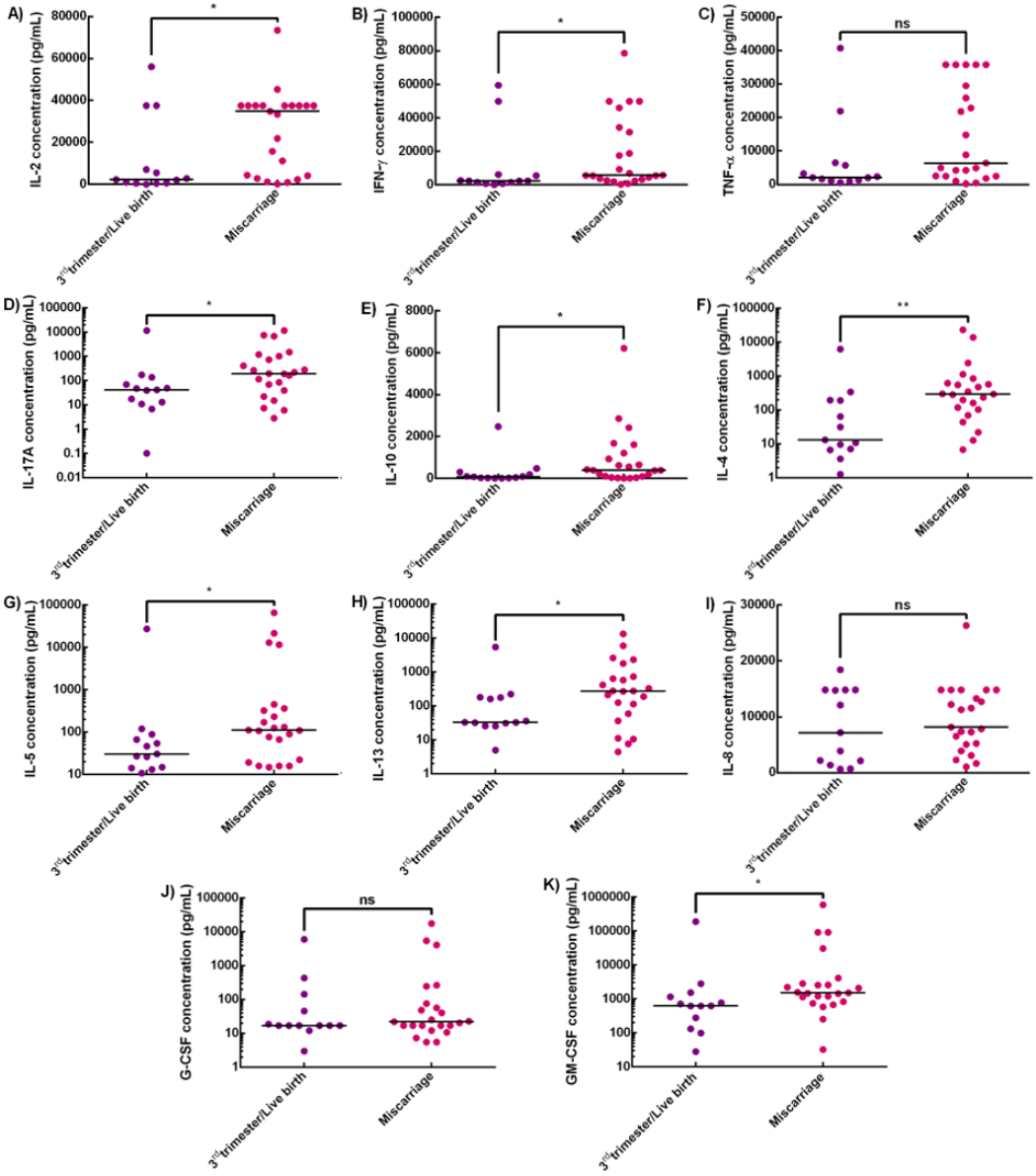


Figure 132. Protein concentration (pg/mL) in stimulated peripheral blood mononuclear cell (PBMC) cultures derived from women with recurrent pregnancy loss (RPL), who were either in the 3rd trimester of their subsequent pregnancy or had a live birth, and in those with a subsequent miscarriage. *The levels of A) interleukin (IL)-2, B) interferon (IFN)-γ, C) tumor necrosis factor (TNF)-α, D) IL-17A, E) IL-10, F) IL-4, G) IL-5, H) IL-13, I) IL-8, J) granulocyte colony-stimulating factor (G-CSF), and K) granulocyte-macrophage colony-stimulating factor (GM-CSF) secretion by PBMCs isolated from women with RPL belonging to the 3rd trimester/Live birth subgroup (N=13) and of those belonging to the miscarriage subgroup (N=23) is depicted. Mann Whitney test performed, median illustrated. ns: non-significant, *: p≤0.05, **: p≤0.01*

9.1.5 Summary

Table 32. Overview of changes in cytokine production in the peripheral blood of women with recurrent pregnancy loss (RPL) compared to control women. *Alterations in cytokine production by unstimulated (U) and stimulated (S) T helper (T_H) cells and total and $CD56^{dim}CD16^+$ Natural Killer (NK) cells detected by flow cytometry are displayed. IFN: interferon, IL: interleukin, MFI: median fluorescence intensity, TNF: tumor necrosis factor, ↓: decreased, ↑: increased, ns: non-significant, *: p≤0.05, **: p≤0.01, ***: p≤0.001, ****: p≤0.0001*

Cell type	Cytokine marker	Change in RPL compared to control group (significance)
T_H cells (U)	IL-2^+ cell prevalence (%)	ns
	IFN-γ^+ cell prevalence (%)	ns
	TNF-α^+ cell prevalence (%)	↓ (****)
	IL-10^+ cell prevalence (%)	↓ (****)
	IL-$17A^+$ cell prevalence (%)	ns
	IL-2 expression levels (MFI)	ns
	IFN-γ expression levels (MFI)	ns
	TNF-α expression levels (MFI)	↑ (****)
	IL-10 expression levels (MFI)	ns
	IL-17A expression levels (MFI)	ns
T_H cells (S)	IL-2^+ cell prevalence (%)	↓ (**)
	IFN-γ^+ cell prevalence (%)	ns
	TNF-α^+ cell prevalence (%)	↓ (****)
	IL-10^+ cell prevalence (%)	↓ (****)
	IL-$17A^+$ cell prevalence (%)	↓ (*)
	IL-2 expression levels (MFI)	↓ (*)
	IFN-γ expression levels (MFI)	ns
	TNF-α expression levels (MFI)	↑ (**)
	IL-10 expression levels (MFI)	↑ (****)
	IL-17A expression levels (MFI)	ns
	IL-2^+/IL-10^+ cell prevalence	↑ (****)
	IFN-γ^+/IL-10^+ cell prevalence	↑ (****)
	TNF-α^+/IL-10^+ cell prevalence	↑ (****)
	IL-$17A^+$/IL-10^+ cell prevalence	↑ (****)
	IL-2^+/IL-$17A^+$ cell prevalence	ns
	IFN-γ^+/IL-$17A^+$ cell prevalence	ns
	TNF-α^+/IL-$17A^+$ cell prevalence	↓ (*)
	IL-2/IL-10 expression levels	↓ (****)
	IFN-γ/IL-10 expression levels	↓ (****)
	TNF-α/IL-10 expression levels	↓ (*)
	IL-17A/IL-10 expression levels	↓ (****)
	IL-2/IL-17A expression levels	↓ (**)
	IFN-γ/IL-17A expression levels	ns
	TNF-α/IL-17A expression levels	↑ (**)
NK cells (U)	IFN-γ^+ cell prevalence (%)	ns

	TNF-α^{+} cell prevalence (%)	↓ (****)
	IL-10^{+} cell prevalence (%)	↓ (*)
	IFN-γ expression levels (MFI)	ns
	TNF-α expression levels (MFI)	ns
	IL-10 expression levels (MFI)	ns
CD56^{dim}CD16^{+} NK cells (U)	IFN-γ^{+} cell prevalence (%)	ns
	TNF-α^{+} cell prevalence (%)	↓ (**)
	IL-10^{+} cell prevalence (%)	ns
	IFN-γ expression levels (MFI)	ns
	TNF-α expression levels (MFI)	↓ (**)
	IL-10 expression levels (MFI)	ns
NK cells (S)	IFN-γ^{+} cell prevalence (%)	ns
	TNF-α^{+} cell prevalence (%)	↓ (****)
	IL-10^{+} cell prevalence (%)	↓ (***)
	IFN-γ expression levels (MFI)	↓ (***)
	TNF-α expression levels (MFI)	↑ (****)
	IL-10 expression levels (MFI)	↓ (*)
	IFN-γ^{+}/IL-10^{+} cell prevalence	ns
	TNF-α^{+}/IL-10^{+} cell prevalence	ns
	IFN-γ/IL-10 expression levels	↓ (**)
	TNF-α/IL-10 expression levels	ns
CD56^{dim}CD16^{+} NK cells (S)	IFN-γ^{+} cell prevalence (%)	ns
	TNF-α^{+} cell prevalence (%)	ns
	IL-10^{+} cell prevalence (%)	ns
	IFN-γ expression levels (MFI)	↓ (*)
	TNF-α expression levels (MFI)	ns
	IL-10 expression levels (MFI)	ns
	IFN-γ^{+}/IL-10^{+} cell prevalence	ns
	TNF-α^{+}/IL-10^{+} cell prevalence	ns
	IFN-γ/IL-10 expression levels	ns
	TNF-α/IL-10 expression levels	ns

Table 33. Overview of changes in cytokine, chemokine, and growth factor secretion in the peripheral blood of women with recurrent pregnancy loss (RPL) compared to control women. *Alterations in protein concentration (pg/mL) in unstimulated (U) and stimulated (S) peripheral blood mononuclear cell (PBMC) cultures assessed using the enzyme-linked immunosorbent assay are shown. G-CSF: granulocyte colony stimulating factor, GM-CSF: granulocyte-macrophage colony-stimulating factor, IFN: interferon, IL: interleukin, TNF: tumor necrosis factor, ↓: decreased, ↑: increased, ns: non-significant, *: p≤0.05, **: p≤0.01, ***: p≤0.001, ****: p≤0.0001*

Culture type	Protein marker	Change in RPL compared to control group (significance)
PBMCs (U)	IL-2 concentration (pg/mL)	↓ (**)
	IFN-γ concentration (pg/mL)	ns
	TNF-α concentration (pg/mL)	↑ (*)
	IL-17A concentration (pg/mL)	↑ (****)
	IL-10 concentration (pg/mL)	ns
	IL-4 concentration (pg/mL)	ns
	IL-5 concentration (pg/mL)	↓ (****)
	IL-13 concentration (pg/mL)	ns
	IL-8 concentration (pg/mL)	↑ (***)
	G-CSF concentration (pg/mL)	ns
	GM-CSF concentration (pg/mL)	↑ (**)
PBMCs (S)	IL-2 concentration (pg/mL)	ns
	IFN-γ concentration (pg/mL)	ns
	TNF-α concentration (pg/mL)	ns
	IL-17A concentration (pg/mL)	ns
	IL-10 concentration (pg/mL)	ns
	IL-4 concentration (pg/mL)	ns
	IL-5 concentration (pg/mL)	↓ (**)
	IL-13 concentration (pg/mL)	↓ (**)
	IL-8 concentration (pg/mL)	↑ (*)
	G-CSF concentration (pg/mL)	ns
	GM-CSF concentration (pg/mL)	ns
	IL-2/IL-10 concentration	ns
	IFN-γ/IL-10 concentration	ns
	TNF-α/IL-10 concentration	ns
	IL-17A/IL-10 concentration	ns
	IL-2/IL-4 concentration	ns
	IFN-γ/IL-4 concentration	ns
	TNF-α/IL-4 concentration	ns
	IL-17A/IL-4 concentration	ns
	IL-2/IL-5 concentration	ns
	IFN-γ/IL-5 concentration	ns
	TNF-α/IL-5 concentration	↑ (*)
	IL-17A/IL-5 concentration	ns

	IL-2/IL-13 concentration	↑ (*)
	IFN-γ/IL-13 concentration	↑ (**)
	TNF-α/IL-13 concentration	↑ (****)
	IL-17A/IL-13 concentration	ns

9.2 Discussion

Cytokines are molecules essential for the orchestration of immune activity and thus their levels can provide valuable information in regards to the strength and direction of immune responses. T_H cells are primary cytokine producers and their endometrial levels are thought to be increased in women with RPL,[167, 174] indicating a contribution of T_H cell cytokine production in the pathogenesis of this condition. It has long been suggested that a shift towards anti-inflammatory responses is associated with healthy pregnancy, while a pro-inflammatory shift is linked to pregnancy loss.[398] Even though this shift in immune activity is thought to primarily affect decidual populations, it is also detectable in circulation prior to conception.[404, 407, 408]

Cytokine expression on peripheral blood T_H cells was examined using flow cytometry in the absence and following cell stimulation to assess constitutive and inducible production. Interestingly, T_H cell production of all cytokines of interest was found to be increased in both the RPL and control participant groups upon stimulation, indicating that T_H responsiveness to PMA and ionomycin is not affected in RPL (Figures 85, 86). IFN-γ production appeared unaltered in women with RPL, regardless of the T_H cell stimulation state (Figures 83B, 84B, 87B, 88B). In the absence of stimulation, IL-2 production was also unaltered in women with RPL compared to controls (Figures 83A, 84A), but upon stimulation a reduction of this cytokine was evident in the RPL group (Figures 87A, 88A). Conflicting findings in

regards to TNF-α production by T_H cells were obtained, with the prevalence of TNF-α^+ cells being reduced but the expression intensity of this cytokine being augmented on both unstimulated and stimulated cells of participants with RPL (Figures 83C, 84C, 87C, 88C). Thus, in contrast to previous findings, an increase in T_H1-associated cytokine production was not evident in the circulation of non-pregnant women with RPL.[412, 413] However, in agreement to the present findings, unaltered IFN-γ and TNF-α production by peripheral blood T_H cells in women with RPL pre-conception has also been reported.[743] Similarly, although IL-10^+ T_H cell prevalence was decreased in both the absence and following stimulation in women with RPL (Figures 83D, 87D), in agreement to prior studies,[413, 414, 423] IL-10 expression levels on stimulated T_H cells were increased (Figure 88D). These findings indicate a decrease in T_H2 cell and/or Treg proportion in women with RPL, accompanied by increased production of IL-10 by individual cells upon stimulation. Moreover, following stimulation a reduction in IL-$17A^+$ T_H cell prevalence was seen in the RPL group (Figure 87E). This finding contradicts previous studies, reporting an augmentation of the T_H17 population in the peripheral blood of non-pregnant women with RPL.[423, 743, 744]

IFN-γ/IL-10 and TNF-α/IL-10 production ratios are examined in some RPL clinics, in order to diagnose “immunological” RPL. These ratios were examined alongside IL-2/IL-10, IL-17A/IL-10, IL-2/IL-17A, IFN-γ/IL-17A, and TNF-α/IL-17A to detect potential shifts in the balance between the T_H1, T_H17, and T_H2-Treg subsets in women with RPL. Interestingly, pro-/anti-inflammatory cytokine-producing T_H cell prevalence was augmented in women with RPL (Figures 89A-89D), indicating a shift towards the T_H1 and T_H17 populations, in agreement to the Type 1/Type 2

hypothesis and previous findings.[427] However, all respective ratios representing pro-/anti-inflammatory cytokine expression intensity on individual T_H cells were reduced in women with RPL (Figures 90A-90D), suggesting a reduction in cytokine production by T_H1 and T_H17 cells and/or an increased production by T_H2/Treg cells. Similarly, although the TNF-α^+/IL-17A$^+$ T_H cell prevalence and the IL-2/IL-17A production were found to be reduced in women with RPL, indicating a shift of pro-inflammatory T_H cell-mediated responses towards T_H17 activity, the TNF-α/IL-17A production levels were elevated in this participant group (Figures 89G, 90E, 90G). Thus, examination of cytokine secretion patterns was essential to determine whether alterations in the cytokine repertoire promote aberrant immunity in RPL.

As NK cells are considered primary immune mediators in pregnancy their pro- and anti-inflammatory cytokine production in women with RPL was also examined. Although the CD56^{bright}CD16$^-$ subset is thought to be predominantly responsible for cytokine production, this phenotype was not detectable using the NK cell cytokine flow cytometry panel. Hence, cytokine production by total and CD56^{dim}CD16$^+$ pNK cells was assessed. In the absence of stimulation, both total and CD56^{dim}CD16$^+$ pNK cell production of IFN-γ in women with RPL appeared unaffected (Figures 91A, 91D, 92A, 92D), compared to that of controls, in contrast to previous studies reporting an enhanced IFN-γ production pre-conception by unstimulated total and CD56^{dim}CD16$^+$ pNK cells in RPL.[190, 333] Upon stimulation similar levels of IFN-γ$^+$ total and CD56^{dim}CD16$^+$ pNK cells were detected between women with RPL and controls (Figures 97A, 97D), in agreement to prior findings.[194] However, following stimulation a reduction was detected in IFN-γ expression intensity in women with RPL (Figures 98A, 98D), indicating that even though pNK cells are capable of

responding to stimulation, synthesizing IFN-γ, they tend to produce lower amounts of these cytokines in women with RPL, not contributing as efficiently to pro-inflammatory immune activation. IFN-γ-mediated induction of HLA expression on embryonic tissues has also been described highlighting a potential NK cell self-regulating mechanism,[406] which could be affected in women with RPL. Conversely, TNF-α^+ pNK cell prevalence appeared reduced in participants with RPL upon stimulation but the expression levels of this cytokine were elevated (Figures 97B, 98B), suggesting that in these women a smaller NK cell number responds to stimulation through the production of TNF-α, synthesizing however a larger amount of this cytokine. TNF-α production by stimulated $CD56^{dim}CD16^+$ pNK cells in the RPL group appeared unaltered (Figures 97E, 98E), in agreement to previous findings,[194] suggesting that changes in the total pNK cell population were mostly driven by the $CD56^{bright}CD16^-$ subset.

In unstimulated samples, IL-10^+ pNK cell prevalence was reduced in women with RPL (Figure 91C), in agreement to the Type 1 hypothesis in RPL, but in contrast to previous findings reporting elevated proportions of these cells.[333] The levels of IL-10 expression by both total and $CD56^{dim}CD16^+$ pNK cells appeared significantly augmented following stimulation, but only in the control group and not participants with RPL (Figures 94G-94I, 96G-96I). As a result, reduced IL-10 production by total, but not $CD56^{dim}CD16^+$ stimulated pNK cells was detected in women with RPL (Figures 97C, 97F, 98C, 98F). It is thus possible that circulating NK cells with an anti-inflammatory activity, mostly belonging to the $CD56^{bright}CD16^-$ subset, are less responsive to stimulation in women with RPL, resulting to inadequate IL-10 secretion. In agreement to this hypothesis a decreased IL-4^+IL-10^+ $CD56^{bright}$ pNK

cells prevalence has been reported in women with RPL following stimulation.[194] Interestingly, in contrast to the Type 1/Type 2 hypothesis, IFN-γ/IL-10 expression levels on NK cells were found to be reduced in participants with RPL (Figure 100A), indicating an overall anti-inflammatory contribution of these cells in the periphery of women with this condition.

Even though RPL clinics offering immunological testing mostly focus on cytokine production, changes in cytokine secretion patterns are primarily orchestrating changes in immune activity. Augmented TNF-α, IL-17A, IL-8, and GM-CSF secretion by unstimulated PBMCs of women with RPL was detected (Figures 101C, 101D, 101I, 101K), in contrast to a previous study reporting reduced plasma levels of these proteins in non-pregnant women with RPL.[333] In a different study, a non-significant elevation in TNF-α levels in the blood of those women has however been observed.[412] On the other hand, decreased IL-2 and IL-5 release by the PBMCs of participants with RPL was seen in the absence of stimulation (Figures 101A, 101G). A reduction in IL-5 plasma levels in women with RPL was previously detected in agreement to this finding, accompanied however by unaltered IL-2 levels.[333] Although the secretion of most proteins of interest was found to be enhanced through stimulation, TNF-α and IL-8 levels were only increased in control participants, but not women with RPL (Figures 102G-102I, 104A-104C). Similarly, IL-10 levels were decreased upon stimulation in women with RPL, but not controls (Figures 103A-103C). Interestingly, in a previous study utilizing K562 cells as stimulants, TNF-α and IL-10 levels were reduced following stimulation in the RPL, but not control group, suggesting an increased consumption of these cytokines by

activated cells and thus highlighting another parameter of immune cell activity that should be examined in the context of RPL.[333]

Following stimulation, secreted levels of most cytokines, including IFN-γ, TNF-α, IL-4 and IL-10, appeared unaltered in women with RPL (Figure 105), parallel to prior findings.[396] However, in contrast to these findings, in a study on PBMCs stimulated with trophoblast extract, IFN-γ and TNF-α secretion was detected in PBMC cultures derived from women with RPL, but not in control ones, while detectable IL-4 and IL-10 levels were observed in cultures from fertile women but in very few cultures from non-pregnant participants with RPL.[414] A reduction in IL-5 and IL-13 secretion and an elevation in IL-8 secretion by stimulated PBMCs of women with RPL was also observed in the present study (Figures 105G-105I), contradicting previous reports of unaltered secretion of these molecules.[396, 413] Additionally, although most pro- to anti-inflammatory cytokine secretion ratios by stimulated PBMCs did not appear to be affected in the RPL compared to the control group, the IL-2/IL-13, IFN-γ/IL-13, TNF-α/IL-13, and TNF-α/IL-5 ratios were enhanced (Figure 106), in agreement to the Type 1/Type 2 hypothesis.

Overall, most changes in T_H cell-associated pro-/anti-inflammatory cytokine production ratios detected the idiopathic and non-idiopathic RPL populations were also seen in the total RPL cohort, with the exception of TNF-α^+/IL-17A$^+$ T_H cell prevalence that appeared unaltered in both the idiopathic and non-idiopathic subpopulations and TNF-α/IL-10 expression intensity, which was unaltered in women with non-idiopathic RPL (Figures 107, 109). Similarly, changes in NK cell cytokine production in these subpopulations, mostly reflected those in the original RPL cohort (Figures 108, 110). However, IL-10 expression intensity appeared

unaltered in both women with idiopathic and non-idiopathic RPL and IL-10$^+$ NK cell prevalence and IFN-γ expression intensity were not significantly different between women with non-idiopathic RPL and controls (Figures 108F, 110B, 110E, 110F). Hence, the absence of underlying RPL associated risk-factors did not appear to be clearly linked to the presence of underlying immune abnormalities in regards to cytokine production by T_H and NK cells. However, further large-cohort studies are required to evaluate differences between subpopulations of women with various underlying pathologies.

Additionally, significant alterations in T_H and NK cell-mediated cytokine production detected in women with RPL and at least five losses were also seen when comparing the total RPL cohort to controls. However, multiple parameters, including TNF-α$^+$/IL-17A$^+$ T_H cell levels, IFN-γ/IL-10, TNF-α/IL-10, IL-17A/IL-10, and TNF-α/IL-17A expression intensity on T_H cells, TNF-α$^+$ and IL-10$^+$ NK cell prevalence, and IFN-γ and IL-10 expression levels on NK cells that were found to be significantly altered in the total RPL cohort, were not significantly different in women with RPL and at least five losses compared to controls (Figures 111, 112). The reason behind such variation could be associated with the lower numbers of women in the higher order loss subgroup. In summary, women with higher order losses did not display a more intense dysregulation of immune activity.

Furthermore, most parameters associated with T_H and NK cell cytokine production did not appear to be altered between the different age-associated subgroups of the control population (Figures 113, 114). However, IL-2$^+$/IL-17A$^+$ and IFN-γ$^+$/IL-17A$^+$ T_H cell prevalence appeared elevated in control women older than 40 years of age compared to women in the ≤30 age subgroup, while TNF-α/IL-10 expression levels

on T_H cells and TNF-α^+ NK cell levels were increased in the 31-35, compared to the ≤30 subgroup (Figures 113F, 113I, 113K, 114C). These findings indicate a T_H1 pro-inflammatory shift in cytokine production in higher age groups, in agreement to the inflammaging theory, suggesting a tendency towards pro-inflammatory phenotypes throughout the aging process.[745] On the other hand, no differences in T_H and NK cell cytokine production patterns could be detected between the age-based subgroups of women with RPL (Figures 115, 116), indicating that a lack of age-associated changes in cytokine production could be linked to the pathogenesis of this condition.

Most of these parameters also appeared unaltered between the ethnicity-associated subgroups of the control cohort, with the exception of IFN-γ/IL-10 and TNF-α/IL-10 expression levels on T_H cells that were reduced in women of a Mixed ethnic background and the IFN-γ/IL-17A levels on these cells that were elevated in White compared to Black control women (Figures 117, 118). However, as this analysis could not be performed in women with RPL of Black and Mixed Ethnic origin and no significant difference could be detected between Asian and White women with RPL (Figures 119, 120), the potential influence of ethnicity on T_H and NK cell-mediated cytokine production in RPL remains unclear. In order to account for ethnic variation, cytokine-associated parameters that were found to be significantly different between the total RPL and control cohorts were assessed in White subpopulations. Even though most significant changes between women with RPL and controls were reflected by the White-only subpopulations, certain parameters, including but not restricted to TNF-α/IL-10 expression levels on T_H cells, IL-10^+ NK cell percentage and IL-10 expression intensity, TNF-α and IFN-γ levels on $CD56^{dim}CD16^+$ NK cells,

and GM-CSF and TNF-α secretion by unstimulated PBMCs, were not significantly altered in White women with RPL compared to White controls (Figures 121-124). These results highlight a potential influence of ethnic variation on immune differences between the total RPL and control populations. Hence, in future studies the use of ethnicity-controlled cohorts would be advisable.

Accordingly, multiple cytokine markers significantly altered between women with RPL and controls also displayed a significant difference when comparing only the subpopulations of these women consuming low levels of alcohol. However, numerous cytokine-associated parameters altered in the RPL population compared to controls appeared unaltered when comparing women with RPL consuming low levels of alcohol to controls with similar alcohol consumption habits. These parameters included, but were not restricted to IL-2^+/IL-10^+, TNF-α^+/IL-10^+, and TNF-α^+/IL-$17A^+$ T_H cell prevalence, IL-2/IL-10, IFN-γ/IL-10, TNF-α/IL-10, IL-2/IL-17A expression levels on T_H cells, IL-10^+ and TNF-α^+ NK cell prevalence, IFN-γ/IL-10 expression levels on NK cells, as well as IL-8, IL-2/IL-13, IFN-γ/IL-13, and TNF-α/IL-5 secretion by stimulated PBMCs (Figures 125-128). Thus, the significance of multiple cytokine-associated alterations in women with RPL could have been influenced by variation in alcohol consumption rates detected between these women and controls. Present findings should serve as an indication that alcohol influence on immune activity prior to and during early pregnancy warrants further investigation.

Regarding the prognostic value of cytokine immune parameters, the assessment of T_H cell pro-/anti-inflammatory cytokine production ratios and IFN-γ, TNF-α, and IL-10 production by NK cells revealed no predictive potential (Figures 129, 130).

However in women with RPL and a following miscarriage augmented TNF-α secretion by unstimulated PBMCs and elevated GM-CSF, IL-2, IL-4, IL-5, IL-10, IL-13, IL-17A, and IFN-γ secretion by stimulated PBMCs was detected compared to women that were either in the 3rd trimester of their subsequent pregnancy at the time of the follow-up or had a live birth (Figures 131, 132). In contrast to these findings, in pregnant women with RPL, IFN-γ, IL-10, and IL-4 secretion by PBMCs was reported not to be significantly different between women with a subsequent miscarriage and those with a live birth.(449) Pre-conception circulating TNF-α, IL-4, IL-10, and IFN-γ levels did not appear predictive of pregnancy outcome in women with RPL.(175, 746) Moreover, in these women no prognostic potential of endometrial IL-4, and IFN-γ secretion assessment could be detected.(421) On the other hand, in the circulation of women with this condition, decreased TNF-α levels post-conception have been linked to a following miscarriage.(449) Hence, although contradicting findings have been displayed in regards to the prognostic value of cytokine evaluation in RPL, a predictive potential of elevated pro- and anti-inflammatory protein secretion pre-conception was seen and should be further investigated.

To sum up, disturbances in cytokine expression in women with RPL were observed. Defective pro- and anti-inflammatory cytokine production by NK cells could result to inadequate support to pregnancy establishment. NK cells' IFN-γ, TNF-α, and IL-10 secretion is thought to contribute to spiral artery remodelling and angiogenesis and control trophoblast invasion.(141, 194) Dysregulation of these processes could result to placentation defects, inadequate oxygen and nutrient supply, and thus fetal demise. The T_H1 shift in secreted cytokine levels observed in women with RPL could

promote the activation of cellular immunity hindering the establishment of systemic tolerance to the fetal semi-allograft. In addition, enhanced secretion of TNF-α and IL-8 could facilitate blood clot formation threatening pregnancy maintenance.[406] Increased secreted levels of both pro- and anti-inflammatory cytokines also appeared predictive of subsequent loss in women with RPL. Although the pathogenic mechanism behind such association remains to be elucidated, this change in cytokine secretion patterns could indicate the presence of an over-active immune system, with aberrant responses underlying early pregnancy, possibly interfering with embryo selection, implantation, and local remodelling.

9.2.1 Limitations and future research

The assessment of cytokine synthesis and release patterns could provide a valuable insight in the immune pathogenesis underlining RPL. In the flow cytometry assay, which is most commonly used in clinical practice, T_H cells were defined according to their $CD3^+CD8^-$ phenotype, due to CD4 downregulation by mitogenic stimulation.[608] This gating however, may allow the inclusion of cytokine production by other cell types, like NKT and γδT cells. Another gating issue was encountered in the NK cell cytokine panel, with the $CD56^{bright}CD16^-$ subset not being present at detectable levels. As a $CD56^+CD16^+$ subpopulation was detectable, these cells were characterised as $CD56^{dim}CD16^+$, resulting in the absence of a $CD56^{bright}CD16^-$ subpopulation (Figure 14). PMA and ionomycin stimulation or the fixation/permeabilization procedure could have possibly induced phenotypic changes to NK cell subsets. For instance, reduced CD56 expression on NK cells upon ionomycin treatment has been observed,[747] while PMA was shown to induce CD16 shedding, significantly down-modulating CD16 expression on these cells.[748]

Thus, the combination of these stimulants could impede subset identification, even though the respective protocol was meticulously optimised and validated (Appendices, Chapters 13.5-13.7). Other commonly used NK cell stimulants, including IL-2 and IL-15, could also affect NK cell phenotype, promoting CD16 expression.[749] Due to the central role of the $CD56^{bright}CD16^{-}$ subset in cytokine production, with its prevalence being remarkably elevated in the uterus, further examination of the effects of different stimulation conditions and fixation/permeabilization protocols would be valuable to accurately identify and study this NK subpopulation.

In addition to flow cytometry, ELISA could provide a useful technique for the identification of cytokine markers in the peripheral blood of women with RPL. In this study, ELISA was used to examine PBMCs' secretion patterns to evaluate the extent of pro- or an anti-inflammatory changes in RPL. The whole PBMC population was examined due to the limited number of cells available, but individual assessment of NK and T_H cells in future studies would be beneficial. These experiments would be particularly helpful in cases where an increased prevalence and a reduced expression intensity of a cytokine, and vice versa, was detected by flow cytometry. Serum or plasma ELISAs could be also utilised for the direct assessment of the levels of these cytokines in the circulation.

PMA and ionomycin were used in this study as NK and T_H cell stimulants. PMA and ionomycin are commonly used for the stimulation of T_H cell cytokine production and can also be employed for NK cell stimulation.[194, 370, 585] A combination of IL-2 and IL-18 is often used for NK cell activation by a weaker, more physiological stimulus.[750] As cytokine levels in women with RPL is potentially altered, unspecific

stimulation with PMA and ionomycin was preferred. However, the use of different stimulants, like K562 cells, embryonic cells, trophoblast debri, and cytokines could also be evaluated to determine whether differences in cytokine production observed in women with RPL are affected by the type of stimulation.

The number of RPL and control samples examined for cytokine production and secretion does not reflect the total cohorts recruited due to the inadequate amount of blood available in certain cases. Assessment via flow cytometry was also limited by elevated cell death rates (>40%) in a number of samples (*N*=26). Investigation of the $CD56^{dim}CD16^{+}$ NK cells' cytokine production patterns was not always feasible due to the small prevalence of this population. Analysis of samples with low $CD56^{dim}CD16^{+}$ NK cell numbers (<100 cells) would disproportionately skew the cytokine data and was thus avoided.

10 IMMUNE BIOMARKERS FOR THE IDENTIFICATION OF WOMEN WITH RPL

10.1 Results

Of 111 potential markers analysed (Supplementary Table 2), 18 were highlighted via the combination of EN and LASSO modelling methods (Figures 133, 134). Specifically, reduced $CD3^+$ T (p=5.2e-08) and $CD56^{bright}CD16^-$ NK (p=0.0013) cell prevalence was detected in women with RPL, accompanied by decreased total (p=1.4e-07) and $CD56^{dim}CD16^+$ (p=0.00063) NK cell activation and reduced granzyme A secretion by stimulated PBMCs (p=1.4e-09) (Figure 135). However, the levels of NK cells (p=9.5e-09) and their degranulation capacity (p=0.016) appeared augmented in women with this condition (Figure 135). The RPL cohort displayed diminished IFN-γ (p=9.6e-05) and elevated TNF-α (p=6e-06) expression on stimulated NK cells, as well as reduced TNF-α production by unstimulated T_H cells (p=2.6e-06) and decreased TNF-α (p=3.8e-07), IL-10 (p=5e-11), IL-17A/IL-10 (p=1.1e-06), TNF-α/IL17A (p=0.047), and IL-2/IL-10 (p=1e-08) production by stimulated T_H cells (Figure 135). IL-8 (p=0.00059) and TNF-α (p=0.029) secretion by unstimulated PBMCs of women with RPL appeared increased, while IL-10 secretion was non-significantly reduced (Figure 135). The model built using a combination of these markers exhibited a significant diagnostic capacity for RPL, achieving a mean area under curve (AUC) value of 0.90 (Supplementary Figure 38).

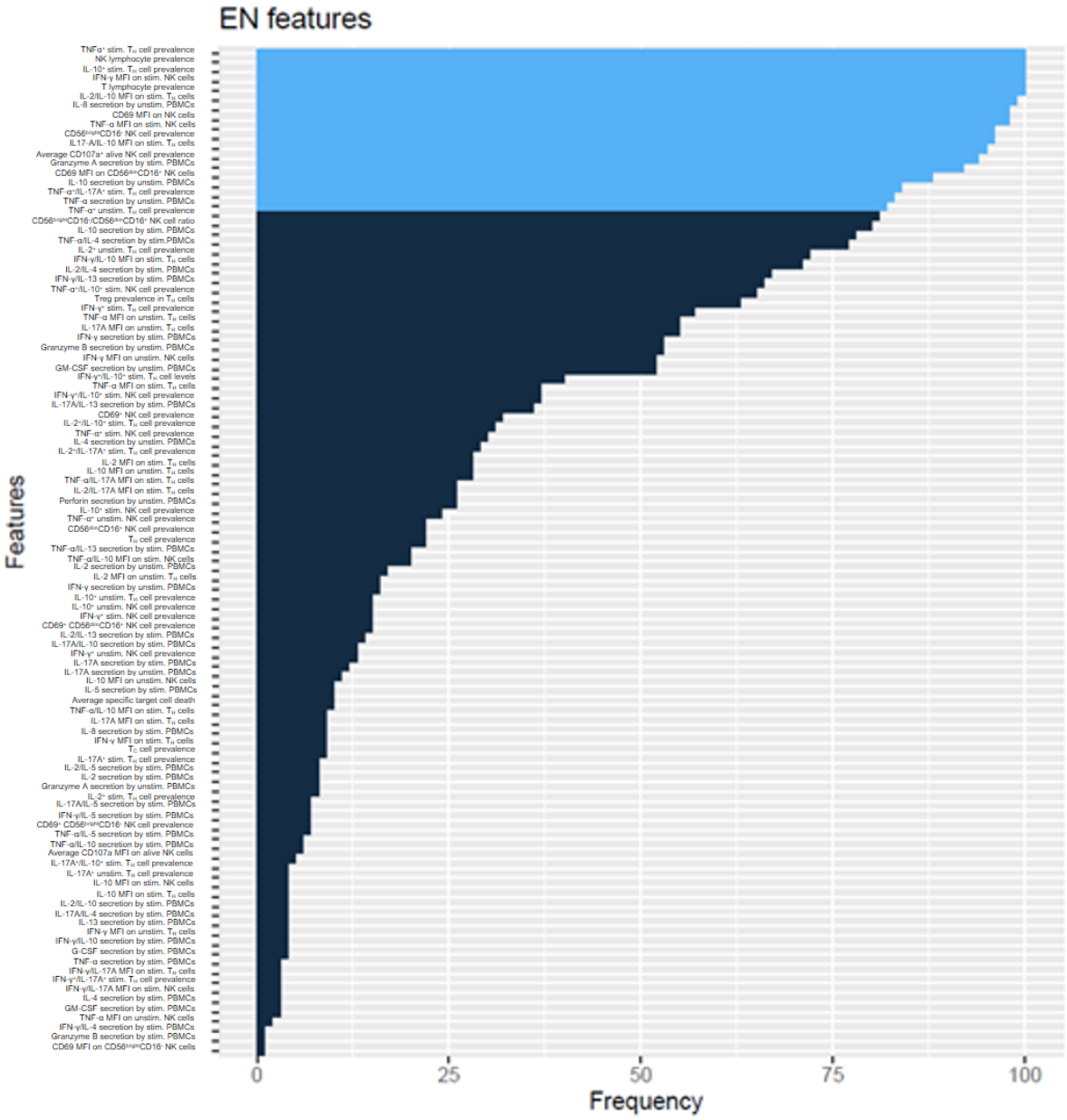


Figure 133. Elastic Net (EN) analysis results for the identification of women with recurrent pregnancy loss (RPL). *The EN algorithm was run 100 times. The number of times (frequency) each marker was selected is displayed. The 1st quartile of markers is highlighted (light blue). G-CSF: granulocyte colony stimulating factor, GM-CSF: granulocyte-macrophage colony-stimulating factor, IFN: interferon, IL: interleukin, MFI: median fluorescence intensity, NK cells: natural killer cells, T_C cells: cytotoxic T cells, T_H cells: T helper cells, TNF: tumor necrosis factor, Treg: regulatory T cell*

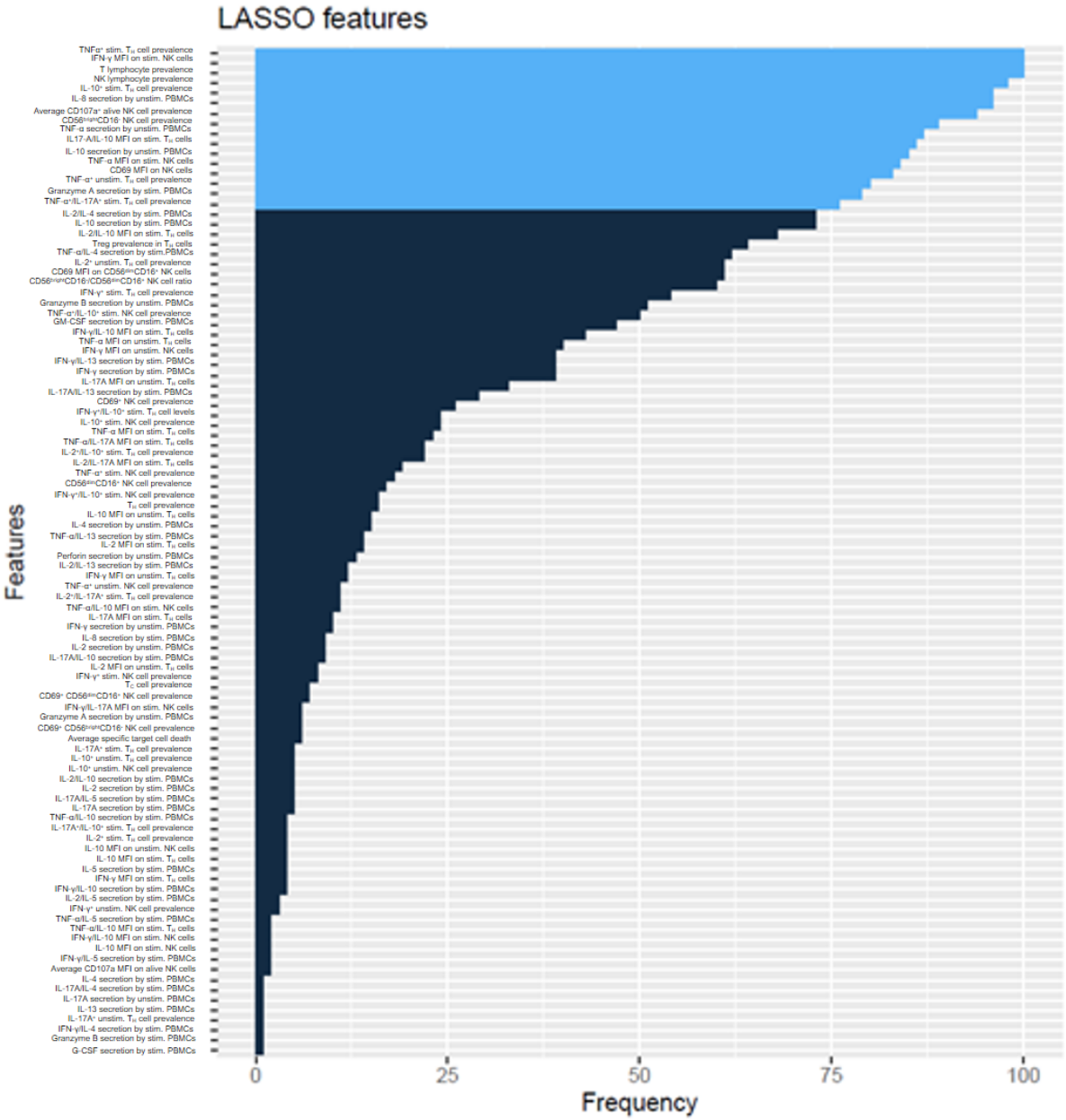


Figure 134. Least Absolute Shrinkage and Selection Operator (LASSO) analysis results for the identification of women with recurrent pregnancy loss (RPL). *The LASSO algorithm was run 100 times. The number of times (frequency) each marker was selected is displayed. The 1st quartile of markers is highlighted (light blue). CD: cluster of differentiation, G-CSF: granulocyte colony stimulating factor, GM-CSF: granulocyte-macrophage colony-stimulating factor, IFN: interferon, IL: interleukin, MFI: median fluorescence intensity, NK cells: natural killer cells, T_C cells: cytotoxic T cells, T_H cells: T helper cells, TNF: tumor necrosis factor, Treg: regulatory T cell*

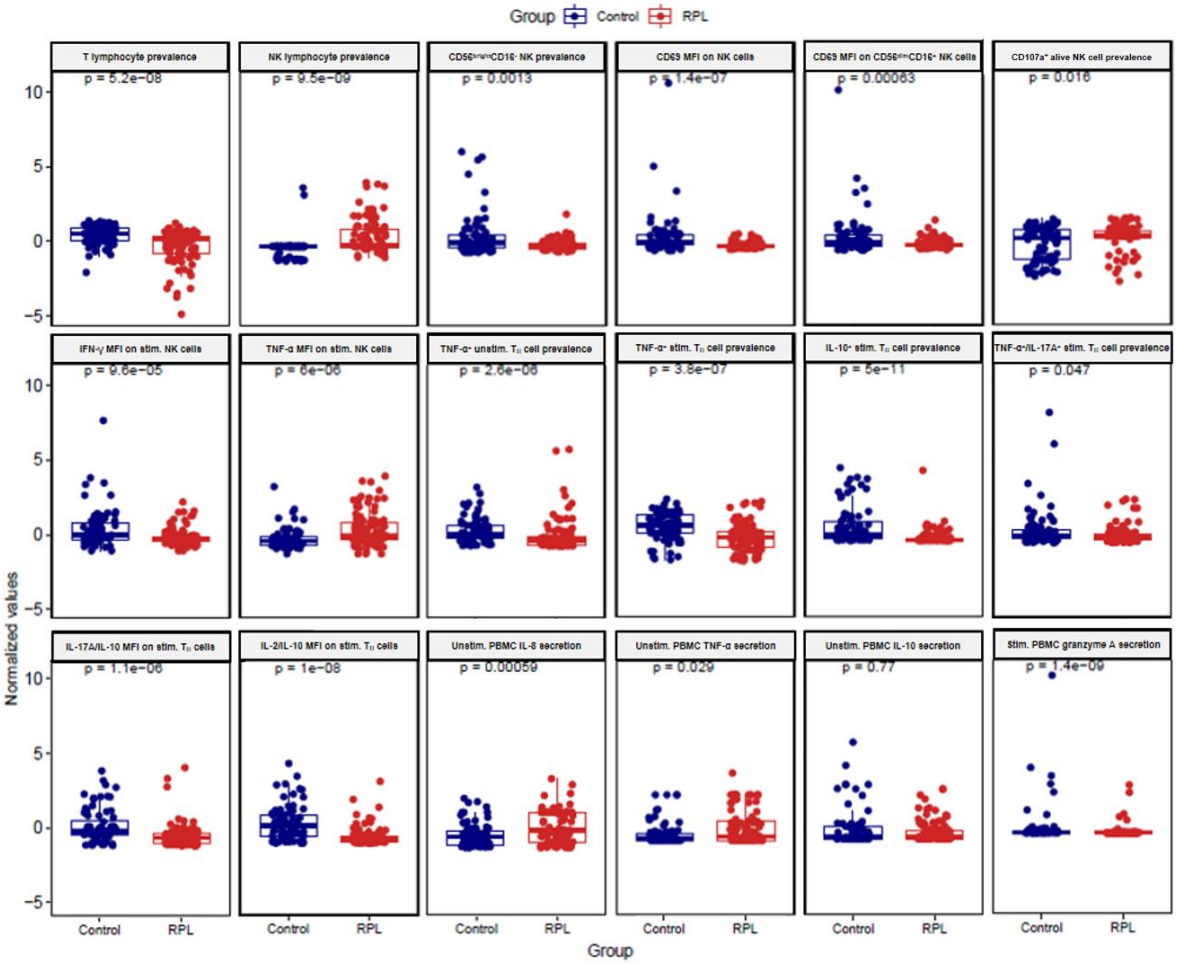


Figure 135. Box plots depicting the distribution of features selected through the combination of Elastic Net (EN) and Least Absolute Shrinkage and Selection Operator (LASSO) methods in the recurrent pregnancy loss (RPL) and control cohorts. *Normalised data for features including T cell and natural killer (NK) cell prevalence in lymphocytes, $CD56^{bright}CD16^{-}$ cell prevalence in NK cells, CD69 median fluorescence intensity (MFI) on total and $CD56^{dim}CD16^{+}$ NK cells, mean $CD107a^{+}$ alive NK cell prevalence in NK:K562 co-cultures, interferon (IFN)-γ and tumor necrosis factor (TNF)-α MFI on stimulated NK cells, $TNF\text{-}\alpha^{+}$ cell prevalence in unstimulated and stimulated T helper (T_H) cells, interleukin (IL)-10^{+} and $TNF\text{-}\alpha^{+}/IL\text{-}17A^{+}$ cell prevalence in stimulated T_H cells, IL-17A/IL-10 and IL-2/IL-10 MFI on stimulated T_H cells, as well as IL-8, TNF-α, and IL-10 secretion by unstimulated peripheral blood mononuclear cells (PBMCs) and granzyme A secretion by stimulated PBMCs are illustrated. The Wilcoxon signed-ranked test was used and the False Discovery Rate (FDR)-corrected p values (Benjamini-Hochberg method) are displayed.*

Of the 18 markers highlighted, T and NK cell prevalence in lymphocytes, and CD56^{bright}CD16^{-} cell prevalence in NK cells were further analysed due to their high score and clinical utility. The NK/T cell prevalence ratio was also taken into consideration during further analysis. NK cell levels and NK/T cell ratio appeared elevated in women with RPL, compared to controls while T and CD56^{bright}CD16^{-} NK cell prevalence was found to be reduced (Figure 136). The combination of these biomarkers displayed a significant diagnostic benefit (AUC=0.83) (Supplementary Figure 39), with NK/T cell ratio resulting to the highest AUC value (Figure 137).

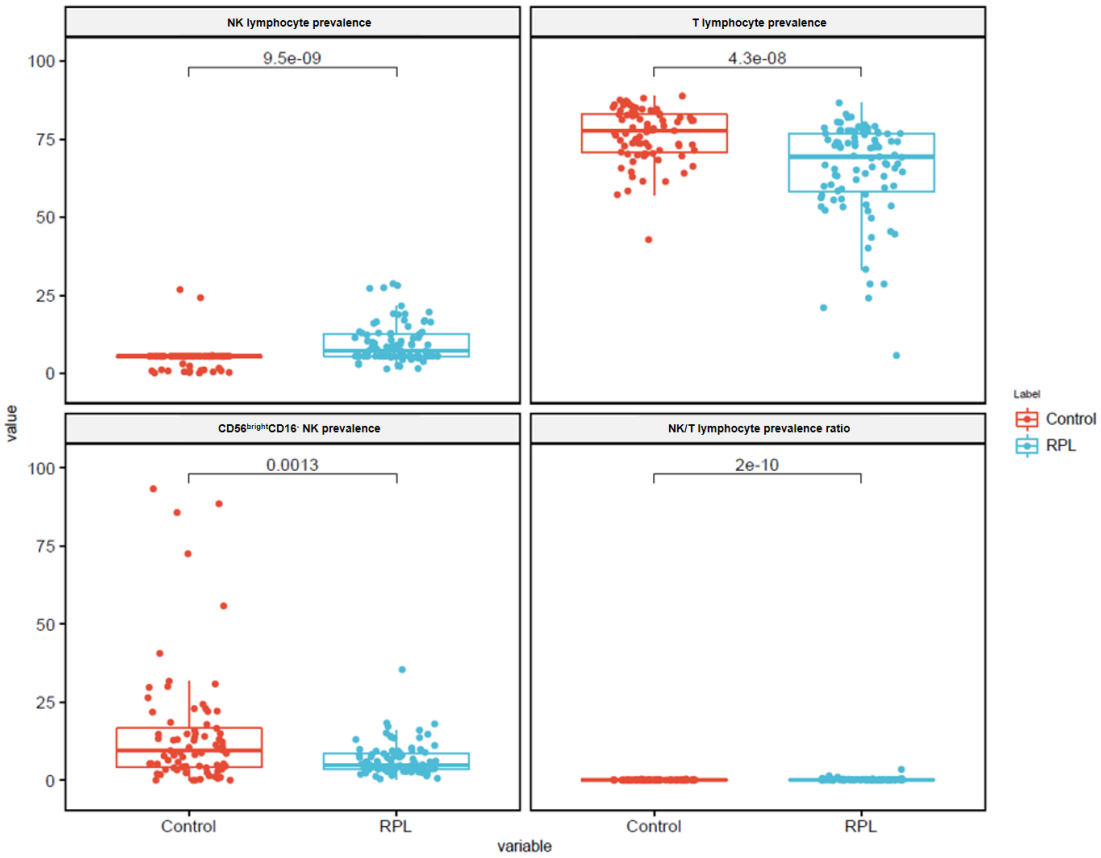


Figure 136. Box plots displaying the levels of the manually selected features in women with recurrent pregnancy loss (RPL) and controls. *The prevalence (%) of natural killer (NK) cells and T cells in lymphocytes and CD56^{bright}CD16^{-} cells in NK cells, as well as the ratio of NK to T cells in women with RPL and controls is shown. The Wilcoxon signed-ranked test was used and the resulting p values are included.*

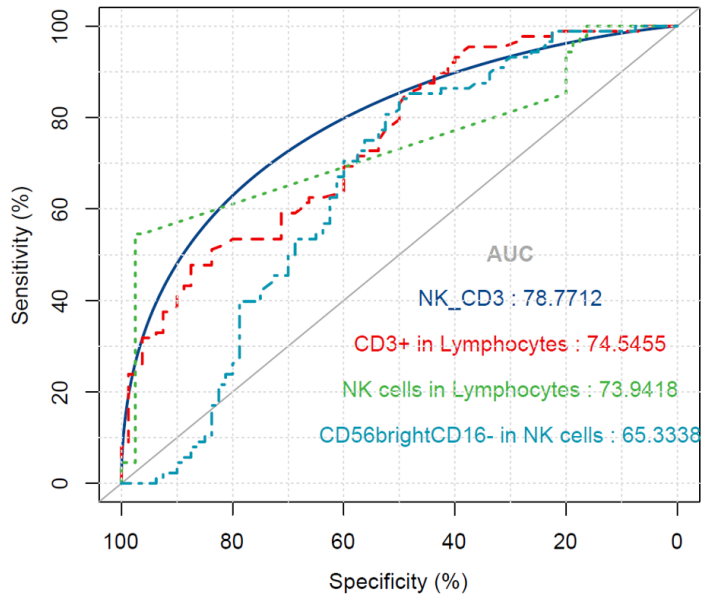


Figure 137. Receiver operating characteristic (ROC) curve illustrating the sensitivity versus the specificity of each of the 4 markers selected for the identification of women with recurrent pregnancy loss (RPL). *Markers included represent the ratio between Natural Killer (NK) and T cell prevalence (NK_CD3), T (CD3+ in Lymphocytes) and NK (NK cells in Lymphocytes) cell prevalence in lymphocytes, and CD56^{bright}CD16^{-} cell prevalence in NK cells (CD56brightCD16- cell in NK cells). The area under curve (AUC) value for each marker is shown as a percentage.*

10.2 Discussion

Through a translational approach immune biomarkers that could be utilised for the early identification of women with RPL were studied. 18 markers with diagnostic potential were automatically selected via the EN and LASSO modelling techniques (Figures 133, 134). Decreased T and CD56^{bright}CD16^{-} NK cell prevalence as well as elevated NK cell levels displayed diagnostic potential in regards to the identification of women with RPL (Figure 133-135). The interdependence between changes in T and NK cell prevalence should however be highlighted, with changes in NK cell levels potentially influenced by the reduced T cell absolute counts (Figure 38A). The

reduction in cytolytic activity, as displayed via the diminished CD69 expression by total and $CD56^{dim}CD16^{+}$ NK cells, the reduced granzyme A secretion by PBMCs, as well as the elevated NK cell degranulation capacity, also appeared as significant candidate biomarkers identifying participants with RPL (Figures 133-135). Importantly, in contrast to the findings suggesting aggravated NK cell cytotoxicity in RPL and the resulting use of this assay in RPL clinics,[168, 187, 191] target cell death in co-cultures with NK cells did not display significant diagnostic potential. Furthermore, alterations in cytokine production, most notably reduced TNF-α and IL-10 expression on T_H cells and decreased IFN-γ on NK cells have arisen as candidate RPL biomarkers (Figures 133-135), in contrast to studies highlighting a shift towards IFN-γ and TNF-α production in RPL.[370, 412, 413, 746]

Although the 18 marker combination appeared effective in the characterization of RPL cases (Supplementary Figure 38), 4 markers were chosen for additional analysis due to their clinical utility. As time-consuming stimulation assays are not likely to be introduced into routine clinical practice, T cell, NK cell, and $CD56^{bright}CD16^{-}$ NK cell enumeration was examined. According to further univariate analysis, the ratio between NK and T cell levels appeared as the optimum biomarker for the identification of women with RPL (Figures 136, 137).

10.2.1 Limitations and future research

Data assessed was collected via the flow cytometry and cytotoxicity assays and ELISA, while mass cytometry data was not included in this analysis due to difficulties in clinical application. The development of a flow cytometry panel examining markers of interest highlighted via the mass cytometry assay would allow the

identification of additional candidate biomarkers that could potentially be introduced in routine clinical practice. Analysis of biomarkers in subpopulations of women with different order losses, as well as in women with idiopathic RPL could contribute in optimizing the timing of such examination in miscarriage clinics. Furthermore, additional recruitment would permit investigation of markers excluded due to a high number of missing values. Recruitment of additional participants, comprising the validation cohort, is also required for the verification of present findings. Last but not least, further research is needed to evaluate the biological relevance of these biomarkers and elucidate the pathological mechanism of RPL.

11 FINAL DISCUSSION

RPL affects a significant percentage of women and often results in severe psychological distress to couples trying to conceive.[9] The impact of RPL is exacerbated by a lack of well-established RPL causes.[81] An implication of aberrant immune activity in RPL pathogenesis has been proposed, with aggravated NK cell activity and a shift towards anti-inflammatory cytokine secretion by T_H cells commonly referenced.[171, 191, 398, 406, 408] Although the potential role of the immune system in RPL has not been elucidated, immunological testing and immunomodulatory treatments are sometimes offered to women with multiple pregnancy losses.

Using an online questionnaire distributed to RPL clinics nationwide, large variation was seen in regards to the diagnostic criteria for this condition and the tests used to identify RPL-associated risk factors. In two NHS and one private clinic immunological testing was offered, against official ESHRE and RCOG recommendations.[1, 5] Large variation was also seen in regards to the management of idiopathic RPL, with immunomodulatory agents such as aspirin and prednisolone offered in some clinics. On the other hand, the therapeutic benefit of progesterone and folic acid was underlined by multiple participants. As findings were mostly representative of NHS practice, with responses from only one private clinic obtained, a follow-up survey directed to the private sector would be required to fully assess the use of immunological testing and whether this is the primary interest of women seeking private care. However, these findings highlight the increasing clinical need for identification of immune biomarkers in women with RPL. The potential pathogenic immune mechanism underlying RPL should be clarified prior to the

introduction of immunomodulatory treatments in clinical practice, as research outcomes remain contentious.

Comprehensive immunophenotyping was performed using peripheral blood samples obtained from a large cohort of non-pregnant women with RPL and healthy controls. An elevation in the total NK cell population prevalence and a shift towards the primarily cytotoxic $CD56^{dim}CD16^{+}$ NK cell subset was discovered in women with this condition in agreement to previous studies.[164, 185, 187, 191] This was accompanied by a T cell reduction and unaltered T cell subset prevalence. Although not evident through flow cytometry, utilizing a novel mass cytometry panel, a Treg-like subset reduction was detected, in line with past findings,[383, 440] suggesting a defect in pre-conception systemic immunosuppression in women with RPL. Consistent with this hypothesis, most T cell subsets reduced in RPL exhibited a TIGIT/Tim-3^{+}PD-1^{+} phenotype, while those increased were TIGIT/Tim-3^{-}PD-1^{-}, indicating than in these women the mechanism behind T cell exhaustion and suppression may be compromised.[286, 374, 751] Such defects could facilitate systemic inflammation, with the total T cell population being more prone to re-activation, exhibiting enhanced cytokine production and effector activity. Using mass cytometry, a reduction in a regulatory-like B cell subset was also seen, accompanied by an increase in a plasma cell-like subset, consistent with the hypothesis suggesting a systemic inflammatory state in women with RPL. However, as the mass cytometry panel was designed with a focus on NK cells, validation of these findings through the use of additional T and B cell markers is required. Furthermore, investigation of additional immune cell populations, such as DCs and macrophages is essential in uncovering the full extent of immune dysregulation in RPL.

No difference in the killing capacity of NK cells could be seen between women with RPL and controls. Although the cytotoxicity assay was developed based on previously established protocols,[161, 187, 752] extensive optimization was required. Both the insignificant findings as well as the need for optimization, highlight the lack of a strong scientific rationale behind the use of this assay in miscarriage clinics. On the other hand, upon their stimulation with target cells, NK cells of women with RPL exhibited an enhanced degranulation capacity. This would be expected to lead to increased target cell death, which was however not seen, possibly due to a reduction in the overall amount of cytolytic molecules released. Even though cytolytic molecule secretion by NK cells could not be evaluated due to the limited amount of blood available, reduced granzyme A and B and perforin secretion by the PBMCs of women with RPL was indeed seen. Furthermore, through the assessment of CD69 expression via flow cytometry, a reduction in the activation status of total and $CD56^{dim}CD16^{+}$ NK cells was seen, accompanied by an increase in the prevalence of activated primarily cytokine-producing $CD56^{bright}CD16^{-}$ NK cells. On the other hand, elevated CD215 expression on circulating total and $CD56^{dim}CD16^{+}$ NK cells of women with RPL was also detected, expected to facilitate enhanced NK cell activation through IL-15-mediated signalling.[717] Even though findings remain controversial, the increase in NK cell levels could result in an overall elevation in NK cell activity, partially supporting the concept of aggravated NK cell-mediated immunity in RPL.[168, 189, 191, 262]

To our knowledge this was the first study focusing on activating and inhibitory receptor expression on circulating NK cells of women with RPL, using a detailed mass cytometry antibody panel. Interestingly, CD57 appeared as the marker most

clearly separating NK cell subpopulations. An increase in NK cell subsets expressing high CD57 levels was seen in women with RPL, underlining a shift of the NK cell population towards more mature subsets with augmented cytotoxic capacity.[271] Fascinatingly, NK cell subsets elevated in women with RPL appeared to lack inhibitory KIR, ILT, NCR, and NKG2 receptor expression, highlighting a potential deficiency in the inhibitory signalling pathways, resulting to an NK cell population more prone to respond to activating signals. This would be expected to lead to enhanced target cell death, which was however not seen through the cytotoxicity assay. Due to the alterations in HLA-C-, HLA-E-, and HLA-G-specific receptor expression on the surface of NK cells of women with RPL, the use of HLA^- K562 targets may not reflect NK cell cytotoxicity in the context of pregnancy. To more accurately assess NK cell activity in RPL, $HLA\text{-}C^+HLA\text{-}E^+HLA\text{-}G^+$ trophoblast cells, or cell lines with a similar HLA expression pattern, could be utilised as targets in future studies.

Another mass cytometry finding that requires further investigation was the lack of CXCR3 and CXCR4 expression on most of the over-represented NK cell subsets in women with RPL, suggesting a deficiency in uterine migration,[314, 318, 321, 739] potentially leading to inadequate local support during decidualization and placentation. Examination of NK and chemokine levels in the endometrium and decidua of women with RPL, as well as NK cell migration assays could be utilised to further examine these findings.

One of the principal theories describing immune activity in RPL is the “Type-1/Type-2” hypothesis, proposing a pro-inflammatory shift in T_H cell cytokine production in the periphery and uterus of women with RPL.[406-408] Upon individual cytokine

examination by flow cytometry, no clear pro- or anti-inflammatory pattern in cytokine production could be seen. When the ratios of pro- to anti-inflammatory cytokine-expressing T_H cell prevalence were measured an inflammatory shift was evident, supporting the use of this test in RPL clinics. However, when the respective ratios regarding the levels of these cytokines on individual T_H cells were investigated, an anti-inflammatory shift was displayed, challenging the biological relevance of the previously described pro-inflammatory shift.

On the other hand, both pro- and anti-inflammatory cytokine production by NK cells appeared overall deficient in women with RPL. Unfortunately, while the $CD56^{dim}CD16^{+}$ NK cell subset was evident by flow cytometry, the primarily cytokine-producing $CD56^{bright}CD16^{-}$ subset was not clearly seen and thus cytokine production by this subpopulation could not be separately analysed. As these cells constitute the dominant subpopulation in the decidua and enhanced $CD56^{bright}CD16^{-}$ NK cell activation in women with RPL was detected in the present study,[159] additional experiments assessing cytokine production by this subset in healthy pregnancy and RPL are needed.

To examine the extent of immune dysregulation in RPL, evaluation of cytokine secretion was required. Potential alterations in pro-/anti-inflammatory cytokine secretion patterns could influence the overall immune activity. In the absence of stimulation an increase in pro-inflammatory TNF-α, IL-17A, GM-CSF, and IL-8 levels was seen, while upon stimulation the T_H2-associated IL-5 and IL-13 levels appeared reduced, resulting in an elevation of T_H1-/T_H2-associated cytokine ratios. Interestingly, this finding was observed pre-conception, suggesting that the Type-1 shift might be a cause of RPL, rather than a result of miscarriage. On the one hand,

overproduction of IL-17, GM-CSF, and IL-8 could result in excessive trophoblast proliferation and uncontrollable invasion of the maternal vasculature.[406, 753-755] On the other hand, increased TNF-α levels could promote trophoblast apoptosis, exacerbating inflammation and obstructing the establishment of the fetal-placental unit.[406, 463] As these cytokines could exert opposite effects on fetal trophoblast growth and invasion, a combination of these cytokines could be used to examine their overall impact using proliferation, apoptosis, and Matrigel invasion assays. To more accurately examine the mechanisms behind RPL, serum from 1st-trimester pregnant women with RPL could be used to determine the relative cytokine concentrations during early gestation. Moreover, cytokine secretion by isolated T_H and NK cells could also be separately assessed to evaluate the impact of these populations on the overall immune activity in RPL.

The presence of underlying pathologies did not appear to influence immune activity in women with RPL. According to ESHRE, for none of the miscarriage risk factors has a relationship of causality been clearly displayed.[9] Hence, to investigate whether the potential immunological miscarriage mechanism is active in all RPL cases, large-cohort studies examining immune markers in women with different RPL-associated risk factors are required. In case of introduction of immunological testing in RPL clinics, such studies would be central in developing a protocol for diagnostic testing. In addition, women with higher order loss did not appear more likely to present with underlying immune dysregulation.

In control women belonging in higher age subgroups, a pro-inflammatory shift in cytokine production was seen, compared to women up to 30 years of age. These differences however, were not evident in the RPL group, suggesting that a lack of

age-associated changes in cytokine production could be linked to the pathogenesis of this condition. Further examination using age-matched RPL and control cohorts is required for the validation of these findings.

On the other hand, an anti-inflammatory shift in cytokine expression levels on T_H cells was seen in control women of Mixed ethnic origin, while an increased T_H1/T_H17 ratio was detected in White compared to Black controls. This analysis could not be performed in the RPL group due to the small number of women of Mixed or Black ethnic backgrounds. As the risk of miscarriage is significantly increased in Black women,[3] further investigation is required. According to the ethnicity-matched subpopulation analysis, the difference in some immune parameters between women with RPL and controls was possibly influenced by the ethnic diversity between groups. Thus, the potential influence of ethnicity should be taken into consideration when designing studies assessing the immune activity of women with RPL.

Similarly, according to the alcohol intake-matched analysis, the difference in some markers between women with RPL and controls could have been affected by variation in alcohol consumption. Hence, additional research is required to evaluate the influence of alcohol consumption on the immune activity of women with this condition.

Importantly, multiple biomarkers, including elevated NK and reduced T cell levels appeared capable of effectively distinguishing women with RPL from the control population. The NK/T cell ratio was highlighted as the most accurate immune biomarker for RPL that could be easily introduced in routine clinical practice. Thus,

upon validation this ratio could provide a useful marker for the identification of women with RPL in miscarriage clinics. Furthermore, TNF-α secretion levels by unstimulated PBMC and the levels of GM-CSF, IFN-γ, IL-2, IL-4, IL-5, IL-10, IL-13, and IL-17A in stimulated PBMC cultures appeared predictive of subsequent pregnancy outcome in women with RPL, with elevated concentrations being linked to miscarriage. Upon validation, such findings could be central in the development of assays used for miscarriage prognosis, potentially highlighting the cases in which therapeutic intervention may be required.

The present study was focused on the assessment of immune activity in the peripheral blood of women with RPL, as endometrial assessment is unlikely to be introduced into routine clinical practice due to its invasive nature. However, it should be underlined that although peripheral immune activity may influence early pregnancy due to trophoblast invasion of maternal vasculature,[109-111] it does not necessarily reflect *in utero* immunity. Hence, to fully elucidate the role of the immune system in RPL pathogenesis, further studies evaluating local immune activity utilizing high-throughput methods are required.[160, 192, 207, 548] Moreover, the investigation of paired peripheral and endometrial samples would allow the identification of peripheral biomarkers that could be used to assess local activity. Finally, although analysis revealed an immune dysregulation in non-pregnant women with RPL, immune activity is altered during early pregnancy.[272, 336, 360, 362, 373] It should thus be determined whether the identification of diagnostic and prognostic biomarkers pre- or post-conception is preferable.

12 LIST OF REFERENCES

1. Royal College of Obstetricians & Gynaecologists. The Investigation and Treatment of Couples with Recurrent First-trimester and Second-trimester Miscarriage. Green-top Guideline. 2011; 17: 1-18.
2. National Institute for Health and Care Excellence. Miscarriage 2020 [Available from: https://cks.nice.org.uk/topics/miscarriage/.
3. Quenby S, Gallos ID, Dhillon-Smith RK, Podesek M, Stephenson MD, Fisher J, Brosens JJ, Brewin J, Ramhorst R, Lucas ES, et al. Miscarriage matters: the epidemiological, physical, psychological, and economic costs of early pregnancy loss. Lancet. 2021; 397(10285): 1658-67.
4. Stirrat GM. Recurrent miscarriage I: definition and epidemiology. Lancet. 1990; 336(8716): 673-5.
5. The ESHRE Guideline Group on RPL, Atik RB, Christiansen OB, Elson J, Kolte AM, Lewis S, Middeldorp S, Nelen W, Peramo B, Quenby S, et al. ESHRE guideline: recurrent pregnancy loss. Hum Reprod Open. 2018; 2018(2): hoy004.
6. van den Boogaard E, Kaandorp SP, Franssen MT, Mol BW, Leschot NJ, Wouters CH, van der Veen F, Korevaar JC, Goddijn M. Consecutive or non-consecutive recurrent miscarriage: is there any difference in carrier status? Hum Reprod. 2010; 25(6): 1411-4.
7. The American College of Obstetricians and Gynecologists. Early pregnancy loss. ACOG practice bulletin. 2018.
8. European Society of Human Reproduction and Embryology. Information for couples with Recurrent Pregnancy Loss. Patient leaflet based on the ESHRE Guideline on Recurrent Pregnancy Loss. 2017: 1-19.
9. ESHRE Early Pregnancy Guideline development Group. Recurrent Pregnancy Loss. European Society of Human Reproduction and Embryology; 2017. p. 1-153.
10. Rai R, Regan L. Recurrent miscarriage. Lancet. 2006; 368(9535): 601-11.
11. Jauniaux E, Farquharson RG, Christiansen OB, Exalto N. Evidence-based guidelines for the investigation and medical treatment of recurrent miscarriage. Hum Reprod. 2006; 21(9): 2216-22.
12. National Institute for Health and Care Excellence. Miscarriage: How common is it? 2020 [Available from: https://cks.nice.org.uk/topics/miscarriage/background-information/prevalence/.
13. Nynas J, Narang P, Kolikonda MK, Lippmann S. Depression and Anxiety Following Early Pregnancy Loss: Recommendations for Primary Care Providers. Prim Care Companion CNS Disord. 2015; 17(1).
14. Farren J, Mitchell-Jones N, Verbakel JY, Timmerman D, Jalmbrant M, Bourne T. The psychological impact of early pregnancy loss. Hum Reprod Update. 2018; 24(6): 731-49.
15. Serrano F, Lima ML. Recurrent miscarriage: psychological and relational consequences for couples. Psychol Psychother. 2006; 79(Pt 4): 585-94.
16. Kolte AM, Olsen LR, Mikkelsen EM, Christiansen OB, Nielsen HS. Depression and emotional stress is highly prevalent among women with recurrent pregnancy loss. Hum Reprod. 2015; 30(4): 777-82.
17. Tavoli Z, Mohammadi M, Tavoli A, Moini A, Effatpanah M, Khedmat L, Montazeri A. Quality of life and psychological distress in women with recurrent miscarriage: a comparative study. Health Qual Life Outcomes. 2018; 16(1): 150.
18. National Institute for Health and Care Excellence. Miscarriage: What are the causes and risk factors? 2020 [Available from: https://cks.nice.org.uk/topics/miscarriage/background-information/causes-risk-factors/.
19. Regan L, Braude PR, Trembath PL. Influence of past reproductive performance on risk of spontaneous abortion. BMJ. 1989; 299(6698): 541–5.
20. Knudsen UB, Hansen V, Juul S, Secher NJ. Prognosis of a new pregnancy following previous spontaneous abortions. Eur J Obstet Gynecol Reprod Biol. 1991; 39(1): 31-6.
21. Parazzini F, Acaia B, Ricciardiello O, Fedele L, Liati P, Candiani GB. Short-term reproductive prognosis when no cause can be found for recurrent miscarriage. Br J Obstet Gynaecol. 1988; 95(7): 654-8.
22. Nybo Andersen AM, Wohlfahrt J, Christens P, Olsen J, Melbye M. Maternal age and fetal loss: population based register linkage study. BMJ. 2000; 320(7251): 1708-12.
23. Quenby SM, Farquharson RG. Predicting recurring miscarriage: what is important? Obstet Gynecol. 1993; 82(1): 132-8.
24. Magnus MC, Wilcox AJ, Morken NH, Weinberg CR, Håberg SE. Role of maternal age and pregnancy history in risk of miscarriage: prospective register based study. BMJ. 2019; 364: l869.

25. Katano K, Suzuki S, Ozaki Y, Suzumori N, Kitaori T, Sugiura-Ogasawara M. Peripheral natural killer cell activity as a predictor of recurrent pregnancy loss: a large cohort study. Fertil Steril. 2013; 100(6): 1629-34.
26. Lashen H, Fear K, Sturdee DW. Obesity is associated with increased risk of first trimester and recurrent miscarriage: matched case-control study. Hum Reprod. 2004; 19(7): 1644-6.
27. Chatenoud L, Parazzini F, di Cintio E, Zanconato G, Benzi G, Bortolus R, La Vecchia C. Paternal and maternal smoking habits before conception and during the first trimester: relation to spontaneous abortion. Ann Epidemiol. 1998; 8(8): 520-6.
28. Kline J, Levin B, Kinney A, Stein Z, Susser M, Warburton D. Cigarette smoking and spontaneous abortion of known karyotype. Precise data but uncertain inferences. Am J Epidemiol. 1995; 141(5): 417-27.
29. Ness RB, Grisso JA, Hirschinger N, Markovic N, Shaw LM, Day NL, Kline J. Cocaine and tobacco use and the risk of spontaneous abortion. N Engl J Med. 1999; 340(5): 333-9.
30. Domínguez-Rojas V, de Juanes-Pardo JR, Astasio-Arbiza P, Ortega-Molina P, Gordillo-Florencio E. Spontaneous abortion in a hospital population: are tobacco and coffee intake risk factors? Eur J Epidemiol. 1994; 10(6): 665-8.
31. Windham GC, Von Behren J, Fenster L, Schaefer C, Swan SH. Moderate maternal alcohol consumption and risk of spontaneous abortion. Epidemiology. 1997; 8(5): 509-14.
32. Rasch V. Cigarette, alcohol, and caffeine consumption: risk factors for spontaneous abortion. Acta Obstet Gynecol Scand. 2003; 82(2): 182-8.
33. Parazzini F, Chatenoud L, Di Cintio E, Mezzopane R, Surace M, Zanconato G, Fedele L, Benzi G. Coffee consumption and risk of hospitalized miscarriage before 12 weeks of gestation. Hum Reprod. 1998; 13(8): 2286-91.
34. Cnattingius S, Signorello LB, Annerén G, Clausson B, Ekbom A, Ljunger E, Blot WJ, McLaughlin JK, Petersson G, Rane A, et al. Caffeine intake and the risk of first-trimester spontaneous abortion. N Engl J Med. 2000; 343(25): 1839-45.
35. Andersen LB, Jørgensen JS, Jensen TK, Dalgård C, Barington T, Nielsen J, Beck-Nielsen SS, Husby S, Abrahamsen B, Lamont RF, et al. Vitamin D insufficiency is associated with increased risk of first-trimester miscarriage in the Odense Child Cohort. Am J Clin Nutr. 2015; 102(3): 633-8.
36. Khattak S, K-Moghtader G, McMartin K, Barrera M, Kennedy D, Koren G. Pregnancy outcome following gestational exposure to organic solvents: a prospective controlled study. JAMA. 1999; 281(12): 1106-9.
37. Ocak Z, Özlü T, Ozyurt O. Association of recurrent pregnancy loss with chromosomal abnormalities and hereditary thrombophilias. Afr Health Sci. 2013; 13(2): 447-52.
38. Hyde KJ, Schust DJ. Genetic considerations in recurrent pregnancy loss. Cold Spring Harb Perspect Med. 2015; 5(3): a023119.
39. Silver RM, Branch DW. Sporadic and Recurrent Pregnancy Loss. In: Reece EA, Hobbins JC, editors. Clinical obstetrics: The fetus & mother. 3rd edition ed. Boston: Wiley-Blackwell; 2007. p. 143-60.
40. Christiansen OB, Mathiesen O, Lauritsen JG, Grunnet N. Idiopathic recurrent spontaneous abortion. Evidence of a familial predisposition. Acta Obstet Gynecol Scand. 1990; 69(7-8): 597-601.
41. Ogasawara M, Aoki K, Okada S, Suzumori K. Embryonic karyotype of abortuses in relation to the number of previous miscarriages. Fertil Steril. 2000; 73(2): 300-4.
42. Carp H, Toder V, Aviram A, Daniely M, Mashiach S, Barkai G. Karyotype of the abortus in recurrent miscarriage. . Fertil Steril. 2001; 75(4): 678-82.
43. Warburton D, Kline J, Stein Z, Hutzler M, Chin A, Hassold T. Does the karyotype of a spontaneous abortion predict the karyotype of a subsequent abortion? Evidence from 273 women with two karyotyped spontaneous abortions. . Am J Hum Genet. 1987; 41(3): 465-83.
44. Rad IA. The impact of consanguinity on fetal loss. Medical Journal of Islamic World Academy of Sciences. 2010; 18(4): 151-4.
45. Yang CJ, Stone P, Stewart AW. The epidemiology of recurrent miscarriage: a descriptive study of 1214 prepregnant women with recurrent miscarriage. Aust N Z J Obstet Gynaecol. 2006; 46(4): 316-22.
46. Ibrahim Y, Johnstone E. The male contribution to recurrent pregnancy loss. Transl Androl Urol. 2018; 7(Suppl 3): S317-S27.
47. Regan L, Rai R. Epidemiology and the medical causes of miscarriage. Best Pract Res Clin Obstet Gynaecol. 2000; 14(5): 839-54.

48. Ford HB, Schust DJ. Recurrent Pregnancy Loss: Etiology, Diagnosis, and Therapy. Rev Obstet Gynecol. 2009; 2(2): 76-83.
49. Carrington B, Sacks G, Regan L. Recurrent miscarriage: pathophysiology and outcome. Curr Opin Obstet Gynecol. 2005; 17(6): 591-7.
50. Laird SM, Tuckerman EM, Cork BA, Linjawi S, Blakemore AI, Li TC. A review of immune cells and molecules in women with recurrent miscarriage. Hum Reprod Update. 2003; 9(2): 163-74.
51. Clifford K, Rai R, Watson H, Regan L. An informative protocol for the investigation of recurrent miscarriage: preliminary experience of 500 consecutive cases. Hum Reprod. 1994; 9(7): 1328-32.
52. Fox-Lee L, Schust DJ. Recurrent pregnancy loss. In: Berek JS, editor. Berek and Novak's Gynecology. Philadelphia: Lippincott Williams & Wilkins; 2007. p. 1277-322.
53. Miodovnik M, Skillman C, Holroyde JC, Butler JB, Wendel JS, Siddiqi TA. Elevated maternal glycohemoglobin in early pregnancy and spontaneous abortion among insulin-dependent diabetic women. Am J Obstet Gynecol. 1985; 153(4): 439-42.
54. Mills JL, Simpson JL, Driscoll SG, Jovanovic-Peterson L, Van Allen M, Aarons JH, Metzger B, Bieber FR, Knopp RH, Holmes LB, et al. Incidence of spontaneous abortion among normal women and insulin-dependent diabetic women whose pregnancies were identified within 21 days of conception. N Engl J Med. 1988; 319(25): 1617-23.
55. Nielsen GL, Sørensen HT, Nielsen PH, Sabroe S, Olsen J. Glycosylated hemoglobin as predictor of adverse fetal outcome in type 1 diabetic pregnancies. Acta Diabetol. 1997; 34(3): 217-22.
56. Hanson U, Persson B, Thunell S. Relationship between haemoglobin A1C in early type 1 (insulin-dependent) diabetic pregnancy and the occurrence of spontaneous abortion and fetal malformation in Sweden. Diabetologia. 1990; 33(2): 100-4.
57. Rai R, Cohen H, Dave M, Regan L. Randomised controlled trial of aspirin and aspirin plus heparin in pregnant women with recurrent miscarriage associated with phospholipid antibodies (or antiphospholipid antibodies). BMJ. 1997; 314(7076): 253-7.
58. Stray-Pedersen B, Stray-Pedersen S. Etiologic factors and subsequent reproductive performance in 195 couples with a prior history of habitual abortion. Am J Obstet Gynecol. 1984; 148(2): 140-6.
59. Rai RS, Regan L, Clifford K, Pickering W, Dave M, Mackie I, McNally T, Cohen H. Antiphospholipid antibodies and beta 2-glycoprotein-I in 500 women with recurrent miscarriage: results of a comprehensive screening approach. Hum Reprod. 1995; 10(8): 2001-5.
60. Oshiro BT, Silver RM, Scott JR, Yu H, Branch DW. Antiphospholipid antibodies and fetal death. Obstet Gynecol. 1996; 87(4): 489-93.
61. Santos TDS, Ieque AL, de Carvalho HC, Sell AM, Lonardoni MVC, Demarchi IG, de Lima Neto QA, Teixeira JJV. Antiphospholipid syndrome and recurrent miscarriage: A systematic review and meta-analysis. J Reprod Immunol. 2017; 123: 78-87.
62. Tektonidou MG, Andreoli L, Limper M, Amoura Z, Cervera R, Costedoat-Chalumeau N, Cuadrado MJ, Dörner T, Ferrer-Oliveras R, Hambly K, et al. EULAR recommendations for the management of antiphospholipid syndrome in adults. Ann Rheum Dis. 2019; 78(10): 1296-304.
63. Lockshin MD, Kim M, Laskin CA, Guerra M, Branch DW, Merrill J, Petri M, Porter TF, Sammaritano L, Stephenson MD, et al. Prediction of adverse pregnancy outcome by the presence of lupus anticoagulant, but not anticardiolipin antibody, in patients with antiphospholipid antibodies. Arthritis Rheum. 2012; 64(7): 2311-8.
64. Chaturvedi S, Brodsky RA, McCrae KR. Complement in the Pathophysiology of the Antiphospholipid Syndrome. Front Immunol. 2019; 10: 449.
65. Abrahams VM, Chamley LW, Salmon JE. Emerging Treatment Models in Rheumatology: Antiphospholipid Syndrome and Pregnancy: Pathogenesis to Translation. Arthritis Rheumatol. 2017; 69(9): 1710-21.
66. Tang W, Mao J, Li KT, Walker JS, Chou R, Fu R, Chen W, Darville T, Klausner J, Tucker JD. Pregnancy and fertility-related adverse outcomes associated with Chlamydia trachomatis infection: a global systematic review and meta-analysis. Sex Transm Infect. 2019; [Epub ahead of print].
67. Silasi M, Cardenas I, Kwon JY, Racicot K, Aldo P, Mor G. Viral infections during pregnancy. Am J Reprod Immunol. 2015; 73(3): 199-213.
68. Baud D, Goy G, Jaton K, Osterheld MC, Blumer S, Borel N, Vial Y, Hohlfeld P, Pospischil A, Greub G. Role of Chlamydia trachomatis in Miscarriage. Emerg Infect Dis. 2011; 17(9): 1630-5.

69. Ahmadi A, Khodabandehloo M, Ramazanzadeh R, Farhadifar F, Nikkhoo B, Soofizade N, Rezaii M. Association between Ureaplasma urealyticum endocervical infection and spontaneous abortion. Iran J Microbiol. 2014; 6(6): 392-7.
70. Cao CJ, Wang YF, Fang DM, Hu Y. Relation between mycoplasma infection and recurrent spontaneous abortion. Eur Rev Med Pharmacol Sci. 2018; 22(8): 2207-11.
71. Naessens A, Foulon W, Cammu H, Goossens A, Lauwers S. Epidemiology and pathogenesis of ureaplasma urealyticum in spontaneous abortion and early preterm labor. Acta Obstet Gynecol Scand. 1987; 66(6): 513-6.
72. Quinn PA, Petric M, Barkin M, Butany J, Derzko C, Gysler M, Lie KI, Shewchuck AB, Shuber J, Ryan E, et al. Prevalence of antibody to Chlamydia trachomatis in spontaneous abortion and infertility. Am J Obstet Gynecol. 1987; 156(2): 291-6.
73. Harger JH, Archer DF, Marchese SG, Muracca-Clemens M, Garver KL. Etiology of recurrent pregnancy losses and outcome of subsequent pregnancies. Obstet Gynecol. 1983; 62(5): 574-81.
74. Cicinelli E, Matteo M, Tinelli R, Pinto V, Marinaccio M, Indraccolo U, De Ziegler D, Resta L. Chronic endometritis due to common bacteria is prevalent in women with recurrent miscarriage as confirmed by improved pregnancy outcome after antibiotic treatment. Reprod Sci. 2014; 21(5): 640-7.
75. McQueen DB, Bernardi LA, Stephenson MD. Chronic endometritis in women with recurrent early pregnancy loss and/or fetal demise. Fertil Steril. 2014; 101(4): 1026-30.
76. Kitaya K. Prevalence of chronic endometritis in recurrent miscarriages. Fertil Steril. 2011; 95(3): 1156-8.
77. McQueen DB, Perfetto CO, Hazard FK, Lathi RB. Pregnancy outcomes in women with chronic endometritis and recurrent pregnancy loss. Fertil Steril. 2015; 104(4): 927-31.
78. Bouet PE, El Hachem H, Monceau E, Gariépy G, Kadoch IJ, Sylvestre C. Chronic endometritis in women with recurrent pregnancy loss and recurrent implantation failure: prevalence and role of office hysteroscopy and immunohistochemistry in diagnosis. Fertil Steril. 2016; 105(1): 106-10.
79. Warwick Clinical Trials Unit. CERM Overview 2020 [Available from: https://warwick.ac.uk/fac/sci/med/research/ctu/trials/cerm/.
80. Tommy's. Your feelings and emotions after miscarriage 2019 [Available from: https://www.tommys.org/baby-loss-support/miscarriage-information-and-support/support-after-miscarriage/your-feelings-and-emotions-after-miscarriage.
81. Ewington LJ, Tewary S, Brosens JJ. New insights into the mechanisms underlying recurrent pregnancy loss. J Obstet Gynaecol Res. 2019; 45(2): 258-65.
82. Practice Committee of the American Society for Reproductive Medicine. Evaluation and treatment of recurrent pregnancy loss: a committee opinion. Fertil Steril. 2012; 98(5): 1103-11.
83. Carp H, Salomon O, Seidman D, Dardik R, Rosenberg N, Inbal A. Prevalence of genetic markers for thrombophilia in recurrent pregnancy loss. Hum Reprod. 2002; 17(6): 1633-7.
84. Medawar PB. Some immunological and endocrinological problems raised by the evolution of viviparity in vertebrates. . Symp Soc Exp Biol. 1953; 7: 320-38.
85. Billington WD. The immunological problem of pregnancy: 50 years with the hope of progress. A tribute to Peter Medawar. J Reprod Immunol. 2003; 60(1): 1-11.
86. Mor G, Aldo P, Alvero AB. The unique immunological and microbial aspects of pregnancy. Nat Rev Immunol. 2017; 17(8): 469-82.
87. Okada H, Tsuzuki T, Murata H. Decidualization of the human endometrium. Reprod Med Biol. 2018; 17(3): 220–7.
88. Moffett-King A. Natural killer cells and pregnancy. Nat Rev Immunol. 2002; 2(9): 656-63.
89. Ander SE, Diamond MS, Coyne CB. Immune responses at the maternal-fetal interface. Sci Immunol. 2019; 4(31): eaat6114.
90. Liu S, Diao L, Huang C, Li Y, Zeng Y, Kwak-Kim JYH. The role of decidual immune cells on human pregnancy. J Reprod Immunol. 2017; 124: 44-53.
91. Tilburgs T, Crespo AC, van der Zwan A, Rybalov B, Raj T, Stranger B, Gardner L, Moffett A, Strominger JL. Human HLA-G+ extravillous trophoblasts: Immune-activating cells that interact with decidual leukocytes. Proc Natl Acad Sci U S A. 2015; 112(23): 7219-24.
92. Braud VM, Allan DS, O'Callaghan CA, Söderström K, D'Andrea A, Ogg GS, Lazetic S, Young NT, Bell JI, Phillips JH, et al. HLA-E binds to natural killer cell receptors CD94/NKG2A, B and C. Nature. 1998; 391(6669): 795-9.

93. Lee N, Llano M, Carretero M, Ishitani A, Navarro F, López-Botet M, Geraghty DE. HLA-E is a major ligand for the natural killer inhibitory receptor CD94/NKG2A. Proc Natl Acad Sci U S A. 1998; 95(9): 5199-204.
94. Boyington JC, Brooks AG, Sun PD. Structure of killer cell immunoglobulin-like receptors and their recognition of the class I MHC molecules. Immunol Rev. 2001; 181: 66-78.
95. Long EO, Barber DF, Burshtyn DN, Faure M, Peterson M, Rajagopalan S, Renard V, Sandusky M, Stebbins CC, Wagtmann N, et al. Inhibition of natural killer cell activation signals by killer cell immunoglobulin-like receptors (CD158). Immunol Rev. 2001; 181: 223-33.
96. Vilches C, Parham P. KIR: diverse, rapidly evolving receptors of innate and adaptive immunity. Annu Rev Immunol. 2002; 20: 217-51.
97. Hiby SE, Walker JJ, O'shaughnessy KM, Redman CW, Carrington M, Trowsdale J, Moffett A. Combinations of maternal KIR and fetal HLA-C genes influence the risk of preeclampsia and reproductive success. J Exp Med. 2004; 200(8): 957-65.
98. Apps R, Murphy SP, Fernando R, Gardner L, Ahad T, Moffett A. Human leucocyte antigen (HLA) expression of primary trophoblast cells and placental cell lines, determined using single antigen beads to characterize allotype specificities of anti-HLA antibodies. Immunology. 2009; 127(1): 26-39.
99. Storkus WJ, Howell DN, Salter RD, Dawson JR, Cresswell P. NK susceptibility varies inversely with target cell class I HLA antigen expression. J Immunol. 1987; 138(6): 1657-9.
100. King A, Boocock C, Sharkey AM, Gardner L, Beretta A, Siccardi AG, Loke YW. Evidence for the expression of HLAA-C class I mRNA and protein by human first trimester trophoblast. J Immunol. 1996; 156(6): 2068-76.
101. Apps R, Gardner L, Moffett A. A critical look at HLA-G. Trends Immunol. 2008; 29(7): 313-21.
102. Sharkey AM, Gardner L, Hiby S, Farrell L, Apps R, Masters L, Goodridge J, Lathbury L, Stewart CA, Verma S, et al. Killer Ig-like receptor expression in uterine NK cells is biased toward recognition of HLA-C and alters with gestational age. J Immunol. 2008; 181(1): 39-46.
103. Parham P, Moffett A. Variable NK cell receptors and their MHC class I ligands in immunity, reproduction and human evolution. Nat Rev Immunol. 2013; 13(2): 133-44.
104. Hutter H, Hammer A, Dohr G, Hunt JS. HLA expression at the maternal-fetal interface. Dev Immunol. 1998; 6(3-4): 197-204.
105. King A, Allan DS, Bowen M, Powis SJ, Joseph S, Verma S, Hiby SE, McMichael AJ, Loke YW, Braud VM. HLA-E is expressed on trophoblast and interacts with CD94/NKG2 receptors on decidual NK cells. Eur J Immunol. 2000; 30(6): 1623-31.
106. King A, Hiby SE, Gardner L, Joseph S, Bowen JM, Verma S, Burrows TD, Loke YW. Recognition of trophoblast HLA class I molecules by decidual NK cell receptors--a review. Placenta. 2000; 21(Suppl A): S81-S5.
107. Zhang J, Dunk CE, Kwan M, Jones RL, Harris LK, Keating S, Lye SJ. Human dNK cell function is differentially regulated by extrinsic cellular engagement and intrinsic activating receptors in first and second trimester pregnancy. Cell Mol Immunol. 2017; 14(2): 203–13.
108. Tarrade A, Lai Kuen R, Malassiné A, Tricottet V, Blain P, Vidaud M, Evain-Brion D. Characterization of human villous and extravillous trophoblasts isolated from first trimester placenta. Laboratory Investigation. 2001; 81(9): 1199-211.
109. Monin L, Whettlock EM, Male V. Immune responses in the human female reproductive tract. Immunology. 2020; 160(2): 106-15.
110. Trundley A, Moffett A. Human uterine leukocytes and pregnancy. Tissue Antigens. 2004; 63(1): 1-12.
111. Jones CJP, Aplin JD. Glycosylation at the Fetomaternal Interface: Does the Glycocode Play a Critical Role in Implantation? Glycoconj J. 2009; 26(3): 359-66.
112. Sargent IL, Borzychowski AM, Redman CW. NK cells and human pregnancy – an inflammatory view. Trends Immunol. 2006; 27(9): 399-404.
113. Hunt JS, Fishback JL, Chumbley G, Loke YW. Identification of class I MHC mRNA in human first trimester trophoblast cells by in situ hybridization. J Immunol. 1990; 144(11): 4420-5.
114. Marchal-Bras-Goncalves R, Rouas-Freiss N, Connan F, Choppin J, Dausset J, Carosella ED, Kirszenbaum M, Guillet J. A soluble HLA-G protein that inhibits natural killer cell-mediated cytotoxicity. Transplant Proc. 2001; 33(3): 2355-9.

115. Solier C, Aguerre-Girr M, Lenfant F, Campan A, Berrebi A, Rebmann V, Grosse-Wilde H, Le Bouteiller P. Secretion of pro-apoptotic intron 4-retaining soluble HLA-G1 by human villous trophoblast. Eur J Immunol. 2002; 32(12): 3576-86.
116. Ishitani A, Sageshima N, Lee N, Dorofeeva N, Hatake K, Marquardt H, Geraghty DE. Protein expression and peptide binding suggest unique and interacting functional roles for HLA-E, F, and G in maternal-placental immune recognition. J Immunol. 2003; 171(3): 1376-84.
117. van der Meer A, Lukassen HG, van Cranenbroek B, Weiss EH, Braat DD, van Lierop MJ, Joosten I. Soluble HLA-G promotes Th1-type cytokine production by cytokine-activated uterine and peripheral natural killer cells. Mol Hum Reprod. 2007; 13(2): 123-33.
118. Brighton PJ, Maruyama Y, Fishwick K, Vrljicak P, Tewary S, Fujihara R, Muter J, Lucas ES, Yamada T, Woods L, et al. Clearance of senescent decidual cells by uterine natural killer cells in cycling human endometrium. eLife. 2017; 6: e31274.
119. Windsperger K, Dekan S, Pils S, Golletz C, Kunihs V, Fiala C, Kristiansen G, Knöfler M, Pollheimer J. Extravillous trophoblast invasion of venous as well as lymphatic vessels is altered in idiopathic, recurrent, spontaneous abortions. Hum Reprod. 2017; 32(6): 1208-17.
120. Quenby S, Vince G, Farquharson R, Aplin J. Recurrent Miscarriage: A Defect in Nature's Quality Control? Hum Reprod. 2002; 17(8): 1959-63.
121. Weimar CHE, Kavelaars A, Brosens JJ, Gellersen B, de Vreeden-Elbertse JMT, Heijnen CJ, Macklon NS. Endometrial stromal cells of women with recurrent miscarriage fail to discriminate between high- and low-quality human embryos. . PLoS One. 2012; 7(7): e41424.
122. Mor G, Cardenas I, Abrahams V, Guller S. Inflammation and pregnancy: the role of the immune system at the implantation site. Ann N Y Acad Sci. 2011; 1221: 80-7.
123. Fukui A, Funamizu A, Yokota M, Yamada K, Nakamua R, Fukuhara R, Kimura H, Mizunuma H. Uterine and circulating natural killer cells and their roles in women with recurrent pregnancy loss, implantation failure and preeclampsia. J Reprod Immunol. 2011; 90(1): 105-10.
124. Van Acker HH, Capsomidis A, Smits EL, Van Tendeloo VF. CD56 in the Immune System: More Than a Marker for Cytotoxicity? Front Immunol. 2017; 8: 892.
125. Yovel G, Shakhar K, Ben-Eliyahu S. The effects of sex, menstrual cycle, and oral contraceptives on the number and activity of natural killer cells. Gynecol Oncol. 2001; 81(2): 254-62.
126. Vargas ML, Sántos JL, Ruiz C, Montes MJ, Alemán P, García-Tortosa C, García-Olivares E. Comparison of the proportions of leukocytes in early and term human decidua. Am J Reprod Immunol. 1993; 29(3): 135-40.
127. Haller H, Radillo O, Rukavina D, Tedesco F, Candussi G, Petrović O, Randić L. An immunohistochemical study of leucocytes in human endometrium, first and third trimester basal decidua. J Reprod Immunol. 1993; 23(1): 41-9.
128. Jabrane-Ferrat N. Features of Human Decidual NK Cells in Healthy Pregnancy and During Viral Infection. Front Immunol. 2019; 10: 1397.
129. Tuckerman E, Laird SM, Prakash A, Li TC. Prognostic value of the measurement of uterine natural killer cells in the endometrium of women with recurrent miscarriage. Hum Reprod. 2007; 22(8): 2208-13.
130. Angelo LS, Banerjee PP, Monaco-Shawver L, Rosen JB, Makedonas G, Forbes LR, Mace EM, Orange JS. Practical NK cell phenotyping and variability in healthy adults. Immunol Res. 2015; 62(3): 341-56.
131. Cooper MA, Fehniger TA, Turner SC, Chen KS, Ghaheri BA, Ghayur T, Carson WE, Caligiuri MA. Human natural killer cells: a unique innate immunoregulatory role for the CD56(bright) subset. Blood. 2001; 97(10): 3146-51.
132. Jacobs R, Hintzen G, Kemper A, Beul K, Kempf S, Behrens G, Sykora KW, Schmidt RE. CD56bright cells differ in their KIR repertoire and cytotoxic features from CD56dim NK cells. Eur J Immunol. 2001; 31(10): 3121-7.
133. Lanier LL, Le AM, Civin CI, Loken MR, Phillips JH. The relationship of CD16 (Leu-11) and Leu-19 (NKH-1) antigen expression on human peripheral blood NK cells and cytotoxic T lymphocytes. J Immunol. 1986; 136(12): 4480-6.
134. Tamblyn JA, Jeffery LE, Susarla R, Lissauer DM, Coort SL, Garcia AM, Knoblich K, Fletcher AL, Bulmer JN, Kilby MD, et al. Transcriptomic analysis of vitamin D responses in uterine and peripheral NK cells. Reproduction. 2019; 158(2): 211-21.
135. Cooper MA, Fehniger TA, Caligiuri MA. The biology of human natural killer-cell subsets. Trends Immunol. 2001; 22(11): 633-40.

136. Long EO, Kim HS, Liu D, Peterson ME, Rajagopalan S. Controlling natural killer cell responses: integration of signals for activation and inhibition. Annu Rev Immunol. 2013; 31: 227-58.
137. Fauriat C, Long EO, Ljunggren HG, Bryceson YT. Regulation of human NK-cell cytokine and chemokine production by target cell recognition. Blood. 2010; 115(11): 2167-76.
138. Gómez Román VR, Murray JC, Weiner LM. Chapter 1 - Antibody-Dependent Cellular Cytotoxicity (ADCC). In: Ackerman ME, Nimmerjahn F, editors. Antibody Fc: Linking Adaptive and Innate Immunity2014.
139. Mandal A, Viswanathan C. Natural killer cells: In health and disease. Hematol Oncol Stem Cell Ther. 2015; 8(2): 47-55.
140. Fu B, Li X, Sun R, Tong X, Ling B, Tian Z, Wei H. Natural killer cells promote immune tolerance by regulating inflammatory TH17 cells at the human maternal-fetal interface. Proc Natl Acad Sci U S A. 2013; 110(3): E231-E40.
141. Ticconi C, Pietropolli A, Di Simone N, Piccione E, Fazleabas A. Endometrial Immune Dysfunction in Recurrent Pregnancy Loss. Int J Mol Sci. 2019; 20(21): 5332.
142. PrabhuDas M, Bonney E, Caron K, Dey S, Erlebacher A, Fazleabas A, Fisher S, Golos T, Matzuk M, McCune JM, et al. Immune mechanisms at the maternal-fetal interface: perspectives and challenges. Nat Immunol. 2015; 16(4): 328-34.
143. Lash GE, Schiessl B, Kirkley M, Innes BA, Cooper A, Searle RF, Robson SC, Bulmer JN. Expression of angiogenic growth factors by uterine natural killer cells during early pregnancy. J Leukoc Biol. 2006; 80(5): 572-80.
144. Moffett A, Regan L, Braude P. Natural killer cells, miscarriage, and infertility. BMJ. 2004; 329(7477): 1283–5.
145. Santoni A, Carlino C, Gismondi A. Uterine NK cell development, migration and function. Reprod Biomed Online. 2008; 16(2): 202-10.
146. King A, Birkby C, Loke YW. Early human decidual cells exhibit NK activity against the K562 cell line but not against first trimester trophoblast. Cell Immunol. 1989; 118(2): 337-44.
147. Abadía-Molina AC, Ruiz C, Montes MJ, King A, Loke YW, Olivares EG. Immune phenotype and cytotoxic activity of lymphocytes from human term decidua against trophoblast. J Reprod Immunol. 1996; 31(1-2): 109-23.
148. Rouas-Freiss N, Gonçalves RM, Menier C, Dausset J, Carosella ED. Direct evidence to support the role of HLA-G in protecting the fetus from maternal uterine natural killer cytolysis. Proc Natl Acad Sci U S A. 1997; 94(21): 11520-5.
149. Hanna J, Goldman-Wohl D, Hamani Y, Avraham I, Greenfield C, Natanson-Yaron S, Prus D, Cohen-Daniel L, Arnon TI, Manaster I, et al. Decidual NK cells regulate key developmental processes at the human fetal-maternal interface. Nat Med. 2006; 12(9): 1065-74.
150. Kennedy PR, Chazara O, Gardner L, Ivarsson MA, Farrell LE, Xiong S, Hiby S, Colucci F, Sharkey AM, Moffett A. Activating KIR2DS4 Is Expressed by Uterine NK Cells and Contributes to Successful Pregnancy. J Immunol. 2016; 197(11): 4292-300.
151. Xiong S, Sharkey AM, Kennedy PR, Gardner L, Farrell LE, Chazara O, Bauer J, Hiby SE, Colucci F, Moffett A. Maternal uterine NK cell-activating receptor KIR2DS1 enhances placentation. J Clin Invest. 2013; 123(10): 4264-72.
152. Moffett A, Loke C. Immunology of placentation in eutherian mammals. Nat Rev Immunol. 2006; 6(8): 584-94.
153. Arcuri F, Cintorino M, Carducci A, Papa S, Riparbelli MG, Mangioni S, Di Blasio AM, Tosi P, Viganò P. Human decidual natural killer cells as a source and target of macrophage migration inhibitory factor. Reproduction. 2006; 131(1): 175-82.
154. Saito S, Nishikawa K, Morii T, Enomoto M, Narita N, Motoyoshi K, Ichijo M. Cytokine production by CD16-CD56bright natural killer cells in the human early pregnancy decidua. Int Immunol. 1993; 5(5): 559-63.
155. Smith SD, Dunk CE, Aplin JD, Harris LK, Jones RL. Evidence for Immune Cell Involvement in Decidual Spiral Arteriole Remodeling in Early Human Pregnancy. Am J Pathol. 2009; 174(5): 1959-71.
156. Sourav P, Lal G. The Molecular Mechanism of Natural Killer Cells Function and Its Importance in Cancer Immunotherapy. Front Immunol. 2017; 8: 1124.
157. Kayisli UA, Mahutte NG, Arici A. Uterine chemokines in reproductive physiology and pathology. Am J Reprod Immunol. 2002; 47(4): 213-21.
158. Gaynor LM, Colucci F. Uterine Natural Killer Cells: Functional Distinctions and Influence on Pregnancy in Humans and Mice. Front Immunol. 2017; 8: 467.

159. Koopman LA, Kopcow HD, Rybalov B, Boyson JE, Orange JS, Schatz F, Masch R, Lockwood CJ, Schachter AD, Park PJ, et al. Human decidual natural killer cells are a unique NK cell subset with immunomodulatory potential. J Exp Med. 2003; 198(8): 1201-12.
160. Vento-Tormo R, Efremova M, Botting RA, Turco MY, Vento-Tormo M, Meyer KB, Park JE, Stephenson E, Polański K, Goncalves A, et al. Single-cell reconstruction of the early maternal-fetal interface in humans. Nature. 2018; 563(7731): 347-53.
161. Yamada H, Morikawa M, Kato EH, Shimada S, Kobashi G, Minakami H. Pre-conceptional natural killer cell activity and percentage as predictors of biochemical pregnancy and spontaneous abortion with normal chromosome karyotype. Am J Reprod Immunol. 2003; 50(4): 351-4.
162. Coulam CB, Goodman C, Roussev RG, Thomason EJ, Beaman KD. Systemic CD56+ cells can predict pregnancy outcome. Am J Reprod Immunol. 1995; 33(1): 40-6.
163. Adib Rad H, Basirat Z, Mostafazadeh A, Faramarzi M, Bijani A, Nouri HR, Soleimani Amiri S. Evaluation of peripheral blood NK cell subsets and cytokines in unexplained recurrent miscarriage. J Chin Med Assoc. 2018; 81(12): 1065-70.
164. Beer AE, Kwak JY, Ruiz JE. Immunophenotypic profiles of peripheral blood lymphocytes in women with recurrent pregnancy losses and in infertile women with multiple failed in vitro fertilization cycles. Am J Reprod Immunol. 1996; 35(4): 376-82.
165. Emmer PM, Veerhoek M, Nelen WL, Steegers EA, Joosten I. Natural killer cell reactivity and HLA-G in recurrent spontaneous abortion. Transplant Proc. 1999; 31(4): 1838-40.
166. Kwak JY, Kwak FM, Ainbinder SW, Ruiz AM, Beer AE. Elevated peripheral blood natural killer cells are effectively downregulated by immunoglobulin G infusion in women with recurrent spontaneous abortions. Am J Reprod Immunol. 1996; 35(4): 363-9.
167. Quenby S, Bates M, Doig T, Brewster J, Lewis-Jones DI, Johnson PM, Vince G. Pre-implantation endometrial leukocytes in women with recurrent miscarriage. Hum Reprod. 1999; 14(9): 2386-91.
168. Aoki K, Kajiura S, Matsumoto Y, Ogasawara M, Okada S, Yagami Y, Gleicher N. Preconceptional natural-killer-cell activity as a predictor of miscarriage. Lancet. 1995; 345(8961): 1340-2.
169. Morikawa M, Yamada H, Kato EH, Shimada S, Ebina Y, Yamada T, Sagawa T, Kobashi G, Fujimoto S. NK cell activity and subsets in women with a history of spontaneous abortion. Cause, number of abortions, and subsequent pregnancy outcome. Gynecol Obstet Invest. 2001; 52(3): 163-7.
170. Yamada H, Kato EH, Kobashi G, Ebina Y, Shimada S, Morikawa M, Sakuragi N, Fujimoto S. High NK cell activity in early pregnancy correlates with subsequent abortion with normal chromosomes in women with recurrent abortion. Am J Reprod Immunol. 2001; 46(2): 132-6.
171. Emmer PM, Nelen WL, Steegers E, Hendriks JC, Veerhoek M, Joosten I. Peripheral natural killer cytotoxicity and CD56(pos)CD16(pos) cells increase during early pregnancy in women with a history of recurrent spontaneous abortion. Hum Reprod. 2000; 15(5): 1163-9.
172. Tang AW, Alfirevic Z, Quenby S. Natural killer cells and pregnancy outcomes in women with recurrent miscarriage and infertility: a systematic review. Hum Reprod. 2011; 26(8): 1971-80.
173. Michimata T, Ogasawara MS, Tsuda H, Suzumori K, Aoki K, Sakai M, Fujimura M, Nagata K, Nakamura M, Saito S. Distributions of endometrial NK cells, B cells, T cells, and Th2/Tc2 cells fail to predict pregnancy outcome following recurrent abortion. Am J Reprod Immunol. 2002; 47(4): 196-202.
174. Lachapelle MH, Miron P, Hemmings R, Roy DC. Endometrial T, B, and NK cells in patients with recurrent spontaneous abortion. Altered profile and pregnancy outcome. J Immunol. 1996; 156(10): 4027-34.
175. Kolanska K, Dabi Y, Dechartres A, Cohen J, Ben Kraiem Y, Selleret L, Mathieu d'Argent E, Placais L, Cheloufi M, Johanet C, et al. Unexplained recurrent miscarriages: predictive value of immune biomarkers and immunomodulatory therapies for live birth. Am J Reprod Immunol. 2021: e13425.
176. Williams PJ, Searle RF, Robson SC, Innes BA, Bulmer JN. Decidual leucocyte populations in early to late gestation normal human pregnancy. J Reprod Immunol. 2009; 82(1): 24-31.
177. Mahmoud F, Abul H, Omu A, Al-Rayes S, Haines D, Whaley K. Pregnancy-associated changes in peripheral blood lymphocyte subpopulations in normal Kuwaiti women. Gynecol Obstet Invest. 2001; 52(4): 232-6.
178. Mosimann B, Wagner M, Shehata H, Poon LC, Ford B, Nicolaides KH, Bansal AS. Natural killer cells and their activation status in normal pregnancy. Int J Reprod Med. 2013; 2013: 906813.

179. Perricone R, Di Muzio G, Perricone C, Giacomelli R, De Nardo D, Fontana L, De Carolis C. High levels of peripheral blood NK cells in women suffering from recurrent spontaneous abortion are reverted from high-dose intravenous immunoglobulins. Am J Reprod Immunol. 2006; 55(3): 232-9.
180. Kühnert M, Strohmeier R, Stegmüller M, Halberstadt E. Changes in lymphocyte subsets during normal pregnancy. Eur J Obstet Gynecol Reprod Biol. 1998; 76(2): 147-51.
181. Thum MY, Bhaskaran S, Abdalla HI, Ford B, Sumar N, Shehata H, Bansal AS. An increase in the absolute count of $CD56^{dim}CD16^{+}CD69^{+}$ NK cells in the peripheral blood is associated with a poorer IVF treatment and pregnancy outcome. Hum Reprod. 2004; 19(10): 2395-400.
182. Kwak JY, Beaman KD, Gilman-Sachs A, Ruiz JE, Schewitz D, Beer AE. Up-regulated expression of CD56+, CD56+/CD16+, and CD19+ cells in peripheral blood lymphocytes in pregnant women with recurrent pregnancy losses. Am J Reprod Immunol. 1995; 34(2): 93-9.
183. Perricone C, De Carolis C, Giacomelli R, Zaccari G, Cipriani P, Bizzi E, Perricone R. High levels of NK cells in the peripheral blood of patients affected with anti-phospholipid syndrome and recurrent spontaneous abortion: a potential new hypothesis. Rheumatology. 2007; 46(10): 1574-8.
184. Seshadri S, Sunkara SK. Natural killer cells in female infertility and recurrent miscarriage: a systematic review and meta-analysis. Hum Reprod Update. 2014; 20(3): 429-38.
185. King K, Smith S, Chapman M, Sacks G. Detailed analysis of peripheral blood natural killer (NK) cells in women with recurrent miscarriage. Hum Reprod. 2010; 25(1): 52-8.
186. Shakhar K, Ben-Eliyahu S, Loewenthal R, Rosenne E, Carp H. Differences in number and activity of peripheral natural killer cells in primary versus secondary recurrent miscarriage. Fertil Steril. 2003; 80(2): 368-75.
187. Yoo JH, Kwak-Kim J, Han AR, Ahn H, Cha SH, Koong MK, Kang IS, Yang KM. Peripheral blood NK cell cytotoxicities are negatively correlated with CD8(+) T cells in fertile women but not in women with a history of recurrent pregnancy loss. Am J Reprod Immunol. 2012; 68(1): 38-46.
188. Prado-Drayer A, Teppa J, Sánchez P, Camejo MI. Immunophenotype of peripheral T lymphocytes, NK cells and expression of CD69 activation marker in patients with recurrent spontaneous abortions, during the mid-luteal phase. Am J Reprod Immunol. 2008; 60(1): 66-74.
189. Ghafourian M, Karami N, Khodadadi A, Nikbakht R. Increase of CD69, CD161 and CD94 on NK cells in women with recurrent spontaneous abortion and in vitro fertilization failure. Iran J Immunol. 2014; 11(2): 84-96.
190. Zhu L, Aly M, Wang H, Karakizlis H, Weimer R, Morath C, Kuon RJ, Toth B, Ekpoom N, Opelz G, et al. Increased natural killer cell subsets with inhibitory cytokines and inhibitory surface receptors in patients with recurrent miscarriage and decreased or normal subsets in kidney transplant recipients late post-transplant. Clin Exp Immunol. 2018; 193(2): 241-54.
191. Karami N, Boroujerdnia MG, Nikbakht R, Khodadadi A. Enhancement of peripheral blood $CD56^{dim}$ cell and NK cell cytotoxicity in women with recurrent spontaneous abortion or in vitro fertilization failure. J Reprod Immunol. 2012; 95(1-2): 87-92.
192. Wang F, Jia W, Fan M, Shao X, Li Z, Liu Y, Ma Y, Li YX, Li R, Tu Q, et al. Single-cell Immune Landscape of Human Recurrent Miscarriage. Genomics, Proteomics & Bioinformatics. 2021; S1672-0229(21): 00003-6.
193. Wang Q, Li TC, Wu YP, Cocksedge KA, Fu YS, Kong QY, Yao SZ. Reappraisal of peripheral NK cells in women with recurrent miscarriage. Reprod Biomed Online. 2008; 17(6): 814-9.
194. Fukui A, Kwak-Kim J, Ntrivalas E, Gilman-Sachs A, Lee SK, Beaman K. Intracellular cytokine expression of peripheral blood natural killer cell subsets in women with recurrent spontaneous abortions and implantation failures. Fertil Steril. 2008; 89(1): 157-65.
195. Zhang Y, Huang C, Lian R, Xu J, Fu Y, Zeng Y, Tu W. The low cytotoxic activity of peripheral blood NK cells may relate to unexplained recurrent miscarriage. Am J Reprod Immunol. 2021; 85(6): e13388.
196. Zhang YN, Huang CY, Lian RC, Xu J, Fu YF, Zeng Y, Tu WW. Relationship between the cytotoxic activity of peripheral blood natural killer cells and recurrent miscarriage. Authorea. 2020: 1-16.
197. Kolanska K, Suner L, Cohen J, Ben Kraiem Y, Placais L, Fain O, Bornes M, Selleret L, Delhommeau F, Feger F, et al. Proportion of Cytotoxic Peripheral Blood Natural Killer Cells and T-Cell Large Granular Lymphocytes in Recurrent Miscarriage and Repeated Implantation Failure: Case-Control Study and Meta-analysis. Arch Immunol Ther Exp. 2019; 67(4): 225-36.
198. Clifford K, Flanagan AM, Regan L. Endometrial CD56+ natural killer cells in women with recurrent miscarriage: a histomorphometric study. Hum Reprod. 1999; 14(11): 2727-30.

199. Quenby S, Kalumbi C, Bates M, Farquharson R, Vince G. Prednisolone reduces preconceptual endometrial natural killer cells in women with recurrent miscarriage. Fertil Steril. 2005; 84(4): 980-4.
200. Kwak JY, Beer AE, Kim SH, Mantouvalos HP. Immunopathology of the implantation site utilizing monoclonal antibodies to natural killer cells in women with recurrent pregnancy losses. Am J Reprod Immunol. 1999; 41(1): 91-8.
201. Marron K, Walsh D, Conor Harrity C. Detailed endometrial immune assessment of both normal and adverse reproductive outcome populations. J Assist Reprod Genet. 2019; 36(2): 199-210.
202. Melsen JE, Lugthart G, Lankester AC, Schilham MW. Human Circulating and Tissue-Resident CD56^{bright} Natural Killer Cell Populations. Front Immunol. 2016; 7: 262.
203. Manaster I, Mandelboim O. The unique properties of uterine NK cells. Am J Reprod Immunol. 2010; 63(6): 434-44.
204. Shimada S, Kato EH, Morikawa M, Iwabuchi K, Nishida R, Kishi R, Onoé K, Minakami H, Yamada H. No difference in natural killer or natural killer T-cell population, but aberrant T-helper cell population in the endometrium of women with repeated miscarriage. Hum Reprod. 2004; 19(4): 1018-24.
205. Lucas ES, Vrljicak P, Muter J, Diniz-da-Costa MM, Brighton PJ, Kong CS, Lipecki J, Fishwick KJ, Odendaal J, Ewington LJ, et al. Recurrent pregnancy loss is associated with a pro-senescent decidual response during the peri-implantation window. Commun Biol. 2020; 3: 37.
206. Rodrigues MN, Favaron PO, Dombrowski JG, de Souza RM, Miglino MA. Role of natural killer (NK) cells during pregnancy: A review. Open J Anim Sci. 2013; 3(2): 138-44.
207. Guo C, Cai P, Jin L, Sha Q, Yu Q, Zhang W, Jiang C, Liu Q, Zong D, Li K, et al. Single-cell profiling of the human decidual immune microenvironment in patients with recurrent pregnancy loss. Cell Discovery. 2021; 7(1): 1.
208. Huhn O, Ivarsson MA, Gardner L, Hollinshead M, Stinchcombe JC, Chen P, Shreeve N, Chazara O, Farrell LE, Theorell J, et al. Distinctive phenotypes and functions of innate lymphoid cells in human decidua during early pregnancy. Nature Communications. 2020; 11(1): 381.
209. Guerrero B, Hassouneh F, Delgado E, Casado JG, Tarazona R. Natural killer cells in recurrent miscarriage: An overview. J Reprod Immunol. 2020; 142: 103209.
210. Del Zotto G, Marcenaro E, Vacca P, Sivori S, Daniela Pende D, Della Chiesa M, Moretta F, Ingegnere T, Mingari MC, Moretta A, et al. Markers and function of human NK cells in normal and pathological conditions. Cytometry B Clin Cytom. 2017; 92(2): 100-14.
211. Pegram HJ, Andrews DM, Smyth MJ, Darcy PK, Kershaw MH. Activating and inhibitory receptors of natural killer cells. Immunology & Cell Biology. 2011; 89(2): 216-24.
212. Vargas RG, Bompeixe EP, França PP, Marques de Moraes M, da Graça Bicalho M. Activating killer cell immunoglobulin-like receptor genes' association with recurrent miscarriage. Am J Reprod Immunol. 2009; 62(1): 34-43.
213. Rajagopalan S, Fu J, Long EO. Cutting edge: induction of IFN-gamma production but not cytotoxicity by the killer cell Ig-like receptor KIR2DL4 (CD158d) in resting NK cells. J Immunol. 2001; 167(4): 1877-81.
214. Rajagopalan S, Long EO. A human histocompatibility leukocyte antigen (HLA)-G-specific receptor expressed on all natural killer cells. J Exp Med. 1999; 189(7): 1093-100.
215. Faure M, Long EO. KIR2DL4 (CD158d), an NK cell-activating receptor with inhibitory potential. The Journal of Immunology. 2002; 168(12): 6208-14.
216. Cristiani CM, Palella E, Sottile R, Tallerico R, Garofalo C, Carbone E. Human NK Cell Subsets in Pregnancy and Disease: Toward a New Biological Complexity. Front Immunol. 2016; 7: 656.
217. Male V, Sharkey A, Masters L, Kennedy PR, Farrell LE, Moffett A. The effect of pregnancy on the uterine NK cell KIR repertoire. Eur J Immunol. 2011; 41(10): 3017-27.
218. Hiby SE, Apps R, Sharkey AM, Farrell LE, Gardner L, Mulder A, Claas FH, Walker JJ, Redman CW, Morgan L, et al. Maternal activating KIRs protect against human reproductive failure mediated by fetal HLA-C2. J Clin Invest. 2010; 120(11): 4102-10.
219. Moffett A, Chazara O, Colucci F, Johnson MH. Variation of maternal KIR and fetal HLA-C genes in reproductive failure: too early for clinical intervention. Reprod Biomed Online. 2016; 33(6): 763-9.

220. Feyaerts D, Kuret T, van Cranenbroek B, van der Zeeuw-Hingrez S, van der Heijden OWH, van der Meer A, Joosten I, van der Molen RG. Endometrial natural killer (NK) cells reveal a tissue-specific receptor repertoire. Hum Reprod. 2018; 33(3): 441-51.
221. Marlin R, Duriez M, Berkane N, de Truchis C, Madec Y, Rey-Cuille MA, Cummings JS, Cannou C, Quillay H, Barré-Sinoussi F, et al. Dynamic shift from CD85j/ILT-2 to NKG2D NK receptor expression pattern on human decidual NK during the first trimester of pregnancy. PLoS One. 2012; 7(1): e30017.
222. Hollenbach JA, Nocedal I, Ladner MB, Single RM, Trachtenberg EA. Killer cell immunoglobulin-like receptor (KIR) gene content variation in the HGDP-CEPH populations. Immunogenetics. 2012; 64(10): 719-37.
223. Hiby SE, Regan L, Lo W, Farrell L, Carrington M, Moffett A. Association of maternal killer-cell immunoglobulin-like receptors and parental HLA-C genotypes with recurrent miscarriage. Hum Reprod. 2008; 23(4): 972-6.
224. Sacks G, Finkelstein E. Natural killer cells and reproductive success. Am J Reprod Immunol. 2020; 85(4): e13291.
225. Wang S, Zhao YR, Jiao YL, Wang LC, Li JF, Cui B, Xu CY, Shi YH, Chen ZJ. Increased activating killer immunoglobulin-like receptor genes and decreased specific HLA-C alleles in couples with recurrent spontaneous abortion. Biochem Biophys Res Commun. 2007; 360(3): 696-701.
226. Faridi RM, Agrawal S. Killer immunoglobulin-like receptors (KIRs) and HLA-C allorecognition patterns implicative of dominant activation of natural killer cells contribute to recurrent miscarriages. Hum Reprod. 2011; 26(2): 491-7.
227. Su N, Wang H, Zhang B, Kang Y, Guo Q, Xiao H, Yang H, Liao S. Maternal natural killer cell immunoglobulin receptor genes and human leukocyte antigen-C ligands influence recurrent spontaneous abortion in the Han Chinese population. Experimental and Therapeutic Medicine. 2018; 15(1): 327-37.
228. Yang X, Yang E, Wang WJ, He Q, Jubiz G, Katukurundage D, Dambaeva S, Beaman K, Kwak-Kim J. Decreased HLA-C1 alleles in couples of KIR2DL2 positive women with recurrent pregnancy loss. J Reprod Immunol. 2020; 142: 103186.
229. Flores AC, Marcos CY, Paladino N, Arruvito L, Williams F, Middleton D, Fainboim L. KIR receptors and HLA-C in the maintenance of pregnancy. Tissue Antigens. 2007; 69(Suppl 1): 112-3.
230. Dambaeva SV, Lee DH, Sung N, Chen CY, Bao S, Gilman-Sachs A, Kwak-Kim J, Beaman KD. Recurrent Pregnancy Loss in Women with Killer Cell Immunoglobulin-Like Receptor KIR2DS1 is Associated with an Increased HLA-C2 Allelic Frequency. Am J Reprod Immunol. 2016; 75(2): 94-103.
231. Witt CS, Goodridge J, Gerbase-Delima MG, Daher S, Christiansen FT. Maternal KIR repertoire is not associated with recurrent spontaneous abortion. Hum Reprod. 2004; 19(11): 2653-7.
232. Hong Y, Wang X, Lu P, Song Y, Lin Q. Killer immunoglobulin-like receptor repertoire on uterine natural killer cell subsets in women with recurrent spontaneous abortions. Eur J Obstet Gynecol Reprod Biol. 2008; 140(2): 218-23.
233. Borges L, Cosman D. LIRs/ILTs/MIRs, inhibitory and stimulatory Ig-superfamily receptors expressed in myeloid and lymphoid cells. Cytokine & Growth Factor Reviews. 2000; 11(3): 209-17.
234. Colonna M, Nakajima H, Cella M. Inhibitory and activating receptors involved in immune surveillance by human NK and myeloid cells. J Leukoc Biol. 1999; 66(5): 718-22.
235. Ponte M, Cantoni C, Biassoni R, Tradori-Cappai A, Bentivoglio G, Vitale C, Bertone S, Moretta A, Moretta L, Mingari MC. Inhibitory receptors sensing HLA-G1 molecules in pregnancy: decidua-associated natural killer cells express LIR-1 and CD94/NKG2A and acquire p49, an HLA-G1-specific receptor. Proc Natl Acad Sci U S A. 1999; 96(10): 5674-9.
236. M. LG, Seiler C, Kay AW, Bayless NL, Starosvetsky E, Moore L, Shen-Orr SS, Aziz N, Khatri P, Dekker CL, et al. Pregnancy-Induced Alterations in NK Cell Phenotype and Function. Front Immunol. 2019; 10: 2469.
237. Allan DSJ, Mcmichael AJ, Braud VM. The ILT Family of Leukocyte Receptors. Immunobiology. 2000; 202(1): 34-41.
238. Navarro F, Llano M, Bellón T, Colonna M, Geraghty DE, López-Botet M. The ILT2(LIR1) and CD94/NKG2A NK cell receptors respectively recognize HLA-G1 and HLA-E molecules co-expressed on target cells. Eur J Immunol. 1999; 29(1): 277-83.

239. Favier B, Lemaoult J, Lesport E, Carosella ED. ILT2/HLA-G interaction impairs NK-cell functions through the inhibition of the late but not the early events of the NK-cell activating synapse. FASEB J. 2010; 24(3): 689-99.
240. Bulmer JN, Lash GE. Uterine natural killer cells: Time for a re-appraisal? F1000Res. 2019; 8: F1000 Faculty Rev-999.
241. Sivori S, Parolini S, Marcenaro E, Millo R, Bottino C, Moretta A. Triggering receptors involved in natural killer cell-mediated cytotoxicity against choriocarcinoma cell lines. Hum Immunol. 2000; 61(11): 1055-8.
242. Jones DC, Kosmoliaptsis V, Apps R, Lapaque N, Smith I, Kono A, Chang C, Boyle LH, Taylor CJ, Trowsdale J, et al. HLA class I allelic sequence and conformation regulate leukocyte Ig-like receptor binding. J Immunol. 2011; 186(5): 2990-7.
243. Fukui A, Funamizu A, Fukuhara R, Shibahara H. Expression of natural cytotoxicity receptors and cytokine production on endometrial natural killer cells in women with recurrent pregnancy loss or implantation failure, and the expression of natural cytotoxicity receptors on peripheral blood natural killer cells in pregnant women with a history of recurrent pregnancy loss. J Obstet Gynaecol Res. 2017; 43(11): 1678-86.
244. Vitale M, Falco M, Castriconi R, Parolini S, Zambello R, Semenzato G, Biassoni R, Bottino C, Moretta L, Moretta A. Identification of NKp80, a novel triggering molecule expressed by human NK cells. Eur J Immunol. 2001; 31(1): 233-42.
245. Vacca P, Mingari MC, Moretta L. Natural killer cells in human pregnancy. J Reprod Immunol. 2013; 97(1): 14-9.
246. Fukui A, Kamoi M, Funamizu A, Fuchinoue K, Chiba H, Yokota M, Fukuhara R, Mizunuma H. NK cell abnormality and its treatment in women with reproductive failures such as recurrent pregnancy loss, implantation failures, preeclampsia, and pelvic endometriosis. Reprod Med Biol. 2015; 14(4): 151-7.
247. Moretta A, Bottino C, Vitale M, Pende D, Cantoni C, Mingari MC, Biassoni R, Moretta L. Activating receptors and coreceptors involved in human natural killer cell-mediated cytolysis. Annu Rev Immunol. 2001; 19: 197-223.
248. Loza MJ, Perussia B. Final steps of natural killer cell maturation: a model for type 1-type 2 differentiation? Nat Immunol. 2001; 2(10): 917-24.
249. Horton NC, Mathew SO, Mathew PA. Novel interaction between proliferating cell nuclear antigen and HLA I on the surface of tumor cells inhibits NK cell function through NKp44. PLoS One. 2013; 8(3): e59552.
250. Morvan MG, Lanier LL. NK cells and cancer: you can teach innate cells new tricks. Nature Reviews Cancer. 2016; 16(1): 7-19.
251. Acar N, Ustunel I, Demir R. Uterine natural killer (uNK) cells and their missions during pregnancy: a review. Acta Histochem. 2011; 113(2): 82-91.
252. Vacca P, Cantoni C, Prato C, Fulcheri E, Moretta A, Moretta L, Mingari MC. Regulatory role of NKp44, NKp46, DNAM-1 and NKG2D receptors in the interaction between NK cells and trophoblast cells. Evidence for divergent functional profiles of decidual versus peripheral NK cells. Int Immunol. 2008; 20(11): 1395-405.
253. El Costa H, Casemayou A, Aguerre-Girr M, Rabot M, Berrebi A, Parant O, Clouet-Delannoy M, Lombardelli L, Jabrane-Ferrat N, Rukavina D, et al. Critical and differential roles of NKp46- and NKp30-activating receptors expressed by uterine NK cells in early pregnancy. The Journal of Immunology. 2008; 181(5): 3009-17.
254. Wallace AE, Whitley GS, Thilaganathan B, Cartwright JE. Decidual natural killer cell receptor expression is altered in pregnancies with impaired vascular remodeling and a higher risk of pre-eclampsia. J Leukoc Biol. 2015; 97(1): 79-86.
255. El Costa H, Tabiasco J, Berrebi A, Parant O, Aguerre-Girr M, Piccinni MP, Le Bouteiller P. Effector functions of human decidual NK cells in healthy early pregnancy are dependent on the specific engagement of natural cytotoxicity receptors. J Reprod Immunol. 2009; 82(2): 142-7.
256. Zhang Y, Zhao A, Wang X, Shi G, Jin H, Lin Q. Expressions of natural cytotoxicity receptors and NKG2D on decidual natural killer cells in patients having spontaneous abortions. Fertil Steril. 2008; 90(5): 1931-7.
257. Fukui A, Ntrivalas E, Gilman-Sachs A, Kwak-Kim J, Lee SK, Levine R, Beaman K. Expression of natural cytotoxicity receptors and a2V-ATPase on peripheral blood NK cell subsets in women with recurrent spontaneous abortions and implantation failures. Am J Reprod Immunol. 2006; 56(5-6): 312-20.

258. Giuliani E, Parkin KL, Lessey BA, Young SL, Fazleabas AT. Characterization of uterine NK cells in women with infertility or recurrent pregnancy loss and associated endometriosis. Am J Reprod Immunol. 2014; 72(3): 262-9.
259. Zingoni A, Palmieri G, Morrone S, Carretero M, Lopez-Botel M, Piccoli M, Frati L, Santoni A. CD69-triggered ERK activation and functions are negatively regulated by CD94 / NKG2-A inhibitory receptor. Eur J Immunol. 2000; 30(2): 644-51.
260. Sáez-Borderías A, Romo N, Magri G, Gumá M, Angulo A, López-Botet M. IL-12-dependent inducible expression of the CD94/NKG2A inhibitory receptor regulates CD94/NKG2C+ NK cell function. The Journal of Immunology. 2009; 182(2): 829-36.
261. O'Leary JG, Goodarzi M, Drayton DL, von Andrian UH. T Cell- And B Cell-Independent Adaptive Immunity Mediated by Natural Killer Cells. Nat Immunol. 2006; 7(5): 507-16.
262. Ntrivalas EI, Kwak-Kim JY, Gilman-Sachs A, Chung-Bang H, Ng SC, Beaman KD, Mantouvalos HP, Beer AE. Status of peripheral blood natural killer cells in women with recurrent spontaneous abortions and infertility of unknown aetiology. Hum Reprod. 2001; 16(5): 855-61.
263. Hò GGT, Celik AA, Huyton T, Hiemisch W, Blasczyk R, Simper GS, Bade-Doeding C. NKG2A/CD94 Is a New Immune Receptor for HLA-G and Distinguishes Amino Acid Differences in the HLA-G Heavy Chain. Int J Mol Sci. 2020; 21(12): 4362.
264. Kusumi M, Yamashita T, Fujii T, Nagamatsu T, Kozuma S, Taketani Y. Expression patterns of lectin-like natural killer receptors, inhibitory CD94/NKG2A, and activating CD94/NKG2C on decidual CD56bright natural killer cells differ from those on peripheral CD56dim natural killer cells. J Reprod Immunol. 2006; 70(1-2): 33-42.
265. Raulet DH, Gasser S, Gowen BG, Deng W, Jung H. Regulation of ligands for the NKG2D activating receptor. Annu Rev Immunol. 2013; 31: 413-41.
266. Apps R, Gardner L, Traherne J, Male V, Moffett A. Natural-killer cell ligands at the maternal-fetal interface: UL-16 binding proteins, MHC class-I chain related molecules, HLA-F and CD48. Hum Reprod. 2008; 23(11): 2535-48.
267. Abdian Asl A, Vaziri Nezamdoust F, Fesahat F, Astani A, Barati M, Raee P, Asadi-Saghandi A. Association between rs1049174 *NKG2D* gene polymorphism and idiopathic recurrent spontaneous abortion in Iranian women: a case-control study. J Obstet Gynaecol. 2021; 41(5): 774-8.
268. Hayashi T, Imai K, Morishita Y, Hayashi I, Kusunoki Y, Nakachi K. Identification of the NKG2D haplotypes associated with natural cytotoxic activity of peripheral blood lymphocytes and cancer immunosurveillance. Cancer Research. 2006; 66(1): 563-70.
269. Furue H, Matsuo K, Kumimoto H, Hiraki A, Suzuki T, Yatabe Y, Komori K, Kanemitsu Y, Hirai T, Kato T, et al. Decreased risk of colorectal cancer with the high natural killer cell activity NKG2D genotype in Japanese. Carcinogenesis. 2008; 29(2): 316-20.
270. Björkström NK, Riese P, Heuts F, Andersson S, Fauriat C, Ivarsson MA, Björklund AT, Flodström-Tullberg M, Michaëlsson J, Rottenberg ME, et al. Expression patterns of NKG2A, KIR, and CD57 define a process of CD56dim NK-cell differentiation uncoupled from NK-cell education. Blood. 2010; 116(19): 3853-64.
271. Lopez-Vergès S, Milush JM, Pandey S, York VA, Arakawa-Hoyt J, Pircher H, Norris PJ, Nixon DF, Lanier LL. CD57 defines a functionally distinct population of mature NK cells in the human CD56dimCD16+ NK-cell subset. Blood. 2010; 116(19): 3865-74.
272. Hidaka Y, Amino N, Iwatani Y, Kaneda T, Mitsuda N, Morimoto Y, Tanizawa O, Miyai K. Changes in natural killer cell activity in normal pregnant and postpartum women: increases in the first trimester and postpartum period and decrease in late pregnancy. J Reprod Immunol. 1991; 20(1): 73-83.
273. Mallone R, Funaro A, Zubiaur M, Baj G, Ausiello CM, Tacchetti C, Sancho J, Grossi C, Malavasi F. Signaling through CD38 induces NK cell activation. Int Immunol. 2001; 13(4): 397–409.
274. Deaglio S, Zubiaur M, Gregorini A, Bottarel F, Ausiello CM, Dianzani U, Sancho J, Malavasi F. Human CD38 and CD16 are functionally dependent and physically associated in natural killer cells. Blood. 2002; 99(7): 2490-598.
275. Le Gars M, Seiler C, Kay AW, Bayless NL, Starosvetsky E, Moore L, Shen-Orr SS, Aziz N, Khatri P, Dekker CL, et al. CD38 is a key regulator of enhanced NK cell immune responses during pregnancy through its role in immune synapse formation. BioRxiv. 2018; Version 1.
276. Silva A, Andrews DM, Brooks AG, Smyth MJ, Hayakawa Y. Application of CD27 as a marker for distinguishing human NK cell subsets. Int Immunol. 2008; 20(4): 625-30.

277. Vossen MTM, Matmati M, Hertoghs KML, Baars PA, Gent MR, Leclercq G, Hamann J, Kuijpers TW, van Lier RAW. CD27 defines phenotypically and functionally different human NK cell subsets. The Journal of Immunology. 2008; 180(6): 3739-45.
278. Kurioka A, Cosgrove C, Simoni Y, van Wilgenburg B, Geremia A, Björkander S, Sverremark-Ekström E, Thurnheer C, Günthard HF, Khanna N, et al. CD161 Defines a Functionally Distinct Subset of Pro-Inflammatory Natural Killer Cells. Front Immunol. 2018; 9: 486.
279. Kim HP, Imbert J, Leonard WJ. Both integrated and differential regulation of components of the IL-2/IL-2 receptor system. Cytokine & Growth Factor Reviews. 2006; 17(5): 349-66.
280. Carson WE, Giri JG, Lindemann MJ, Linett ML, Ahdieh M, Paxton R, Anderson D, Eisenmann J, Grabstein K, Caligiuri MA. Interleukin (IL) 15 is a novel cytokine that activates human natural killer cells via components of the IL-2 receptor. J Exp Med. 1994; 180(4): 1395-403.
281. Sharma R, Das A. IL-2 mediates NK cell proliferation but not hyperactivity. Immunol Res. 2018; 66(1): 151-7.
282. Gasteiger G, Hemmers S, Firth MA, Le Floc'h A, Huse M, Sun JC, Rudensky AY. IL-2-dependent tuning of NK cell sensitivity for target cells is controlled by regulatory T cells. J Exp Med. 2013; 210(6): 1167-78.
283. Henney CS, Kuribayashi K, Kern DE, Gillis S. Interleukin-2 augments natural killer cell activity. Nature. 1981; 291(5813): 335-8.
284. Wu Y, Tian Z, Wei H. Developmental and Functional Control of Natural Killer Cells by Cytokines. Front Immunol. 2017; 8: 930.
285. MacLean MA, Wilson R, Jenkins C, Miller H, Walker JJ. Interleukin-2 receptor concentrations in pregnant women with a history of recurrent miscarriage. Hum Reprod. 2002; 17(1): 219-20.
286. Arruga F, Guerra G, Baev D, Hoofd C, Coscia M, D'Arena GF, Gaidano G, Furman RR, Deaglio S. Expression of the Tigit/CD226/CD155 Receptors/Ligand System in Chronic Lymphocytic Leukemia. Blood. 2019; 134: 5454.
287. Zhang Z, Wu N, Lu Y, Davidson D, Colonna M, Veillette A. DNAM-1 controls NK cell activation via an ITT-like motif. J Exp Med. 2015; 212(12): 2165-82.
288. Shibuya A, Campbell D, Hannum C, Yssel H, Franz-Bacon K, McClanahan T, Kitamura T, Nicholl J, Sutherland GR, Lanier LL, et al. DNAM-1, a novel adhesion molecule involved in the cytolytic function of T lymphocytes. Immunity. 1996; 4(6): 573-81.
289. Beldi-Ferchiou A, Lambert M, Dogniaux S, Vély F, Vivier E, Olive D, Dupuy S, Levasseur F, Zucman D, Lebbé C, et al. PD-1 mediates functional exhaustion of activated NK cells in patients with Kaposi sarcoma. Oncotarget. 2016; 7(45): 72961-77.
290. Della Chiesa M, Pesce S, Muccio L, Carlomagno S, Sivori S, Moretta A, Marcenaro E. Features of Memory-Like and PD-1(+) Human NK Cell Subsets. Front Immunol. 2016; 7: 351.
291. Pesce S, Greppi M, Tabellini G, Rampinelli F, Parolini S, Olive D, Moretta L, Moretta A, Marcenaro E. Identification of a subset of human natural killer cells expressing high levels of programmed death 1: A phenotypic and functional characterization. Journal of Allergy and Clinical Immunology. 2017; 139(1): 335-46.
292. Wang F, Hou H, Wu S, Tang Q, Liu W, Huang M, Yin B, Huang J, Mao L, Lu Y, et al. TIGIT expression levels on human NK cells correlate with functional heterogeneity among healthy individuals. Eur J Immunol. 2015; 45(10): 2886-97.
293. Wang Y, Li D, Yu T, Hu M, Xing J, Bai S, Qu W, Tong X. Dynamics of TIGIT and PD-1 expression on NK cells during the course of normal pregnancy. Immunology Letters. 2021; 230: 42-8.
294. Fu W, Ma Z, Lei C, Ding M, Hu S. TIGIT-Fc Promote Immune Tolerance at the Feto-maternal Interface. bioRxiv. 2019.
295. Liu S, Zhang H, Li M, Hu D, Li C, Ge B, Jin B, Fan Z. Recruitment of Grb2 and SHIP1 by the ITT-like motif of TIGIT suppresses granule polarization and cytotoxicity of NK cells. Cell Death And Differentiation. 2013; 20(3): 456-64.
296. Li M, Xia P, Du Y, Liu S, Huang G, Chen J, Zhang H, Hou N, Cheng X, Zhou L, et al. T-cell immunoglobulin and ITIM domain (TIGIT) receptor/poliovirus receptor (PVR) ligand engagement suppresses interferon-γ production of natural killer cells via β-arrestin 2-mediated negative signaling. Journal of Biological Chemistry. 2014; 289(25): 17647-57.
297. Stanietsky N, Simic H, Arapovic J, Toporik A, Levy O, Novik A, Levine Z, Beiman M, Dassa L, Achdout H, et al. The interaction of TIGIT with PVR and PVRL2 inhibits human NK cell cytotoxicity. Proc Natl Acad Sci U S A. 2009; 106(42): 17858-63.

298. Meggyes M, Miko E, Lajko A, Csiszar B, Sandor B, Matrai P, Tamas P, Szereday L. Involvement of the PD-1/PD-L1 Co-Inhibitory Pathway in the Pathogenesis of the Inflammatory Stage of Early-Onset Preeclampsia. Int J Mol Sci. 2019; 20(3): 583.
299. Zheng Y, Li Y, Lian J, Yang H, Li F, Zhao S, Qi Y, Zhang Y, Huang L. TNF-α-induced Tim-3 expression marks the dysfunction of infiltrating natural killer cells in human esophageal cancer. Journal of Translational Medicine volume. 2019; 17: 165.
300. Xu L, Huang Y, Tan L, Yu W, Chen D, Lu C, He J, Wu G, Liu X, Zhang Y. Increased Tim-3 expression in peripheral NK cells predicts a poorer prognosis and Tim-3 blockade improves NK cell-mediated cytotoxicity in human lung adenocarcinoma. International Immunopharmacology. 2015; 29(2): 635-41.
301. Li Y, Zhang J, Zhang D, Hong X, Tao Y, Wang S, Xu Y, Piao H, Yin W, Yu M, et al. Tim-3 signaling in peripheral NK cells promotes maternal-fetal immune tolerance and alleviates pregnancy loss. Science Signaling. 2017; 10(498): eaah4323.
302. Gallois A, Silva I, Osman I, Bhardwaj N. Reversal of natural killer cell exhaustion by TIM-3 blockade. OncoImmunology. 2015; 3(12): e946365.
303. da Silva IP, Gallois A, Jimenez-Baranda S, Khan S, Anderson AC, Kuchroo VK, Osman I, Bhardwaj N. Reversal of NK-cell exhaustion in advanced melanoma by Tim-3 blockade. Cancer Immunology Research. 2014; 2(4): 410-22.
304. Ndhlovu LC, Lopez-Vergès S, Barbour JD, Jones RB, Jha AR, Long BR, Schoeffler EC, Fujita T, Nixon DF, Lanier LL. Tim-3 marks human natural killer cell maturation and suppresses cell-mediated cytotoxicity. Blood. 2012; 119(16): 3734-43.
305. Gleason MK, Lenvik TR, McCullar V, Felices M, O'Brien MS, Cooley SA, Verneris MR, Cichocki F, Holman CJ, Panoskaltsis-Mortari A, et al. Tim-3 is an inducible human natural killer cell receptor that enhances interferon gamma production in response to galectin-9. Blood. 2012; 119(13): 3064-72.
306. Li Y, Li D, Du M. TIM-3: a crucial regulator of NK cells in pregnancy. Cell Mol Immunol. 2017; 14(11): 948-50.
307. Meggyes M, Miko E, Polgar B, Bogar B, Farkas B, Illes Z, Szereday L. Peripheral blood TIM-3 positive NK and CD8+ T cells throughout pregnancy: TIM-3/galectin-9 interaction and its possible role during pregnancy. PLoS One. 2014; 9(3): e92371.
308. Li YH, Zhou WH, Tao Y, Wang SC, Jiang YL, Zhang D, Piao HL, Fu Q, Li DJ, Du MR. The Galectin-9/Tim-3 pathway is involved in the regulation of NK cell function at the maternal-fetal interface in early pregnancy. Cell Mol Immunol. 2016; 13(1): 73-81.
309. Sun J, Yang M, Ban Y, Gao W, Song B, Wang Y, Zhang Y, Shao Q, Kong B, Qu X. Tim-3 Is Upregulated in NK Cells during Early Pregnancy and Inhibits NK Cytotoxicity toward Trophoblast in Galectin-9 Dependent Pathway. PLoS One. 2016; 11(1): e0147186.
310. Meggyes M, Lajko A, Palkovics T, Totsimon A, Illes Z, Szereday L, Miko E. Feto-maternal immune regulation by TIM-3/galectin-9 pathway and PD-1 molecule in mice at day 14.5 of pregnancy. Placenta. 2015; 36(10): 1153-60.
311. Li J, Li FF, Zuo W, Zhou Y, Hao HY, Dang J, Jiang M, He MZ, Deng DR. Up-regulated expression of Tim-3/Gal-9 at maternal-fetal interface in pregnant woman with recurrent spontaneous abortion. Journal of Huazhong University of Science and Technology. 2014; 34(4): 586-90.
312. Zhang T, Zhu W, Zhao Y, Cheung WC, Liu Y, Chen X, Du Y, Leung KT, Chan YL, Wang CC, et al. Early transient suppression of immune checkpoint proteins T-cell immunoglobulin mucin-3 and programmed cell death-1 in peripheral blood lymphocytes after blastocyst transfer is associated with successful implantation. Fertil Steril. 2020; 114(2): 426-35.
313. Campbell JJ, Qin S, Unutmaz D, Soler D, Murphy KE, Hodge MR, Wu L, Butcher EC. Unique subpopulations of CD56+ NK and NK-T peripheral blood lymphocytes identified by chemokine receptor expression repertoire. J Immunol. 2001; 166(11): 6477-82.
314. Hanna J, Wald O, Goldman-Wohl D, Prus D, Markel G, Gazit R, Katz G, Haimov-Kochman R, Fujii N, Yagel S, et al. CXCL12 expression by invasive trophoblasts induces the specific migration of CD16- human natural killer cells. Blood. 2003; 102(5): 1569-77.
315. Lima M, Leander M, Santos M, Santos AH, Lau C, Queirós ML, Gonçalves M, Fonseca S, Moura J, Teixeira MDA, et al. Chemokine Receptor Expression on Normal Blood CD56(+) NK-Cells Elucidates Cell Partners That Comigrate during the Innate and Adaptive Immune Responses and Identifies a Transitional NK-Cell Population. Journal of Immunology Research. 2015; 2015: 839684.
316. Freud AG, Mundy-Bosse BL, Yu J, Caligiuri MA. The Broad Spectrum of Human Natural Killer Cell Diversity. Immunity. 2017; 47(5): 820-33.

317. Robertson MJ. Role of chemokines in the biology of natural killer cells. J Leukoc Biol. 2002; 71(2): 173-83.
318. Carlino C, Stabile H, Morrone S, Bulla R, Soriani A, Agostinis C, Bossi F, Mocci C, Sarazani F, Tedesco F, et al. Recruitment of circulating NK cells through decidual tissues: a possible mechanism controlling NK cell accumulation in the uterus during early pregnancy. Blood. 2008; 111(6): 3108-15.
319. Huang Y, Zhu XY, Du MR, Li DJ. Human trophoblasts recruited T lymphocytes and monocytes into decidua by secretion of chemokine CXCL16 and interaction with CXCR6 in the first-trimester pregnancy. The Journal of Immunology. 2008; 180(4): 2367-75.
320. Berahovich RD, Lai NL, Wei Z, Lanier LL, Schall TJ. Evidence for NK cell subsets based on chemokine receptor expression. The Journal of Immunology. 2006; 177(11): 7833-40.
321. Sentman CL, Meadows SK, Wira CR, Eriksson M. Recruitment of uterine NK cells: induction of CXC chemokine ligands 10 and 11 in human endometrium by estradiol and progesterone. J Immunol. 2004; 173(11): 6760-6.
322. Hirota Y, Osuga Y, Koga K, Yoshino O, Hirata T, Morimoto C, Harada M, Takemura Y, Nose E, Yano T, et al. The expression and possible roles of chemokine CXCL11 and its receptor CXCR3 in the human endometrium. The Journal of Immunology. 2006; 177(12): 8813-21.
323. Jones RL, Hannan NJ, Kaitu'u TJ, Zhang J, Salamonsen LA. Identification of chemokines important for leukocyte recruitment to the human endometrium at the times of embryo implantation and menstruation. The Journal of Clinical Endocrinology & Metabolism. 2004; 89(12): 6155-67.
324. Red-Horse K, Drake PM, Gunn MD, Fisher SJ. Chemokine ligand and receptor expression in the pregnant uterus: reciprocal patterns in complementary cell subsets suggest functional roles. Am J Pathol. 2001; 159(6): 2199-213.
325. Hannan NJ, Jones RL, Critchley HOD, Kovacs GJ, Rogers PAW, Affandi B, Salamonsen LA. Coexpression of fractalkine and its receptor in normal human endometrium and in endometrium from users of progestin-only contraception supports a role for fractalkine in leukocyte recruitment and endometrial remodeling. The Journal of Clinical Endocrinology & Metabolism. 2004; 89: 6119-29.
326. Drake PM, Red-Horse K, Fisher SJ. Reciprocal chemokine receptor and ligand expression in the human placenta: implications for cytotrophoblast differentiation. Developmental Dynamics. 2004; 229(4): 877-85.
327. Wu X, Jin LP, Yuan MM, Zhu Y, Wang MY, Li DJ. Human first-trimester trophoblast cells recruit CD56brightCD16- NK cells into decidua by way of expressing and secreting of CXCL12/stromal cell-derived factor 1. The Journal of Immunology. 2005; 175(1): 61-8.
328. Wu X, Li DJ, Yuan MM, Zhu Y, Wang MY. The expression of CXCR4/CXCL12 in first-trimester human trophoblast cells. Biol Reprod. 2004; 70(6): 1877-85.
329. Kuang H, Chen Q, Zhang Y, Zhang L, Peng H, Ning L, Cao Y, Duan E. The cytokine gene CXCL14 restricts human trophoblast cell invasion by suppressing gelatinase activity. Endocrinology. 2009; 150(12): 5596-605.
330. Huang Y, Zhu XY, Du MR, Wu X, Wang MY, Li DJ. Chemokine CXCL16, a scavenger receptor, induces proliferation and invasion of first-trimester human trophoblast cells in an autocrine manner. Hum Reprod. 2006; 21(4): 1083-91.
331. Drake PM, Gunn MD, Charo IF, Tsou CL, Zhou Y, Huang L, Fisher SJ. Human placental cytotrophoblasts attract monocytes and CD56(bright) natural killer cells via the actions of monocyte inflammatory protein 1alpha. J Exp Med. 2001; 193(10): 1199-212.
332. Parveen F, Faridi RM, Singh B, Agrawal S. Analysis of CCR5 and CX3CR1 gene polymorphisms in association with unexplained recurrent miscarriages among north Indian women. Cytokine. 2011; 56(2): 239-44.
333. Zhu L, Aly M, Kuon RJ, Toth B, Wang H, Karakizlis H, Weimer R, Morath C, Ibrahim E, Ekpoom N, et al. Patients with idiopathic recurrent miscarriage have abnormally high TGFß+ blood NK, NKT and T cells in the presence of abnormally low TGFß plasma levels. BMC Immunol. 2019; 20(1): 10.
334. Topham NJ, Hewitt EW. Natural killer cell cytotoxicity: how do they pull the trigger? Immunology. 2009; 128(1): 7-15.
335. Souza SS, Castro FA, Mendonça HC, Palma PV, Morais FR, Ferriani RA, Voltarelli JC. Influence of menstrual cycle on NK activity. J Reprod Immunol. 2001; 50(2): 151-9.
336. Okamura K, Furukawa K, Nakakuki M, Yamada K, Suzuki M. Natural killer cell activity during pregnancy. Am J Obstet Gynecol. 1984; 149(4): 396-9.

337. Lanier LL, Buck DW, Rhodes L, Ding A, Evans E, Barney C, Phillips JH. Interleukin 2 activation of natural killer cells rapidly induces the expression and phosphorylation of the Leu-23 activation antigen. J Exp Med. 1988; 167(5): 1572-85.
338. Moretta A, Poggi A, Pende D, Tripodi G, Orengo AM, Pella N, Augugliaro R, Bottino C, Ciccone E, Moretta L. CD69-mediated pathway of lymphocyte activation: anti-CD69 monoclonal antibodies trigger the cytolytic activity of different lymphoid effector cells with the exception of cytolytic T lymphocytes expressing T cell receptor alpha/beta. J Exp Med. 1991; 174(6): 1393-8.
339. Dons'koi BV, Chernyshov VP, Osypchuk DV. Measurement of NK activity in whole blood by the CD69 up-regulation after co-incubation with K562, comparison with NK cytotoxicity assays and CD107a degranulation assay. J Immunol Methods. 2011; 372(1-2): 187-95.
340. Clausen J, Vergeiner B, Enk M, Petzer AL, Gastl G, Gunsilius E. Functional Significance of the Activation-Associated Receptors CD25 and CD69 on Human NK-cells and NK-like T-cells. . Immunobiology. 2003; 207(2): 85-93.
341. Borrego F, Robertson MJ, Ritz J, Peña J, Solana R. CD69 is a stimulatory receptor for natural killer cell and its cytotoxic effect is blocked by CD94 inhibitory receptor. Immunology. 1999; 97(1): 159-65.
342. Borrego F, Peña J, Solana R. Regulation of CD69 expression on human natural killer cells: differential involvement of protein kinase C and protein tyrosine kinases. Eur J Immunol. 1993; 23(5): 1039-43.
343. Craston R, Koh M, Mc Dermott A, Ray N, Prentice HG, Lowdell MW. Temporal dynamics of CD69 expression on lymphoid cells. J Immunol Methods. 1997; 209(1): 37-45.
344. Higuchi K, Aoki K, Kimbara T, Hosoi N, Yamamoto T, Okada H. Suppression of natural killer cell activity by monocytes following immunotherapy for recurrent spontaneous aborters. Am J Reprod Immunol. 1995; 33(3): 221-7.
345. Coulam CB, Roussev RG. Correlation of NK cell activation and inhibition markers with NK cytoxicity among women experiencing immunologic implantation failure after in vitro fertilization and embryo transfer. J Assist Reprod Genet. 2003; 20(2): 58-62.
346. Pérez-Villar JJ, Melero I, Rodríguez A, Carretero M, Aramburu J, Sivori S, Orengo AM, Moretta A, López-Botet M. Functional ambivalence of the Kp43 (CD94) NK cell-associated surface antigen. J Immunol. 1995; 154(11): 5779-88.
347. Azargoon A, Mirrasouli Y, Shokrollahi Barough M, Barati M, Kokhaei P. The State of Peripheral Blood Natural Killer Cells and Cytotoxicity in Women with Recurrent Pregnancy Loss and Unexplained Infertility. Int J Fertil Steril. 2019; 13(1): 12-7.
348. Kodama T, Hara T, Okamoto E, Kusunoki Y, Ohama K. Characteristic changes of large granular lymphocytes that strongly express CD56 in endometrium during the menstrual cycle and early pregnancy. Hum Reprod. 1998; 13(4): 1036-43.
349. Zhu L, Aly M, Wang H, Karakizlis H, Weimer R, Morath C, Kuon RJ, Toth B, Opelz G, Daniel V. Decreased NK cell immunity in kidney transplant recipients late post-transplant and increased NK-cell immunity in patients with recurrent miscarriage. PLoS One. 2017; 12(10): e0186349.
350. Souza SS, Ferriani RA, Santos CM, Voltarelli JC. Immunological evaluation of patients with recurrent abortion. J Reprod Immunol. 2002; 56(1-2): 111-21.
351. Roussev RG, Dons'koi BV, Stamatkin C, Ramu S, Chernyshov VP, Coulam CB, Barnea ER. Preimplantation factor inhibits circulating natural killer cell cytotoxicity and reduces CD69 expression: implications for recurrent pregnancy loss therapy. Reprod Biomed Online. 2013; 26(1): 79-87.
352. Quack KC, Vassiliadou N, Pudney J, Anderson DJ, Hill JA. Leukocyte activation in the decidua of chromosomally normal and abnormal fetuses from women with recurrent abortion. Hum Reprod. 2001; 16(5): 949-55.
353. Vassiliadou N, Bulmer JN. Functional studies of human decidua in spontaneous early pregnancy loss: effect of soluble factors and purified CD56+ lymphocytes on killing of natural killer- and lymphokine-activated killer-sensitive targets. Biol Reprod. 1998; 58(4): 982-7.
354. Gunturi A, Berg RE, Forman J. The role of CD94/NKG2 in innate and adaptive immunity. Immunol Res. 2004; 30(1): 29-34.
355. Peritt D, Robertson S, Gri G, Showe L, Aste-Amezaga M, Trinchieri G. Differentiation of human NK cells into NK1 and NK2 subsets. J Immunol. 1998; 161(11): 5821-4.
356. Hoshino T, Winkler-Pickett RT, Mason AT, Ortaldo JR, Young HA. IL-13 production by NK cells: IL-13-producing NK and T cells are present in vivo in the absence of IFN-gamma. J Immunol. 1999; 162(1): 51-9.

357. Warren HS, Kinnear BF, Phillips JH, Lanier LL. Production of IL-5 by human NK cells and regulation of IL-5 secretion by IL-4, IL-10, and IL-12. J Immunol. 1995; 154(10): 5144-52.
358. Mehrotra PT, Donnelly RP, Wong S, Kanegane H, Geremew A, Mostowski HS, Furuke K, Siegel JP, Bloom ET. Production of IL-10 by human natural killer cells stimulated with IL-2 and/or IL-12. J Immunol. 1998; 160(6): 2637-44.
359. Gray JD, Hirokawa M, Ohtsuka K, Horwitz DA. Generation of an inhibitory circuit involving CD8+ T cells, IL-2, and NK cell-derived TGF-beta: contrasting effects of anti-CD2 and anti-CD3. J Immunol. 1998; 160(5): 2248-54.
360. Higuma-Myojo S, Sasaki Y, Miyazaki S, Sakai M, Siozaki A, Miwa N, Saito S. Cytokine profile of natural killer cells in early human pregnancy. Am J Reprod Immunol. 2005; 54(1): 21-9.
361. Lidström C, Matthiesen L, Berg G, Sharma S, Ernerudh J, Ekerfelt C. Cytokine secretion patterns of NK cells and macrophages in early human pregnancy decidua and blood: implications for suppressor macrophages in decidua. Am J Reprod Immunol. 2003; 50(6): 444-52.
362. Veenstra van Nieuwenhoven AL, Bouman A, Moes H, Heineman MJ, de Leij LF, Santema J, Faas MM. Cytokine production in natural killer cells and lymphocytes in pregnant women compared with women in the follicular phase of the ovarian cycle. Fertil Steril. 2002; 77(5): 1032-7.
363. Fonseca BM, Cunha SC, Gonçalves D, Mendes A, Braga J, Correia-da-Silva G, Teixeira NA. Decidual NK cell-derived conditioned medium from miscarriages affects endometrial stromal cell decidualisation: endocannabinoid anandamide and tumour necrosis factor-α crosstalk. Hum Reprod. 2020; 35(2): 265-74.
364. Liu J, Dong P, Jia N, Wen X, Luo L, Wang S, Li J. The expression of intracellular cytokines of decidual natural killer cells in unexplained recurrent pregnancy loss. The Journal of Maternal-Fetal and Neonatal Medicine. 2020: 1-7.
365. Taima A, Fukui A, Yamaya A, Yokota M, Fukuhara R, Yokoyama Y. A semen-based stimulation method to analyze cytokine production by uterine CD56 bright natural killer cells in women with recurrent pregnancy loss. J Reprod Immunol. 2020; 142: 103206.
366. Saito S, Nakashima A, Myojo-Higuma S, Shiozaki A. The balance between cytotoxic NK cells and regulatory NK cells in human pregnancy. J Reprod Immunol. 2008; 77(1): 14-22.
367. Lash GE, Naruse K, Robson A, Innes BA, Searle RF, Robson SC, Bulmer JN. Interaction between uterine natural killer cells and extravillous trophoblast cells: effect on cytokine and angiogenic growth factor production. Hum Reprod. 2011; 26(9): 2289-95.
368. De Oliveira LG, Lash GE, Murray-Dunning C, Bulmer JN, Innes BA, Searle RF, Sass N, Robson SC. Role of interleukin 8 in uterine natural killer cell regulation of extravillous trophoblast cell invasion. Placenta. 2010; 31(7): 595-601.
369. Chen X, Liu Y, Cheung WC, Zhao Y, Huang J, Chung JPW, Wang CC, Li TC. Increased expression of angiogenic cytokines in CD56+ uterine natural killer cells from women with recurrent miscarriage. Cytokine. 2018; 110: 272-6.
370. Ng SC, Gilman-Sachs A, Thaker P, Beaman KD, Beer AE, Kwak-Kim J. Expression of intracellular Th1 and Th2 cytokines in women with recurrent spontaneous abortion, implantation failures after IVF/ET or normal pregnancy. Am J Reprod Immunol. 2002; 48(2): 77-86.
371. Bulmer JN, Morrison L, Longfellow M, Ritson A, Pace D. Granulated lymphocytes in human endometrium: histochemical and immunohistochemical studies. Hum Reprod. 1991; 6(6): 791-8.
372. Tilburgs T, Claas FHJ, Scherjon SA. Elsevier Trophoblast Research Award Lecture: Unique Properties of Decidual T Cells and Their Role in Immune Regulation During Human Pregnancy. Placenta. 2010; 31 Suppl: S82-6.
373. Reinhard G, Noll A, Schlebusch H, Mallmann P, Ruecker AV. Shifts in the TH1/TH2 balance during human pregnancy correlate with apoptotic changes. Biochem Biophys Res Commun. 1998; 245(3): 933-8.
374. Lozano E, Dominguez-Villar M, Kuchroo V, Hafler DA. The TIGIT/CD226 axis regulates human T cell function. The Journal of Immunology. 2012; 188(8): 3869-75.
375. Tsushima F, Yao S, Shin T, Flies A, Flies S, Xu H, Tamada K, Pardoll DM, Chen L. Interaction between B7-H1 and PD-1 determines initiation and reversal of T-cell anergy. Blood. 2007; 110(1): 180-5.
376. Moldenhauer LM, Hayball JD, Robertson SA. Utilising T Cell Receptor Transgenic Mice to Define Mechanisms of Maternal T Cell Tolerance in Pregnancy. J Reprod Immunol. 2010; 87(1-2): 1-13.

377. Shimada S, Iwabuchi K, Kato EH, Morikawa M, Sakuragi N, Onoé K, Minakami H, Yamada H. No difference in natural-killer-T cell population, but Th2/Tc2 predominance in peripheral blood of recurrent aborters. Am J Reprod Immunol. 2003; 50(4): 334-9.
378. Zhao Y, Chen X, Zhang T, Chan LKY, Liu Y, Chung JPW, Kwong J, Li TC. The use of multiplex staining to measure the density and clustering of four endometrial immune cells around the implantation period in women with recurrent miscarriage: comparison with fertile controls. Journal of Molecular Histology. 2020; 51(5): 593-603.
379. Carbone J, Sarmiento E, Gallego A, Lanio N, Navarro J, García S, Fernandez-Cruz E. Peripheral blood T- and B-cell immunophenotypic abnormalities in selected women with unexplained recurrent miscarriage. J Reprod Immunol. 2016; 113: 50-3.
380. Vassiliadou N, Searle RF, Bulmer JN. Elevated expression of activation molecules by decidual lymphocytes in women suffering spontaneous early pregnancy loss. Hum Reprod. 1999; 14(5): 1194-200.
381. Du M, Yu N, Ding Q, Chen X, Frempong ST, Cai X, Bao S. Elevated percentage of $CD3^+$ T cells and pregnancy outcome in women with recurrent pregnancy loss. Clin Chim Acta. 2018; 486: 341-6.
382. Yahata T, Kurabayashi T, Honda A, Takakuwa K, Tanaka K, Abo T. Decrease in the proportion of granulated CD56+ T-cells in patients with a history of recurrent abortion. J Reprod Immunol. 1998; 38(1): 63-73.
383. Wang WJ, Salazar Garcia MD, Deutsch G, Sung N, Yang X, He Q, Jubiz G, Bilal M, Dambaeva S, Gilman-Sachs A, et al. PD-1 and PD-L1 expression on T-cell subsets in women with unexplained recurrent pregnancy losses. Am J Reprod Immunol. 2020; 83(5): e13230.
384. Wang WJ, Hao CF, Yi-Lin, Yin GJ, Bao SH, Qiu LH, Lin QD. Increased prevalence of T helper 17 (Th17) cells in peripheral blood and decidua in unexplained recurrent spontaneous abortion patients. J Reprod Immunol. 2010; 84(2): 164-70.
385. Mamedaliyeva NM, Kurmanova AM, Lokshin VN, Kurmanova GM, Sh Issenova S. Clinical and immunological parallels in pregnancy loss. Gynecol Endocrinol. 2017; 33(sup1): 5-7.
386. Ali S, Majid S, Niamat Ali M, Taing S. Evaluation of T cell cytokines and their role in recurrent miscarriage. International Immunopharmacology. 2020; 82: 106347.
387. Pennock ND, White JT, Cross EW, Cheney EE, Tamburini BA, Kedl RM. T cell responses: naive to memory and everything in between. Advances in Physiology Education. 2013; 37(4): 273-83.
388. Wissinger E. CD8+ T Cells. Bitesized immunology: British Society for Immunology.
389. Saito S, Nishikawa K, Morii T, Narita N, Enomoto M, Ichijo M. Expression of activation antigens CD69, HLA-DR, interleukin-2 receptor-alpha (IL-2R alpha) and IL-2R beta on T cells of human decidua at an early stage of pregnancy. Immunology. 1992; 75(4): 710-2.
390. Lissauer D, Piper K, Goodyear O, Kilby MD, Moss PA. Fetal-specific CD8+ cytotoxic T cell responses develop during normal human pregnancy and exhibit broad functional capacity. J Immunol. 2012; 189(2): 1072-80.
391. Tsuda S, Nakashima A, Shima T, Saito S. New Paradigm in the Role of Regulatory T Cells During Pregnancy. Front Immunol. 2019; 10: 573.
392. Wang SC, Li YH, Piao HL, Hong XW, Zhang D, Xu YY, Tao Y, Wang Y, Yuan MM, Li DJ, et al. PD-1 and Tim-3 pathways are associated with regulatory CD8+ T-cell function in decidua and maintenance of normal pregnancy. Cell Death Dis. 2015; 6: e1738.
393. Clark DA, Chaouat G, Mogil R, Wegmann TG. Prevention of spontaneous abortion in DBA/2-mated CBA/J mice by GM-CSF involves CD8+ T cell-dependent suppression of natural effector cell cytotoxicity against trophoblast target cells. Cell Immunol. 1994; 154(1): 143-52.
394. Ghafourian M, Abuhamidy A, Karami N. Increase of peripheral blood TCD8+ cells in women with recurrent miscarriage. J Obstet Gynaecol. 2014; 34(1): 36-9.
395. Yang KM, Ntrivalas E, Cho HJ, Kim NY, Beaman K, Gilman-Sachs A, Kwak-Kim J. Women With Multiple Implantation Failures and Recurrent Pregnancy Losses Have Increased Peripheral Blood T Cell Activation. Am J Reprod Immunol. 2010; 63(5): 370-8.
396. Kuon RJ, Schaumann J, Goeggl T, Strowitzki T, Sadeghi M, Opelz G, Daniel V, Toth B. Patients with idiopathic recurrent miscarriage show higher levels of DR+ activated T-cells that are less responsive to mitogens. J Reprod Immunol. 2015; 112: 82-7.
397. Jin LP, Chen QY, Zhang T, Guo PF, Li DJ. The CD4+CD25 bright regulatory T cells and CTLA-4 expression in peripheral and decidual lymphocytes are down-regulated in human miscarriage. Clin Immunol. 2009; 133(3): 402-10.

398. Calleja-Agius J, Brincat MP. Recurrent miscarriages: What is the role of cytokines? Gynecol Endocrinol. 2008; 24(12): 663-8.
399. Saini V, Arora S, Yadav A, Bhattacharjee J. Cytokines in recurrent pregnancy loss. Clin Chim Acta. 2011; 412(9-10): 702-8.
400. Alberts B, Johnson A, Lewis J, Raff M, Roberts K, Walter P. Helper T Cells and Lymphocyte Activation. New York: Garland Science; 2002. 1410-23 p.
401. Raghupathy R, Makhseed M, Azizieh F, Hassan N, Al-Azemi M, Al-Shamali E. Maternal Th1- and Th2-type reactivity to placental antigens in normal human pregnancy and unexplained recurrent spontaneous abortions. Cell Immunol. 1999; 196(2): 122-30.
402. Wegmann TG, Lin H, Guilbert L, Mosmann TR. Bidirectional cytokine interactions in the maternal-fetal relationship: is successful pregnancy a TH2 phenomenon? Immunol Today. 1993; 14(7): 353-6.
403. Raghupathy R. Th1-type immunity is incompatible with successful pregnancy. Immunol Today. 1997; 18(10): 478-82.
404. Marzi M, Vigano A, Trabattoni D, Villa ML, Salvaggio A, Clerici E, Clerici M. Characterization of type 1 and type 2 cytokine production profile in physiologic and pathologic human pregnancy. Clin Exp Immunol. 1996; 106(1): 127-33.
405. Piccinni MP, Beloni L, Livi C, Maggi E, Scarselli G, Romagnani S. Defective production of both leukemia inhibitory factor and type 2 T-helper cytokines by decidual T cells in unexplained recurrent abortions. Nat Med. 1998; 4(9): 1020-4.
406. Carp H. Cytokines in recurrent miscarriage. Lupus. 2004; 13(9): 630-4.
407. Makhseed M, Raghupathy R, Azizieh F, Al-Azemi MM, Hassan NA, Bandar A. Mitogen-induced cytokine responses of maternal peripheral blood lymphocytes indicate a differential Th-type bias in normal pregnancy and pregnancy failure. Am J Reprod Immunol. 1999; 42(5): 273-81.
408. Raghupathy R, Makhseed M, Azizieh F, Omu A, Gupta M, Farhat R. Cytokine production by maternal lymphocytes during normal human pregnancy and in unexplained recurrent spontaneous abortion. Hum Reprod. 2000; 15(3): 713-8.
409. Korn T, Bettelli E, Oukka M, Kuchroo VK. IL-17 and Th17 Cells. Annu Rev Immunol. 2009; 27: 485-517.
410. Roomandeh N, Saremi A, Arasteh J, Pak F, Mirmohammadkhani M, Kokhaei P, Zare A. Comparing Serum Levels of Th17 and Treg Cytokines in Women with Unexplained Recurrent Spontaneous Abortion and Fertile Women. Iran J Immunol. 2018; 15(1): 59-67.
411. Moore KW, de Waal Malefyt R, Coffman RL, O'Garra A. Interleukin-10 and the interleukin-10 receptor. Annu Rev Immunol. 2001; 19: 683-765.
412. Daher S, de Arruda Geraldes Denardi K, Blotta MH, Mamoni RL, Reck AP, Camano L, Mattar R. Cytokines in recurrent pregnancy loss. J Reprod Immunol. 2004; 62(1-2): 151-7.
413. Hossein H, Mahroo M, Abbas A, Firouzeh A, Nadia H. Cytokine production by peripheral blood mononuclear cells in recurrent miscarriage. Cytokine. 2004; 28(2): 83-6.
414. Hill JA, Polgar K, Anderson DJ. T-helper 1-type immunity to trophoblast in women with recurrent spontaneous abortion. JAMA. 1995; 273(24): 1933-6.
415. Wilson R, Moor J, Jenkins C, Miller H, Walker JJ, McLean MA, Norman J, McInnes IB. Abnormal first trimester serum interleukin 18 levels are associated with a poor outcome in women with a history of recurrent miscarriage. Am J Reprod Immunol. 2004; 51(2): 156-9.
416. Wilson R, McInnes I, Leung B, McKillop JH, Walker JJ. Altered interleukin 12 and nitric oxide levels in recurrent miscarriage. Eur J Obstet Gynecol Reprod Biol. 1997; 75(2): 211-4.
417. Shaarawy M, Nagui AR. Enhanced expression of cytokines may play a fundamental role in the mechanisms of immunologically mediated recurrent spontaneous abortion. Acta Obstet Gynecol Scand. 1997; 76(3): 205-11.
418. Makhseed M, Raghupathy R, Azizieh F, Farhat R, Hassan N, Bandar A. Circulating cytokines and CD30 in normal human pregnancy and recurrent spontaneous abortions. Hum Reprod. 2000; 15(9): 2011-7.
419. Liu Y, Chen H, Feng L, Zhang J. Interactions between gut microbiota and metabolites modulate cytokine network imbalances in women with unexplained miscarriage. Nature Portfolio Journal Biofilms and Microbiomes. 2021; 7(1): 24.
420. Rezaei A, Dabbagh A. T-helper (1) cytokines increase during early pregnancy in women with a history of recurrent spontaneous abortion. Medical Science Monitor. 2002; 8(8): CR607-CR10.
421. Lim KJ, Odukoya OA, Ajjan RA, Li TC, Weetman AP, Cooke ID. The role of T-helper cytokines in human reproduction. Fertil Steril. 2000; 73(1): 136-42.

422. Michimata T, Sakai M, Miyazaki S, Ogasawara MS, Suzumori K, Aoki K, Nagata K, Saito S. Decrease of T-helper 2 and T-cytotoxic 2 cells at implantation sites occurs in unexplained recurrent spontaneous abortion with normal chromosomal content. Hum Reprod. 2003; 18(7): 1523-8.
423. Abdolmohammadi Vahid S, Ghaebi M, Ahmadi M, Nouri M, Danaei S, Aghebati-Maleki L, Mousavi Ardehaie R, Yousefi B, Hakimi P, Hojjat-Farsangi M, et al. Altered T-cell subpopulations in recurrent pregnancy loss patients with cellular immune abnormalities. J Cell Physiol. 2019; 234(4): 4924-33.
424. Kamali-Sarvestani E, Zolghadri J, Gharesi-Fard B, Sarvari J. Cytokine gene polymorphisms and susceptibility to recurrent pregnancy loss in Iranian women. J Reprod Immunol. 2005; 65(2): 171-8.
425. Reid JG, Simpson NA, Walker RG, Economidou O, Shillito J, Gooi HC, Duffy SR, Walker JJ. The carriage of pro-inflammatory cytokine gene polymorphisms in recurrent pregnancy loss. Am J Reprod Immunol. 2001; 45(1): 35-40.
426. Daher S, Shulzhenko N, Morgun A, Mattar R, Rampim GF, Camano L, DeLima MG. Associations between cytokine gene polymorphisms and recurrent pregnancy loss. J Reprod Immunol. 2003; 58(1): 69-77.
427. Kwak-Kim JY, Chung-Bang HS, Ng SC, Ntrivalas EI, Mangubat CP, Beaman KD, Beer AE, Gilman-Sachs A. Increased T helper 1 cytokine responses by circulating T cells are present in women with recurrent pregnancy losses and in infertile women with multiple implantation failures after IVF. Hum Reprod. 2003; 18(4): 767-73.
428. Makhseed M, Raghupathy R, Azizieh F, Omu A, Al-Shamali E, Ashkanani L. Th1 and Th2 cytokine profiles in recurrent aborters with successful pregnancy and with subsequent abortions. Hum Reprod. 2001; 16(10): 2219-26.
429. Mueller-Eckhardt G, Mallmann P, Neppert J, Lattermann A, Melk A, Heine O, Pfeiffer R, Zingsem J, Domke N, Mohr-Pennert A. Immunogenetic and serological investigations in nonpregnant and in pregnant women with a history of recurrent spontaneous abortions. German RSA/IVIG Study Group. J Reprod Immunol. 1994; 27(2): 95-109.
430. Jenkins C, Roberts J, Wilson R, MacLean MA, Shilito J, Walker JJ. Evidence of a T(H) 1 type response associated with recurrent miscarriage. Fertil Steril. 2000; 73(6): 1206-8.
431. Calleja-Agius J, Muttukrishna S, Pizzey AR, Jauniaux E. Pro- and antiinflammatory cytokines in threatened miscarriages. Am J Obstet Gynecol. 2011; 205(1): 83.e8-.e16.
432. Kleinewietfeld M, Hafler DA. The plasticity of human Treg and Th17 cells and its role in autoimmunity. Semin Immunol. 2013; 25(4): 305-12.
433. Kimura A, Kishimoto T. IL-6: regulator of Treg/Th17 balance. Eur J Immunol. 2010; 40(7): 1830-5.
434. Zhu L, Chen H, Liu M, Yuan Y, Wang Z, Chen Y, Wei J, Su F, Zhang J. Treg/Th17 Cell Imbalance and IL-6 Profile in Patients With Unexplained Recurrent Spontaneous Abortion. Reprod Sci. 2017; 24(6): 882-90.
435. Razdaibiedina A, Khobzey M, Tkachenko V, Vorobiova I. Effects of Single-Nucleotide Polymorphisms in Cytokine, Toll-Like Receptor, and Progesterone Receptor Genes on Risk of Miscarriage. Obstetrics and Gynecology International. 2018; 2018: 9272749.
436. Qian J, Zhang N, Lin J, Wang C, Pan X, Chen L, Li D, Wang L. Distinct pattern of Th17/Treg cells in pregnant women with a history of unexplained recurrent spontaneous abortion. BioScience Trends. 2018; 12(2): 157-67.
437. Gao Y, Wang P, Zou T, Zhang Z, Liang W. Increased Th17 and reduced Treg cells in patients with unexplained recurrent spontaneous abortion. Clinical and Experimental Obstetrics & Gynecology. 2019; 46(3): 458-60.
438. Ji J, Zhai H, Zhou H, Song S, Mor G, Liao A. The role and mechanism of vitamin D-mediated regulation of Treg/Th17 balance in recurrent pregnancy loss. Am J Reprod Immunol. 2019; 81(6): e13112.
439. Wang WJ, Liu FJ, Qu HM, Hao CF, Qu QL, Xiong-Wang W, Bao HC, Wang XR. Regulation of the expression of Th17 cells and regulatory T cells by IL-27 in patients with unexplained early recurrent miscarriage. J Reprod Immunol. 2013; 99(1-2): 39-45.
440. Sereshki N, Gharagozloo M, Ostadi V, Ghahiri A, Roghaei MA, Mehrabian F, Andalib AA, Hassanzadeh A, Hosseini H, Rezaei A. Variations in T-helper 17 and Regulatory T Cells during The Menstrual Cycle in Peripheral Blood of Women with Recurrent Spontaneous Abortion. Int J Fertil Steril. 2014; 8(1): 59-66.

441. Wang WJ, Hao CF, Qu QL, Wang X, Qiu LH, Lin QD. The deregulation of regulatory T cells on interleukin-17-producing T helper cells in patients with unexplained early recurrent miscarriage. Hum Reprod. 2010; 25(10): 2591-6.
442. Bansal AS. Joining the immunological dots in recurrent miscarriage. Am J Reprod Immunol. 2010; 64(5): 307-15.
443. Yockey LJ, Iwasaki A. Interferons and Proinflammatory Cytokines in Pregnancy and Fetal Development. Immunity. 2018; 49(3): 397-412.
444. Cheng SB, Sharma S. Interleukin-10: a pleiotropic regulator in pregnancy. Am J Reprod Immunol. 2015; 73(6): 487-500.
445. Choi BC, Polgar K, Xiao L, Hill JA. Progesterone inhibits in-vitro embryotoxic Th1 cytokine production to trophoblast in women with recurrent pregnancy loss. Hum Reprod. 2000; 15(Suppl 1): 46-59.
446. AbdulHussain G, Azizieh F, Makhseed M, Raghupathy R. Effects of Progesterone, Dydrogesterone and Estrogen on the Production of Th1/Th2/Th17 Cytokines by Lymphocytes from Women with Recurrent Spontaneous Miscarriage. J Reprod Immunol. 2020; 140: 103132.
447. Zenclussen AC, Fest S, Busse P, Joachim R, Klapp BF, Arck PC. Questioning the Th1/Th2 paradigm in reproduction: peripheral levels of IL-12 are down-regulated in miscarriage patients. Am J Reprod Immunol. 2002; 48(4): 245-51.
448. Arora R, Rathee A, Sachdeva M, Agrawal U. Unexplained repeated pregnancy loss and T helper cells. Eur J Obstet Gynecol Reprod Biol. 2020; 254: 277-83.
449. Bates MD, Quenby S, Takakuwa K, Johnson PM, Vince GS. Aberrant cytokine production by peripheral blood mononuclear cells in recurrent pregnancy loss? Hum Reprod. 2002; 17(9): 2439-44.
450. Mor G, Cardenas I. The immune system in pregnancy: a unique complexity. Am J Reprod Immunol. 2010; 63(6): 425-33.
451. Daher S, Fonseca F, Ribeiro OG, Musatti CC, Gerbase-DeLima M. Tumor necrosis factor during pregnancy and at the onset of labor and spontaneous abortion. Eur J Obstet Gynecol Reprod Biol. 1999; 83(1): 77-9.
452. Hunt JS, Chen HL, Miller L. Tumor necrosis factors: pivotal components of pregnancy? Biol Reprod. 1996; 54(3): 554-62.
453. Ashkar AA, Croy BA. Interferon-gamma contributes to the normalcy of murine pregnancy. Biol Reprod. 1999; 61(2): 493-502.
454. Ashkar AA, Croy BA. Functions of uterine natural killer cells are mediated by interferon gamma production during murine pregnancy. Semin Immunol. 2001; 13(4): 235-41.
455. Ashkar AA, Di Santo JP, Croy BA. Interferon gamma contributes to initiation of uterine vascular modification, decidual integrity, and uterine natural killer cell maturation during normal murine pregnancy. J Exp Med. 2000; 192(2): 259-70.
456. Torchinsky A, Shepshelovich J, Orenstein H, Zaslavsky Z, Savion S, Carp H, Fain A, Toder V. TNF-alpha protects embryos exposed to developmental toxicants. Am J Reprod Immunol. 2003; 49(3): 159-68.
457. Otun HA, Lash GE, Innes BA, Bulmer JN, Naruse K, Hannon T, Searle RF, Robson SC. Effect of tumour necrosis factor-α in combination with interferon-γ on first trimester extravillous trophoblast invasion. J Reprod Immunol. 2011; 88(1): 1-11.
458. Lash GE, Otun HA, Innes BA, Kirkley M, De Oliveira L, Searle RF, Robson SC, Bulmer JN. Interferon-gamma inhibits extravillous trophoblast cell invasion by a mechanism that involves both changes in apoptosis and protease levels. The FASEB Journal. 2006; 20(14): 2512-8.
459. Nakashima A, Ito M, Yoneda S, Shiozaki A, Hidaka T, Saito S. Circulating and decidual Th17 cell levels in healthy pregnancy. Am J Reprod Immunol. 2010; 63(2): 104-9.
460. Wang S, Qian J, Sun F, Li M, Ye J, Li M, Du M, Li D. Bidirectional regulation between 1st trimester HTR8/SVneo trophoblast cells and in vitro differentiated Th17/Treg cells suggest a fetal-maternal regulatory loop in human pregnancy. Am J Reprod Immunol. 2019; 81(5): e13106.
461. Guilbert LJ. There is a bias against type 1 (inflammatory) cytokine expression and function in pregnancy. J Reprod Immunol. 1996; 32(2): 105-10.
462. Haimovici F, Hill JA, Anderson DJ. The effects of soluble products of activated lymphocytes and macrophages on blastocyst implantation events in vitro. Biol Reprod. 1991; 44(1): 69-75.
463. Yui J, Garcia-Lloret M, Wegmann TG, Guilbert LJ. Cytotoxicity of tumour necrosis factor-alpha and gamma-interferon against primary human placental trophoblasts. Placenta. 1994; 15(8): 819-35.

464. Lissauer D, Eldershaw SA, Inman CF, Coomarasamy A, Moss PAH, Kilby MD. Progesterone promotes maternal-fetal tolerance by reducing human maternal T-cell polyfunctionality and inducing a specific cytokine profile. Eur J Immunol. 2015; 45(10): 2858-72.
465. Care AS, Bourque SL, Morton JS, Hjartarson EP, Robertson SA, Davidge ST. Reduction in Regulatory T Cells in Early Pregnancy Causes Uterine Artery Dysfunction in Mice. Hypertension. 2018; 72(1): 177-87.
466. Mei S, Tan J, Chen H, Chen Y, Zhang J. Changes of CD4+CD25high regulatory T cells and FOXP3 expression in unexplained recurrent spontaneous abortion patients. Fertil Steril. 2010; 94(6): 2244-7.
467. Yang H, Qiu L, Chen G, Ye Z, Lü C, Lin Q. Proportional change of CD4+CD25+ regulatory T cells in decidua and peripheral blood in unexplained recurrent spontaneous abortion patients. Fertil Steril. 2008; 89(3): 656-61.
468. Somerset DA, Zheng Y, Kilby MD, Sansom DM, Drayson MT. Normal human pregnancy is associated with an elevation in the immune suppressive CD25+ CD4+ regulatory T-cell subset. Immunology. 2004; 112(1): 38-43.
469. Zhao JX, Zeng YY, Liu Y. Fetal alloantigen is responsible for the expansion of the CD4(+)CD25(+) regulatory T cell pool during pregnancy. J Reprod Immunol. 2007; 75(2): 71-81.
470. Ramhorst R, Fraccaroli L, Aldo P, Alvero AB, Cardenas I, Leirós CP, Mor G. Modulation and recruitment of inducible regulatory T cells by first trimester trophoblast cells. Am J Reprod Immunol. 2012; 67(1): 17-27.
471. Zheng Y, Josefowicz S, Chaudhry A, Peng XP, Forbush K, Rudensky AY. Role of Conserved Non-Coding DNA Elements in the Foxp3 Gene in Regulatory T-cell Fate Nature. 2010; 463(7282): 808-12.
472. Samstein RM, Josefowicz SZ, Arvey A, Treuting PM, Rudensky AY. Extrathymic Generation of Regulatory T Cells in Placental Mammals Mitigates Maternal-Fetal Conflict. Cell. 2012; 150(1): 29-38.
473. Aluvihare VR, Kallikourdis M, Betz AG. Regulatory T cells mediate maternal tolerance to the fetus. Nat Immunol. 2004; 5(3): 266-71.
474. Zenclussen AC, Gerlof K, Zenclussen ML, Sollwedel A, Bertoja AZ, Ritter T, Kotsch K, Leber J, Volk HD. Abnormal T-cell reactivity against paternal antigens in spontaneous abortion: adoptive transfer of pregnancy-induced CD4+CD25+ T regulatory cells prevents fetal rejection in a murine abortion model. Am J Pathol. 2005; 166(3): 811-22.
475. Winger EE, Reed JL. Low circulating CD4(+) CD25(+) Foxp3(+) T regulatory cell levels predict miscarriage risk in newly pregnant women with a history of failure. Am J Reprod Immunol. 2011; 66(4): 320-8.
476. Petri M, Howard D, Repke J. Frequency of lupus flare in pregnancy. The Hopkins Lupus Pregnancy Center experience. Arthritis Rheum. 1991; 34(12): 1538-45.
477. Ruiz-Irastorza G, Lima F, Alves J, Khamashta MA, Simpson J, Hughes GR, Buchanan NM. Increased rate of lupus flare during pregnancy and the puerperium: a prospective study of 78 pregnancies. Br J Rheumatol. 1996; 35(2): 133-8.
478. Ostensen M, Husby G. A prospective clinical study of the effect of pregnancy on rheumatoid arthritis and ankylosing spondylitis. Arthritis Rheum. 1983; 26(9): 1155-9.
479. Nelson JL, Ostensen M. Pregnancy and rheumatoid arthritis. Rheum Dis Clin North Am. 1997; 23(1): 195-212.
480. Johnson PM, Christmas SE, Vince GS. Immunological aspects of implantation and implantation failure. Hum Reprod. 1999; 14: 26-36.
481. Kamat BR, Isaacson PG. The immunocytochemical distribution of leukocytic subpopulations in human endometrium. Am J Pathol. 1987; 127(1): 66-73.
482. King A, Wellings V, Gardner L, Loke YW. Immunocytochemical characterization of the unusual large granular lymphocytes in human endometrium throughout the menstrual cycle. Hum Immunol. 1989; 24(3): 195-205.
483. Gardner L, Moffett A. Dendritic cells in the human decidua. Biol Reprod. 2003; 69(4): 1438-46.
484. Lima J, Martins C, Leandro MJ, Nunes G, Sousa MJ, Branco JC, Borrego LM. Characterization of B cells in healthy pregnant women from late pregnancy to post-partum: a prospective observational study. . BMC Pregnancy Childbirth. 2016; 16(1): 139.
485. Muzzio D, Zenclussen AC, Jensen F. The role of B cells in pregnancy: the good and the bad. Am J Reprod Immunol. 2013; 69(4): 408-12.

486. Fettke F, Schumacher A, Costa SD, Zenclussen AC. B cells: the old new players in reproductive immunology. Front Immunol. 2014; 5: 285.
487. Soares RR, Antinarelli LMR, Abramo C, Macedo GC, Coimbra ES, Scopel KKG. What do we know about the role of regulatory B cells (Breg) during the course of infection of two major parasitic diseases, malaria and leishmaniasis? Pathog Glob Health. 2017; 111(3): 107-15.
488. Blair PA, Noreña LY, Flores-Borja F, Rawlings DJ, Isenberg DA, Ehrenstein MR, Mauri C. CD19(+)CD24(hi)CD38(hi) B cells exhibit regulatory capacity in healthy individuals but are functionally impaired in systemic Lupus Erythematosus patients. Immunity. 2010; 32(1): 129-40.
489. Griffin DO, Holodick NE, Rothstein TL. Human B1 cells in umbilical cord and adult peripheral blood express the novel phenotype CD20+ CD27+ CD43+ CD70-. J Exp Med. 2011; 208(1): 67-80.
490. Quách TD, Rodríguez-Zhurbenko N, Hopkins TJ, Guo X, Hernández AM, Li W, Rothstein TL. Distinctions among Circulating Antibody-Secreting Cell Populations, Including B-1 Cells, in Human Adult Peripheral Blood. J Immunol. 2016; 196(3): 1060-9.
491. Parra D, Takizawa F, Sunyer JO. Evolution of B cell immunity. Annu Rev Anim Biosci. 2013; 1: 65-97.
492. Holodick NE, Tumang JR, Rothstein TL. Immunoglobulin secretion by B1 cells: differential intensity and IRF4-dependence of spontaneous IgM secretion by peritoneal and splenic B1 cells. Eur J Immunol. 2010; 40(11): 3007-16.
493. Baumgarth N, Herman OC, Jager GC, Brown L, Herzenberg LA, Herzenberg LA. Innate and acquired humoral immunities to influenza virus are mediated by distinct arms of the immune system. Proc Natl Acad Sci U S A. 1999; 96(5): 2250-5.
494. Hayakawa K, Hardy RR, Honda M, Herzenberg LA, Steinberg AD, Herzenberg LA. Ly-1 B cells: functionally distinct lymphocytes that secrete IgM autoantibodies. Proc Natl Acad Sci U S A. 1984; 81(8): 2494-8.
495. Choi YS, Dieter JA, Rothaeusler K, Luo Z, Baumgarth N. B-1 cells in the bone marrow are a significant source of natural IgM. Eur J Immunol. 2012; 42(1): 120-9.
496. Baumgarth N, Herman OC, Jager GC, Brown LE, Herzenberg LA, Chen J. B-1 and B-2 cell-derived immunoglobulin M antibodies are nonredundant components of the protective response to influenza virus infection. J Exp Med. 2000; 192(2): 271-80.
497. Haas KM, Poe JC, Steeber DA, Tedder TF. B-1a and B-1b cells exhibit distinct developmental requirements and have unique functional roles in innate and adaptive immunity to S. pneumoniae. Immunity. 2005; 23(1): 7-18.
498. Coutinho A, Kazatchkine MD, Avrameas S. Natural autoantibodies. Curr Opin Immunol. 1995; 7(6): 812-8.
499. Casali P, Schettino EW. Structure and function of natural antibodies. Curr Top Microbiol Immunol. 1996; 210: 167-79.
500. Holodick NE, Rodríguez-Zhurbenko N, Hernández AM. Defining Natural Antibodies. Front Immunol. 2017; 8: 872.
501. Casali P, Notkins AL. Probing the human B-cell repertoire with EBV: polyreactive antibodies and CD5+ B lymphocytes. Annu Rev Immunol. 1989; 7(513-535): 513.
502. Burastero SE, Casali P, Wilder RL, Notkins AL. Monoreactive high affinity and polyreactive low affinity rheumatoid factors are produced by CD5+ B cells from patients with rheumatoid arthritis. J Exp Med. 1988; 168(6): 1979-92.
503. Casali P, Burastero SE, Nakamura M, Inghirami G, Notkins AL. Human lymphocytes making rheumatoid factor and antibody to ssDNA belong to Leu-1+ B-cell subset. Science. 1987; 236(4797): 77-81.
504. Mantovani L, Wilder RL, Casali P. Human rheumatoid B-1a (CD5+ B) cells make somatically hypermutated high affinity IgM rheumatoid factors. J Immunol. 1993; 151(1): 473-88.
505. Duan B, Morel L. Role of B-1a cells in autoimmunity. Autoimmun Rev. 2006; 5(6): 403-8.
506. Nakamura M, Burastero SE, Notkins AL, Casal P. Human monoclonal rheumatoid factor-like antibodies from CD5 (Leu-1)+ B cells are polyreactive. J Immunol. 1988; 140(12): 4180-6.
507. Jensen F, Wallukat G, Herse F, Budner O, El-Mousleh T, Costa SD, Dechend R, Zenclussen AC. CD19+CD5+ cells as indicators of preeclampsia. Hypertension. 2012; 59(4): 861-8.
508. Kasaian MT, Ikematsu H, Casali P. Identification and analysis of a novel human surface CD5- B lymphocyte subset producing natural antibodies. J Immunol. 1992; 148(9): 2690-702.
509. Kasaian MT, Casali P. Analysis of the human CD5- CD45RAlow B-cell subset. Ann N Y Acad Sci. 1992; 651: 59-69.

510. Bhat NM, Mithal A, Bieber MM, Herzenberg LA, Teng NN. Human CD5+ B lymphocytes (B-1 cells) decrease in peripheral blood during pregnancy. J Reprod Immunol. 1995; 28(1): 53-60.
511. Watanabe M, Iwatani Y, Kaneda T, Hidaka Y, Mitsuda N, Morimoto Y, Amino N. Changes in T, B, and NK lymphocyte subsets during and after normal pregnancy. Am J Reprod Immunol. 1997; 37(5): 368-77.
512. Nielsen HS, Witvliet MD, Steffensen R, Haasnoot GW, Goulmy E, Christiansen OB, Claas F. The presence of HLA-antibodies in recurrent miscarriage patients is associated with a reduced chance of a live birth. J Reprod Immunol. 2010; 87(1-2): 67-73.
513. Taylor PV, Hancock KW. Antigenicity of trophoblast and possible antigen-masking effects during pregnancy. Immunology. 1975; 28(5): 973–82.
514. Gelabert A, Balasch J, Ercilla G, Vanrell JA, Vives J, González-Merlo J, Castillo R. Abortion may sensitize the mother to HLA antigens. Tissue Antigens. 1981; 17(4): 353-6.
515. Yang X, Zhang C, Chen G, Sun C, Li J. Antibodies: The major participants in maternal–fetal interaction. J Obstet Gynaecol Res. 2018; 45(1): 1-8.
516. Margni RA, Perdigón G, Abatángelo C, Gentile T, Binaghi RA. Immunobiological behaviour of rabbit precipitating and non-precipitating (co-precipitating) antibodies. Immunology. 1980; 41(3): 681-6.
517. Gentile T, Borel IM, Angelucci J, Miranda S, Margni RA. Preferential synthesis of asymmetric antibodies in rats immunized with paternal particulate antigens. Effect on pregnancy. J Reprod Immunol. 1992; 22(2): 173-83.
518. Malan Borel I, Gentile T, Angelucci J, Pividori J, Guala MC, Binaghi RA, Margni RA. IgG asymmetric molecules with antipaternal activity isolated from sera and placenta of pregnant human. J Reprod Immunol. 1991; 20(2): 129-40.
519. Eblen AC, Gercel-Taylor C, Shields LB, Sanfilippo JS, Nakajima ST, Taylor DD. Alterations in humoral immune responses associated with recurrent pregnancy loss. Fertil Steril. 2000; 73(2): 305-13.
520. Zenclussen AC, Gentile T, Kortebani G, Mazzolli A, Margni R. Asymmetric antibodies and pregnancy. Am J Reprod Immunol. 2001; 45(5): 289-94.
521. Barrientos G, Fuchs D, Schröcksnadel K, Ruecke M, Garcia MG, Klapp BF, Raghupathy R, Miranda S, Arck PC, Blois SM. Low levels of serum asymmetric antibodies as a marker of threatened pregnancy. J Reprod Immunol. 2009; 79(2): 201-10.
522. Yanaba K, Bouaziz JD, Haas KM, Poe JC, Fujimoto M, Tedder TF. A regulatory B cell subset with a unique CD1dhiCD5+ phenotype controls T cell-dependent inflammatory responses. Immunity. 2008; 28(5): 639-50.
523. Moulin V, Andris F, Thielemans K, Maliszewski C, Urbain J, Moser M. B lymphocytes regulate dendritic cell (DC) function in vivo: increased interleukin 12 production by DCs from B cell-deficient mice results in T helper cell type 1 deviation. J Exp Med. 2000; 192(5): 475-82.
524. Flores-Borja F, Bosma A, Ng D, Reddy V, Ehrenstein MR, Isenberg DA, Mauri C. CD19+CD24hiCD38hi B cells maintain regulatory T cells while limiting TH1 and TH17 differentiation. Sci Transl Med. 2013; 5(173): 173ra23.
525. Mizoguchi A, Bhan AK. A case for regulatory B cells. J Immunol. 2006; 176(2): 705-10.
526. Shen P, Roch T, Lampropoulou V, O'Connor RA, Stervbo U, Hilgenberg E, Ries S, Dang VD, Jaimes Y, Daridon C, et al. IL-35-producing B cells are critical regulators of immunity during autoimmune and infectious diseases. Nature. 2014; 507(7492): 366-70.
527. Wang RX, Yu CR, Dambuza IM, Mahdi RM, Dolinska MB, Sergeev YV, Wingfield PT, Kim SH, Egwuagu CE. Interleukin-35 induces regulatory B cells that suppress autoimmune disease. Nat Med. 2014; 20(6): 633-41.
528. Mauri C, Menon M. Human regulatory B cells in health and disease: therapeutic potential. J Clin Invest. 2017; 127(3): 772-9.
529. Busse M, Campe KNJ, Nowak D, Schumacher A, Plenagl S, Langwisch S, Tiegs G, Reinhold A, Zenclussen AC. IL-10 producing B cells rescue mouse fetuses from inflammation-driven fetal death and are able to modulate T cell immune responses. Sci Rep. 2019; 9: 9335.
530. Slawek A, Lorek D, Kedzierska AE, Chelmonska-Soyta A. Regulatory B cells with IL-35 and IL-10 expression in a normal and abortion-prone murine pregnancy model. Am J Reprod Immunol. 2020; 83(3): e13217.
531. Jensen F, Muzzio D, Soldati R, Fest S, Zenclussen AC. Regulatory B10 cells restore pregnancy tolerance in a mouse model. Biol Reprod. 2013; 89(4): 90.

532. Danaii S, Ghorbani F, Ahmadi M, Abbaszadeh H, Koushaeian L, Soltani-Zangbar MS, Mehdizadeh A, Hojjat-Farsangi M, Kafil HS, Aghebati-Maleki L, et al. IL-10-producing B cells play important role in the pathogenesis of recurrent pregnancy loss. International Immunopharmacology. 2020; 87: 106806.
533. Faas MM, De Vos P. Innate immune cells in the placental bed in healthy pregnancy and preeclampsia. Placenta. 2018; 69: 125-33.
534. Miyazaki S, Tsuda H, Sakai M, Hori S, Sasaki Y, Futatani T, Miyawaki T, Saito S. Predominance of Th2-promoting dendritic cells in early human pregnancy decidua. J Leukoc Biol. 2003; 74(4): 514-22.
535. Steinman RM. The dendritic cell system and its role in immunogenicity. Annu Rev Immunol. 1991; 9: 271-96.
536. Ehrentraut S, Sauss K, Neumeister R, Luley L, Oettel A, Fettke F, Costa SD, Langwisch S, Zenclussen AC, Schumacher A. Human Miscarriage Is Associated With Dysregulations in Peripheral Blood-Derived Myeloid Dendritic Cell Subsets. Front Immunol. 2019; 10: 2440.
537. Della Bella S, Giannelli S, Cozzi V, Signorelli V, Cappelletti M, Cetin C, Villa ML. Incomplete activation of peripheral blood dendritic cells during healthy human pregnancy. Clin Exp Immunol. 2011; 164(2): 180-92.
538. Karoline Sauss K, Stefanie Ehrentraut S, Ana Claudia Zenclussen AC, Anne Schumacher A. The pregnancy hormone human chorionic gonadotropin differentially regulates plasmacytoid and myeloid blood dendritic cell subsets. Am J Reprod Immunol. 2018; 79(4): e12837.
539. Rieger L, Honig A, Sütterlin M, Kapp M, Dietl J, Ruck P, Kämmerer U. Antigen-presenting cells in human endometrium during the menstrual cycle compared to early pregnancy. J Soc Gynecol Investig. 2004; 11(7): 488-93.
540. Volchek M, Girling JE, Lash GE, Cann L, Kumar B, Robson SC, Bulmer JN, Rogers PAW. Lymphatics in the human endometrium disappear during decidualization. Hum Reprod. 2010; 25(10): 2455-64.
541. Tagliani E, Erlebacher A. Dendritic cell function at the maternal-fetal interface. Expert Review of Clinical Immunology. 2011; 7(5): 593-602.
542. Kämmerer U, Eggert AO, Kapp M, McLellan AD, Geijtenbeek TBH, Dietl J, van Kooyk Y, Kämpgen E. Unique appearance of proliferating antigen-presenting cells expressing DC-SIGN (CD209) in the decidua of early human pregnancy. . Am J Pathol. 2003; 162(3): 887-96.
543. Shima T, Nakashima A, Yasuda I, Ushijima A, Inada K, Tsuda S, Yoshino O, Tomura M, Saito S. Uterine CD11c+ cells induce the development of paternal antigen-specific Tregs via seminal plasma priming. J Reprod Immunol. 2020; 141: 103165.
544. Leno-Durán E, Muñoz-Fernández R, Olivares EG, Tirado-González I. Liaison between natural killer cells and dendritic cells in human gestation. Cell Mol Immunol. 2014; 11(5): 449-55.
545. Kwiatek M, Gęca T, Krzyżanowski A, Malec A, Kwaśniewska A. Peripheral Dendritic Cells and CD4+CD25+Foxp3+ Regulatory T Cells in the First Trimester of Normal Pregnancy and in Women with Recurrent Miscarriage. PLoS One. 2015; 10(5): e0124747.
546. Askelund K, Liddell HS, Zanderigo AM, Fernando NS, Khong TY, Stone PR, Chamley LW. $CD83^+$ dendritic cells in the decidua of women with recurrent miscarriage and normal pregnancy. . Placenta. 2004; 25(2-3): 140-5.
547. Liu S, Wei H, Li Y, Huang C, Lian R, Xu J, Chen L, Zeng Y. Downregulation of $ILT4^+$ dendritic cells in recurrent miscarriage and recurrent implantation failure. Am J Reprod Immunol. 2018; 80(4): e12998.
548. Lucas ES, Vrljicak P, Muter J, Diniz-da-Costa MM, Brighton PJ, Kong CS, Lipecki J, Fishwick KJ, Odendaal J, Ewington LJ, et al. Recurrent pregnancy loss is associated with a pro-senescent decidual response during the peri-implantation window. Commun Biol. 2020; 3(1): 37.
549. Gordon S, Plüddemann A. Tissue macrophages: heterogeneity and functions. . BMC Biol. 2017; 15(1): 53.
550. Hirayama D, Iida T, Nakase H. The Phagocytic Function of Macrophage-Enforcing Innate Immunity and Tissue Homeostasis. Int J Mol Sci. 2018; 19(1): 92.
551. Fest S, Aldo PB, Abrahams VM, Visintin I, Alvero A, Chen R, Chavez SL, Romero R, Mor G. Trophoblast-macrophage interactions: a regulatory network for the protection of pregnancy. Am J Reprod Immunol. 2007; 57(1): 55-66.
552. Renaud SJ, Graham CH. The role of macrophages in utero-placental interactions during normal and pathological pregnancy. Immunol Invest. 2008; 37(5): 535-64.

553. De M, Wood GW. Influence of oestrogen and progesterone on macrophage distribution in the mouse uterus. J Endocrinol. 1990; 126(3): 417-24.
554. Jensen AL, Collins J, Shipman EP, Wira CR, Guyre PM, Pioli PA. A subset of human uterine endometrial macrophages is alternatively activated. . Am J Reprod Immunol. 2012; 68(5): 374-86.
555. Clark GF. Functional glycosylation in the human and mammalian uterus. . Fertil Res Pract. 2015; 1: 17.
556. Lash GE, Pitman H, Morgan HL, Innes BA, Agwu CN, Bulmer JN. Decidual macrophages: key regulators of vascular remodeling in human pregnancy. J Leukoc Biol. 2016; 100(2): 315-25.
557. Ning F, Liu H, Lash GE. The Role of Decidual Macrophages During Normal and Pathological Pregnancy. Am J Reprod Immunol. 2016; 75(3): 298-309.
558. Gori S, Soczewski E, Fernández L, Grasso E, Gallino L, Merech F, Colado A, Borge M, Pérez Leirós C, Salamone G, et al. Decidualization Process Induces Maternal Monocytes to Tolerogenic IL-10-Producing Dendritic Cells (DC-10). Front Immunol. 2020; 11: 1571.
559. Shakhawat A, Shaikly V, Elzatma E, Mavrakos E, Jabeen A, Fernández N. Interaction between HLA-G and monocyte/macrophages in human pregnancy. J Reprod Immunol. 2010; 85(1): 40-6.
560. Hofmeister V, Weiss EH. HLA-G modulates immune responses by diverse receptor interactions. Seminars in Cancer Biology. 2003; 13(5): 317-23.
561. Tang MX, Hu XH, Liu ZZ, Kwak-Kim J, Liao AH. What are the roles of macrophages and monocytes in human pregnancy? J Reprod Immunol. 2015; 112: 73-80.
562. Parasar P, Guru N, Nayak NR. Contribution of macrophages to fetomaternal immunological tolerance. Hum Immunol. 2021; S0198-8859(21): 00063-X.
563. Heikkinen J, Möttönen M, Komi J, Alanen A, Lassila O. Phenotypic characterization of human decidual macrophages. Clin Exp Immunol. 2003; 131(3): 498-505.
564. Jena MK, Nayak N, Chen K, Nayak NR. Role of Macrophages in Pregnancy and Related Complications. Arch Immunol Ther Exp. 2019; 67(5): 295-309.
565. Co EC, Gormley M, Kapidzic M, Rosen DB, Scott MA, Stolp HAR, McMaster M, Lewis L Lanier LL, Bárcena A, Fisher SJ. Maternal decidual macrophages inhibit NK cell killing of invasive cytotrophoblasts during human pregnancy. Biol Reprod. 2013; 88(6): 155.
566. Ding J, Yin T, Yan N, Cheng Y, Yang J. FasL on decidual macrophages mediates trophoblast apoptosis: A potential cause of recurrent miscarriage. International Journal of Molecular Medicine. 2019; 43(6): 2376-86.
567. Brown MB, von Chamier M, Allam AB, Reyes L. M1/M2 Macrophage Polarity in Normal and Complicated Pregnancy. Front Immunol. 2014; 5: 606.
568. Yao Y, Xu XH, Jin L. Macrophage Polarization in Physiological and Pathological Pregnancy. Front Immunol. 2019; 10: 792.
569. Tonello A, Poli G. Tubal ectopic pregnancy: macrophages under the microscope. . Hum Reprod. 2007; 22(10): 2577-84.
570. Tsao FY, Wu MY, Chang YL, Wu CT, Ho HN. M1 macrophages decrease in the deciduae from normal pregnancies but not from spontaneous abortions or unexplained recurrent spontaneous abortions. J Formos Med Assoc. 2018; 117(3): 204-11.
571. Ding J, Yang C, Cheng Y, Wang J, Zhang S, Yan S, He F, Yin T, Yang J. Trophoblast-derived IL-6 serves as an important factor for normal pregnancy by activating Stat3-mediated M2 macrophages polarization. International Immunopharmacology. 2021; 90: 106788.
572. Guenther S, Vrekoussis T, Heublein S, Bayer B, Anz D, Knabl J, Navrozoglou I, Dian D, Friese K, Makrigiannakis A, et al. Decidual macrophages are significantly increased in spontaneous miscarriages and over-express FasL: a potential role for macrophages in trophoblast apoptosis. Int J Mol Sci. 2012; 13(7): 9069-80.
573. Care AS, Diener KR, Jasper MJ, Brown HM, Ingman WVSAR, S.A. Macrophages regulate corpus luteum development during embryo implantation in mice. J Clin Invest. 2013; 123(8): 3472-87.
574. Shimada S, Ebina Y, Iijima N, Deguchi M, Yamada H. Decidual $CD68^{+}HLA\text{-}DR^{+}CD163^{-}$ M1 macrophages increase in miscarriages with normal fetal chromosome. Am J Reprod Immunol. 2018; 79(2): 1-6.
575. National Institute for Health and Care Excellence. Miscarriage: Scenario: Managing recurrent miscarriage 2020 [Available from: https://cks.nice.org.uk/topics/miscarriage/management/managing-recurrent-miscarriage/.

576. Queensland Clinical Guidelines. Early pregnancy loss. Maternity and Neonatal Clinical Guideline. 2018: 1-39.
577. Ministry of Health & Family Welfare Government of India. STANDARD TREATMENT GUIDELINES: Management of Recurrent Spontaneous Abortion. 2017: 1-20.
578. Huchon C, Deffieux X, Beucher G, Capmas P, Carcopino X, Costedoat-Chalumeau N, Delabaere A, Gallot V, Iraola E, Lavoue V, et al. Pregnancy loss: French clinical practice guidelines. Eur J Obstet Gynecol Reprod Biol. 2016; 201: 18-26.
579. Toth B, Würfel W, Bohlmann M, Zschocke J, Rudnik-Schöneborn S, Nawroth F, Schleußner E, Rogenhofer N, Wischmann T, von Wolff M, et al. Recurrent Miscarriage: Diagnostic and Therapeutic Procedures. Guideline of the DGGG, OEGGG and SGGG (S2k-Level, AWMF Registry Number 015/050). Geburtshilfe und Frauenheilkunde. 2018; 78(4): 364-81.
580. Sacks G, Yang Y, Gowen E, Smith S, Fay L, Chapman M. Detailed analysis of peripheral blood natural killer cells in women with repeated IVF failure. Am J Reprod Immunol. 2012; 67(5): 434-42.
581. Bisset LR, Lung TL, Kaelin M, Ludwig E, Dubs RW. Reference values for peripheral blood lymphocyte phenotypes applicable to the healthy adult population in Switzerland. Eur J Haematol. 2004; 72(3): 203-12.
582. Gounder SS, Abdullah BJJ, Radzuanb NEIBM, Zain FDBMZ, Sait NBM, Chua C, Subramani B. Effect of Aging on NK Cell Population and Their Proliferation at Ex Vivo Culture Condition. Anal Cell Pathol. 2018; 2018: 7871814.
583. Ilavská S, Horváthová M, Szabová M, Nemessányi T, Jahnová E, Tulinská J, Líšková A, Wsolová L, Staruchová M, Volkovová K. Association between the human immune response and body mass index. Hum Immunol. 2012; 73(5): 480-5.
584. Arjona A, Sarkar DK. Evidence supporting a circadian control of natural killer cell function. Brain Behav Immun. 2006; 20(5): 469-76.
585. Lee S, Kim J, Jang B, Hur S, Jung U, Kil K, Na B, Lee M, Choi Y, Fukui A, et al. Fluctuation of peripheral blood T, B, and NK cells during a menstrual cycle of normal healthy women. J Immunol. 2010; 185(1): 756-62.
586. Flynn L, Byrne B, Carton J, Kelehan P, O'Herlihy C, O'Farrelly C. Menstrual cycle dependent fluctuations in NK and T-lymphocyte subsets from non-pregnant human endometrium. Am J Reprod Immunol. 2000; 43(4): 209-17.
587. Sulke AN, Jones DB, Wood PJ. Variation in natural killer activity in peripheral blood during the menstrual cycle. Br Med J (Clin Res Ed). 1985; 290(6472): 884-6.
588. Landmann RM, Müller FB, Perini C, Wesp M, Erne P, Bühler FR. Changes of immunoregulatory cells induced by psychological and physical stress: relationship to plasma catecholamines. Clin Exp Immunol. 1984; 58(1): 127-35.
589. Targan S, Britvan L, Dorey F. Activation of human NKCC by moderate exercise: increased frequency of NK cells with enhanced capability of effector--target lytic interactions. Clin Exp Immunol. 1981; 45(2): 352-60.
590. Edwards AJ, Bacon TH, Elms CA, Verardi R, Felder M, Knight SC. Changes in the populations of lymphoid cells in human peripheral blood following physical exercise. Clin Exp Immunol. 1984; 58(2): 420-7.
591. Brahmi Z, Thomas JE, Park M, Park M, Dowdeswell IR. The effect of acute exercise on natural killer-cell activity of trained and sedentary human subjects. J Clin Immunol. 1985; 5(5): 321-8.
592. Deuster PA, Curiale AM, Cowan ML, Finkelman FD. Exercise-induced changes in populations of peripheral blood mononuclear cells. Med Sci Sports Exerc. 1988; 20(3): 276-80.
593. Suzui M, Kawai T, Kimura H, Takeda K, Yagita H, Okumura K, Shek PN, Shephard RJ. Natural killer cell lytic activity and CD56(dim) and CD56(bright) cell distributions during and after intensive training. J Appl Physiol. 2004; 96(6): 2167-73.
594. Oshida Y, Yamanouchi K, Hayamizu S, Sato Y. Effect of acute physical exercise on lymphocyte subpopulations in trained and untrained subjects. Int J Sports Med. 1988; 9(2): 137-40.
595. Fiatarone MA, Morley JE, Bloom ET, Benton D, Solomon GF, Makinodan T. The effect of exercise on natural killer cell activity in young and old subjects. J Gerontol. 1989; 44(2): 37-45.
596. Tvede N, Pedersen BK, Hansen FR, Bendix T, Christensen LD, Galbo H, Halkjaer-Kristensen J. Effect of physical exercise on blood mononuclear cell subpopulations and in vitro proliferative responses. Scand J Immunol. 1989; 29(3): 383-9.

597. Espersen GT, Elbaek A, Ernst E, Toft E, Kaalund S, Jersild C, Grunnet N. Effect of physical exercise on cytokines and lymphocyte subpopulations in human peripheral blood. APMIS. 1990; 98(5): 395-400.
598. Kendall A, Hoffman-Goetz L, Houston M, MacNeil B, Arumugam Y. Exercise and blood lymphocyte subset responses: intensity, duration, and subject fitness effects. J Appl Physiol. 1990; 69(1): 251-60.
599. Field CJ, Gougeon R, Marliss EB. Circulating mononuclear cell numbers and function during intense exercise and recovery. J Appl Physiol. 1991; 71(3): 1089-97.
600. Kappel M, Tvede N, Galbo H, Haahr PM, Kjaer M, Linstow M, Klarlund K, Pedersen BK. Evidence that the effect of physical exercise on NK cell activity is mediated by epinephrine. J Appl Physiol. 1991; 70(6): 2530-4.
601. Gabriel H, Schwarz L, Steffens G, Kindermann W. Immunoregulatory hormones, circulating leucocyte and lymphocyte subpopulations before and after endurance exercise of different intensities. Int J Sports Med. 1992; 13(5): 359-66.
602. Caggiula AR, McAllister CG, Matthews KA, Berga SL, Owens JF, Miller AL. Psychological stress and immunological responsiveness in normally cycling, follicular-stage women. J Neuroimmunol. 1995; 59(1-2): 103-11.
603. Benschop RJ, Geenen R, Mills PJ, Naliboff BD, Kiecolt-Glaser JK, Herbert TB, van der Pompe G, Miller GE, Matthews KA, Godaert GL, et al. Cardiovascular and immune responses to acute psychological stress in young and old women: a meta-analysis. Psychosom Med. 1998; 60(3): 290-6.
604. Schedlowski M, Jacobs R, Stratmann G, Richter S, Hädicke A, Tewes U, Wagner TO, Schmidt RE. Changes of natural killer cells during acute psychological stress. J Clin Immunol. 1993; 13(2): 119-26.
605. Aoki K, Furukawa T, Ogasawara M, Hori S, Kitamura T. Psychosocial factors in recurrent miscarriages. Acta Obstet Gynecol Scand. 1998; 77(5): 572-3.
606. Zhang J, Dunk C, Croy AB, Lye SJ. To serve and to protect: the role of decidual innate immune cells on human pregnancy. Cell and Tissue Research. 2016; 363(1): 249-65.
607. Powell RM, Lissauer D, Tamblyn J, Beggs A, Cox P, Moss P, Kilby MD. Decidual T Cells Exhibit a Highly Differentiated Phenotype and Demonstrate Potential Fetal Specificity and a Strong Transcriptional Response to IFN. J Immunol. 2017; 199(10): 3406-17.
608. Lissauer D, Goodyear O, Khanum R, Moss PA, Kilby MD. Profile of maternal CD4 T-cell effector function during normal pregnancy and in women with a history of recurrent miscarriage. Clin Sci. 2014; 126(5): 347-54.
609. Homer HA. Modern management of recurrent miscarriage. Aust N Z J Obstet Gynaecol. 2019; 59(1): 36-44.
610. Carp H. Immunotherapy for recurrent pregnancy loss. Best Pract Res Clin Obstet Gynaecol. 2019; 60: 77-86.
611. Wong LF, Porter TF, Scott JM. Immunotherapy for recurrent miscarriage. Cochrane Database Syst Rev. 2014; 2014(10): CD000112.
612. Roepke ER, Hellgren M, Hjertberg R, Blomqvist L, Matthiesen L, Henic E, Lalitkumar S, Strandell A. Treatment efficacy for idiopathic recurrent pregnancy loss - a systematic review and meta-analyses. Acta Obstet Gynecol Scand. 2018.
613. Jeve YB, Davies W. Evidence-based management of recurrent miscarriages. J Hum Reprod Sci. 2014; 7(3): 159-69.
614. Porter TF, LaCoursiere Y, Scott JR. Immunotherapy for recurrent miscarriage. Cochrane Database Syst Rev. 2006; 2: CD000112.
615. Christiansen OB. A fresh look at the causes and treatments of recurrent miscarriage, especially its immunological aspects. Hum Reprod Update. 1996; 2(4): 271-93.
616. Duhem C, Dicato MA, Ries F. Side-effects of intravenous immune globulins. Clin Exp Immunol. 1994; 97(Suppl 1): 79-83.
617. The Recurrent Miscarriage Immunotherapy Trialists Group, Coulam CB, Clark DA, Collins J, Scott JR, Schlesselman JS, Aoki K, Carp HJA, Cauchi MN, Lim D, et al. Worldwide collaborative observational study and meta-analysis on allogenic leukocyte immunotherapy for recurrent spontaneous abortion. Recurrent Miscarriage Immunotherapy Trialists Group. Am J Reprod Immunol. 1994; 32(2): 55-72.
618. Puckett Y, Gabbar A, Bokhari AA. Prednisone. 2020. In: StatPearls [Internet] [Internet]. Treasure Island (FL): StatPearls Publishing.

619. Christiansen OB, Mathiesen O, Husth M, Lauritsen JG, Grunnet N. Placebo-controlled trial of active immunization with third party leukocytes in recurrent miscarriage. Acta Obstet Gynecol Scand. 1994; 73(3): 261-8.
620. Gerriets V, Bansal P, Goyal A, Khaddour K. Tumor Necrosis Factor (TNF) Inhibitors. 2020. In: StatPearls [Internet] [Internet]. Treasure Island (FL): StatPearls Publishing.
621. Ahmadi M, Ghaebi M, Abdolmohammadi-Vahid S, Abbaspour-Aghdam S, Hamdi K, Abdollahi-Fard S, Danaii S, Mosapour P, Koushaeian L, Dolati S, et al. NK cell frequency and cytotoxicity in correlation to pregnancy outcome and response to IVIG therapy among women with recurrent pregnancy loss. J Cell Physiol. 2019; 234(6): 9428-37.
622. Stray-Pedersen B, Stray-Pedersen S. Recurrent abortion: the role of psychotherapy. In: Sharp F, Beard RW, editors. Early Pregnancy Loss. London: Springer; 1988. p. 433-40.
623. Clifford K, Rai R, Regan L. Future pregnancy outcome in unexplained recurrent first trimester miscarriage. Hum Reprod. 1997; 12(2): 387-9.
624. Liddell HS, Pattison NS, Zanderigo A. Recurrent miscarriage--outcome after supportive care in early pregnancy. Aust N Z J Obstet Gynaecol. 1991; 31(4): 320-2.
625. Sacks G. Enough! Stop the arguments and get on with the science of natural killer cell testing. Hum Reprod. 2015; 30(7): 1526-31.
626. Moffett A, Shreeve N. First do no harm: uterine natural killer (NK) cells in assisted reproduction. Hum Reprod. 2015; 30(7): 1519-25.
627. Laird SM, Lash GE, Li TC, Bulmer JN. The Role of Natural Killer Cells in Human Fertility. Royal College of Obstetricians and Gynaecologists. 2016; Scientific Impact Paper No. 53: 1-11.
628. Tommy's. Why did I miscarry and was it my fault? 2020 [updated December 14th, 2019.
629. Nemoto T, Beglar D, editors. Developing Likert-Scale Questionnaires. JALT2013 Conference Proceedings; 2014; Tokyo.
630. Coomarasamy A, Devall AJ, Cheed V, Harb H, Middleton LJ, Gallos ID, Williams H, Eapen AK, Roberts T, Ogwulu CC, et al. A Randomized Trial of Progesterone in Women with Bleeding in Early Pregnancy. . N Engl J Med. 2019; 380(19): 1815-24.
631. Coomarasamy A, Williams H, Truchanowicz E, Seed PT, Small R, Quenby S, Gupta P, Dawood F, Koot YEM, Atik RB, et al. A Randomized Trial of Progesterone in Women with Recurrent Miscarriages. . N Engl J Med. 2015; 373(22): 2141-8.
632. Yu N, Li X, Song W, Li D, Yu D, Zeng X, Li M, Leng X, Li X. CD4(+)CD25 (+)CD127 (low/-) T cells: a more specific Treg population in human peripheral blood. Inflammation. 2012; 35(6): 1773-80.
633. Liu W, Putnam AL, Xu-Yu Z, Szot GL, Lee MR, Zhu S, Gottlieb PA, Kapranov P, Gingeras TR, Fazekas de St Groth B, et al. CD127 expression inversely correlates with FoxP3 and suppressive function of human CD4+ T reg cells. J Exp Med. 2006; 203(7): 1701-11.
634. Golubovskaya V, Wu L. Different Subsets of T Cells, Memory, Effector Functions, and CAR-T Immunotherapy. Cancers. 2016; 8(3): 36.
635. BioLegend. Natural Killer Cells 2018 [Available from: https://www.biolegend.com/natural_killer
636. Becton DaC. FlowJo™ Software version 10.6.2. 2021.
637. Monaco G, Chen H, Poidinger M, Chen J, de Magalhães JP, Larbi A. flowAI: automatic and interactive anomaly discerning tools for flow cytometry data. Bioinformatics. 2016; 32(16): 2473-80.
638. Corporation M. Microsoft Excel. 2016.
639. GraphPad. GraphPad Prism version 6.0.0. 2021.
640. Spitzer MH, Nolan GP. Mass Cytometry: Single Cells, Many Features. Cell. 2016; 165(4): 780-91.
641. Hartmann FJ, Simonds EF, Bendall SC. A Universal Live Cell Barcoding-Platform for Multiplexed Human Single Cell Analysis. Sci Rep. 2018; 8: 10770.
642. Fluidigm. Normalization of Mass Cytometry Data Using EQ Four Element Calibration Beads. Fluidigm Technical Note. 1-13.
643. Lozzio BB, Lozzio CB. Properties and usefulness of the original K-562 human myelogenous leukemia cell line. Leuk Res. 1979; 3(6): 363-70.
644. Bryceson YT, March ME, Barber DF, Ljunggren HG, Long EO. Cytolytic granule polarization and degranulation controlled by different receptors in resting NK cells. J Exp Med. 2005; 202(7): 1001-12.

645. Jang YY, Cho D, Kim SK, Shin DJ, Park MH, Lee JJ, Shin MG, Shin JH, Suh SP, Ryang DW. An improved flow cytometry-based natural killer cytotoxicity assay involving calcein AM staining of effector cells. Ann Clin Lab Sci. 2012; 42(1): 42-9.
646. Kim GG, Donnenberg VS, Donnenberg AD, Gooding W, Whiteside TL. A novel multiparametric flow cytometry-based cytotoxicity assay simultaneously immunophenotypes effector cells: comparisons to a 4 h 51Cr-release assay. J Immunol Methods. 2007; 325(1-2): 51-66.
647. Team R. RStudio: Integrated Development for R. RStudio. Boston, MA2020.
648. Team RC. R: A language and environment for statistical computing. R Foundation for Statistical Computing. Vienna, Austria2020.
649. Crowell HL, Robinson MD. Differential discovery with CATALYST. 2021.
650. Nowicka M, Krieg C, Crowell HL, Weber LM, Hartmann FJ, Guglietta S, Becher B, Levesque MP, Robinson MD. CyTOF workflow: differential discovery in high-throughput high-dimensional cytometry datasets. F1000Res. 2017; 6: 748.
651. Crowell HL, Zanotelli VRT, Chevrier S, Robinson MD. CATALYST: Cytometry dATa anALYSis Tools. R package version 1.14.0. 2020.
652. Wilke CO. cowplot: Streamlined Plot Theme and Plot Annotations for 'ggplot2'. R package version 1.1.0. 2020.
653. Ellis B, Haaland P, Hahne F, Le Meur N, Gopalakrishnan N, Spidlen J, Jiang M, Finak G. flowCore: flowCore: Basic structures for flow cytometry data. R package version 2.2.0. 2020.
654. Weber LM. diffcyt: Differential discovery in high-dimensional cytometry via high-resolution clustering. R package version 1.10.0. 2020.
655. McCarthy DJ, Campbell KR, Lun ATL, Wills QF. Scater: pre-processing, quality control, normalization and visualization of single-cell RNA-seq data in R. Bioinformatics. 2017; 33(8): 1179-86.
656. Amezquita RA, Lun ATL, Becht E, Carey VJ, Carpp LN, Geistlinger L, Marini F, Rue-Albrecht K, Risso D, Soneson C, et al. Orchestrating single-cell analysis with Bioconductor. Nature Methods. 2020; 17(2): 137-45.
657. Konopka T. umap: Uniform Manifold Approximation and Projection. R package version 0.2.7.0. 2020.
658. Melville J. uwot: The Uniform Manifold Approximation and Projection (UMAP) Method for Dimensionality Reduction. R package version 0.1.9. 2020.
659. Weber LM, Nowicka M, Soneson C, Robinson MD. diffcyt: Differential discovery in high-dimensional cytometry via high-resolution clustering. Commun Biol. 2019; 2: 183.
660. Liaw A, Wiener M. Classification and Regression by randomForest. R News. 2002; 2(3): 18-22.
661. Wickham H. ggplot2: Elegant Graphics for Data Analysis. New York: Springer-Verlag; 2016.
662. Kuhn M. The caret Package. 2019.
663. Chong J, Soufan O, Li C, Caraus I, Li S, Bourque G, Wishart DS, Xia J. MetaboAnalyst 4.0: towards more transparent and integrative metabolomics analysis. Nucleic Acids Research. 2018; 46(W1): W486-W94.
664. Bravo-Merodio L, Williams JA, Gkoutos GV, Acharjee A. -Omics biomarker identification pipeline for translational medicine. Journal of Translational Medicine. 2019; 17(155).
665. Bravo-Merodio L, Acharjee A, Hazeldine J, Bentley C, Foster M, Gkoutos GV, Lord JM. Machine learning for the detection of early immunological markers as predictors of multi-organ dysfunction. Scientific Data. 2019; 6(328).
666. Regan L, Rai R, Saravelos S, Li TC, Gynaecologists RCoO. Investigation and Treatment of Recurrent First-Trimester and one or more Second-Trimester Miscarriage. Green-top Guideline. 2021; 17 (Peer Review Draft): 1-48.
667. Meaney S, Corcoran P, Spillane N, O'Donoghue K. Experience of miscarriage: an interpretative phenomenological analysis. BMJ Open. 2017; 7(3): e011382.
668. Coomarasamy A, Dhillon-Smith RK, Papadopoulou A, Al-Memar M, Brewin J, Abrahams VM, Maheshwari A, Christiansen OB, Stephenson MD, Goddijn M, et al. Recurrent miscarriage: evidence to accelerate action. Lancet. 2021; 397(10285): 1675-82.
669. van Dijk MM, Kolte AM, Limpens J, Kirk E, Quenby S, van Wely M, Goddijn M. Recurrent pregnancy loss: diagnostic workup after two or three pregnancy losses? A systematic review of the literature and meta-analysis. Hum Reprod Update. 2020; 26(3): 356-67.

670. Manning R, Iyer J, Bulmer JN, Maheshwari A, Choudhary M. Are we managing women with Recurrent Miscarriage appropriately? A snapshot survey of clinical practice within the United Kingdom. J Obstet Gynaecol. 2021; 41(5): 807-14.
671. Saccone G, Schoen C, Franasiak JM, Scott RT, Berghella V. Supplementation with progestogens in the first trimester of pregnancy to prevent miscarriage in women with unexplained recurrent miscarriage: a systematic review and meta-analysis of randomized, controlled trials. Fertil Steril. 2017; 107(2): 430-8.
672. de Jong PG, Kaandorp S, Di Nisio M, Goddijn M, Middeldorp S. Aspirin and/or heparin for women with unexplained recurrent miscarriage with or without inherited thrombophilia. Cochrane Database of Systematic Reviews. 2014; 2014(7): CD004734.
673. Hazeldine J, Lord JM. The impact of ageing on natural killer cell function and potential consequences for health in older adults. Ageing Res Rev. 2013; 12(4): 1069-78.
674. Choong ML, Ton SH, Cheong SK. Influence of race, age and sex on the lymphocyte subsets in peripheral blood of healthy Malaysian adults. Annals of Clinical Biochemistry. 1995; 32(Pt 6): 532-9.
675. Haralambieva IH, Salk HM, Lambert ND, Ovsyannikova IG, Kennedy RB, Warner ND, Pankratz VS, Poland GA. Associations between race, sex and immune response variations to rubella vaccination in two independent cohorts. Vaccine. 2014; 32(17): 1946-53.
676. Romeo J, Wärnberg J, Nova E, Díaz LE, Gómez-Martinez S, Marcos A. Moderate alcohol consumption and the immune system: a review. British Journal of Nutrition. 2007; 98(Suppl 1): S111-5.
677. Labrecque N, Cermakian N. Circadian Clocks in the Immune System. J Biol Rhythms. 2015; 30(4): 277-90.
678. Tommy's. Electronic cigarettes and vaping 2020 [Available from: https://www.tommys.org/pregnancy-information/im-pregnant/smoking-and-pregnancy/electronic-cigarettes-and-vaping.
679. Goodier MR, Jonjić S, Riley EM, Juranić Lisnić V. CMV and natural killer cells: shaping the response to vaccination. Eur J Immunol. 2018; 48(1): 50-65.
680. Siewiera J, El Costa H, Tabiasco J, Berrebi A, Cartron G, Le Bouteiller P, Jabrane-Ferrat N. Human cytomegalovirus infection elicits new decidual natural killer cell effector functions. PLoS Pathogens. 2013; 9(4): e1003257.
681. Feyaerts D, van der Meer A, Joosten I, van der Molen RG. Selective Expansion and CMV-dependency in Pregnancy Trained Human Endometrial NK Cells. Cell Mol Immunol. 2019; 16(4): 410-1.
682. Lin X, Chen Y, Fang Z, Chen Q, Chen L, Han Q, Yan J. Effects of cytomegalovirus infection on extravillous trophoblast cells invasion and immune function of NK cells at the maternal-fetal interface. Journal of Cellular and Molecular Medicine. 2020; 24(19): 11170-6.
683. Michel KG, Huijbregts RPH, Gleason JL, Richter HE, Hel Z. Effect of hormonal contraception on the function of plasmacytoid dendritic cells and distribution of immune cell populations in the female reproductive tract. Journal of Acquired Immune Deficiency Syndromes. 2015; 68(5): 511-8.
684. Sinaye Ngcapu S, Lindi Masson L, Sengeziwe Sibeko S, Lise Werner L, Lyle R McKinnon LR, Koleka Mlisana K, Muki Shey M, Natasha Samsunder N, Karim SA, Karim QA, et al. Lower concentrations of chemotactic cytokines and soluble innate factors in the lower female genital tract associated with the use of injectable hormonal contraceptive. J Reprod Immunol. 2015; 110: 14-21.
685. Konstantinus IN, Balle C, Jaumdally SZ, Galmieldien H, Pidwell T, Masson L, Tanko RF, Happel AU, Sinkala M, Myer L, et al. Impact of Hormonal Contraceptives on Cervical T-helper 17 Phenotype and Function in Adolescents: Results from a Randomized, Crossover Study Comparing Long-acting Injectable Norethisterone Oenanthate (NET-EN), Combined Oral Contraceptive Pills, and Combined Contraceptive Vaginal Rings. Clinical Infectious Diseases. 2020; 71(7): e76-e87.
686. Williams WV. Hormonal contraception and the development of autoimmunity: A review of the literature. The Linacre Quarterly. 2017; 84(3): 275-95.
687. Auerbach L, Hafner T, Huber JC, Panzer S. Influence of low-dose oral contraception on peripheral blood lymphocyte subsets at particular phases of the hormonal cycle. Fertil Steril. 2002; 78(1): 83-9.
688. Pascal V, Schleinitz N, Brunet C, Ravet S, Bonnet E, Lafarge X, Touinssi M, Reviron D, Viallard JF, Moreau JF, et al. Comparative analysis of NK cell subset distribution in normal and lymphoproliferative disease of granular lymphocyte conditions. Eur J Immunol. 2004; 34(10): 2930-40.

689. Schlums H, Cichocki F, Tesi B, Theorell J, Beziat V, Holmes TD, Han H, Chiang SCC, Foley B, Mattsson K, et al. Cytomegalovirus Infection Drives Adaptive Epigenetic Diversification of NK Cells With Altered Signaling and Effector Function. Immunity. 2015; 42(3): 443-56.
690. Liang Q, Tong L, Xiang L, Shen S, Pan C, Liu C, Zhang H. Distinct changes of in BTLA, ICOS, PD-1, and TIGIT expression on peripheral blood and decidual CD8+ T cells in women with unexplained recurrent spontaneous abortion. Biol Reprod. 2020; 103(5): 1012-7.
691. Mahmoud F, Diejomaoh M, Omu A, Abul H, Haines D. Effect of IgG therapy on lymphocyte subpopulations in the peripheral blood of Kuwaiti women experiencing recurrent pregnancy loss. Gynecol Obstet Invest. 2004; 58(2): 77-83.
692. Tang R, Rangachari M, Kuchroo VK. Tim-3: A co-receptor with diverse roles in T cell exhaustion and tolerance. Semin Immunol. 2019; 42: 101302.
693. Dunham RM, Cervasi B, Brenchley JM, Albrecht H, Weintrob A, Sumpter B, Engram J, Gordon S, Klatt NR, Frank I, et al. CD127 and CD25 expression defines CD4+ T cell subsets that are differentially depleted during HIV infection. The Journal of Immunology. 2008; 180(8): 5582-92.
694. Kmieciak M, Gowda M, Graham L, Godder K, Bear HD, Marincola FM, Manjili MH. Human T cells express CD25 and Foxp3 upon activation and exhibit effector/memory phenotypes without any regulatory/suppressor function. Journal of Translational Medicine. 2009; 7: 89.
695. Fuhrman CA, Yeh WI, Seay HR, Saikumar Lakshmi P, Chopra G, Zhang L, Perry DJ, McClymont SA, Yadav M, Lopez MC, et al. Divergent Phenotypes of Human Regulatory T Cells Expressing the Receptors TIGIT and CD226. The Journal of Immunology. 2015; 195(1): 145-55.
696. Francisco LM, Salinas VH, Brown KE, Vanguri VK, Freeman GJ, Kuchroo VK, Sharpe AH. PD-L1 regulates the development, maintenance, and function of induced regulatory T cells. J Exp Med. 2009; 206(13): 3015-29.
697. Cai J, Wang D, Zhang G, Guo X. The Role Of PD-1/PD-L1 Axis In Treg Development And Function: Implications For Cancer Immunotherapy. OncoTargets and Therapy. 2019; 12: 8437-45.
698. Huang Z, Qi G, Miller JS, Zheng SG. CD226: An Emerging Role in Immunologic Diseases. Frontiers in Cell and Developmental Biology. 2020; 8: 564.
699. Shibuya K, Shirakawa J, Kameyama T, Honda SI, Tahara-Hanaoka S, Miyamoto A, Onodera M, Sumida T, Nakauchi H, Miyoshi H, et al. CD226 (DNAM-1) is involved in lymphocyte function-associated antigen 1 costimulatory signal for naive T cell differentiation and proliferation. J Exp Med. 2003; 198(12): 1829-39.
700. Iwata Y, Matsushita T, Horikawa M, Dilillo DJ, Yanaba K, Venturi GM, Szabolcs PM, Bernstein SH, Magro CM, Williams AD, et al. Characterization of a rare IL-10-competent B-cell subset in humans that parallels mouse regulatory B10 cells. Blood. 2011; 117(2): 530-41.
701. Morandi F, Horenstein AL, Costa F, Giuliani N, Pistoia V, Malavasi F. CD38: A Target for Immunotherapeutic Approaches in Multiple Myeloma. Front Immunol. 2018; 9: 2722.
702. Bona CA, Bonilla FA. Textbook of Immunology. Second ed. Boca Raton, Florida: CRC Press; 2019. 300 p.
703. Brisslert M, Bokarewa M, Larsson P, Wing K, Collins LV, Tarkowski A. Phenotypic and functional characterization of human CD25+ B cells. Immunology. 2006; 117(4): 548-57.
704. Amu S, Tarkowski A, Dörner T, Bokarewa M, Brisslert M. The human immunomodulatory CD25+ B cell population belongs to the memory B cell pool. Scand J Immunol. 2007; 66(1): 77-86.
705. Zhao J, Lei Z, Liu Y, Li B, Zhang L, Fang H, Song C, Wang X, Zhang GM, Feng ZH, et al. Human pregnancy up-regulates Tim-3 in innate immune cells for systemic immunity. The Journal of Immunology. 2009; 182(10): 6618-24.
706. Zahran AM, Hetta HF, Rayan A, Eldin AS, Hassan EA, Fakhry H, Soliman A, El-Badawy O. Differential expression of Tim-3, PD-1, and CCR5 on peripheral T and B lymphocytes in hepatitis C virus-related hepatocellular carcinoma and their impact on treatment outcomes. Cancer Immunology, Immunotherapy. 2020; 69(7): 1253-63.
707. Mahmudul Hasan M, Wang Y, Blaji U, Gu J, Nattamai D, Nyarige V, Thompson-Snipes L, Klintmalm GB, O'Leary JG, Wang J, et al. Critical roles of TIGIT+ human regulatory B cells in the suppression of antibody-mediated allograft rejection. The Journal of Immunology. 2020; 204(1): 87-110.
708. Thibult ML, Mamessier E, Gertner-Dardenne J, Pastor S, Just-Landi S, Xerri L, Chetaille B, Olive D. PD-1 is a novel regulator of human B-cell activation. Int Immunol. 2013; 25(2): 129-37.
709. Toth B, Vomstein K, Togawa R, Böttcher B, Hudalla H, Strowitzki T, Daniel V, Kuon RJ. The impact of previous live births on peripheral and uterine natural killer cells in patients with recurrent miscarriage. Reproductive Biology and Endocrinology. 2019; 17: 72.

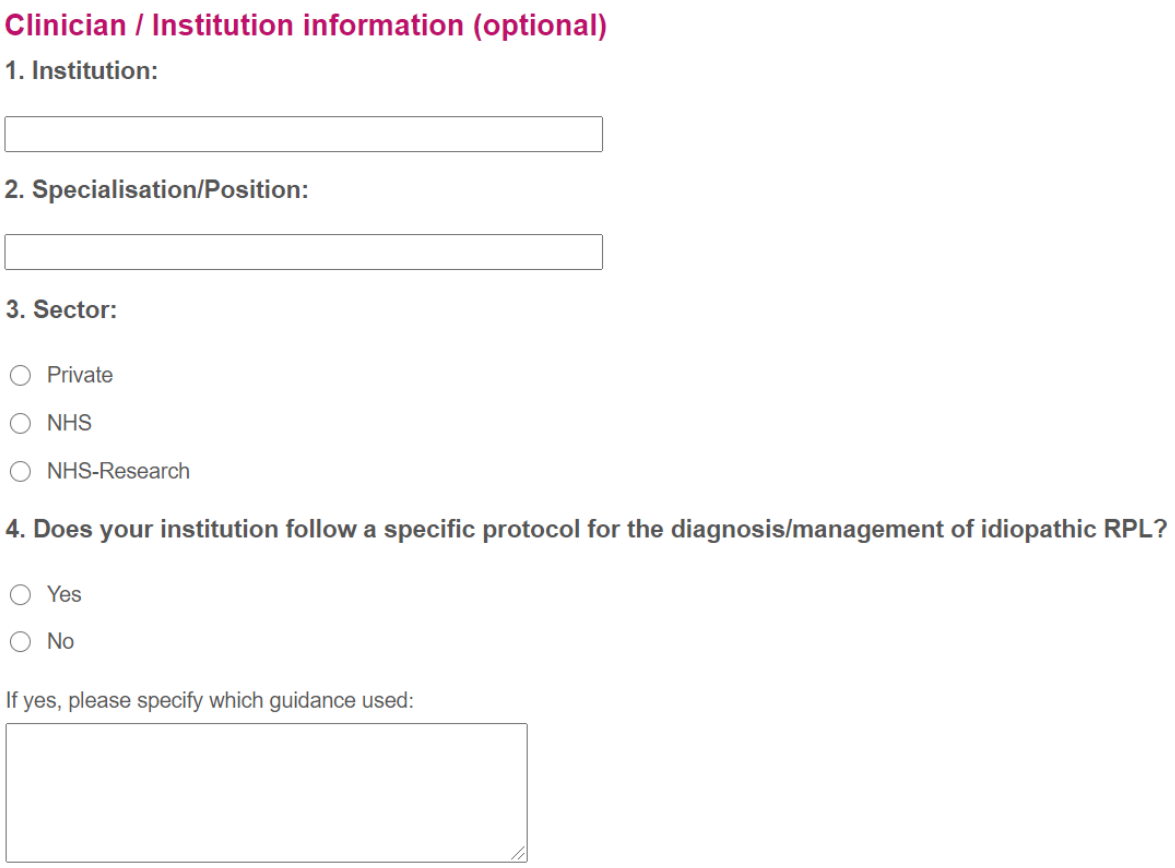
710. Kuon RJ, Vomstein K, Weber M, Müller F, Seitz C, Wallwiener S, Strowitzki T, Schleussner E, Markert UR, Daniel V, et al. The "killer cell story" in recurrent miscarriage: Association between activated peripheral lymphocytes and uterine natural killer cells. J Reprod Immunol. 2017; 119: 9-14.
711. Gounder SS, Basri Johan Jeet Abdullah BJJ, Radzuanb NEIBM, Zain FDBM, Sait NBM, Chua C, Subramani B. Effect of Aging on NK Cell Population and Their Proliferation at Ex Vivo Culture Condition. Anal Cell Pathol. 2018; 2018: 7871814.
712. Haynes L, Maue AC. Effects of aging on T cell function. Curr Opin Immunol. 2009; 21(4): 414-7.
713. Tollerud DJ, Brown LM, Blattner WA, Hoover RN. The Influence of Race on T-Cell Subset Distributions. Berlin, Heidelberg: Springer; 1991.
714. Cooper S, Laird SM, Mariee N, Li TC, Metwally M. The effect of prednisolone on endometrial uterine NK cell concentrations and pregnancy outcome in women with reproductive failure. A retrospective cohort study. J Reprod Immunol. 2019; 131: 1-6.
715. Chowdhury D, Lieberman J. Death by a thousand cuts: granzyme pathways of programmed cell death. Annu Rev Immunol. 2008; 26: 389-420.
716. Mikkelsen AP, Egerup P, Ebert JFM, Kolte AM, Nielsen HS, Lidegaarda Ø. Pregnancy Loss and Cancer Risk: A Nationwide Observational Study. EClinicalMedicine. 2019; 15: 80–8.
717. Zanoni I, Spreafico R, Bodio C, Di Gioia M, Cigni C, Broggi A, Gorletta T, Caccia M, Chirico G, Sironi L, et al. IL-15 cis presentation is required for optimal NK cell activation in lipopolysaccharide-mediated inflammatory conditions. Cell Rep. 2013; 4(6): 1235-49.
718. Rudnicka K, Matusiak A, Chmiela M. CD25 (IL-2R) expression correlates with the target cell induced cytotoxic activity and cytokine secretion in human natural killer cells. Acta Biochim Pol. 2015; 62(4): 885-94.
719. Skak K, Frederiksen KS, Lundsgaard D. Interleukin-21 activates human natural killer cells and modulates their surface receptor expression. Immunology. 2008; 123(4): 575-83.
720. Fu B, Tian Z, Wei H. Subsets of human natural killer cells and their regulatory effects. Immunology. 2014; 141(4): 483-9.
721. Seay K, Church C, Zheng JH, Deneroff K, Ochsenbauer C, Kappes JC, Liu B, Jeng EK, Wong HC, Goldstein H. In Vivo Activation of Human NK Cells by Treatment with an Interleukin-15 Superagonist Potently Inhibits Acute In Vivo HIV-1 Infection in Humanized Mice. J Virol. 2015; 89(12): 6264-74.
722. Castillo EF, Schluns KS. Regulating the immune system via IL-15 transpresentation. Cytokine. 2012; 59(3): 479-90.
723. Varla-Leftherioti M, Spyropoulou-Vlachou M, Niokou D, Keramitsoglou T, Darlamitsou A, Tsekoura C, Papadimitropoulos M, Lepage V, Balafoutas C, Stavropoulos-Giokas C. Natural killer (NK) cell receptors' repertoire in couples with recurrent spontaneous abortions. Am J Reprod Immunol. 2003; 49(3): 183-91.
724. Goruroglu Ozturk O, Sahın G, Karacor ED, Kucukgoz U. Evaluation of KIR genes in recurrent miscarriage. J Assist Reprod Genet. 2012; 29(9): 933-8.
725. Ntrivalas EI, Bowser CR, Kwak-Kim J, Beaman KD, Gilman-Sachs A. Expression of killer immunoglobulin-like receptors on peripheral blood NK cell subsets of women with recurrent spontaneous abortions or implantation failures. Am J Reprod Immunol. 2005; 53(5): 215-21.
726. Fukui A, Ntrivalas E, Fukuhara R, Fujii S, Mizunuma H, Gilman-Sachs A, Beaman K, Kwak-Kim J. Correlation between natural cytotoxicity receptors and intracellular cytokine expression of peripheral blood NK cells in women with recurrent pregnancy losses and implantation failures. Am J Reprod Immunol. 2009; 62(6): 371-80.
727. Bottino C, Castriconi R, Pende D, Rivera P, Nanni M, Carnemolla B, Cantoni C, Grassi J, Marcenaro S, Reymond N, et al. Identification of PVR (CD155) and Nectin-2 (CD112) as cell surface ligands for the human DNAM-1 (CD226) activating molecule. J Exp Med. 2003; 198(4): 557-67.
728. Stannard KA, Lemoine S, Waterhouse NJ, Vari F, Chatenoud L, Gandhi MK, Martinet L, Smyth MJ, Guillerey C. Human peripheral blood DNAM-1neg NK cells are a terminally differentiated subset with limited effector functions. Blood Advances. 2019; 3(11): 1681–94.
729. Ishiyama T, Watanabe K, Fukuchi K, Yajima K, Koike M, Tomoyasu S, Tsuruoka N. The presence of CD5LOW+NK cells in normal controls and patients with pulmonary tuberculosis. Immunology Letters. 1993; 37(2-3): 139-44.
730. Ishiyama T, Watanabe K, Fukuchi K, Yajima K, Koike M, Tomoyasu S, Tsuruoka N. The increase of CD5LOW+NK cells in patients with multiple myeloma and plasmacytoma. Anticancer Research. 1994; 14(2B): 725-30.

731. Bernstein HB, Plasterer MC, Schiff SE, Kitchen CMR, Kitchen S, Zack JA. CD4 expression on activated NK cells: ligation of CD4 induces cytokine expression and cell migration. The Journal of Immunology. 2006; 177(6): 3669-76.
732. Abel AM, Yang C, Thakar MS, Malarkannan S. Natural Killer Cells: Development, Maturation, and Clinical Utilization. Front Immunol. 2018; 9: 1869.
733. Terry LA, DiSanto JP, Small TN, Flomenberg N. Differential expression and regulation of the human CD8 alpha and CD8 beta chains. Tissue Antigens. 1990; 35(2): 82-91.
734. Moebius U, Kober G, Griscelli AL, Hercend T, Meuer SC. Expression of different CD8 isoforms on distinct human lymphocyte subpopulations. Eur J Immunol. 1991; 21(8): 1793-800.
735. Addison EG, North J, Bakhsh I, Marden C, Haq S, Al-Sarraj S, Malayeri R, Wickremasinghe RG, Davies JK, Lowdell MW. Ligation of CD8alpha on human natural killer cells prevents activation-induced apoptosis and enhances cytolytic activity. Immunology. 2005; 116(3): 354-61.
736. Srour EF, Leemhuis T, Jenski L, Redmond R, Jansen J. Cytolytic activity of human natural killer cell subpopulations isolated by four-color immunofluorescence flow cytometric cell sorting. Cytometry. 1990; 11(3): 442-6.
737. Geng J, Raghavan M. CD8αα homodimers function as a coreceptor for KIR3DL1. Proc Natl Acad Sci U S A. 2019; 116(36): 17951-6.
738. Contini P, Ghio M, Poggi A, Filaci G, Indiveri F, Ferrone S, Puppo F. Soluble HLA-A,-B,-C and -G molecules induce apoptosis in T and NK CD8+ cells and inhibit cytotoxic T cell activity through CD8 ligation. Eur J Immunol. 2003; 33(1): 125-34.
739. Hanna J, Mandelboim O. When killers become helpers. Trends Immunol. 2007; 28(5): 201-6.
740. Romagnani P, Lasagni L, Annunziato F, Serio M, Romagnani S. CXC chemokines: the regulatory link between inflammation and angiogenesis. Trends Immunol. 2004; 25(4): 201-9.
741. Horowitz A, Strauss-Albee DM, Leipold M, Kubo J, Nemat-Gorgani N, Dogan OC, Dekker CL, Mackey S, Maecker H, Swan GE, et al. Genetic and environmental determinants of human NK cell diversity revealed by mass cytometry. Sci Transl Med. 2013; 5(208): 208ra145.
742. Ebina Y, Nishino Y, Deguchi M, Maesawa Y, Nakashima Y, Yamada H. Natural killer cell activity in women with recurrent miscarriage: Etiology and pregnancy outcome. J Reprod Immunol. 2017; 120: 42-7.
743. Lee SK, Kim JY, Hur SE, Kim CJ, Na BJ, Lee M, Gilman-Sachs A, Kwak-Kim J. An imbalance in interleukin-17-producing T and Foxp3^{+} regulatory T cells in women with idiopathic recurrent pregnancy loss. Hum Reprod. 2011; 26(11): 2964-71.
744. Saifi B, Rezaee SA, Tajik N, Ahmadpour ME, Ashrafi M, Vakili R, SoleimaniAsl S, Aflatoonian R, Mehdizadeh M. Th17 cells and related cytokines in unexplained recurrent spontaneous miscarriage at the implantation window. Reprod Biomed Online. 2014; 29(4): 481-9.
745. Rea IM, Gibson DS, McGilligan V, McNerlan SE, Alexander HD, Ross OA. Age and Age-Related Diseases: Role of Inflammation Triggers and Cytokines. Front Immunol. 2018; 9: 586.
746. Wilson R, Jenkins C, Miller H, McInnes IB, Moore J, McLean MA, Walker JJ. Abnormal cytokine levels in non-pregnant women with a history of recurrent miscarriage. Eur J Obstet Gynecol Reprod Biol. 2004; 115(1): 51-4.
747. Romera-Cárdenas G, Thomas LM, Lopez-Cobo S, García-Cuesta EM, Long EO, Reyburn HT. Ionomycin Treatment Renders NK Cells Hyporesponsive. PLoS One. 2016; 11(3): e0150998.
748. Peruzzi G, Femnou L, Gil-Krzewska A, Borrego F, Weck J, Krzewski K, Coligan JE. Membrane-type 6 matrix metalloproteinase regulates the activation-induced downmodulation of CD16 in human primary NK cells. The Journal of Immunology. 2013; 191(4): 1883-94.
749. Dunne J, Lynch S, O'Farrelly C, Todryk S, Hegarty JE, Feighery C, Doherty DG. Selective expansion and partial activation of human NK cells and NK receptor-positive T cells by IL-2 and IL-15. The Journal of Immunology. 2001; 167(6): 3129-38.
750. Stegmann KA, Robertson F, Hansi N, Gill U, Pallant C, Christophides T, Pallett LJ, Peppa D, Dunn C, Fusai G, et al. CXCR6 Marks a Novel Subset of T-bet^{lo}Eomes^{hi} Natural Killer Cells Residing in Human Liver Sci Rep. 2016; 6: 26157.
751. Sakuishi K, Apetoh L, Sullivan JM, Blazar BR, Kuchroo VK, Anderson AC. Targeting Tim-3 and PD-1 pathways to reverse T cell exhaustion and restore anti-tumor immunity. J Exp Med. 2010; 207(10): 2187-94.
752. Gilman-Sachs A, DuChateau BK, Aslakson CJ, Wohlgemuth GP, Kwak JY, Beer AE, Beaman KD. Natural killer (NK) cell subsets and NK cell cytotoxicity in women with histories of recurrent spontaneous abortions. Am J Reprod Immunol. 1999; 41(1): 99-105.

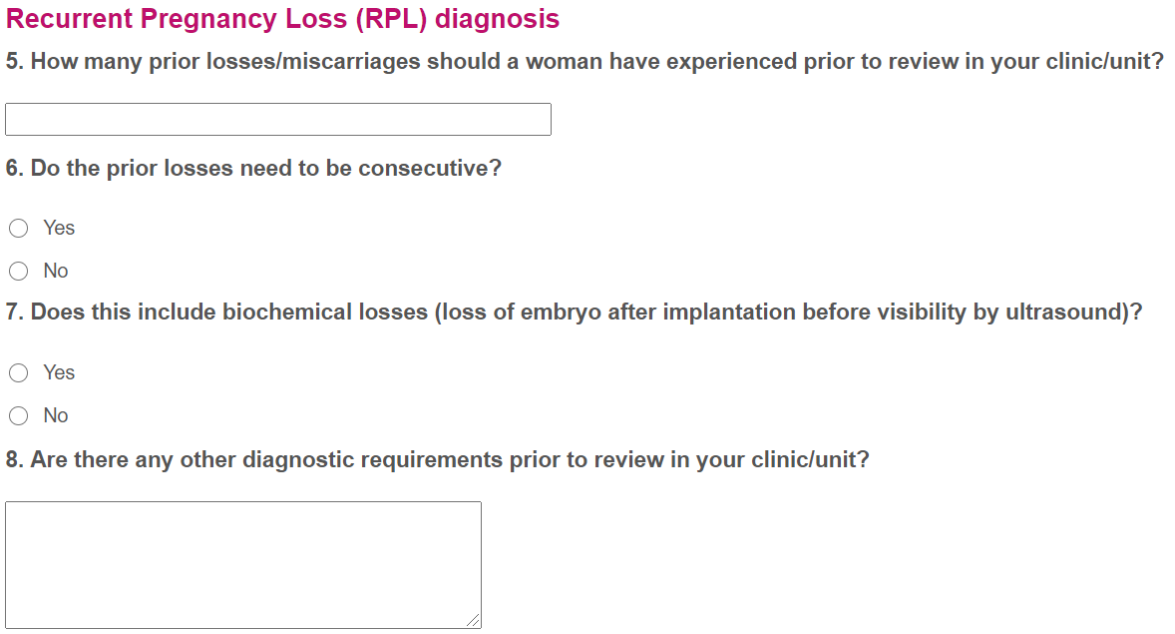
753. Pongcharoen S, Niumsup P, Sanguansermsri D, Supalap K, Butkhamchot P. The effect of interleukin-17 on the proliferation and invasion of JEG-3 human choriocarcinoma cells. Am J Reprod Immunol. 2006; 55(4): 291-300.
754. Wu HX, Jin LP, Xu B, Liang SS, Li DJ. Decidual stromal cells recruit Th17 cells into decidua to promote proliferation and invasion of human trophoblast cells by secreting IL-17. Cell Mol Immunol. 2014; 11(3): 253-62.
755. Jovanović M, Stefanoska I, Radojcić L, Vićovac L. Interleukin-8 (CXCL8) stimulates trophoblast cell migration and invasion by increasing levels of matrix metalloproteinase (MMP)2 and MMP9 and integrins alpha5 and beta1. Reproduction. 2010; 139(4): 789-98.
756. Mei HE, Leipold MD, Maecker HT. Platinum-conjugated antibodies for application in mass cytometry. Cytometry A. 2016; 89(3): 292-300.
757. Chao KH, Yang YS, Ho HN, Chen SU, Chen HF, Dai HJ, Huang SC, Gill TJr. Decidual natural killer cytotoxicity decreased in normal pregnancy but not in anembryonic pregnancy and recurrent spontaneous abortion. Am J Reprod Immunol. 1995; 34(5): 274-80.
758. Mao B, Huang S, Lu X, Sun W, Zhou Y, Pan X, Yu J, Lai M, Chen B, Zhou Q, et al. Early Development of Definitive Erythroblasts from Human Pluripotent Stem Cells Defined by Expression of Glycophorin A/CD235a, CD34, and CD36. Stem Cell Reports. 2016; 7(5): 869-83.
759. Samsel L, McCoy JPJ. Imaging flow cytometry for the study of erythroid cell biology and pathology. J Immunol Methods. 2015; 423: 52-9.
760. Zamai L, Mariani AR, Zauli G, Rodella L, Rezzani R, Manzoli FA, Vitale M. Kinetics of in vitro natural killer activity against K562 cells as detected by flow cytometry. 1998; 32(4): 280-5.
761. Hara N, Fujii T, Okai T, Taketani Y. Histochemical demonstration of interleukin-2 in decidua cells of patients with preeclampsia. Am J Reprod Immunol. 1995; 34(1): 44-51.

13 APPENDICES

13.1 Questionnaire designed and distributed to explore current practice for the diagnosis and management of idiopathic RPL



Supplementary Figure 1. Questions 1-4 of questionnaire distributed through SmartSurvey™ to recurrent pregnancy loss (RPL) clinics nationwide. *Questions included on this page were focused on obtaining information on the clinicians completing their survey and the institution in which the clinics belong to.*



Supplementary Figure 2. Questions 5-8 of questionnaire distributed through SmartSurvey™ to recurrent pregnancy loss (RPL) clinics nationwide. *Questions on this page were designed to collect information in regards to the criteria used to diagnose RPL and thus recruit women in RPL clinics.*

Idiopathic RPL definition

9. Which of the following tests are offered in your unit/clinic to investigate an underlying anatomical cause of RPL?

	Routinely	When clinically indicated
Pelvic ultrasonography	☐	☐
Hysteroscopy	☐	☐
Hysterosalpingography (HSG)	☐	☐
None	☐	☐

Other (please specify)

10. Which of the following tests are offered in your unit/clinic to investigate an underlying Hypothalamic-pituitary-adrenal axis-associated cause of RPL?

	Routinely	When clinically indicated
Progesterone	☐	☐
Luteinizing hormone (LH)	☐	☐
Prolactin	☐	☐
Follicle-stimulating hormone (FSH)	☐	☐
Anti-Müllerian hormone (AMH)	☐	☐
Oestrogen	☐	☐
Testosterone	☐	☐
Free androgen index	☐	☐
Sex hormone binding globulin (SHBG)	☐	☐
Inhibin B	☐	☐
None	☐	☐

Other (please specify)

11. Which of the following tests are offered in your unit/clinic to investigate an underlying genetic/chromosomal cause of RPL?

	Routinely	When clinically indicated
Maternal karyotyping	☐	☐
Paternal karyotyping	☐	☐
Foetal karyotyping	☐	☐
None	☐	☐

Other (please specify)

Supplementary Figure 3. Questions 9-11 of questionnaire distributed through SmartSurvey™ to recurrent pregnancy loss (RPL) clinics nationwide. *Questions on this page were designed to collect information in regards to the tests performed to identify anatomical, hypothalamic-pituitary-adrenal axis-associated, and genetic/chromosomal RPL risk factors.*

Idiopathic RPL definition

12. Which of the following tests are offered in your unit/clinic to investigate haematological RPL causes?

	Routinely	When clinically indicated
Anti-β glycoprotein antibodies	☐	☐
Anti-cardiolipin antibodies	☐	☐
Lupus anticoagulant	☐	☐
Antiphosphatidic acid	☐	☐
Antiphosphatidyl serine	☐	☐
Antiphosphatidyl ethanolamine	☐	☐
Antiphosphatidyl choline	☐	☐
Antiphosphatidyl glycerol	☐	☐
Antiphosphatidyl inositol	☐	☐
Prothrombin Time (PT)	☐	☐
Activated Partial Thromboplastin Time (aPTT)	☐	☐
Activated protein C resistance	☐	☐
Protein C deficiency	☐	☐
Protein S deficiency	☐	☐
Factor V Leiden	☐	☐
Antithrombin (III) deficiency	☐	☐
MTHFR Gene Mutation	☐	☐
Prothrombin gene mutation	☐	☐
None	☐	☐

Other (please specify)

Supplementary Figure 4. Question 12 of questionnaire distributed through SmartSurvey™ to recurrent pregnancy loss (RPL) clinics nationwide. *The question on this page was generated to obtain information on the tests performed to identify haematological RPL risk factors.*



Idiopathic RPL definition

13. Which of the following tests are offered in your unit/clinic to investigate thyroid-associated RPL causes?

	Routinely	When clinically indicated
Anti-thyroid peroxidase (anti-TPO) antibodies	☐	☐
Anti-thyroglobulin (anti-Tg) antibodies	☐	☐
T3	☐	☐
T4	☐	☐
TSH	☐	☐
None	☐	☐

Other (please specify)

14. Which of the following tests are offered in your unit/clinic to investigate diabetes-associated causes of RPL?

	Routinely	When clinically indicated
Random venous glucose	☐	☐
Glycated haemoglobin (HbA1c)	☐	☐
None	☐	☐

Other (please specify)

15. Which of the following tests are offered in your unit/clinic to investigate infection-associated causes of RPL?

	Routinely	When clinically indicated
Low vaginal microbiology swab	☐	☐
High vaginal swab (endocervical)	☐	☐
High vaginal swab (ectocervical)	☐	☐
None	☐	☐

Other (please specify)

16. Which other tests are performed in your unit/clinic to investigate RPL causes?

	Routinely	When clinically indicated
Anti-nuclear antibodies (ANA) (e.g. anti-DNA, anti-histone, anti-Sm, anti-ribonucleoprotein, anti-Jo, anti-Scl, anti-SSA/Ro, anti-SSB/La)	☐	☐
Anti-smooth muscle antibodies	☐	☐
Anti-sperm antibodies (maternal)	☐	☐
Anti-sperm antibodies (paternal)	☐	☐
Sperm DNA fragmentation	☐	☐
Vitamin D (25OHD3) levels	☐	☐
Homocysteine levels	☐	☐
None	☐	☐

Other (please specify)

Supplementary Figure 5. Questions 13-16 of questionnaire distributed through SmartSurvey™ to recurrent pregnancy loss (RPL) clinics nationwide. *Questions on this page were designed to collect information on the tests performed to identify thyroid-associated, diabetes-associated, infection-associated, and other known RPL risk factors.*

Immunological testing in RPL

17. Is further immunological testing offered in your unit/clinic? *

- ○ Yes
- ○ No

18. If yes, which immunological tests are offered in your unit/clinic?

	Routinely	When clinically indicated
Natural Killer (NK), T, and B cell immunophenotyping	☐	☐
Assessment of Natural Killer (NK) cell cytotoxicity	☐	☐
Helper CD4(+) (Th) and cytotoxic CD8(+) (Tc) T cell immunophenotyping	☐	☐
Regulatory T cell (Treg) immunophenotyping	☐	☐
Examination of T helper (Th) cell cytokine production	☐	☐
CD5(+) (B-1) and CD5(-) (B-2) B cell immunophenotyping	☐	☐
Anti-HLA antibody screening	☐	☐
Anti-HY antibody screening	☐	☐
Anti-paternal blocking antibody screening	☐	☐
Human Leukocyte Antigen (HLA)-typing (DQα sharing)	☐	☐
None	☐	☐

Other (please specify)

19. Does your unit/clinic offer any endometrial immunological tests?

- ○ Yes
- ○ No

If yes, which ones?

Supplementary Figure 6. Questions 17-19 of questionnaire distributed through SmartSurvey™ to recurrent pregnancy loss (RPL) clinics nationwide. *Questions on this page were created to collect information in regards to the use of immunological tests in RPL clinics.*

Recurrent Pregnancy Loss (RPL) management

20. Which of the following treatments may be offered in your unit/clinic to women with idiopathic/immunological RPL?

	Offered
Aspirin	☐
Prednisone	☐
Prednisolone	☐
Progesterone	☐
Human chorionic gonadotrophin (hCG)	☐
Anti-Tumour Necrosis Factor (TNF)-α agents	☐
Granulocyte-colony stimulating factor (G-CSF)	☐
Hydroxychloroquine	☐
Heparin	☐
Intravenous immunoglobulin (IVIg)	☐
Paternal cell immunization	☐
Third-party donor leukocyte immunization	☐
Trophoblast membrane infusion	☐
Intralipid infusion	☐
Endometrial scratching	☐
Folic acid	☐
Vitamin D supplementation	☐
Multivitamin supplementation	☐
Psychotherapy	☐
Supportive care	☐
Lifestyle changes (e.g. in case of obesity, high alcohol intake, illicit drug use, smoking)	☐
None	☐

Other (please specify)

21. If appropriate please give some additional information about the treatment dose and timing (prior to or during pregnancy):

Supplementary Figure 7. Questions 20-21 of questionnaire distributed through SmartSurvey™ to recurrent pregnancy loss (RPL) clinics nationwide. *Questions on this page were created to collect information in regards to the treatments used for the management of idiopathic RPL.*

Treatment outcome

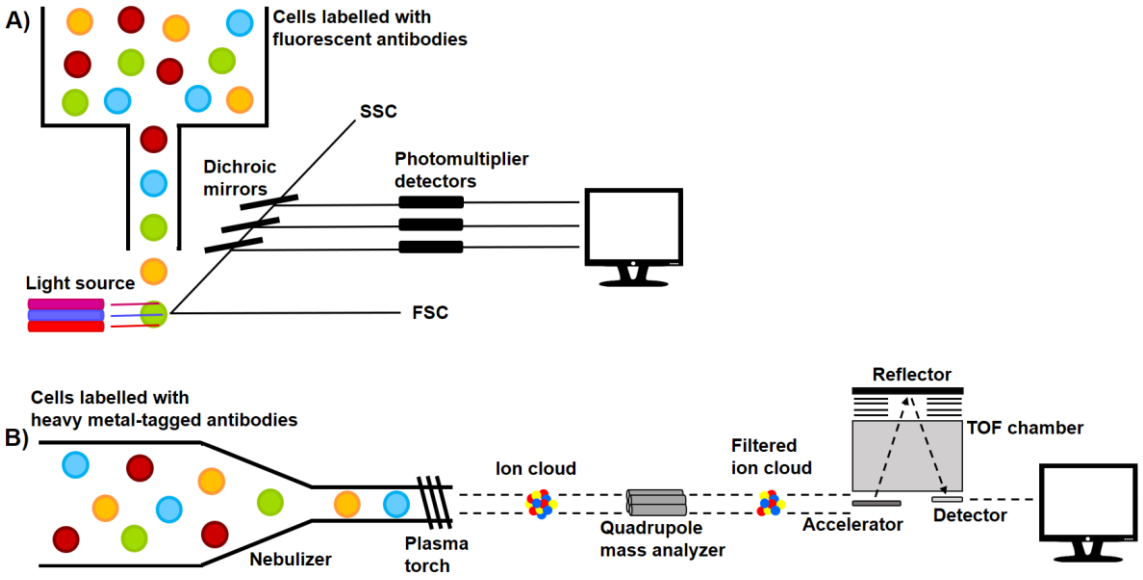
22. Finally, if possible please provide your perspective in the following treatments used (how effective they were / how likely it is that you would suggest it as an option to idiopthic RPL patients?).

	Very effective / Would definitely suggest	Often effective / Would probably suggest	Somewhat effective / Could suggest depending on the case	Rarely effective / Would probably not suggest	Not effective / Would not suggest
Aspirin	○	○	○	○	○
Other non-steroidal anti-inflammatory drugs	○	○	○	○	○
Prednisone	○	○	○	○	○
Prednisolone	○	○	○	○	○
Other steroids	○	○	○	○	○
Progesterone	○	○	○	○	○
Human chorionic gonadotrophin (hCG)	○	○	○	○	○
Other hormonal treatment	○	○	○	○	○
Anti-Tumour Necrosis Factor (TNF)-α agents	○	○	○	○	○
Granulocyte-colony stimulating factor (G-CSF)	○	○	○	○	○
Hydroxychloroquine	○	○	○	○	○
Heparin	○	○	○	○	○
Intravenous immunoglobulin (IVIg)	○	○	○	○	○
Paternal cell immunization	○	○	○	○	○
Third-party donor leukocyte immunization	○	○	○	○	○
Trophoblast membrane infusion	○	○	○	○	○
Intralipid infusion	○	○	○	○	○
Endometrial scratching	○	○	○	○	○
Folic acid	○	○	○	○	○
Vitamin D supplementation	○	○	○	○	○
Multivitamin supplementation	○	○	○	○	○

Supplementary Figure 8. Question 22 of questionnaire distributed through SmartSurvey™ to recurrent pregnancy loss (RPL) clinics nationwide. *The question on this page was design to collect information on the responders' opinion in regards to the effectiveness of the different treatments for idiopathic RPL and thus the likelihood to suggest them to women with this condition.*

13.2 Flow and mass cytometry

Both flow and mass cytometry were utilised for the phenotypic assessment of peripheral blood lymphocytes in women with RPL. Flow-based assays are widely applied and are utilised in certain clinics as part of RPL investigations. Such assays are however limited by fluorescent signal overlap, restricting the number of parameters simultaneously examined (Supplementary Figure 9A). On the other hand, the mass cytometry assay allows the concurrent investigation of a higher number of markers as the use of stable heavy metals results in little signal overlap (Supplementary Figure 9B). Thus, the flow cytometry assay was employed as an easily accessible potential clinical test assessing the major peripheral lymphocyte populations and subpopulations in women with RPL, while the mass cytometry assay was utilised as an exploratory test focused on the detailed investigation of NK cell phenotype.



Supplementary Figure 9. Basic principles of the flow and mass cytometry techniques utilised. *A) During cell examination by flow cytometry, fluorescently stained cells pass through a light source. In the BD FACSCanto™ II cell analyzer (BD Biosciences) the light source consists of three excitation lasers, a violet, a blue, and a red, which produce light beams at 405nm, 488nm, and 633nm respectively. The resulting forward scatter (FSC) signal measures light parallel to the laser beam, indicating cell size, while the side scatter (SSC) measures diffraction of light at a 90^{o} angle from the beam, indicating structural complexity and granularity of the cell. Dichroic mirrors partition light and direct certain wavelengths to the appropriate detector. The photomultiplier detectors amplify the signal, enabling the detection and quantification of emitted light of different wavelengths. Signals are converted to a digital readout and are analysed. This set-up allows the simultaneous assessment of 8 colours and thus the examination of ≤8 parameters on each cell. B) During mass cytometry, cells labelled with heavy metals pass through a nebulizer, creating aerosol, and a plasma torch, vaporizing cells and generating an ion cloud. Low mass ions, such as biological molecules and environmental contaminants, are removed by a quadrupole mass analyser. The filtered heavy ions are accelerated and enter a time-of-flight (TOF) chamber, being separated according to their mass-to-charge ratio and reflected towards a detector. The detector measures a mass spectrum, representing each isotope's identity and quantity. This Helios Cytometry by Time-Of-Flight (Fluidigm) set-up allows the simultaneous investigation of >40 parameters on each cell.*

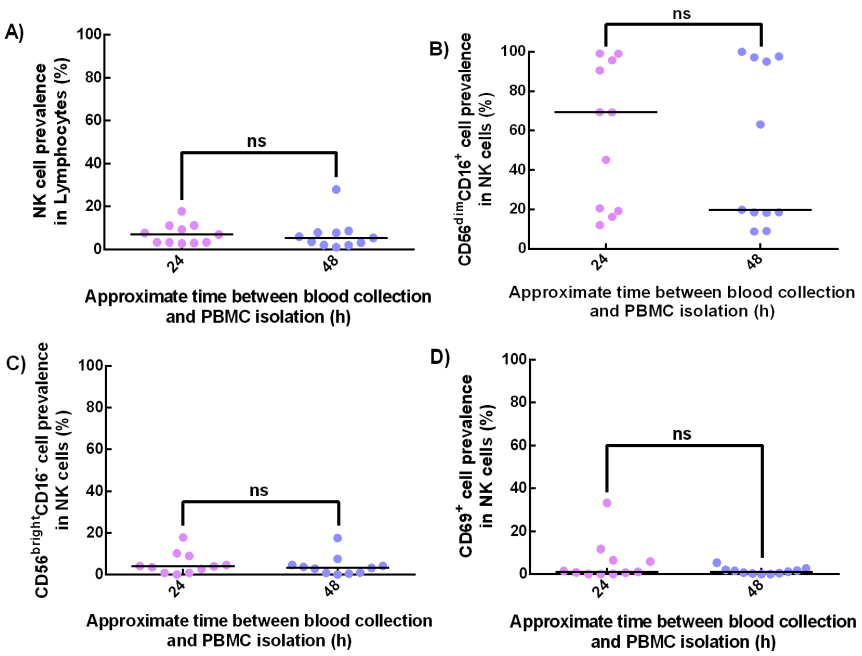
13.3 Flow cytometer set-up and quality control

The BD FACSCanto™ II cell analyzer (BD Biosciences), used for the TBNK, flow, and cytotoxicity assays was calibrated daily and the quality of runs was closely monitored by Mr Steven Dix, Ms Genevieve Panaro, and Ms Kamila Silverio Fernadez. On a daily basis 7-color setup beads (BD Biosciences) were used to achieve the target median fluorescence intensity for each detector, optimize detector sensitivity, and calculate compensation. A mixture of 4μm and 6μm beads, labelled with one fluorophore each or unlabelled, were included in tubes in the form of a lyophilized pellet. The pellet was rehydrated immediately prior to use with BD FACS setup bead diluent and vortexed. The manufacturer-defined target mean fluorescence intensity and spectral overlap values were input and the voltages were automatically adjusted by the BD FACSCanto™ Software (BD Biosciences) in order to achieve the optimal mean fluorescent intensity for each detector. Compensation values were also calculated by the software based on the spectral overlap values. Furthermore, quality control was performed using the CD-Chex Plus® material (Streck), consisting of normal human erythrocytes and peripheral blood leukocytes. The controls provided were used with each daily run to ensure that target ranges for the $CD3^+$, $CD4^+$, and $CD8^+$ T cell, $CD19^+$ B cell, and $CD3^-CD56/CD16^+$ NK cell populations were met, allowing detection of systematic errors.

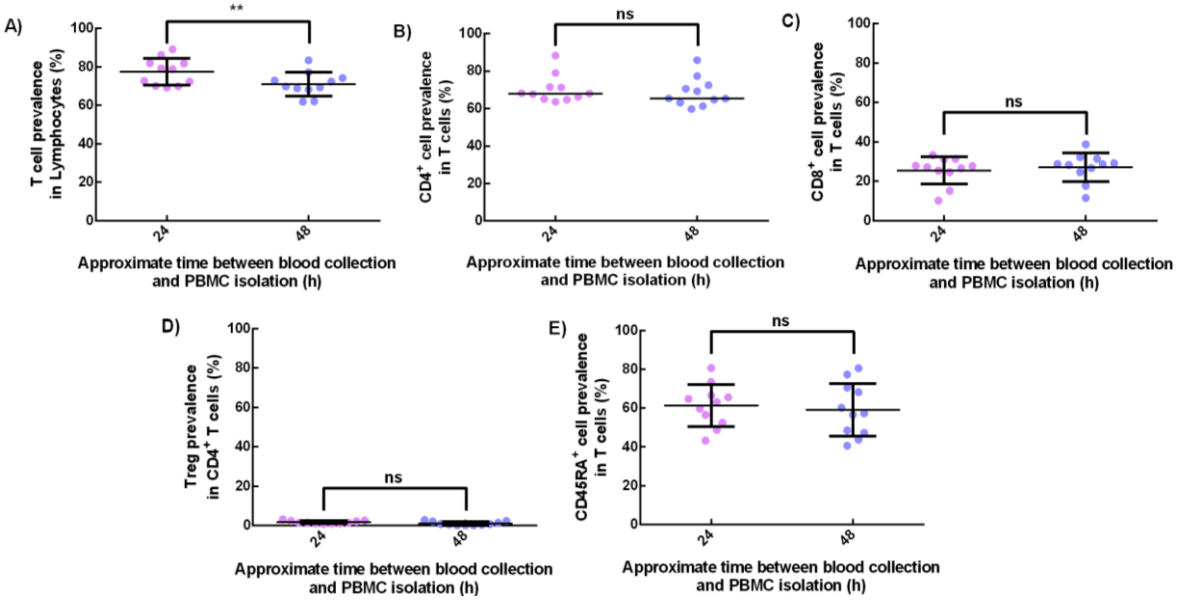
13.4 Peripheral blood mononuclear cell isolation time optimization

Control samples (*N*=11) were used to examine the effects of the time period between blood collection time and PBMC isolation. More specifically, using the flow assay, the effect of isolating cells 24h and 48h after blood collection was assessed,

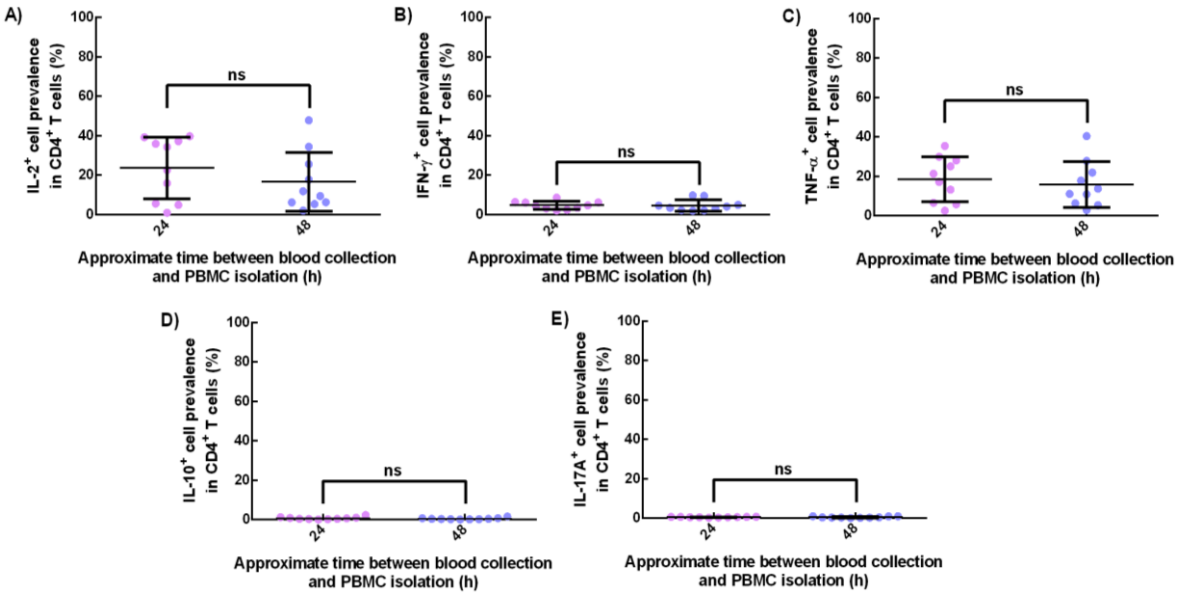
examining differences in NK and T cell population and subpopulation prevalence. Additionally, the effect of isolation time on the number of cytokine-producing T_H and NK cells was examined after PBMC stimulation. The number of NK cells expressing CD25 and CD215 after stimulation was also examined. As it can be seen in Supplementary Figures 10-13, only T cell prevalence in Lymphocytes was found to be significantly affected by the difference in PBMC isolation time, with T cells levels being slightly reduced after 48h (p=0.0049). As no further differences were observed, samples from which PBMCs were isolated at both these time points were included in this study.



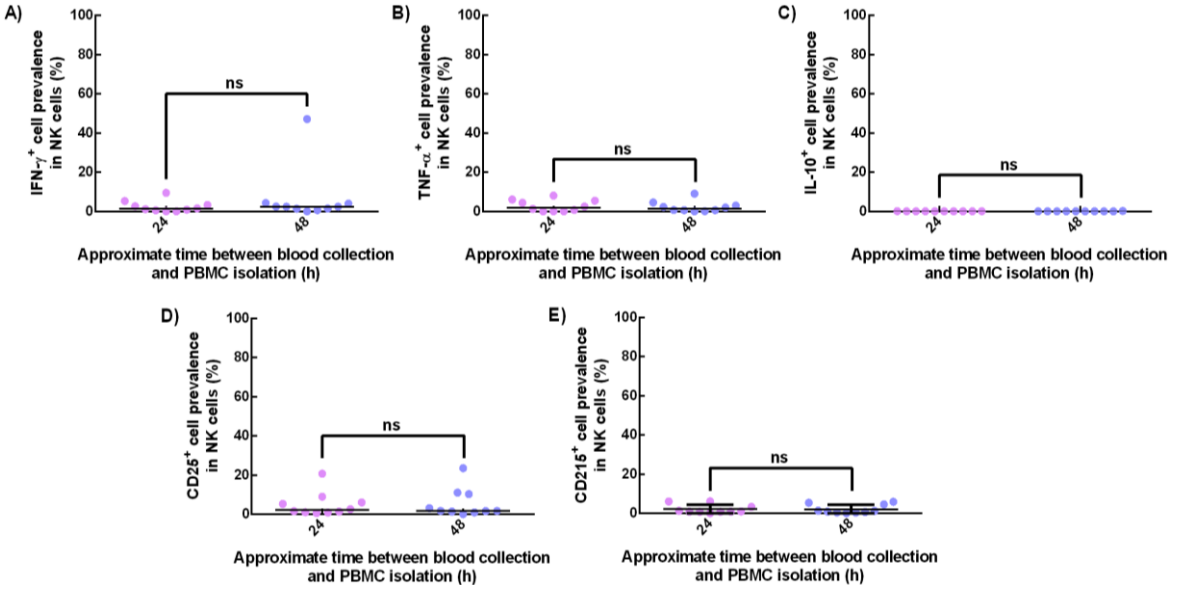
Supplementary Figure 10. Effect of Peripheral Blood Mononuclear Cell (PBMC) isolation time on Natural Killer (NK) cells. *A) NK cell prevalence in Lymphocytes (%), B) $CD56^{dim}CD16^{+}$ cell prevalence in NK cells (%), C) $CD56^{bright}CD16^{-}$ cell prevalence in NK cells (%), and D) $CD69^{+}$ cell prevalence in NK cells (%) are displayed in two paired groups, one for PBMCs isolation 24h after blood collection and one for PBMCs isolation 48h after blood collection (N=11). The median value for each group is shown. Wilcoxon matched-pairs signed rank test performed. ns: non-significant*



Supplementary Figure 11. Effect of peripheral blood mononuclear cell (PBMC) isolation time on T cells. *A) T cell prevalence in Lymphocytes (%), B) CD4⁺ cell prevalence in T cells (%), C) CD8⁺ cell prevalence in T cells (%), D) regulatory T cell (Treg) prevalence in CD4⁺ T cells, and E) CD45RA⁺ cell prevalence in T cells (%) are depicted in two paired groups, one for PBMCs isolation 24h after blood collection and one for PBMCs isolation 48h after blood collection (N=11). Normally distributed datasets (A, C, D, E): Paired t test performed, mean and standard deviation displayed. Non-normally distributed datasets (B): Wilcoxon matched-pairs signed rank test used, median illustrated. ns: non-significant, **: p≤0.01*



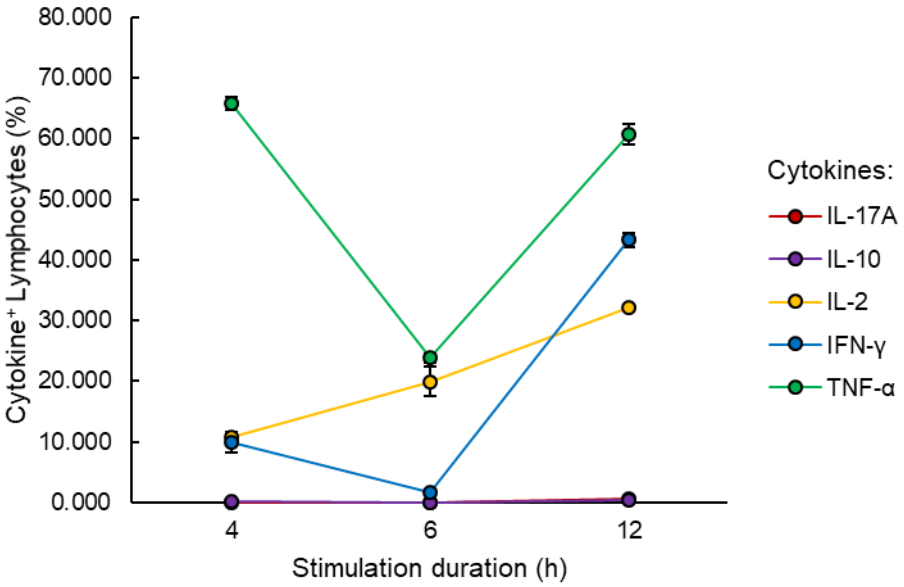
Supplementary Figure 12. Effect of peripheral blood mononuclear cell (PBMC) isolation time on cytokine production by CD4⁺ T helper cells. *A) IL-2⁺ cell prevalence in CD4⁺ T cells (%), B) IFN-γ⁺ cell prevalence in CD4⁺ T cells (%), C) TNF-α⁺ cell prevalence in CD4⁺ T cells (%), D) IL-10⁺ cell prevalence in CD4⁺ T cells (%), and E) IL-17A⁺ cell prevalence in CD4⁺ T cells (%) are displayed in two paired groups, one for PBMCs isolation 24h after blood collection and one for PBMCs isolation 48h after blood collection (N=11). Normally distributed datasets (A, B, C, E): Paired t test used, mean and standard deviation shown. Non-normally distributed datasets (D): Wilcoxon matched-pairs signed rank test performed, median depicted. ns: non-significant*



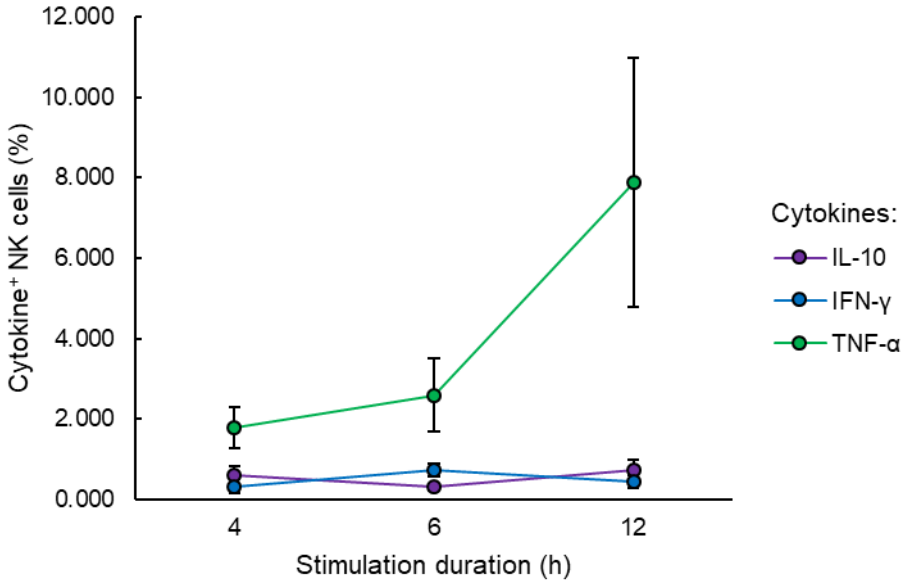
Supplementary Figure 13. Effect of peripheral blood mononuclear cell (PBMC) isolation time on cytokine production and cytokine receptor expression by Natural Killer (NK) cells. *A) IFN-γ$^+$ cell prevalence in NK cells (%), B) TNF-α$^+$ cell prevalence in NK cells (%), C) IL-10$^+$ cell prevalence in NK cells (%), D) CD25$^+$ cell prevalence in NK cells (%), and E) CD215$^+$ cell prevalence in NK cells (%) are depicted in two paired groups, one for PBMCs isolation 24h after blood collection and one for PBMCs isolation 48h after blood collection (N=11). Normally distributed datasets (E): Paired t test performed, mean and standard deviation illustrated. Non-normally distributed datasets (A, B, C, D): Wilcoxon matched-pairs signed rank test used, median shown. ns: non-significant*

13.5 Peripheral blood mononuclear cell stimulation optimization

Prior to the establishment of the previously described stimulation protocol, stimulation conditions were optimized using the cytokine panels of the flow cytometry assay. Initially, three different stimulation durations, including 4h, 6h, and 12h were tested. The number of samples used (*N*=2) were not adequate to perform statistical analyses, but as it can be seen in Supplementary Figures 14 and 15 the 12h stimulation period was found to induce the highest production of most cytokines of interest.



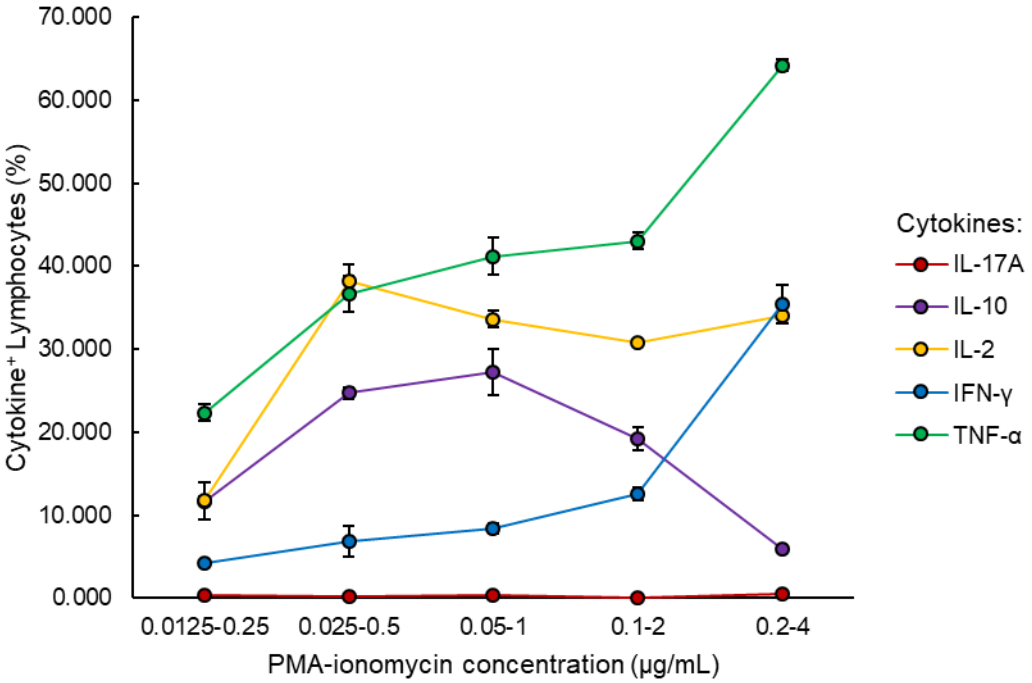
Supplementary Figure 14. Percentage of lymphocytes expressing each cytokine of interest, following stimulation with 0.05µg/mL phorbol 12-myristate 13-acetate and 1µg/mL ionomycin for 4h, 6h, and 12h. *The mean prevalence of cells expressing IL-17A, IL-10, IL-2, IFN-γ, and TNF-α in the total lymphocyte population is illustrated (N=2), with the error bars representing standard deviation.*



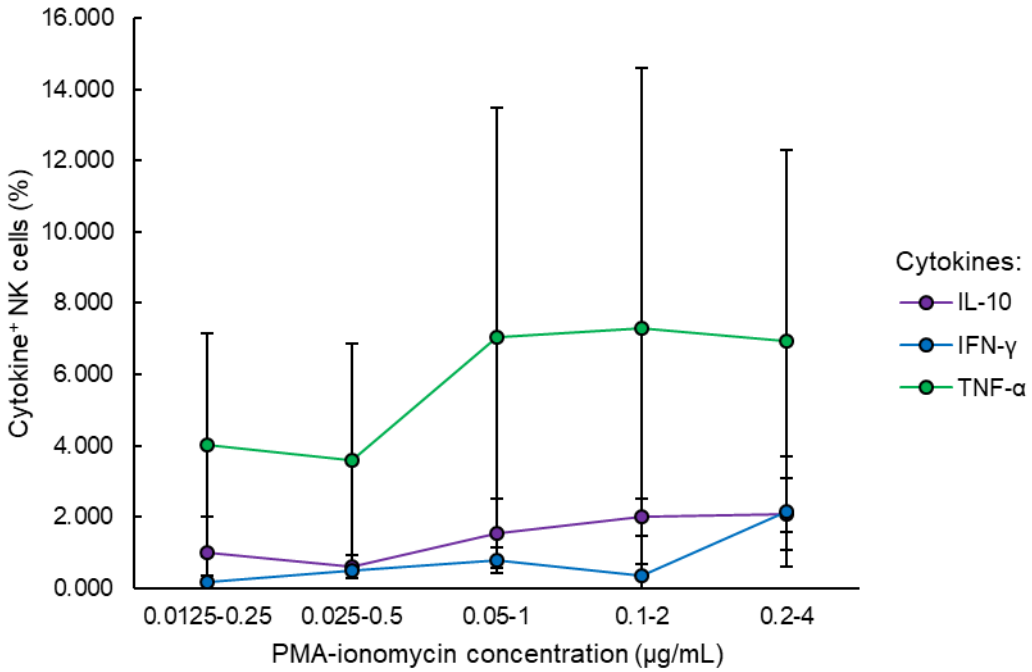
Supplementary Figure 15. Percentage of Natural Killer (NK) cells expressing each cytokine of interest, following stimulation with 0.05μg/mL phorbol 12-myristate 13-acetate and 1μg/mL ionomycin for 4h, 6h, and 12h. *The mean prevalence of cells expressing IL-10, IFN-γ, and TNF-α in the total $CD3^+CD56^-$ NK cell population is illustrated (N=2), while error bars representing standard deviation are also shown.*

The amount of PMA and ionomycin used was also optimized. Five different combinations of stimulant concentrations were tested, including 0.0125μg/mL and 0.25μg/mL, 0.025μg/mL and 0.5μg/mL, 0.05μg/mL and 1μg/mL, 0.1μg/mL and 2μg/mL, and 0.2μg/mL and 4μg/mL PMA and ionomycin, respectively. Stimulated PBMCs were stained and examined by flow cytometry. Statistical analysis was not performed due to the sample number (*N*=2), but according to the expression of cytokines of interest, shown in Supplementary Figures 16 and 17, 0.025μg/mL PMA and 0.5μg/mL ionomycin and 0.05μg/mL PMA and 1μg/mL were found to induce production of all cytokines at an adequate level. However, as both stimulants were diluted in DMSO (Sigma-Aldrich), which is potentially toxic to PBMCs, the percentage of cell death following stimulation with these stimulant concentrations

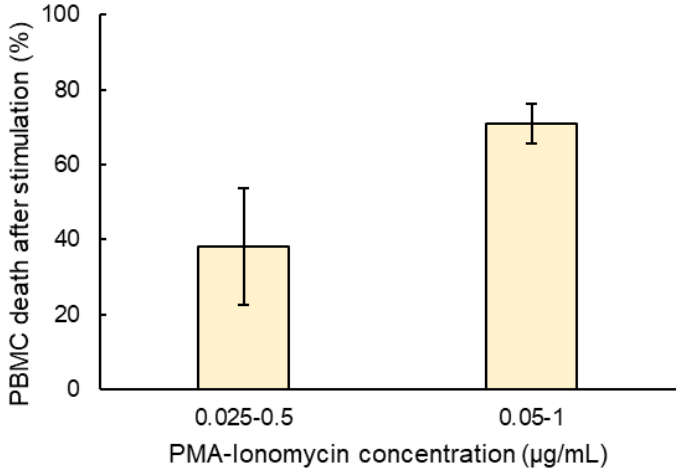
was examined by light microscopy using Trypan blue (Thermo Fisher Scientific) for dead cell staining (*N*=2). According to these findings, 0.025μg/mL PMA and 0.5μg/mL ionomycin were used for PBMC stimulation, as lower death levels were induced (Supplementary Figure 18).



Supplementary Figure 16. Percentage of lymphocytes expressing each cytokine of interest, following stimulation with different concentrations of phorbol 12-myristate 13-acetate (PMA) and ionomycin for 12h. *The mean prevalence of cells expressing IL-17A, IL-10, IL-2, IFN-γ, and TNF-α in the total lymphocyte population is depicted (N=2), with the error bars representing standard deviation.*



Supplementary Figure 17. Percentage of Natural Killer (NK) cells expressing each cytokine of interest, following stimulation with different concentrations of phorbol 12-myristate 13-acetate (PMA) and ionomycin for 12h. *The mean prevalence of cells expressing IL-10, IFN-γ, and TNF-α in the total $CD3^+CD56^-$ NK cell population is illustrated (N=2), while error bars representing standard deviation are also depicted.*



Supplementary Figure 18. Percentage of peripheral blood mononuclear cell (PBMCs) death following 12h stimulation with 0.025µg/mL-0.5µg/mL and 0.05µg/mL-1µg/mL phorbol 12-myristate 13-acetate (PMA)-ionomycin concentrations. *The mean cell death is displayed (N=2), while the standard deviation is shown in the form of error bars.*

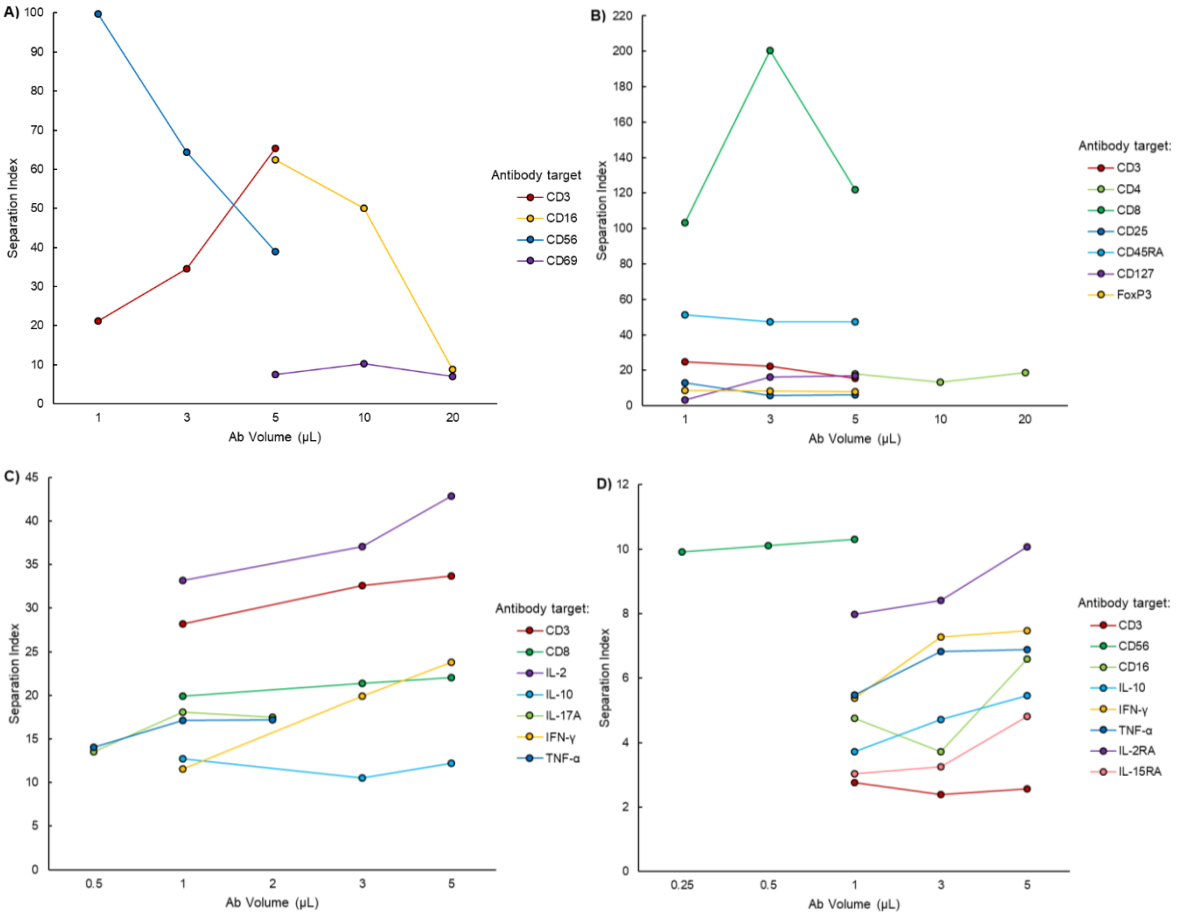
13.6 Flow cytometry assay optimization

All antibodies and dyes used in flow cytometry panels were titrated (*N*=1). 10^6 PBMCs were stained, according to the respective protocol, with the suggested amount of each antibody. Only one antibody was added per tube to avoid interference and reduce background noise. For each antibody titrated, two additional tubes with PBMCs were generated, in which ~½ and ¼ of the suggested amount was added. The Zombie Green™ dye was also titrated. A 1:100 Zombie dilution was generated, as previously described, and 10^6 PBMCs were stained with 100µL, 50µL, or 25µL dilution. The optimum amount for each stain was decided according to the separation index resulting from each titre. The separation index was calculated according to the following equation:

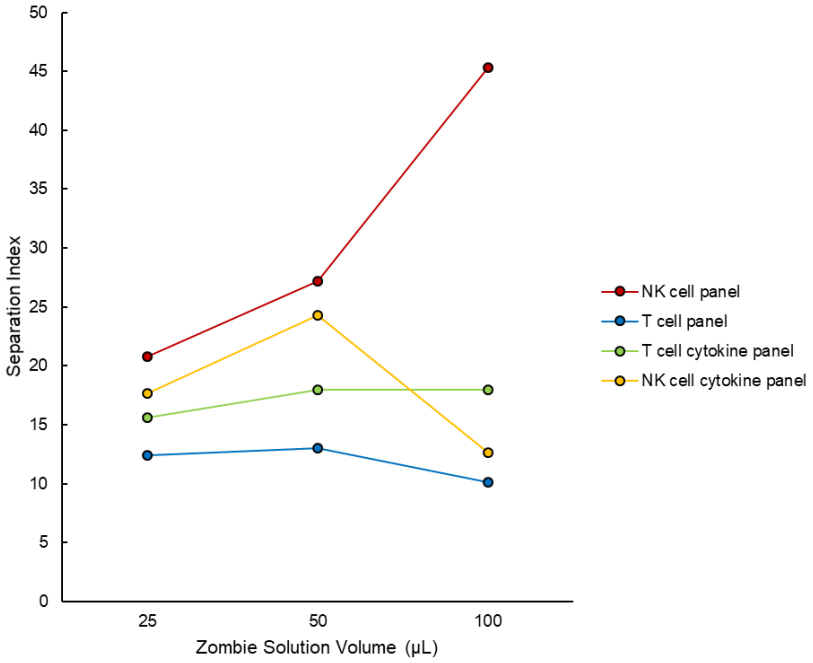
Separation Index=$(MFI_{pos}–MFI_{neg})/[(84\%_{neg}–MFI_{neg})/0.995]$, where MFI_{pos} and MFI_{neg} represent the median fluorescence intensity of cells positive and negative for the stain of interest and $84\%_{neg}$ represents the 84^{th} percentile of negative cells.

In the NK cell panel, 1µL anti-CD56, 5µL anti-CD3, 5µL anti-CD16, and 10µL of anti-CD69 antibody resulted to the highest separation indices and hence these amounts were used (Supplementary Figure 19A). In regards to the T cell panel, 3µL of anti-CD8 antibody resulted in the highest separation index. 3µL of anti-CD3 and anti-CD45RA antibodies and 5µL of anti-CD4 were also preferred as no pronounced difference between the separation indices could be detected. 3µL anti-CD127 were used, as separation indices for 3µL and 5µL were found to be similar. Lastly, as the $CD25^+$ and $FoxP3^+$ populations appeared limited, the suggested volumes of these antibodies, equal to 5µL, were preferred (Supplementary Figure 19B). In the T_H cell

cytokine panel, 5μL anti-CD3, anti-CD8, anti-IL-2, and anti-IFN-γ antibodies and 2μL of anti-TNF-α antibody were found to result to the highest separation index and were thus chosen, while the suggested volumes of anti-IL-10 and anti-IL-17A, equal to 5μL and 2μL respectively, were preferred due to the low prevalence of these cells (Supplementary Figure 19C). In the NK cell cytokine panel, the suggested amount of all antibodies was chosen. For most antibodies this amount was shown to result in the highest separation index. When examining anti-CD3, the highest amount was chosen due to the lack of pronounced differences in separation indices. Hence, 5μL anti-CD3, anti-CD16, anti-IL-10, anti-IFN-γ, anti-TNF-α, anti-CD25, and anti-CD215 and 1μL of the anti-CD56 antibody were used in this panel (Supplementary Figure 19D). 50μL of Zombie solution appeared adequate for the staining of 10^6 cells (Supplementary Figure 20).

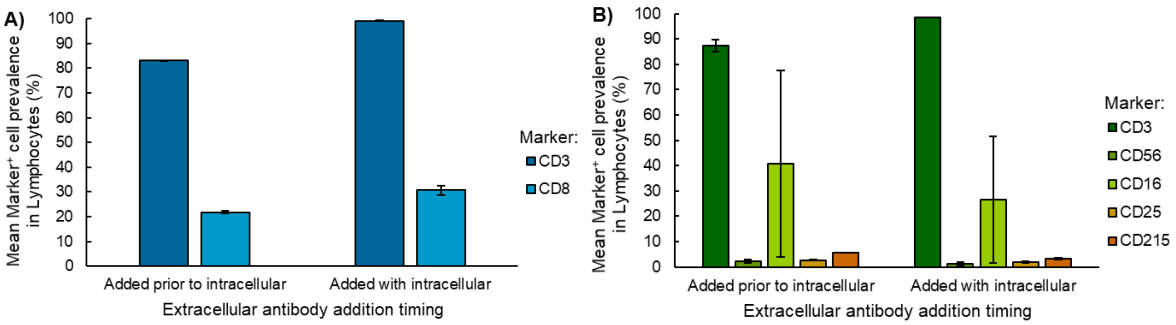


Supplementary Figure 19. Titration of antibodies used in the flow cytometry assay. *The separation indices resulting from the use of different titres of the antibodies included in the A) Natural Killer (NK) cell, B) T cell, C) T helper cell cytokine, and D) NK cell cytokine panel are displayed.*



Supplementary Figure 20. Titration of the Zombie dead cell stain used in the flow cytometry assay. *The separation indices resulting from the use of various amounts of the dye solution for the staining of cells that were processed according to the protocols of the different panels are illustrated*

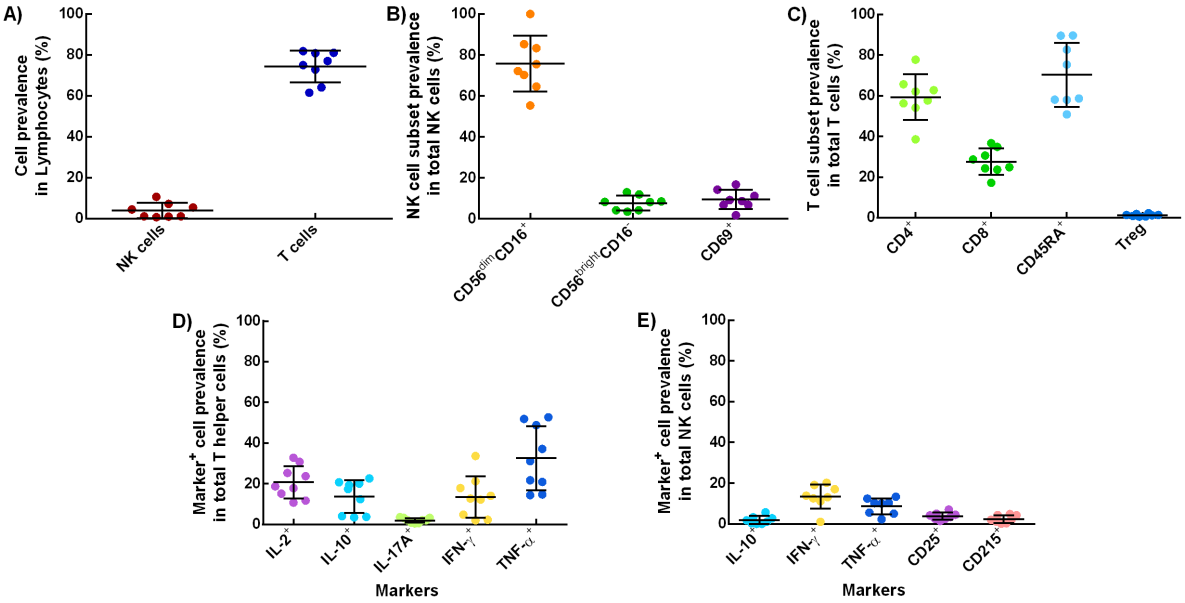
In the cytokine panels the timing of extracellular antibody addition was also optimized (*N*=2). As shown in Supplementary Figure 21A the levels of $CD3^+$ and $CD8^+$ cells stained with the T_H cell cytokine panel were reduced when the respective antibodies were added prior to fixation/permeabilization and hence in the resulting protocol, PBMCs were stained with both extracellular and intracellular antibodies after the fixation/permeabilization. On the other hand, apart from anti-CD3, antibodies used in the NK cell cytokine panel were not negatively affected by the fixation/permeabilization process, and as CD56, CD25, and CD215 expression was relatively low the protocol was not altered to ensure detection of these markers (Supplementary Figure 21B).



Supplementary Figure 21. Optimization of extracellular antibody addition timing in the cytokine panels of the flow-cytometry based assay. *Average percentage of cells positive for each marker targeted by the extracellular antibodies used in the A) T helper (T_H) cell cytokine and B) Natural Killer cell cytokine panels are shown (N=2), in relation to the timing of their addition. Specifically, marker expression on cells stained with extracellular antibodies prior to fixation, permeabilization, and intracellular antibody addition and on cells stained with both intracellular and extracellular antibodies after the fixation and permeabilization process is depicted. Error bars representing standard deviation are included.*

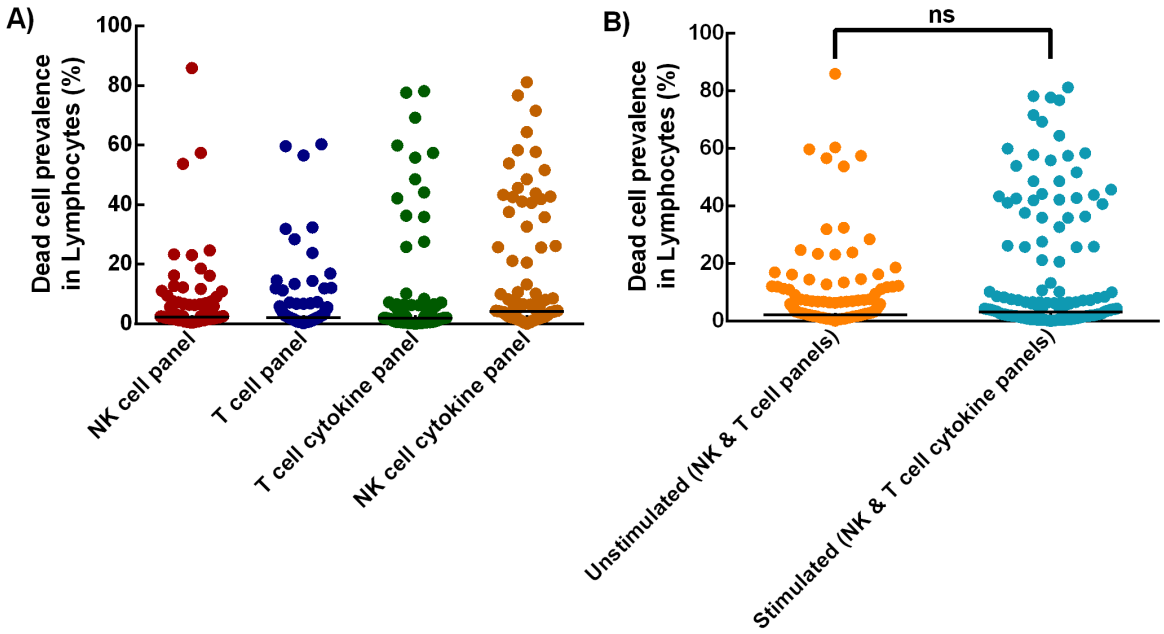
13.7 Flow cytometry assay validation

In order to validate the flow cytometry assay, control samples (*N*=8) were used. PBMCs were isolated and stained according to the optimized protocol, and the expression of all markers of interest was assessed (Supplementary Figure 22).



Supplementary Figure 22. Flow cytometry assay validation. *The prevalence of A) Natural Killer (NK) and T lymphocytes, B) CD56^{dim}CD16^{+}, CD56^{bright}CD16^{-}, CD69^{+} NK cell subsets, C) CD4^{+}, CD8^{+}, CD45RA^{+}, and regulatory (Treg) T cell subsets, D) IL-10^{+}, IL-17A^{+}, IFN-γ^{+}, and TNF-α^{+} T helper cells, and E) IL-10^{+}, IFN-γ^{+}, TNF-α^{+}, CD25^{+}, and CD215^{+} NK cells is illustrated (N=8). The mean and standard deviation of each dataset is shown.*

13.8 Cell death evaluation following staining with the different flow cytometry panels



Supplementary Figure 23. Dead cell prevalence in the peripheral blood mononuclear cell populations stained with the different panels of the flow cytometry assay. *Samples isolated in from women with recurrent pregnancy loss and controls were stained for cell death with Zombie Green and processed according to the Natural Killer (NK) (N=116) and T (N=117) cell panel protocol, not having undergone prior stimulation, or the T (N=113) and NK (N=109) cell cytokine panel protocol, being previously stimulated with phorbol 12-myristate 13-acetate and ionomycin. Zombie Green⁺ dead cell prevalence A) in each panel and B) in panels not requiring prior stimulation compared to those requiring pre-stimulation is depicted. Mann-Whitney test used, median illustrated. ns: non-significant*

13.9 Compensation tube preparation for flow cytometry

Compensation was performed using OneComp eBeads™ compensation beads (Thermo Fisher Scientific). More specifically, one compensation tube was generated per antibody used. Half the amount of each antibody used in the sample tube was added in the compensation tube. A negative control containing no antibody was also created. Beads were vortexed and one drop was added in each compensation tube.

The tubes were incubated for 30min at 4ºC in the dark and were then washed with 2mL CellWash buffer (BD Biosciences) by 5min centrifugation at 500g. Supernatant was removed and 400μL CellWash buffer were added. Tubes were vortexed, stored at 4ºC, and run on the BD FACSCanto™ II (BD Biosciences) cytometer prior to sample runs.

13.10 Mass cytometry antibody conjugations

Multiple antibodies included were manually conjugated. More specifically, for the conjugation of Lanthanides and Indium metals the Maxpar® X8 Antibody Labeling Kits and the respective protocol (Fluidigm) were utilised. According to the protocol, for each conjugation, the Maxpar® X8 polymer (Fluidigm) was thawed and diluted in 95μL L-Buffer. 5μL 50mM metal was added and the mixture was incubated for 40min at 37ºC. The polymer-metal solution and 200μL L-Buffer were added in a 3kDa centrifugal filter column placed on a collection tube (Merck Millipore), which was then centrifuged for 25min at 12000g. The metal-loaded polymer was washed with 400μL C-Buffer by 30min centrifugation at 12000g and diluted in 60μL C-Buffer. During the metal-loaded polymer preparation, the respective antibody was also prepared for conjugation. 100μg of antibody were added in a 50kDa centrifugal filter column placed on a collection tube (Merck Millipore), which was then filled up to 400μL with R-Buffer and was centrifuged for 10min at 12000g. 100μL freshly prepared 4mM Bond-Breaker™ TCEP solution (Thermo Fisher Scientific), diluted in R-Buffer, was added to the antibody column and the mixture was incubated at 37ºC for 30min. Following incubation, 300μL C-Buffer was added and the column was centrifuged at 12000g for 10min. The antibody was then washed with 400μL C-Buffer by 10min centrifugation at 12000g. The diluted metal-loaded polymer was

transferred in the 50kDa antibody column and the mixture was incubated for 90min at 37ºC to allow conjugation. The conjugated antibody was washed once with 200μL W-Buffer and three times with 400μL W-Buffer by 10min centrifugations at 12000g. To determine yield, 80μL W-Buffer was added and 2μL of the mixture were used to measure absorbance at 280nm against a W-Buffer-only blank, on the NanoDrop™ Spectrophotometer (Thermo Fisher Scientific). The W-Buffer was then removed through a 10min centrifugation at 12000g and Antibody Stabilizer PBS (Candor), supplemented with 0.05% Sodium azide (Merck Millipore) for the prevention of microbial contamination, was added to obtain a 0.5mg/mL final conjugated antibody concentration. Finally, in order to collect the antibody, the column was inverted on a sterile graduated skirted tube (STARLAB) that was centrifuged for 2min at 1000g and the flow-through was stored at 4ºC.

For antibody conjugation with Cadmium metals Maxpar® MCP9 Antibody Labeling Kits and the respective protocol (Fluidigm) were used. For each conjugation performed, the Maxpar® MCP9 polymer (Fluidigm) was thawed and diluted in 87μL L-Buffer. 13μL 50mM metal was added to the dilution. The mixture was incubated for 60min at 37ºC. Similar to the Lanthanide and Indium conjugation protocol, the polymer-metal solution diluted in 200μL L-Buffer was added in a 3kDa column placed on a collection tube (Merck Millipore). The tube was centrifuged at 12000g for 25min and the metal-loaded polymer was washed with 300μL L-Buffer by 30min centrifugation at 12000g and with 400μL C-Buffer by 45min centrifugation at 12000g. Finally, the metal-loaded polymer was diluted in 60μL C-Buffer. Concurrently with the metal-loaded polymer, the antibody was prepared. 100μg antibody was added in a 50kDa column placed on a collection tube (Merck

Millipore). The column was filled up to 400μL with R-Buffer and was centrifuged at 12000g for 10min. The antibody was washed twice with 400μL R-Buffer by 10min centrifugation at 12000g. 100μL 4mM TCEP solution (Thermo Fisher Scientific), diluted in R-Buffer, was added to the column and the antibody mixture was incubated for 30min at 37ºC. After incubation, the antibody was washed twice, once with 300μL C-Buffer and once with 400μL C-Buffer by 10min centrifugations at 12000g. The metal-loaded polymer, diluted in C-Buffer, was transferred in the 50kDa antibody column. To facilitate conjugation the mixture was incubated at 37ºC for 90min. 300μL W-Buffer was then added to the mixture, which was then transferred in a 100kDa centrifugal filter column placed on a collection tube (Merck Millipore). The column was centrifuged at 5000-8000g for 10min. The conjugated antibody was washed three times with 400μL W-Buffer by 10min centrifugations at 5000-8000g. As mentioned previously, the final conjugated antibody yield was determined using the NanoDrop™ Spectrophotometer (Thermo Fisher Scientific). HRP Protector™ (Candor) was added to obtain a final conjugated antibody concentration equal to 0.5mg/mL. To collect the antibody, the column was inverted on a tube, which was centrifuged at 1000g for 2min. The flow-through was transferred on a sterile graduated skirted tube (STARLAB) and was stored at 4ºC.

Antibody conjugation with platinum metals is based on direct metal binding to the antibody and thus no polymer is required. These conjugations were performed using a protocol adapted from Mei, Leipold, and Maecker (2016) and buffers from Maxpar® kits (Fluidigm).[756] 100μg antibody was added in a 50kDa column placed on a collection tube (Merck Millipore) and diluted in R-Buffer at a final volume equal to 400μL. The column was centrifuged for 10min at 12000g. 100μL freshly prepared

4mM TCEP (Thermo Fisher Scientific), diluted in R-Buffer, was added to the column, which was then incubated at 37ºC for 30min. The antibody was washed twice with 300μL and subsequently with 400μL C-Buffer by 10min centrifugation at 12000g. 20μL platinum metal was added in a sterile microcentrifuge tube (Thermo Fisher Scientific) and diluted in 580μL C-Buffer. The antibody was also diluted in 400μL of C-Buffer and was transferred in the metal tube. The antibody and metal mixture was incubated at 37ºC for 90min. Following incubation, the mixture was transferred in a new 50kDa column-collection tube assembly, was centrifuged at 12000g for 10min, and was washed once with 200μL W-Buffer and three times with 400μL W-Buffer by 10min centrifugation at 12000g. Antibody yield was determined using the NanoDrop™ Spectrophotometer (Thermo Fisher Scientific), as previously described. Subsequently, Antibody Stabilizer PBS (Candor) supplemented with 0.05% Sodium azide (Merck Millipore) was added in order to obtain a 0.5mg/mL final antibody concentration. The antibody was collected through inversion of the 50kDa column on a sterile graduated skirted tube (STARLAB), which was then centrifuged for 2min at 1000g. The flow-through was stored at 4ºC.

13.11 Mass cytometry antibody titrations

The antibodies used were titrated in groups to determine optimal amounts to be used. More specifically, multiple antibodies were titrated in the same tube, ensuring however the absence of spillover between metal channels combined. Barcodes discriminating between antibody concentrations were used to allow pooling of samples. PBMCs were defrosted, as previously described, and diluted in 100μL Maxpar® cell staining buffer (Fluidigm). 5μL of Fc receptor blocking solution were added, to prevent non-specific binding, and PBMCs were incubated for 10min at

room temperature. A backbone cocktail was generated and added (Supplementary Table 1). Certain antibodies included in the backbone cocktail were excluded from certain titrations and when possible were replaced by the same antibody conjugated to a different metal, to prevent spillover to channels of interest. To facilitate staining, PBMCs were incubated for 25min at room temperature. Subsequently, cells were stained with 10μL 5% Cisplatin-194Pt, diluted in PBS, incubated for 3min at room temperature, and washed with 4mL staining buffer by 5min centrifugation at 300g. PBMCs were resuspended in staining buffer and 90μL were transferred in tubes prepared for each titre. A cocktail including the antibodies for titration was generated and an appropriate amount was added in each tube. This resulted in PBMCs stained with 0.2μL, 0.5μL, 0.75μL, and 1μL of each antibody, while for CD57 a volume equal to 0.05μL was also tested. In each tube a barcode was then added and tubes were incubated for 30min at room temperature and washed with 4mL staining buffer by 5min centrifugation at 300g. The different titres were then pooled into one combined tube. The tube was then centrifuged at 300g for 5min for buffer removal. 200μL of PBS and 300μL of 3.2% paraformaldehyde, diluted in PBS were added. Cells were incubated for 15min at room temperature, protected from light, and were washed with 3mL staining buffer by 4min centrifugation at 800g. 2μL Rh103 DNA intercalator (Fluidigm) was diluted in 0.5mL of Maxpar® Fix and Perm Buffer (Fluidigm) and the solution was added to the pelleted cells, which were then vortexed and incubated overnight at 4^{o}C. On the day of acquisition, cells were prepared as described in the Materials and Methods and run on the Helios CyTOF system (Fluidigm).

Supplementary Table 1. Backbone cocktail used in antibody titrations for the mass cytometry assay. *The antibodies added in the backbone cocktail, defined by their target molecule and metal tag, are included alongside the amount of each used per 100µL of peripheral blood mononuclear cell sample. CD: cluster of differentiation*

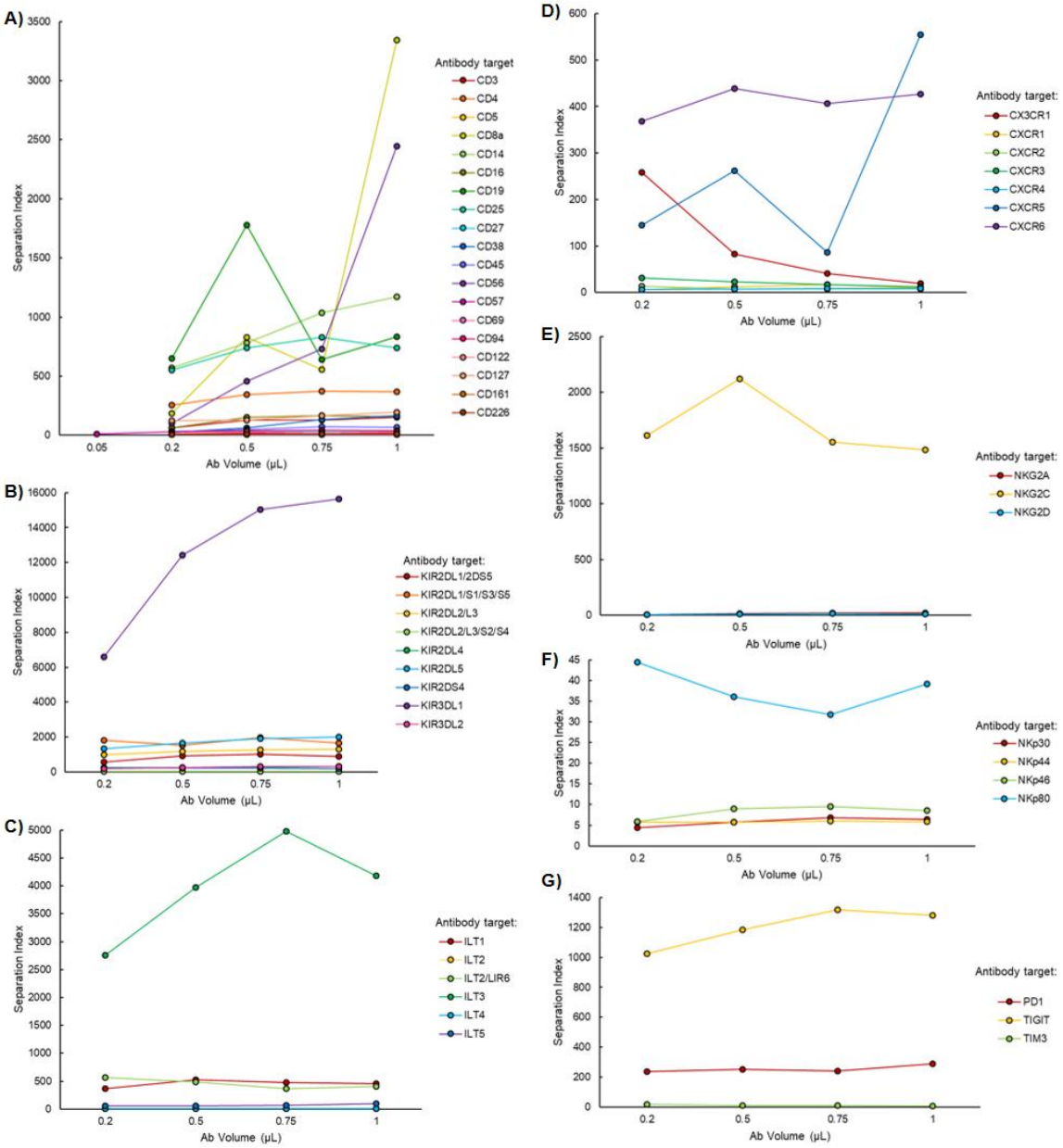
Antibody	µL
CD3 - 141Pr or 154Sm	0.40
CD4 - 145Nd	0.40
CD14 - 160Gd or 175Lu	0.30
CD16 - 209Bi	0.20
CD19 - 142Nd	0.80
CD45 - 89Y	1.00
CD56 - 155Gd or 163Dy	0.20

The protocol for analysis of titration data was similar to the one used for samples. The .fcs files were normalized using the CyTOF® Software v7.0 (Fluidigm, 2019) and data was cleaned-up and debarcoded on Cytobank (Beckman Coulter). Expression of most markers was examined in the $CD45^+CD3^-CD14^-CD19^-CD56^+$ NK cell population, which was the main population of interest. CD45 expression was assessed on total cells, while lineage marker expression, including CD3, CD14, CD19, and CD56, was examined on in $CD45^+$ leukocytes. CD4 and CD8 expression was assessed on the $CD45^+CD3^+$ T cell population and CD5 expression was examined on $CD45^+CD3^-CD14^-CD19^+$ B cells. Median metal intensity (MMI) of the populations negative and positive for each marker and 84^{th} percentile of the negative population were calculated and exported to Excel 2016.[638] The separation index was calculated according to the following equation:

$$\text{Separation Index}=(MMI_{pos}–MMI_{neg})/[(84\%_{neg}–MMI_{neg})/0.995]$$

The titres resulting in the highest separation index, without inducing significant spillover to the -1, +1, and +2 channels, as well as the +16 channel, where spillover

due to oxidation can be observed, were selected to be used for staining RPL and control samples (Supplementary Figure 24).



Supplementary Figure 24. Titrations of antibodies used in the mass cytometry assay. *The separation indices resulting from the use of different titres of the antibodies included in the mass cytometry panel are displayed. Antibodies titrated are separated into A) anti-cluster of differentiation (CD), B) anti-killer-cell immunoglobulin-like receptor (KIR), C) anti- immunoglobulin-like transcript (ILT) receptor, D) anti-chemokine receptor, E) anti-natural killer group (NKG)2 receptor, F) anti-natural cytotoxicity receptor, and G) anti-inhibitory immune checkpoint receptor antibodies, according to their target molecules.*

13.12 Mass cytometry assay validation

In order to validate the mass cytometry assay the staining protocol, including the complete antibody panel, was tested on healthy control samples (*N*=3), stored at -80^{o}C. Normalization, data clean-up, and debarcoding were also performed according to protocol. The different gating strategies applied for the titrations were again used to ensure adequate performance of all antibodies. No issues could be detected and thus no alterations were made.

13.13 Mass cytometry data analysis pipeline

The R script utilised for the analysis of mass cytometry data is included below, using the NK cell panel as an example:

```
#packages
if (!requireNamespace("BiocManager", quietly = TRUE))
  install.packages("BiocManager")
BiocManager::install("CATALYST")
if (!requireNamespace("BiocManager", quietly = TRUE))
  install.packages("BiocManager")
BiocManager::install("diffcyt")
if (!requireNamespace("BiocManager", quietly = TRUE))
  install.packages("BiocManager")
BiocManager::install("scater")
BiocManager::install("uwot")
#analysis code
library(CATALYST)
library(cowplot)
library(flowCore)
library(diffcyt)
library(scater)
```

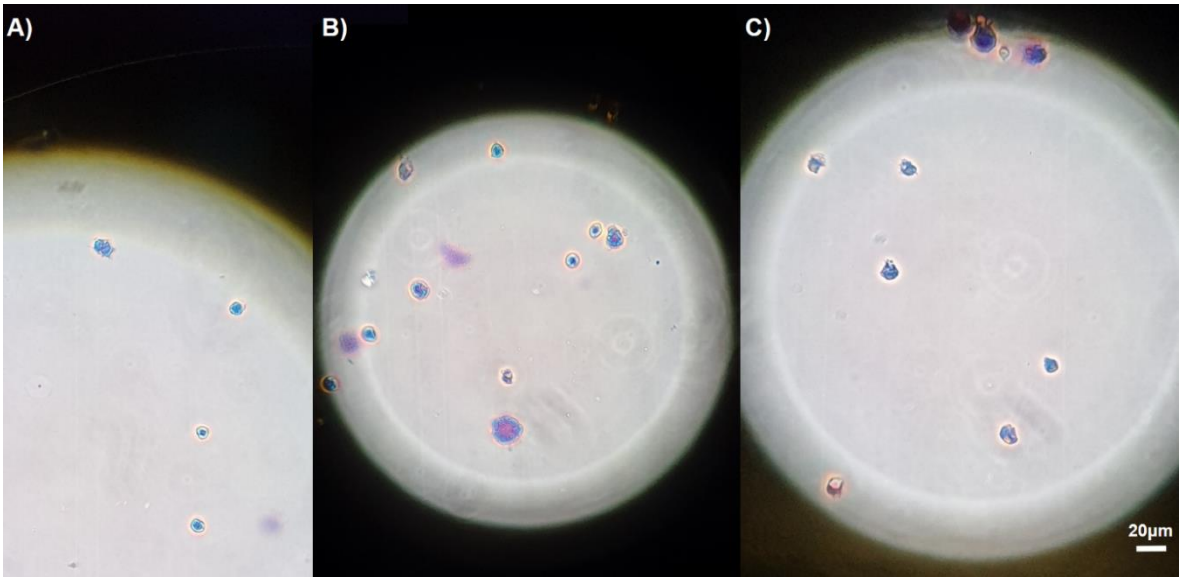
```
library(SingleCellExperiment)
library(umap)
library(uwot)
#import data
library(readxl)
NK_panel <- read_excel("C:/Users/Danai/Desktop/PhD/Results/R Data/Catalyst algorithm/NK_panel.xlsx")
View(NK_panel)
head(NK_panel)
library(readxl)
NK_md <- read_excel("C:/Users/Danai/Desktop/PhD/Results/R Data/Catalyst algorithm/NK_md.xlsx")
View(NK_md)
head(NK_md)
#set working directory (open folder with files, more, set working directory)
fcs <- list.files(pattern = ".fcs$")
fs <- read.flowSet(fcs, transformation = FALSE, truncate_max_range = FALSE)
#data preparation
(sce <- prepData(fs, NK_panel, NK_md))
all(NK_panel$fcs_colname %in% colnames(fs))
n_cells(sce)
#plots
plotCounts(sce, group_by = "sample_id", color_by = "condition")
pbMDS(sce, color_by = "condition", label_by = "sample_id")
plotCounts(sce,
        prop = TRUE,
        group_by = "condition",
        color_by = "patient_id")
#clustering
sce <- cluster(sce, features = "type",
            xdim = 10, ydim = 10, maxK = 20,
```

```
          verbose = TRUE, seed = 1234)
delta_area(sce)
sce <- mergeClusters(sce, k = "meta20", table = merging_table, id = "merging1")
head(cluster_codes(sce))[, seq_len(10)]
pbMDS(sce, by = "both", k = "meta20",
     shape_by = "condition", size_by = TRUE)
#dimensionality reduction
set.seed(1601)
sce <- runDR(sce, dr = "UMAP", cells = 1000, features = "type")
reducedDimNames(sce)
head(reducedDim(sce, "UMAP"))
p <- plotDR(sce, color_by = "meta20", facet_by = "condition")
p$facet$params$ncol <- 4; p
plotAbundances(sce, k = "meta20", by = "cluster_id",
             group_by = "condition", shape_by = "patient_id")
plotExprHeatmap(sce, features = "type",
              by = "cluster_id", k = "meta20",
              scale = "first", q = 0.01, perc = TRUE, col_dend = FALSE)
#create design & constrast matrix
design <- createDesignMatrix(ei(sce), cols_design = "condition")
contrast <- createContrast(c(0, 1))
#differential abundance (DA) of clusters
res_DA <- diffcyt(sce, clustering_to_use = "meta20",
                analysis_type = "DA", method_DA = "diffcyt-DA-edgeR",
                design = design, contrast = contrast, verbose = TRUE)
#extract result tables
tbl_DA <- rowData(res_DA$res)
tbl_DA
plotDiffHeatmap(sce, tbl_DA, all = TRUE, fdr = 0.05)
plotDiffHeatmap(sce, tbl_DA, all = TRUE, col_anno = FALSE,
              hm_pal = c("purple2", "snow1", "orange1"),
```

```
        fdr_pal = c("grey60", "lawngreen"),
        lfc_pal = c("coral2", "snow1", "turquoise3"))
#cluster Counts per Sample
counts <- assay(res_DA$d_counts)
```

13.14 Cytotoxicity assay optimization and troubleshooting

Even though the cytotoxicity assay utilizing PBMCs and K562 cells is commonly used for the assessment of NK cell cytotoxicity in both the research setting and in private clinics,[752, 757] extensive troubleshooting was required. Prior to optimization, PBMC-K562 co-cultures were visualised using Cytospin and Giemsa staining to examine the morphological state of these cells. Samples containing freshly isolated PBMCs, K562 cells, or a combination of both at a 3:1 ratio, were diluted at a 10^6 cells/mL concentration in RPMI. A microscopic slide (Fisher Scientific) was prepared per sample. A filter card (Thermo Fisher Scientific) was added on top of the glass slide and a Cytofunnel™ (Thermo Fisher Scientific) was placed on the card. The slide-filter card-funnel assembly was inserted into a Cytoclip™ (Thermo Fisher Scientific), which was then placed in Cytospin 2 (Shandon). 80μL CellWash buffer (BD Biosciences) and 20μL diluted sample were added into the funnel and spun at 500rpm for 3min. The assembly was removed and the slide was separated and air dried for 10min. Aerospray® Hematology Pro (ELITechGroup) was used for staining with eosin (ELITechGroup), binding to positively charge cytoplasmic proteins, and thiazine (ELITechGroup), dying acidic cellular components like nucleoproteins and nucleic acids. After staining, three drops of Coverquick 2000 mounting media (VWR) were added on the slide and a coverslip (Fisher Scientific) was placed. The sample was left to dry and was examined by light microscopy (Supplementary Figure 25).



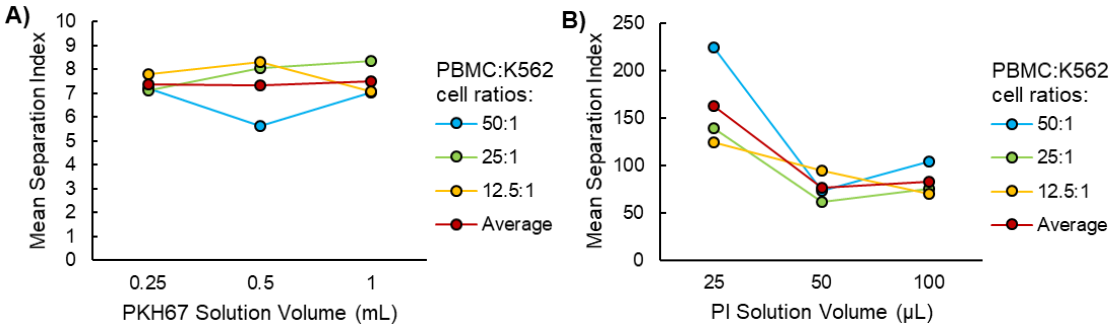
Supplementary Figure 25. Peripheral blood mononuclear cell (PBMC) and K562 cell visualization by Giemsa staining and light microscopy. *Cells in A) PBMC-only samples, B) co-cultures containing PBMC and K562 cells at a 3:1 ratio, and C) K562-only cell cultures are displayed.*

The PKH67 and PI dyes used for K562 and dead cell identification, respectively, were titrated (*N*=1). 50:1, 25:1, and 12.5:1 PBMC:K562 cell co-cultures were generated in duplicates according to protocol and were incubated for 4h. For each titration, cells were only stained with the dye of interest. Both dye solutions were prepared as previously described and the suggested amount, alongside ½ and ¼ of it were used. The MFI of cells positive and negative for the dye of interest and the 84th percentile of negative cells were measure. The separation index for each dye amount used was calculated according to the following equation:

$$\text{Separation Index}=(MFI_{pos}-MFI_{neg})/[(84\%_{neg}-MFI_{neg})/0.995]$$

As duplicates of co-cultures were generated, the mean separation index was calculated. As illustrated in Supplementary Figure 26A, the separation indices resulting from the different PKH67 solution volumes used did not appear to greatly

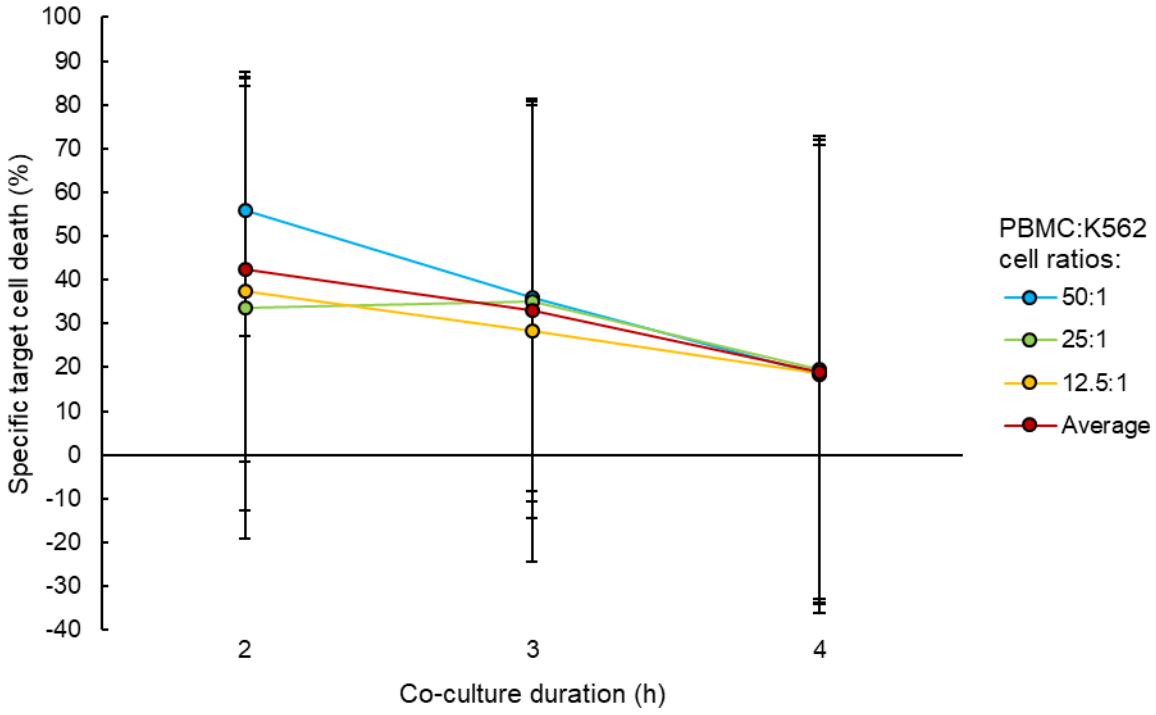
differ and thus the lower amount was preferred. On the other hand, the use of the lowest PI solution volume was found to result to the highest separation index and thus this volume was utilised (Supplementary Figure 26B).



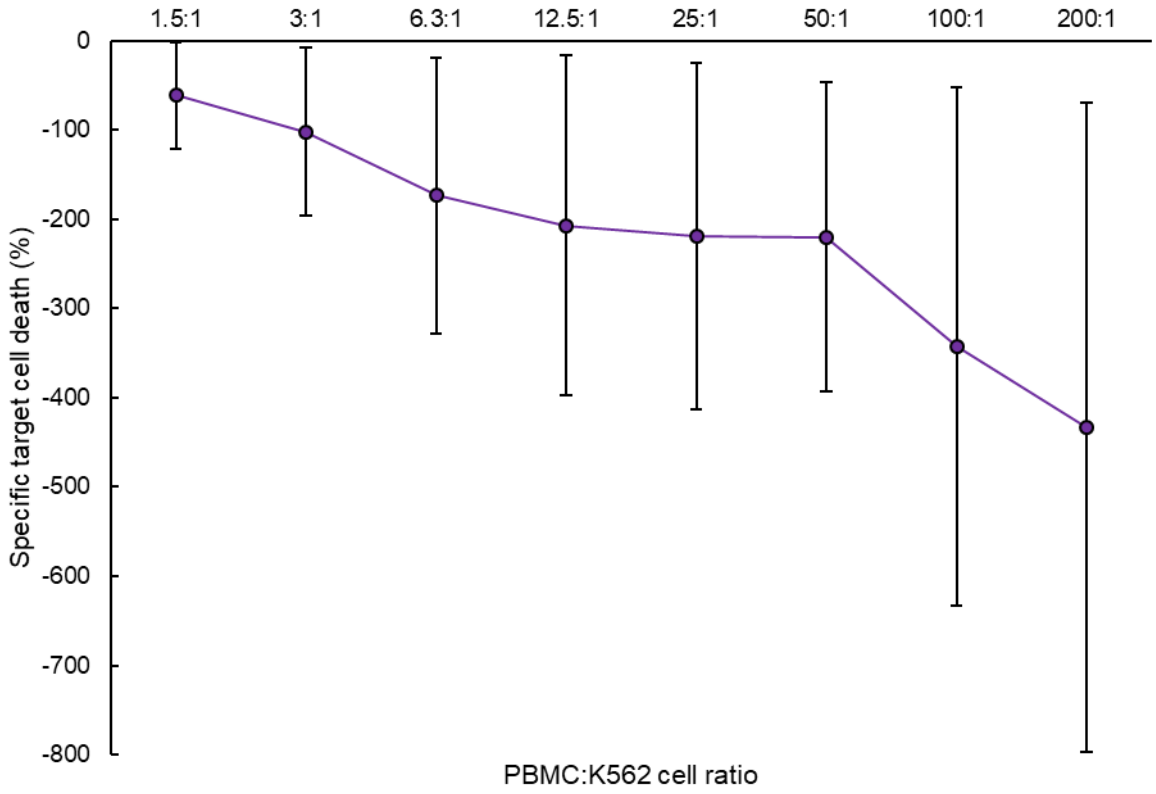
Supplementary Figure 26. Titration of dyes used in the cytotoxicity assay. *The mean separation indices, resulting from the use of different amounts of A) PKH67 or B) propidium iodide (PI) solution, in duplicated of peripheral blood mononuclear cell (PBMC):K562 cell co-cultures, including different ratios of these cells, are illustrated. An average of the results obtained by the use different ratios is also shown.*

Co-culture incubation time (*N*=2) and PBMC:K562 cell ratio (*N*=2) were also optimized. For both experiments, K562 cells were stained with the suggested amount of PKH67, equal to 4µL diluted in 1mL of Diluent C, while dead cells were stained with the suggested 0.5mg/mL PI solution volume, equal to 100µL. To optimize incubation time PBMC:K562 cell ratios equal to 50:1, 25:1, and 12.5:1 were used, while for optimization of cell ratios co-cultures were incubated for 4h. As it can be seen in Supplementary Figure 27, specific target cell death was reduced when the co-cultures were incubated for longer time periods. This finding could possibly be explained by an increase in spontaneous K562 cell death upon longer incubation. Thus, 2h incubation was used. In cultures used for the PBMC:K562 ratio optimization negative specific target cell death values were obtained due to high death rates in K562-only cultures (Supplementary Figure 28). The experiment was

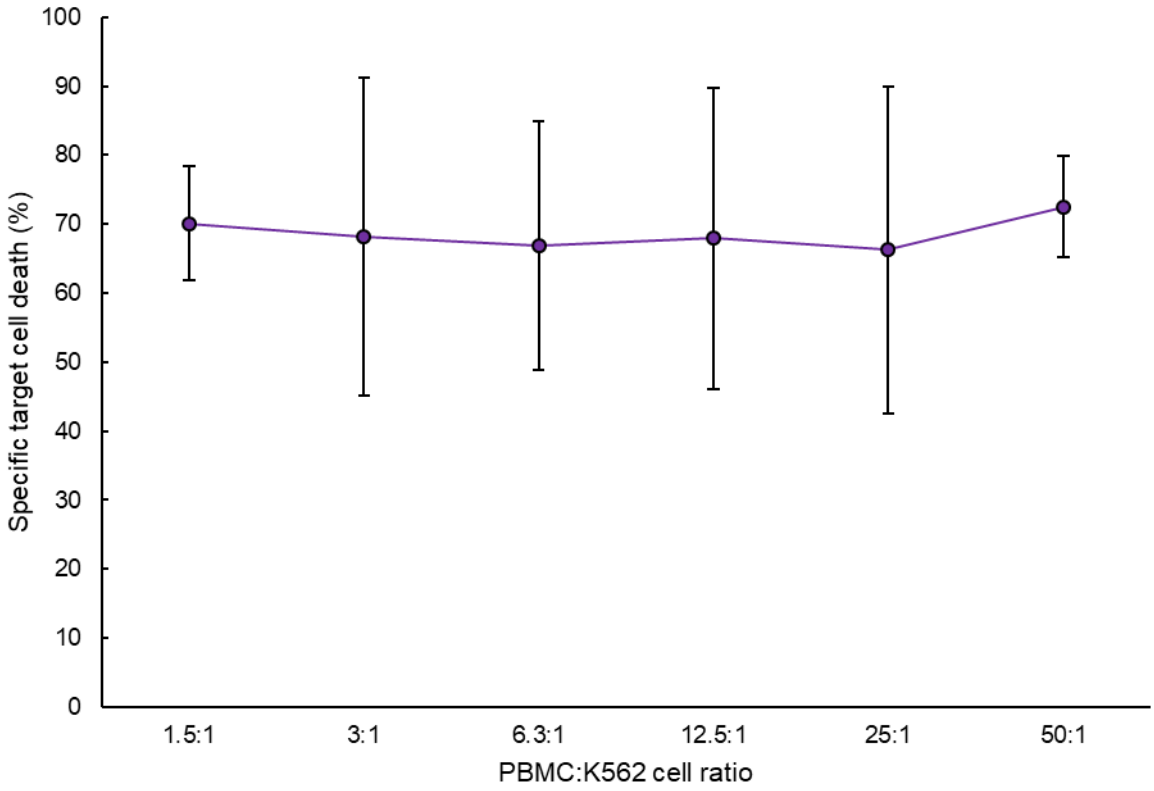
repeated, maintaining a constant co-culture volume. In that case specific target cell death was observed but values appeared relatively constant between cultures including the different PBMC:K562 cell ratios (Supplementary Figure 29). Thus, the 50:1, 25:1, and 12.5:1 ratios that are most commonly used were chosen. As the efficiency of NK cell killing appeared to be affected by co-culture volume, the final volume was maintained at a constant level between co-cultures containing the different cell ratios and controls in all subsequent experiments.



Supplementary Figure 27. Optimization of peripheral blood mononuclear cell (PBMC):K562 cell co-culture duration. *Mean specific K562 target cell death (%) in co-cultures including different PBMC:K562 cell ratios is illustrated in relation to the co-culture duration (h) (N=2). An average of specific target cell death in co-cultures including different cell ratios is also shown for each co-culture duration. Error bars representing standard deviation are included.*



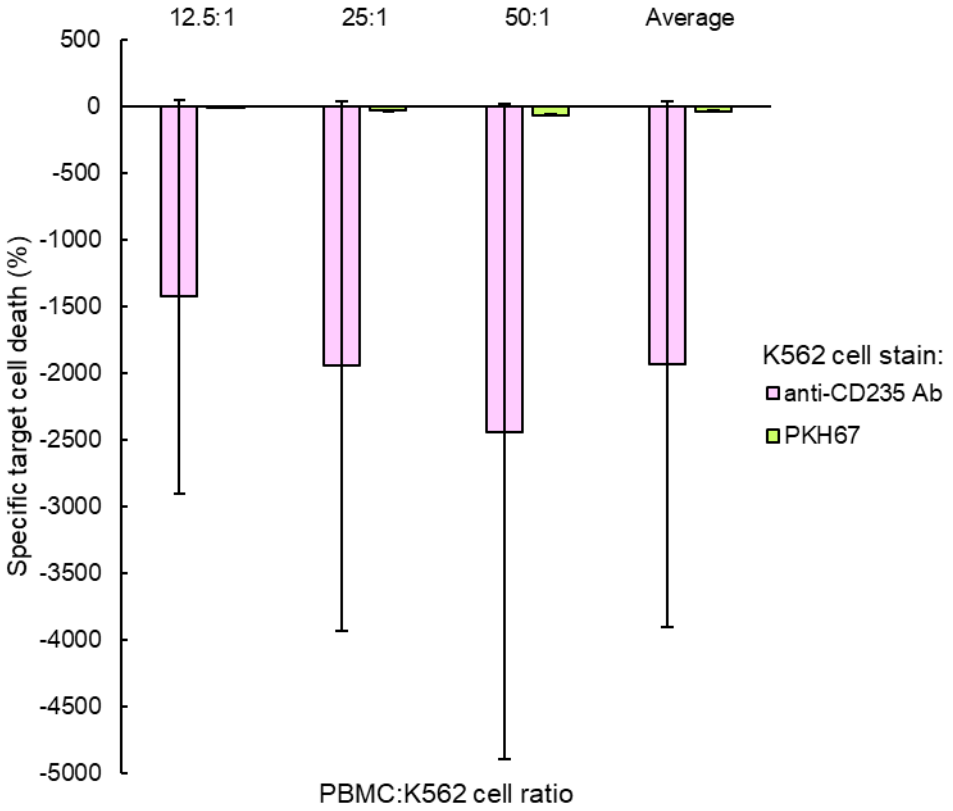
Supplementary Figure 28. Optimization of peripheral blood mononuclear cell (PBMC):K562 cell ratios used in co-cultures. *Mean specific K562 target cell death (%) in PBMC:K562 cell co-cultures, in which different ratios of these cells were used, is displayed (N=2). Error bars representing standard deviation are also shown.*



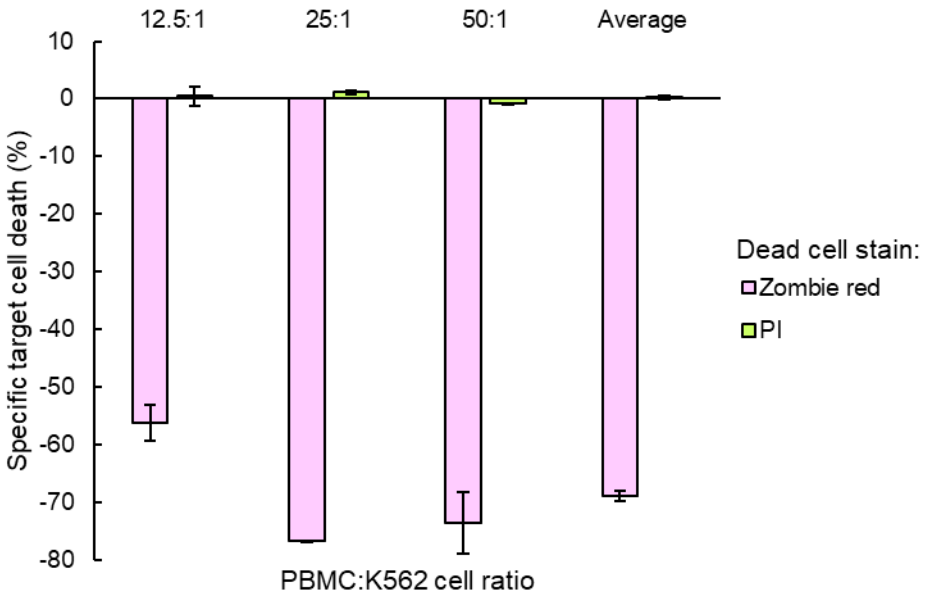
Supplementary Figure 29. Optimization of peripheral blood mononuclear cell (PBMC):K562 cell ratios used in co-cultures, in which a constant final volume is maintained. *Mean specific K562 target cell death (%) in PBMC:K562 cell co-cultures, in which different ratios of these cells were used maintaining a constant final volume, is depicted (N=2). Error bars representing standard deviation are also displayed.*

Further experiments were performed to try and identify factors possibly inducing death in K562-only control cultures. At first the effect of staining with PKH67 and PI was examined by replacing each dye. In both cases the optimized protocol was used, with PBMCs and K562 cells being co-incubated for 2h at ratios equal to 50:1, 25:1, and 12.5:1. Specifically, K562 cells were pre-stained using 5μL of an anti-CD235a antibody (Thermo Fisher Scientific), targeting Glycophorin A, a protein present on cells of the erythroid lineage and K562 cells (*N*=2).[643, 758, 759] Dead cells were stained with PI and control co-cultures with PKH67-labelled K562 cells were also generated using the same samples. Similarly, PI staining was replaced by

100µL of Zombie Red™ solution, including Zombie Red™ dye (BioLegend) diluted 1:100 in phosphate-buffered saline (*N*=2). In these cultures K562 cells were pre-stained with PKH67 and control co-cultures, in which dead cells were stained with PI, were also generated using the same samples. As shown in Supplementary Figures 30 and 31, use of alternative stains did not improve spontaneous K562 death. Hence, the original dyes were not replaced.



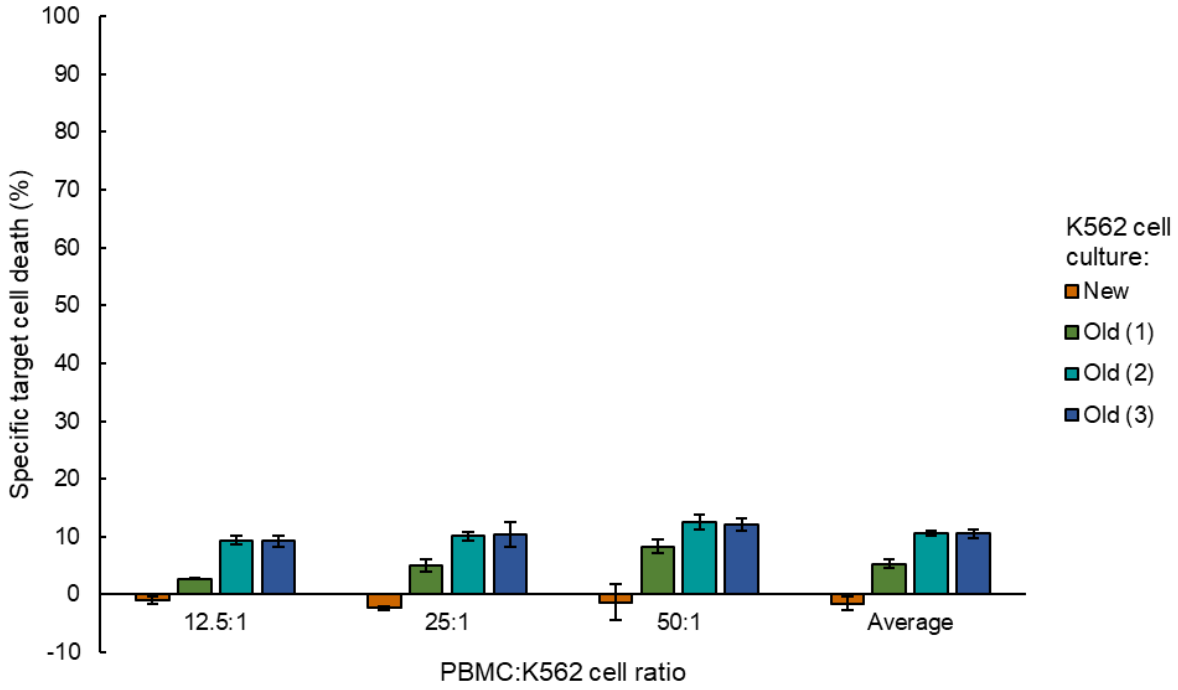
Supplementary Figure 30. Optimization of K562 cell staining performed during the cytotoxicity assay. *Mean specific K562 target cell death (%) in peripheral blood mononuclear cell (PBMC):K562 cell co-cultures, in which an anti-CD235 antibody or PKH67 were used for labelling K562 cells, is illustrated (N=2). Co-cultures used included different PBMC:K562 cell ratios and an average of specific target cell death across these co-cultures is also displayed. Error bars representing standard deviation are shown.*



Supplementary Figure 31. Optimization of dead cell staining performed during the cytotoxicity assay. *Mean specific K562 target cell death (%) in peripheral blood mononuclear cell (PBMC):K562 cell co-cultures, in which Zombie red or propidium iodide (PI) were used for dead cell staining is displayed (N=2). Co-cultures used included different PBMC:K562 cell ratios and an average of specific target cell death across these co-cultures is also shown. Error bars representing standard deviation are included.*

K562 cells originally used in the cytotoxicity assay optimization were kindly provided by Dr Farhat Latif Khanim's laboratory in the University of Birmingham School of Biosciences. The identity of the cells had been validated by short tandem repeat profiling. However, HLA class I expression on these cells was assessed to ensure that NK cell cytotoxicity was not inhibited by these molecules. K562 cells were stained with 5µL anti-HLA-A,B,C antibody (BD Biosciences) and examined by flow cytometry. No HLA-A,B,C expression was detected. Additionally, to ensure that the high spontaneous death was a result of the cells used, a new K562 cell line was obtained (Sigma-Aldrich) and the cytotoxicity assay was repeated (*N*=2), using the

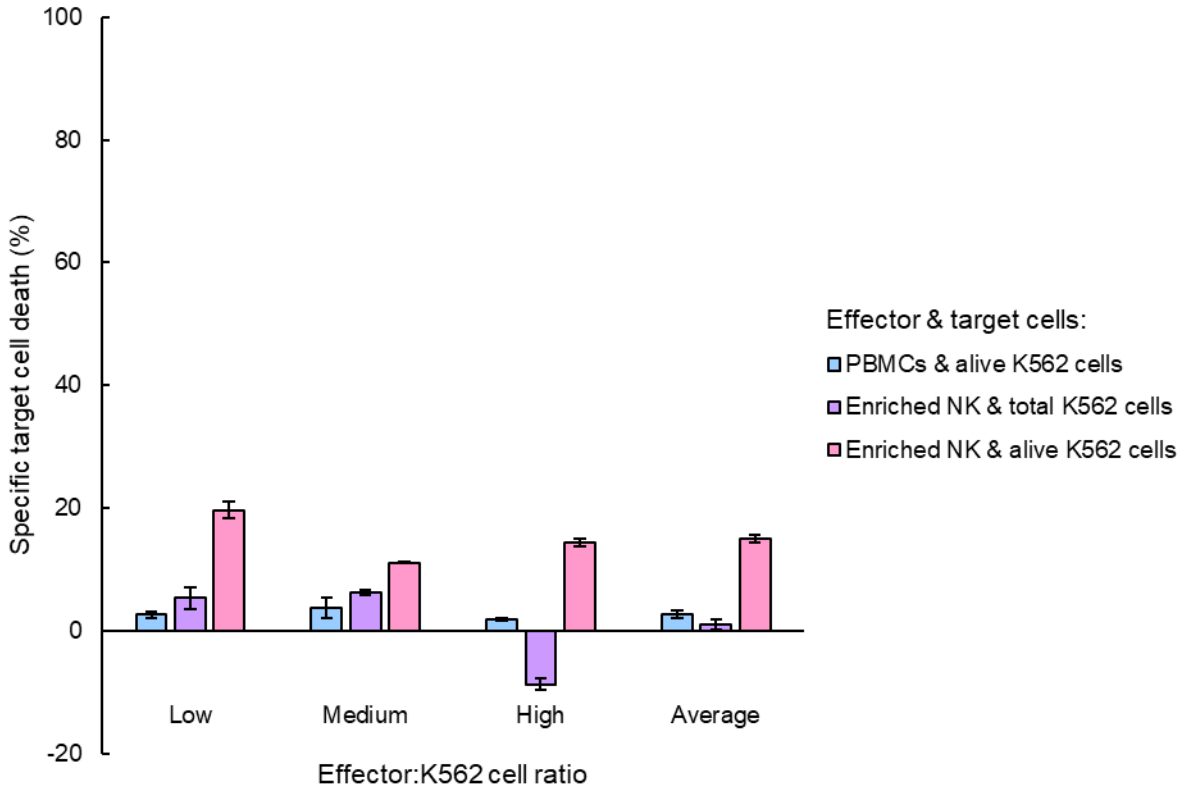
original K562 cell cultures as controls. The use of new cells however did not improve specific target cell death rates (Supplementary Figure 32).



Supplementary Figure 32. Cytotoxicity assay optimization using a new K562 target cell line. *Mean specific K562 target cell death (%) in co-cultures including different peripheral blood mononuclear cell (PBMC):K562 cell ratios, using K562 cells derived from new or older cultures is illustrated (N=2). An average of specific target cell death in co-cultures including different cell ratios is also shown. Error bars representing standard deviation are depicted.*

In an effort to eliminate influence from other PBMCs, NK cells were isolated using the EasySep™ Human NK Cell Isolation Kit (STEMCELL Technologies) and were used in co-cultures at a NK:K562 cell ratio equal to 0.5:1, 1:1, and 2:1. Additionally, dead K562 cell removal was performed using the Dead Cell Removal Kit (Miltenyi Biotec) prior to co-culture generation to ensure that alive target cells were mostly present at the start of the co-culture period. Hence, PBMC-alive K562, enriched NK-total K562, and enriched NK-alive K562 co-cultures were generated and the assay was performed according to the optimized protocol (*N*=2). As illustrated in

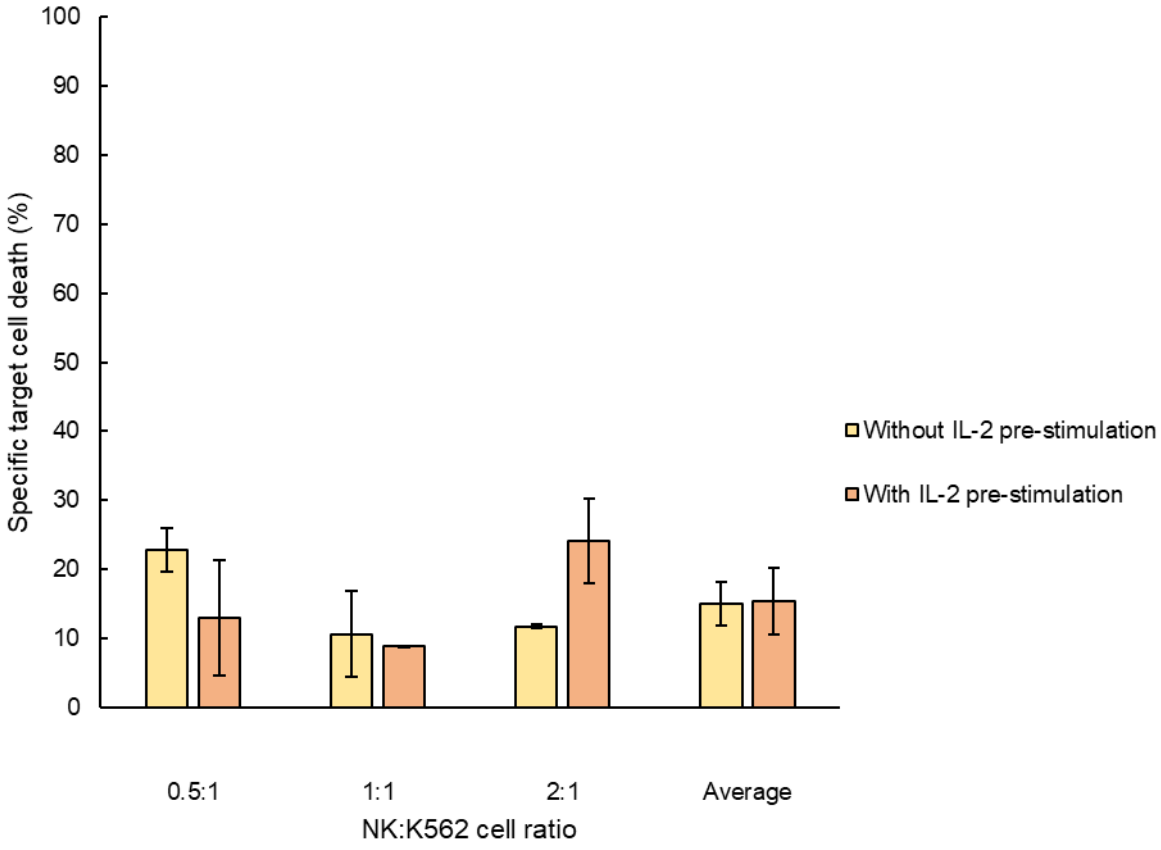
Supplementary Figure 33, the combination of enriched NK cells with alive K562 cells resulted in the higher specific target cell death and thus this method was used to study NK cell cytotoxicity in women with RPL and controls.



Supplementary Figure 33. Cytotoxicity assay optimization using Natural Killer (NK) cell enrichment and dead K562 cell removal. *Mean specific K562 target cell death (%) in co-cultures containing peripheral blood mononuclear cells (PBMCs) and alive K562 cells, enriched NK and total K562 cells, and enriched NK cells and alive K562 cells is shown (N=2). In co-cultures including PBMCs the effector:target cell ratios used were equal to 12.5:1 (Low), 25:1 (Medium), and 50:1 (High), while the average specific K562 target cell death observed in each of these conditions was calculated. In co-cultures including NK cells, 0.5:1 (Low), 1:1 (Medium), and 2:1 (High) effector:target cell ratios were used, and the average value was again included. Error bars representing standard deviation are displayed.*

Lastly, IL-2-mediated NK cell pre-stimulation was employed as it is often used to enhance NK cell cytotoxicity.[760] Specifically, enriched NK cells were washed and

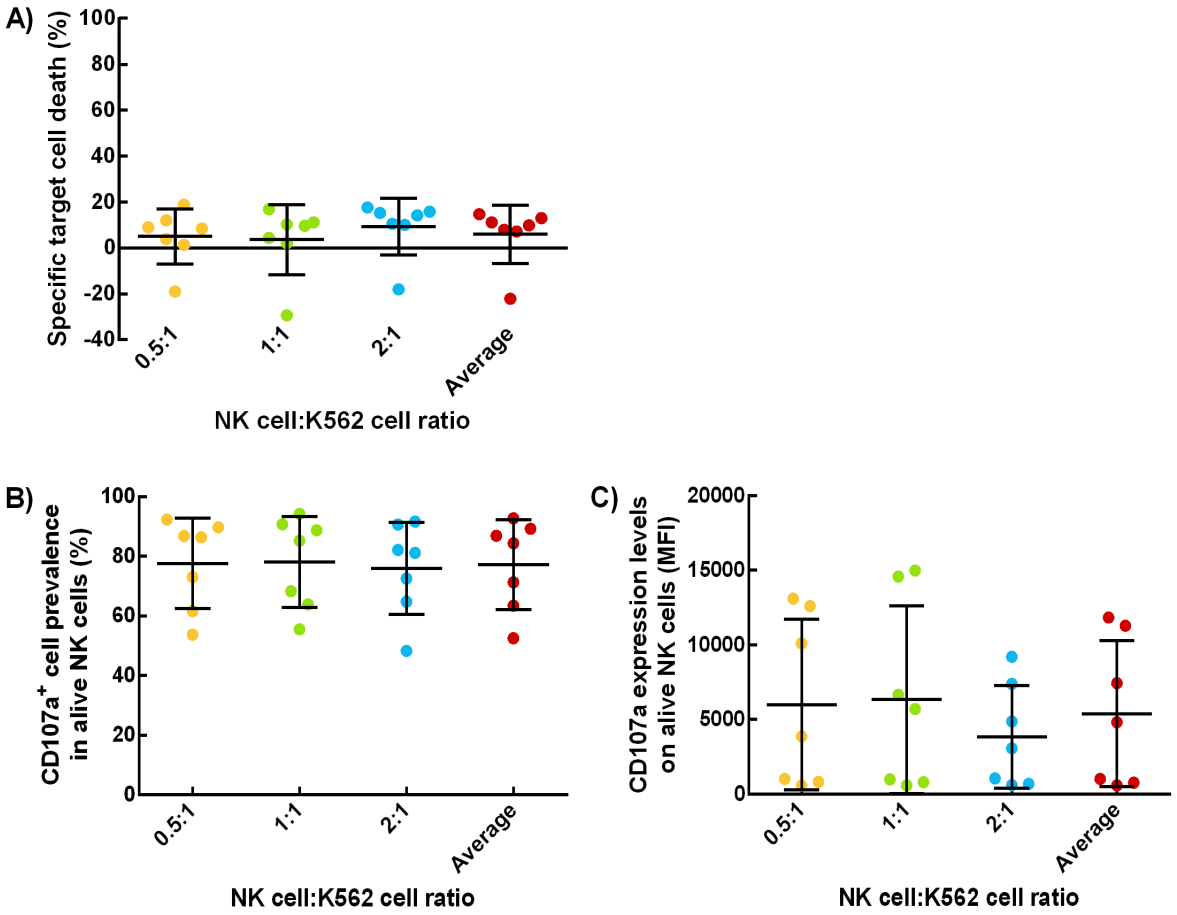
cultured at a $5*10^5$-10^6 concentration in complete RPMI (*N*=2). 200U human recombinant IL-2 (Sigma-Aldrich) was added per mL of culture, while control unstimulated cultures were also generated. Cells were incubated for 18h and were washed with 5mL complete RPMI medium prior to their co-incubation with alive K562 cells. Specific target cell death was only increased by IL-2 pre-stimulation in the culture containing NK and K562 cells at a 2:1 ratio (Supplementary Figure 34). As no or low IL-2 levels have been detected in the endometrium and decidua of healthy women,[421, 761] IL-2 pre-stimulation was not implemented.



Supplementary Figure 34. Cytotoxicity assay optimization by interleukin (IL)-2 pre-stimulation of Natural Killer (NK) cells. *Mean specific K562 target cell death (%) in co-cultures including different NK:K562 cell ratios, following or in the absence of IL-2-mediated NK cell pre-stimulation is illustrated (N=2). An average of specific target cell death in co-cultures including different cell ratios is also displayed. Error bars representing standard deviation are included.*

13.15 Cytotoxicity assay validation

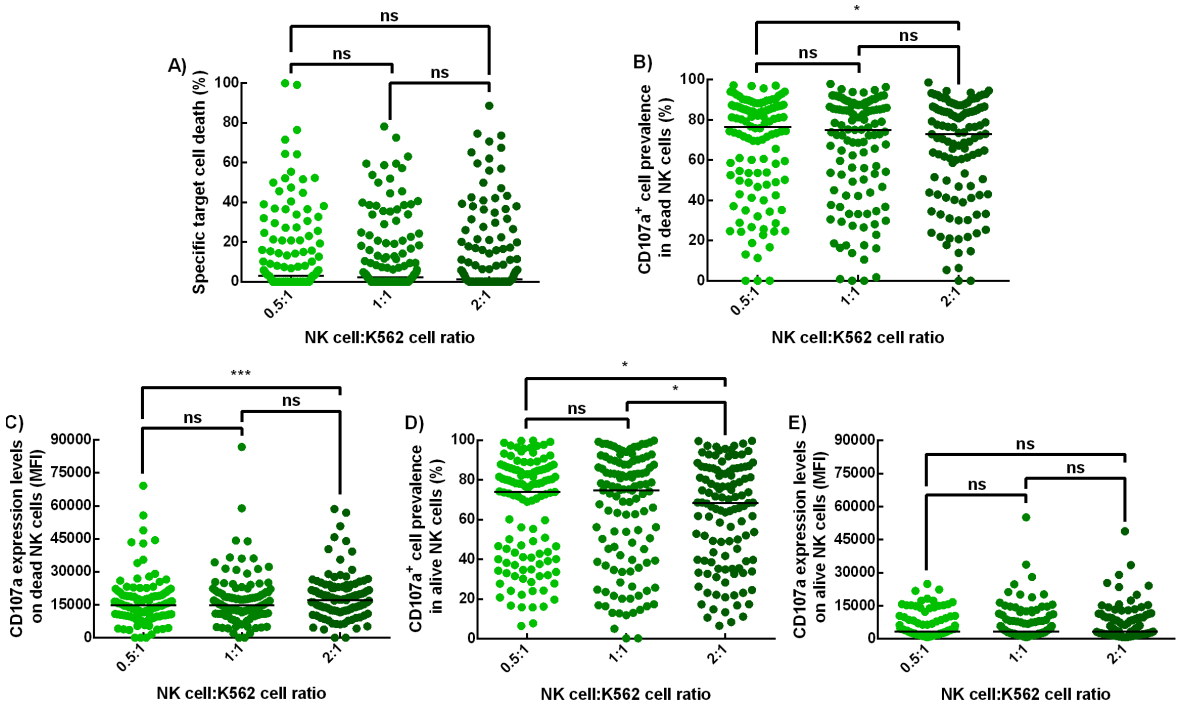
To validate the cytotoxicity assay, control samples (*N*=7) were obtained and processed according to the optimized protocol described in the Material and Methods chapter. Specific target cell death levels, $CD107a^{+}$ alive NK cell prevalence, and CD107 expression intensity on these cells was evaluated (Supplementary Figure 35). Negative specific target cell death values were only detected in one sample and thus no further optimization was performed.



Supplementary Figure 35. Cytotoxicity assay validation. *A) Specific K562 target cell death (%), B) CD107a⁺ cell prevalence in alive Natural Killer (NK) cells (%), and C) CD107a expression levels on alive NK cells, represented by the median fluorescence intensity (MFI), in co-cultures containing different NK:K562 cell ratios are illustrated (N=7). For each of these parameters of NK cell activity the average of the values obtained from the different co-culture conditions for each sample is also shown. The mean and standard deviation of each dataset is displayed.*

13.16 Effect of NK cell:K562 cell ratio on specific target cell death

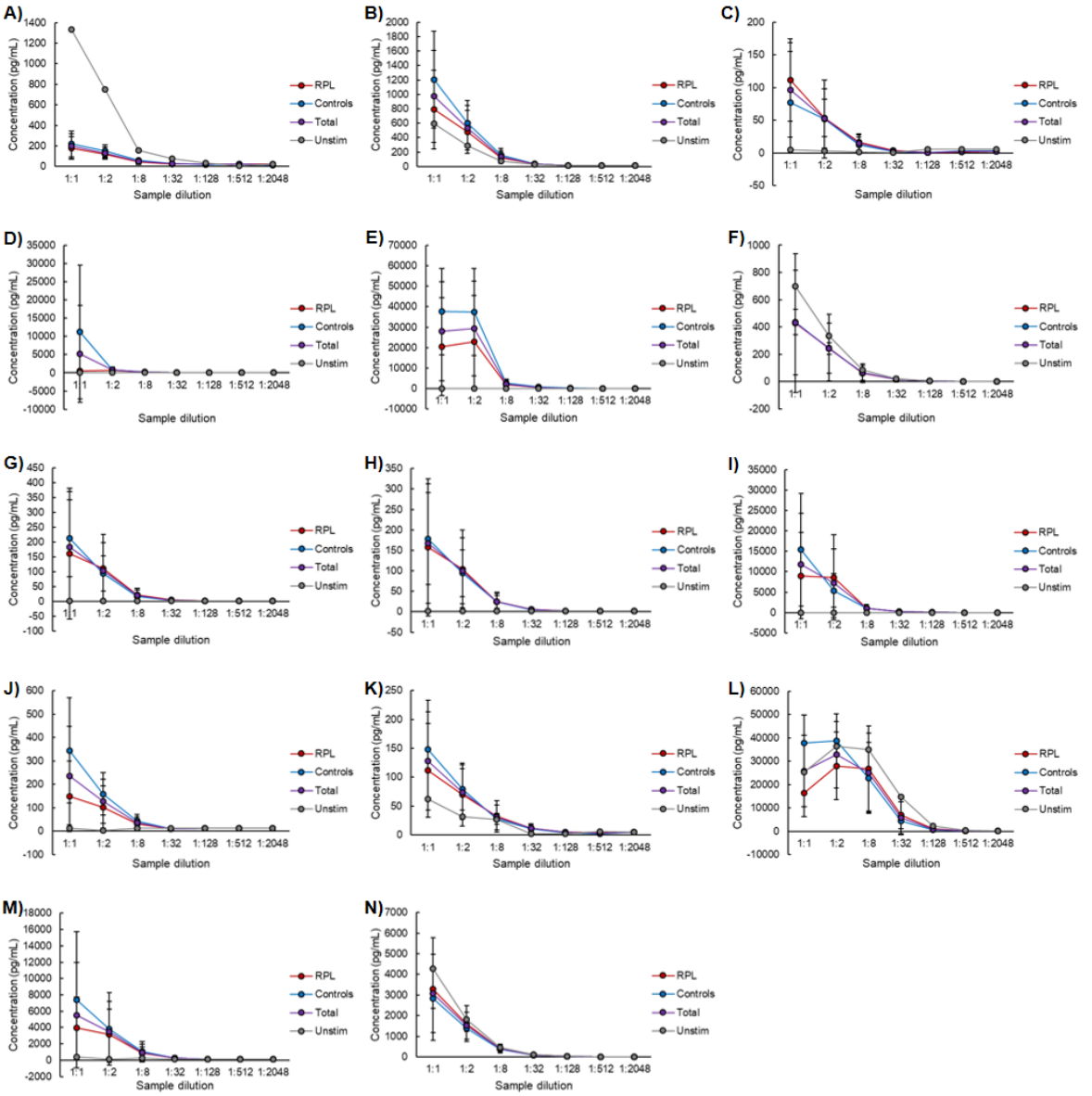
The levels of specific target cell death were compared between the 0.5:1, 1:1, and 2:1 NK cell:K562 cell co-cultures (*N*=135), and were not found to be affected by the NK cell:K562 cell ratio (Supplementary Figure 36A). Similarly, CD107a expression on dead and alive NK cells was measured and compared between co-cultures containing different NK cell:K562 cell ratios (*N*=116). $CD107a^+$ dead NK cell prevalence was found to be elevated in co-cultures containing 0.5:1 NK cells:K562 cells compared to co-cultures containing a 2:1, ratio of these cells (adjusted p=0.0286) (Supplementary Figure 36B), while CD107a expression intensity on dead NK cells was reduced in 0.5:1 compared to the 2:1 (adjusted p=0.0004) co-cultures (Supplementary Figure 36C). Furthermore, $CD107a^+$ cell prevalence in the alive NK cell population was decreased in the 2:1 NK cell:K562 cell co-cultures, compared to both the 0.5:1 (adjusted p=0.0498) and the 1:1 (adjusted p=0.0345) ones (Supplementary Figure 36D), while CD107a expression intensity on alive NK cells was not found to be affected by the effector:target cell ratio (Supplementary Figure 36E).



Supplementary Figure 36. Effect of Natural Killer (NK) cell:K562 cell ratios used in co-cultures for the evaluation of specific target cell death and CD107a expression. *The A) specific K562 cell death (N=135), B) CD107a$^+$ dead NK cell prevalence (N=116), C) CD107a expression intensity on dead NK cells, represented by the median fluorescence intensity (MFI) (N=116), D) CD107a$^+$ alive NK cell prevalence (N=116), and E) CD107a expression intensity on alive NK cells (N=116) in co-cultures including different ratios of NK cells:K562 cells are depicted. NK cells used were derived from both women with recurrent pregnancy loss (RPL) and controls. Friedman test was performed, accompanied by the Dunn's test for multiple comparisons, median displayed. ns: non-significant, *: adjusted p≤0.05, ***: adjusted p≤0.001*

13.17 Enzyme-linked immunosorbent assay optimization and validation

ELISA optimization and validation were simultaneously performed, using stimulated samples from control women (*N*=4) and women with RPL (*N*=5), as well as one unstimulated control sample. All the samples were titrated to determine the optimal concentration to be used. 4-fold dilutions of each sample, including 1:2, 1:8, 1:32, 1:128, 1:512, and 1:2048, were tested. 75µL sample and 75µL cell culture medium were added to the 1:2 tube and serial dilutions were performed. Undiluted controls were also used. The protocol described in the Materials and Methods section was utilised. ProcartaPlex™ Multiplex Immunoassay User Guide (ThermoFisher Scientific) suggested shaking at 500rpm but speed was increased at 700rpm as small microsphere aggregates could be detected. 1:1 and 1:2 sample dilutions were found to result in the highest concentration of most cytokines, without surpassing the detection limit (Supplementary Figure 37). Both concentrations were tested in the first assay and as quite a few markers were reported to be below the detection limit when the 1:2 dilution was used, undiluted samples were used in the following assays. The assay was validated (*N*=9), ensuring the detection of all cytokines.



Supplementary Figure 37. Enzyme-linked immunosorbent assay optimization. *Mean concentration (pg/mL) of A) granulocyte colony-stimulating factor (G-CSF), B) granulocyte-macrophage colony-stimulating factor (GM-CSF), C) granzyme A, D) granzyme B, E) interferon (IFN)-γ, F) interleukin (IL)-10, G) IL-13, H) IL-17A, I) IL-2, J) IL-4, K) IL-5, L) IL-8, M) perforin, and N) tumor necrosis factor (TNF)-α as detected by the enzyme-linked immunosorbent assay, in samples diluted 1:1, 1:2, 1:8, 1:32, 1:128, 1:512, 1:2048 in cell culture medium, is illustrated. Concentration in samples obtained by women with recurrent pregnancy loss (RPL) (N=5), healthy controls (N=4), total samples from women with RPL and controls (N=9), and an unstimulated control (N=1) are displayed in the form of different groups. Error bars representing standard deviation are included.*

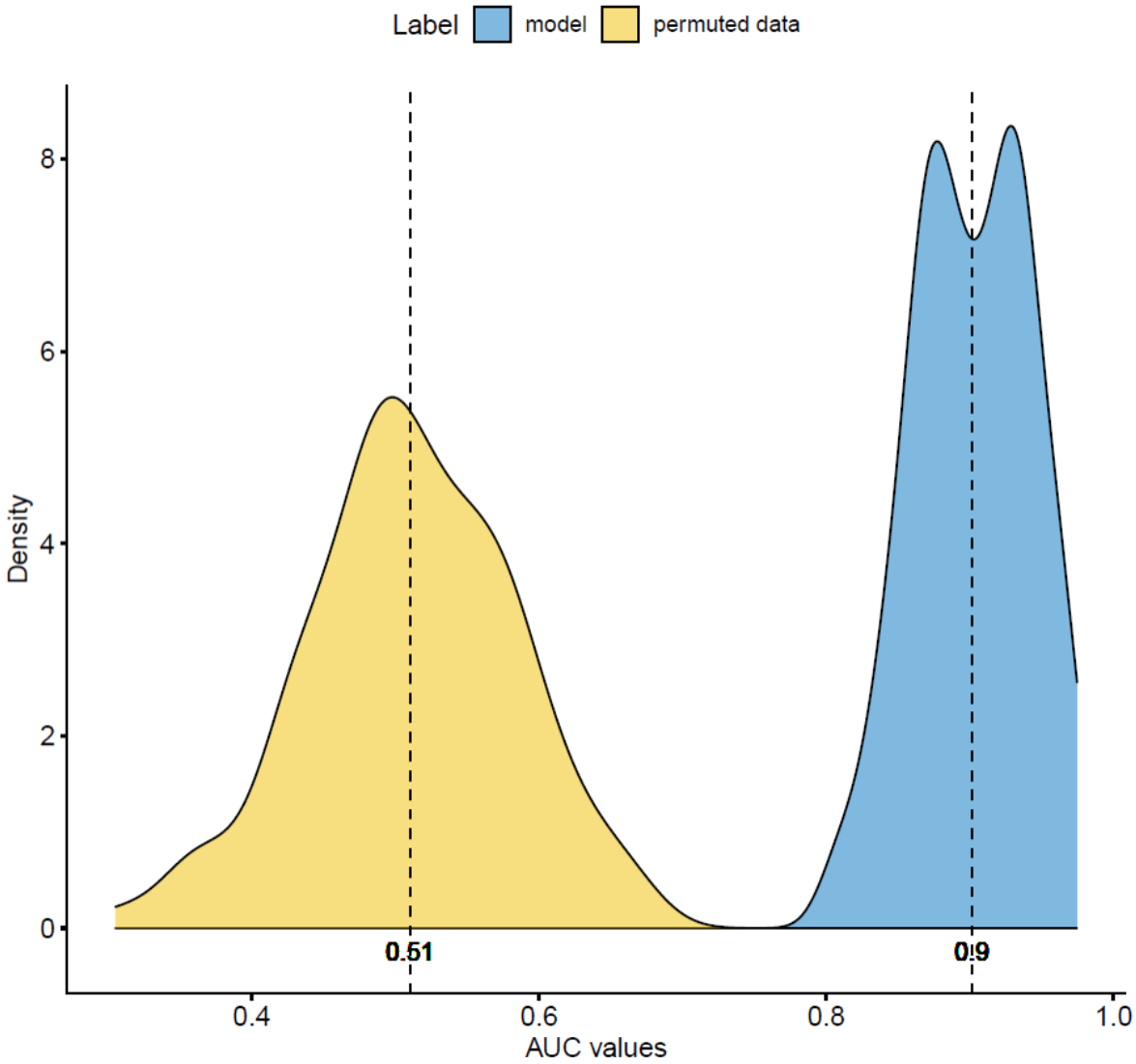
13.18 Data utilised for biomarker identification

Supplementary Table 2. Markers investigated for the identification of candidate immunological biomarkers distinguishing women with RPL. *Each marker examined and the respective assay used for data collection is depicted. CD: cluster of differentiation, G-CSF: granulocyte-colony stimulating factor, GM-CSF: granulocyte-macrophage colony-stimulating factor, IFN: interferon, IL: interleukin, MFI: median fluorescence intensity, NK: Natural Killer cells, PBMC: peripheral blood mononuclear cell, T_H cells: T helper cells, TNF: tumor necrosis factors, Treg: regulatory T cell*

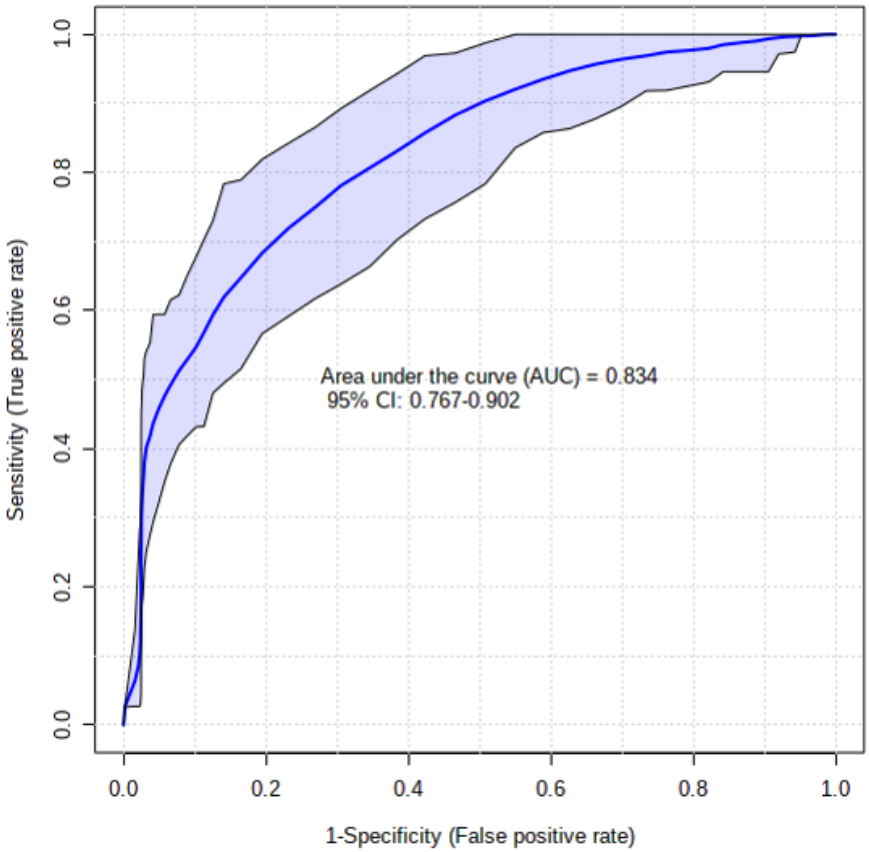
Assay	Marker	Assay	Marker
Flow cytometry assay	NK cells prevalence in lymphocytes (%)	Cytotoxicity assay	Average specific cell death (%)
	$CD56^{dim}CD16^{+}$ prevalence in NK cells (%)		Average $CD107a^{+}$ alive NK cell prevalence (%)
	$CD56^{bright}CD16^{-}$ prevalence in NK cells (%)		Average CD107a MFI on alive NK cells
	$CD56^{bright}/CD56^{dim}$ NK cell ratio	Enzyme-linked Immunosorbent assay	G-CSF concentration (pg/mL) in stimulated PBMC cultures
	$CD69^{+}$ cell prevalence in NK cells (%)		GM-CSF concentration (pg/mL) in stimulated PBMC cultures
	CD69 MFI on NK cells		IL-2 concentration (pg/mL) in stimulated PBMC cultures
	$CD69^{+}$ cell prevalence in $CD56^{dim}CD16^{+}$ NK cells (%)		IL-4 concentration (pg/mL) in stimulated PBMC cultures
	CD69 MFI on $CD56^{dim}CD16^{+}$ NK cells		IL-5 concentration (pg/mL) in stimulated PBMC cultures
	$CD69^{+}$ cell prevalence in $CD56^{bright}CD16^{-}$ NK cells (%)		IL-8 concentration (pg/mL) in stimulated PBMC cultures
	CD69 MFI on $CD56^{bright}CD16^{-}$ NK cells		IL-10 concentration (pg/mL) in stimulated PBMC cultures
	$CD3^{+}$ cell prevalence in lymphocytes (%)		IL-13 concentration (pg/mL) in stimulated PBMC cultures
	$CD4^{+}$ cell prevalence in T cells (%)		IL-17A concentration (pg/mL) in stimulated PBMC cultures
	$CD8^{+}$ cell prevalence in T cells (%)		IFN-γ concentration (pg/mL) in stimulated PBMC cultures
	Treg prevalence in T_H cells (%)		TNF-α concentration (pg/mL) in stimulated PBMC cultures
	$IL\text{-}2^{+}$ cell prevalence in stimulated T_H cells (%)		Granzyme A concentration (pg/mL) in stimulated PBMC cultures
	IL-2 MFI on stimulated T_H cells		Granzyme B concentration (pg/mL) in stimulated PBMC cultures
	$IFN\text{-}\gamma^{+}$ cell prevalence in stimulated T_H cells (%)		Perforin concentration (pg/mL) in stimulated PBMC cultures
	IFN-γ MFI on stimulated T_H cells		G-CSF concentration (pg/mL) in unstimulated PBMC cultures
	$TNF\text{-}\alpha^{+}$ cell prevalence in stimulated T_H cells (%)		GM-CSF concentration (pg/mL) in unstimulated PBMC cultures
	TNF-α MFI on stimulated T_H cells		IL-2 concentration (pg/mL) in unstimulated PBMC cultures
	$IL\text{-}10^{+}$ cell prevalence in stimulated T_H cells (%)		IL-4 concentration (pg/mL) in unstimulated PBMC cultures
	IL-10 MFI on stimulated T_H cells		IL-5 concentration (pg/mL) in unstimulated PBMC cultures
	$IL\text{-}17A^{+}$ cell prevalence in stimulated T_H cells (%)		IL-8 concentration (pg/mL) in unstimulated PBMC cultures
	IL-17A MFI on stimulated T_H cells		IL-10 concentration (pg/mL) in unstimulated PBMC cultures

	IL-2$^+$ cell prevalence in unstimulated T_H cells (%)		IL-13 concentration (pg/mL) in unstimulated PBMC cultures
	IL-2 MFI on unstimulated T_H cells		IL-17A concentration (pg/mL) in unstimulated PBMC cultures
	IFN-γ$^+$ cell prevalence in unstimulated T_H cells (%)		IFN-γ concentration (pg/mL) in unstimulated PBMC cultures
	IFN-γ MFI on unstimulated T_H cells		TNF-α concentration (pg/mL) in unstimulated PBMC cultures
	TNF-α$^+$ cell prevalence in unstimulated T_H cells (%)		Granzyme A concentration (pg/mL) in unstimulated PBMC cultures
	TNF-α MFI on unstimulated T_H cells		Granzyme B concentration (pg/mL) in unstimulated PBMC cultures
	IL-10$^+$ cell prevalence in unstimulated T_H cells (%)		Perforin concentration (pg/mL) in unstimulated PBMC cultures
	IL-10 MFI on unstimulated T_H cells		IL-2/IL-10 concentration ratio
	IL-17A$^+$ cell prevalence in unstimulated T_H cells (%)		IFN-γ/IL-10 concentration ratio
	IL-17A MFI on unstimulated T_H cells		TNF-α/IL-10 concentration ratio
	IL-2$^+$/IL-10$^+$ T_H cell ratio		IL-17A/IL-10 concentration ratio
	IL-2/IL-10 MFI ratio on T_H cells		IL-2/IL-13 concentration ratio
	IFN-γ$^+$/IL-10$^+$ T_H cell ratio		IFN-γ/IL-13 concentration ratio
	IFN-γ/IL-10 MFI ratio on T_H cells		TNF-α/IL-13 concentration ratio
	TNF-α$^+$/IL-10$^+$ T_H cell ratio		IL-17A/IL-13 concentration ratio
	TNF-α/IL-10 MFI ratio on T_H cells		IL-2/IL-4 concentration ratio
	IL-17A$^+$/IL-10$^+$ T_H cell ratio		IFN-γ/IL-4 concentration ratio
	IL-17A/IL-10 MFI ratio on T_H cells		TNF-α/IL-4 concentration ratio
	IL-2$^+$/IL-17A$^+$ T_H cell ratio		IL-17A/IL-4 concentration ratio
	IL-2/IL-17A MFI ratio on T_H cells		IL-2/IL-5 concentration ratio
	IFN-γ$^+$/IL-17A$^+$ T_H cell ratio		IFN-γ/IL-5 concentration ratio
	IFN-γ/IL-17A MFI ratio on T_H cells		TNF-α/IL-5 concentration ratio
	TNF-α$^+$/IL-17A$^+$ T_H cell ratio		IL-17A/IL-5 concentration ratio
	TNF-α/IL-17A MFI ratio on T_H cells		
	IFN-γ$^+$ cell prevalence in stimulated NK cells (%)		
	IFN-γ MFI on stimulated NK cells		
	TNF-α$^+$ cell prevalence in stimulated NK cells (%)		
	TNF-α MFI on stimulated NK cells		
	IL-10$^+$ cell prevalence in stimulated NK cells (%)		
	IL-10 MFI on stimulated NK cells		
	IFN-γ$^+$ cell prevalence in unstimulated NK cells (%)		
	IFN-γ MFI on unstimulated NK cells		
	TNF-α$^+$ cell prevalence in unstimulated NK cells (%)		
	TNF-α MFI on unstimulated NK cells		
	IL-10$^+$ cell prevalence in unstimulated NK cells (%)		
	IL-10 MFI on unstimulated NK cells		
	IFN-γ$^+$/IL-10$^+$ NK cell ratio		
	IFN-γ/IL-10 MFI ratio on NK cells		
	TNF-α$^+$/IL-10$^+$ NK cell ratio		
	TNF-α/IL-10 MFI ratio on NK cells		

13.19 Effectiveness of models built for the identification of women with RPL



Supplementary Figure 38. Density plot of the area under curve (AUC) values of the 18 marker-based model for the identification of women with recurrent pregnancy loss (RPL), run 1000 times using permuted and non-permuted data. *The mean AUC values for each dataset is highlighted (bold). The 18 markers taken into consideration represent the 18 features selected by the Elastic Net (EN) and Least Absolute Shrinkage and Selection Operator (LASSO) methods.*



Supplementary Figure 39. Receiver operating characteristic (ROC) curve of the 4 marker-based model for the identification of women with recurrent pregnancy loss (RPL). *The area under curve (AUC) and the 95% confidence interval (CI) values are displayed.*

14 PUBLICATIONS ARISING FROM THE PRESENT THESIS

Bagkou Dimakou D, Lissauer D, Tamblyn J, Coomarasamy A, Richter A. Understanding human immunity in idiopathic Recurrent Pregnancy Loss. Eur J Obstet Gynecol Reprod Biol.

Bagkou Dimakou D, Tamblyn J, Chu J, Coomarasamy A, Richter A. Diagnosis and management of idiopathic recurrent pregnancy loss (RPL): Current immune testing and immunomodulatory treatment practice in the United Kingdom. J Reprod Immunol.